Current Chemistry Letters 13 (2024) 359–366

Contents lists available at GrowingScience

Current Chemistry Letters

homepage: www.GrowingScience.com

Chitosan – hydrogen iodide salt supported graphite electrode: A simple and novel electrode for the reduction of nitro group under electrochemical condition

P. L. Deena[a*], Savariraj Joseph Selvaraj[b] and K. Joby Thomas[c]

[a]*Department of Chemistry, St. Joseph's College (Autonomous), Tiruchirappalli, 620 002, Tamil Nadu, India*
[b]*Affiliated to Bharathidasan University, Tiruchirappalli 620 024, Tamilnadu, India*
[c]*Department of Chemistry, St. Thomas' College (Autonomous), Thrissur- 680 001, Kerala, India*

C H R O N I C L E

Article history:
Received March 20, 2023
Received in revised form
June 17, 2023
Accepted November 1, 2023
Available online
November 1, 2023

Keywords:
Chemoselective reduction
Quaternary ammonium chloride
Chitosan
Acetic acid
Nitro group

A B S T R A C T

The present investigation provides a unique, simple, selective and efficient method for the electrochemical reduction of aromatic nitro groups into amines using chitosan-hydrogen iodide salt supported graphite electrode. 3:1 tetrabutyl ammonium chloride and acetic acid mixture was used as the medium for electrolytic process and a constant voltage of 5 V applied between the modified electrodes. The reaction was found to be selective and further reduction of amines was not observed. The purity of the products was checked with HPLC and characterized using spectroscopic tools. The electrochemical synthesis resulted in moderate to good yields of amino compounds which were higher than the reduction using conventional graphite electrodes. Quaternary ammonium chloride behaved as supporting electrolyte during synthesis and the reaction did not progress in the absence of acetic acid. The redox characteristic of the process was studied by cyclic voltammetry of the reaction mixture.

1. Introduction

The widespread application of aromatic amines in different industries, including agrochemicals, textile dyes, medicines, the rubber industry, fine chemicals etc. demonstrates their great utility as intermediates and building blocks in organic synthesis.[1-5] One of the most prevalent techniques for getting various aromatic amines is via reducing nitro groups.[6, 7]

The conversion of a nitro group ($-NO_2$) to an aromatic amine ($-NH_2$) can be accomplished in organic chemistry in a variety of ways. The most widely used technique for converting nitro groups into aromatic amines is catalytic hydrogenation. It involves the use of a metal catalyst (usually Pd, Pt or Ni) and hydrogen gas under high pressure and temperature.[8] In the iron reduction process, nitro groups are transformed into aromatic amines using iron powder and an acid (typically acetic acid).[9] Zinc reduction involves the use of zinc dust and an acid (usually hydrochloric acid) to reduce nitro groups to aromatic amines.[10-12] Under benign conditions, aromatic nitro compounds are converted to amines via the sodium borohydride reduction technique, which uses $NaBH_4$ and an acid (often acetic acid).[13,14]

In spite of the requirement of high pressure, possibility for potential accident and costly catalyst/reagent, these reductions are more preferred in the synthetic laboratories. Nitro compounds and their derivatives are important in biological, pharmaceutical and industrial fields.[15,16] The reduction of nitro group under electrochemical conditions is another approach that has been widely explored but is not as frequently used. The reaction can be carried out under mild conditions and is often utilized to reduce nitro compounds that are challenging to reduce using alternative techniques.[17-19]

* Corresponding author.
E-mail address shanplsabs@gmail.com (P. L. Deena)

doi: 10.5267/j.ccl.2023.11.001

In addition to the conventional techniques, electrochemically stimulated reactions in organic synthesis have created novel avenues for synthetic transformation.[20-24] Making the reaction as environmentally friendly as possible while adhering to green chemistry principles is of the utmost importance.[25-27] It is a powerful method for selectively reducing benzyl groups in organic molecules, providing a versatile tool for the synthesis of a wide range of benzylic compounds.[28-30] Oxidation of toluene, benzyl alcohol, benzyl chloride, 3-phenylpropene are just a few examples of electrochemical oxidation reactions.[31-33] The electrochemical reduction of organic compounds is a versatile and promising field that continues to be explored for various applications, contributing to both chemical synthesis advancements and sustainable technologies. Electrosynthesis of alcohols, electrochemical hydrogenation, electrochemical reduction of α,β-unsaturated ketones etc. are the few examples which showcase the diverse applications of electrochemical reduction in various fields, ranging from chemical synthesis to environmental remediation and energy storage.[34] By adjusting the applied current or voltage, electrochemical reactions enable control of chemoselectivity.

Chitosan is a polymer of carbohydrate which is made up of β- linked D- glucosamine and N-acetyl D-glucosamine units. It is obtained from the basic hydrolysis of chitin (**Fig. 1**) isolated from the shells of shrimp. The -NH_2 unit present in the chitosan is the central focus of the chemists and is modified to specific applications particularly to serve as ligand for several transition metals. Commercially available chitosan is categorized as low, medium and high based on their molecular weight.

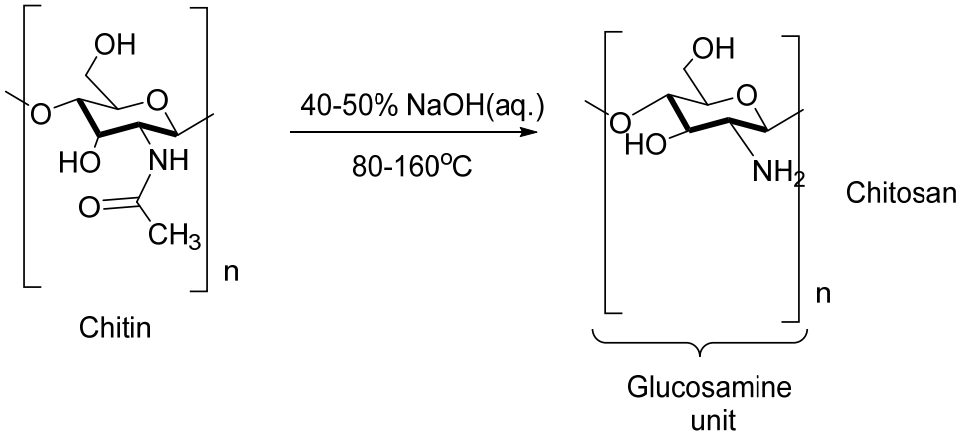

Fig. 1. Chitosan Preparation from chitin

Chitosan, due to its unique chemical structure, has several properties such as biocompatibility, biodegradability and adsorption capability, making it useful in various biomedical applications.[35-37] However, chitosan is not conductive, which limits its use in electronic applications. In contrast, graphite is advantageous for use in electronic equipment because it is an excellent conductor of electricity and has a wide surface area. By impregnating chitosan with graphite, the resulting composite material has improved adsorption properties of chitosan and the conductivity of graphite. In the acid, the free -NH_2 group of chitosan gets protonated, and the resulted salt is soluble in water. Upon evaporation the dissolved chitosan-acid salt results in a translucent film with high tensile strength. We envisaged that this film could be used as electrode by impregnating graphite powder (G-Ch).

In this communication, we report the preparation of a novel electrode in which graphite is impregnated on Chitosan – Hydrogen iodide salt and investigated the use of this electrode for the reduction of nitro group under electrochemical conditions. This electrode can act both as the reservoir of H^+ ions and supplier of electrons. We anticipate that under mild conditions, the H^+ ions in the electrode will facilitate the reduction. Furthermore, enhanced surface area of the electrode may boost current flow through the medium. The yield of the amino compounds was compared with the yield obtained by the reduction using graphite electrode.

2. Results and discussion

2.1. SEM analysis of the G-Ch film

Though the film looks homogeneous with even distribution of graphite, the SEM image clearly shows that the graphite powder is randomly distributed, and the surfaces are not uniform and smooth (**Fig. 2**). In the SEM image, it is observed that small flakes of chitosan –HI is adhered on the surface which is around 20 μm in size.

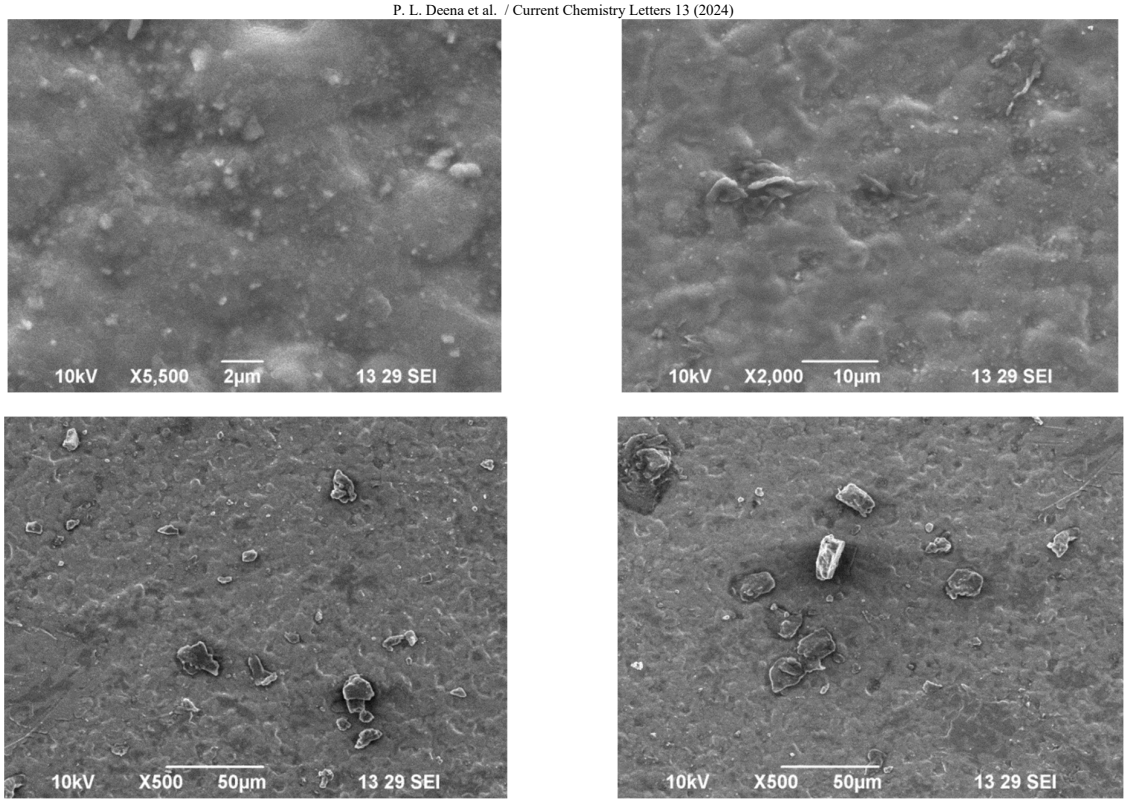

Fig. 2. SEM image of the graphite impregnated chitosan (1g of graphite/1g of chitosan)

2.2. XRD studies of the G-Ch film

The diffractogram of the Chitosan-graphite film displayed two sharp peaks at 2θ = 26.795° and 54.826° which is attributed to the peaks of crystalline chitosan (130) and graphite (004). The appearance of sharp peaks is an indication of crystalline behaviour of the composite material than pure low molecular weight chitosan.[38] The XRD spectrum of G-Ch is depicted in **Fig. 3.**

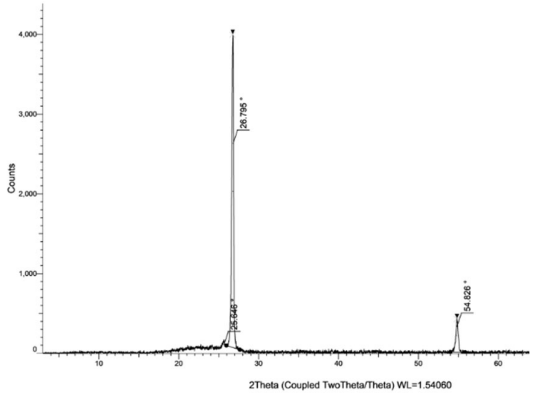

Fig. 3. X-ray diffractogram of chitosan-graphite composite material

2.3. FTIR spectral studies

FTIR spectrum of chitosan and the composite film (G-Ch) is shown in **Fig. 4.** The O-H and N-H stretching frequencies appeared at 3340 and 2878 cm^{-1} respectively in the spectrum of G-Ch. These peaks were slightly shifted to low energy region when compared to IR spectrum of chitosan. This confirms the interaction of chitosan-HI salt with graphite. C-N stretching frequencies of the composite film (1622 and 1525.5 cm^{-1}) also appeared in the lower frequency region of the FTIR spectrum when compared to the peaks of pure low molecular weight chitosan. The strong spectral peak of chitosan corresponds to C-O-C vibrations (1077 cm^{-1}) were also shifted to lower frequency side in the composite film spectrum (1062 and 1020 cm^{-1}).

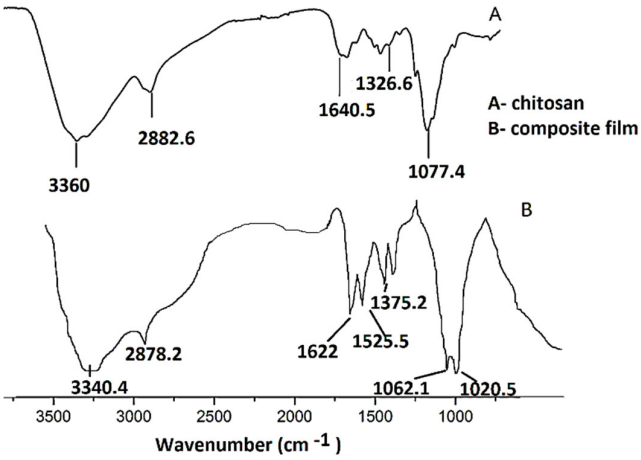

Fig. 4. FTIR spectrum of A) chitosan and B) composite film

2.4. Conductivity of composite film

Initially we studied the conductivity of the films prepared (2 x 5 cm) using $nBu_4N^+Cl^-$: AcOH (3:1mmol) as electrolyte and MeOH (30 ml) as solvent (**Table 1**). Additionally, we attempted to find out conductivity in EtOH. In the methanol medium, conductivity values were seen to be relatively superior. Moreover, we chose MeOH solvent since it has high dielectric constant and does not dissolve the chitosan-HI film. A constant voltage of 5 V was applied between the graphite impregnated chitosan–HI films. The current flow was found to increase slightly as the amount of graphite is increased in the film. A slight fluctuation of the current was observed during measurement.

Table. 1. Conductivity study of the graphite impregnated polymer film

Sl. No	Chitosan (g):Graphite (g)	Solvent	Current (A)
1	10:1	MeOH	0.03
2	10:2	MeOH	0.05
3	10:4	MeOH	0.06
4	10:5	MeOH	0.08
5	10:10	MeOH	0.08
6	10:1	EtOH	0.02
7	10:2	EtOH	0.05
8	10:4	EtOH	0.06
9	10:5	EtOH	0.07
10	10:10	EtOH	0.07

2.5 Electrochemical synthesis

Same reaction condition was applied to a number of substituted aromatic nitro compounds and the outcome is shown in **Table 2**. 3mmol nitro compounds were subjected to electrochemical reduction using $nBu_4N^+Cl^-$: AcOH (3:1 mmol) and MeOH (30 ml) as electrolyte and solvent respectively. Modified electrodes (1g graphite : 1g chitosan : 800 mg HI) having dimensions (2 x 5cm) were used for all investigation. A constant potential of 5 V was applied between the electrodes for a period of 8 h. The purity of the products was checked with HPLC and characterized using NMR and FTIR spectroscopic tools. The efficiency of the processes in the presence of the conventional graphite electrode was also determined parallelly and reported in **Table 2.**

From the experimental data, it was noticed that majority of nitro compounds gave higher yields of reduced amino form in the presence of G-Ch electrodes during electrochemical transformation than the reduction using graphite electrodes. Exceptionally very high yield of 2-nitro aniline was obtained when compared to the synthesis using conventional graphite electrodes. Slightly low yield was noticed for the reduction of 4-methoxy nitro compound when compared to the electrochemical synthesis using graphite electrodes. The increased efficiency of the G-Ch electrodes in converting the aromatic nitro compounds into the corresponding amino compounds may be due to the potency of the electrodes to supply the H^+ ions (from HI) readily from their surface which is an essential condition of reduction.

In the absence of acetic acid, it was also observed that the electrochemical synthesis did not advance. It can be assumed that repeated release of H^+ ions from the G-Ch surface and the absorption of protons from the acetic acid continuous till the completion of the reaction. The G-Ch electrode (cathode) itself acted as the reservoirs of both H^+ ions and electrons for the reduction of nitro compounds.

Table. 2. Substrate scope for nitro reduction under electrochemical condition

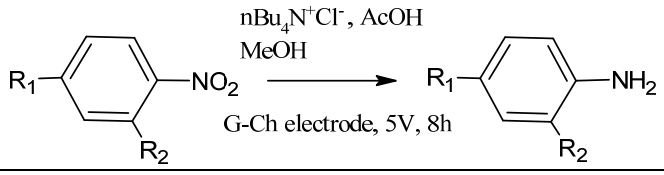

Sl. No	R_1, R_2	Yield (%) G-Ch electrode	Yield (%) Graphite electrode
1	R_1=H, R_2=H	89	85
2	R_1=Cl, R_2=H	87	82
3	R_1= NH_2, R_2=H	81	81
4	R_1=H, R_2=NH_2	92	76
5	R_1= OMe, R_2=H	65	68
6	R_1=F, R_2=H	78	75
7	R_1=H, R_2= F	79	68

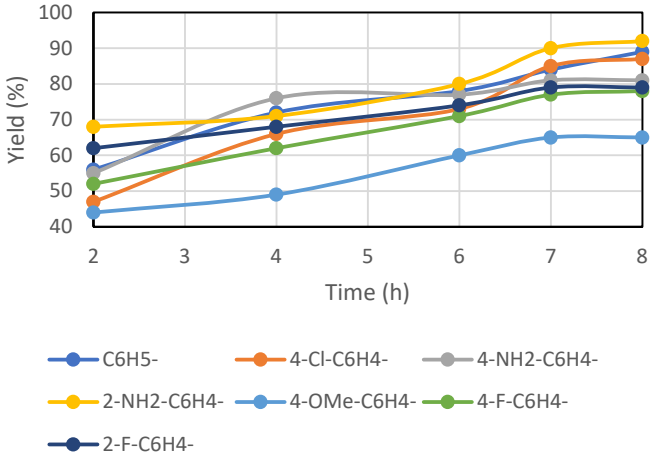

Fig. 5. Variation of reaction time with the yield of amino compounds

The approximate duration of the electrochemical process was also estimated in this work. It was found that the entire electrochemical reduction process took 6 to 8 hours to complete. The optimal time for the synthesis of aromatic amino compounds was determined to be 8 hours. The variation of reaction time with the yield of the aromatic amino compounds is depicted in **Fig. 5**. It is understandable that the molecules such as 4-amino nitrobenzene, 4-methoxy nitrobenzene and 2-fluoro nitrobenzene underwent complete reduction at 7 h.

For the electrochemical reduction of nitro compounds, it was also examined how the applied voltage (1–5 V) varied with the yield of product **(Table 3)**. Since there was a good yield of the products and a discernible rate of reaction at 5 V potential, this voltage was selected to be the optimum condition for the reduction.

Table 3. Variation of the applied potential with the yield (%) of the product

Compound	1V	3V	5V
aniline	78	84	89
p-chloroaniline	79	83	87
p-phenylenediamine	72	79	81
o-phenylenediamine	78	86	92
4-methoxy aniline	60	63	65
4-Fluoroaniline	68	74	78
2-Fluoroaniline	67	75	79

The resulting anilines were pure as demonstrated by chromatographic and spectroscopic methods.

The NMR spectral data and the M. P/B. P of various amino compounds are listed below.

C_6H_5-NH_2: B. P. 185.2 ^{0}C; ^{1}Hnmr (ppm): δ 6.64-7.13 (Ar-H), 3.54 (-NH_2); ^{13}Cnmr (ppm): δ 115.1, 118.5, 129.4, 146.5. **4-Cl-C_6H_4- NH_2**: M. P. 73.1 ^{0}C; ^{1}Hnmr (ppm): δ 6.57-7.11 (Ar-H), 3.57 (-NH_2); ^{13}Cnmr (ppm): δ 145.07, 116.22, 122.9, 129.07. **4-NH_2-C_6H_4-NH_2**: M. P. 140.3 ^{0}C; ^{1}Hnmr (ppm): δ 6.54 (Ar-H), 3.37 (-NH_2); ^{13}Cnmr (ppm): δ 138.68, 116.65. **2-NH_2-C_6H_4-NH_2:** M. P. 104.5 ^{0}C; ^{1}Hnmr (ppm): δ 6.34, 6.57 (Ar-H), 4.37 (-NH_2); ^{13}Cnmr (ppm): δ 116.38, 147.32. **4-OMe-**

C_6H_4-NH_2: M. P. 58.1 ^{0}C; ^{1}Hnmr (ppm): δ 6.77, 6.92 (Ar-H), 3.43 (-NH_2), 3.73 (-OCH_3) ; ^{13}Cnmr (ppm): δ 56.31, 114.32, 116.41, 140.82, 152.33. **4-F- C_6H_4-NH_2**: B. P. 187.5 ^{0}C; ^{1}Hnmr (ppm): δ 6.53, 6.83 (Ar-H), 3.46 (-NH_2); ^{13}Cnmr (ppm): δ 115.4.31, 116.7, 148.22, 156.72 **2-F- C_6H_4-NH_2:** 182.2 ^{0}C; ^{1}Hnmr (ppm): δ 6.92-7.62 (Ar-H), 3.71 (-NH_2); ^{13}Cnmr (ppm): δ 111.62, 116.42, 126.33, 129.64, 134.5, 154.51

The electrode remains undissolved in the reaction medium. After the reaction, the electrode was washed with methanol and air dried. It had the same nature after two hours and its usability had been verified. It is worthwhile to mention that almost the same yield of the amino compounds was obtained for the second process.

2.6. Cyclic voltametric studies

The mechanism of nitro group reduction under electrochemical method had been thoroughly investigated by cyclic voltammetry studies. We performed CV studies using G-Ch electrodes and Ag/AgCl reference electrode. 2-nitroaniline (1 mmol) was chosen as the substrate (**Fig. 6**). Initially, the reaction mixture was scanned over a potential range of -2 to +2 V to observe the active regions. After that the experiment was repeated with a fresh mixture in the potential range -2.0 to 0 V which found as the active region of the electrochemical process. The curve shown in the figure represents the cyclic voltammogram for the reduction of 2-nitro aniline. The voltammogram displayed three small reduction peaks at -0.68, -1.2 and -1.41 V which corresponds to three stage reduction of the nitro group. A strong oxidation peak at -0.66 V was also visible in the CV diagram. Based on CV investigations, the reduction mechanism for the nitro group can be explained as depicted in **Scheme 1**.

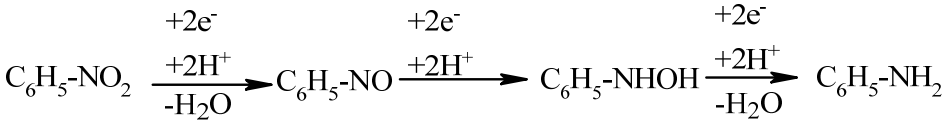

Scheme 1. Mechanism of nitro group reduction under electrochemical conditions

The G-Ch electrode initially provides two electrons and two H^+ ions to the nitro group, which then changes into $C_6H_5N(OH)_2$ at -0.68 V. Due to the initial product's instability, it loses one water molecule and converts into aromatic nitroso compound (C_6H_5NO). The nitroso compound further captures two electrons and two H^+ ions from the electrode to form the hydroxyl amine (C_6H_5NHOH). This process took place at -1.2 V. The third step of the reduction process occurred at -1.4 V, when the hydroxyl amine accepts two H^+ ions and electrons from the G-Ch electrode to produce the corresponding amino compound.

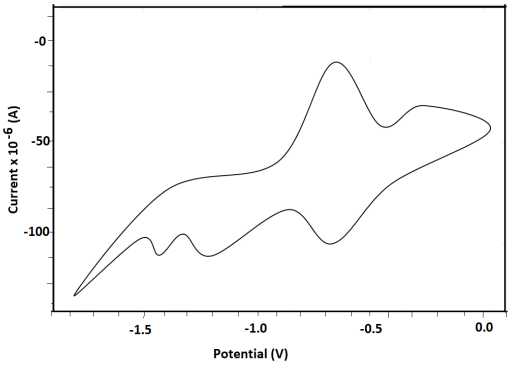

Fig. 6. Cyclic voltammogram of 2-nitro aniline

3. Conclusion

In conclusion, we have developed chitosan-HI supported graphite electrode and used it for the reduction of nitro group of aromatic compounds. We have demonstrated the effectiveness of G-Ch electrodes in reducing the nitro group into amino group and compared with that of conventional reduction using graphite electrodes. The electrode acted as the reservoir for both electrons and H^+ ions. Most of the nitro compounds gave better yields of amines compared to the reduction using graphite electrodes. Presence of $nBu_4N^+Cl^-$: AcOH (3 : 1) electrolyte in MeOH gave better results for the reduction of nitro compounds using 1g graphite : 1g chitosan : 800 mg HI composite electrode. Among the investigated reductions, the 2-nitroaniline reduction at 5 V for 8 h displayed the highest yield of o-phenylenediamine (92 %). The three-stage reduction process involved in the electrochemical reduction was verified using cyclic voltametric studies. The reusability of the G-Ch electrode was checked after cleaning it with methanol. Almost same yield of the amines was obtained when the reduction was conducted again using the same electrode.

4. Experimental

4.1. Preparation of chitosan-hydrogen iodide salt supported graphite electrode

Commercially available low molecular weight chitosan (Sisco Research Lab) was taken in 100 ml beaker and added 30ml water. To this suspension, stoichiometric amount of hydrogen iodide (Merck Millipore) is added dropwise with constant stirring. Chitosan gets dissolved completely to produce highly viscous gelatin like chitosan – HI salt. To this viscous material graphite powder (purchased from Aldrich) was added and stirred with mechanical stirrer for 30 minutes to ensure complete dissolution of chitosan and proper mixing of graphite powder. After 30 minutes, the viscous black colour liquid was poured into petri dish covered with perforated filter paper and allowed to dry in the in the open atmosphere. (Oven drying alters the nature of film that is produced). After two days of drying, the film is peeled off from the petri dish and cut into the desired shape and size (2 x 5 cm). The graphite powder was discovered to be well bound within the film and washing with an organic solvent did not remove any graphite powder from the film. Following this method, we impregnated 100 mg, 200 mg, 400 mg, 500 mg and 1000 mg of graphite in 1000 mg of chitosan. The film was found to be insoluble in CH_2Cl_2, $CHCl_3$, THF, MeOH and ethanol. The film with less graphite (100 mg – 500 mg) undergoes deformation and is flexible when dipped in ethanol. Better rigidity is obtained when 1000 mg of graphite powder was impregnated on the polymer.

4.2 Spectroscopy, microscopy and XRD studies

Shimadzu prestige 20 FT-IR spectrophotometer was used to record IR spectra with NaCl crystal as the sample holder. The Attenuated Total Reflection (ATR) method was used to perform FTIR analysis. SEM was performed using SEM EDX MB.1051. XRD of chitosan-hydrogen iodide salt supported graphite electrode were recorded by DW-XRD-2700A instrument. Utilizing a Bruker 300 MHz FT-NMR apparatus, the NMR spectra of the products were determined.

4.3 Cyclic voltammetric studies

Cyclic voltammetric studies of the reaction mixture were performed using G-Ch electrodes (0.5 x 3 cm) and Ag/AgCl reference electrode. 2-nitroaniline (1 mmol) was chosen as the substrate in order to analyze the overall behaviour of the nitro reduction process. Voltammetric studies were performed using electrochemical workstation (CH instrument, Model: CH1660D) at a scan rate of 50 mV/s in 3:1 quaternary ammonium chloride and acetic acid mixture as the electrolytic medium. Total volume of the electrolytic solution was 8 ml.

4.4. Procedure for the selective nitro reduction

Due to its reasonable rigidity and resistance to deformation in organic solvent, we selected 1g graphite powder impregnated chitosan HI (1g graphite: 1g chitosan: 800 mg HI) sheet as the electrodes. The electrode was taken as a rectangle with dimensions of 2 cm width and 5 cm height. The weight of the rectangle film was around 650 mg-700 mg.

In a typical experiment, the electrolytic cell is charged with nitro compound (3 mmol), MeOH (30 ml) and 3: 1 tetrabutyl ammonium chloride (TBAC) and acetic acid mixture as electrolyte (40 ml). During synthesis, TBAC acted as a supportive electrolyte. The best agents for a significant dissolution of the reactants were TBAC, AcOH and MeOH in combination. The modified electrodes were immersed in the reaction mixture and a constant voltage (5V) was applied for 8 h. During the reaction the colour of the solution turns brown, and the colour deepens as the reaction progressed. In order to assure sufficient current flow to convert the reaction intermediates into amines, we conducted the reaction for a period of 8 h. After completion of the reaction, as identified by the TLC, the reaction mixture was evaporated, and aniline was separated by acid-base treatment and then purified by column chromatography using alumina.

To compare the efficiency of graphite impregnated chitosan electrode with that of pure graphite electrode, we conducted the reduction of various nitro compounds using graphite electrode (1.5 cm diameter and 5 cm height) in the same electrolytic conditions.

References

1. Koutros S., Lynch C. F., Ma X., Lee W. J., Hoppin J. A., Christensen C. H., Andreotti G., Freeman L. B., Rusiecki J. A., Hou L., Sandler D. P., Alavanja M. C. **(2009)** Heterocyclic aromatic amine pesticide use and human cancer risk: results from the U.S. Agricultural Health Study. *Int. J. Cancer.,* 124 (5) 1206-1212.
2. Pinheiro H. M.,Touraud E., and Thomas O. **(2004)** Aromatic amines from azo dye reduction: status review with emphasis on direct UV spectrophotometric detection in textile industry waste waters. *Dyes Pigments,* 61 (2) 121-139.
3. Sakai T. **(2001)** Stepwise determination of quaternary ammonium salts and aromatic amines in pharmaceuticals by ion association titration. *Anal. Sci.,* 17, 1379–1382.
4. Radomski. J. **(1979)** The primary aromatic amines: their biological properties and structure-activity relationships. *Ann. Rev. Pharmacol. Toxicol.,* 19, 129-157.
5. Ning X. A., Liang J. Y., Li R. J., Hong Z.,Wang Y. J., Chang K. L., Zhang Y. P., Yang Z. Y. **(2015)** Aromatic amine contents, component distributions and risk assessment in sludge from 10 textile-dyeing plants. *Chemosphere,* 134, 367-373.

6. Wienhofer G., Sorribes I., Boddien A., Westerhaus F., Junge K., Junge H., Llusar R., Beller M. **(2011)** General and selective iron-catalyzed transfer hydrogenation of nitroarene without base. *J. Am. Chem. Soc.,* 133 (32) 12875-12879.
7. Jagadeesh R.V., Wienhofer G., Westerhaus F. A., Surkus A. E., Pohl M. M., Junge H., Junge K., and Beller M. **(2011)** Efficient and highly selective iron-catalyzed reduction of nitroarenes. *Chem. Commun.,* 47, 10972-10974.
8. Zengin N., Goksu H., Sen F. **(2021)** Chemoselective hydrogenation of aromatic nitro compo- unds in the presence of homogeneous Pd based catalysts. *Chemosphere,* 282, 130887.
9. Gamble A. B., Garner J., Gordon C. P., O'Conner S. M. J., and Keller P. A. **(2007)** Aryl nitro reduction with iron powder or stannous chloride under ultrasonic irradiation, *Synthetic Com- munications,* 37 (16) 2777-2786.
10. Kumar P., and Rai K. L. **(2012)** Reduction of aromatic nitro compounds to amines using zinc and aqueous chelating ethers: mild and efficient method for zinc activation. *Chemical Papers,* 66 (8) 772-778.
11. Gowda D. C., Mahesh B., and Gowda S. **(2001)** Zinc-catalyzed ammonium formate reductions: rapid and selective reduction of aliphatic and aromatic nitro compounds. *ChemInform,* 32 (23) 75-77.
12. Khan F. A., Dash J., Sudheer C., and Gupta R. K. **(2003)** Chemoselective reduction of arom- atic nitro and azo compounds in ionic liquids using zinc and ammonium salts. *Tetrahedron Letters,* 44 (42) 7783-7787.
13. Gohain S., Prajapati D., and Sandhu J. S. **(1995)** A new and efficient method for the selective reduction of nitroarenes: use of ammonium sulphate-sodium borohydride. *Chemistry Letters,* 1995, 725-726.
14. Zhou Z. H., Xu Y. B., Wu S. M., Ling W. J., Zhang L., and Wang Z. Q. **(2022)** Selective nitro reduction of ester substituted nitroarenes by $NaBH_4$-$FeCl_2$. *Pharmaceutical Fronts,* 04 (03) e151-e156.
15. Czubara A. B., Kula K., Wnorowski A., Biernasiuk A.,Popiołek L., Miodowski D., Demchuk O. M., and Jasinski R. **(2019)** Novel functionalized β-nitrostyrenes: promising candidates for new antibacterial drugs. *Saudi. Pharm. J.,* 27 (4) 593-601.
16. Kula K., Dresler E., Demchuk O., Jasinski R. **(2015)** New aldimine N-oxides - precursors for preparation of heterocycles with potential biological activity. *Przem. Chem.* 94 (8) 1385.
17. Rodrigo E., and Waldvogel S. R. **(2018)** Simple electrochemical reduction of nitrones to amines. *Chem. Sci.,* 10, 2044-2047.
18. Burge H. D., Collins D. J., and Davis B. H. **(1980**) Intermediates in the Raney nickel catalysed hydrogenation of nitrobenzene to aniline. *Ind. Eng. Chem. Prod. Res. Dev.,* 19 (3) 389-391.
19. Liu M., Li Y. P., Cao H. B., and Zhang Y. **(2007)** Electrochemical reduction of nitrobenzene at carbon nanotube electrode. *J. Hazard Mater.,* 148 (1-2) 158–163.
20. Liu J., Lu L., Wood D., and Lin S. **(2020)** New redox strategies in organic synthesis by means of electrochemistry and photochemistry. *ACS Cent Sci.,* 6 (8) 1317-1340.
21. Mohle S., Zirbes M., Rodrigo E., Gieshoff T., Wiebe A., and Waldvogel S R. **(2018)** Modern electrochemical aspects for the synthesis of value-added organic products. *Angew. Chem. Int. Ed. Engl.,* 57 (21) 6018-6041.
22. Wiebe A., Gieshoff T., Mohle S., Rodrigo E., Zirbes M., and Waldvogel S. R. **(2018)** Electrif- ying organic synthesis. *Angew. Chem. Int. Ed. Engl.,* 57 (20) 5594-5619.
23. Schotten C., Nicholls T. P., Bourne R. A., Kapur N., Nguyen B. N., and Willans C. E. **(2020)** Making electrochemistry easily accessible to the synthetic chemist. *Green Chem.,* 22, 3358-3375.
24. Pollok D., and Waldvogel S.R. **(2020)** Electro-organic synthesis – a 21st century technique. *Chem. Sci.,* 11, 12386-12400.
25. Lund H., and Hammerich O. **(2001)** *Organic Electrochemistry*, 4th Ed, Marcel Dekker, New York.
26. Yount J., Piercey D. G. **(2022)** Electrochemical synthesis of high-nitrogen materials and energetic materials. *Chem. Rev.,* 122 (9) 8809-8840.
27. Anastas P. T., and Warner J. C. **(1998)** *Green Chemistry: Theory and Practice,* 14th Ed, Oxford University Press, Oxford (England).
28. Isse A. A., Giusti A. D., Gennaro A., and Falciola L. **(2006)** Electrochemical reduction of benzyl halides at a silver electrode**.** *Electrochimica Acta.* 51 (23) 4956-4964.
29. Gurtner C., Wun A. W., and Sailor M. J. **(1999)** Surface modification of porous silicon by electrochemical reduction of organo halides. *Angew. Chem. Int. Ed.,* 38 (13-14) 1966-1968.
30. Torben L., and Henning L. **(1987)** Indirect electrochemical reduction of some benzyl chlorides. *Acta Chemica Scandinavica*. 41b, 93-102.
31. Tomat R., and Rigo A. **(1984)** Electrochemical oxidation of toluene promoted by OH radicals. *J. Appl. Electrochem.,* 14 (1) 1–8.
32. Wang D., Wang P., Wang S., Chen Y. H., Zhang H., and Lei A. **(2019)** Direct electrochemical oxidation of alcohols with hydrogen evolution in continuous-flow reactor. *Nat. Commun*. 10 (1) 2796.
33. Zhao G., Jiang T., Wu W., Han B., Liu Z., and Gao H. **(2004)** Electro-oxidation of benzyl alcohol in a biphasic system consisting of supercritical co_2 and ionic liquids. *Journal of Physical Chemistry B,* 108, 13052-13057.
34. Bender M. T.,Yuan X.,Goetz M. K., and Choi K. S. **(2022)** Electrochemical hydrogenation, hydrogenolysis, and dehydrogenation for reductive and oxidative biomass upgrading using 5-hydroxymethylfurfural as a model system. *ACS Catal.* 12 (19) 12349–12368.
35. Vunain E., Mishra A. K., and Mamba B. B. **(2017)** Fundamentals of chitosan for biomedical applications. *Chitosan Based Biomaterials,* 1, 3-30.
36. Aibani N., Rai R., Patel P., Cuddihy G., and Wasan E. K. **(2021)** Chitosan nanoparticles at the biological interface: implications for drug delivery. *Pharmaceutics,* 13 (10) 1686.
37. Riofrio A., Alcivar T., and Baykara H. **(2021)** Environmental and economic viability of chitosan production in guayas-ecuador: a robust investment and life cycle analysis. *ACS Omega,* 6 (36) 23038–23051.
38. Saeed A., Zahid S., Sajid M., Ud Din S., Alam M. K., Chaudhary F. A., Kaleem M., Alswairki H.J., and Abutayyem H. **(2022**) Physico-mechanical properties of commercially available tissue conditioner modified with synthesized chitosan oligosaccharide. *polymers* 14 (6) 1233.

ChemPhotoChem

Research Article
doi.org/10.1002/cptc.202300211

Chemistry Europe
European Chemical Societies Publishing

www.chemphotochem.org

Converting Conventional Host to TADF Sensitizer and Hot-Exciton Emitter in Donor-Adamantane-Acceptor Triads for Blue OLEDs: A Computational Study

Ramalingam Mahaan,[a] Aruljothy John Bosco,*[a] and A. Irudaya Jothi[b]

Exploiting triplet excitons in TADF sensitizers and hot-exciton emitters has attracted considerable attention and interest in recent studies on the design and development of blue OLEDs. The structural and optical property relationship of adamantane (Ad) core appended with four different strengths of donor and seven acceptor units were investigated using DFT and TD-DFT methods. The theoretical studies revealed that increased donor and acceptor strength on adamantane building block leads to: (i) a decrease in ionization potentials and an increase in electron affinities, (ii) a decrease in singlet energies (E_S) and the S_1-T_1 energy gaps (ΔE_{ST}); (iii) decreased SOC magnitudes between S_1-T_1 states; (iv) increased RISC rate from the T_n to S_1 states, demonstrating an increased tendency for upconversion of triplet excitons from the T_n to S_1 state. In addition, low exchange energy causes excited state characteristics of molecules to shift from HLCT to CT nature in the S_1 state. In contrast, the T_1 states retain their LE character, resulting in higher triplet energies (E_T). The adamantane molecular systems appended with P-DMAC-Donor-Ad-P-DMB and Donor-Ad-P-BODIPY based triads exhibit promising TADF sensitizer and hot-exciton characteristics to find application as potential candidates for blue OLEDs when compared to experimentally reported conventional host.

Introduction

Organic light emitting diodes (OLEDs) have significantly contributed to display technology over the past decade due to their low energy consumption, high efficiency, and simpler technology.[1,2] First-generation traditional fluorescence emitters could only yield theoretically up to 25% of the internal quantum efficiency (IQE) by utilizing photons from the singlet state (S_1) due to their inability to exploit 75% of the remaining triplet excitons radiatively.[3,4] The transition metal's high spin-orbit coupling (SOC) property allows second-generation phosphorescent emitters to achieve 100% IQE as phosphorescence decay through the intersystem crossing (ISC) process.[5] However, the toxicity and cost restrict their widespread usage and applications. In 2012, Adachi and co-workers reported that third-generation thermally activated delayed fluorescence (TADF) emitters utilizing organic molecules surpassed the efficiency limit of traditional fluorescence emitters and achieved 100% IQE.[6] TADF emitters typically have their frontier molecular orbitals (FMOs) twisted in a configuration with the lowest energy gap (ΔE_{ST}) between S_1 and triplet (T_1) states influenced by the donor and acceptor units. The TADF mechanism relies on thermal energy to elevate the T_1 state to isoenergetic with the emissive S_1 state by enabling the reverse intersystem crossing (RISC) process to harvest the triplet excitons efficiently.[7] The TADF molecular systems are constructed in such a way that the molecules have a significant spatial separation between the highest occupied (HOMO) and lowest unoccupied (LUMO) molecular orbitals, respectively, resulting in smaller exchange energy (J) and minimal ΔE_{ST} values. Moreover, though purely organic TADF materials have gained significant prominence since Adachi's pioneering research in 2012, they often necessitate robust charge transfer (CT) states. These states serve to minimize exchange energy and energy splitting (ΔE_{ST}) between the first singlet (S_1) and triplet (T_1) excited states. However, this can lead to diminished oscillator strength and reduced radiative rates for the S_1 states. To overcome this issue, employ hot exciton materials. These materials utilize reverse intersystem crossing from higher triplet (T_2, T_n) to singlet states, effectively harnessing non-radiative triplet excitons.[8] Later, Adachi et al. introduced the fourth-generation hyperfluorescence approach to improve color purity and material stability in TADF emitters. By embedding a TADF sensitizer with a fluorescent emitter into a wide energy gap host matrix, excitons transfer between them, resulting in enhanced efficiency and overcoming emission broadening and stability issues in third-generation TADF emitters (refer to Figure 1, which illustrates the energy transfer mechanism occurring in hyperfluorescent OLEDs and hot-exciton emitters.).[9–11] Moreover, a pure dopant in the emissive layer generally decreases device

[a] R. Mahaan, A. J. Bosco
Advanced Materials Chemistry Laboratory, Department of Chemistry, Faculty of Engineering and Technology, SRM Institute of Science and Technology, Kattankulathur – 603 203, Tamil Nadu, India
Mobile number: +91-9840757430
E-mail: johnbosa@srmist.edu.in
sambosco@gmail.com
msmahaanr333@gmail.com
mr3388@srmist.edu.in

[b] A. I. Jothi
Department of Chemistry, St. Joseph's College, (Affiliated to Bharathidasan University) Tiruchirappalli – 620 024, Tamil Nadu, India
E-mail: irudayajyothi@gmail.com

Supporting information for this article is available on the WWW under https://doi.org/10.1002/cptc.202300211

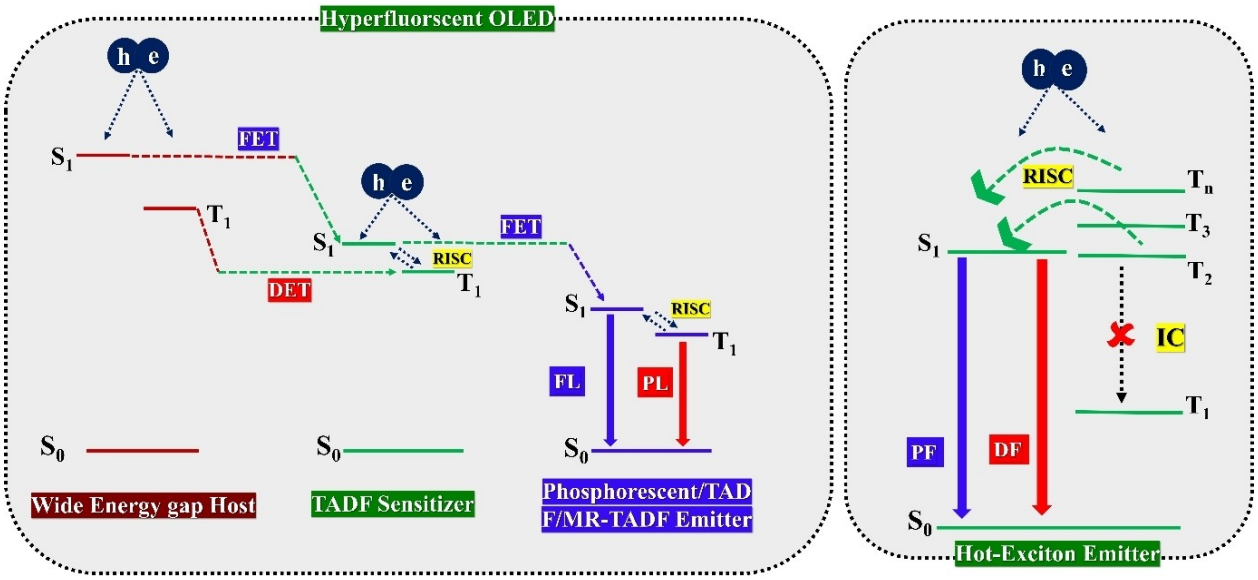

Figure 1. Energy transfer process of hyperfluorescent OLEDs and Hot-exciton emitters.

efficiency due to concentration quenching, singlet-singlet annihilation, triplet-triplet annihilation, etc.[12] Hence, pure emitters must be doped with appropriate TADF sensitizer in the emissive layer to increase the device's efficiency by reducing the excited state collisions. In order to design a TADF sensitizer for blue hyperfluorescent OLEDs, the molecular systems should meet the following requirements: (i). TADF sensitizer should have a higher E_T (2.80–3.00 eV) than the dopant to prevent backward energy transfer from the dopant and lower than the wide energy gap host (> 3.00 eV)[13] (ii). The ΔE_{ST} should be lower than 0.5 eV[14] (iii). Reasonable charge and carrier transport properties are crucial[15] (iv). The HOMO and LUMO energies must be aligned with that of the HOMO and LUMO energies of the adjacent hole transport (HT) and electron transport (ET) layers in order to minimize the driving voltage[16] (v). High thermal and morphological stability contribute to a more extended device lifetime.[17] For hot-exciton emitters, (i). Small energy splitting between S_1 and T_2 states promotes the efficient triplet exciton upconversion from higher triplet states (ii). A more significant energy gap between the T_2 and T_1 state to suppress triplet-triplet internal conversion (iii). High SOC and RISC rate between S_1 and T_2 states. Thus, the design of the TADF sensitizer and hot-exciton emitter is exceedingly challenging, especially for applying blue OLEDs.

Over the last few years, prominent research has focused on the molecule triplet energies and the corresponding energy barriers.[18] Hence, electron donor and acceptor units have been incorporated into the non-conjugated materials such as silicon derivatives,[19] acridine-based molecules,[20] and adamantane[21,22] core units to produce high E_T energy molecules. In 2019, Z Ma et al. reported two adamantane core-based dendritic molecules with high E_T energies of 2.83–2.95 eV for blue TADF OLEDs with 18.3% external quantum efficiency (EQE).[23] Recently, W Li and his team demonstrated a ~29% higher device efficiency via adamantane moiety substitution on the acridine donor unit with the dual fluorescence emission.[24] In 2022, W Xu et al. demonstrated aggregation-induced and clustering-triggered emission based on the adamantane and carborane molecular systems in solution and solid states.[25] The adamantane moiety is widely used to develop host molecules,[21,23] electron and hole transport materials,[22,26] and emitters[24] for OLED device applications. In 2015, Yu Gu et al. reported adamantane-based wide-bandgap host material (CzCN–Ad) for blue electrophosphorescence devices with high E_T (3.03 eV) and glass transition temperatures.[21] Molecular systems with adamantane core units exhibit high E_T energies, causing conjugation breaking, but their ΔE_{ST} energy remains high. However, long-range Forster energy transfer from the TADF sensitizers improves device efficiencies with a lower doping ratio by reducing the exciton density. This achievement is limited to TADF-sensitizers or exciplex-type molecules.[14,27] A systematic study on the effect of adamantane building blocks and subunits on optoelectronic properties is essential to identify potential multifunctional materials for OLEDs.

To our knowledge, the excited-state photophysical properties of adamantane building blocks have not been studied systematically. Although adamantane-based molecules have higher E_T energies and glass transition temperatures, only limited research has been conducted into the exclusive photophysical properties of these building blocks. The adamantane building blocks possess only sigma bonds, which prevent conjugation and the intramolecular charge transfer process between electron donor and acceptor units. Therefore, adamantane building blocks are expected to exhibit higher E_T energies. Despite its low molecular weight, the adamantane building block has high thermal and decomposition stability, which is beneficial for easy device fabrication and a longer lifetime. The primary objective of this research is to investigate how substituting different donor and acceptor units on the adamantane core affects the electronic properties of newly

designed molecules. In order to accomplish this, 28 molecules were designed by four donor units, namely phenylcarbazole (P-CBZ), phenyl-*tertiary*-butylcarbazole (P-*t*-Bu-CBZ), phenyldiphenylacridine (P-DPAC), and phenyldimethylacridine (P-DMAC). Seven acceptor units: phenyl-γ-carboline (P-γ-CBN), phenyltriazole (P-TZ), phenylphenthiazole (P-PTZ), phenylpyridine (P-PY), phenylcyanide (P-CN), and dimesitylborane (P-DMB), phenylborondipyrromethene (P-BODIPY)[28] have systematically substituted in the R_1 and R_2 positions of the adamantane core unit (Scheme 1 and Figure S1–S3). All donor and acceptor units used herein are well known and reported,[27,29–31] and they are arranged in order of increasing strength of electron-donating (P-CBZ < P-t-Bu-CBZ < P-DPAC < P-DMAC) and accepting (P- γ-CBN < P-TZ < P-PTZ < P-PY < P-CN < P-DMB < P-BODIPY) nature. Since CzCN–Ad is an experimentally reported molecule (molecule 5), it was selected as the reference molecule for this study. In this reference molecule, P-CBZ donor and P-CN acceptor subunits are attached at the R_1 and R_2 positions of the adamantane building block.[21] As the computed results, we intend to examine how the different strengths of donor and acceptor units influence the ground and excited state properties of newly designed molecules, such as HOMO (IP), LUMO (EA), H-L gap (HOMO-LUMO gap), hole injection and electron transport properties, nature of singlet, triplet states, ΔE_{ST}, SOC, and K_{rISC} values.

Computational Details

The ground state geometries of all newly designed molecules were optimized using the Becke, 3-parameter, Lee-Yang-Parr (B3LYP) functional with a 6-31 + G* basis set.[32] The absence of imaginary frequencies confirms that molecular structures have minimum energies. In order to optimize the ground state geometry of the reference molecule, a benchmark study was conducted using different Hatree-Fock functionals with a range of 0–100% (Table S1). Only the B3LYP functional exhibited the lowest deviations from the reference molecule's experimentally measured HOMO and LUMO energies. However, the LUMO energy values obtained from theoretical calculations are often higher than experimental values due to the greater difficulty in accurately predicting the behavior of virtual orbitals compared to occupied orbitals. Hence B3LYP functional were selected to optimize the ground-state geometries of the newly designed molecules. In the same way, excited state energies for the reference molecule were also calculated using popularly proposed functionals (B3LYP, PBE0, M06, M06-2X, CAM–B3LYP, WB97X, Lc-wPBE, M06-HF) with 6-31 + G* basis set (Table S2). Nevertheless, only the B3LYP,[32] PBE0,[33] and M06[34] functionals have values close to the experimentally obtained excitation energies. So, the excited state calculations of newly designed molecules were evaluated using these three functionals (B3LYP, PBE0, and M06). We computed the designed molecule's ionization potential (IP) and electron affinities (EA) based on their respective ionic geometries using the B3LYP/6-31 + G* level of theory.[35] Natural transition orbital (NTO) analyses were performed using the B3LYP, PBE0, and M06 functionals with a 6-31 + G* basis set to study the characteristics of excited states.[36] The adiabatic triplet energies of the molecules were computed using the PBE0 functional, combined with the 6-31G* basis set. All the calculations were performed with the polarizable continuum model (PCM) in the toluene solvent medium. Furthermore, the SOC values between the excited states were calculated in their T_1 geometry using ORCA software at the PBE0/def2-SVP level of theory.[37] A mean separation distance (r) and overlap extent (l) values were calculated using Multiwfn software in S_1 and T_1 states.[38] The semi-classical Marcus equation was used to calculate the RISC values between excited states.[39]

$$k = \frac{2\pi}{\hbar g} |V|^2 \frac{1}{\sqrt{4\pi k_B T \lambda}} \exp\left(\frac{(\lambda + \Delta E_{ST})^2}{4\lambda k_B T}\right)$$

Where T, λ, k_B, and *V* denote the temperature, reorganization energy, Boltzmann constant, and SOC, respectively.[39] In this study, the value of g (degeneracy) is set to 3 for RISC values T at 300 K. All these calculations were carried out using the Gaussian16 package.[40]

We choose Bis[2-(4,6-difluorophenyl)pyridinato-C2,N](picolinato)iridium (III) (FIrPic), 10,10′-(4,4′-Sulfonylbis(4,1-phenylene)) bis(9,9-dimethyl-9,10-dihydroacridine (DMAC-DPS), and BN-CP2 as the reference blue, phosphorescent, TADF and MR-TADF emitters, respectively. 4-(1-{4-[bis(4-methylphenyl)amino]phenyl} cyclohexyl)-N,N-bis(4-methylphenyl)aniline (TAPC) and N,N′-Di(1-naphthyl)-N,N′-diphenyl-(1,1′-biphenyl)-4,4′-diamine (NPB) as the

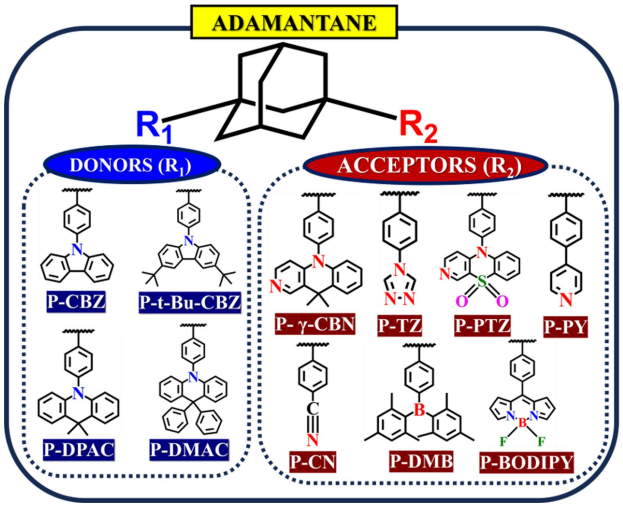

Molecules	R_1	R_2	Molecules	R_1	R_2
1	P-CBZ	P- γ-CBN	13	P-DPAC	P- γ-CBN
2	P-CBZ	P-TZ	14	P-DPAC	P-TZ
3	P-CBZ	P-PTZ	15	P-DPAC	P-PTZ
4	P-CBZ	P-PY	16	P-DPAC	P-PY
5	P-CBZ	P-CN	17	P-DPAC	P-CN
6	P-CBZ	P-DMB	18	P-DPAC	P-DMB
7	P-t-Bu-CBZ	P- γ-CBN	19	P-DMAC	P- γ-CBN
8	P-t-Bu-CBZ	P-TZ	20	P-DMAC	P-TZ
9	P-t-Bu-CBZ	P-PTZ	21	P-DMAC	P-PTZ
10	P-t-Bu-CBZ	P-PY	22	P-DMAC	P-PY
11	P-t-Bu-CBZ	P-CN	23	P-DMAC	P-CN
12	P-t-Bu-CBZ	P-DMB	24	P-DMAC	P-DMB
25	P-CBZ	P-BODIPY	27	P-DPAC	P-BODIPY
26	P-t-Bu-CBZ	P-BODIPY	28	P-DMAC	P-BODIPY

Scheme 1. Chemical structures of core and subunits are used to design new molecules

reference hole transport layers (HTL), 2,2′,2″-(1,3,5-Benzinetriyl)-tris(1-phenyl-1-H-benzimidazole) (TPBi) and 1,3,5-Tris(3-pyridyl-3-phenyl)benzene (TmPyPB) as the reference electron transport materials (ETM), respectively and we choose commonly used 1,3-Bis(N-carbazolyl)benzene (mCP) as a reference host material.[41–43] In the case of the FIrpic emitter, calculations were performed with LANL2DZ effective core potential (ECP) for Ir and 6-31 + G* for the remaining atoms.[42–48]

Results and Discussion

Geometrical Parameters

Geometrical parameters and electronic structures influence the energy difference between ΔE_{ST} and the relevant ISC and RISC processes.[49] The calculated bond length (d_1 and d'_1), dihedral angle values (δ_1 and δ'_1), and the indices marked on the molecular structures are given in Table S3 and Figure S1. On the adamantane core, the strength of the donor and acceptor units shows a slight effect on bond lengths and a significant impact on dihedral angle values. Molecules containing DPAC and DMAC donor units have a slightly higher bond length (1.436 to 1.438 Å) between the donor and phenyl ring of the adamantane core (N2-C3) than molecules containing CBZ and t-Bu-CBZ donor units (1.421 to 1.424 Å). Similarly, when examining the bond lengths between the acceptor unit and phenyl ring of the adamantane core (C2′-N3′), molecules containing PTZ (1.444 Å), PY (1.484 Å), and DMB (1.571 Å) acceptor units have higher values than other acceptor-based molecules (1.425 to 1.434 Å). Furthermore, the dihedral angle value between the donor and phenyl ring of the adamantane core (C1-N2-C3-C4) increases with increasing the donor strength in order from t-Bu-CBZ (57.21° to 58.59°) to CBZ (59.90° to 61.46°) to DMAC (89.45° to 90.05°) to DPAC (96.60° to 98.03°). As a result, the dihedral angle values for DPAC and DMAC-based molecules are perpendicular (~90°) to that of the adamantane core; they are expected to have smaller ΔE_{ST} values.[50] The dihedral angle values between the acceptors and the phenyl ring of the adamantane core are lower for DMB acceptor-based molecules (C1′-C2′-B3′-C4′) than other acceptor-based molecules. In addition, the order of the dihedral angle values increases from DMB (23.14° to 23.79°) to PY (37.12° to 37.13°) to TZ (46.09° to 46.22°) to CN (56.53° to 80.44°) to CBN (62.34° to 62.59°) to PTZ (86.08° to 89.81°) acceptor units in the molecules. In the case of molecules incorporating a BODIPY acceptor unit, there is a notable elevation in dihedral angle values observed between the donor and phenyl ring (ranging from 89.93° to 122.31°), as well as between the phenyl ring and BODIPY unit (approximately ~124°).

Frontier Molecular Orbital (FMO)

The calculated HOMO and LUMO energies of the molecules play a vital factor in determining the driving voltage of the OLED devices (Table 1).[16] Herein, we studied the evolution of the molecule's HOMO and LUMO energies with their isolated donor and acceptor moieties (Table S4). The HOMO and LUMO energies are generally destabilized and stabilized according to the strength of their donor and acceptor units. HOMO energies of molecules with P-CBZ donor units (1–6) range from −5.56 to −5.66 eV, molecules with P-t-Bu-CBZ donor units (7–12) range from −5.35 to −5.43 eV, molecules with P-DPAC donor units (13–18) range from −5.29 to −5.39 eV, while molecules with P-DMAC donor units (19–24) range from −5.08 to −5.20 eV. Herein, we observed that the HOMO energies are systematically destabilized to increase the strength of the donor units from P-CBZ to P-t-Bu-CBZ to P-DPAC to P-DMAC. The LUMO energies of molecules containing P-CBZ donor units **(1–6)** and **25** are systematically stabilized as their acceptor strength increased from −1.23 to −1.27 to −1.38 to −1.53 to −1.80 to −1.84 and −3.13 eV, respectively (P-γ-CBN to P-TZ to P-PTZ to P-PY to P-CN to P-DMB to P-BODIPY). Similar trends can be observed in LUMO energies for other donor unit-based molecules, albeit with differences in their energies. A systematic destabilization of HOMO energies and stabilization of LUMO energies led to a systematic decrease in the H-L gaps for the first six and **25** molecules from 4.40 to 4.39 to 4.26 to 4.06 to 3.86 to 3.72 eV and 2.51 eV and the same trend is observed for other sets of molecules **(except for molecule 8)**, only differing in their energies. In addition, it is imperative to examine how IP and EA energies correlate with their corresponding HOMO and LUMO energies of the molecules (Table 1).[35] Generally, high HOMO energies have lower IP values, whereas low LUMO energies have higher EA values. The IP values decreased as their HOMO energy increased with increasing donating strength of donor units, about 6.95 to 6.25 eV. Consequently, the EA values in P-CBZ-donor and P-BODIPY-based molecules increase by about 0.29 to 0.51 eV and ~1.87 eV **(except molecule 5)** as the LUMO energy stabilizes, and the same trend of EA values has been observed for other P-t-Bu-CBZ, P-DPAC, and P-DMAC donor unit-based molecules. The distribution of HOMO-LUMO wave-functions of the designed molecules and subunits are depicted in Figures 2 & S3–S5. HOMO-LUMO distributions confirmed that all the molecules have a localized HOMO and LUMO distribution on their respective donor and acceptor units. Specifically, the LUMO distribution of molecules **1**, **3**, **7**, **9**, **13**, **15**, **19**, and **21** are more prominently localized in the CBN and PTZ moieties. Furthermore, molecular orbital contribution (MOC) analysis of the molecules comprising donor (R_1), core, and acceptor (R_2) units are computed in Table S5.[38] The MOC analysis shows that 99.30% to 99.97% of HOMO distribution is localized to their respective donor units, whereas 89.47% to 99.99% of LUMO distribution is localized to their respective acceptor units. Comparatively, molecules containing P-TZ, P-CN, and P-TZ acceptors account for only 4% to 5% of LUMO distributions on the adamantane core units. The finding of this study illustrates that all molecules possess effective HOMO-LUMO separation when adamantane is the building block and are expected to have minimal electron transport and hole injection properties.

Table 1. Calculated HOMO and LUMO energies, adiabatic ionization potential (IP) and electron affinity (EA), reorganization energies for the hole (λ_h) and electron (λ_e), the difference between λ_h and λ_e ($\Delta\lambda$) at B3LYP/6-31 + G* level of theory. (All values are in eV).

Molecules	HOMO	LUMO	$\Delta E_{H\text{-}L}$	IP	EA	λ_h	λ_e	$\Delta\lambda$
1	−5.63	−1.23	4.40	6.67	0.29	0.09	0.10	0.01
2	−5.66	−1.27	4.39	6.95	0.29	0.12	0.18	0.06
3	−5.64	−1.38	4.26	6.72	0.41	0.07	0.15	0.08
4	−5.59	−1.53	4.06	6.85	0.51	0.12	0.30	0.19
5	−5.66	−1.80	3.86	6.95	0.45	0.13	0.15	0.02
6	−5.56	−1.84	3.72	6.69	0.83	0.09	0.19	0.11
7	−5.40	−1.22	4.18	6.46	0.28	0.09	0.10	0.01
8	−5.43	−1.24	4.19	6.62	0.28	0.12	0.18	0.05
9	−5.41	−1.37	4.04	6.50	0.40	0.08	0.15	0.07
10	−5.37	−1.52	3.85	6.55	0.49	0.12	0.30	0.18
11	−5.43	−1.66	3.77	6.62	0.43	0.13	0.15	0.03
12	−5.35	−1.83	3.52	6.47	0.82	0.09	0.19	0.11
13	−5.35	−1.22	4.13	6.40	0.23	0.13	0.08	0.05
14	−5.38	−1.25	4.13	6.53	0.25	0.20	0.17	0.02
15	−5.39	−1.37	4.02	6.45	0.37	0.13	0.13	0.00
16	−5.32	−1.52	3.80	6.46	0.46	0.20	0.32	0.12
17	−5.36	−1.66	3.70	6.51	0.41	0.20	0.15	0.04
18	−5.29	−1.83	3.46	6.37	0.81	0.09	0.21	0.12
19	−5.15	−1.23	3.92	6.34	0.17	0.08	0.10	0.02
20	−5.18	−1.26	3.92	6.48	0.18	0.11	0.23	0.12
21	−5.20	−1.34	3.86	6.29	0.40	0.08	0.16	0.08
22	−5.12	−1.52	3.60	6.41	0.43	0.11	0.38	0.26
23	−5.16	−1.67	3.49	6.46	0.36	0.11	0.20	0.09
24	−5.08	−1.83	3.25	6.25	0.81	0.08	0.23	0.15
25	−5.64	−3.13	2.51	6.77	1.88	0.08	0.27	0.19
26	−5.43	−3.11	2.33	6.54	1.86	0.09	0.27	0.18
27	−5.36	−3.13	2.24	6.45	1.88	0.14	0.27	0.13
28	−5.16	−3.12	2.05	6.40	1.87	0.08	0.27	0.19

Reorganization Energies

The efficiency of electrode-based devices depends on the charge transport rate and the alignment of the layers between the electrodes. Thus, reorganization energies (λ) can provide insight into how the charge transport rate evolves in the molecules. Molecules with higher λ energies have lower charge transport rates, while molecules with lower λ energies have higher charge transport rates.[15,51] The computed electron (λ_e) and hole (λ_h) reorganization energies for all the molecules are given in Table 1. It can be found from the table that λ_h energies have low values ranging from 0.07 to 0.14, which indicates that all the molecules have high hole mobility. Notably, molecules containing P-DPAC donor units have high λ_h values of 0.20 except for molecules **13**, **15**, and **18**. The calculated reorganization energies of isolated donor and acceptor units are given in Table S6. The results demonstrated that higher λ_h energies of molecules containing P-DPAC donor units are attributed to the higher λ_h energies of their individual P-DPAC donor units (**λ_h = 0.19**). In contrast, all molecules have relatively higher electron mobilities, ranging from 0.08 to 0.38, which results in moderate electron transport in the device. Moreover, molecules containing P-PY and P-BODIPY acceptor units have higher λ_e energies than other acceptor-based molecules, ranging from 0.27 to 0.38 due to the higher λ_e energies of the individual P-PY and P-BODIPY acceptor units (**0.55 and 0.43**). Hence, from these results, the electron transport barrier is expected to be higher when compared to the hole transport in the molecules. Nevertheless, the difference between the λ_e and λ_h of all the molecules ($\Delta\lambda$) has minimal values, except those with P-PY and P-BODIPY acceptor-based molecules, ranging from 0.00 to 0.15. As a result of the slight difference in $\Delta\lambda$ values, it can be inferred that all the molecules can function as ambipolar nature.

Excited State Properties

The excitation parameters such as singlet (E_S), triplet (E_T), and ΔE_{ST} energies need to be investigated.[52] Examining the

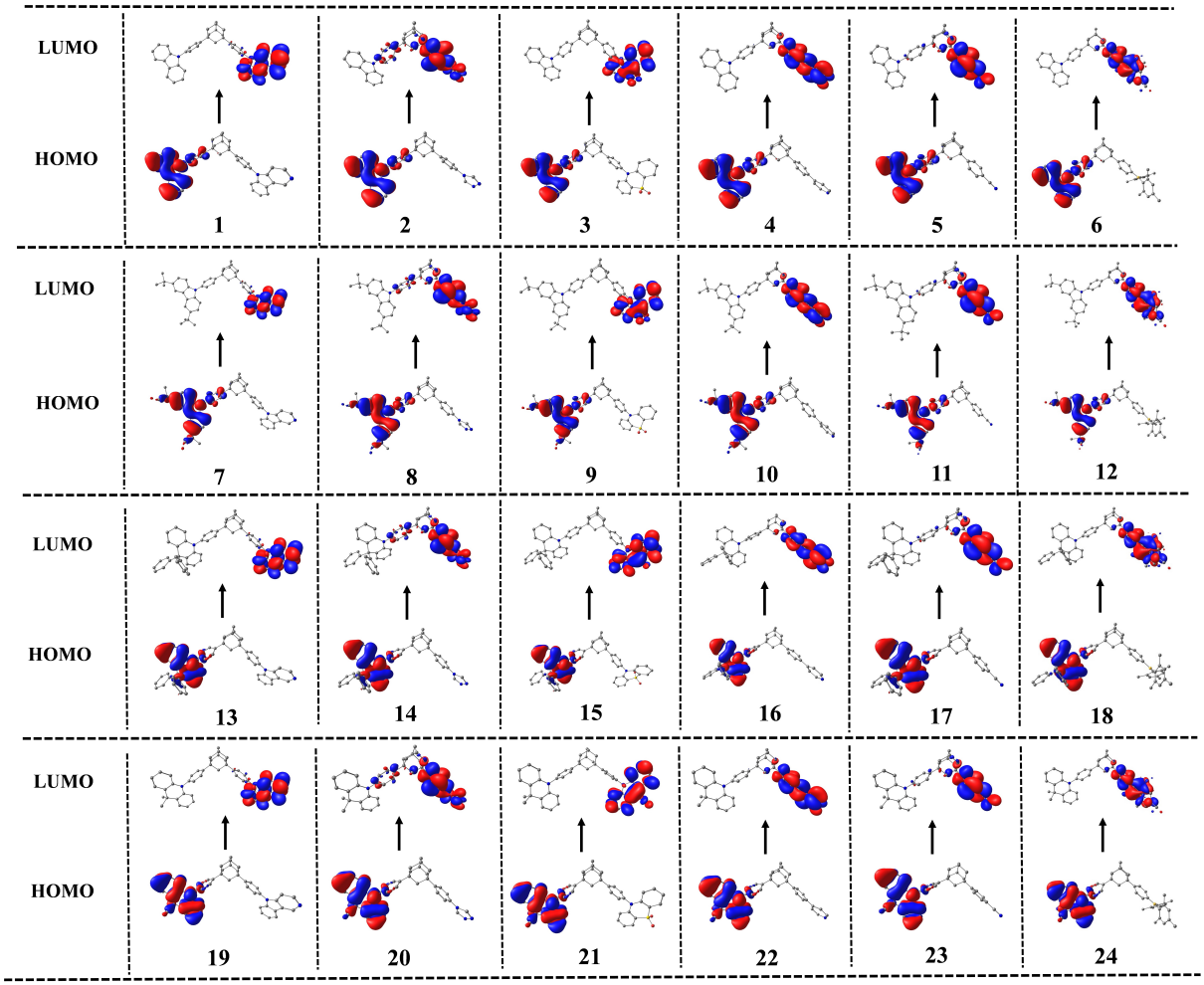

Figure 2. FMO contour plots of newly designed molecules (iso-surface value = 0.02 au). Here, hydrogen atoms are omitted for clarity.

molecules's S_1 and T_1 energy levels is crucial to characterize their photophysical properties. The molecule's calculated vertical S_1, T_1 (PBE0), and adiabatic T_1 energies are given in Tables 2 and S7–S8, and their energy level alignment of the lowest ten singlet and triplet states is shown in Figure 3. The S_1 energies of the molecules decrease systematically as the strength of donor and acceptor units increase from P-CBZ (4.03–2.55 eV) to P-t-Bu-CBZ (3.91-2.35 eV) to P-DPAC (3.88–2.27 eV) to P-DMAC (3.70–

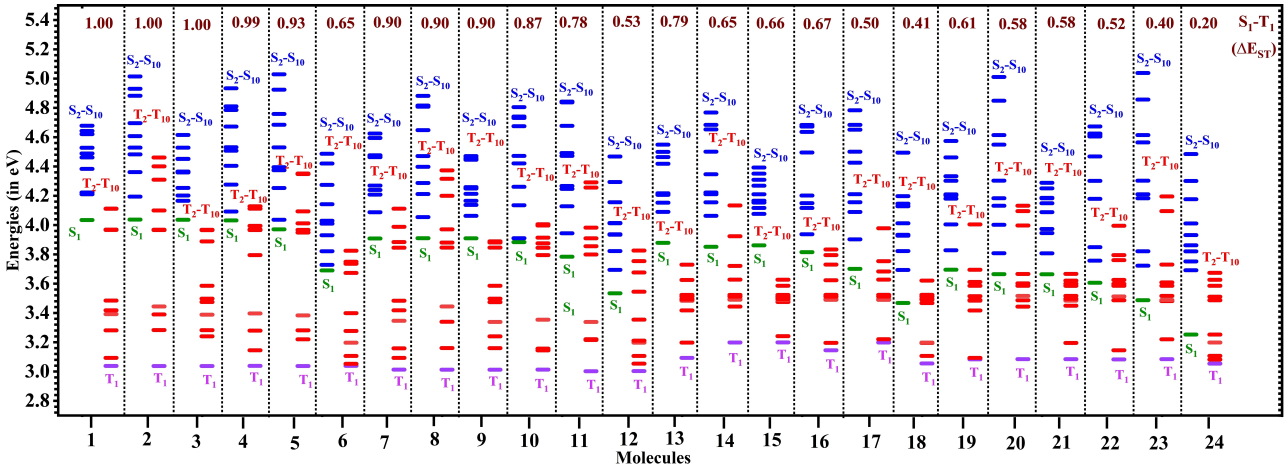

Figure 3. Excited state energy diagram of newly designed molecules calculated at PBE0/6-31 + G* level of theory.

Table 2. Calculated vertical singlet (S_1) and triplet (T_1) energies, vertical singlet-triplet energy differences (ΔE_{ST}) and SOC constant (in cm^{-1}), and RISC rate (in s^{-1}) between S_1 and T_1 excited states. (All values are in eV).

	B3LYP			PBE0					M06		
Molecules	S_1	T_1	ΔE_{ST}	S_1	T_1	ΔE_{ST}	SOC	k_{rISC} (T_1-S_1)	S_1	T_1	ΔE_{ST}
1	3.92	3.15	0.77	4.03	3.04	1.00	0.59	3.52×10^{-28}	3.97	3.01	0.96
2	3.92	3.15	0.77	4.04	3.04	1.00	0.59	3.53×10^{-28}	3.98	3.01	0.97
3	3.92	3.15	0.77	4.04	3.04	1.00	0.59	3.57×10^{-28}	3.98	3.01	0.97
4	3.81	3.15	0.66	4.03	3.04	0.99	0.57	1.36×10^{-27}	3.97	3.01	0.96
5	3.69	3.15	0.54	4.01	3.04	0.97	0.58	4.77×10^{-24}	3.97	3.01	0.96
6	3.47	3.13	0.34	3.69	3.04	0.65	0.24	7.29×10^{-11}	3.69	3.01	0.68
7	3.80	3.13	0.66	3.91	3.01	0.90	0.31	6.57×10^{-23}	3.84	2.97	0.87
8	3.80	3.13	0.66	3.91	3.01	0.90	0.35	8.45×10^{-23}	3.85	2.97	0.87
9	3.80	3.13	0.66	3.91	3.01	0.90	0.36	8.72×10^{-23}	3.85	2.97	0.87
10	3.61	3.13	0.48	3.88	3.01	0.87	0.35	3.69×10^{-21}	3.84	2.97	0.87
11	3.50	3.17	0.34	3.78	3.00	0.78	0.35	1.68×10^{-16}	3.85	2.96	0.89
12	3.28	3.11	0.17	3.53	3.00	0.53	0.21	3.18×10^{-06}	3.68	2.96	0.72
13	3.72	3.21	0.51	3.88	3.09	0.79	0.26	3.04×10^{-17}	3.87	3.07	0.80
14	3.69	3.29	0.40	3.85	3.20	0.65	0.37	1.74×10^{-10}	3.85	3.18	0.67
15	3.70	3.29	0.41	3.86	3.20	0.66	0.28	3.85×10^{-11}	3.85	3.18	0.68
16	3.55	3.28	0.27	3.82	3.15	0.67	0.27	1.30×10^{-11}	3.85	3.14	0.72
17	3.43	3.29	0.14	3.70	3.20	0.50	0.25	4.81×10^{-05}	3.76	3.18	0.59
18	3.22	3.13	0.09	3.47	3.06	0.41	0.23	3.33×10^{-02}	3.62	3.02	0.60
19	3.54	3.17	0.37	3.70	3.08	0.61	0.40	9.36×10^{-09}	3.70	3.07	0.62
20	3.50	3.17	0.33	3.67	3.08	0.58	0.39	1.38×10^{-07}	3.67	3.09	0.58
21	3.55	3.28	0.27	3.66	3.08	0.58	0.38	1.33×10^{-07}	3.66	3.09	0.57
22	3.35	3.16	0.18	3.61	3.08	0.52	0.39	2.43×10^{-05}	3.67	3.09	0.58
23	3.22	3.17	0.05	3.49	3.08	0.40	0.25	8.02×10^{-02}	3.85	3.18	0.68
24	3.01	3.01	0.00	3.25	3.05	0.20	0.18	$3.20\times10^{+03}$	3.42	3.02	0.40

2.07 eV). Whereas the T_1 energies of molecules range between 3.00 and 3.20 eV, particularly molecules containing P-DPAC donor units have higher T_1 energies of about ~3.20 eV, except for molecules **13** and **18** and molecules containing P-BODIPY-acceptor units have lower T_1 energies about 1.55 eV. The evolution of S_1 and T_1 energies of the molecules are understood by examining their NTOs[53] and the overlap extent (I_S & I_T) between holes and electrons at the S_1 and T_1 states (Table S9 & Figures 4 and 5 and S6).[54,55] The NTOs of molecules **1**, **2**, **3**, **4**, **7**, **8**, and **9** have delocalized transition over the donor units at the S_1 state **(except molecule 6)**. Because these molecules have higher overlap extent values ranging from 54.09% to 68.24%, resulting in hybridized local and charge transfer (HLCT) features in their S_1 states. On the other hand, the NTOs of molecule **6** have delocalized on the DMB acceptor unit with an HLCT nature. Furthermore, molecules **13**, **14**, **15**, **19**, **20**, and **21** exhibit CT characteristics with localized hole and electron NTO transitions on their respective donor units with low overlap extent values ranging from 18.41% to 25.33%. In particular, the NTOs of molecules **5**, **10**–**12**, **16**–**18**, and **22**–**28** exhibited pure CT character with shallow overlap extent values ranging from 0.00% to 12.75%. The above analysis showed that the S_1 excitation states switched the nature from HLCT to CT characteristics as donor and acceptor strength increased. When examining the hole-electron NTOs at the T_1 state, all the molecules have localized transitions on their respective donor and acceptor units, exhibiting the LE characteristic due to high overlap extent values ranging from 46.38% to 76.27% except P-BODIPY-based molecules with HLCT nature. However, the NTOs of molecules **13**, **16**, **18**, and **24** are mainly localized on their acceptor units. Since the NTO distribution of the T_1 state indicates that all the molecules have the localized transition on their donor and acceptor units, their T_1 energies tend to be close to the respective isolated donor and acceptor units. Figures S7-S10 display the NTOs calculated with other B3LYP and M06 functionals, and these results exhibit a similar pattern to the NTOs obtained through the PBE0 functional. The absorption wavelengths of molecules are directly related to their HOMO and LUMO gaps. The calculated absorption and emission wavelengths for P-DMB acceptor unit-based molecules **(molecules 6**, **12**, **18**, **24)** are shown in Table 3 as obtained from the PBE0/6-31G* level of theory. In order to increase the donating strength of the molecules, the absorption wavelength increases from 333 nm to 375 nm in accordance with the linear decrease of HOMO-LUMO gaps. Similarly, the emission wavelength increases from 380 nm to 426 nm as the strength of the

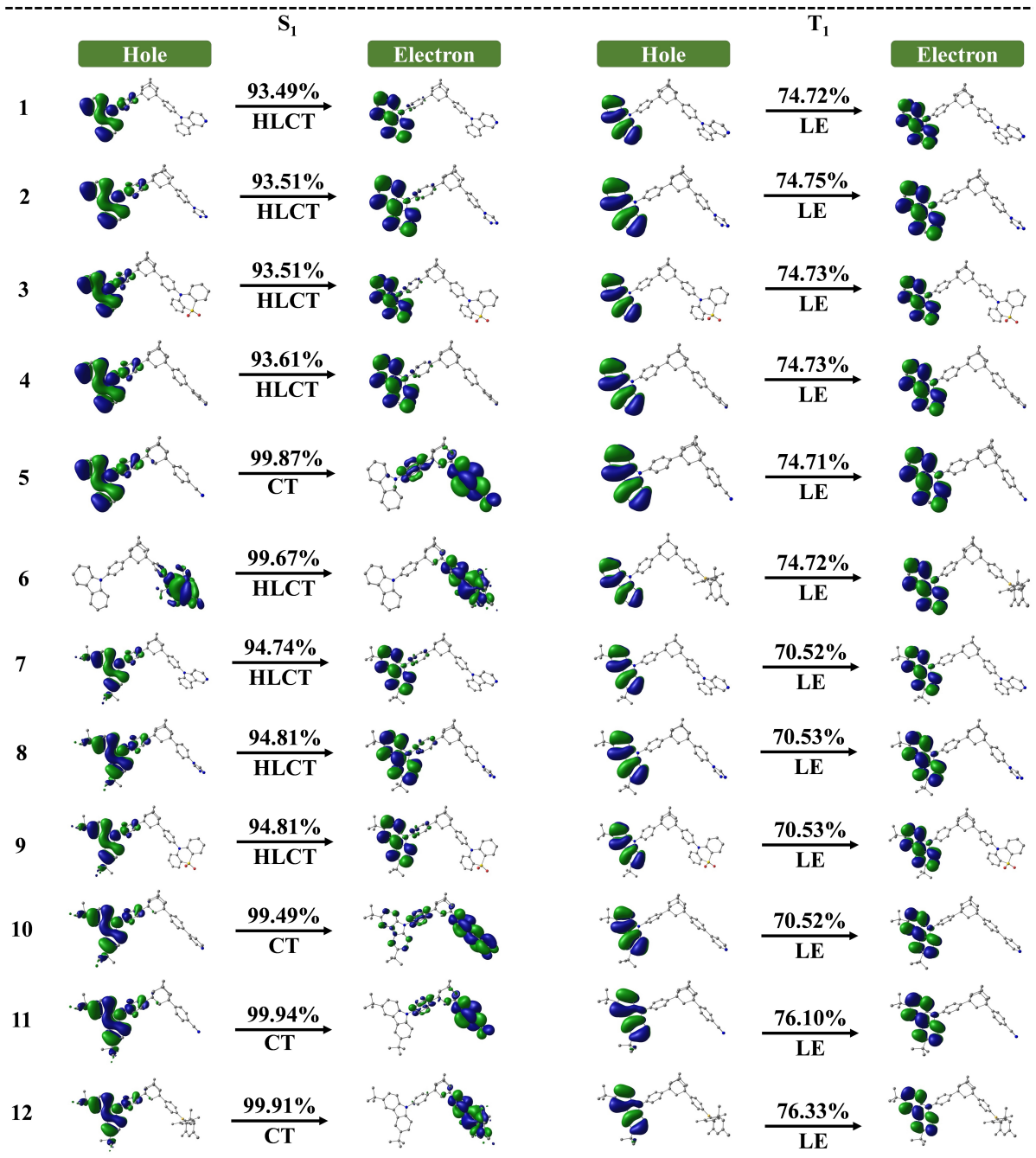

Figure 4. Hole-particle NTOs (iso-surface value = 0.02 au.) of 1 to 12 molecules with excited state transition character obtained from PBE0/6-31 + G* level of theory. The hydrogen atoms are omitted here for clarity.

Table 3. Calculated HOMO-LUMO gaps (in eV), absorption, and emission wavelengths (in nm) of some inspirational molecules (DMB acceptor unit-based molecules).

Molecules	$\Delta E_{H\text{-}L}$	Absorption λ	Emission λ
6	3.72	333	380
12	3.52	346	388
18	3.46	352	407
24	3.25	375	426

donor units increases in the molecules., i.e., the violet-blue region. The absorption and emission vary smoothly from lower to higher wavelengths depending on electron-donating strength in the P-DMB acceptor unit-based molecules.

The ΔE_{ST} values of the molecules are considered the most crucial parameter in the device efficiency and driving voltage of the OLEDs.[52] On the adamantane core unit, substituting different strengths of donor and acceptor units would cause significant changes in the ΔE_{ST} values, particularly the ΔE_{ST} values systematically decreased as the strength of the donor

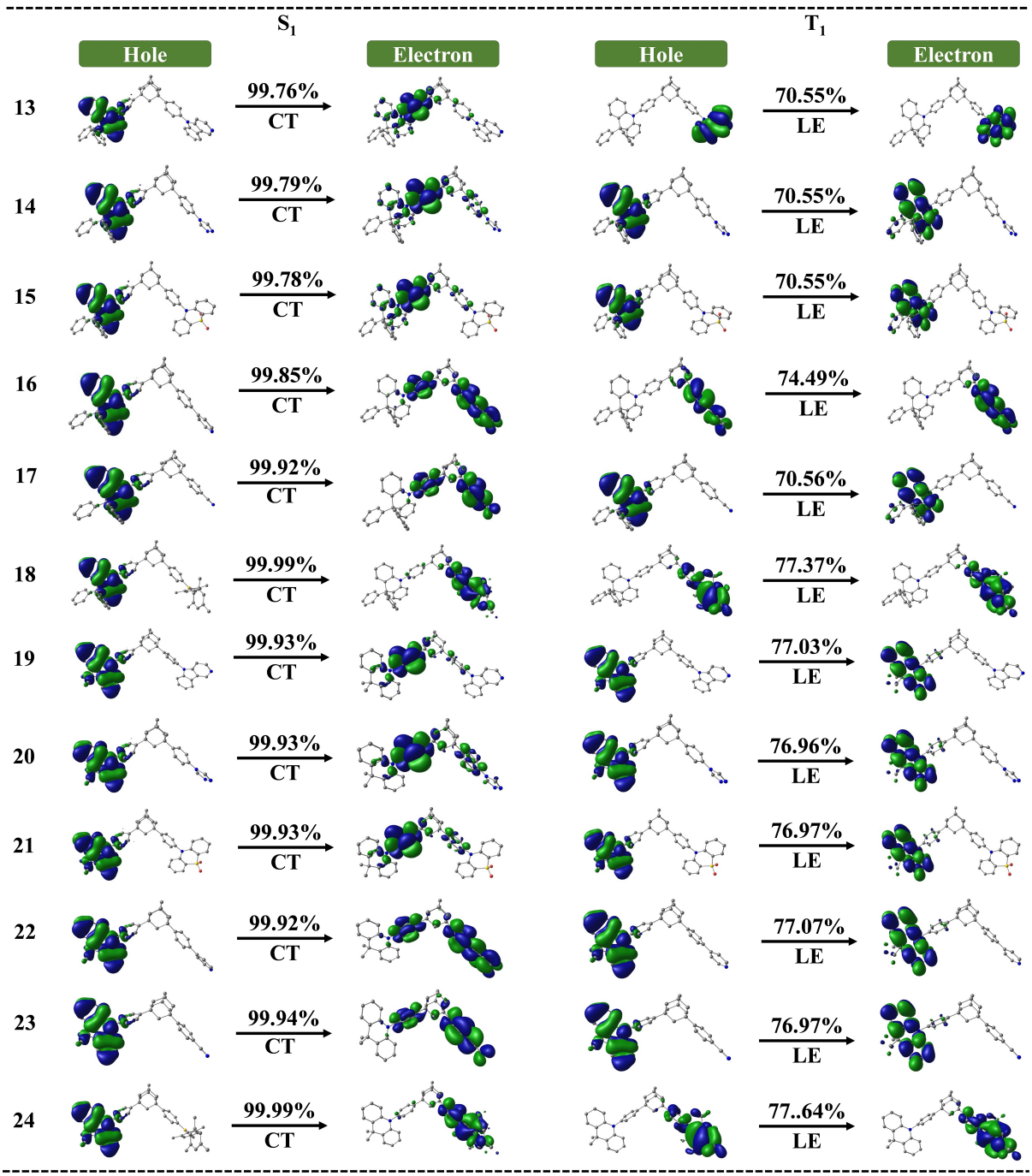

Figure 5. Hole-particle NTOs (iso-surface value = 0.02 au.) of 13 to 24 molecules with excited state transition character obtained from PBE0/6-31 + G* level of theory. The hydrogen atoms are omitted here for clarity.

and acceptor units increased (Table 2 & Figure 6). The ΔE_{ST} energies of molecules with P-CBZ donor units range from 1.00 to 0.52 eV, molecules with P-t-Bu-CBZ donor units range from 0.90 to 0.53 eV, molecules with P-DPAC donor units range from 0.79 to 0.41 eV, while molecules with P-DMAC donor units range from 0.61 to 0.20 eV. In particular, the molecules with P-DMB- acceptor (0.65 to 0.20 eV), P-DPAC, and P-DMAC donor unit-based (0.79 to 0.20 eV) molecules have lower ΔE_{ST} values than molecules with other acceptor and donor units. The increased CT characteristics of the hole and electron NTO distributions at S_1 states significantly caused the systematic decrease in ΔE_{ST} values. Furthermore, the overlap extent (l_S/l_T) and separation distance (r_S/r_T) between the hole and electron parameters provide further insight into the molecule's ΔE_{ST} values. Table S9 shows the calculated overlap extent and mean separation distance between the holes and electrons at the S_1 and T_1 states. Lower ΔE_{ST} values are generally associated with smaller overlap extents and higher mean separation distances between holes and electrons in the S_1 and T_1 states.[54,55] All the T_1 states show higher l_T (46.38 % to 78.87 %) and lower r_T (0.12 Å

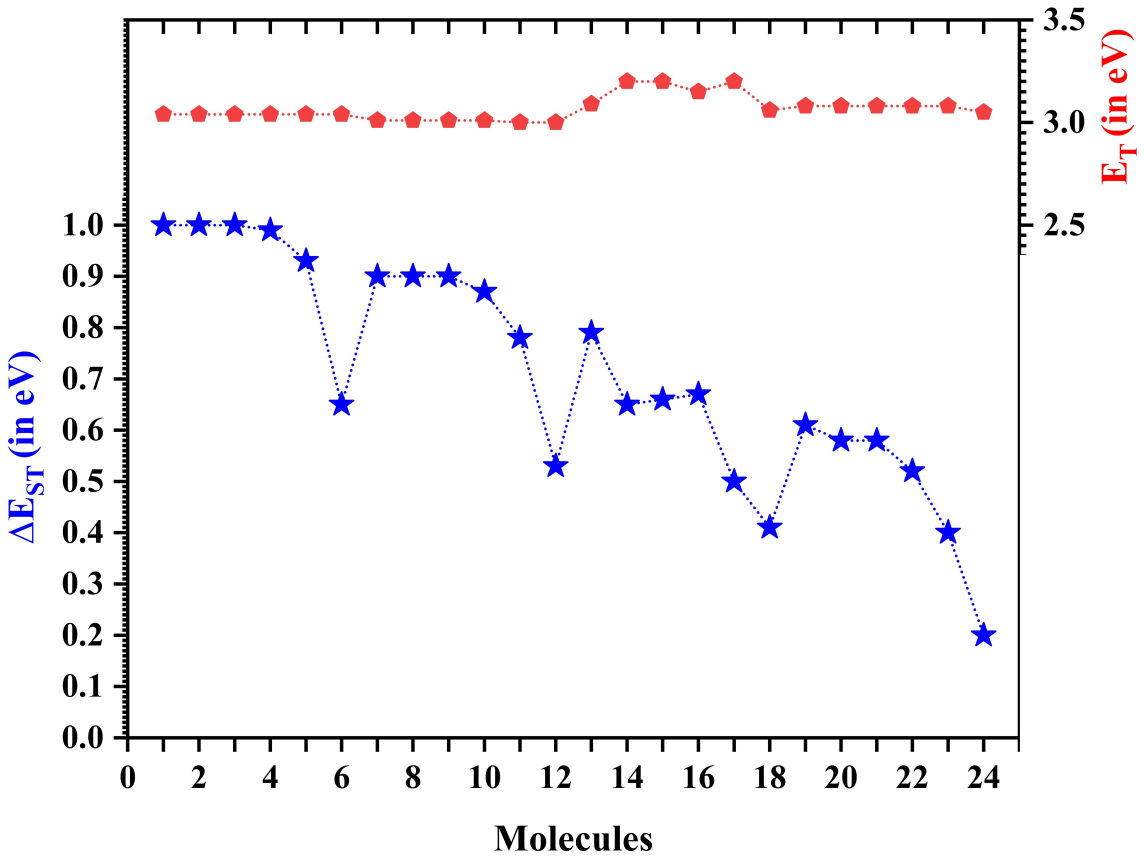

Figure 6. Evolution of singlet-triplet energy differences (ΔE_{ST}) and their Triplet (T_1) energies.

to 4.05 Å) values because the NTOs are localized on their respective donor and acceptor units. Thus, the evolution of the ΔE_{ST} values of the molecules is only understood by looking at the r_S values in the S_1 state. The r_S values at the S_1 state increased as the strength of the donor and acceptor units increased. The r_S value of molecules with P-CBZ donor range from 0.63 to 13.28 Å, molecules with P-t-Bu-CBZ donor units range from 0.64 to 13.32 Å, molecules with P-DPAC donor units range from 4.96 to 13.44 Å and, molecules with P-DMAC donor units range from 5.43 to 13.59 Å. In addition, higher mean separation distance values (10.65 to 12.33 Å) account for lower ΔE_{ST} values (0.65 to 0.20 eV) of P-DMB acceptor unit-based molecules.

The SOC $\langle S_1 | \widehat{H_{SO}} | T_n \rangle$ and ΔE_{ST} descriptors are crucial for determining the organic luminescent rates, such as K_{RISC}.[56] According to El-Sayed rule, the SOC $\langle S_1 | \widehat{H_{SO}} | T_n \rangle$ values are influenced by the electronic configuration of excited states and the attribution of the ΔE_{ST} factors.[57,58] The general mechanism is by reducing the ΔE_{ST} energy difference and increasing the SOC values between excited states (^{1}CT→^{3}LE/^{3}CT), which enables the excitons to be upconverted from T_n to S_1 state and, finally, the excitons to be transferred to emitters with reduced exciton losses. The SOC $\langle S_1 | \widehat{H_{SO}} | T_1 \rangle$ values (Tables 2 and S10) decrease systematically with increasing the strength of donor and acceptor units on the adamantane core. Nevertheless, it is noteworthy that the acceptor unit's strength substantially impacts SOC values more than the donor units. For instance, P-CBZ-containing molecules had maximum SOC $\langle S_1 | \widehat{H_{SO}} | T_1 \rangle$ values ranging from 0.24 to 0.59 cm^{-1} and molecules containing other donor moieties ranging from 0.18 to 0.40 cm^{-1}, except P-BODIPY-based molecules. Therefore, HLCT and LE characteristics between S_1 and T_1 states of the molecules show higher SOC values, whereas CT and LE characteristics between excited states show lower SOC values. In addition, the contributions to the SOC magnitudes between excited states are diminished for molecules featuring strong acceptor units. This observation persists even with distinct NTO configurations, owing to the vanished exchange energy, resulting in relatively small ΔE_{ST} values. However, P-BODIPY acceptor unit-based molecules show poor SOC magnitudes between S_1 and T_1 states. Furthermore, Table 4 includes SOC values between ^{1}CT and ^{3}LE states $\langle S_1 | \widehat{H_{SO}} | T_{2,3,4} \rangle$ for a more detailed understanding of vibronic effects because considering the two-state model (S_1 and T_1) is insufficient to describe the up-conversion mechanism. The vibronic coupling effect between the S_1 and higher T_n excited states considerably influences the SOC coupling values between the ^{1}CT state and ^{3}LE (T_2, T_4 states). The SOC values (S_1-$T_{2\text{-}4}$) show higher values for P-DMB acceptor-based molecules. The calculated rate constants between S_1 and T_1 states (K_{rISC}) are

Table 4. Calculated SOC values between S_1 and T_n ($T_n \geq 4$) excited states. (All values are in cm^{-1}).

Molecules	$\langle S_1 \lvert \widehat{H_{SO}} \rvert T_2 \rangle$	$\langle S_1 \lvert \widehat{H_{SO}} \rvert T_3 \rangle$	$\langle S_1 \lvert \widehat{H_{SO}} \rvert T_4 \rangle$
1	0.23	0.00	0.13
2	0.21	0.13	0.01
3	0.21	0.01	0.13
4	0.24	0.01	0.13
5	0.21	0.00	0.13
6	0.38	0.71	0.78
7	0.33	0.00	0.16
8	0.29	0.15	0.01
9	0.29	0.00	0.17
10	0.30	0.00	0.17
11	0.29	0.01	0.15
12	0.26	0.32	0.30
13	0.18	0.36	0.47
14	0.29	0.36	0.01
15	0.35	0.46	0.13
16	0.21	0.34	0.45
17	0.26	0.07	0.24
18	0.23	0.35	0.97
19	0.44	0.00	0.24
20	0.36	0.22	0.00
21	0.44	0.00	0.22
22	0.43	0.01	0.23
23	0.34	0.04	0.25
24	0.21	0.20	0.21

given in Table 2 & S10. The RISC rates systematically increase as the strength of both donor and acceptor units increases on the adamantane core due to the linear reduction of ΔE_{ST} values. The RISC rates of molecules with P-CBZ donor units range from $\sim 10^{-28}$ to $\sim 10^{-11}\,s^{-1}$, molecules with P-t-Bu-CBZ donor units range from $\sim 10^{-23}$ to $\sim 10^{-06}\,s^{-1}$, molecules with P-DPAC donor units range from $\sim 10^{-17}$ to $\sim 10^{-02}\,s^{-1}$, while molecules with P-DMAC donor units range from $\sim 10^{-09}$ to $\sim 10^{+03}\,s^{-1}$, respectively. Particularly, molecules containing P-BODIPY acceptors exhibit lower RISC rates between T_1 and S_1 ($\sim 10^{-63}\,s^{-1}$) due to higher singlet-triplet energy differences between S_1 and T_1 states.

TADF Sensitizer for Blue Hyperfluorescent OLEDs

The HOMO and LUMO energies of the TADF sensitizer should be aligned with the neighboring HT, ET, and emissive layers, as described in the criteria for potential TADF sensitizer. The HOMO energies of the TADF sensitizer should lie between the HOMO energies of the HT layer and the emitter and also closer to the HT layer for adequate hole transportation. In contrast, the molecules must have minimal deviations from the LUMO energies of the ET layer to ensure effective electron transport between the ETL and the TADF sensitizer.[16] HOMO-LUMO energy barrier diagram of the newly designed molecules with HT and ET layers and emitters is depicted in Figure 7. The HOMO energies of all the molecules lie between the HOMO energies of the HT layer and emitter (except for the DMAC-DPS and BN-CP2 emitters). Therefore, all the molecules are expected to have minimal hole transport barriers between the FIrpic emitter and the HT layer. When probed with the DMAC-DPS and BN-CP2 emitters, only molecules containing P-DMAC donor units **(molecules 19–24)** have HOMO energies between the HOMO energies of the HT layer and the DMAC-DPS and BN-CP2 emitters. The development of molecules with minimal hole transport and electron injection barriers for DMAC-DPS and MR-TADF emitters is challenging. However, molecules containing P-

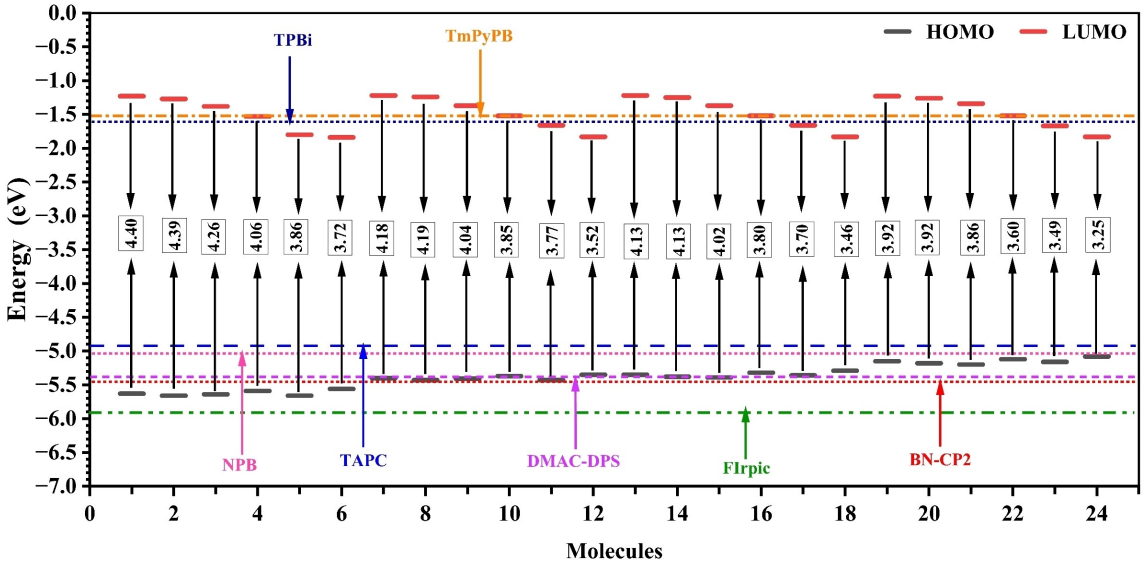

Figure 7. HOMO and LUMO energy levels (in eV) and HOMO-LUMO energy gap of newly designed molecules and reference HTL (TAPC, NPB), ETL (TmPyPB, TmPyPB), and emitters (DMAC-DPS/FIrpic/BN-CP2) as obtained at the B3LYP/6-31 + G* level of theory.

DMAC donor units are expected to have a minimal hole transport barrier on the DMAC-DPS and BN-CP2 emitters. In addition, when examining the energy barriers with LUMO orbitals, only molecules with P-PY **(molecules 4**, **10**, **16**, **22)**, P-CN **(molecules 5**, **11**, **17**, **23)**, and P-DMB **(molecules 6**, **12**, **18**, **24)** acceptor units (a total of 12 molecules) have lower deviations from the LUMO energies of the ET layer, so these molecules are expected to have lower electron injection barriers. In contrast, it is noteworthy that molecules containing P-γ-CBN, P-TZ, and P-PTZ acceptor units have higher electron injection barriers when used as the sensitizer. Besides blue emitters, the TADF sensitizers should have E_T above ~2.80 eV to prevent backward energy transfer from guests to the TADF sensitizers.[13] Therefore, all molecules have a higher E_T (3.00 to 3.20 eV) (Figure 6) (except P-BODIPY acceptor-based molecules) than emitters (DMAC-DPS/FIrPic/BN-CP2//2.56/2.85/2.44 eV), which allows excitons to be transported efficiently to emitters, which is compatible with the E_T of the universal unipolar mCP host (3.03 eV).

Studies conducted earlier have provided evidence that molecules with ΔE_{ST} values below 0.5 eV with higher triplet energies (> 2.80 eV) can effectively serve as TADF sensitizers for blue hyperfluorescent OLEDs. Because of the small ΔE_{ST} energies, these TADF sensitizers can increase the efficiency and lifespan of OLED devices by reducing the density of long-life triplet excitons and excited state collisions. As a result, the ΔE_{ST} energies of molecules **17**, **18**, **23**, and **24** are less than 0.5 eV, demonstrating that these molecules can function as TADF sensitizers. In contrast to the mCP and experimental molecule, the designed molecules differ by, at most, 0.82 eV in their ΔE_{ST} energies. The P-DMB acceptor unit substituted **(molecules 18 and 24)** and molecule **23** demonstrated the lowest ΔE_{ST} of 0.20 to 0.41 eV with higher triplet energy (3.05 to 3.08 eV) and reasonable SOC values of 0.18 to 0.21 cm^{-1}, allowing for a fast RISC rate of up to 3.33×10^{-02} to $3.20\times10^{+03}$ s^{-1} for the efficient FET mechanism by the TADF sensitizers in blue hyperfluorescent OLEDs. Still, the RISC rate is significantly lower due to its moderate ΔE_{ST} values. In order to increase the RISC rate in the molecules, two and three P-DMB acceptor units are attached to the potential system number 24 (Table S11, Figures S11–S12). The results reveal that when the number of boron atoms increased from one to two to three on the adamantane core, the ΔE_{ST} values systematically decreased, which increases the RISC rate by about ~10^{+05} s^{-1}.

Hot-Exciton Emitter

For hot exciton emitter, the general criteria are the high energy difference between T_2 and T_1 states to avoid the internal conversion (IC), the T_2 and T_n states should degenerate with or higher than the S_1 state to enable the up-conversion of high-lying triplet hot excitons (^{3}LE/^{3}CT→^{1}CT), excitons are upconverted from T_2 and T_n states to S_1 state and, finally, TADF emission originates from the S_1 state into the ground state as delayed fluorescence. Thus, we selected molecules containing BODIPY acceptor units **(25 to 28)** applicable for hot exciton emitters along with desired criteria based on the above-mentioned mechanism.[59] As a result, molecules **25 to 28** containing the P-BODIPY unit have higher energy differences between S_1-T_1 and T_2-T_1 states. When increasing the donor strength on the adamantane core with BODIPY moiety, the S_1, T_2, T_2-T_1, and S_1-T_1 energies systematically deceased, while T_1 energies remain constant (Tables S7 and S12–S13). Generally, many hot-exciton materials are reported using hybrid M06-2X functional, which overestimates the T_2 energies. In this study, we calculated the excitation energies of the BODIPY-based molecules with B3LYP, PBE0, M06, and M06-2X functionals (Figures S13-S17). All the DFT functionals predict similar energy level alignments and trends, albeit with the energies. The hole and electrons NTOs show pure CT nature at S_1 and T_2 states by the PBE0 functional, which results in degenerate energies for S_1 and T_2 states, while the T_1 state shows HLCT nature (Figure S6). Nevertheless, M06-2X functional shows HLCT nature for S_1, T_1, and T_2 states and results in similar energies for all the BODIPY-based molecules, even if it modifies the donating strength (Figure S13). The B3LYP. PBE0 and M06 functionals predict the S_1-T_2 energy levels close to zero because of vanished exchange energy, which results in weak SOC magnitudes. Thus, we utilized the M06-2X functional to calculate the SOC values only for BODIPY-based molecules with the same basis set (Table S10). The BODIPY-based molecules have higher SOC $\langle S_1 \left| \widehat{H_{SO}} \right| T_2 \rangle$ values of about 0.57 to 0.59 cm^{-1} with lower S_1-T_2 energy difference values of about 0.07 eV exhibit a higher RISC rate of about ~10^{+06} s^{-1} between S_1 and T_2 states. These molecules show lower RISC values between S_1 and T_1 states, about ~10^{-63} s^{-1}, and SOC magnitudes of about 0.07 cm^{-1} due to high S_1-T_1 energy differences of about 1.45 eV, which inhibit the exciton up-conversion from the T_1 state to S_1 state.

Conclusions

This study attempts to understand how the adamantane building block controls the electronic properties of the molecules by varying the strength of donor and acceptor units. The molecules containing P-PY **(molecules 4**, **10**, **16**, **22)**, P-CN **(molecules 5**, **11**, **17**, **23)**, and P-DMB **(molecules 6**, **12**, **18**, **24)** acceptor units exhibit lower hole transport and electron injection barriers than other molecules. In addition, only the molecules containing P-DMAC donor units **(molecules 22**–**24)** have lower hole transport barriers on the DMAC-DPS and BN-CP2 emitters. Hence, it is demonstrated that increasing the strength of donor and acceptor units on the adamantane core results in a gradual reduction in the hole transport and electron injection barriers. The fact that the adamantane core unit is an effective non-conjugated building block ensures its efficient HOMO and LUMO separation resulting in lower reorganization energies. Furthermore, all the molecules yield higher E_T due to the localized NTO distribution on their respective donor and acceptor units with LE character. A systematic and significant decrease in ΔE_{ST} and the SOC ($\langle S_1 \left| \widehat{H_{SO}} \right| T_1 \rangle$) coupling values

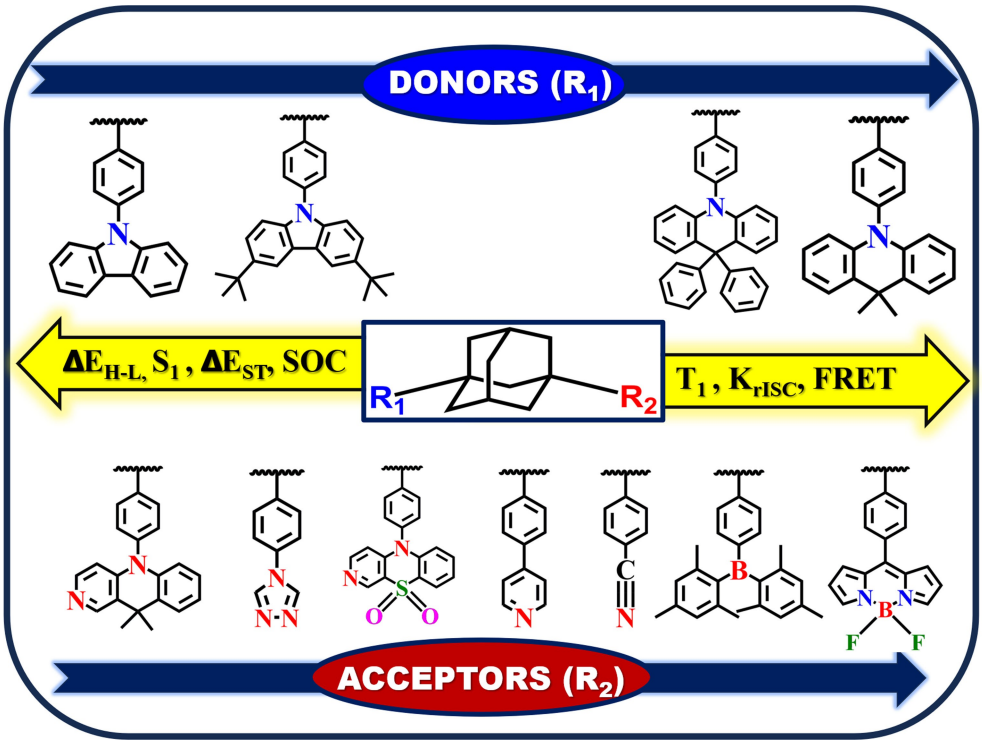

Figure 8. The overall notable trends in the crucial parameters examined.

were observed when increasing the strength of the donor and acceptor units on the adamantane core. Similarly, the RISC values increase significantly, indicating an increase in the long-range Forster/Resonance energy transfer process from the TADF sensitizers to the emitter. Moreover, when boron atoms are increased from one to two to three on the adamantane core, the ΔE_{ST} values are further decreased, which enhances the RISC rate. Moreover, the molecules containing P-BODIPY acceptor units have the potential criteria, making them good candidates for hot-exciton emitters with adamantane core. Therefore, molecules **24**, **2B**, **3B**, and **25**–**28** exhibit strong potential as TADF sensitizers and hot exciton emitters out of the 30 systems examined. Their advantageous attributes include notably low ΔE_{ST} values and favorable SOC and RISC values, highlighting their significant prospects for achieving efficient performance. In Figure 8, we summarize the most salient findings of this study. In this theoretical attempt, we demonstrate that changing the strength of donors and acceptors on the adamantane core greatly influences the molecule's structure and electronic properties. The results of our study are thus expected to benefit the development and applications of adamantane core, BODIPY, and DMB acceptor unit-based materials for optoelectronic devices.

Acknowledgements

R. M. acknowledges the SRMIST fellowship for pursuing this research, and the authors also thank the High-Performance Computing Centre (HPCC), SRM Institute of Science and Technology for providing the computational facility.

Conflict of Interests

The authors declare no competing financial interest.

Data Availability Statement

The data that support the findings of this study are available from the corresponding author upon reasonable request.

Keywords: TADF sensitizer · conventional host · adamantane core · dimesitylborane · hot-exciton

[1] M. A. Baldo, S. Lamansky, P. E. Burrows, M. E. Thompson, S. R. Forrest, *Appl. Phys. Lett.* **1999**, *75*, 4.
[2] M. A. Baldo, D. F. O'Brien, Y. You, A. Shoustikov, S. Sibley, M. E. Thompson, S. R. Forrest, *Nature* **1998**, *395*, 151.
[3] C. Adachi, T. Tsutsui, S. Saito, *Appl. Phys. Lett.* **1990**, *56*, 799.
[4] C. W. Tang, S. A. Vanslyke, *Appl. Phys. Lett.* **1987**, *51*, 913.
[5] J. Wang, C. Jiang, C. Liu, H. Liu, C. Yao, *Mater. Lett.* **2018**, *233*, 149.
[6] H. Uoyama, K. Goushi, K. Shizu, H. Nomura, C. Adachi, *Nature* **2012**, *492*, 234.
[7] Q. Zhang, J. Li, K. Shizu, S. Huang, S. Hirata, H. Miyazaki, C. Adachi, *J. Am. Chem. Soc.* **2012**, *134*, 14706.
[8] I. Danyliv, K. Ivaniuk, Y. Danyliv, I. Helzhynskyy, V. Andruleviciene, D. Volyniuk, P. Stakhira, G. V. Baryshnikov, J. V. Grazulevicius, *ACS Appl. Electron. Mater.* **2023**, *5*, 4174.
[9] R. Braveenth, H. Lee, J. D. Park, K. J. Yang, S. J. Hwang, K. R. Naveen, R. Lampande, J. H. Kwon, *Adv. Funct. Mater.* **2021**, *31*, 2105805.

[10] K. R. Naveen, H. Lee, R. Braveenth, D. Karthik, K. J. Yang, S. J. Hwang, J. H. Kwon, *Adv. Funct. Mater.* **2022**, *32*, 2110356.
[11] Y. Wang, J. H. Yun, L. Wang, J. Y. Lee, *Adv. Funct. Mater.* **2021**, *31*, 2008332.
[12] M. A. Baldo, C. Adachi, S. R. Forrest, *Phys. Rev. B: Condens. Matter Mater. Phys.* **2000**, *62*, 10967.
[13] M. A. Baldo, D. F. O'Brien, Y. You, A. Shoustikov, S. Sibley, M. E. Thompson, S. R. Forrest, *Nature* **1998**, *395*, 151.
[14] B. Sun, K. N. Tong, X. Chen, J. L. He, H. Liu, M. K. Fung, J. Fan, *J. Mater. Chem. C* **2021**, *9*, 7706.
[15] S. Yin, Y. Yi, Q. Li, G. Yu, Y. Liu, Z. Shuai, *J. Phys. Chem. A* **2006**, *110*, 7138.
[16] D. Kim, L. Zhu, J.-L. Brédas, *Chem. Mater.* **2012**, *24*, 2604.
[17] Y. Wang, J. H. Yun, L. Wang, J. Y. Lee, *Adv. Funct. Mater.* **2021**, *31*, 2008332.
[18] T. Chatterjee, K.-T. Wong, *Adv. Opt. Mater.* **2019**, *7*, 1800565.
[19] W.-S. Han, H.-J. Son, K.-R. Wee, K.-T. Min, S. Kwon, I.-H. Suh, S.-H. Choi, D. H. Jung, S. O. Kang, *J. Phys. Chem. C* **2009**, *113*, 19686.
[20] F. Rodella, S. Bagnich, E. Duda, T. Meier, J. Kahle, S. Athanasopoulos, A. Köhler, P. Strohriegl, *Front. Chem.* **2020**, *8*, 1.
[21] Y. Gu, L. Zhu, Y. Li, L. Yu, K. Wu, T. Chen, M. Huang, F. Wang, S. Gong, D. Ma, J. Qin, C. Yang, *Chem. Eur. J.* **2015**, *21*, 8250.
[22] H. Fukagawa, N. Yokoyama, S. Irisa, S. Tokito, *Adv. Mater.* **2010**, *22*, 4775.
[23] Z. Ma, W. Dong, J. Hou, Q. Duan, S. Shao, L. Wang, *J. Mater. Chem. C* **2019**, *7*, 11845.
[24] W. Li, X. Cai, B. Li, L. Gan, Y. He, K. Liu, D. Chen, Y. Wu, S. Su, *Angew. Chem. Int. Ed.* **2019**, *58*, 582.
[25] W. Xu, D. Hu, Z. Wang, G. Wang, K. Liu, J. Liang, R. Miao, Y. Fang, *J. Phys. Chem. Lett.* **2022**, 5358.
[26] M. A. B. Gapol, D. H. Kim, *Phys. Chem. Chem. Phys.* **2019**, *21*, 3857.
[27] Y. K. Wang, S. H. Li, S. F. Wu, C. C. Huang, S. Kumar, Z. Q. Jiang, M. K. Fung, L. S. Liao, *Adv. Funct. Mater.* **2018**, *28*, 1.
[28] L. Wan, Z. Cheng, F. Liu, P. Lu, *Mater. Chem. Front.* **2023**, 4420.
[29] X. Y. Liu, H. T. Ge, Y. Zhao, D. Zhao, J. Fan, L. S. Liao, H. Lee, J. H. Park, K. J. Yang, S. J. Hwang, R. Braveenth, T. H. Ha, M. I. Han, C. W. Lee, J. H. Kwon, *J. Mater. Chem. C* **2021**, *9*, 4300.
[30] J. S. Moon, D. H. Ahn, S. W. Kim, S. Y. Lee, J. Y. Lee, J. H. Kwon, *RSC Adv.* **2018**, *8*, 17025.
[31] Y. Xia, Z. Liu, J. Li, C. Fan, G. Li, B. Zhao, Y. Wu, H. Wang, K. Guo, *Org. Electron.* **2020**, *85*, 105826.
[32] J. Tirado-Rives, W. L. Jorgensen, *J. Chem. Theory Comput.* **2008**, *4*, 297.
[33] C. Adamo, V. Barone, *J. Chem. Phys.* **1999**, *110*, 6158.
[34] R. Valero, R. Costa, I. de P. R. Moreira, D. G. Truhlar, F. Illas, *J. Chem. Phys.* **2008**, *128*, 114103.
[35] S. Salman, D. Kim, V. Coropceanu, J.-L. Brédas, *Chem. Mater.* **2011**, *23*, 5223.
[36] R. L. Martin, *J. Chem. Phys.* **2003**, *118*, 4775.
[37] F. Neese, *WIREs Comput. Mol. Sci.* **2018**, *8*, e1327.
[38] T. Lu, F. Chen, *J. Comput. Chem.* **2012**, *33*, 580.
[39] J.-L. Brédas, D. Beljonne, V. Coropceanu, J. Cornil, *Chem. Rev.* **2004**, *104*, 4971.
[40] M. J. Frisch, G. W. Trucks, H. B. Schlegel, G. E. Scuseria, M. a. Robb, J. R. Cheeseman, G. Scalmani, V. Barone, G. a. Petersson, H. Nakatsuji, X. Li, M. Caricato, a. V Marenich, J. Bloino, B. G. Janesko, R. Gomperts, B. Mennucci, H. P. Hratchian, J. V Ortiz, a. F. Izmaylov, J. L. Sonnenberg, Williams, F. Ding, F. Lipparini, F. Egidi, J. Goings, B. Peng, A. Petrone, T. Henderson, D. Ranasinghe, V. G. Zakrzewski, J. Gao, N. Rega, G. Zheng, W. Liang, M. Hada, M. Ehara, K. Toyota, R. Fukuda, J. Hasegawa, M. Ishida, T. Nakajima, Y. Honda, O. Kitao, H. Nakai, T. Vreven, K. Throssell, J. a. Montgomery Jr., J. E. Peralta, F. Ogliaro, M. J. Bearpark, J. J. Heyd, E. N. Brothers, K. N. Kudin, V. N. Staroverov, T. a. Keith, R. Kobayashi, J. Normand, K. Raghavachari, a. P. Rendell, J. C. Burant, S. S. Iyengar, J. Tomasi, M. Cossi, J. M. Millam, M. Klene, C. Adamo, R. Cammi, J. W. Ochterski, R. L. Martin, K. Morokuma, O. Farkas, J. B. Foresman, D. J. Fox, *Gaussian 16*, **2016**, p. Gaussian 16, Revision C.01, Gaussian, Inc., Wallin.
[41] D. Zhang, M. Cai, Y. Zhang, D. Zhang, L. Duan, *Mater. Horiz.* **2016**, *3*, 145.
[42] J. Luo, S. Gong, Y. Gu, T. Chen, Y. Li, C. Zhong, G. Xie, C. Yang, *J. Mater. Chem. C* **2016**, *4*, 2442.
[43] S. Tokito, T. Iijima, Y. Suzuri, H. Kita, T. Tsuzuki, F. Sato, *Appl. Phys. Lett.* **2003**, *83*, 569.
[44] A. Ejigu, D. A. Walsh, *J. Phys. Chem. C* **2014**, *118*, 7414.
[45] R. J. Holmes, S. R. Forrest, Y.-J. Tung, R. C. Kwong, J. J. Brown, S. Garon, M. E. Thompson, *Appl. Phys. Lett.* **2003**, *82*, 2422.
[46] T. D. Anthopoulos, J. P. J. Markham, E. B. Namdas, I. D. W. Samuel, S.-C. Lo, P. L. Burn, *Appl. Phys. Lett.* **2003**, *82*, 4824.
[47] J. Pan, F. Fang, J. Xie, L. Wang, J. Chen, J. Chang, W. Lei, W. Zhang, D. Zhao, *J. Mater. Chem. C* **2020**, *8*, 5572.
[48] R. K. Konidena, K. R. Naveen, *Adv. Photonics. Res.* **2022**, *3*, 2200201.
[49] E. E. Bas, P. Ulukan, A. Monari, V. Aviyente, S. Catak, *J. Phys. Chem. A* **2022**, *126*, 473.
[50] Y. Shi, H. Ma, Z. Sun, W. Zhao, G. Sun, Q. Peng, *Angew. Chem. Int. Ed.* **2022**, *61*.
[51] D. P. McMahon, A. Troisi, *J. Phys. Chem. Lett.* **2010**, *1*, 941.
[52] J. Wu, Y. Liao, S.-X. Wu, H.-B. Li, Z.-M. Su, *Phys. Chem. Chem. Phys.* **2012**, *14*, 1685.
[53] D. Kim, L. Zhu, J.-L. Brédas, *Chem. Mater.* **2012**, *24*, 2604.
[54] R. Chen, Y. Tang, Y. Wan, T. Chen, C. Zheng, Y. Qi, Y. Cheng, W. Huang, *Sci. Rep.* **2017**, *7*.
[55] T. Chen, L. Zheng, J. Yuan, Z. An, R. Chen, Y. Tao, H. Li, X. Xie, W. Huang, *Sci. Rep.* **2015**, *5*, 1.
[56] X.-K. Chen, D. Kim, J.-L. Brédas, *Acc. Chem. Res.* **2018**, *51*, 2215.
[57] M. A. El-Sayed, R. G. Brewer, *J. Chem. Phys.* **1963**, *39*, 1623.
[58] W. Zhao, Z. He, J. W. Y. Lam, Q. Peng, H. Ma, Z. Shuai, G. Bai, J. Hao, B. Z. Tang, *Chem.* **2016**, *1*, 592.
[59] X. Nie, Z. Mahmood, D. Liu, M. Li, D. Hu, W. Chen, L. Xing, S. Su, Y. Huo, S. Ji, *Energy Environ.* **2023**, e12597.

Manuscript received: September 8, 2023
Revised manuscript received: October 29, 2023
Accepted manuscript online: November 27, 2023
Version of record online: ■■, ■■

RESEARCH ARTICLE

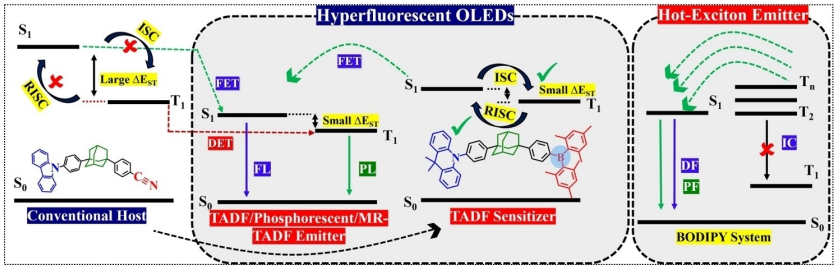

R. Mahaan, A. J. Bosco, A. I. Jothi*

1 – 15

Converting Conventional Host to TADF Sensitizer and Hot-Exciton Emitter in Donor-Adamantane-Acceptor Triads for Blue OLEDs: A Computational Study

TADF Sensitizer and Hot-Exciton Emitter: The conventional host molecule undergoes a conversion into a TADF sensitizer and a Hot-Exciton emitter via distinct donor and acceptor unit substitutions on the adamantane core. Molecules incorporating acceptor units such as DMB and BODIPY, which feature boron atoms, have the potential to serve as TADF sensitizers and Hot-exciton emitters for OLED applications, respectively.

Surfaces and Interfaces 40 (2023) 103020

Contents lists available at ScienceDirect

Surfaces and Interfaces

journal homepage: www.sciencedirect.com/journal/surfaces-and-interfaces

High-performance electrochemical sensor based on neodymium molybdate/reduced graphene oxide ($Nd_2Mo_3O_{12}$/RGO) for rapid detection of carcinogenic organic pollutants in water samples

Santhiyagu Sahayaraj Rex Shanlee [a], Ruspika Sundaresan [a], Shen-Ming Chen [a,*], Ramachandran Balaji [b,*], Tharini Jeyapragasam [c], Jing- Yi Peng [a], A. Irudaya Jothi [d]

[a] Department of Chemical Engineering and Biotechnology, National Taipei University of Technology, No.1, Section 3, Chung-Hsiao East Road, Taipei 106, Taiwan
[b] Department of Electronics and Communication Engineering, Koneru Lakshmaiah Education Foundation, Andhra Pradesh 522302, India
[c] Department of Science and Humanities, Solaimalai College of Engineering, Veerapanjan, Madurai 625020, India
[d] Department of Chemistry, St. Joseph's College (Autonomous), (Affiliated to Bharathidasan University, Tiruchirappali 620024), Tiruchirappalli, Tamilnadu 620002, India

ARTICLE INFO

Keywords:
Rare earth molybdate
RGO
Metol
Electrochemistry
Real-world analysis

ABSTRACT

Reasonable design, rapid, and reliable high-performance catalyst for the electrochemical sensor determination of carcinogenic photographic developing agent metol (ML) which is identified as a water and environment contaminant. This research investigation is based on the development of rare earth molybdate ($Nd_2Mo_3O_{12}$) embedded with reduced graphene oxide, synthesized through the co-precipitation method for electrochemical sensing of ML. The highly conducting carbon-based material improved the electronic conductivity of metal molybdate. The synthesized nanocomposite was thoroughly characterized by various techniques to affirm its surface morphology, topography, crystal structure, surface area, and elemental composition. Taking advantage of a huge electroactive surface area and fast electron transfer rate and strong electrocatalytic ability of NdMO, the fabricated NdMO/RGO sensor displays sensitivity for the quantitative analysis of ML. Their limit of detection (LOD) of 0.005 μM with a linear range of 0.01 – 1770 μM respectively. Beyond that, the developed sensor exhibits good catalytic activity, stability, reproducibility, and selectivity toward the detection of ML. The proposed sensor was employed for the water sample analysis and appreciable recovery results were obtained.

1. Introduction

Metol (ML) (N-methyl-p-aminophenol sulfate) is an important organic molecule containing an amino functional group and a hydroxyl functional group [1]. It is predominantly used as a monochromic material for photographic development and hair dye. Due to the advancement of information technology, photographic techniques have grown excellently over the last two decades. Photographers use photosensitive materials for the conversation of latent images to visible images in photographic techniques. ML is the main organic compound that converts latent images to visible images. It is used as an excellent developing agent for tone developer applications for a century [2,3]. After finishing the photographic development, ML is released into the water bodies namely rivers, ponds, lakes, streams, and seas. ML is the sulfate salt of N-methylaminophenol. It causes great concern for the environment and hence affects human beings, plants, and animals [4]. It causes skin problems, and eye problems, and affects the important organs of the human body. It is malignant to aquatic life and carcinogenic [5]. Hence, it is a need of the situation to fabricate a simple, rapid, low-cost, sensitive, and convenient technique for ML determination in water bodies. Different kinds of a method for the detection of biological samples includes analytical methods[6] such as the mass-chromatogram spectrum [7], gas chromatography [8], mass spectrometry [9] and electroanalytical methods[10] in which the potentiometric sensors[11], amperometry [12]. There are certain methods such as spectrophotometry [13], an electrochemical method [2], Fenton reagent [5], ceric oxidimetry [2], and photolysis [14] have been used to determine ML. However, some other methods need a lot of time, affluent equipment, hazardous solvents, and extensive labor. However, electrochemical methods offer simple, low-cost, highly selective, and quick responses and an excellent

* Corresponding authors.
E-mail addresses: smchen78@ms15.hinet.net (S.-M. Chen), rbalaji@kluniversity.in (R. Balaji).

https://doi.org/10.1016/j.surfin.2023.103020
Received 27 April 2023; Received in revised form 25 May 2023; Accepted 5 June 2023
Available online 14 June 2023

linear range.

Due to their exceptional optical, magnetic, and electrical capabilities, rare earth molybdates are a fascinating family of rare-earth-based compounds that have been thoroughly researched [15–17]. Rare earth metals show good chemical stability, thermal stability, good catalytic, mechanical, and electrical properties [18,19]. It has good fluorescent properties and piezoelectric and ferro elastic properties. Rare earth metals have extensive applications in the field of electrocatalysis, photocatalysts for the degradation of organic water pollutants, limit emitting diodes, biosensors, optical fibers, chemical sensors, energy storage, and magnetic materials [20,21]. Among the various rare earth molybdates, neodymium (Nd) and their oxides, carbonates, phosphates, chromates, and zirconates show good magnetic, electrical, optical, high laser power, and ferroelectric properties [22]. Muthuraj et al., prepared yttrium molybdate nanosheets using simple wet chemical methods which show remarkable photocatalytic properties and electrocatalytic properties towards acebutolol [23] and photocatalytic activity towards paraoxonethyl [24]. These works indicate that rare earth molybdate has the potential to be a promising electrochemical sensing material.

Neodymium is the fourth member of the lanthanides series with excellent ferromagnetic properties and electrical properties [25]. Neodymium (Nd)-based composite find applications in the field of magnetism, ceramic materials, photocatalysis, energy storage devices, and sensor applications [26,27]. Molybdates have been used in numerous physical and chemical applications recently because of their distinctive physical and chemical characteristics. [28]. Molybdates can easily combine with Neodymium due to their good hosting medium for the last ions [29]. Reduced graphene oxide (RGO) is the atomically thin carbon sheet with the functional group which could be easily prepared on the large scale with low cost and higher yield from the simple precursor (graphitic oxide) [30,31]. RGO has been decorated with different nanoparticles such as Ag, Au, ZnO, TiO_2, and polymers to form novel multifunctional hybrid materials [32,33]. These multifunctional hybrid materials show excelling electric, magnetic, and catalytic properties compared to RGO [34,35]. In the present work, we prepared neodymium molybdate with reduced graphene oxide (NdMO/RGO) using a simple hydrothermal method. Our report is the primary study to date for the determination of ML using NdMO/RGO nanocomposite. There are a few materials namely $CuCo_2O_4$ [1], $CaSnO_3$ [36], MoS_2 [37], ionic liquid [2], gold nanoparticle [38], $LiCoO_2$ [5], ZrO_2 [39], $CoMoSe_2$ [40] were explored for the sensing of ML. RGO a well-known material for electrochemical sensing applications with very good electrical conductivity and chemical stability, was chosen as the carbon support in this paper. The electrocatalytic materials are undeniably bound to RGO, which plays an important role in increasing the active area[41].

In this study, we prepare a novel $Nd_2Mo_3O_{12}$ with RGO nanocomposite via the co-precipitation method for ML detection. As prepared NdMO/RGO shows higher catalytic sites, high surface area, and higher catalytic activities compared to NdMO and RGO. In comparison to the bare GCE, NdMO modified GCE, high electrocatalytic activity was obtained at the NdMO/RGO modified electrode due to the synergetic effects of RGO and NdMO nanomaterials. With our investigative results, NdMO/RGO-based sensors can be recommended for onsite monitoring of ML.

2. Experiment section

2.1. Chemical reagents

The reagents and the material characterization were explained in the supplementary document (SI).

2.2. Synthesis of GO and RGO

The detailed procedure for the preparation of GO and RGO was explained in SI.

2.3. Synthesis procedure NdMO nanoparticle and NdMO/RGO composite

NdMO was synthesized by using a similar protocol similar to previous literature [27]. First 0.1 M of $Nd(NO_3)_2$ and Na_2MoO_4 are liquified in 60 ml of DI H_2O and stirred for 15 min constantly. After 15 min, 0.5 g of urea was introduced and then 10 ml of ethylene glycol was introduced. To the mixture, GO was added and stirred at 70 °C for 1 h. Then the attained precipitate was centrifuged using DI H_2O and ethanol to eliminate the impurities and then dried for 24 h and calcined for about 6 h at 650 °C. Then the powder was ground and named NdMO/RGO and used for the characterizations and electrochemical analysis. For the synthesis of NdMO, the same procedure was followed without adding GO. Scheme 1 depicts the graphical illustration of synthesis procedure of NdMO/RGO.

3. Result and discussion

3.1. Physio-chemical characterization

X-ray diffraction (XRD) pattern was scrutinized to understand the crystallinity of the NdMO, RGO, and NdMO/RGO composite. In Fig. 1A (a) there are several peaks located in the XRD lattice planes and it was found that those were similar to the XRD pattern of $Nd_2(MoO_4)_3$ [JCPDS. NO: 00–025–1174] and the peaks appeared at 22.1, 24.2, 25.2, 26.8, 28.5, 30.7, 38.5, and 43.2 corresponds to (−204), (312), (−132), (−404), (223), (040), (−244), and (514) planes respectively. Fig. 1A(b) shows the XRD pattern of RGO in which it shows the broad peak at 24.1 which corresponds to the (002) plane indicating it is amorphous. Fig. 1A (c) exhibits the XRD pattern of NdMO/RGO, on comparing the peaks of NdMO and RGO it was evident that the location of the peaks of NdMO/RGO was almost identical to NdMO and RGO peaks which indicates the crystallinity of the prepared NdMO/RGO composite. Fig. 1B represents the Raman spectra of RGO and NdMO/RGO composite to give information about the carbonaceous material [42]. Two peaks were detected for the carbon material D band and G band. The Raman spectra of RGO and NdMO/RGO exhibit peaks around 1360 and 1590 cm^{-1}. The observed I_D/I_G ratio of RGO is found to be 0.96. It was found that the I_D/I_G ratio increased to 0.98 for NdMO/RGO. On comparing the RGO and NdMO/RGO the I_D/I_G of the D and G bands was higher for NdMO/RGO indicating that the NdMO/RGO composite has higher surface defects. These results prove the successful formation of NdMO/RGO composite material.

3.2. Structural characterizations of NdMO/RGO composite

The surface morphology and topography of NdMO, RGO, and NdMO/RGO were characterized through field emission scanning electron microscopy (FE-SEM) and high-resolution transmission electron microscopy (HR-TEM) at various magnifications Fig. 2(A-E). It was clear from Fig. 2A, that the prepared NdMO/RGO has a particle-like morphology. Fig. 2B depicts the thin sheet-like layer structure of RGO. In the FE-SEM image (Fig. 2D&E) of NdMO/RGO, the NdMO nanoparticle was anchored on the surface of RGO which proves the synergetic effect between the NdMO and RGO heterojunctions which will enhance the electrochemical activity for the detection of ML. The HR-TEM image in Fig. 3A&B explored the particle-like topography of NdMO which is complimentary to the FE-SEM image. Fig. 3C&D presents the HR-TEM image of NdMO/RGO in which the NdMO nano-particle was anchored over the thin sheets of RGO forming a heterojunction. From this figure, we can understand the intimate interaction between the NdMO and RGO heterojunction which ultimately boosts the electron transfer rate. The elemental mapping of NdMO/RGO composite is revealed in Fig. 3E–H which shows the NdMO/RGO composite was enriched with elements Nd (yellow), Mo (blue), O (green), and C (red). Fig. 3(I) depicts the SAED pattern of the NdMO/RGO composite. Fig. 3(J) depicts the lattice fringe of the NdMO/RGO composite from which the D-spacing was calculated

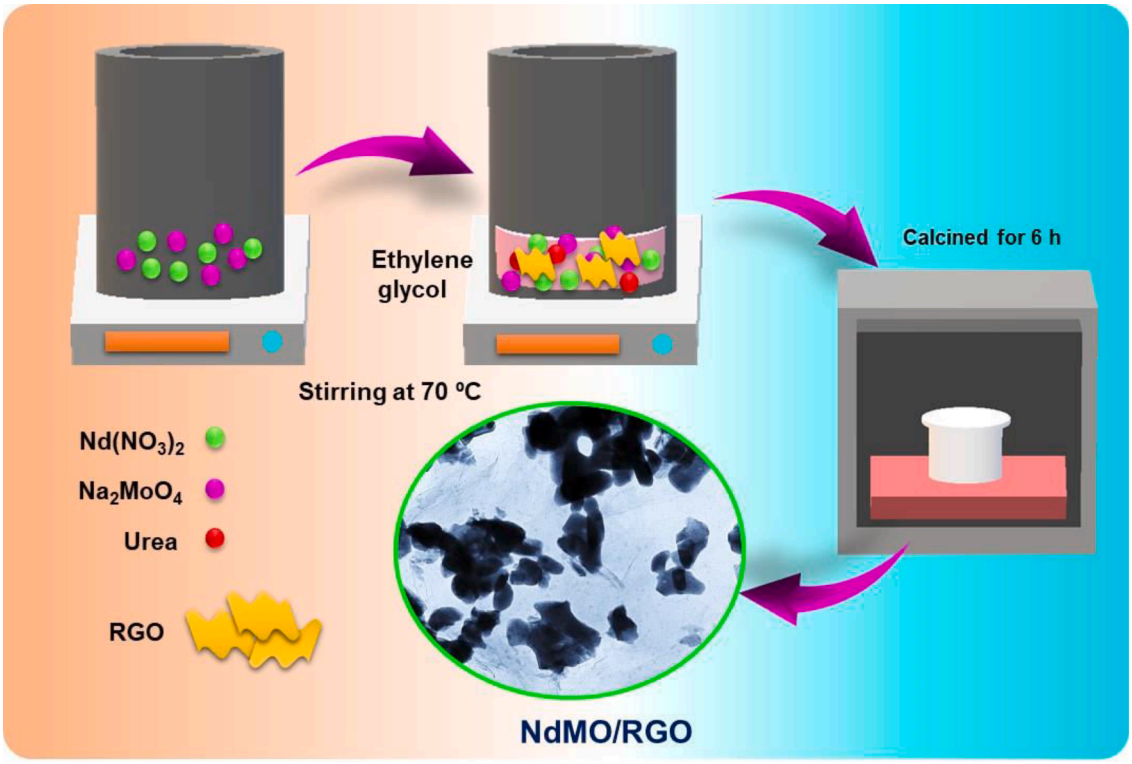

Scheme 1. Graphic depiction of the preparation of NdMO/RGO composite.

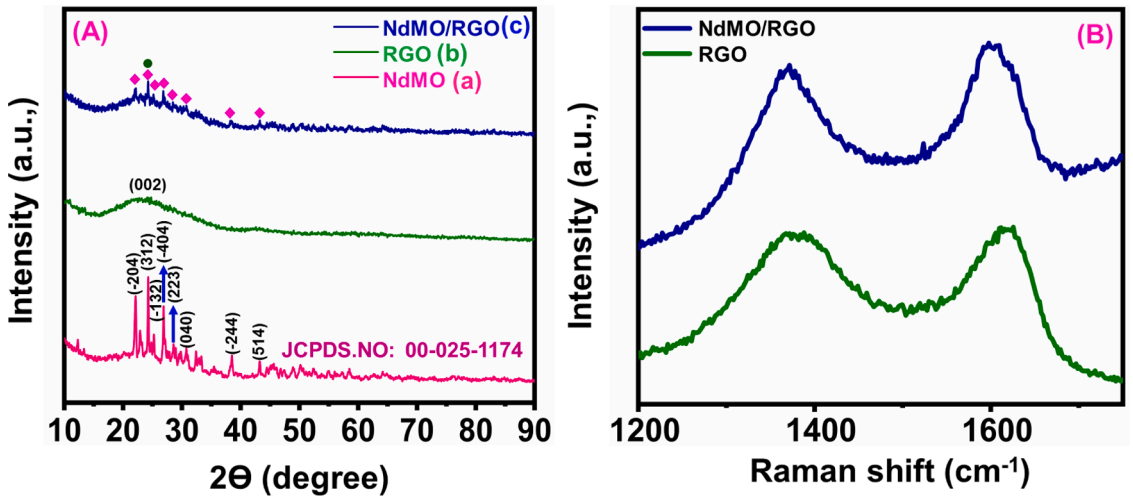

Fig. 1. (A) XRD pattern NdMO, RGO, and NdMO/RGO and (B) Raman spectra of RGO, NdMO/RGO composite.

to be 0.366 nm corresponds to the (312) plane. The EDS spectrum in Fig. 3(K) displays the intense peak ascribed to the elements Nd, Mo, O, and C respectively. Thus, the results endorse the formation of NdMO/RGO composite.

3.3. XPS investigation of NdMO/RGO composites

X-ray photoelectron spectroscopy (XPS) measurement is a selective and sensitive characterization technique used to analyze the chemical composition, electronic state, and interaction of the NdMO/RGO composite [43]. XPS survey spectrum in Fig. 4A shows that the NdMO/RGO mainly consists of neodymium (Nd), Molybdenum (Mo), oxygen (O), and carbon (C) in agreement with elemental mapping results. From Fig. 4B, the enlarged view of the Nd 3d spectrum portrayed the prominent peak centered at 989.17 and 1001.95 eV for $3d_{5/2}$ and $3d_{3/2}$ which confirms the +3 oxidation state of Nd [44]. The high-resolution Mo spectrum of NdMO has depicted in Fig. 4C in which the peaks centered at 234.11 and 237.31 eV which are attributed to $3d_{5/2}$ and $3d_{3/2}$ correspond to the characteristics Mo^{6+} [45]. The occurrence of the O1s peak at 531.91 eV depicted in Fig. 4D is attributed to the Nd-O/Mo-O bond [45]. The high-resolution C1S spectrum (Fig. 4E) of NdMO/RGO gets deconvoluted into three peaks. The peaks centered at 288.34, 289.92, and 292.32 eV attributed to C = O, C–O, and C–C/C = C respectively [46]. These results concluded the existence of Nd, Mo, O, and C which unambitiously revealed the successful formation of NdMO/RGO composite.

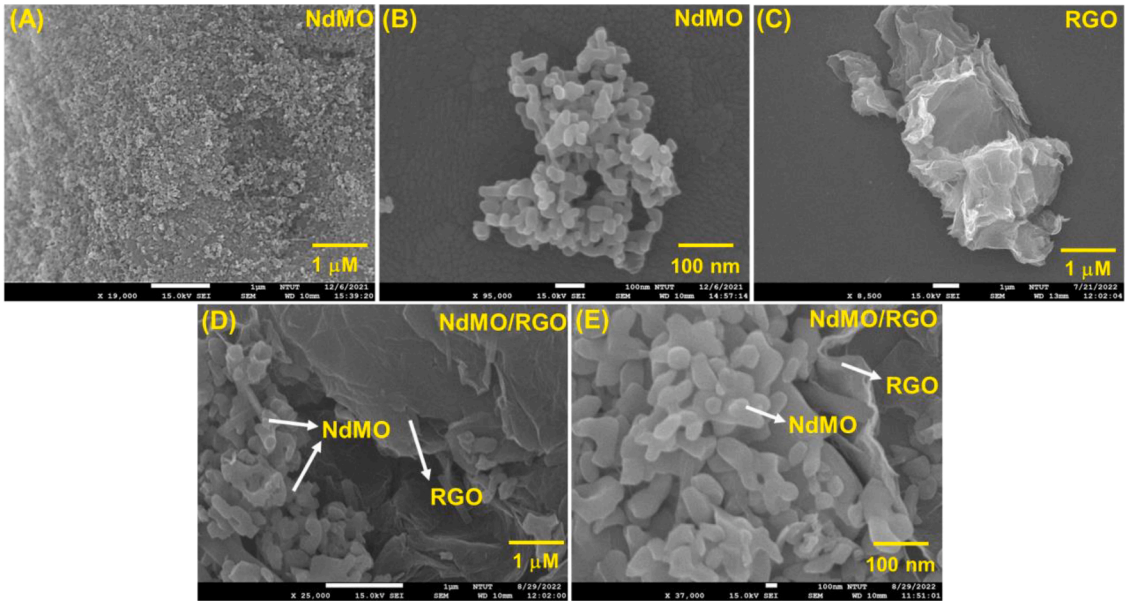

Fig. 2. FESEM image of (A&B) NdMO, (C) RGO, and (D&E) NdMO/RGO composite.

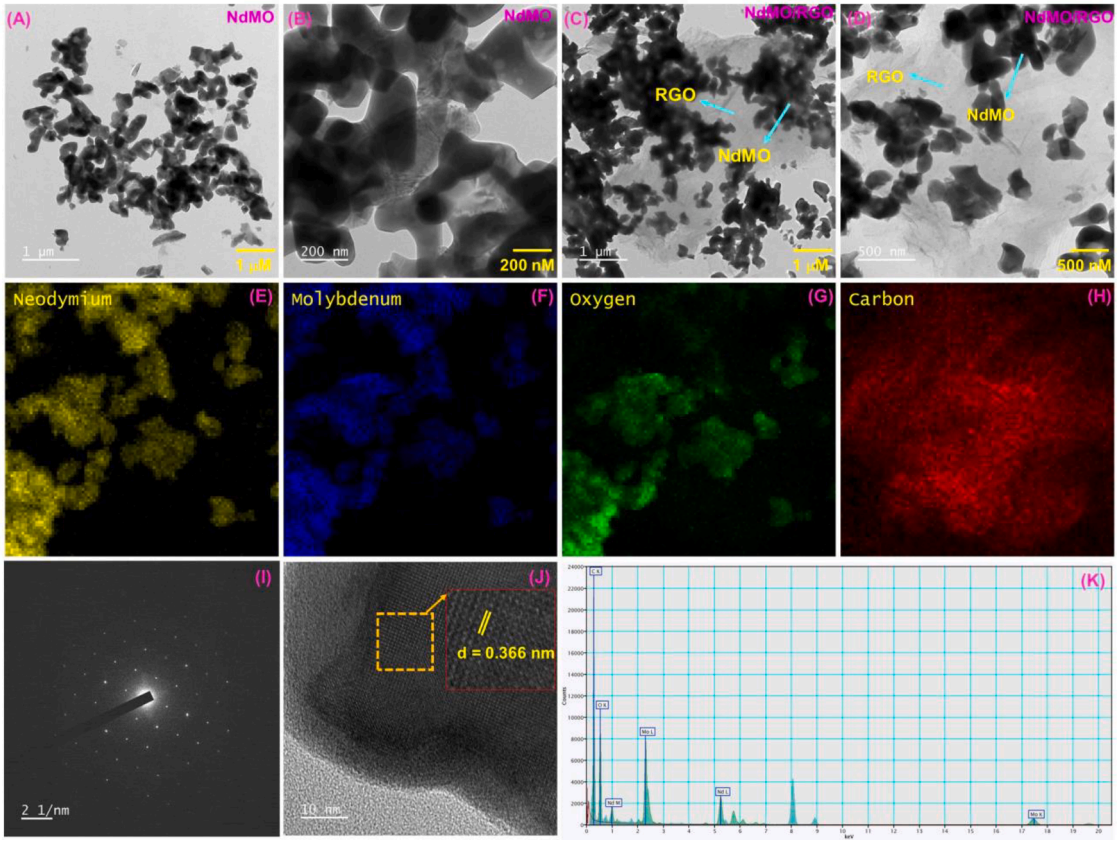

Fig. 3. TEM image of (A&B) NdMO, (C&D) NdMO/RGO composite, (E-H) elemental mapping image of neodymium, molybdenum, oxygen, and carbon, (I) SAED pattern of NdMO/RGO, (J) HR-TEM image of NdMO/RGO composite, and (K) EDS spectra of NdMO/RGO composite.

3.2. Electrocatalytic activity

3.2.1. Conductivity and charge transfer kinetics of the fabricated sensor

The NdMO/RGO/GCE was analyzed through a series of Cyclic voltammetry (CV) and Electrochemical impedance spectroscopy (EIS) measurements in 5 mM $[Fe(CN)_6]^{3-/4-}$ (FC system) and 0.1 M KCl was chosen as a redox coupling electrolyte to scrutinize the electrocatalytic activity [47]. Fig. 5A shows the Nyquist plot in a small semicircle for NdMO/RGO/GCE (R_{ct} = 58.1 Ω) compared to that of other modified electrodes RGO/GCE (R_{ct} = 253.93 Ω), NdMO/GCE (R_{ct} = 606.52 Ω), and bare GCE (R_{ct} =705.1 Ω) respectively. A high R_{ct} value of unmodified GCE indicates a reduced electrocatalytic activity due to its poor

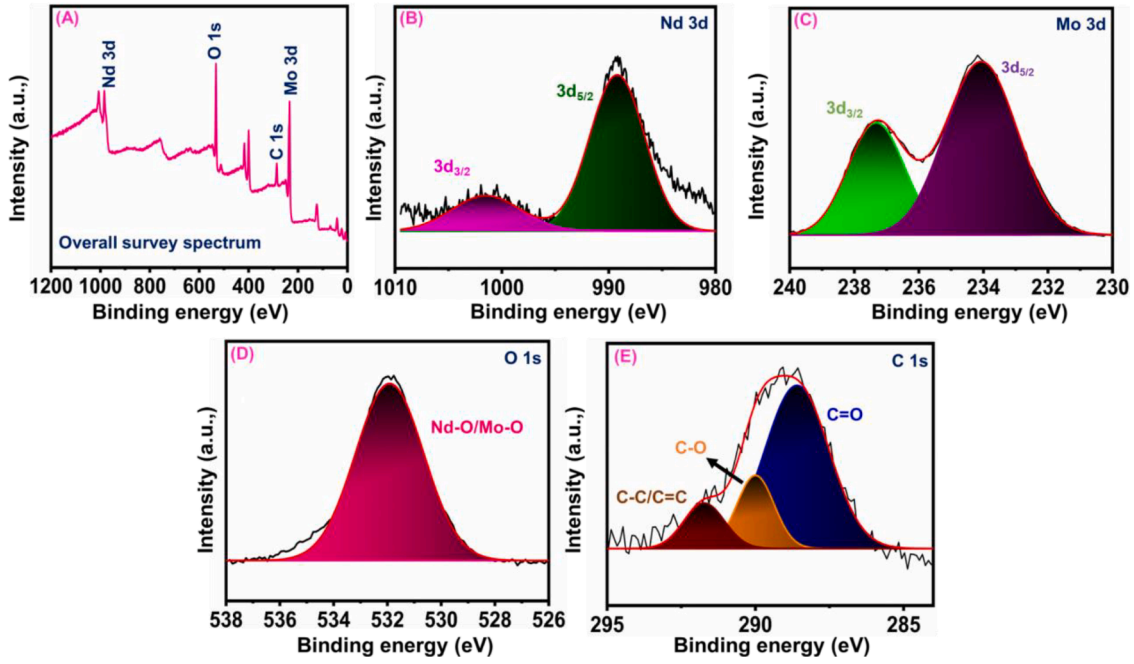

Fig. 4. XPS analysis of NdMO/RGO (A) Overall survey spectra and high-resolution spectrum of (B) Nd, (C) Mo, (D) O, and (E) C respectively.

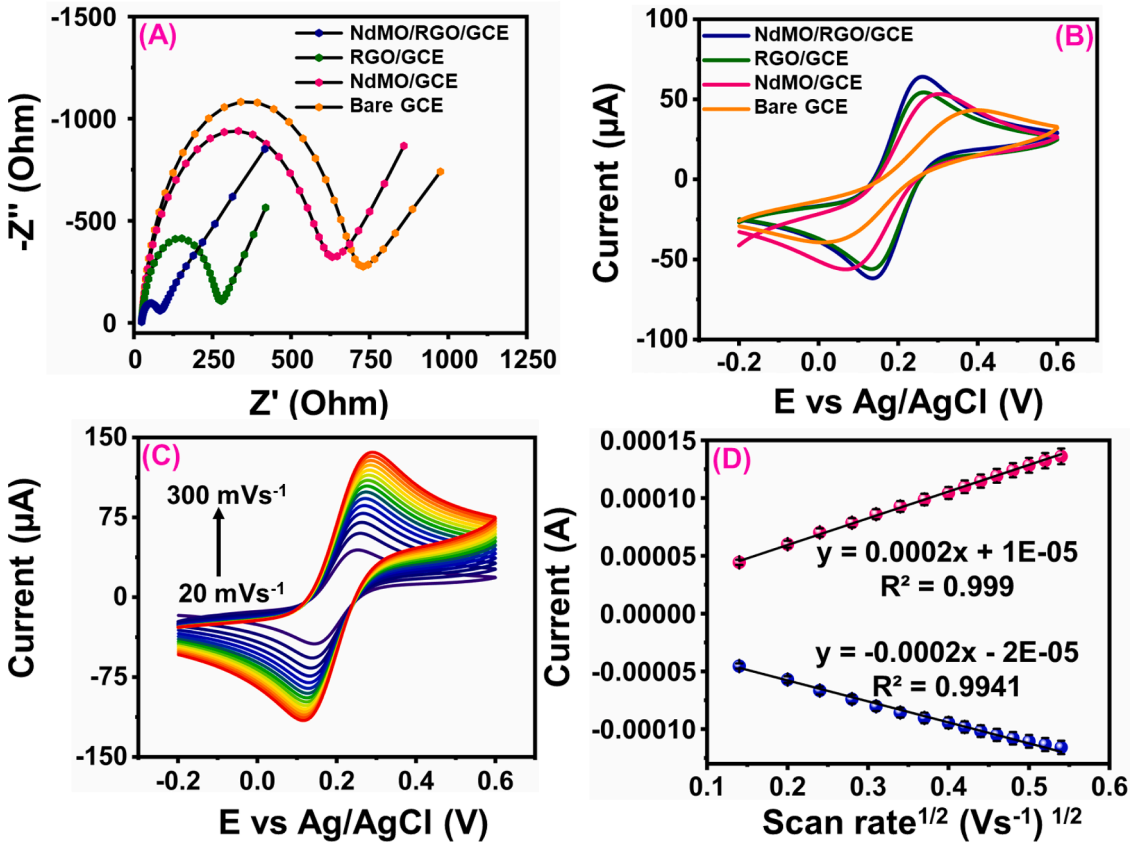

Fig. 5. (A&B) EIS Nyquist plot and CV response of bare GCE, NdMO/GCE, RGO/GCE, and NdMO/RGO/GCE, (C) CV plot of NdMO/RGO/GCE at various scan rate, and (D) corresponding linear plot of current vs square root of scan rate.

electron transfer which results in reduced electronic conductivity. So, the unmodified GCE undergoes some modification with bimetal oxide. NdMO/GCE shows a lower R_{ct} value which proves the enhanced conductivity which is due to the presence of more active sites resulting in fast electron transport. Thus, the detection of NdMO/GCE/GCE proves its suitability as an efficient electrocatalyst.

The conductivity and effectiveness of the bare GCE, NdMO/GCE, RGO/GCE, and NdMO/RGO/GCE have been tested in 0.1 M KCl and FC

systems through CV analysis. As seen from Fig. 5B, it was clear that the bare GCE shows a well-defined redox peak with a poor peak-to-peak separation. As the NdMO modified electrode shows an increased peak current. The high conductivity nature of graphene causes it to show a higher peak current for the electrode modified with RGO. When the NdMO/RGO was combined it shows a much higher redox current which induces the electron transfer ability between the electrode and electrolyte due to its highly electro-active nature. Further, the effect of scan rate varies from 20 mVs^{-1} – 300 mVs^{-1} depicted in Fig. 5C in the presence of 0.1 M KCl and FC system. Fig. 5D shows a linearity corresponding to the peak current and square root of the scan rate, which is a diffusion-controlled process. As the scan rate increases redox peak current increases. The electrochemical active surface area (EASA) was calculated by using the formula [48,49],

$$\mathbf{Ip} = \left(2.69 \times 10^5\right) \boldsymbol{n}^{3/2} \boldsymbol{D}^{1/2} \boldsymbol{A} \boldsymbol{v}^{1/2} \boldsymbol{C} \quad (1)$$

The EASA of bare GCE, NdMO/GCE, RGO/GCE, and NdMO/RGO/GCE was calculated to be 0.075, 0.089, 0.115, and 0.125 cm^2. The above results reveal that the synergetic interaction between the NdMO and RGO heterojunction gives a higher active surface to NdMO/RGO/GCE composite. The increase in electrode surface area of NdMO/RGO/GCE facilitates electrochemical detection.

3.2.3. Electrochemical response of NdMO/GCE/RGO toward detection

Initially, the electrocatalytic activity of NdMO/RGO/GCE towards ML detection was determined through CV analysis. Fig. 6A depicts the CV peak of bare GCE, NdMO/RGO, RGO/GCE, and NdMO/RGO/GCE in 0.1 M PBS presence of 100 μM of ML. From Fig. 6A it was found that a redox peak was obtained which indicates the electrochemical current response for the detection of ML. Accordingly, bare GCE showed a low peak current due to its poor electron mobility at bare GCE. Interestingly, NdMO/RGO/GCE shows an enhanced redox peak current with a shift in potential than the other modified electrodes which confirms the synergistic interaction of RGO and NdMO heterojunction which enhances the electrocatalytic activity of NdMO/RGO/GCE. Fig. 6B depicts a bar graph of different modified electrodes to their current response. In electrochemical measurements, pH of the supporting electrolyte plays a crucial role. The experiment was conducted in a range of pH (3 – 11) in the presence of 100 μM of ML at a fixed scan rate of 50 mVs^{-1} to assess the pH influence of the 0.1 M PBS. The pH optimization of NdMO/RGO/GCE was depicted in Fig. 6C.The acidic medium typically raises the peak potential towards more positive potential due to maximum proton transformation, whereas less proton transformation shifts the peak potential towards more negative potential. From pH 3 the peak current gets enhanced but a higher peak current was obtained for pH 7 and beyond pH 7 the peak current was decreased. Thus, the overall pH study shows that pH 7 is most suitable for electrochemical detection. Fig. 6D depicts the corresponding plot for pH against the current response. Scheme 2 represents the electrochemical redox mechanism of ML in which first the ML was oxidized with a loss of two electron and two protons forms 4-(methylamino)cyclohexane-2.5-dien-1-one sulfate then it gained with 2 electron and a 2 proton to form ML.

3.2.4. Effect of different concentrations and different scan rates

The electrochemical response of NdMO/RGO/GCE was investigated at various concentrations of ML from 20 μM – 100 μM at a fixed scan rate of 50 mVs^{-1}. Fig. 7A depicts the current response of NdMO/RGO/GCE at different concentrations. Thus, the findings demonstrate that as the ML

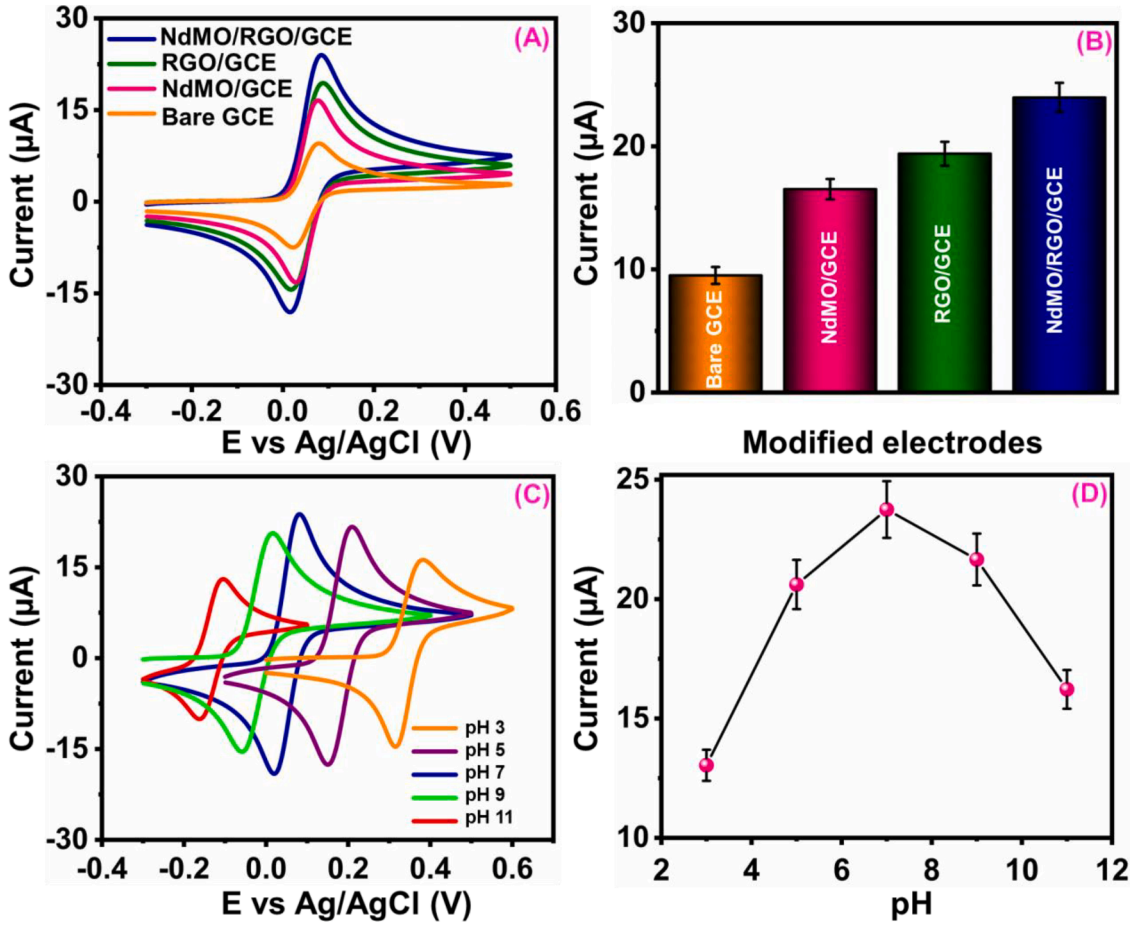

Fig. 6. (A) CV curves of modified electrodes, (B) corresponding bar diagram for different modified electrodes against current response, (C) CV response of different pH from 3 –11, and (D) corresponding calibration plot for various pH against current response.

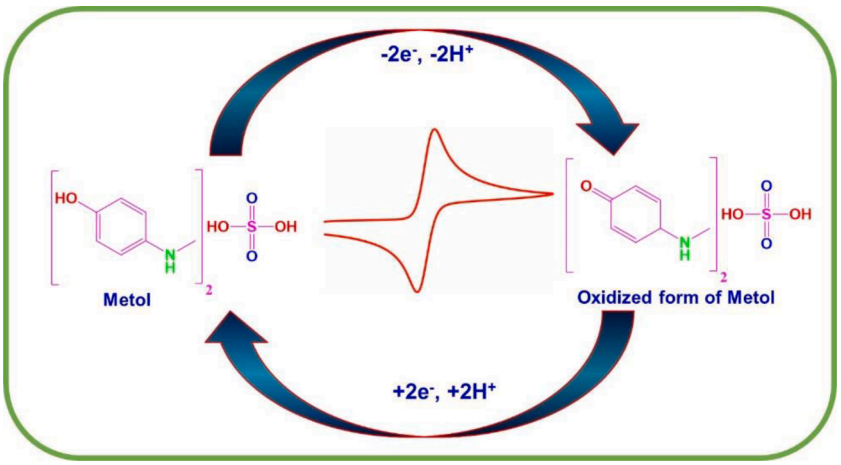

Scheme 2. Electrochemical redox mechanism of ML.

concentration increases the peak current gets increases simultaneously. Fig. 7B shows the strong linear relationship between the concentration of ML and peak current with a linear regression equation $I_{pa}(\mu A)$ = 0.1243(μM) + 8.272, R^2 = 0.9971, $I_{pc}(\mu A)$ = −0.1359(μM) - 4.643, R^2 = 0.9941 respectively. This result exhibits excellent electrocatalytic activity of NdMO/RGO/GCE towards the detection of ML. The dynamic behavior of redox on NdMO/RGO/GCE was scrutinized by varying scan rates from 20 mVs^{-1} – 200 mVs^{-1}. Fig. 7C displays an increase in scan rate increases the redox current response of ML increases. Fig. 7D displays the linearity of the calibration plot of the I_{pa} and I_{pc} against the $\upsilon^{1/2}$ and the equation could be described as $I_{pa}(\mu A)$= 108.74 $\upsilon^{1/2}(Vs^{-1})$ + 17.705, R^2 = 0.9944, $I_{pc}(\mu A)$ = −76.904 $\upsilon^{1/2}(Vs^{-1})$- 17.129, R^2 = 0.9962 respectively.

3.3. Quantitative detection of ML using NdMo/RGO/GCE

Differential pulse voltammetry (DPV) analysis was used to estimate the proposed NdMO/RGO/GCE sensor's analytical performance for the

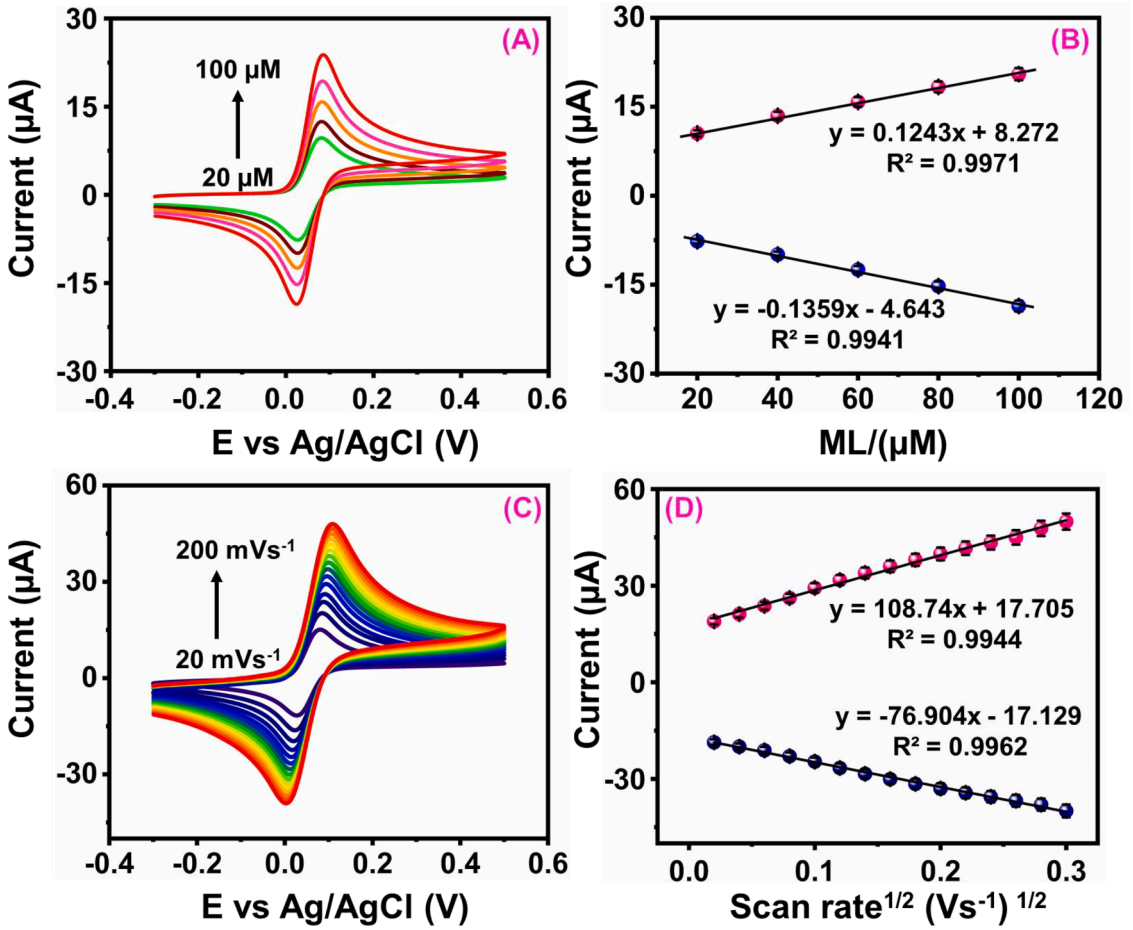

Fig. 7. (A) CV response of NdMO/RGO/GCE at increasing concentrations, (B) corresponding linear plot for increasing concentration against its current response, (C) CV response of NdMO/RGO/GCE at various scan rates, and (D) corresponding linear plot for the square root of scan rate against its current response.

detection of ML. Fig. 8**A** depicts the DPV response of modified GCE with the increase in the concentration range from 0.01 μM – 60, 70 – 1770 μM of ML in 0.1 M PBS at a fixed scan rate of 50 mVs^{-1}. The DPV results show that the ML is oxidized too well and a sharp oxidation peak is distinguished. As the concentration of ML increases the peak current gets increases showing a good linear relationship displayed in Fig. 8**B** with a regression equation $I_{pa} = 0.1089$ μM + 0.3828, $R^2 = 0.9986$, and I_{pa}= 0.0301 μM + 6.9945, $R^2 = 0.9977$ respectively. By using the slope from the equation, the LOD of NdMO/RGO were found to be **0.005** μm using the formula LOD =3 s/q[41] where "S" denotes the standard deviation of three blank signals and "q" denotes the slope value of the calibration plot, and sensitivity of **1.5873** μA μM^{-1} cm^{-2} respectively. The obtained results were compared with the previously reported literature shown in **Table.S2**. Selectivity of the specified analyte was determined in the presence of some other interfering compounds as depicted in Fig. 8C. It was conducted in the presence of 100 μM of ML with interfering reagents such as ascorbic acid (AA), glucose (GLU), urea (UA), catechol (CT), K^+, Na^+, and Fe^{3+} which does not affect the oxidation peak current of ML. This demonstrates the NdMO/RGO/GCE's anti-interfering ability to identify ML in the presence of some interfering substances. A corresponding bar diagram of the current response of the interfering species was displayed in Fig. 8D. To investigate the stability of the NdMO/RGO/GCE, the DPV response was examined in 0.1 M PBS at 100 μM of ML depicted in **Fig.S2**(A). The experiment was prolonged for about 15 days showing a stable current response demonstrating the excellent stability of the proposed sensor for the detection of ML. The reproducibility test was performed by DPV analysis depicted in **Fig.S2**(B). Hence, no significant variation in ML response on repetitive measurements was noticed. Hence these results demonstrate that the prepared NdMO/RGO credits have better stability and reproducibility.

3.4. Real sample analysis

To understand the practicability of the proposed ML sensor based on NdMO/RGO/GCE, the electrochemical experiments were performed in tap water and river water using the standard addition method. The real sample preparation was explained in SI. Moreover, a known concentration of ML (5, 10, 15 μM) was spiked into the water sample. The recovery results were shown in **Table. S**3, the recoveries were within the range of 99.6 – 99.0%. These results confirm that the proposed sensor was accurate and sensitive toward the detection of ML in a real sample and it was employed for the further detection of ML.

4. Conclusion

In summary, the rare-earth molybdate was effectively synthesized by a co-precipitation method. Various techniques were used to characterize the NdMO/RGO composite. NdMO/RGO was used for the effective, sensitive, and selective detection of carcinogenic contaminant ML. Even in the presence of other interfering agents NdMO/RGO demonstrates remarkable electrocatalytic activity. The NdMO/RGO shows prominent catalytic activity ascribed to the high surface area, optimum electronic property, and high electron transfer rates due to the synergetic effect between the NdMO and RGO. The proposed sensor exhibits a wide linear range, low LOD, appreciable sensitivity, and stability. Finally, this

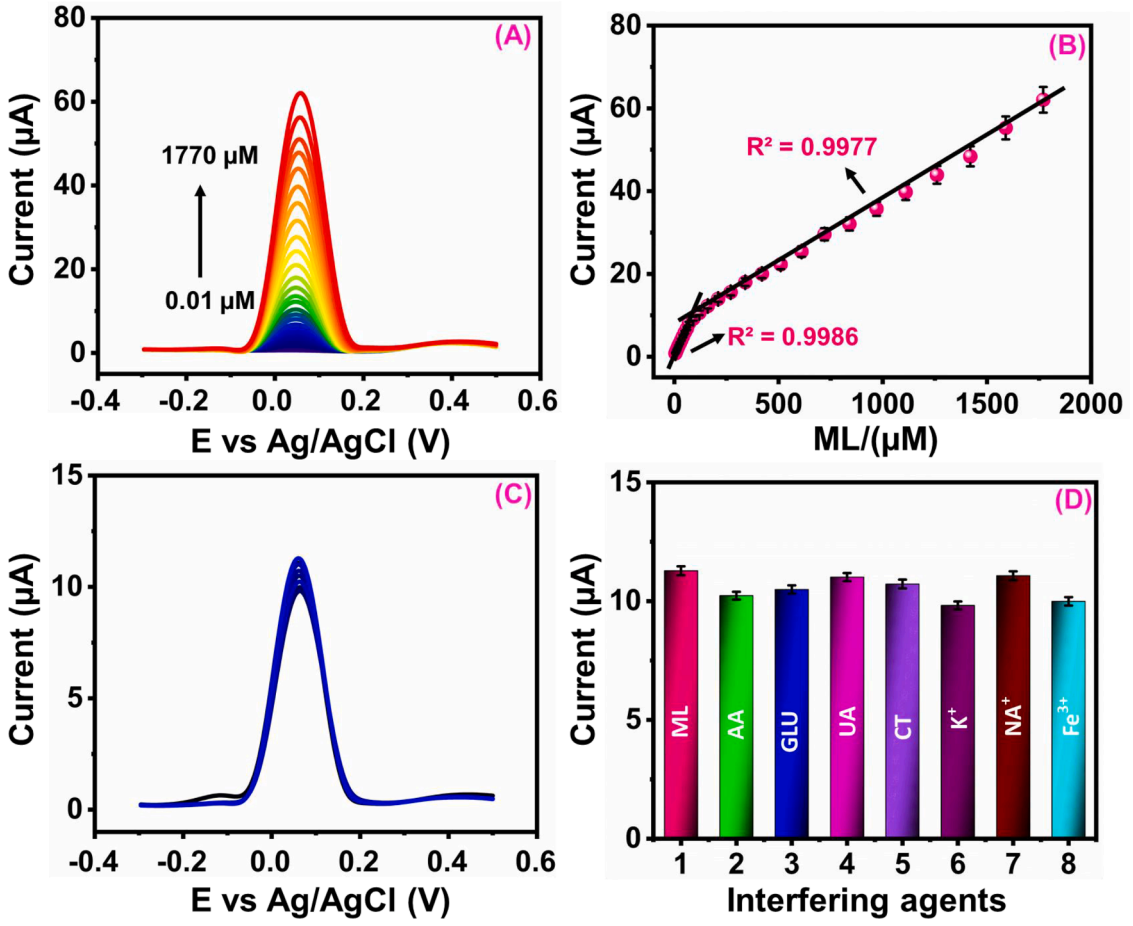

Fig. 8. (A) DPV at NdMO/RGO/GCE with various concentration levels of ML from 0.01 – 1770 μM, (B) calibration linear plot of concentration against oxidation current response, (C) DPV response with 10-fold concentrations of various interfering reagents, and (D) corresponding bar diagram of various interfering reagents against current response.

proposed sensor was applied to tap and river water which shows excellent recovery results. As a result, the suggested sensor has the potential to be used in environmental applications and future research on electrochemical sensors. The development of carbon-based molybdate with electrochemical sensor applications is discussed in this paper in a novel way.

Funding

The authors are grateful for the financial support from the Ministry of Science and Technology (MOST), Taiwan, Project no. MOST 111–2113-M-027–002.

CRediT authorship contribution statement

Santhiyagu Sahayaraj Rex Shanlee: Conceptualization, Methodology, Investigation, Writing – original draft, Visualization. **Ruspika Sundaresan:** Conceptualization, Supervision, Methodology, Investigation, Writing – original draft, Writing – review & editing, Visualization. **Shen-Ming Chen:** Conceptualization, Validation, Supervision, Project administration, Funding acquisition. **Ramachandran Balaji:** Conceptualization, Writing – original draft, Visualization. **Tharini Jeyapragasam:** Writing – original draft. **Jing- Yi Peng:** Writing – original draft. **A. Irudaya Jothi:** .

Declaration of Competing Interest

The authors declare that they have no known competing financial interests or personal relationships that could have appeared to influence the work reported in this paper.

Supplementary materials

Supplementary material associated with this article can be found, in the online version, at doi:10.1016/j.surfin.2023.103020.

References

[1] S. Samanta, R. Srivastava, CuCo2O4 based economical electrochemical sensor for the nanomolar detection of hydrazine and metol, J. Electroanal. Chem. 777 (2016) 48–57.
[2] W. Sun, Q. Jiang, K. Jiao, Electrochemical behaviors of metol on ionic-liquid-modified carbon paste electrode and its analytical application, J. Solid State Electrochem. 13 (8) (2009) 1193–1199.
[3] L. Lunar, D. Sicilia, S. Rubio, D. Pérez-Bendito, U. Nickel, Degradation of photographic developers by Fenton's reagent: condition optimization and kinetics for metol oxidation, Water Res. 34 (6) (2000) 1791–1802.
[4] L. Lunar, D. Sicilia, S. Rubio, D. Pérez-Bendito, U. Nickel, Identification of metol degradation products under Fenton's reagent treatment using liquid chromatography-mass spectrometry, Water Res. 34 (13) (2000) 3400–3412.
[5] W. Sun, Y. Deng, J. Liu, et al., Electrochemical behavior and voltammetric determination of p-methylaminophenol sulfate using LiCoO2 nanosphere modified electrode, Thin Solid Films 564 (2014) 379–383.
[6] T.A. Ternes, Analytical methods for the determination of pharmaceuticals in aqueous environmental samples, TrAC Trends Anal. Chem. 20 (8) (2001) 419–434.
[7] H.A. Medien, S.M. Khalil, Kinetics of the oxidative decolorization of some organic dyes utilizing Fenton-like reaction in water, J. King Saud Univ. Sci. 22 (3) (2010) 147–153.
[8] T. McCarthy, B. Brodie, J. Milner, R. Bevill, Improved method for selenium determination in biological samples by gas chromatography, J. Chromatogr. B Biomed. Sci. Appl. 225 (1) (1981) 9–16.
[9] F. Hernandez, J. Sancho, O. Pozo, Critical review of the application of liquid chromatography/mass spectrometry to the determination of pesticide residues in biological samples, Anal. Bioanal. Chem. 382 (2005) 934–946.
[10] S. Kumar, A. Awasthi, M.D. Sharma, K. Singh, D. Singh, Functionalized multiwall carbon nanotube-molybdenum disulphide nanocomposite based electrochemical ultrasensitive detection of neurotransmitter epinephrine, Mater. Chem. Phys. 290 (2022), 126656.
[11] O. Özbek, C. Berkel, Ö. Isildak, Applications of potentiometric sensors for the determination of drug molecules in biological samples, Crit. Rev. Anal. Chem. 52 (4) (2022) 768–779.
[12] T. Thomas, R.J. Mascarenhas, O.J. D'Souza, P. Martis, J. Dalhalle, B.K. Swamy, Multi-walled carbon nanotube modified carbon paste electrode as a sensor for the amperometric detection of L-tryptophan in biological samples, J. Colloid Interface Sci. 402 (2013) 223–229.
[13] R.R. Krishna, C. Sastry, Spectrophotometric determination of p-methylaminophenol sulphate (metol), Fresenius' Z. anal. Chem. 296 (1) (1979) 46. -46.
[14] R. Andreozzi, V. Caprio, A. Insola, R. Marotta, The oxidation of metol (N-methyl-p-aminophenol) in aqueous solution by UV/H2O2 photolysis, Water Res. 34 (2) (2000) 463–472.
[15] Z. Chen, W. Bu, N. Zhang, J. Shi, Controlled construction of monodisperse La2 (MoO4) 3: yb, Tm microarchitectures with upconversion luminescent property, J. Phys. Chem. C 112 (11) (2008) 4378–4383.
[16] B. Ponomarev, A. Zhukov, Magnetic and magnetoelectric properties of rare earth molybdates, Phys. Res. Int. 2012 (2012).
[17] P. Gall, N. Barrier, R. Gautier, GP. Synthesis, Structural trends, and physical and electronic properties of the reduced molybdenum oxides R4Mo4O11 (R= Nd– Tm and Y) containing infinite chains of trans-edge-shared octahedral clusters, Inorg. Chem. 41 (11) (2002) 2879–2885.
[18] T. Kokulnathan, E.A. Kumar, T.J. Wang, Synthesis of two-dimensional nanosheet like samarium molybdate with abundant active sites: real-time carbendazimin analysis in environmental samples, Microchem. J. 158 (2020), 105227.
[19] P. Sharma, M. Minakshi Sundaram, D. Singh, R. Ahuja, Highly energetic and stable gadolinium/bismuth molybdate with a fast reactive species, redox mechanism of aqueous electrolyte, ACS Appl. Energy Mater. 3 (12) (2020) 12385–12399.
[20] H. Safardoust-Hojaghan, Rare-earth molybdates ceramic nanomaterials. Advanced Rare Earth-Based Ceramic Nanomaterials, Elsevier, 2022, pp. 259–290.
[21] Brixner, L., Barkley, J., Jeitschko, W. Rare earth molybdates (VI). Handbook on the physics and chemistry of rare earths. 1979;3:609–654.
[22] M. Ganesan, R.K. Devi, A.H. Liao, K.Y. Lee, G. Gopalakrishnan, H.C. Chuang, 3D-flower-like porous neodymium molybdate nanostructure for trace level detection of organophosphorus pesticide in food samples, Food Chem. 396 (2022), 133722.
[23] T.W. Chen, J.V. Kumar, S.M. Chen, et al., Rational construction of novel rose petals-like yttrium molybdate nanosheets: a Janus catalyst for the detection and degradation of cardioselective β-blocker agent acebutolol, Chem. Eng. J. 359 (2019) 1472–1485.
[24] R. Karthik, J.V. Kumar, S.M. Chen, T. Kokulnathan, H.Y. Yang, V. Muthuraj, Design of novel ytterbium molybdate nanoflakes anchored carbon nanofibers: challenging sustainable catalyst for the detection and degradation of assassination weapon (Paraoxon-Ethyl), ACS Sustain. Chem. Eng. 6 (7) (2018) 8615–8630.
[25] J. Zhu, D. Zhou, S. Guo, et al., Grain boundary conductivity of high purity neodymium-doped ceria nanosystem with and without the doping of molybdenum oxide, J. Power Sources 174 (1) (2007) 114–123.
[26] H. Li, W. Li, F. Wang, X. Liu, C. Ren, Fabrication of two lanthanides co-doped Bi2MoO6 photocatalyst: selection, design and mechanism of Ln1/Ln2 redox couple for enhancing photocatalytic activity, Appl. Catal. B 217 (2017) 378–387.
[27] J.V. Kumar, R. Karthik, S.M. Chen, et al., Design of novel 3D flower-like neodymium molybdate: an efficient and challenging catalyst for sensing and destroying pulmonary toxicity antibiotic drug nitrofurantoin, Chem. Eng. J. 346 (2018) 11–23.
[28] R. Karthik, J. Vinoth Kumar, S.M. Chen, C. Karuppiah, Y.H. Cheng, V. Muthuraj, A study of electrocatalytic and photocatalytic activity of cerium molybdate nanocubes decorated graphene oxide for the sensing and degradation of antibiotic drug chloramphenicol, ACS Appl. Mater. Interfaces 9 (7) (2017) 6547–6559.
[29] Y. Hu, W. Zhuang, H. Ye, D. Wang, S. Zhang, X. Huang, A novel red phosphor for white light emitting diodes, J. Alloy. Compd. 390 (1–2) (2005) 226–229.
[30] S. Stankovich, D.A. Dikin, G.H. Dommett, et al., Graphene-based composite materials, Nature 442 (7100) (2006) 282–286.
[31] V.C. Tung, L.M. Chen, M.J. Allen, et al., Low-temperature solution processing of graphene– carbon nanotube hybrid materials for high-performance transparent conductors, Nano Lett. 9 (5) (2009) 1949–1955.
[32] C. Xu, X. Wang, J. Zhu, Graphene– metal particle nanocomposites, J. Phys. Chem. C 112 (50) (2008) 19841–19845.
[33] R. Pasricha, S. Gupta, A.K. Srivastava, A facile and novel synthesis of Ag–graphene-based nanocomposites, Small 5 (20) (2009) 2253–2259.
[34] V. Singh, D. Joung, L. Zhai, S. Das, S.I. Khondaker, S. Seal, Graphene based materials: past, present and future, Prog. Mater Sci. 56 (8) (2011) 1178–1271.
[35] B. He, Y. Xu, J. Zhu, X. Zhang, Effects of the doping density of charge-transporting layers on regular and inverted perovskite solar cells: numerical simulations, Adv. Compos. Hybrid Mater. 4 (2021) 1146–1154.
[36] B. Muthukutty, A. Krishnapandi, S.M. Chen, M. Abinaya, A. Elangovan, Innovation of novel stone-like perovskite structured calcium stannate (CaSnO3): synthesis, characterization, and application headed for sensing photographic developing agent metol, ACS Sustain. Chem. Eng. 8 (11) (2020) 4419–4430.
[37] C. Koventhan, V. Vinothkumar, S.M. Chen, et al., Efficient hydrothermal synthesis of flake-like molybdenum disulfide for selective electrochemical detection of metol in water real samples, Int. J. Electrochem. Sci. 15 (2020) 7390–7406.
[38] X. Niu, L. Yan, Z. Wen, et al., Voltammetric determination of metol on a gold nanoparticle modified carbon molecular wire electrode, Anal. Lett. 50 (2) (2017) 325–335.
[39] B. Kaur, B. Satpati, R. Srivastava, ZrO 2 supported Nano-ZSM-5 nanocomposite material for the nanomolar electrochemical detection of metol and bisphenol A, RSC Adv. 6 (70) (2016) 65736–65746.
[40] S. Ramaraj, M. Sakthivel, S.M. Chen, K.C. Ho, Active-site-rich 1T-phase CoMoSe2 integrated graphene oxide nanocomposite as an efficient electrocatalyst for electrochemical sensor and energy storage applications, Anal. Chem. 91 (13) (2019) 8358–8365.

[41] R. Sundaresan, V. Mariyappan, T.W. Chen, et al., One-dimensional rare-earth tungstate nanostructure encapsulated reduced graphene oxide electrocatalyst-based electrochemical sensor for the detection of organophosphorus pesticide, J. Nanostruct. Chem. (2023) 1–14.
[42] A.P. Steffi, R. Balaji, N. Chandrasekar, et al., High-performance anti-corrosive coatings based on rGO-SiO2-TiO2 ternary heterojunction nanocomposites for superior protection for mild steel specimens, Diam Relat. Mater. 125 (2022), 108968.
[43] V. Renganathan, R. Balaji, S.M. Chen, V. Singh, The electrochemical determination of hazardous 4-hydroxynitrobenzene using NiS2 decorated graphene oxide nanocomposite in the river water sample, Microchem. J. 153 (2020), 104502.
[44] Y. Xie, F. Gao, X. Tu, et al., Flake-like neodymium molybdate wrapped with multi-walled carbon nanotubes as an effective electrode material for sensitive electrochemical detection of carbendazim, J. Electroanal. Chem. 855 (2019), 113468.
[45] R. Sundaresan, V. Mariyappan, S.M. Chen, S. Alagarsamy, M. Akilarasan, Fabrication of a new electrochemical sensor based on bimetal oxide for the detection of furazolidone in biological samples, Micromachines 13 (6) (2022) 876 (Basel).
[46] R. Sundaresan, V. Mariyappan, S.M. Chen, M. Keerthi, R. Ramachandran, Electrochemical sensor for detection of tryptophan in the milk sample based on MnWO4 nanoplates encapsulated RGO nanocomposite, Colloids Surf. A 625 (2021), 126889.
[47] S. Vinoth, S.F. Wang, Detection of the neurodegenerative drug in a biological sample using three-dimensional sphere mixed metal oxide tailored with carbon fiber as an electrocatalyst by voltammetry technique, J. Electrochem. Soc. 169 (9) (2022), 097511.
[48] R. Balaji, V. Renganathan, C.P. Chu, Y.C. Liao, C. Kao, S.M. Chen, Periodic Copper Microbead Array on Silver Layer for Dual Mode Detection of Glyphosate, OpenNano (2022), 100105.
[49] S. Vinoth, S.F. Wang, Modification of glassy carbon electrode with manganese cobalt oxide-cubic like structures incorporated graphitic carbon nitride sheets for the voltammetric determination of 2, 4, 6-trichlorophenol, Microchim. Acta 189 (5) (2022) 1–13.

Journal of Molecular Structure 1284 (2023) 135367

Contents lists available at ScienceDirect

Journal of Molecular Structure

journal homepage: www.elsevier.com/locate/molstr

Self-assembled crystals of nonplanar benzimidazole macrocycles: Synthesis, characterization, crystal structure, SEM, and DFT studies

A. Irudaya Jothi [a], P. V. Priyanka [b], V. Alexander [b,*]

[a] Department of Chemistry, St. Joseph's College, Tiruchirappalli 620002 (Affiliated to Bharathidasan University, Tiruchirappalli 620024), Tamil Nadu, India
[b] Department of Chemistry, Loyola College, Chennai 600034, Tamil Nadu, India

ARTICLE INFO

Article history:
Received 17 October 2022
Revised 8 March 2023
Accepted 16 March 2023
Available online 21 March 2023

Keywords:
Benzimidazole macrocycles
Self-assembly
π-π interactions
Nonplanarity
DFT studies

ABSTRACT

Self-assembly of macrocycles driven by non-covalent interactions such as π-π stacking and hydrogen bond is a prominent tool to design and construct supramolecular architectures of different shapes, geometries, and functions. Three structurally similar 11-, 12-, and 14-membered 1,2-fused benzimidazodioxaaza macrocycles are synthesized by the [1 + 1] Schiff base condensation of *ortho*-bridged dibenzaldehydes and 1,2-diaminobenzene. Nonplanarity of the macrocycles plays a key role in the self-assembly of the molecules forming cuboidal cage-like cavities in their crystal structures. 3-D networks of the free and chloroform-solvated macrocycles are stabilized by strong aromatic π-π and CH-π stacking interactions and hydrogen bonds originating from the electrophilic benzimidazole and chloroform units, respectively. The importance of nonplanarity in the formation of 3-D supramolecular motifs in crystals is rationalized from the quantum chemical modelling by the DFT studies and the SEM images of the macrocycles.

1. Introduction

Inherent stability of macrocyclic systems coupled with their well-defined geometry tends to simplify the design, synthesis, and construction of molecular assemblies using macrocycles as supramolecular building blocks [1–5]. In nature, vital biological systems such as heme proteins and vitamin B_{12} coenzyme constitute planar tetrapyrroles such as chlorins, corrins, and porphyrins as their macrocyclic core units [6–8]. Peripheral substitution onto the macrocyclic skeletons in their synthetic analogues introduce nonplanar distortions in the molecular systems [9].

Bis-benzimidazole macrocycles are intrinsically nonplanar in which the in-built benzimidazole moieties infuse nonplanarity [10–12]. Unusual crystal packing interactions directed by nonplanarity in such macrocyclic systems dictate the topology of their supramolecular architectures and the noncovalent interactions have profound effects on their coordination, biochemical, catalytic, and spectroscopic properties [9,13,14].

Electrophilic benzimidazoles promote supramolecular assemblies such as one-dimensional polymeric chains, two-dimensional ladder-like ribbons and channels, three-dimensional networks [15], polymorph aggregates [16], metal complex helicates [17], and coordination polymers [18]. Our interest stems out here to synthesize nonplanar dioxabenzimidazole macrocycles via Schiff base condensation and to study their self-assembling characteristics dictated the noncovalent interactions due to their twisted structure. The important role of Schiff base macrocycles in coordination and supramolecular chemistry, organic synthesis, as well as their biological and medical applications are the reason for their fascinating and highly expanding chemistry over the decades [19]. Schiff base directed macrocyclizations have been applied for the synthesis of macrocycles by optimizing various reaction conditions [3–5,11,19–23].

The synthesis of benzimidazole derivatives is also of great importance for their wide range of biological activities such as antimalarial [24,25], antifilarial [26], anti-parasitic [27], antibacterial [28–30], antifungal [31], antiviral [32], anti-tubercular [33], and anti-inflammatory activities [34–36]. Benzimidazole derivatives are synthesized from *o*-phenylenediamine and aldehydes and display interesting coordination and biological characteristics [37–53].

We report here, the synthesis of 11-, 12-, and 14-membered 1,2-fused benzimidazodioxaaza macrocycles (**5**–**7**) from 1,2-diaminobenzene (**1**) and *ortho*-bridged dibenzaldehydes (**3**–**5**) (also known as two-armed dibenzaldehydes) and the self-assembly of free and solvated crystal structures of these puckered macrocycles. The DFT studies reveal intrinsic nonplanarity of these macrocycles and the possible modes of noncovalent interactions.

* Corresponding author.

https://doi.org/10.1016/j.molstruc.2023.135367
0022-2860/

2. Experimental section

2.1. Reagents and solvents

Salicylaldehyde, 1,2-dibromoethane, 1,3-dibromopropane, and 1,2-diaminobenzene (Aldrich) were used as received for the synthesis of *ortho*-bridged dibenzaldehydes. Sodium borohydride and borax (Merck) and fused calcium chloride and anhydrous sodium sulfate (Merck, India) were used as received. Silica gel (Merck, 230–400 mesh) was used for column chromatography. Chloroform, dichloromethane, THF, DMF, ethyl alcohol, methyl alcohol, acetone, and petroleum ether were purified by the standard procedures [54].

2.2. Spectral studies

Infrared spectra were recorded on a Bruker Tensor II FT-IR spectrometer in the range 4000–400 cm^{-1}. The NMR spectra were recorded using JEOL GSX-400 and Bruker AVANCE III 500 MHz (AV 500) multinuclear NMR spectrometers for ^{1}H and ^{13}C NMR spectra at 298 K. Distortionless Enhancement by Polarization Transfer (DEPT) experiments were run with selection angle parameter of 135° The ESI-TOF mass spectra were run on a Micromass ToF Spec2*E* mass spectrometer. The electronic absorption spectra were recorded on an Agilent UV–Visible spectrophotometer controlled by the ChemStation software in the region 190-1100 nm in ethanol at 298 K using a matched pair of Teflon stoppered quartz cell of path length 1 cm. The emission spectra were recorded on a Fluorolog-3 FL3–221 spectrofluorometer with a 450 W CW Xenon lamp as the excitation source. The band pass for the excitation and double grating emission monochromator was set at 2 nm. The emission spectra of the macrocycles **5**–**7** were recorded in ethanol deaerated by purging argon at 298 K using a quartz cell of path length 10 mm.

2.3. X-ray diffraction

Single crystals suitable for X-ray diffraction were carefully selected under Leica DM LSP polarizing microscope and mounted on a thin glass fiber with cyanoacrylate adhesive. X-ray diffraction data were collected on a Bruker AXS kappa ApexII CCD diffractometer at 293(2) K equipped with graphite monochromatic Mo K_α radiation (λ = 0.71073 Å). The unit cell parameters were determined from 36 data frames collected at different sections of the Ewald sphere. The intensity data were gathered using ω and ϕ scan with a frame width of 0.50. The intensity data were corrected for Lorentz and polarization effects and the empirical absorption correction (multiscan procedure using SADABS) applied. The structures were solved by direct methods, completed with successive difference Fourier synthesis, and refined by full-matrix least square methods based on F^2 using the SHELXL-2014 software. The ORTEP32 in WinGX software package was used for the molecular graphics.

2.4. SEM analysis

The SEM images of the compounds **5**–**7** were obtained on Carel Zeiss EVO 18. The measurements of the particle dimensions were measured using imageJ software.

2.5. DFT studies

The Density Functional Theory (DFT) calculations were performed using Gaussian® 16 Rev A.03, Version x86–64 AVX2-enabled/Linux suite of software programs [55]. Optimized molecular geometries and molecular electrostatic potentials (MEP) map and electronic energy of FMOs are obtained using the hybrid functional B3LYP and 6–31 G(d,p) basis set [56,57].

2.6. General procedure for the preparation of macrocycles 5–7

The *ortho*-bridged dialdehydes 2,2'-[ethane-1,2-diylbis(oxy)] dibenzaldehyde (**2**), 2,2'-[propane-1,3-diylbis(oxy)]dibenzaldehyde (**3**), and 2,2'-[1,2-phenylenebis(methyleneoxy)]- dibenzaldehyde (**4**) were prepared by the *O*-alkylation of salicylaldehyde with dibromoalkanes according to the procedure reported by Armstrong and Lindoy [23]. The 1,2-fused benzimidazo dioxaaza macrocycles **5**–**7** were synthesized by the condensation of the *ortho*-bridged dialdehydes **2–4** with 1,2-diamino-benzene (**1**). A solution of 1,2-diaminobenzene (2.16 g, 20 mmol) in 50 mL absolute ethanol was added to a hot solution of **2** (5.40 g, 20 mmol), **3** (5.68 g, 20 mmol), or **4** (6.92 g, 20 mmol) (for **5, 6**, or **7**, respectively) in 100 mL absolute ethanol, refluxed for 4 h, and cooled to room temperature. The reaction mixture was extracted with 3 × 100 mL portions of chloroform. The organic layer was dried over anhydrous sodium sulfate, filtered, and the volume of the solution reduced to 20 mL in a rotavapor. The concentrated solution was added in drops to hot hexane under stirring whereupon a white powder separated out. The compound was filtered, washed with hot hexane, and dried. Crystals of **5–7** suitable for single crystal X-ray diffraction were obtained by the slow evaporation of their solutions in ethanol (**5** and **7**) and chloroform:hexane, (1:1, v/v) (**5** and **6**) at room temperature.

2.7. 7,19-Dihydro-6H-*dibenzo*[e,j]*benzo[4,5]imidazo[2,1-g][1,4,8]dioxaazacycloundecine (5)*

Yield 85%. ν/cm^{-1} (KBr): 3032 ν_s(C–H)$_{aro}$, 751 δ(C–H)$_{aro}$, 3061 ν_{as}(C–H)$_{ali}$, 2924 ν_s(C–H)$_{ali}$, 1595, 1492 and 1450 ν_s(C=C) and ν_s(C=N), 1282 ν_s(C–N), 1239 ν_{as}(C–O–C), 935 ω(CH_2), 862 τ(CH_2), 834 ρ(CH_2). δ_H/ppm (500 MHz, $CDCl_3$, 298 K): 3.80 (2H, s, $^{a}CH_2$), 4.46 (2H, s, $^{b}CH_2$), 5.25 (2H, s, Ph-$^{c}CH_2$-Bz), 6.70 (1H, d, Ar-H_d), 6.99 (1H, t, Ar-H_e), 7.09–7.25 (5H, m, Ar-H_{f-h}), 7.30–7.77 (4H, m, Ar-H_{i-l}). δ_C/ppm (125 MHz, $CDCl_3$, 298 K): 46.46, 69.34, 73.42, 110.92 (2C), 114.80 (2C), 120.00, 120.87, 121.39 (2C), 121.48, 122.14, 122.46, 124.37, 125.01, 131.22, 131.47, 131.56, 124.37, 125.01, 134.59, 143.38, 151.99, 157.23, 161.16. ESI-TOF MS (*m/z*): 343.18 $[M + H]^+$, 237.15.

2.8. 6,7,8,20-Tetrahydro-dibenzo[f,k]*benzo[4,5]imidazo[2,1-h][1,5,9]dioxaazacyclododecine (6)*

Yield 72%. ν/cm^{-1} (KBr): 3050 ν_s(C–H)$_{aro}$, 742 δ(C–H)$_{aro}$, 3019 ν_{as}(C–H)$_{ali}$, 2979 ν_s(C–H)$_{ali}$, 1603, 1587 and 1492 ν_s(C=C) and ν_s(C=N), 1384 ν_s(C–N), 1245 ν_{as}(C–O–C), 937 ω(CH_2), 854 τ(CH_2), 825 ρ(CH_2). δ_H/ppm (500 MHz, $CDCl_3$, 298 K): 2.75 (2H, m, $^{a}CH_2$), 3.9 (2H, t, $^{b}CH_2$), 4.5 (2H, t, $^{c}CH_2$), 5.1 (2H, s, Ph-$^{d}CH_2$-Bz), 6.8–7.8 (aromatic protons). δ_C/ppm (125 MHz, $CDCl_3$, 298 K): 26.83, 67.06, 68.07, 47.56, 111.4, 111.6, 112.9, 119.8, 120.1, 120.2, 121.4, 121.6, 121.9, 122.9, 130.3, 130.9, 131.6, 132.4, 135.1, 143.5, 152.2, 156.6, 158.0. ESI-TOF MS (*m/z*): 357.13, $[M + H]^+$, 358.13 $[M + 2]^+$.

2.9. 11,23-Dihydro-6H-*tribenzo*[b,g,k]*benzo[4,5]imidazo[2,1-d][1,9,5]dioxaazacyclotridecine (7)*

Yield 80%. ν/cm^{-1} (KBr): 3062 ν_s(C–H)$_{aro}$, 748 δ(C–H)$_{aro}$, 3040 ν_{as}(C–H)$_{ali}$, 2971 ν_s(C–H)$_{ali}$, 1602 and 1522 ν_s(C=C), 1454 ν_s(C=N), 1255 ν_s(C–N), 1223 ν_{as}(C–O–C), 932 ω(CH_2), 854 τ(CH_2), 788 ρ(CH_2). δ_H/ppm (500 MHz, $CDCl_3$, 298 K): 3.9 (2H, s, $^{a}CH_2$), 4.1 (2H, s, $^{b}CH_2$), 5.3 (2H, s, Ph-$^{c}CH_2$-Bz), 6.9–7.9 (aromatic protons). δ_C/ppm (125 MHz, $CDCl_3$, 298 K): 69.14, 69.21, 47.42, 111.05, 113.54 (2C), 113.81, 119.71, 120.61, 121.26, 121.56, 121.97, 124.36, 128.59, 128.98, 129.87, 130.98, 131.20, 131.62, 132.28, 135.08, 135.83,

136.40, 143.40, 156.49, 157.85. ESI-TOF MS (*m/z*): 419.17 $[M + H]^+$, 313.13 $[M\text{-}(C_{21}H_{17}O)]^+$.

3. Results and discussion

3.1. Synthesis of 11-, 12-, and 14-membered 1,2-fused benzimidazo dioxaaza macrocycles (5–7)

The condensation of 1,2-diaminobenzene (**1**) with the *ortho*-bridged dibenzaldehydes, 2,2'-[ethane-1,2-diylbis(oxy)] dibenzaldehyde (**2**), 2,2'-[propane-1,3-diylbis(oxy)]dibenzaldehyde (**3**), or 2,2'-[1,2-phenylenebis(methylenoxy)]dibenzaldehyde (**4**) in absolute ethanol under reflux gives the ring contracted 1,2-fused benzimidazo dioxaaza macrocycles **5, 6**, and **7** respectively (Chart 1). Higher thermodynamic stability of these ring contracted 1,2-fused benzimidazo macrocycles favors their formation [21,23,52,53].

The mechanism of formation of 1,2-fused dioxaaza benzimidazo macrocycles **5, 6**, and **7** via the Schiff bases **5a, 6a**, and **7a** is illustrated in Scheme 1 [21]. The condensation involving both amino- and aldehyde groups forms the macrocycles **5a, 6a**, and **7a** (Step 1). The Schiff base macrocycles **5a, 6a**, and **7a** undergo intramolecular self-redox process to yield the 1,2-fused benzimidazo dioxaaza macrocycles **5**–**7** (Step 2).

3.2. Spectral characterization of 5–7

The macrocycles **5**–**7** are characterized by ^{1}H and ^{13}C NMR spectroscopy and electron spray ionization-Time of Flight (ESI-ToF) mass spectrometry and their spectra are given in Fig. S1-S9.

3.2.1. ^{1}H NMR spectrum of 5

The ^{1}H NMR spectrum of **5** in $CDCl_3$ displays resonances at 5.2, 4.5, and 3.8 ppm due to the H_c, H_b, and H_a methylene protons, respectively. The doublet at 6.7 ppm and the triplet at 7.0 ppm are assignable to the H_d and H_e protons, respectively. The seven resonances in the region 7.1–7.8 ppm are assignable to the H_f-H_l aromatic protons. The ^{1}H NMR spectrum of **5** is shown in Fig. S1.

3.2.2. ^{13}C and DEPT-135 NMR spectra of 5

The ^{13}C NMR spectrum of **5** in $CDCl_3$ displays resonances at 73.4, 69.3, and 46.6 ppm assignable to the C_3, C_2, and C_1 methylene carbons, respectively. The resonances at 110.9, 114.1, 119.9, 120.9, 121.4, 121.6, 122.1, 122.4 129.9, 131.2, 131.5, 131.6 ppm are assignable to the C_4 - C_{11} and C_{14} - C_{17} aromatic carbons, respectively. The resonances at 124.3, 125.0, 157.2, and 161.1 ppm are attributed to the C_{12}, C_{13}, C_{21}, and C_{22} aromatic quaternary carbons, respectively, of the linker. The signals at 134.5, 143.4, and 151.9 ppm are assignable to the C_{18}, C_{19}, and C_{20} aromatic quaternary carbons of the benzimidazole ring. The DEPT-135 NMR spectrum of **5** shows twelve resonances (up) due to the C_4 - C_{11} and C_{14} - C_{17} aromatic carbons and three resonances (down) due to the C_1 - C_3 methylene carbons. The ^{13}C and DEPT-135 and spectra are given in Fig. S2 and S3, respectively.

3.2.3. ESI-TOF mass spectrum of 5

The ESI-TOF mass spectrum of **5** shows a peak at *m/z* 343 corresponding to the molecular ion $[M + H]^+$ $(C_{22}H_{19}N_2O_2)^+$. A peak at *m/z* 237 corresponds to the species $[M\text{-}(C_7H_5O)]^+$ $(C_{15}H_{13}N_2O)^+$ formed by the loss of a $C_6H_4OCH_2$ group from the molecular ion. The ESI-TOF mass spectrum of **5** is shown in Fig. S4.

3.2.4. ^{1}H NMR spectrum of 6

The ^{1}H NMR spectrum of **6** in $CDCl_3$ displays resonances at 2.7, 3.9, 4.4, and 5.1 ppm assignable to the H_a, H_b, H_c, and H_d methylene protons, respectively. The nine resonances in the region 6.8–7.8 ppm are due to the six types of phenylene and three types of the benzimidazole protons. The ^{1}H NMR spectrum of **6** is shown in Fig. S5.

3.2.5. ^{13}C NMR spectrum of 6

The ^{13}C NMR spectrum of **6** in $CDCl_3$ displays resonances at 68, 67, 48, and 27 ppm assignable to the C_4, C_3, C_2, and C_1 methylene carbons, respectively. The nineteen resonances in the region 111-158 ppm correspond to the seven quaternary and twelve *C*H aromatic carbons. The ^{13}C NMR spectrum of **6** is shown in Fig. S5.

3.2.6. ESI-TOF mass spectrum of 6

The ESI-TOF mass spectrum of **6** shows peaks at *m/z* 357 and 358 corresponding to the species $[M + H]^+$ $(C_{23}H_{21}N_2O_2)^+$ and $[M + 2H]^+$ $(C_{23}H_{22}N_2O_2)^+$ formed by the addition of one and two protons, respectively, to the molecular ion (Fig. S6).

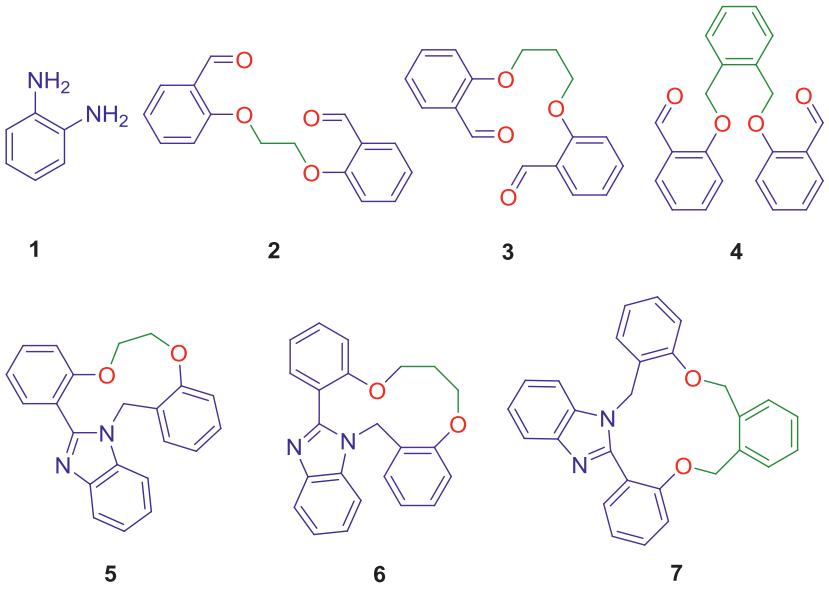

Chart 1. 1,2-Diaminobenzene (**1**), *ortho*-bridged dibenzaldehydes **2–4**, and the ring contracted 1,2-fused dioxaaza benzimidazo macrocycles **5–7**.

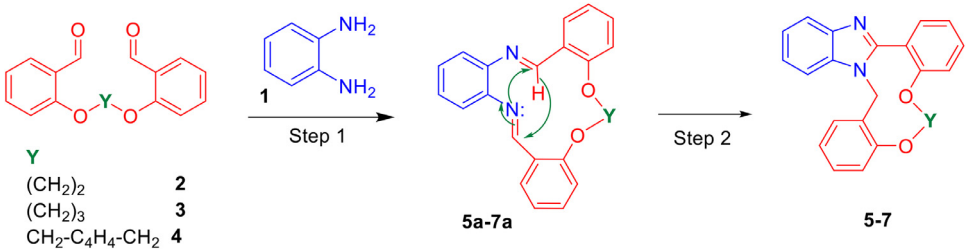

Scheme 1. Synthesis of twisted macrocycles **5**–**7** from dibenzaldehydes **2**–**4** and 1,2-diaminobenzene (**1**) via the Schiff base macrocycles **5a**-**7a** by intramolecular self-redox process.

3.2.7. ^{1}H NMR spectrum of 7

The ^{1}H NMR spectrum of **7** in $CDCl_3$ shown in Fig. S7 displays resonances at 5.3, 4.1, and 3.9 ppm due to the H_c. H_b, and H_c methylene protons, respectively. The resonances in the region 6.9–8.0 ppm correspond to the aromatic protons.

3.2.8. ^{13}C and DEPT-135 spectra of 7

The ^{13}C NMR spectrum of **7** in $CDCl_3$ displays resonances at 69.1, 69.2, and 47.4 ppm assignable to the C_3, C_2, and C_1 methylene carbons, respectively. The resonances in the region 111-157 ppm are assignable to the aromatic carbons. The DEPT-135 NMR spectrum of **7** shows three resonances (up) assignable to the C_1 - C_3 methylene carbons and twelve resonances assignable to the aromatic carbons. The ^{13}C and DEPT-135 NMR spectra of **7** in $CDCl_3$ are presented in Fig. S8.

3.2.9. ESI-TOF mass spectrum of 7

The ESI-TOF mass spectrum of **7** shows a peak at *m/z* 419 corresponding to the molecular ion $[M + H]^+$ $(C_{28}H_{23}N_2O_2)^+$. The peak at *m/z* 313 is assignable to the species $[M\text{-}(C_7H_6O)]^+$ $(C_{21}H_{17}O)^+$ formed by the loss of a $C_6CH_4OCH_2$ group from the molecular ion. The ESI-TOF mass spectrum of **7** is shown in Fig. S9.

3.3. Crystal structures

Crystals suitable for XRD studies are obtained by slow evaporation method. The compounds **5** and **7** crystallize as free macrocycle from their solutions in ethanol, whereas **5** and **6** crystallize as the chloroform solvates from the chloroform-hexane (1:10 v/v) solutions. Besides aromatic π-stacking interactions, intermolecular hydrogen bonding by the polar chloroform molecules in the solvates of **5** and **6** increases their unit cell densities (1.399 and 1.381 mgm^{-3}, respectively). ORTEP and packing diagrams of **5**–**7** are shown in Fig. 1 and 2. The crystallographic data and the structure refinement parameters of the ring contracted 1,2-fused benzimidazo dioxaaza macrocycles **5**–**7** are given in Table S1.

3.4. Crystal structures of free macrocycle 5

The macrocycle **5** crystallizes in the monoclinic system with the space group $P2_1/n$ with four molecules in a unit cell ($z = 4$). The molecules of **5** self-assemble into a one-dimensional infinite chain by head-to-tail arrangement (Fig. 3a) interconnected by intermolecular aromatic CH···π stacking interactions (C10···H1, 2.862 Å) between phenyl rings of benzimidazole and strong CH···π interactions (C16···H2, 2.738 Å and C21···H2, 2.869 Å) between phenyl and benzimidazole units of neighboring macrocycles (Fig. 3b). Two macrocyclic units of adjacent complementary chains make the cuboidal cage-like structures as shown in Fig. 3c (pink and orange; gray and green), wherein the planar benzimidazole units project outside at opposite corners in each cuboidal motif. Van der Waals interactions (H15B···H15B, 2.119 Å) between the methylene protons of the ether linkers in the complementary pairs lie exactly at the middle of the cuboids stabilizing the self-assembly (Fig. 3d). The cuboidal motifs of **5** in 4-fold axis are shown in Fig. 4a. The structural dimension of each cuboidal unit of **5** is described by the distances between the centroids of macrocyclic rings (7.501, 8.806, 5.454, and 15.426 Å, Fig. 4b), benzimidazoles (6.358, 10.612, 7.610, and 17.522 Å, Fig. 4c), and phenyl rings (8.545, 9.905, 10.810, and 14.985 Å, Fig. 4d).

3.5. Crystal structure of chloroform-solvate of 5 (5·$CHCl_3$)

The chloroform-solvate of the macrocycle **5** crystallizes in the triclinic system with the space group *P*-1 with four solvated molecules in a unit cell ($z = 4$). Two solvated macrocycles of a unit cell form half of a triclinic cubic lattice (Fig. 5a), while the other two molecules complement and complete the cuboidal cage (Fig. 5b). The 3-D cylindrical networks formed by the self-assembly with chloroform molecules at alternate corners of each cubical unit (Fig. 5c and 5d).

Hydrogen bonding by the polar chloroform molecules interlinks each macrocycle in the cuboidal cage-like structures. The 3-D cylindrical network is further stabilized by aromatic off-set π-stacking, and van der Waals interactions exerted by chloroform, benzimidazole and phenyl rings, and ether linkers as shown in Fig. 6a-b. Each chloroform molecule in a unit cell exerts four non-covalent interactions (Fig. 6b): (1) with the macrocycle to which it is solvated (N1···H45, 2.392 Å); (2) with the chloroform of the neighboring molecule (Cl2···Cl4, 3.452 Å) in the same cubic unit; (3) with a macrocycle in the neighboring unit cell (Cl1···C41, 3.422 Å); and (4) with a chloroform unit in between the cylindrical networks (Cl3···Cl6, 3.212 Å).

Strong CH···Cl interactions (H22A···Cl4, 2.623 Å) between the methylene protons of the ether linkers and chlorine of the chloroform units significantly contribute to the stability of the supramolecular architecture of **5·$CHCl_3$**. Benzimidazo moieties in the chloroform-solvate of **5** are interconnected by CH···π (aromatic) stacking interactions (C5···H37A, 2.890 Å; C27···H21A, 2.770 Å; and C28···H21A, 2.842 Å), H-bonds originating from the benzimidazole units and methylene protons of the ether linkers (N1···H36A, 2.716 Å), and van der Waals interactions between the methylene protons of the ether linkers of the complementary pairs of macrocycles (H21B···H37B, 2.389 Å). Two half units of the cubic units are connected by a pair of strong off-set CH···π interactions (H25···C11, 2.868 Å) between the benzimidazole and phenyl rings and a pair of strong CH···O bonds (H26···O2, 2.700 Å) between benzimidazole and oxygen of the ether linkers of neighboring units. The distance between centroids of two adjacent puckered macrocyclic rings (5.267, 8.948, 7.896, and 12.380 Å, Fig. 7a) and that of chloroform molecules (6.548, 13.120, 12.238, and 16.740 Å, Fig. 7b), and that the distance between the phenyl rings (8.289, 11.008, 11.214, and 15.937 Å) represent the inner- and outer dimensions of each cuboidal unit.

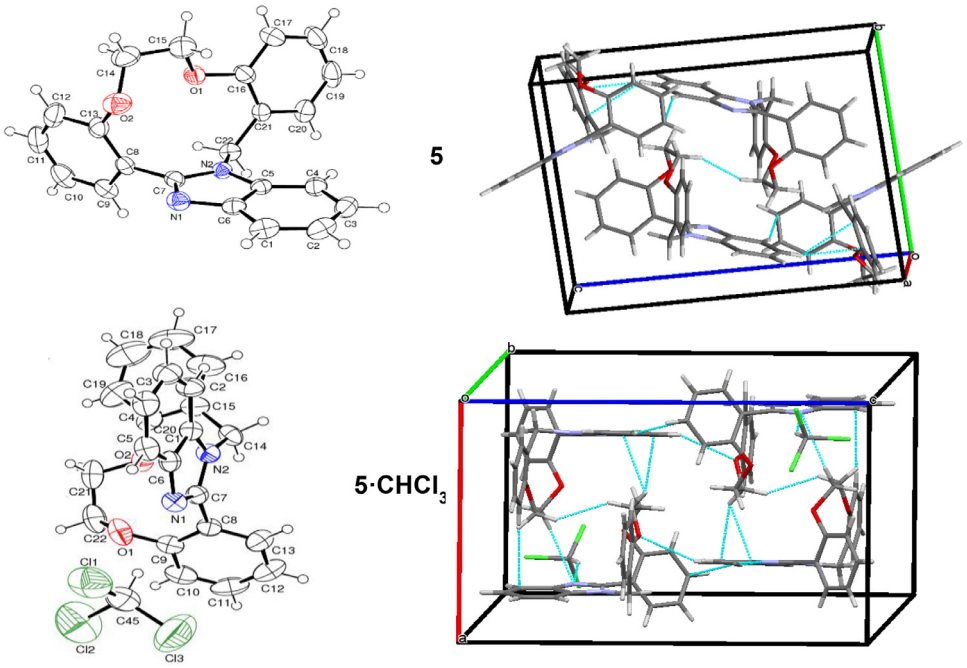

Fig. 1. ORTEP (50% probability) and packing diagrams of macrocycles: **5** (CCDC #1499642) and **5·CHCl$_3$** (CCDC #1499643).

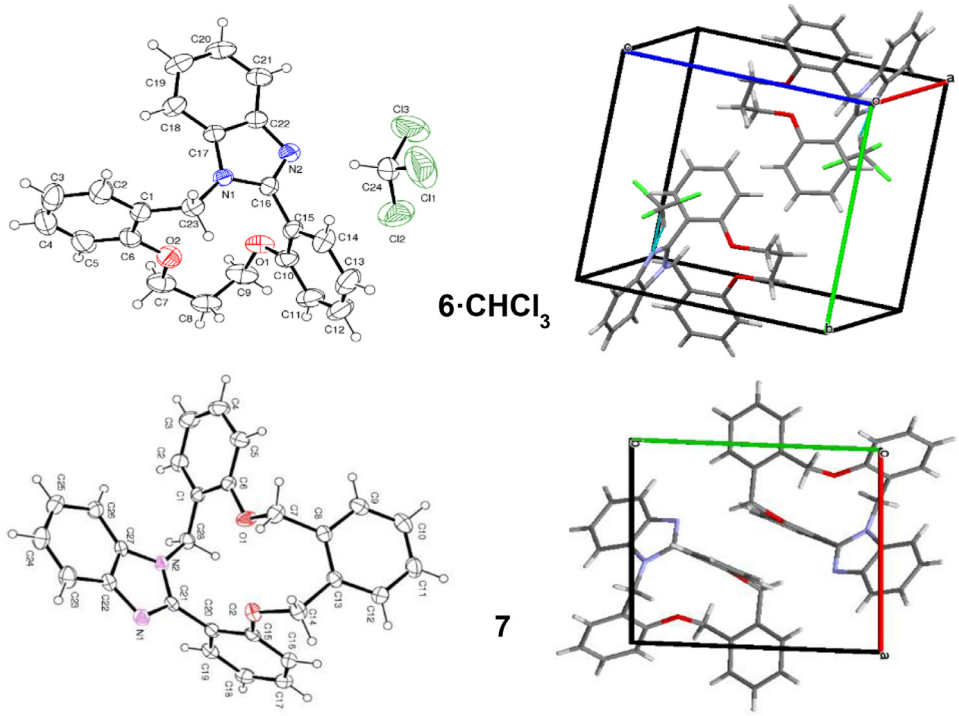

Fig. 2. ORTEP (50% probability) and packing diagrams of macrocycles: **6·CHCl$_3$** (CCDC #1514605); and **7** (CCDC #1529342).

3.6. Crystal structure of chloroform-solvate of macrocycle 6 (6·CHCl$_3$)

The macrocycle **6** crystallizes as its chloroform-solvate in the triclinic system with the space group *P*-1 containing two molecules in a unit cell ($z = 2$) which self-assemble into infinite chains **A** and **B** (Fig. 8a). The macrocycles are in a head-to-tail arrangement in the chains making them to be antiparallel. Aromatic CH···π offset stacking interactions between the phenyl rings **X** and **Y** of the neighboring molecules (C4···H12, 2.8514 Å), hydrogen bonds between chloroform and benzimidazole units in each chain (N2···H24, 2.212 Å), and aromatic CH···π interactions between the planar benzimidazole rings in adjacent chains **A** and **B** (C17···H23A, 2.874 Å) contribute to the close packing of molecules in and between the chains and their stability. Self-intertwining of the antiparallel chains **A** and **B** forms cuboidal blocks (Fig. 8b). Chloroform molecules positioned at the corners of each cuboid define its outer boundaries (Fig. 8b) and the channel-like space between the blocks (Fig. 8c).

The **ABAB** packing of the antiparallel chains **A** and **B** is illustrated by the space-fill models in Fig. 9a (front) and 9b (back). A

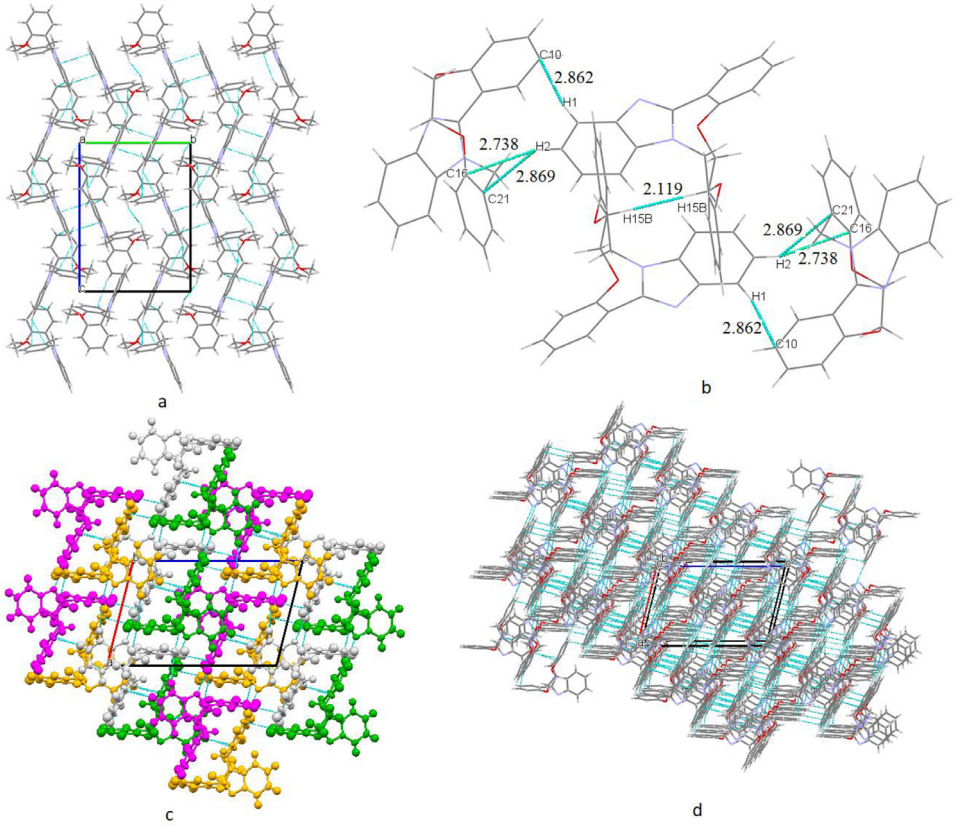

Fig. 3. (a) Antiparallel 1-D chains of macrocycle **5** along axis *b*, (b) strong non-covalent interactions between the macrocycles **5** in an infinite chain, (c) complementary pairs of macrocycles in the antiparallel chains viewed along axis *b*, and (d) view of channels formed between pairs of antiparallel chains of **5**.

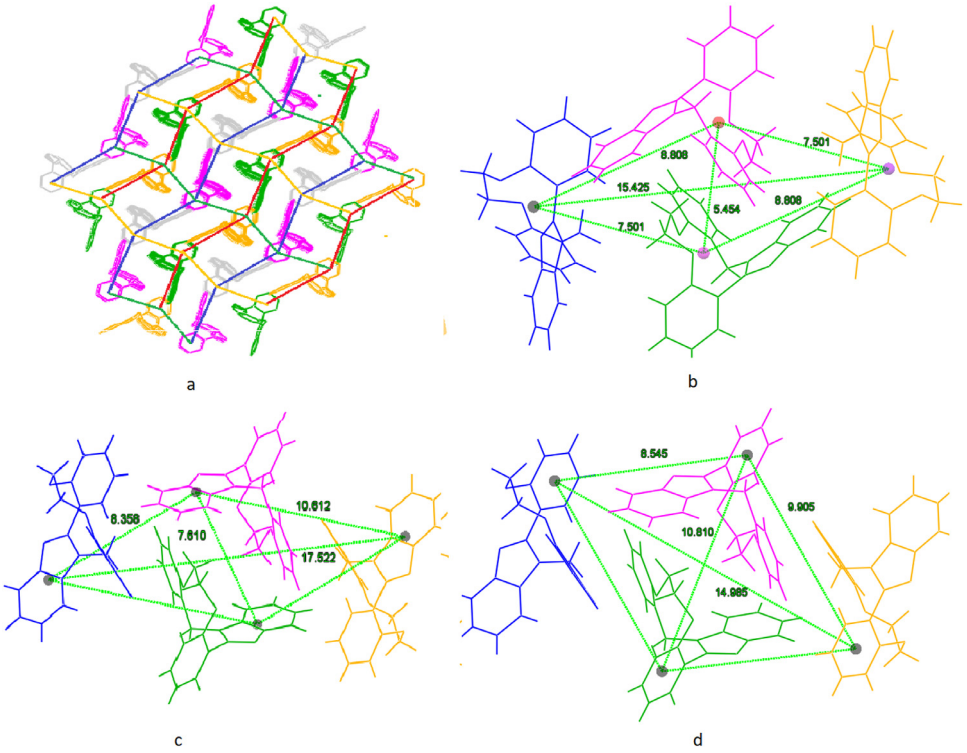

Fig. 4. Cuboidal motifs in the self-assembly of **5** (a), distance (in Å) between the centroids of macrocyclic rings (b), benzimidazoles (c), and phenyl rings (d).

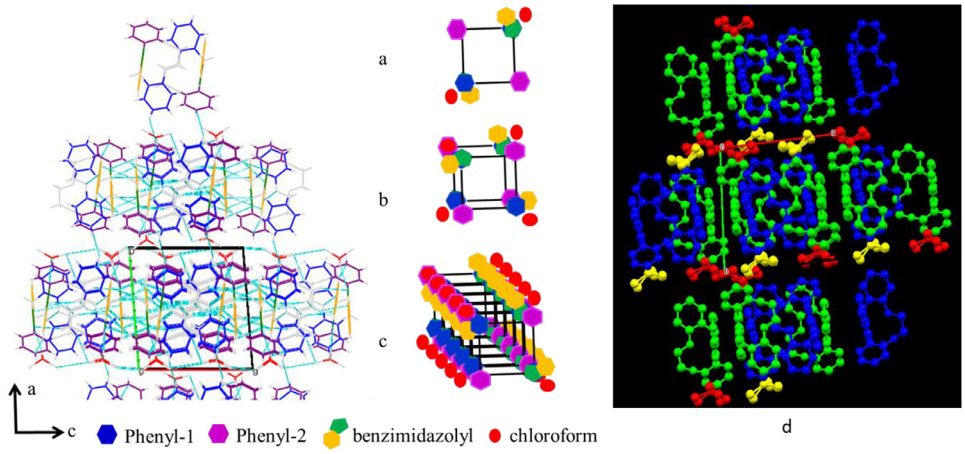

Fig. 5. Chloroform-solvate crystal structure of **5** viewed along axis *c* and its simpler representation of the formation of its self-assembly: (a) macrocycle and chloroform building blocks in 2-D, (b) cubic unit cell, (c) self-assembly by non-covalent interactions, (d) 3-D network with two-fold symmetry axis.

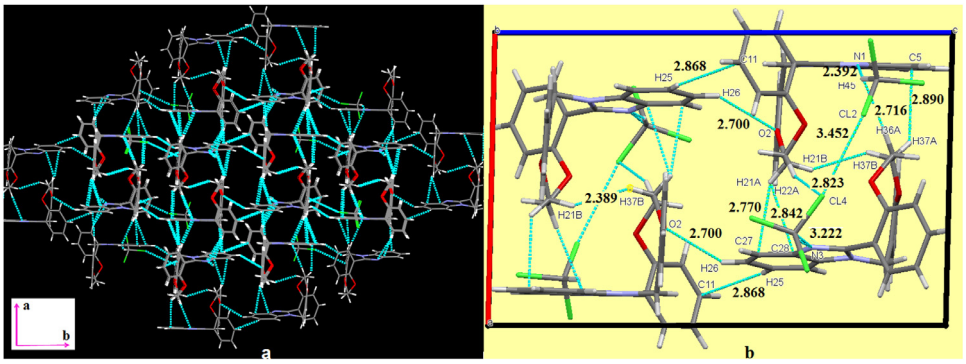

Fig. 6. (a) Intermolecular non-covalent interactions in the 3-D network of chloroform-solvate of **5** and (b) their dimensions (in Å).

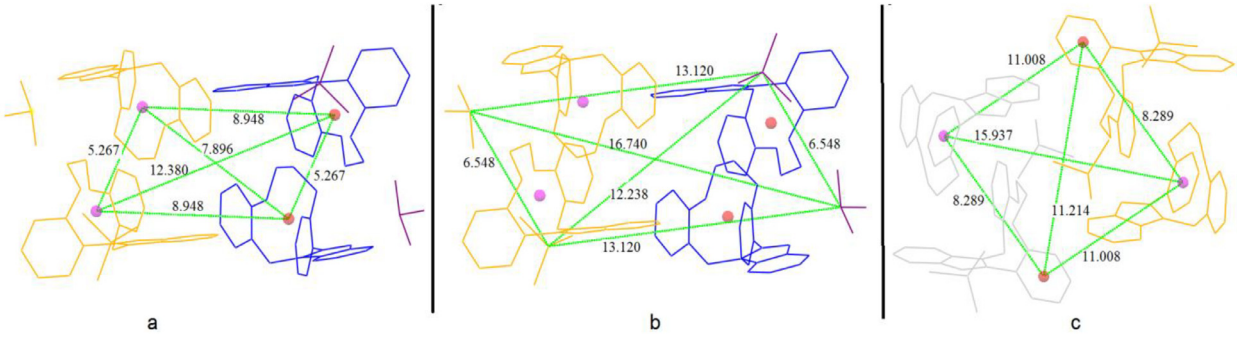

Fig. 7. Distance between the centroids of puckered macrocyclic rings (a), the chloroform molecules (b), and the phenyl rings (c) in the chloroform-solvates of **5**.

closer view of this packing reveals a ladder-like structure wherein the planar benzimidazole rings and ether linkages of chains **A** and **B** form the slide rails and rugs, respectively (Fig. 9c). The outer dimensions of the cuboidal blocks vary depending upon the distances between the chloroform units of two adjacent chains **A** and **B** (9.419, 10.066, and 10.684 Å) as illustrated in Fig. 10a. Similarly, the inner dimensions of the cuboidal blocks are described by the distances between the centroids of macrocyclic rings (10.684 and 4.764 Å) (Fig. 10b) and of the benzimidazole units (10.684 and 4.805 Å) (Fig. 10c). The distances between the phenyl rings **X** and **Y** in a macrocycle, between the neighboring molecules of a chain, and between the molecules in the adjacent chains are 6.352, 5.421, and 7.685 Å, respectively (Fig. 10d). Chloroform molecules in the solvates of **6** significantly promote self-assembly of the molecules in the crystal structure by interconnecting and stabilizing molecular units and 3-D networks by hydrogen bonds. The positions of chloroform molecules in the crystal structure of **6**.CH_3Cl precisely define and significantly contribute to the formation and stabilization of the 3-D network.

3.7. Crystal structure of 7

The macrocycle **7** crystallizes in the triclinic system with the space group *P*-1 with two molecules in a unit cell ($z = 2$). In the crystal structure of **7**, each molecule is connected to another molecule in the same unit cell and to two other molecules in the neighboring unit cells by head-to-tail self-assembly exerting four pairs of weak aromatic CH···π offset stacking interactions with benzimidazole (H24···C7, 2.879 Å; H18···C26, 2.858 Å), phenyl rings

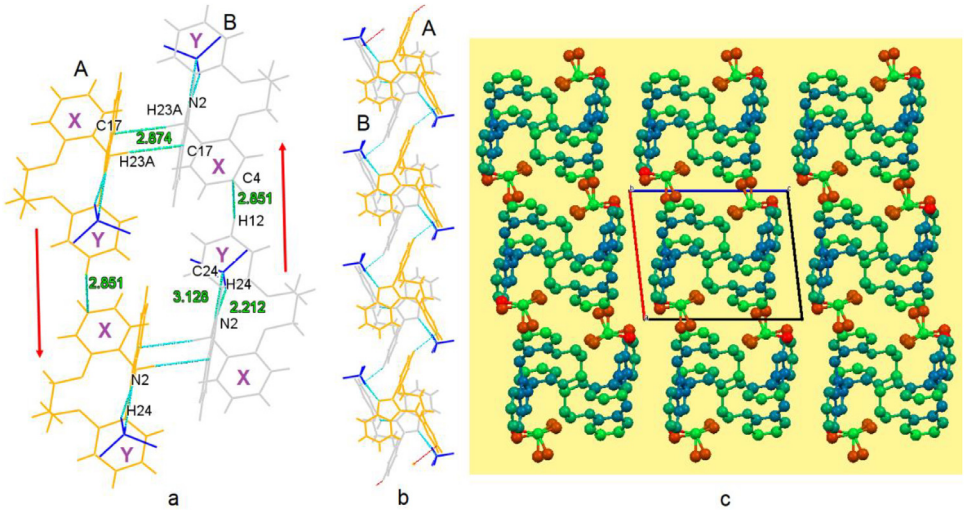

Fig. 8. Crystal structure of chloroform-solvate of macrocycle **6**. (a) aromatic CH···π offset stacking interactions and hydrogen bonds viewed along the axis *a*, (b) cuboidal blocks made up of a pair of macrocycles stacked to each other from chains **A** and **B** with the center of inversion viewed along axis *c*, and (c) the 3-D networks of cuboids viewed with atomic displacement.

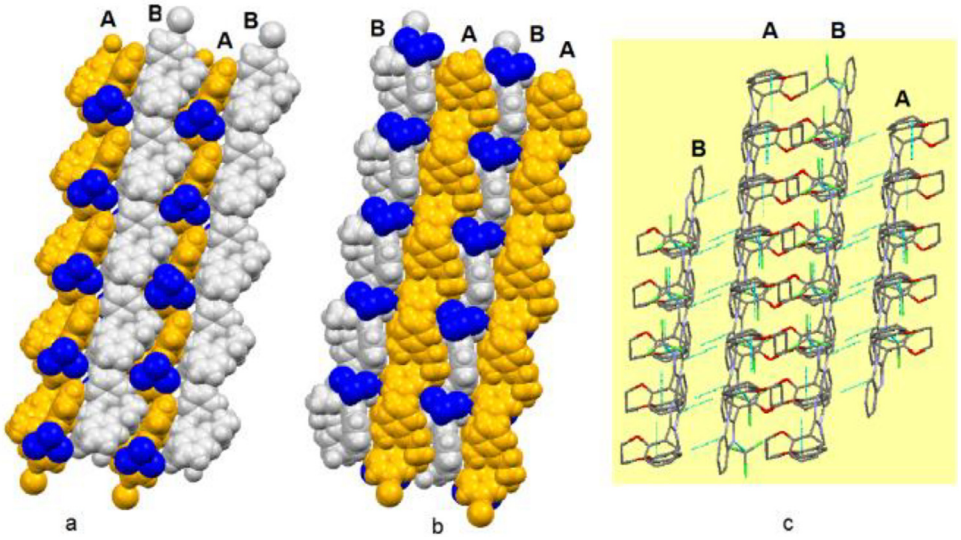

Fig. 9. Space fill model of macrocycle **6** in its chloroform-solvate crystals depicting the cubical arrangement of chloroform units and close packing of the antiparallel chains **A** and **B** along the axis *a*: (a) front and (b) rear view. Ladder structure formed by the antiparallel chains **A** and **B** with the benzimidazole rings as slide rails, ether linkers as rugs, and chloroform molecules above and below the rugs.

(C3···H28B, 2.804 Å), and ether linkages (H28A···H19, 2.396 Å) as shown in Fig. 11.

The macrocycles are packed with an intermolecular distance of 2.804 Å, wherein the head of one molecule in chain **X** is paired with the tail of another molecule in chain **Y** forming cuboidal cages as viewed in Fig. 12a and 12b. The benzimidazole units in each cuboidal cage project outside in the opposite directions at a distance of 2.879 Å, whereas the benzimidazole moieties in the adjacent antiparallel chains **X** and **Y** generate rectangular voids in the 3-D network (Fig. 12c). The distance between the centroids of puckered macrocyclic rings (6.859 Å), benzimidazole rings (9.859 Å), and phenyl rings (9.629 and 7.801 Å) is illustrated in Fig. 13.

3.8. Comparison of the crystal structures and SEM images of 5–7

Self-assembly of these structurally similar ring-contracted 1,2-fused benzimidazodioxaaza macrocycles leads to the formation of exciting three-dimensional networks by non-covalent intra- and intermolecular aromatic π-π stacking and CH···π interactions and NH···H hydrogen bond in the solid state with well-defined conformation and functional characteristics. The nonplanarity of the macrocycles originating from the presence of benzimidazole moiety accounts for the formation of unconventional noncovalent interactions in the free and chloroform solvates of the macrocycles. The orientation of electrophilic benzimidazole units, phenyl rings, and ether linkages in each macrocycle leads to the self-assembly of the molecules into unsymmetrical chains, cuboidal cage-like pores, cuboidal blocks, and channels. The self-assembly of the molecules are stabilized by strong aromatic π-π and CH-π stacking interactions in the free macrocycles **5** and **7**, whereas hydrogen bonds originating from benzimidazole and chloroform units further stabilize the 3-D networks of the solvates of macrocycles **5** and **6**.

The self-assembly of the free macrocycles **5** and **7** and solvates of **5** and **6** originates from two anti-parallel chains stacking on to each other by the π-stacking and hydrogen bonding. Each of these chains are unsymmetrical and the macrocycles are connected by head-to-tail arrangement. The presence of chloroform units in the

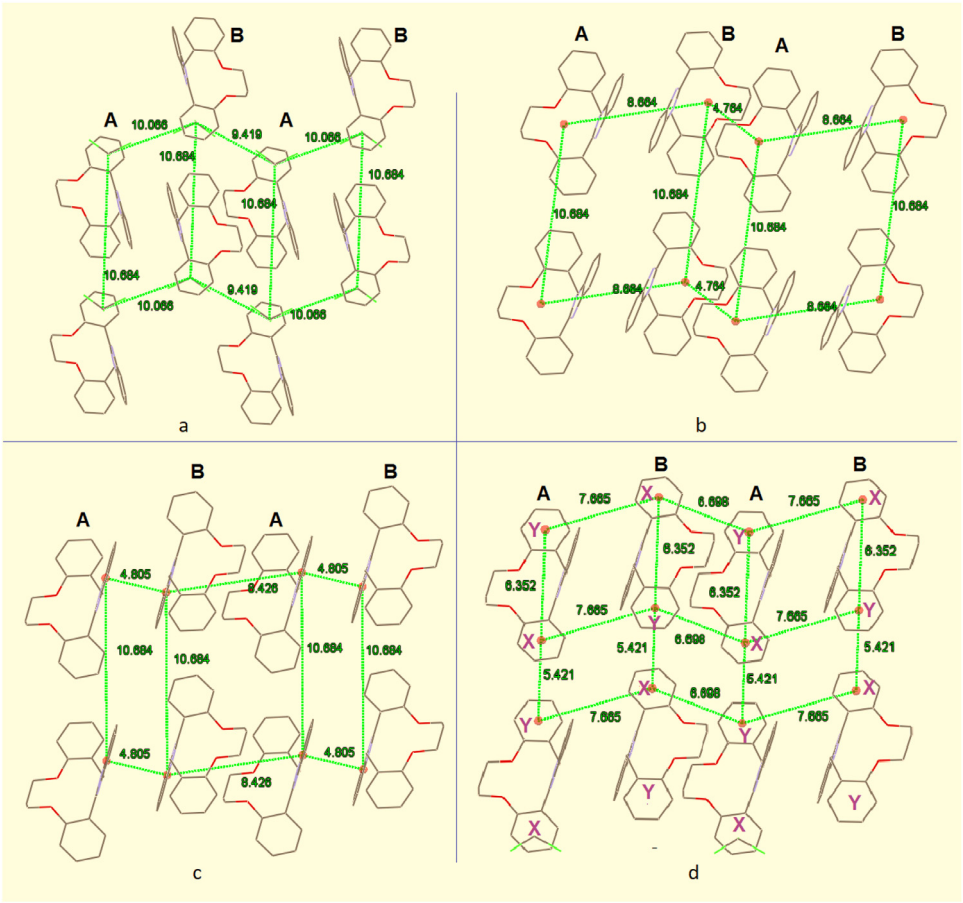

Fig. 10. Distances (Å) between: (a) chloroform units, (b) centroids of puckered macrocyclic rings, (c) centroids of planar benzimidazole rings, and (d) centroids of phenyl rings **X** and **Y** in the crystal structure of **6·CHCl3**. Hydrogen atoms are omitted for clarity.

crystal structures of macrocycles **5** and **6** is crucial in the formation of hydrogen bonds between the macrocycle and the solvent units. The regular cuboidal arrangements of the macrocycles of **5** and **6** in their solvated forms are defined by the presence of chloroform at each corner of the cuboidal units of their networks.

The self-assembly of macrocycles is further evidenced from the SEM images of the macrocycles **5–7** presented in Fig. 14a-f. The SEM images of the macrocycle **5** indicate cuboidal blocks of well-defined geometry with average size of 7.19 μm (Fig. 14a and b). The SEM images of macrocycles **6** (Fig. 14c and d) indicate self-assembly leading to the formation of micro-spheres of average diameter of 472 nm. The cylindrical self-assembly of the macrocycle **6** is observed with different sizes (Fig. 14d). Micro-spheres of **7** with the average diameter 589 nm are observed in the SEM images (Fig. 14e and f). The possible noncovalent interactions originating from the nonplanar macrocycles are the key factors resulting in their different self-assembled structures.

3.9. Electronic absorption spectra of macrocycles 5–7

The electronic absorption spectra of the dioxaaza benzimidazo macrocycles **5, 6**, and **7** in ethanol at 25 °C contain three absorption bands. The strong absorption band at 201 nm corresponds to the π-π^* transitions originating from phenyl rings in the macrocycles. The absorption bands at 258 (**5**) and 283 (**6** and **7**) are assignable to the π-π^* transitions of the benzimidazole rings. The bands at 277 (**5**), 313 (**6**), and 317 nm (**7**) are assignable to the n-π^* transitions of the macrocycles. The electronic absorption spectra of the macrocycles **5–7** are presented in Fig. 15a.

3.10. Emission spectra of macrocycles 5–7

The emission spectra of the macrocycles **5, 6**, and **7** in ethanol at 25 °C contain broad emission bands in the UV region at 356, 369, and 364 nm upon excitation at their excitation maxima at 276, 283, and 282 nm, respectively. The emission and excitation spectra of **5, 6**, and **7** are presented in Fig. 15b-d.

3.11. DFT studies of 5–7

The quantum mechanical based structure-electronic feature relationship of molecules is understood in the light of DFT calculations [58,59]. The energy optimized geometries, molecular electrostatic potentials maps, three-dimensional descriptions of the overlap of atomic orbitals (Fig. 16) and frontier molecular orbitals (FMOs) of **5–7** (Fig. 17) are obtained from the B3LYP functional using the basis set 6–31 G(d,p). The optimized geometry of the macrocycles **5–7** obtained from the DFT calculations is puckered (Fig. 16a) and is in accordance with the geometry of their molecular structures from single crystal XRD studies (Fig. 1). The phenyl- and benzimidazole rings of the macrocycles are not coplanar with each other as well as with the macrocyclic rings as shown in Fig. 16a. The restricted C−−C rotation between the planar *ortho*-fused benzimidazole unit and the phenyl rings is the cause for the puckered geometry of the macrocycles. Consequently, in the optimized geometry the phenyl rings orient above and below the molecular plane and stabilize the molecules. The puckered geometry and the spatial orientation of the aliphatic and aromatic groups of **5–7** account for the formation of head-to-tail arrange-

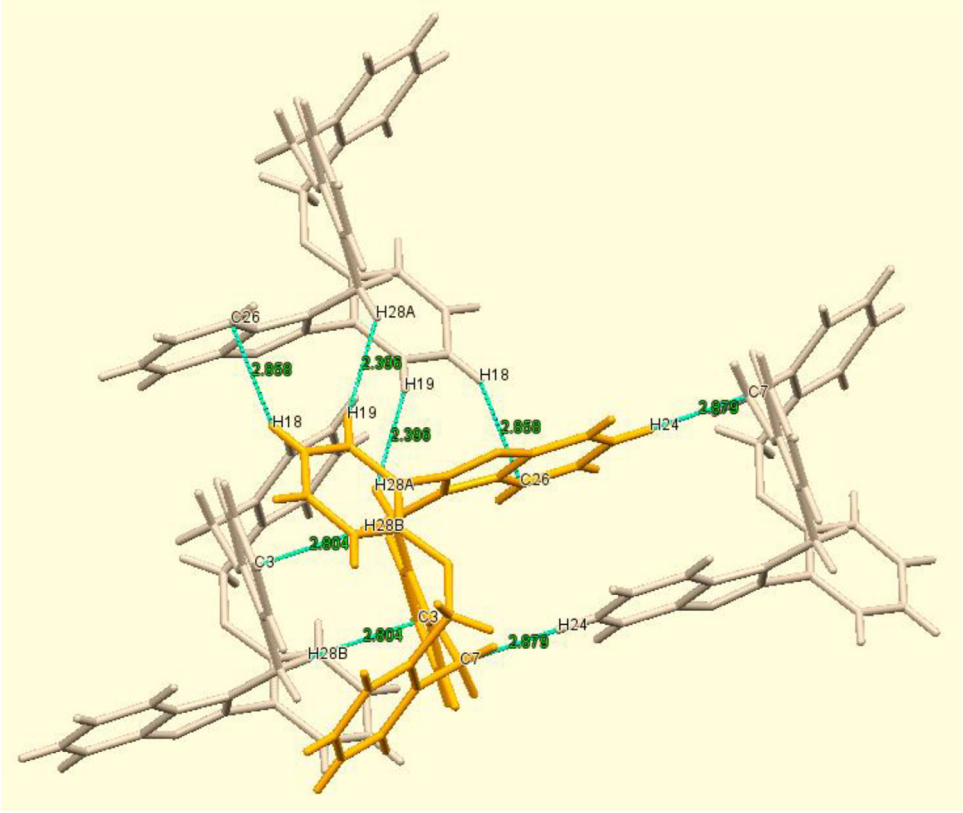

Fig. 11. Intermolecular aromatic CH···π stacking interactions originating from benzimidazole and phenyl rings of macrocycle **7**.

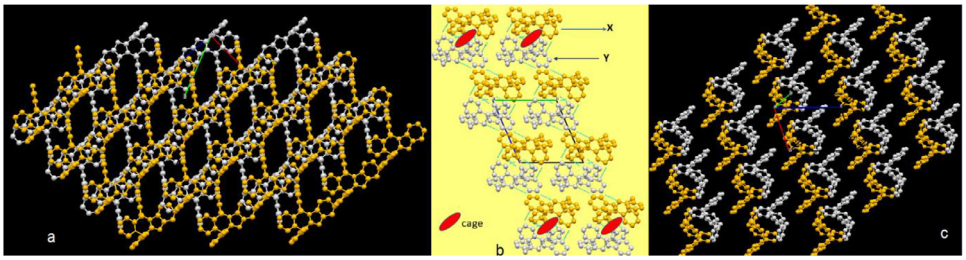

Fig. 12. Crystal structure of **7**. (a) two antiparallel chains **X** and **Y** creating cuboidal cage-like structures viewed along axis *b*, (b) cuboidal cage-like pores shown in red ellipsoids viewed along axis *a*, and (c) view along axis *c* indicating the projection of benzimidazole units of each molecule in the opposite directions.

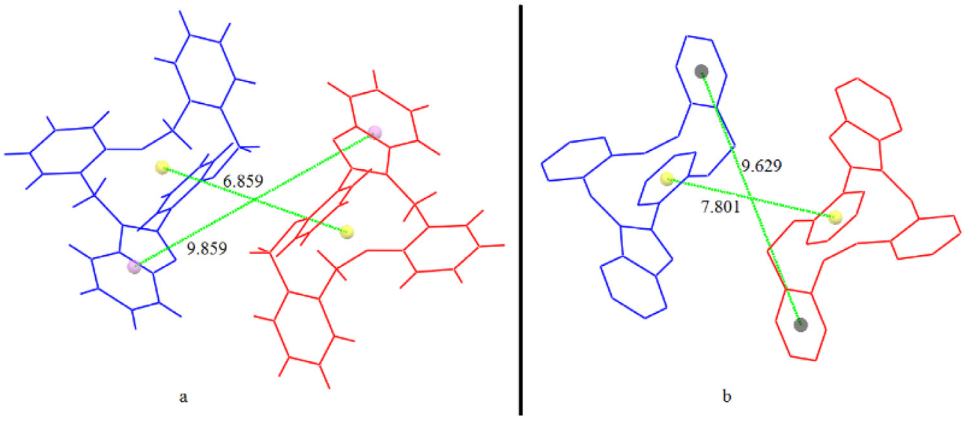

Fig. 13. (a) Distance between centroids of macrocyclic and benzimidazole rings and (b) distance between centroids of phenyl rings in the crystal structure of **7**.

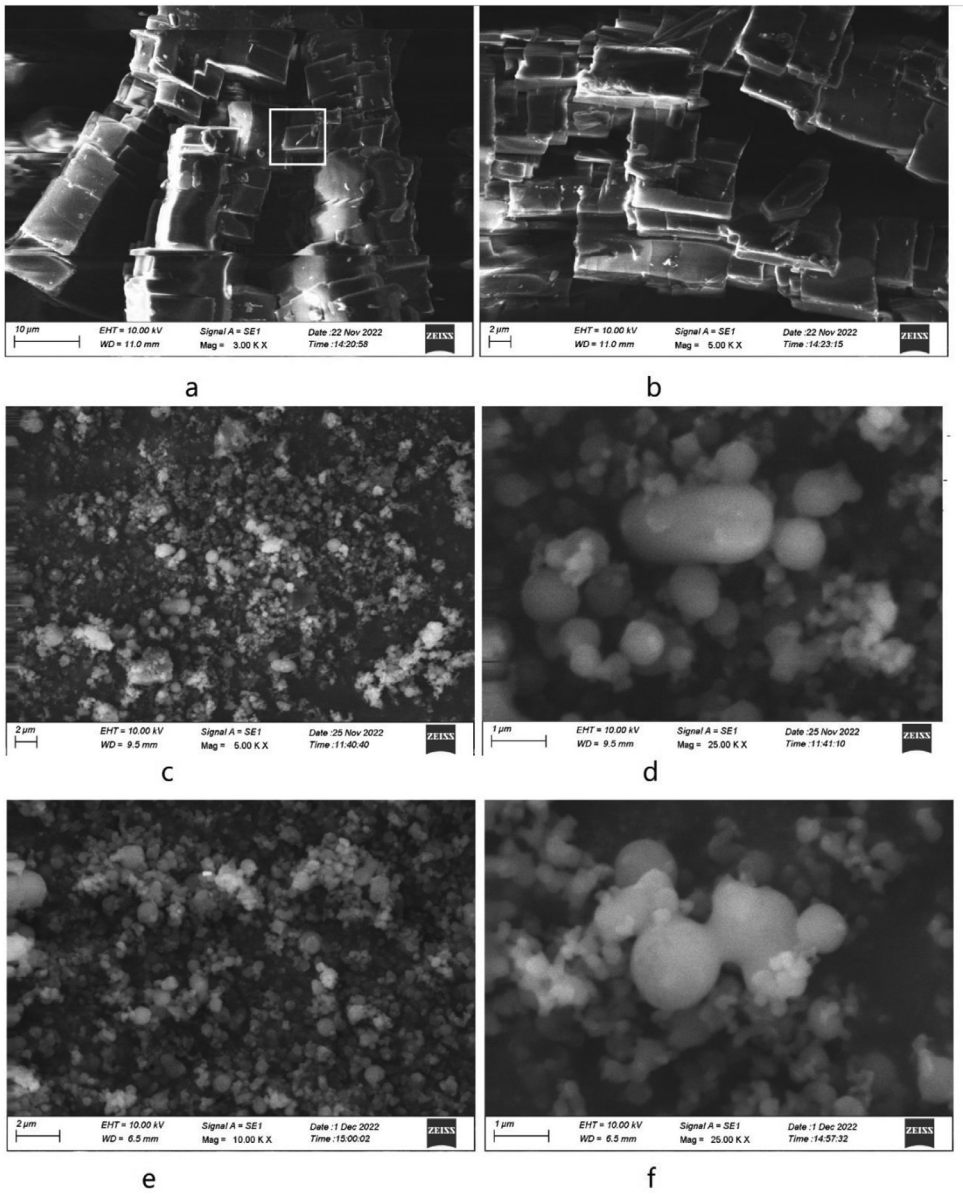

Fig. 14. SEM images of **5** (a and b), **6** (c and d), and **7** (e and f).

ment in the unit cells, anti-parallel chains, cuboidal cages and channels in the 3-D networks, and aromatic π-stacking interactions (Sections 3.3-3.6).

The molecular electrostatic potentials of **5**–**7** mapped onto the electron density surfaces, shown in Fig. 16b and c, describe electronic polarization in the molecules. High electron density regions shown in red are nucleophilic where the electronegative nitrogen and oxygen atoms are present and the lower electron density regions shown in blue are electrophilic. The nucleophilic and electrophilic centers of the macrocycles with proton donor and electron acceptor capabilities are thus identified from the three-dimensional MEP models.

The FMO sketches of the molecules **5**–**7** describe the best overlap between the interacting orbitals and hence the delocalization of electrons (Fig. 17). Greater the overlap between the orbitals, better the delocalization of electrons. HOMOs of macrocycles **5**–**7** reveal localization of electrons onto the benzimidazole rings as shown in Fig. 17. LUMO of **5** indicates delocalization of electrons onto the phenyl and benzimidazole rings, whereas LUMOs of **6** and **7** indicate localization of electrons onto the phenyl rings and *ortho*-xylenyl group, respectively. Similar localization/delocalization of electrons is observed in HOMO-1 and LUMO+1 sketches of the macrocycles **5**–**7.**

Electron delocalization in molecules is significantly influenced by the overlap between the orbitals which is influenced by the electronic and space effects exerted by the functional/substituent groups. Greater the electron delocalization, lower is the energy of the FMOs. The difference in the energy of the FMOs and the energy gap $\Delta E_{HOMO\text{-}LUMO}$ is attributed to the difference in the delocalization of electrons exerted by the electronic and space effects of ethylene, propylene, and *o*-xylenyl moieties of **5, 6**, and **7**, respectively. The aliphatic ethylene and propylene groups in **5** and **6** stabilize the HOMOs, whereas the *ortho*-xylenyl group in **7** stabilizes the LUMO. The energy of the HOMOs (eV) follows the order: **5** (−5.89) > **6** (−5.81) > **7** (−5.79), whereas that of the LUMOs is: **7** (−0.99) > **5** (−0.70 > **6** (−0.66). The ethylene group in **5** stabilizes both the HOMO and LUMO better than the propylene group in **6**. The energy gap $\Delta E_{HOMO\text{-}LUMO}$ (eV) of **5**–**7** follows the

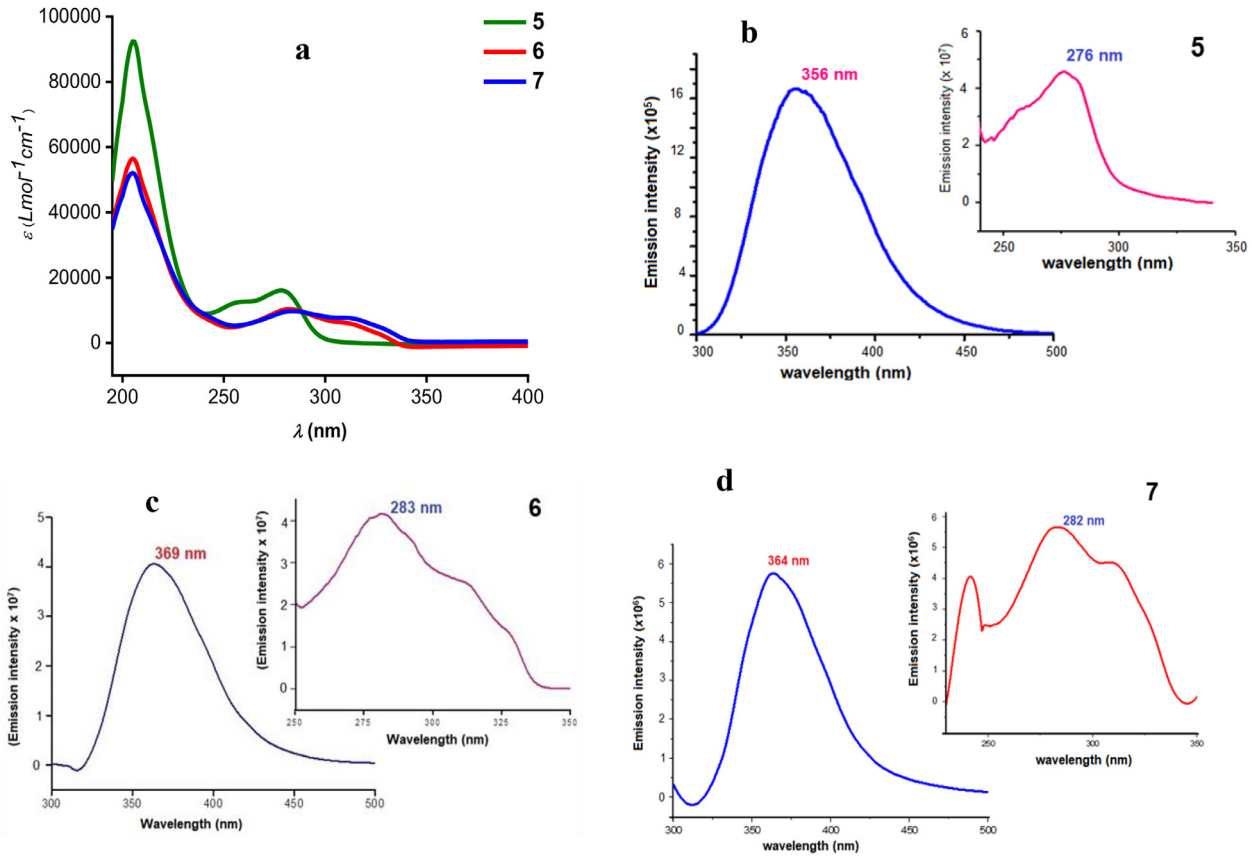

Fig. 15. Electronic absorption spectra of the macrocycles **5–7** in ethanol (a). Emission spectra of **5–7** in ethanol 25 °C at room temperature (b-d). *Inset*: excitation spectra of **5–7**.

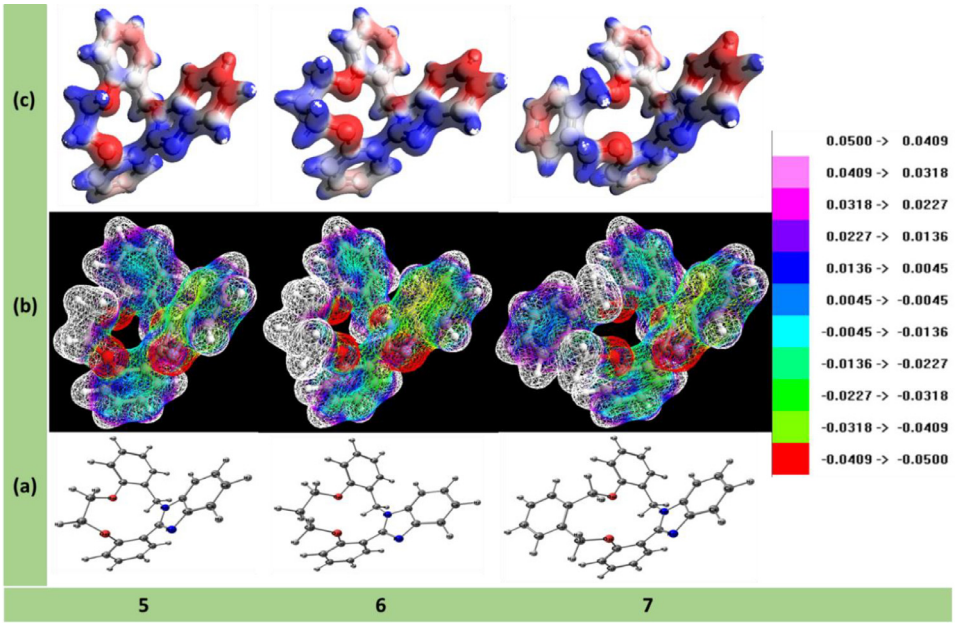

Fig. 16. (a) Optimized geometry, (b) molecular electrostatic potentials map, and (c) description of overlap of molecular orbitals of macrocycles **5–7** derived from the DFT calculations.

order: **5** (5.19) > **6** (5.15) > **7** (4.79) (Fig. S10). The electron rich *o*-xylenyl group contributes more toward the low $\Delta E_{HOMO\text{-}LUMO}$ value of **7** than the aliphatic groups in **5** and **6**. Lower the $\Delta E_{HOMO\text{-}LUMO}$ value, greater is the intramolecular charge transfer in the molecule.

The global molecular electronic and reactivity descriptors such as chemical and ionization potentials, electron affinity, hardness and softness, electrophilicity index, and net electrophilicity of **5, 6**, and **7**, computed from the DFT studies [60,61], are presented in Table S1. The chemical potentials (μ) of the molecules are appre-

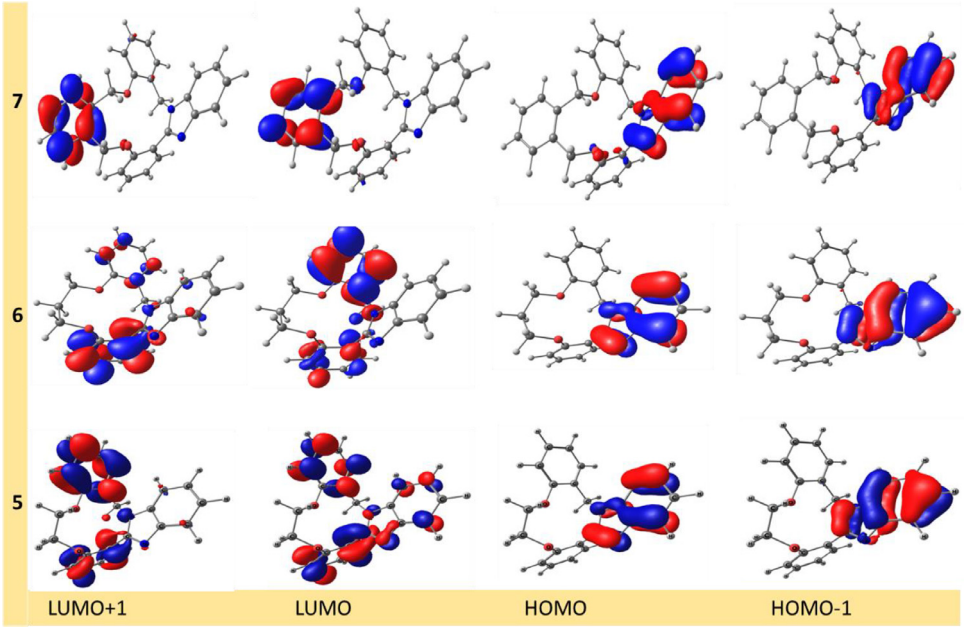

Fig. 17. Sketches of frontier molecular orbitals of **5**–**7** from DFT calculations.

ciably closer to each other (Fig. S10). The chemical hardness (η) of the molecules **5**–**7**, calculated from the $\Delta E_{HOMO\text{-}LUMO}$ values, are 2.59, 2.58, and 2.39, respectively. The calculated softness (σ) of the molecules **5** and **6** is 0.39 and that of **7** is 0.42. Electrons flow from an occupied molecular orbital to an unoccupied molecular orbital and the overlap between the exchanging orbitals is critical in determining the energy of the FMOs and the energy gap, $\Delta E_{HOMO\text{-}LUMO}$. Soft molecules have larger energy gap than hard molecules indicating their greater tendency toward electron transfer [60]. This inference is consistent with the lower energy gap of **7** with smaller hardness value than those of the macrocycles **5** and **6**.

The electrophilicity index of macrocycle **7** ($\omega = 2.39$) is larger than that of **5** ($\omega = 2.10$) and **6** ($\omega = 2.03$) (Table S1) leading to its greater tendency for electron transfer. Macrocycle **7** also exhibits better electron donor capability with larger net electrophilicity ($\omega^{\pm} = 3.39$) than that of **5** ($\omega^{\pm} = 3.30$) and **6** ($\omega^{\pm} = 2.90$) as shown in Fig. S11. The difference in the molecular electronic and reactivity parameters is indicative of the electronic and space effects of the aliphatic and aromatic ether moieties of the benzimidazo macrocycles **5**–**7**. Macrocycle **7** containing electron rich *para*-xylenyloxy group influences its global molecular electronic and reactivity parameters than that of **5** and **6** which contain the aliphatic ethylenoxy and propylenoxy groups, respectively.

4. Conclusion

Self-assembly of three nonplanar benzimidazole macrocycles synthesized from [1 + 1] Schiff base condensation between *ortho*-bridged dibenzaldehydes and *ortho*-phenylenediamine results in highly defined cuboidal cavity-like microscale particles. The noncovalent interactions such as π-π and CH-π stacking interactions principally originating from the electrophilic benzimidazole units lead to the self-assembly of the benzimidazole macrocycles **5** and **7**, whereas in the solvated crystals of **5** and **6** H-bonding originating from the chloroform molecules in addition to the π-stacking interactions promote the self-assembly. The nonplanarity of the benzimidazole macrocycles is an important structural factor for the self-assembly of these nonplanar macrocycles leading to the well-defined structures. The quantum theoretical modeling of the macrocycles **5**–**7** from the DFT studies account for their nonplanarity and molecular electronic properties.

Supporting Information

The ^{1}H and ^{13}C NMR, and ESI-TOF mass spectra of compounds **5**-**7** (Fig. S1-S9) and the chemical parameters computed from the DFT studies (Fig. S10 and Table S1) are presented in the Electronic Supplementary Information.

Declaration of Competing Interest

The authors declare that they have no known competing financial interests or personal relationships that could have appeared to influence the work reported in this paper.

CRediT authorship contribution statement

A. Irudaya Jothi: Conceptualization, Methodology, Investigation, Writing – original draft. **P. V. Priyanka:** Formal analysis, Data curation. **V. Alexander:** Resources, Supervision, Writing – review & editing.

Data availability

No data was used for the research described in the article.

Acknowledgement

We thank the SAIF, IIT Madras, Chennai, for recording NMR and Mass spectra and XRD analysis and ACICI, St. Joseph's College, for UV–Vis, luminescence, and SEM analysis.

Supplementary materials

Supplementary material associated with this article can be found, in the online version, at doi:10.1016/j.molstruc.2023.135367.

References

[1] L.F. Lindoy, K.-.M. Park, S.S. Lee, Metals, macrocycles and molecular assemblies -macrocyclic complexes in metallo-supramolecular chemistry, Chem. Soc. Rev. 42 (2013) 1713–1727.

[2] X.-.Z. Li, C.-.B. Tian, Q.-.F. Sun, Coordination-directed self-assembly of functional polynuclear lanthanide supramolecular architectures, Chem. Rev. 122 (2022) 6374–6458.

[3] H. Chen, C. Huang, Y. Deng, Q. Sun, Q.-.L. Zhang, B.-.X. Zhu, X.-.L. Ni, Solvent-switched Schiff-base macrocycles: self-sorting and self-assembly-dependent unconventional organic particles, ACS Nano 13 (2019) 2840–2848.

[4] H. Chen, C. Huang, Y. Deng, Q. Sun, Q.-.L. Zhang, B.-.X. Zhu, X.-.L. Ni, Organic–core shell shaped micro/nanoparticles from twisted macrocycles in Schiff base reactions, Chem. Sci. 10 (2019) 490–496.

[5] Y. Xiong, C. Huang, H. Liu, R. Yi, B.-.X. Zhu, X.-.L. Ni, Tunable organic particles: an efficient approach from solvent-dependent Schiff base macrocycles, Chin. Chem. Lett. 32 (2021) 3522–3525.

[6] M. Taniguchi, J.S. Lindsey, Synthetic chlorins, possible surrogates for chlorophylls, prepared by derivatization of porphyrins, Chem. Rev. 117 (2017) 344–535.

[7] D. Hodgkin, J. Pickworth, S. Robertson, Structure of Vitamin B_{12}: the crystal structure of the hexacarboxylic acid derived from b_{12} and the molecular structure of the vitamin, Nature 176 (1955) 325–328.

[8] C.J. Matthews, T.A. Leese, W. Clegg, M.R.J. Elsegood, L. Horsburgh, J.C. Lockhart, A route to bis(benzimidazole) ligands with built-in asymmetry: potential models of protein binding sites having histidines of different basicity, Inorg. Chem. 35 (1996) 7563–7571.

[9] T. Fekner, J. Gallucci, M.K. Chan, Ruffling-induced chirality: synthesis, metalation, and optical resolution of highly nonplanar, cyclic, benzimidazole-based ligands, J. Am. Chem. Soc. 126 (2004) 223–236.

[10] W.R. Scheidt, Y.-.J. Lee, Recent advances in the stereochemistry of metallotetrapyrroles, Struct. Bonding 64 (1987) 1–70.

[11] A. Dey, K. Biradha, Anion and guest directed tetracyclic macrocycles of Ag5l4 and Ag6l4 with an arc-shaped ligand containing pyridine and benzimidazole units: reversal of anion selectivity by guest, Cryst. Growth Des. 17 (2017) 5629–5633.

[12] H.-.W. Wu, L.-.W. Lee, P. Thanasekaran, C.-.H. Su, Y.-.H. Liu, T.-.M. Chin, K.-.L. Lu, Weak interactions in imidazole-containing zinc(II)-based metal–organic frameworks, *J. Chin. Chem.* Soc. (2020) 1–7.

[13] W.H. Kwok, H. Zhang, P. Payra, M. Duan, S.-.C. Hung, D.H. Johnston, J. Gallucci, E. S.-Jankun, M.K. Chan, Synthesis and characterization of the dimethyl-substituted bisbenzimidazole ligand and its manganese complex, Inorg. Chem. 39 (2000) 2367–2376.

[14] P. Payra, S.-.C. Hung, W.H. Kwok, D.H. Johnston, J. Gallucci, M.K. Chan, Structural, magnetic and catalytic properties of a self-recognized μ-oxo-bridged diiron(III) bis(benzimidazole) complex, Inorg. Chem. 40 (2001) 4036–4039.

[15] S. Horiuchi, S. Ishibashi, S. Inada, S. Aoyagi, Hydrogen-bonded architectures and field-induced polarization switching in bridged bis(benzimidazole) crystals, Cryst. Growth Des. 19 (2019) 328–335.

[16] W. Zieliński, A. Katrusiak, Hydrogen bonds NH···N in compressed benzimidazole polymorphs, Cryst. Growth Des. 13 (2013) 696–700.

[17] W.-.H. Sun, C. Shao, Y. Chen, H. Hu, R. Sheldon, H. Wang, X. Leng, X. Jin, Controllable supramolecular assembly interactions by π-π: cobalt(II) and copper(II) complexes with benzimidazole derivatives, Organometallics 21 (2002) 4350–4355.

[18] C.-.J. Wang, K.-.F. Yue, Z.-.X. Tu, L.-.L. Xu, Y.-.L. Liu, Y.-.Y. Wang, Syntheses, crystal structures, and properties of a series of coordination polymers based on 2-(*N*-pyridyl)benzimidazole ligands (n = 3,4), Cryst. Growth Des. 11 (2011) 2897–2904.

[19] N.E. Borisova, M.D. Reshetova, Y.A. Ustynyuk, Metal-free methods in the synthesis of macrocyclic Schiff bases, Chem. Rev. 107 (2007) 46–79.

[20] V. Alexander, Design and synthesis of macrocyclic ligands and their complexes of lanthanides and actinides, Chem. Rev. 95 (1995) 273–342.

[21] N.E. Borisova, M.D. Reshetova, Y.A. Ustynyuk, Binuclear and polynuclear transition metal complexes with macrocyclic ligands: new polydentate macrocyclic ligands in reactions of 4-alkyl-2,6-diformylphenols with 1,2-diaminobenzenes, Russ. Chem. Bull. Int. Ed. 53 (2004) 181–188.

[22] K. Ghosh, I. Saha, *ortho*-Phenylenediamine-based open and macrocyclic receptors in selective sensing of $H_2PO_4^-$, ATP and ADP under different conditions, Org. Biomol. Chem. 10 (2012) 9383–9392.

[23] L.G. Armstrong, I.F. Lindoy, Nitrogen-Oxygen Donor Macrocylic Ligands. I. Nickel(II) complexes of a new series of cyclic ligands derived from salicylaldehydes, Inorg. Chem. 14 (1975) 1323–1326.

[24] M. Leshabane, G.A. Dziwornu, D. Coertzen, J. Reader, P. Moyo, M. van der Watt, K. Chisanga, C. Nsanzubuhoro, R. Ferger, E. Erlank, N. Venter, L. Koekemoer, K. Chibale, L.-.M. Birkholtz, Benzimidazole derivatives are potent against multiple life cycle stages of plasmodium falciparum malaria parasites, ACS Infect. Dis. 7 (2021) 1945–1955.

[25] G.A. Dziwornu, D. Coertzen, M. Leshabane, C.M. Korkor, C.K. Cloete, M. Njoroge, L. Gibhard, N. Lawrence, J. Reader, M. van der Watt, S. Wittlin, L.-.M. Birkholtz, K. Chibale, Benzimidazole derivatives incorporating phenolic mannich base side chains inhibit microtubule and hemozoin formation: structure-activity relationship and *in vivo* oral efficacy studies, J. Med. Chem. 64 (2021) 5198–5215.

[26] D.S. Carter, R.T. Jacobs, Y.R. Freund, P.W. Berry, T. Akama, E.E. Easom, C.S. Lunde, F. Rock, R. Stefanakis, J. McKerrow, C. Fischer, C.A. Bulman, K.C. Lim, B.M. Suzuki, N. Tricoche, J.A. Sakanari, S. Lustigman, J.J. Plattner, Benzimidazole-benzoxaborole hybrids as an approach to the treatment of river blindness: part 2. ketone linked analogues, ACS Infect. Dis. 6 (2020) 180–185.

[27] M. Boiani, L. Boiani, A. Denicola, S.T. de Ortiz, E. Serna, N.V. de Bilbao, L. Sanabria, G. Yaluff, H. Nakayama, A.R. de Arias, C. Vega, M. Rolan, A. Gómez-Barrio, H. Cerecetto, M. González, 2*H*-Benzimidazole 1,3-dioxide derivatives: a new family of water-soluble anti-trypanosomatid agents, J. Med. Chem. (49) (2006) 3215–3224.

[28] C. Raynaud, W. Daher, M.D. Johansen, F. Roquet-Banères, M. Blaise, O.K. Onajole, A.P. Kozikowski, J.-.L. Herrmann, J. Dziadek, K. Gobis, L. Kremer, Active benzimidazole derivatives targeting the mmpl3 transporter in mycobacterium abscesses, ACS Infect. Dis. 6 (2020) 324–337.

[29] T.L. Mistry, L. Truong, A.K. Ghosh, M.E. Johnson, S. Mehboob, Benzimidazole-based FabI inhibitors: a promising novel scaffold for anti-staphylococcal drug development, ACS Infect. Dis. 3 (2017) 54–61.

[30] T.C. Kühler, M. Swanson, B. Christenson, B. Klintenberg, B. Lamm, J. Fägerhag, R. Gatti, M. Ölwegård-Halvarsson, V. Shcherbuchin, T. Elebring, J.-.E. Sjöström, Novel structures derived from 2-[[(2-pyridyl)methyl]thio]-1*h*-benzimidazole as anti-helicobacter pylori agents, Part 1, J. Med. Chem. 45 (2002) 4282–4299.

[31] Y.-.B. Bai, A.-.L. Zhang, J.-.J. Tang, J.-.M. Gao, Synthesis and antifungal activity of 2-chloromethyl-1*h*-benzimidazole derivatives against phytopathogenic fungi *in vitro*, J. Agric. Food Chem. 61 (2013) 2789–2795.

[32] Y.-.F. Li, G.-.F. Wang, P.-.L. He, W.-.G. Huang, F.-.H. Zhu, H.-.Y. Gao, W. Tang, Y. Luo, C.-.L. Feng, L.-.P. Shi, Y.-.D. Ren, W. Lu, J.-.P. Zuo, Synthesis and anti-hepatitis B virus activity of novel benzimidazole derivatives, J. Med. Chem. 49 (2006) 4790–4794.

[33] C. Ràfols, E. Bosch, R. Ruiz, K.J. Box, M. Reis, C. Ventura, S. Santos, M.E. Araújo, F. Martins, Acidity and hydrophobicity of several new potential antitubercular drugs: isoniazid and benzimidazole derivatives, J. Chem. Eng. Data 57 (2012) 330–338.

[34] M.K. Kim, H. Shin, K.-.S. Park, H. Kim, J. Park, K. Kim, J. Nam, H. Choo, Y. Chong, Benzimidazole derivatives as potent JAK1-selective inhibitors, J. Med. Chem. 58 (2015) 7596–7602.

[35] G. Chen, Z. Liu, Y. Zhang, X. Shan, L. Jiang, Y. Zhao, W. He, Z. Feng, S. Yang, G. Liang, Synthesis and anti-inflammatory evaluation of novel benzimidazole and imidazopyridine derivatives, ACS Med. Chem. Lett. 4 (2013) 69–74.

[36] J.M. Murray, Z.K. Sweeney, B.K. Chan, M. Balazs, E. Bradley, G. Castanedo, C. Chabot, D. Chantry, M. Flagella, D.M. Goldstein, R. Kondru, J. Lesnick, J. Li, M.C. Lucas, J. Nonomiya, J. Pang, S. Price, L. Salphati, B. Safina, P.P.A. Savy, E.M. Seward, M. Ultsch, D.P. Sutherlin, Potent and highly selective benzimidazole inhibitors of PI3-kinase delta, J. Med. Chem. 55 (2012) 7686–7695.

[37] H. Nimesh, S. Sur, D. Sinha, P. Yadav, P. Anand, P. Bajaj, J.S. Virdi, V. Tandon, Synthesis and biological evaluation of novel bisbenzimidazoles as *Escherichia coli* topoisomerase Ia inhibitors and potential antibacterial agents, J. Med. Chem. 57 (2014) 5238–5257.

[38] B. Das, H. Holla, Y. Srinivas, Efficient (bromodimethyl)sulfonium bromide mediated synthesis of benzimidazoles, Tetrahedron Lett. 48 (2007) 61–64.

[39] Y.X. Chen, L.F. Qian, W. Zhang, B. Han, Efficient aerobic oxidative synthesis of 2-substituted benzoxazoles, benzothiazoles, and benzimidazoles catalyzed by 4-methoxy-TEMPO, Angew. Chem. Int. Ed. 47 (2008) 9330–9333.

[40] J.-.P. Wan, S.-.F. Gan, J.-.M. Wu, Y. Pan, Water mediated chemoselective synthesis of 1,2-disubstituted benzimidazoles using *o*-phenylenediamine and the extended synthesis of quinoxalines, Green Chem. 11 (2009) 1633–1637.

[41] S.V. Ryabukhin, A.S. Plaskon, D.M. Volochnyuk, A.A. Tolmachev, Synthesis of fused imidazoles and benzothiazoles from (hetero)aromatic *ortho*-diamines or *ortho*-aminothiophenol and aldehydes promoted by chlorotrimethylsilane, Synthesis 21 (2006) 3715–3726.

[42] N.D. Kokare, J.N. Sangshetti, D.B. Shinde, One-pot efficient synthesis of 2-aryl-1-arylmethyl-1*H*-benzimidazoles and 2,4,5-triaryl-1*H*-imidazoles using oxalic acid catalyst, Synthesis 18 (2007) 2829–2834.

[43] F.A.S. Alasmary, A.M. Snelling, M.E. Zain, A.M. Alafeefy, A.S. Awaad, N. Karodia, Synthesis and evaluation of selected benzimidazole derivatives as potential antimicrobial agents, Molecules (20) (2015) 15206–15223.

[44] A.E. Sparke, C.M. Fisher, R.E. Mewis, S.J. Archibald, Synthesis, structure and reactivity of 1-(4-nitrobenzyl)-2-chloromethyl benzimidazole, Tetrahedron Lett. 51 (2010) 4723–4726.

[45] J.S. Peng, M. Ye, C.J. Zong, F.Y. Hu, L.T. Feng, X.Y. Wang, Y.F. Wang, C.X. Chen, Copper-catalyzed intramolecular C–N bond formation: a straightforward synthesis of benzimidazole derivatives in water, J. Org. Chem. 76 (2011) 716–719.

[46] N. Zheng, K.W. Anderson, X.H. Huang, H.N. Nguyen, S.L. Buchwald, A palladium-catalyzed regiospecific synthesis of *n*-aryl benzimidazoles, Angew. Chem. Int. Ed. 46 (2007) 7509–7512.

[47] D. Xue, Y.-.Q. Long, Metal-free TEMPO-Promoted C(sp^3)–H amination to afford multisubstituted benzimidazoles, J. Org. Chem. 79 (2014) 4727–4734.

[48] D.N. Kommi, P.S. Jadhavar, D.N. Kumar, A.K. Chakraborti, All-Water" one-pot diverse synthesis of 1,2-disubstituted benzimidazoles: hydrogen bond driven 'synergistic electrophile–nucleophile dual activation' by water, Green Chem. 15 (2013) 798–810.

[49] R. Chebolu, D.N. Kommi, D. Kumar, N. Bollineni, A.K. Chakraborti, Hydrogen-bond-driven electrophilic activation for selectivity control: scope and limitations of fluorous alcohol-promoted selective formation of 1,2-disubstituted benzimidazoles and mechanistic insight for rationale of selectivity, J. Org. Chem. 77 (2012) 10158–10167.

[50] A.K. Chaturvedi, A.S. Negi, P.A. Khare, Simple and straightforward synthesis of substituted 2-arylbenzimidazoles over silica gel, RSC Adv 3 (2013) 4500–4504.

[51] K. Bahrami, M.M. Khodaei, A. Nejati, Synthesis of 1,2-disubstituted benzimidazoles, 2-substituted benzimidazoles and 2-substituted benzothiazoles in SDS micelles, Green Chem 12 (2010) 1237–1241.
[52] J.G. Smith, I. Ho, Organic redox reactions during the interaction of *o*-phenylenediamine with benzaldehyde, Tetrahedron Lett. 38 (1971) 3541–3544.
[53] P.N. Preston, Synthesis, reactions, and spectroscopic properties of benzimidazoles, Chem. Rev. 74 (1974) 279–314.
[54] B.S. Furniss, A.J. Hannaford, P.W.G. Smith, A.R. Tatchell, *Vogel's Textbook* of *Practical Organic Chemistry*, 5th ed., John Wiley and Sons, New York, 1989.
[55] N. Jr. M.J. Frisch, G.W. Trucks, H.B. Schlegel, G.E. Scuseria, M.A. Robb, J.R. Cheeseman, G. Scalmani, V. Barone, G.A. Peterson, H. Nakatsuji, X. Li, M. Caricato, A.V. Marenich, J. Bloino, B.G. Janesko, R. Gomperts, B. Mennucci, H.P. Hratchian, J.V. Ortiz, A.F. Izmaylov, J.L. Sonnenberg, D. Williams-Young, F. Ding, F. Lipparini, F. Egidi, J. Goings, B. Peng, A. Petrone, T. Henderson, D. Ranasinghe, V.G. Zakrzewski, J. Gao, J.E. Peralta, F. Ogliaro, M.J. Bearpark, J.J. Heyd, E.N. Brothers, K.N. Kudin, V.N. Staroverov, T.A. Keith, R. Kobayashi, J. Normand, K. Raghavachari, A.P. Rendell, J.C. Burant, S.S. Iyengar, J. Tomasi, M. Cossi, J.M. Millam, M. Klene, C. Adamo, R. Cammi, J.W. Ochterski, R.L. Martin, K. Morokuma, O. Farkas, J.B. Foresman, D.J. Fox, Gaussian 16, Revision A.03 Gaussian, Inc., Wallingford CT, 2016. N. Jr..
[56] A.D. Becke, Density-Functional Thermochemistry. III. The role of exact exchange, J. Chem. Phys. 98 (1993) 5648–5652.
[57] C. Lee, W. Yang, R.G. Parr, Development of the Colle-Salvetti correlation-energy formula into a functional of the electron density, Phys. Rev. B 37 (1988) 785–789.
[58] J.N. Latosińska, M. Latosińska, J.K. Maurin, A. Orzeszko, Z. Kazimierczuk, Quantum-chemical insight into structure-reactivity relationship in 4,5,6,7-tetrahalogeno-1*H*-benzimidazoles: a combined X-ray, DSC, DFT/QTAIM, Hershfield surface-based, and molecular docking approach, J. Phys. Chem. A 118 (2014) 2089–2106.
[59] J. Pina, J.S.S. de Melo, R.M.F. Batista, S.P.G. Costa, M. Manuela, M. Raposo, Triphenylamine-benzimidazole derivatives: synthesis, excited-state characterization, and DFT Studies, J. Org. Chem. 78 (2013) 11389–11395.
[60] R.G. Pearson, Absolute electronegativity and hardness: applications to inorganic chemistry, Inorg. Chem. 27 (1988) 734–740.
[61] E.E. Elemike, D.C. Onwudiwe, H.U. Nwankwo, E.C. Hosten, Synthesis, crystal structure, electrochemical and anti-corrosion studies of Schiff base derived from *o*-toluidine and *o*-chlorobenzaldehyde, J. Mol. Struc. 1136 (2017) 253–262.

RJC

RASĀYAN *J. Chem.*
Vol. 16 | No. 3 |1462-1472| July - September | 2023
ISSN: 0974-1496 | e-ISSN: 0976-0083 | CODEN: RJCABP
http://www.rasayanjournal.com
http://www.rasayanjournal.co.in

SYNTHESIS AND SPECTRAL CHARACTERIZATION OF HIGH-PERFORMANCE SUPERCAPACITOR ZIF-67@rGO NANOCOMPOSITE ELECTRODE MATERIALS

S. Antony Sakthi[1], K. Priyadarshini[2], C. Mani[3] and S. Rusho Robin Prasad[4]
[1]Department of Chemistry, St. Joseph's College, (Autonomous), Affiliated to Bharathidasan University, Tiruchirappalli-620 002, India
[2]Department of Electronics and Communication Engineering, K.Ramakrishnan College of Engineering, Tiruchirappalli-621 112, India
[3]Dr.C. Mani LABS, Center for Green Energy, Tiruchirappalli-621 112, India
[4] Department of Chemistry, St. Joseph's College, (Autonomous), Affiliated to Bharathidasan University, Tiruchirappalli-620 002, India
Corresponding Author: santonysakthi@gmail.com

ABSTRACT

Over the past two decades, graphite (GO) and reduced graphene oxide (rGO) two-dimensional materials have been found to be very valuable applied materials. Graphene acts as an electron transfer agent and performs well as an electrode material in supercapacitors. However, mass production of graphene remains a major challenge. According to this research paper, naturally occurring graphite from the earth is refined and re-extracted. Hummer's method was used to prepare graphene oxide from well-purified flake graphite with the addition of both H_2SO_4 as a guest and $KMnO_4$ as an oxidizing agent. Recently, ZIF-67@rGO nanocomposites have been widely used due to their high surface area, uniform porosity, and relatively high thermal and chemical stability.When comparing graphite and graphene oxide, graphene oxide spacing distance is much more than graphite. It is well known that graphene oxide contains a large number of oxygen-containing functional groups due to graphite oxidation. Another common feature of rGO is that fold-like structures are observed on both the surface and edges of rGO. Also,ZIF-67@rGO nanocomposite was prepared by mixing equal amounts of crystalline ZIF-67 and very fine rGO powder using a simple hydrothermal and stirring method. Such instruments FT-IR, XRD, UV, and SEM have been used to characterize the consequences of these factors on the structure and attribute of GO, rGO, and ZIF-67@rGO. In general, looking at the results and properties of rGO/ZIF-67 air gel, it is confirmed that this nanocomposite material is an alternative composition for use as an electrode material for electrodes in symmetric supercapacitor storage devices.

Keywords: Synthesis of Nanocomposites, High-Performance Electrode Material, ZIF-67@rGoNanocomposites, Reduced Graphene Oxide, Supercapacitor Storage Devices.

RASĀYAN *J. Chem.*, Vol. 16, No. 3, 2023

INTRODUCTION

Environmental concerns that continue to grow in today's era are currently motivating researchers with energy needs to suggest alternative technology should be developed to save more energy. Li-ion batteries exhibit higher energy density but do not need to have a longer life cycle in an environment where lithium-based rechargeable batteries and EDLC supercapacitors have attracted more attention. Additionally, all things considered, the EDLCs supercapacitor was considered a good alternative. This is because they exhibit high power densities and long-life cycles, but mainly moderate levels of energy density. Realizing both of these makes it clear that only the EDLC supercapacitor will be better suited for future upheavals because this supercapacitor can deliver both high energy and very much high power density.[1-3]

There is no doubt that such supercapacitors are applicable for electronic implementation, hybrid electric vehicles (HEVs), and compact power supply and pulsed electronics devices.[4] Metal-Organic Frameworks, which have been continuously developed since the past, uses like this such as gas storage, and energy storage devices such as a supercapacitor, catalysts, biosensors, and solar cells in general.[5] MOFs are characterized by a variety of unique properties, Significantly higher surface area, more hierarchical pore

http://doi.org/10.31788/RJC.2023.1638206

size distribution, and higher chemical and thermal stability.[6] Currently a wide variety of MOFs have been recommended, due to the high porosity structures at the potential electrodes in the supercapacitor. All previously used MOFs have very low electrical conductivity, and this conclusion states that not all electrodes based on metal-organic frameworks (MOF) give efficient charge transfer to the current collector. MOFs may have certain limitations, which can be remedied by adding their compounds with other carriers such as graphene oxide and polymer conductive materials. This is because the conductive compounds in MOFs have a high surface area, its properties are a positive factor over a competing electrode and another shape of carbon. Salunge*et al*. prepared a nanocomposite material containing integrated metal-organic frameworks (MOF-ZIF-8) and polyaniline (PANI) and then used these composites as electrode materials of a supercapacitor and tested them with 1M H_2SO_4 aqueous electrolyte solution and published their results, and the electrode in this supercapacitor showed capacitance values of 236 Fg-1 at a constant current density of 1A g^{-1}.It is confirmed that this hybrid electrode provides good specific capacitance values by using the UIO-66 composite with the presence of rGO in 1 M KOH electrolyte solution.[7-9] However, this specific capacitance value can only be achieved at very low current densities, for instance, 0.15A g^{-1}.

It is proposed that Mn-Metal Organic Frameworks(MOF) derivational from Mn_3O_4-Grapheneoxide(GO) based on the nanocomposite supercapacitor electrodes can provide a capacitance value it comes to around 546 F g^{-1}at1A g^{-1}.[10-12] Xu *et al.* Issued a statement saying that the ZIF-67/polypropylene nanotubes-based nanocomposite electrode to obtained maximum capacitance values of 597.6Fg^{-1} at 0.5Ag^{-1}(1M Na_2SO_4=electrolyte).[13]Different types of MOF established electrodes was used to design substantial capacitance values of supercapacitor.[14-16] According to literature studies, while most MOF-based supercapacitors were studied in the presence of aqueous electrolytes, the overall performance of the assembled device was not reported.

Generally, the properties of the electrode and electrode materials used in a symmetric supercapacitor significantly affect the output parameters of the asymmetry supercapacitor like energy density, power density, specific capacitance, and cycle life stability to some extent. The overall high achievement of a supercapacitor follows the following characteristics, which demonstrate that electrolytes are important stakeholders in achieving energy density and cycle stability.[17-18]In addition, all the commonly used electrolytes can be listed below, namely, aqueous, organic solution, potassium iodide, $K_3[Fe(CN)_6$, and hydroquinone.[19-20]All these are especially miscible with aqueous electrolytes (eg KOH, H_2SO_4, and Na_2SO_4).[21]To further improve the electrochemical performance in supercapacitors, studies have suggested adding redox additive electrolytes (RAEs) to these symmetric supercapacitor electrodes.[22-23] A number of studies have been carried out on supercapacitor electrode materials; it is based on graphene oxides, metal oxides, and metal hydroxides.[24]As far as we are concerned, any other published data were not available to appraise the achievement of the performance of supercapacitors with the presence of these aqueous electrolytes with MOF or MOF-based composites.

Recent research suggests that the preparation of ZIF-67@rGO nanocomposite is very simple, highly porous, acid-free, agitated, and environment-friendly. When ZIF-67 is mixed with rGO, which gives a high surface area (947m^2g^{-1}), also, the composites also become more porous and have higher electrical conductivity. It is clearly known that ZIF-67@ rGO introduces an enhancement throughout the composite; generally, properties of the mobility of electrons and ion diffusivity are much analogized to the ZIF-67 nanocomposite. The results of our studies on the ZIF-67/rGO redox system revealed that this offers much more specific capacitance values and high energy densities, in addition to outstanding cyclic stability. This research led to the creation of a symmetric supercapacitor by combining two identical electrodes to fabricate a symmetric supercapacitor storage system.

The newly fabricated symmetric supercapacitors offer higher capacitance value and remarkable energy density differentiating from previously published MOF-based supercapacitor storage devices. Also, the electrochemical performance of two separate symmetric supercapacitors with parallel and series connections will be experimentally demonstrated. According to the general opinion and knowledge of researchers and authors, the prepared ZIF-67/rGO nanocomposite is an excellent high-performance supercapacitor which is the first report.

EXPERIMENTAL

Materials

Various chemicals, solvents, reagents, and chemical salts were used for this study without any further purification. Micronized grained fine grade ($Co(NO_3)_2$•$6H_2O$) cobalt nitrate hexahydrate and graphite powder, ($KMnO_4$) Potassium permanganate, (HCl) hydrochloric acid, (H_2SO_4) sulfuric acid and Ethylene glycol all these were procured from SISCOCHEM laboratory chemical company in India, (H_2O_2) hydrogen peroxide, ($NaNO_2$) sodium nitrate,(KOH) potassium hydroxide and (N_2H_4.H_2O) hydrogen hydrates were purchased from Merck, India, and polytetrafluoroethylene (PTFE) from Ecochem, Mumbai.

Methods of Making Graphene Oxide (GO)

GO was prepared using micron-sized flake graphite powder as a raw source using a (modified Hummers method).[25]According to Fig.-1, concisely, graphite powder and $KMnO_4$ the weight ratio of the mixture (1:5) i.e., (2g graphite powder +10g $KMnO_4$) was mixed well, and then added 150ml H_2SO_4 to the above- mentioned contents it causes a reaction and a form of energy is released in the form of heat which is called an (exothermic) reaction and further external heating was applied to the above contents, the temperature of this chemical reaction mixture was slowly increased from 30°C to 35°C. The temperature of these contents was gradually raised to 50°C and continuously stirred at constant temperature for 2 hours. Following this, the heated reaction mixture was equilibrated to room temperature RT (27 ± 1 °C) to cool its temperature, It was then placed in an ice bath to which 30% hydrogen peroxide was added and mixed thoroughly. Eventually, the reaction mixture was subjected to centrifuge for 10 min at 8000rpm to remove all the unwanted elements such as unreacted carbons and acid mineral content. The GO composites thus prepared were thoroughly washed many times with double distilled water followed by two more washes with 30% HCl and finally washed with ethanol. Previously prepared and purified graphene oxide it has been thoroughly desiccated, at 90°C.The well-dried material should be manually crushed and stored at room temperature prior to preservation.

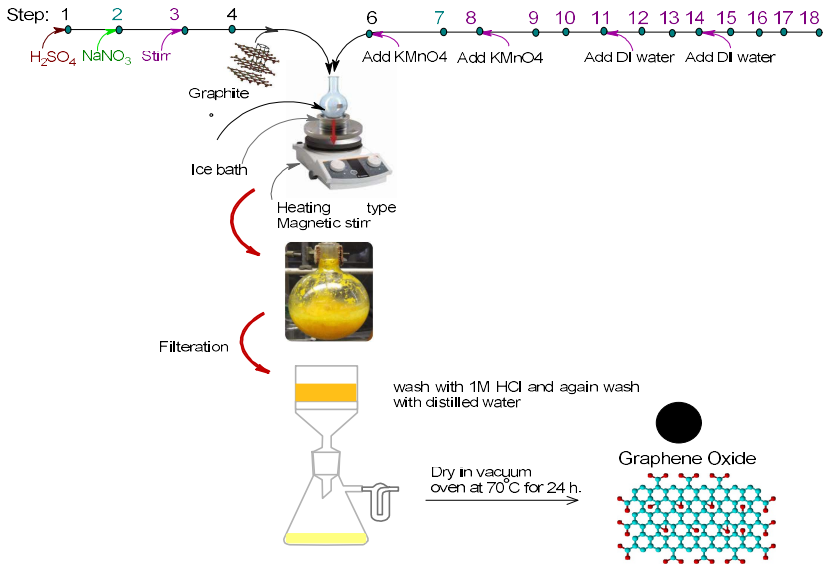

Fig.-1: Schematic Procedure for GO Preparation

Synthesis of rGO

For some comparative studies, graphene oxide was prepared using the reducing agent hydrogen hydrate. 15ml (1 mg mL^{-1}) of hydrogen hydrate was added to an aqueous dispersion of graphene oxide and mixed well, then continuously stirred at 90°C for 6 h at a constant temperature.After the chemical reaction was over, it was centrifuged at 800 rpm for 10 minutes;then the settled black-colored precipitate was separated. Then the separated sample was washed with deionized water several times.

Synthesis of ZIF-67

As shown in Fig.-2, two beakers should be taken separately and thoroughly washed with deionized water, then in the first beaker take 15ml of deionized water and add 500mg of $Co(NO_3)_2.6H_2O$ to dissolve well, in the second beaker take 25ml of deionized water and add 600mg of 2-methylimidazole and dissolve well. After this, the two solutions should be combined and stirred very vigorously at 60°C. After doing this for some time, the well-mixed mixture gradually turned into a milky colloidal dispersion.[26] Then after 20 minutes, the stirring should be stopped completely and then this mixture should be kept undisturbed for 20 hours. After all this, the dispersion was centrifuged and filtered; the filtered mixture was washed thoroughly with methanol and heated continuously at 150°C for 9 hours.

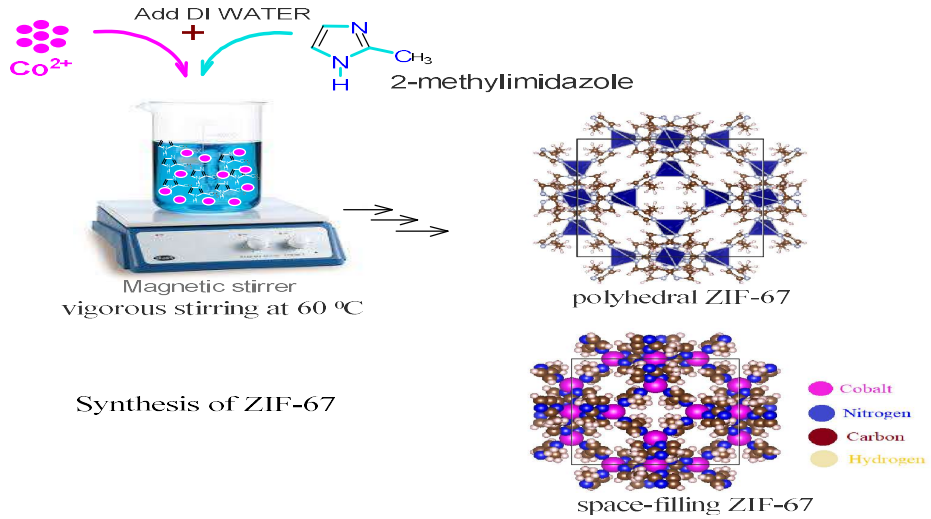

Fig.-2:Schematic Synthesis of the ZIF-67 Material

Preparation of ZIF-67/rGO Composite

Take two beakers separately and add 5mL and 10mL amounts of deionized water in which Cobalt nitrate hexahydrate (500 mg) and graphene oxide (50mg) were dispersed respectively. Graphene oxide should be sonicated for two hours to obtain clear dispersion; this should be followed by the addition of 7-gram 2MI (2-methylimidazole linker). All the ingredients mentioned below, especially the metal solution, graphene oxide, and organic binders were added and heated at a moderate temperature and stirred well continuously for 6 hours.[27-28]Following the completion of all reactions, the ZIF-67@rGO nanocomposite mixture was recovered by centrifugation and then filtered.The filtered mixture was again washed twice with double distilled water and again thoroughly washed with methanol and thoroughly dried under vacuum at 80°C for 2 hours.

RESULTS AND DISCUSSION

MOF-based nanocomposites offer many advantages due to their enormoussurface area and dependence on nano-hierarchical pore size distribution. When graphene oxide and ZIF-67 form a hybrid structure together, they provide synergistic benefits to each other. ZIP-67 with polyhedral crystal structures are decorated with 2D graphene oxide materials, resulting in these composite achieving properties such as more surface area, high porosity, high capacitance value, and emphasizedcharge transfer. Detailed studies about the properties ofprepared nanocomposite and potential applications of electrode materials in supercapacitor electrodes are detailed in the following section.Various nanocrystal structures of ZIF-67 are shown in Fig.-3, 4, and 5, and ZIF-67 XRD structural information is shown in Fig.-6. The nanocrystal structure of nanocomposites is shown in Fig.-7and 8.The reference patterns (XRD) of ZIF-67@rGO nanocomposite are analyzed to obtain structural information such as crystal structures as shown in Fig.-9, and the characteristic diffraction peaks of ZIF-67@rGO MOF are well displayed.This observation of ZIF-67 incorporation into the prepared nano-composite indicates successful integration.Significant peaks when analyzing ZIF-67/rGO by XRD can be identified and listed as follows: 7.0° (011), 10.5° (002), 12.7° (112), 14.5° (022), 16.0° (013), 18.0° (222), 22.1° (114), 24.0° (233), 25.6° (002), 25.0° (134),

29.6° (044), 31.3° (244), 37.0° (235), and 43.1° (100). Specifically, the 2θ very low-intensenesspeak appeared at 25.6°(002) showing the presence of rGOin the Crystallography Open Database (COD-7222297, ZIF-67@rGO). It can be stated as follows that in respect of rGO, many diffraction peaks are not reflected because of its single to few-layered structure. Therefore, the ZIF-67@rGO nanocomposite analyzed by XRD provides detailed evidence of its successful crystal formulation, so it is a special feature.

Summary

$C_{250.33}$ $H_{239.03}$ Co_{24} $N_{125.16}$ $O_{93.65}$
Space Group: C m c e (#64-1)
a = 24.11298 Å α = 90.0000°
b = 16.94684 Å β = 90.0000°
c = 19.73992 Å γ = 90.0000°
V = 8066.4975 Å^3

Title $C_{250.33}H_{239.03}Co_{24}N_{125.16}O_{93.65}$

Lattice type	C
Space group name	C m c e
Space group number	64
Setting number	1

Lattice parameters

a	b	c	α	beta	gamma
24.11298	16.94684	19.73992	90.0000	90. 0000	90.0000

Unit-cell volume = 8066.497458 Å^3

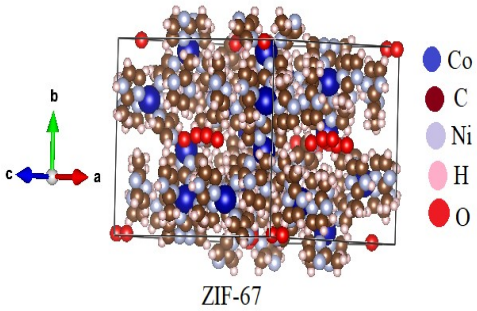

Fig.-3: ZIF-67 Space Filling

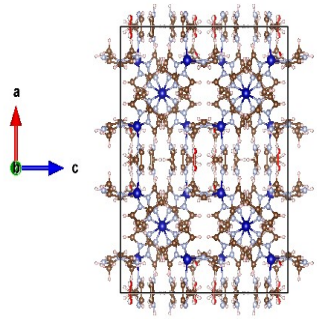

Fig.-4:ZIF-67 Stick and Ball

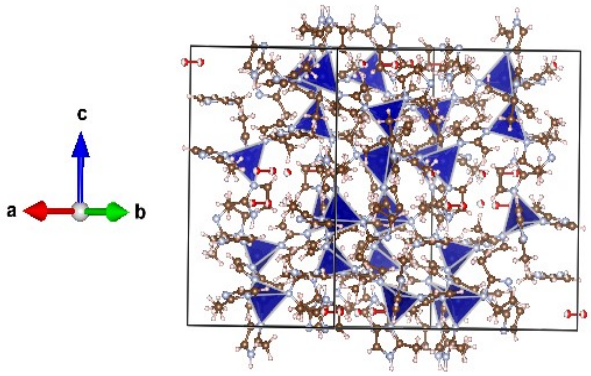

Fig.-5. ZIF-67 Polyhedral

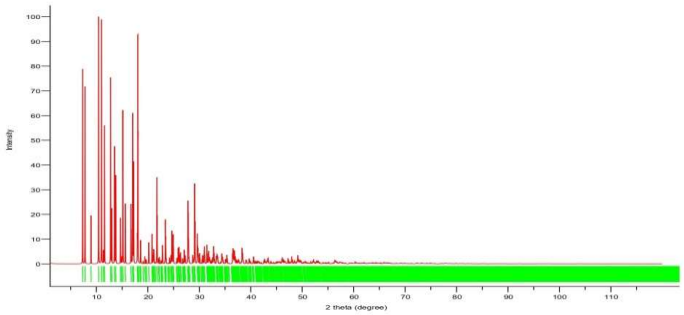

Fig.-6: Prepared ZIF-67Nanocomposite Material XRD Pattern

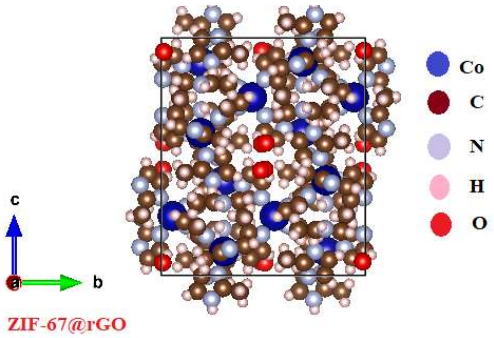

Fig.-7:ZIF-67@rGO Space Filling

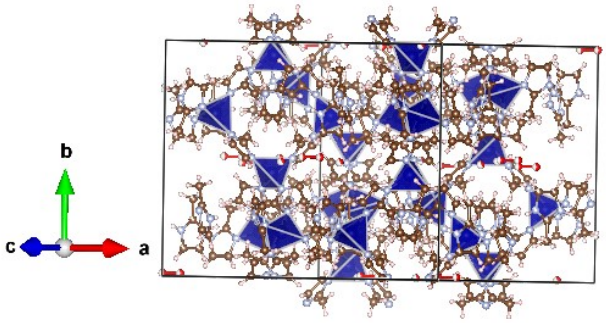

Fig.-8:ZIF-67@rGO Polyhedral

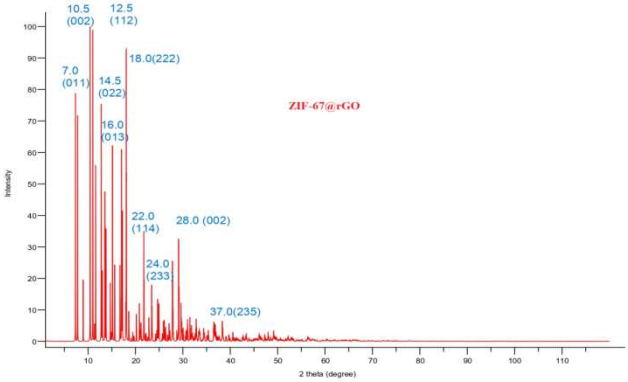

Fig.-9:Detailed XRD Patterns of ZIF-67/rGO

The morphology of the sample was examined by using the field emission scanning electron microscopy (FESEM) technique. Figure-10a, clearly indicates the bulk morphology of nanocomposite with crystalline 3D polyhedral structural shape and the average size of which is 200nm.

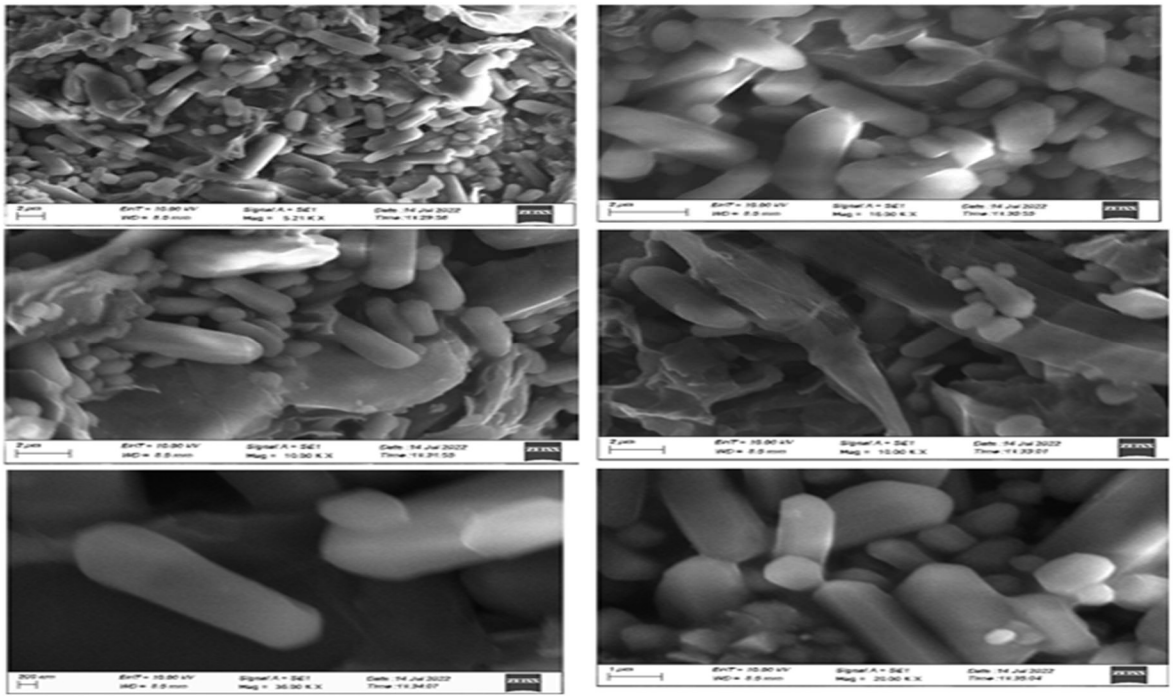

Fig.-10(a): FESEM Images of ZIF-67/rGO

The growth of the ZIF-67/rGO nanocomposite demonstrated that the MOF crystals grew transparently and uniformly on the rGO paper sheet-like surface. FESEM suggests a proposed approach for morphological and micro-structural analysis, the prepared ZIF-67/rGO composites led to the formation of desirable composites that largely preserve the features of both components. A symmetric supercapacitor

ensures instantaneous charge storage in the supercapacitor due to the very quick diffusion of electrolyte ions across the electrodes.The introduction of the high-porosity nanocomposite as the electrode material in supercapacitors further benefits from greatly improved performance.Thevarious structural information such as surface plots of the prepared nanocomposite has been presented in Fig.-11. Area, length, and summary of particle size have been listed in Fig.-12a, Fig.-12b and Fig.-12c.

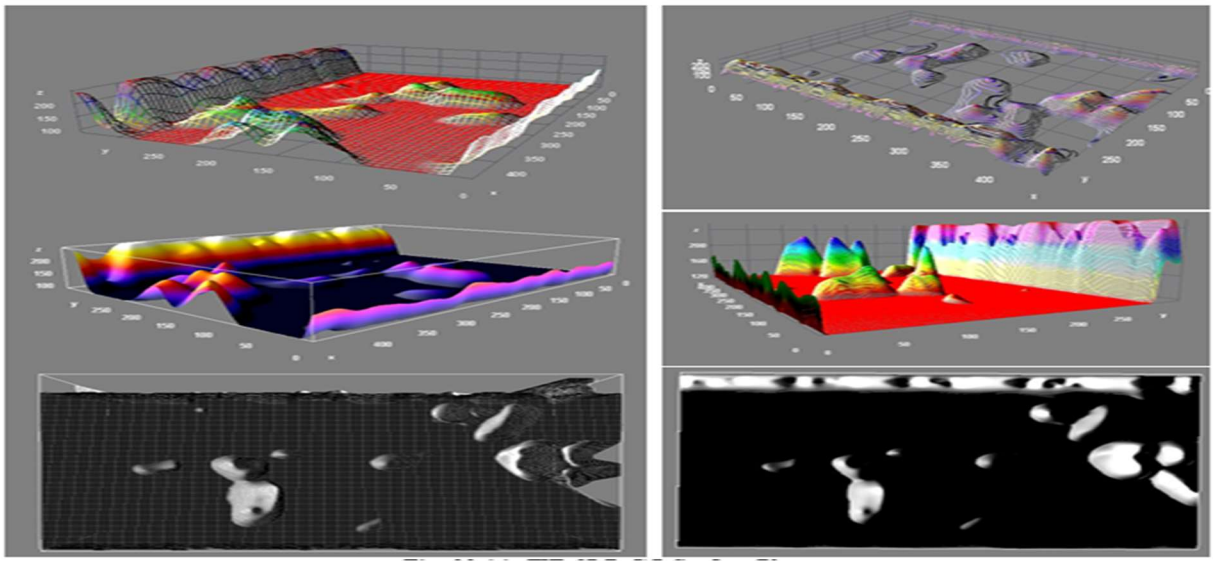

Fig.-11: ZIF-67@rGO Surface Plot

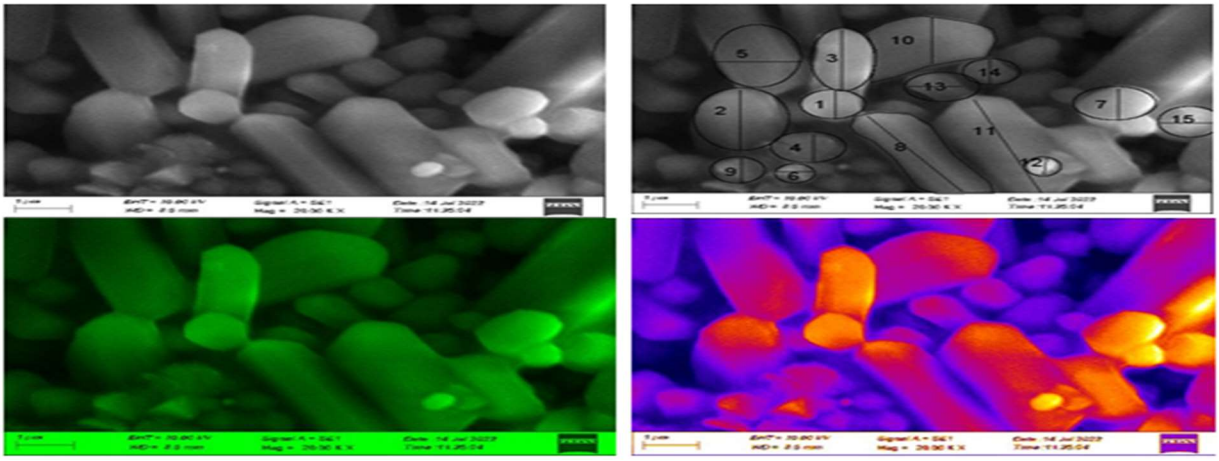

Fig.-12(a): ZIF-67@rGO Nanoparticles

All the functional groups peaks of ZIF-67/rGO nanocomposite are clearly seen in Fig.-13, ZIF-67@rGO composite gives a very strong intensity broad band at 3439 cm^{-1} which indicates the of O-H group. The IR peaks at 2924 cm^{-1} and 2868 cm^{-1} are attributed to C-H stretching and bending in GO respectively.

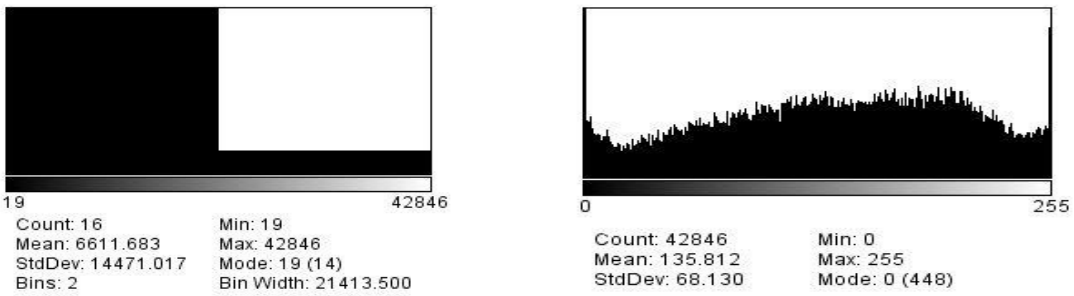

Area Distribution Histogram

Fig.-12(b): ZIF-67@rGO Surface Plot Area Distribution and Histogram

NanoPlus
Common

Intensity Distribution S/N : 411615

User	: Common	Group	:	Repetition	: 1/1
Date	: 09-Sep-22	File Name	: Z1F-67		
Time	: 10:02:19	Sample Information	:		
SOP Name	: SJC Size Method			Security	: No Security

Version 5.22 / 3.00

Intensity Distribution

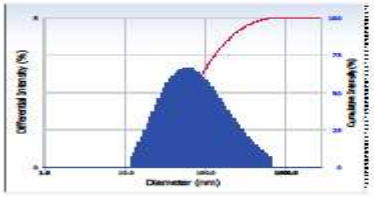

ACF

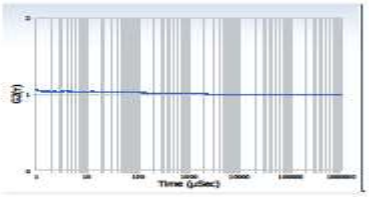

Distribution Results (Contin)

Peak	Diameter (nm)	Std. Dev.
1	112.7	113.5
2	0.0	0.0
3	0.0	0.0
4	0.0	0.0
5	0.0	0.0
Average	112.7	113.5
Residual :	4.971e-002	(N.G)

Cumulants Results

Diameter	(d)	: 111.1	(nm)
Polydispersity Index	(P.I.)	: 0.470	
Diffusion Const.	(D)	: 4.430e-008	(cm²/sec)

Measurement Condition

Temperature	: 25.0	(°C)
Diluent Name	: WATER	
Refractive Index	: 1.3328	
Viscosity	: 0.8878	(cP)
Scattering Intensity	: 30826	(cps)
Attenuator 1	: 7.28	(%)

Intensity Distribution Table

d (nm)	f(%)	f(cum.%)	d (nm)	f(%)	f(cum.%)	d (nm)	f(%)	f(cum.%)	d (nm)	f(%)	f(cum.%)
1.0	0.0	0.0	7.4	0.0	0.0	55.1	3.3	40.8	408.8	0.8	96.8
1.1	0.0	0.0	8.0	0.0	0.0	59.7	3.3	44.2	442.9	0.7	97.5
1.2	0.0	0.0	8.7	0.0	0.0	64.7	3.3	47.5	479.9	0.6	98.2
1.3	0.0	0.0	9.4	0.0	0.0	70.1	3.3	50.8	519.9	0.6	98.8
1.4	0.0	0.0	10.2	0.0	0.0	75.9	3.3	54.1	563.3	0.5	99.2
1.5	0.0	0.0	11.1	0.0	0.0	82.2	3.2	57.2	610.4	0.4	99.6
1.6	0.0	0.0	12.0	0.3	0.3	89.1	3.1	60.4	661.3	0.4	100.0
1.8	0.0	0.0	13.0	0.5	0.8	96.5	3.0	63.4	716.5	0.0	100.0
1.9	0.0	0.0	14.1	0.6	1.5	104.6	2.9	66.3	776.3	0.0	100.0
2.1	0.0	0.0	15.3	0.8	2.3	113.3	2.8	69.1	841.1	0.0	100.0
2.2	0.0	0.0	16.5	1.0	3.3	122.8	2.7	71.8	911.3	0.0	100.0
2.4	0.0	0.0	17.9	1.2	4.5	133.0	2.6	74.4	987.4	0.0	100.0
2.6	0.0	0.0	19.4	1.4	6.0	144.2	2.4	76.9	1069.8	0.0	100.0
2.8	0.0	0.0	21.0	1.7	7.6	156.2	2.3	79.2	1159.2	0.0	100.0
3.1	0.0	0.0	22.8	1.9	9.5	169.2	2.2	81.4	1255.9	0.0	100.0
3.3	0.0	0.0	24.7	2.1	11.6	183.4	2.0	83.4	1360.8	0.0	100.0
3.6	0.0	0.0	26.8	2.3	13.9	198.7	1.9	85.3	1474.3	0.0	100.0
3.9	0.0	0.0	29.0	2.5	16.4	215.2	1.8	87.1	1597.4	0.0	100.0
4.2	0.0	0.0	31.4	2.7	19.0	233.2	1.6	88.7	1730.8	0.0	100.0
4.6	0.0	0.0	34.0	2.8	21.8	252.7	1.5	90.2	1875.3	0.0	100.0
5.0	0.0	0.0	36.9	2.9	24.8	273.8	1.4	91.6	2031.8	0.0	100.0
5.4	0.0	0.0	40.0	3.1	27.8	296.6	1.3	92.9	2201.4	0.0	100.0
5.8	0.0	0.0	43.3	3.2	31.0	321.4	1.1	94.0	2385.2	0.0	100.0
6.3	0.0	0.0	46.9	3.2	34.2	348.2	1.0	95.1	2584.3	0.0	100.0

Fig.-12(c): Intensity Distribution Curve

Alkenes skeleton of C=C bond in graphene oxide, the stretching vibration of this C=C bond usually produces a moderate band around 1621cm^{-1}.A strong intensive peak appears at 1670 cm^{-1}, which is attributed to the C=O stretching vibration of the carbonyl group. The reduction of GO is characterized by FT-IR spectroscopy, and given Fig.-13, the peaks with reduced graphene oxide oxygen-containing functionalities are all reduced compared to graphene oxide. Also shown here is the successful reduction of graphene oxide when a hydrogen-hydrate ($NH_2.NH_2.H_2O$) reducing agent is used.

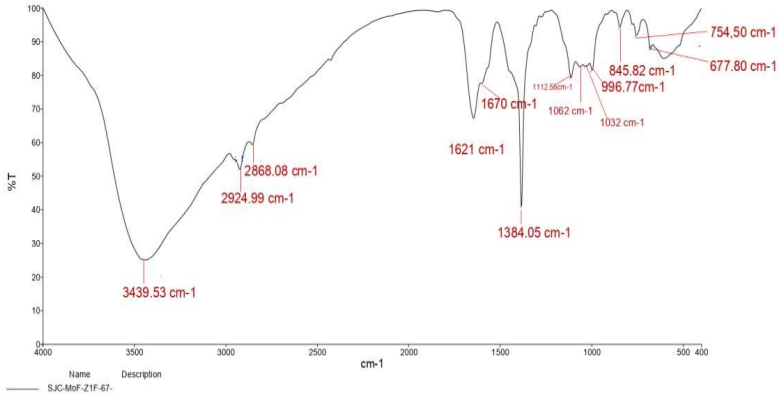

Fig.-13: FTIRSpectra of ZIF-67/rGOComposites

CONCLUSION

It is believed that the newly prepared ZIF-67/rGO nanocomposite can be used as electrode material in symmetric supercapacitor energy storage devices compared to other nanocomposite materials.A simple hydrothermal method was used to prepare these new nanocomposite materials by taking equal amounts of ZIF-67 and rGO. The Hummer method was used for the first time to prepare graphene oxide with this huge surface area, followed by the successful preparation of rGO with the help of $NH_3.H_2O$aqueous and hydrazine hydrate($NH_2.NH_2.H_2O$). It was noted in the Journal of Nanomaterials[5] that the interlayer spacing of graphene oxides was much larger than graphite. The morphology of the graphite powder was completely changed and then completely oxidized; due to this process, many oxygens functional groups were found in the graphene oxide.Typical fold morphologies were observed on both the rGO surface and edge. When compared with the traditional Chemical Vapor Deposition(CVD) method, the recently developed Hummers' method has been proven to be able to synthesize GO on a large scale, and then Rgo-reduced graphene oxide can be prepared using a reducing agent, which has a very low production cost. Briefly described, the overarching objective of this research paper is to focus on the recent advancement based on this consistently controlled synthesis of ZIF-67@rGO-based materials as amalgamated electrode material. The above-indicated ZIF-67@rGO nanocomposite has been a prime choice for comparing different preparation technique and their implementation in earlier times because this composite has many unique features such as more active sites, solid stability, and huge surface area. Generally speaking, all ZIF-67@rGO-based nanocomposites to be prepared are environmentally friendly and have high productivity at a low cost.Based on the above-mentioned statement, this study is seen as the main objective of the paper. Furthermore,the heterogeneous catalyst ZIF-67 can be used for low-cost production for commercial applications. Especially, it meets the economic and environmentally friendly requirements.Taken as a whole, a prerequisite for the widespread use of the Zip-67 heterogeneous catalysts is the high-quality aspect of the compound and the low-cost mass production of its derivatives. Therefore, it is felt that the applications of ZIF-67@rGO nanocomposite-based heterogeneous catalysts in extensive industrial production should be further developed in the future keeping in mind the following objectives for realizing and mass production.(i) Exclusivelymore attention should be given to exploring novel synthetic methods to increase acertain amount of ZIF-67-based nanocomposite materials in the way ofeconomically feasible strategies without high cost and non-toxicity.(ii) Most of the ZIF-67-based nanocomposite materials are nanoporous in size (diameter of the pore < 2nm). It is felt that their applications are restricted due to steric hindrance effects as they contain large molecules. Therefore, it is necessary to integrate micro-, meso-, and macropores of the crystal form of nanoporous ZIF-67-based materials to enhance the reduced mass resistance and diffusion rate. (iii) The immovability and maturity permanence of ZIF-67-based materials especially under harsh conditions must be solved if proper stability, chemical stability, and thermal and mechanical stability are to be used in various modern applications.

ACKNOWLEDGMENTS

A.S., I would like to acknowledge the Department of Chemistry, St, Joseph's College, Tiruchirappalli-620 002, India, for providing infrastructure facilities. K.P. also thanks the Director and Principal of K. Ramakrishnan College of Engineering, Tiruchirappalli-621 112, India, for encouraging research activities. C.M. author also expresses sincere thanks to all Dr.C. Mani *L A B S* team members for their kind co-operations.

CONFLICT OF INTERESTS

All the authors expressly declare that there is no conflict of interest in publishing this research paper in the journal.

AUTHOR CONTRIBUTIONS

All the authors contributed significantly to this manuscript, participated in reviewing/editing and approved the final draft for publication. The research profile of the authors can be verified from their ORCID ids, given below:

S. Antony Sakthi https://orcid.org/0000-0001-6668-9005
K. Priyadarshini https://orcid.org/0000-0002-7513-5028

C. Mani https://orcid.org/0000-0001-5360-8245
S. Rusho Robin Prasad https://orcid.org/0009-0007-0365-0999

REFERENCES

1. P.G. Bruce, S.A. Freunberger, L. J. Hardwick, J. Tarascon, *Nature Materials*, **11(1)**, 19(2012), https://doi.org/10.1038/nmat3191
2. R. Ramachandran, S. M. Chen, G. Kumar, *International Journal of Electrochemical Science*, **10**, 10355(2015)
3. C. Liu, F. Li, L. P. Ma, H. M. Cheng, *Advanced Materials*, **22 (8)**, 28(2010), https://doi.org/10.1002/adma.200903328.
4. E. Frackowiak, F. Beguin, *Carbon*, **40(10)**, 1775(2002), https://doi.org/10.1016/S0008-6223(02)00045-3
5. M. Sharma, S. Sundriyal, A. Panwar, A. Gaur, *Journal of Alloys Compounds*, **766**, 859(2018), https://doi.org/10.1016/j.jallcom.2018.07.019
6. V. Kaur, K. H. Kim, A. K. Paul, A. Deep, *Journal of Material Chemistry A*, **4(11)**, 3991(2016), https://doi.org/10.1039/C5TA09668E
7. S. Sundriyal, V. Shrivastav, H. Kaur, S. Mishra, A. Deep, *ACS Omega*, **3(12)**, 17348(2018), https://doi.org/10.1021/acsomega.8b02065
8. S. Kempahanumakkagari, K. Vellingiri, A. Deep, E.E. Kwon, N. Bolan, K-H.Kim, *Coordination Chemistry Reviews*, **357**, 105(2018),https://doi.org/10.1016/j.ccr.2017.11.028
9. R. R. Salunkhe, J. Tang, N. Kobayashi, J. Kim, Y. Ide, S. Tominaka, J.H. Kim, Y. Yamauchi, *Chemical Sciences*, **7**, 5704(2016), https://doi.org/10.1039/C6SC01429A
10. Y. Zhao, J. Liu, M. Horn, et al., *Science China Materials*, **61**, 159(2018), https://doi.org/10.1007/s40843-017-9153-x
11. K. Zhao, K. Lyu, S. Liu, Q. Gan, Z. He, Z. Zhou, *Journal of Material Science*, **52(1)**, 446(2016), http//doi:10.1007/s10853-016-0344-3
12. X. Xu, J. Tang, H. Qian, S. Hou, Y. Bando, M. S. A. Hossain, L. Pan, Y.Yamauchi, *ACS Applied Materials & Interfaces*, **9**, 38737(2017), https://doi.org/10.1021/acsami.7b09944
13. L. Shao, Q. Wang, Z. Ma, Z. Ji, X. Wang, D. Song, Y. Liu, N. Wang, *Journal of Power Sources*, **379**, 350(2018), https://doi.org/10.1016/j.jpowsour.2018.01.028
14. P. Du, Y. Dong, C. Liu, W. Wei, D. Liu, P. Liu, *Journal of Colloid and Interface Science*, **518**, 57(2018), https://doi.org/10.1016/j.jcis.2018.02.010
15. T. Brousse, D. Belanger, J.W. Long, Journal of the Electrochemical Society, **162(5)**, A5185(2015), https://doi.org/10.1149/2.0201505JES
16. A.Farisabadi, M. Moradi, S. Borhani, S. Hajati, M.A. Kiani, S.A.Tayebifard, *Journal of Materials Science: Materials in Electronics*, **29**, 8421(2018), https://doi.org/10.1007/s10854-018-8853-2
17. K. Jayaramulu, D.P. Dubal, B. Nagar, V. Ranc, O. Tomanec, M. Petr, K. K. R. Datta, R. Zboril, P. Gomez-Romero, R. A. Fischer, *Advanced Materials*, **30**, 1705789(2018), https://doi.org/10.1002/adma.201705789
18. C. Zhao, W. Zheng, X. Wang, H. Zhang, X. Cui, H. Wang, *Scientific Reports*, **3**, 2986(2013), https://doi.org/10.1038/srep02986
19. B.Nagar, D.P. Dubal, L. Pires, A. Merkoci, P. Gomez-Romero, *ChemSusChem*, **11**, 1849(2018), https://doi.org/10.1002/cssc.201800426
20. C. Zhong, Y. Deng, W. Hu, J. Qiao, L. Zhang, J. Zhang, *Chemical Society Reviews*, **44**, 7484(2015), https://doi.org/10.1039/C5CS00303B
21. P. J. Hall, M. Mirzaeian, S.I. Fletcher, F.B. Sillars, A.J.R. Rennie, G. O. Shitta-Bey, G. Wilson, A. Cruden, R. Carter, *Energy & Environmental Science*, **3**, 1238(2010), https://doi.org/10.1039/C0EE00004C

22. S. T. Senthilkumar, R. K. Selvan, J.S. Melo, *Journal of Material Chemistry A*, **1**, 12386(2013), https://doi.org/10.1039/C3TA11959A
23. N. R. Chodankar, D. P. Dubal, A.C. Lokhande, A.M. Patil, J.H. Kim, C.D. Lokhande, *Scientific Reports*, **6**, 39205(2016), https://doi.org/10.1038/srep39205
24. J.-M. Tarascon, M. Armand, *Nature*, **414**, 359(2001), https://doi.org/10.1038/35104644
25. A. Hosseinian, A. Amjad, R.Hosseinzadeh-Khanmiri, E. Ghorbani-Kalhor, M. Babazadeh, E. Vessally, *Journal of Materials Science: Materials in Electronics,* **28**, 18040(2017), https://doi.org/10.1007/s10854-017-7747-z
26. R. Naveen S. K. Shahenoor Bash and M.C. Rao, *Rasayan Journal of Chemistry*, **11(1)**, 195(2018), http://dx.doi.org/10.7324/RJC.2018.1112016
27. Purushotham Endla, *Rasayan Journal of Chemistry*, **12(4)**, 1676(2019), http://dx.doi.org/10.31788/RJC.2019.1245132
28. K. Khairan, Zahraturriaz and Z. Jalil, *Rasayan Journal of Chemistry*, **12(1)**, 50(2019), http://dx.doi.org/10.31788/RJC.2019.1214073

[RJC- 8206/2022]

Chemical Papers
https://doi.org/10.1007/s11696-023-03297-y

ORIGINAL PAPER

Facile green synthesis of gelatin sodium alginate cerium oxide hydrogel nanocomposite and their photocatalytic and its biological applications

A. S. Stella Shalini[1] · L. Shahanaz[1] · P. Rajeswaran[2] · R. Tamilarasan[2] · S. Kumaran[3] · P. Siva Karthik[4]

Received: 18 July 2023 / Accepted: 18 December 2023

Abstract

In this study, we harnessed the potential of a plant extract derived from *Oldenlandia umbellata,* a member of the Rubiaceae family, as a biological reducing agent to create cerium oxide nanoparticles from cerous nitrate hexahydrate. These cerium oxide nanoparticles, in turn, were incorporated into hydrogels composed of gelatin and sodium alginate, resulting in the formation of Gelatin–Sodium Alginate–Cerium Oxide ($GSCeO_2$) nanocomposite hydrogels. UV–visible spectra displayed absorbance peaks at 340 nm and 361 nm for cerium oxide nanoparticles and $GSCeO_2$ nanocomposites, respectively. Fourier-Transform Infrared (FT-IR) spectroscopy was employed to differentiate between various functional groups present in the cerium oxide nanoparticles and $GSCeO_2$ nanocomposites. X-ray Diffraction (XRD) investigations confirmed the face-centered cubic structure with a sharp peak at the (111) plane for both cerium oxide nanoparticles and $GSCeO_2$ nanocomposites. Furthermore, XRD analysis provided the average particle sizes of 16.7 nm and 21.39 nm for 0.1 M cerium oxide nanoparticles and $GSCeO_2$ nanocomposites, respectively. Energy-Dispersive X-ray Analysis confirmed the presence of essential elements in the nanoparticles and nanocomposites. The $GSCeO_2$ nanocomposites exhibited excellent photocatalytic activity against methyl red dye under exposure to ultraviolet–visible light irradiation and demonstrated enhanced antioxidant properties. In vitro cytotoxicity assays conducted on MDA-MB 231 (human breast cancer cells) revealed an IC50 value of 28.69 µg/ml for $GSCeO_2$ nanocomposites. Additionally, $GSCeO_2$ nanocomposites displayed potent antifungal activity against *Aspergillus flavus* and *Candida albicans*.

Keywords Gelatin · Sodium alginate · Hydrogels · Cytotoxicity

Introduction

In recent decades, semiconductor photocatalysis has gained significant attention for its remarkable contributions to environmental and energy applications. This environmentally friendly and pollution-free technology harnesses solar energy directly, making it a popular area of research and innovation (Qamar et al. 2019). As per researchers' findings, nanosized particles exhibit a crucial role in photocatalytic processes owing to their exceptional chemical and physical attributes. Among the diverse array of nanosized particles, metal oxide nanoparticles stand out as captivating entities due to their extraordinary properties and wide-ranging applications. They find applications in catalysis, optics, pharmaceutical drug production, and as agents with antimicrobial properties (Muthuvel et al. 2020a, b). Creating metal oxide nanoparticles from cost-effective and highly efficient biological sources holds significant appeal for researchers

✉ A. S. Stella Shalini
drstellaj28@gmail.com

[1] Department of Chemistry, St. Joseph's College (Autonomous), Affiliated to Bharathidasan University, Tiruchirappalli, Tamil Nadu 620 002, India

[2] Department of Chemistry, Vel Tech High Tech Dr.Rangarajan Dr.Sakunthala Engineering College (Autonomous), Chennai, Tamil Nadu 600 062, India

[3] Department of Electronics and Communication Engineering, Saveetha Engineering College, Thandalam, Chennai 602 105, India

[4] Department of Chemistry, University College of Engineering, Panruti 607 106, India

Published online: 03 February 2024

across disciplines, including chemists, biologists, and material scientists. These metal oxide nanostructures, such as TiO_2, ZnO, CuO, WO_3, and SnO_2, exhibit distinctive features, including magnetic and hydrophobic properties, adding to their allure (Rajeshkumar and Naik 2018). CeO_2 has gained recognition as an excellent photocatalyst due to its high catalytic efficiency, straightforward preparation process, cost-effectiveness, and non-toxicity. Notably, CeO_2 demonstrates efficacy in bacterial resistance and ultraviolet radiation shielding. Moreover, its affordability and suitability for a broad temperature range have led to extensive use in environmental remediation. Cerium, one of the most abundant rare earth elements in the Earth's crust, underscores its accessibility. Additionally, semiconductor cerium oxide is characterized by a wide bandgap energy (3.19 eV) and a high excitation binding energy, enhancing its suitability for diverse applications. Furthermore, cerium oxide nanoparticles exhibit commendable antioxidant properties, showcasing potential in the treatment of stress-related ailments (Arumugam et al. 2015; Caputo et al. 2017). However, the individual performance of CeO_2 remains suboptimal, characterized by several drawbacks. These include a low specific surface area, a wide bandgap resulting in limited absorption in the visible spectrum, especially up to 400 nm, and high electron–hole recombination rates (Lian et al. 2019). Therefore, there is a compelling need to enhance and modify CeO_2 to mitigate these aforementioned limitations. Numerous studies have demonstrated that the photocatalytic activity of CeO_2 can be substantially improved through various strategies, including bandgap engineering, doping, the formation of heterojunctions, and composite materials, among others. Among these strategies, one of the most effective approaches involves creating composites of CeO_2 with materials that exhibit visible light responsiveness and possess lower bandgaps. Notably, materials like gelatin sodium alginate fall into this category, enabling broader solar spectrum absorption and facilitating charge generation and separation, thereby enhancing photocatalytic performance. The methods like co-precipitation (Pujar et al. 2018), spray pyrolysis (Sharma et al. 2010), solvothermal (Bumajdad et al. 2009), hydrothermal (Zhang et al. 2002), template-assisted (Balavi et al. 2013), and sol–gel method (Wang et al. 2002) are used for the synthesis of CeO_2 and its composites. These traditional methods often come with drawbacks such as high cytotoxicity, limited productivity, and ecological concerns. In recent decades, bionanotechnology has been on the rise as it involves the use of non-hazardous, environmentally friendly biological systems like bacteria, fungi, plant leaves, vitamins, and yeast for the synthesis of metal oxide nanoparticles (Muthuvel et al. 2020a, b). Moreover, plant extracts contain a variety of phytochemicals, including phenols, proteins, amino acids, saponins, flavonoids, terpenoids, and carbohydrates. The polyphenolic hydroxyl (OH) groups present in these plant extracts exhibit a strong affinity for metal ions, making them a common choice for their utilization as reducing and stabilizing agents in various applications. In the literature, various plant extracts, including those from sources like *Moringa oleifera* (Kalaiselvi et al. 2018), *Hibiscus sabdariffa* flowers (Thoyhogi et al. 2015), *Azadirachta indica* leaves (Sharma et al. 2017), *Olea europaea* (Maqbool et al. 2016), and *Citrullus lanatus* (Reddy Yadav et al. 2016) have been employed for green synthesis, facilitating the reduction of methylene blue dye in the presence of CeO_2 nanoparticles. *Oldenlandia umbellata*, a medicinal plant from the Rubiaceae family with a history in Indian ayurvedic medicine, has demonstrated potential therapeutic applications for various conditions, and its pharmacological effects, including antibacterial, anti-inflammatory, antipyretic, hepatoprotective, antioxidant, and anti-tissue activity, have been established through research. Furthermore, the plant's aqueous extract contains secondary metabolites such as alkaloids, phenols, flavonoids, terpenoids, steroids, proteins, amino acids, and carbohydrates (Senthilkumar et al. 2017; Behera et al. 2018). Notably, *O. umbellata* in combination with silver nanoparticles exhibits antioxidant, antimicrobial, and biocompatible properties, yet its application in the synthesis of cerium oxide nanoparticles remains unexplored (Reddy 2021; Subramanian et al. 2019). This study aims to utilize *O. umbellata* plant extract for the reduction of cerous nitrate hexahydrate, introducing a green synthesis approach for cerium oxide nanoparticles. Additionally, gelatin and sodium alginate hydrogels are employed to create a hybrid material, gelatin sodium alginate hydrogel Cerium oxide ($GSCeO_2$), which, due to its reduction capabilities, holds promise as a renewable, non-toxic, environmentally friendly material suitable for a wide range of applications, including biological and photocatalytic applications.

Experimental methods

Materials

In this study, a selection of analytical grade chemicals was employed, each with specific details: Cerous nitrate hexahydrate ($Ce(NO_3)_3{\cdot}6H_2O$) sourced from Sigma-Aldrich, boasting a purity of 99.9%. Gelatin ($C_{31}H_{27}NO_4$), ethanol, sodium hydroxide, and methyl red dye were also procured from Sigma-Aldrich, each with a purity rating of 99.9%. These chemicals were utilized as received, without any additional purification steps. Prior to usage, all glassware underwent meticulous cleaning procedures involving an acid wash followed by rinsing with distilled water. Throughout the experiments, exclusive reliance was placed on deionized water.

Plant materials collection

In November 2021, *O. umbellata* plants from the Rubiaceae family were collected from the Pachamalai hills in the Eastern Ghats of Tamil Nadu, South Eastern India, situated at approximately Latitude 11°19′32″ N and Longitude 78°37′55″ E. The collected plant materials were carefully stored and preserved in a cool, dry place away from direct sunlight to maintain their integrity for subsequent use in the study.

Preparation of plant extract

The plant material, once collected, underwent a thorough cleaning process with repeated rinses of deionized water, followed by a ten-day period of air-drying in a shaded environment. After this drying period, the plant material was mechanically ground into a coarse powder and stored in an airtight container. Subsequently, (10 g) of this leaf powder were combined with 100 mL of deionized water in a 250-mL beaker. The mixture was brought to a boil and maintained at a boiling temperature for 20 min before being allowed to cool to room temperature. The plant extract was then separated from any remaining plant materials by passing the mixture through Whatman filter paper No. 1, and the resulting filtered extract was preserved in a refrigerator for future use.

Synthesis of cerium oxide nanoparticles using Oldenlandia umbellata plant extract

A 10-mL aliquot of the plant extract was combined with separate solutions of cerous nitrate hexahydrate at concentrations of 0.1 M, 0.3 M, and 0.5 M. Each mixture was agitated for 3 h at 80 °C. Subsequently, the mixtures underwent centrifugation at 5000 rpm for 30 min to achieve further purification. They were then subjected to multiple washes with deionized water. The resulting material was subsequently subjected to a two-hour treatment in a hot air oven at 120 °C. This process resulted in the formation of a light yellow-colored powder, which was later calcined at 500 °C for 4 h (Altaf et al. 2021). The same procedure was repeated for the preparations at 0.3 M and 0.5 M concentrations, respectively.

Preparation of $GSCeO_2$ nanocomposite hydrogels

In the standard procedure, (2.0 g) of gelatin (G) was individually dissolved in 10 mL of deionized water, and approximately (0.4 g) of sodium alginate was dissolved in 20 mL of water with constant stirring at 50 °C. The hydrogels were formed by thoroughly mixing 8.0 mL of G and 12 mL of SA to create a gelatin-sodium alginate (GS) dispersion. About 100 mg of the prepared cerium oxide NPs was incorporated into this dispersion and stirred vigorously for 30 min before being allowed to cool and placed in a refrigerator for at least 120 min. Subsequently, the hydrogel was prepared, transferred onto a glass plate, and then cured at 60 °C, typically for 30 min. After cooling, a white-colored hydrogel thin-layer film was obtained, and this material was labeled as $GSCeO_2$ hydrogel.

Photocatalytic activity

To assess the photocatalytic efficacy of the $GSCeO_2$ hydrogel nanocomposite, the degradation of methyl red dye was performed under the influence of both a D2 Lamp and a Tungsten Halogen Lamp (W Lamp power: AC 220 V / 50 Hz). The photochemical reaction vessel and the UV source were placed 10 cm apart, and 50 mg of the $GSCeO_2$ nanocomposite was dispersed in 10 mL of a dye solution prepared at a concentration of 0.05 g/L. Following this, the suspension was agitated for 30 min in darkness after the lights were switched on, and the readings were recorded. The assessment of various aqueous suspension concentrations of MR dye in each sample followed a similar procedure.

Antioxidant activity

The $GSCeO_2$ hydrogel nanocomposite's antioxidant activity was evaluated through the 1,1-diphenyl-2-picrylhydrazyl (DPPH) assay. Different concentrations of powdered nanocomposite (10, 50, 100, 250, and 500 gL^{-1}) were prepared using methanol as the solvent. In separate test tubes, 300 µL of each $GSCeO_2$ hydrogel nanocomposite solution was combined with 0.1 mM of DPPH (100 µL). The mixture was vigorously agitated and left at room temperature for 30 min in the absence of light. Each sample was analyzed at least three times. The $GSCeO_2$ hydrogel nanocomposite's ability to scavenge free radicals was demonstrated by the color change from blue to yellow, measured at 517 nm using a UV–visible spectrophotometer. Ascorbic acid served as a standard for comparing the percentage of inhibition of the generated nanoparticles. Indeed, the capacity of the produced nanocomposites to scavenge free radicals is inversely correlated with their absorbance value. The ability of a substance to scavenge the DPPH radical can be quantified using the standard formula as reported in the literature (Nisha et al. 2023).

Antifungal activity

The agar well diffusion method was used to qualitatively assess the antifungal activity of the $GSCeO_2$ nanocomposites. Aspergillus flavus and Candida albicans were cultured in 20 mL of potato dextrose agar medium in petri plates for 24 h. Following this, wells were prepared, and different concentrations of the $GSCeO_2$ sample

(500 µg/mL, 250 µg/mL, 100 µg/mL, and 50 µg/mL) were added. The plates were then incubated for 24 h at 37 °C to observe the size of the inhibition zones that formed around the wells. Amphotericin B was used as a positive control, and the data were analyzed using GraphPad Prism 6.0 (USA).

In vitro cytotoxicity activity

The cytotoxicity of the $GSCeO_2$ sample was evaluated in vitro using the MTT assay and MDA-MB 231 cells. MDA-MB 231 cultured cells were harvested from a 15-mL tube following trypsinization and then seeded into a 96-well tissue culture plate at a density of 1×105 cells/mL (200 µL). The cells were cultured for 24–48 h at 37 °C in DMEM media containing 10% FBS and 1% antibiotic solution. Following a rinse with sterile PBS, different concentrations of the $GSCeO_2$ sample in serum-free DMEM medium were added. Each sample was subjected to three replications during a 24-h culture period at 37 °C in a humidified 5% CO_2 incubator. After the initial incubation, 20 µL of MTT solution at a concentration of 5 mg/mL was added to each well, and the cells were further incubated for 2 to 4 h until purple precipitates were visible under an inverted microscope. Subsequently, the medium and MTT (220 µL) were removed from the wells and washed with 1X PBS (200 µL). Furthermore, 100 µL of DMSO was added, and the plate was agitated for five minutes to dissolve the formazan crystals. The absorbance of each plate was measured at 570 nm using Thermo Fisher Scientific's microplate reader (USA). The IC50 value and the percentage of viable cells were calculated using GraphPad Prism 6.0 software (USA).

Characterization

Powdered X-ray diffraction patterns were acquired using a PANalytical (X'Pert PRO) diffractometer, with CuKα radiation (λ = 0.1541 nm). UV–vis absorption spectra were measured using an ELICO SL-159 spectrophotometer. FT-IR spectra were obtained at room temperature in the range of 4000–400 cm^{-1} using a 5DX FT-IR spectrometer with a spectral resolution of ± 2 cm^{-1}, and a dry KBr pellet was utilized for this purpose. Material morphology was examined with a FESEM (CARL ZEISS) model EV018, and TEM images were captured at room temperature (25 °C) using an electron microscope (JEOL SM-7600 F, Japan) equipped with a field-emission gun operating at an acceleration voltage of 200 kV. Elemental analysis of the composite was conducted using EDAX. The maximum composite diameter was determined by Dynamic Light Scattering (DLS) studies.

Results and discussion

Powder XRD analysis

To confirm the distinct phases of CeO_2 nanoparticles at various concentrations, X-ray diffraction was utilized for the analysis, which included 0.1 M CeO_2, 0.3 M CeO_2, 0.5 M CeO_2, and $GSCeO_2$ (Fig. 1). In all nanoparticle and nanocomposite concentrations, the peak values were consistent. Specifically, peaks at 2Θ values of 28.450, 32.000, 47.380, 56.250, 58.960, 69.300, 76.630, 67.870, and 78.960 were associated with crystal planes (111), (200), (220), (311), (222), (400), (311), and (420), respectively. The obtained diffraction peaks were compared to data from the JCPDS card No. 34-0394, revealing a match with the face-centered

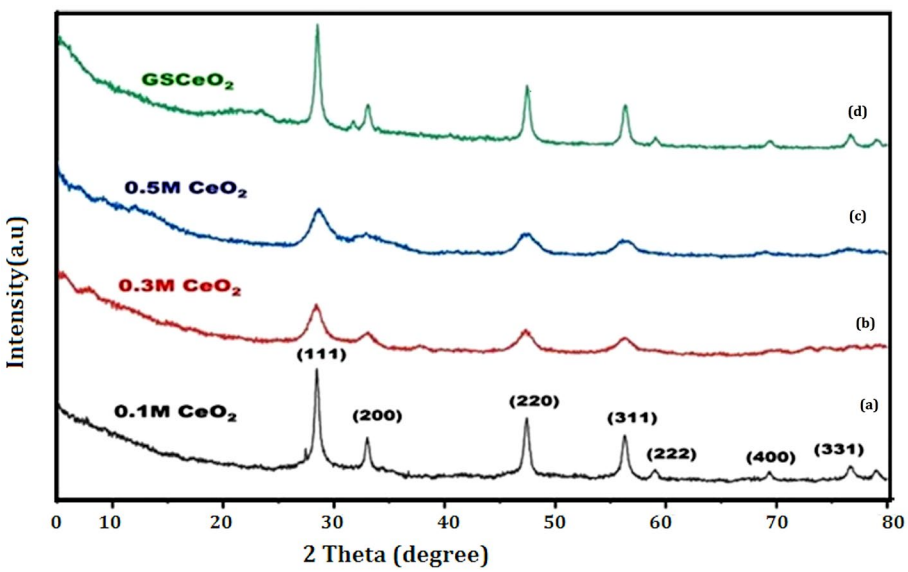

Fig. 1 Powder XRD pattern of **a** 0.1 M CeO_2, **b** 0.3 M CeO_2, **c** 0.5 M CeO_2, and **d** $GSCeO_2$ nanocomposite

cubic structure (Ahmad et al. 2020). Notably, strong and narrow peaks, particularly the (111) plane, at the highest concentrations, indicated that the cerium oxide nanoparticles were highly crystalline. The Debye–Scherer formula was applied to determine the typical size of CeO_2 nanoparticles (Thamizhazhagan et al. 2021). The normal crystalline sizes were found to be in the following range: 0.1 M CeO_2—26.7 ± 3 nm, 0.3 M CeO_2—18.0 ± 2 nm, and 0.5 M CeO_2—15.60 ± 3 nm, respectively. When comparing these three different concentrations, it became evident that 0.1 M CeO_2 exhibited a particularly intense peak. The average particle size of the $GSCeO_2$ nanocomposite was determined to be 21.39 nm.

SEM analysis

To understand the surface morphology of the samples, SEM analysis was performed, and the results are depicted in Fig. 2. Figure 2a–d depicts SEM images of the CeO_2 and $GSCeO_2$ hydrogel nanocomposite. The morphology of the cerium oxide CeO_2 nanoparticles revealed a spherical shape. In the $GSCeO_2$ composite sample, CeO_2 nanoparticles were consistently distributed throughout the hydrogel, showing no signs of aggregation. To further elucidate the elemental composition within the $GSCeO_2$ hydrogel nanocomposites, we employed EDAX. As illustrated in Fig. 2e, the EDAX spectra provide clear evidence of the presence of both cerium and oxygen atoms in the biosynthesized nanocomposites, evident from the robust signals emanating from cerium and oxygen. The elemental analysis indicates that cerium comprises approximately 85.22% of the composition, with oxygen constituting the remaining 14.78%. Importantly, the entire scanning range revealed no indications of impurity peaks, affirming the high purity of the synthesized nanocomposites.

TEM and SAED analysis

To provide detailed insights into the size, shape, crystallography, and quality of nanoparticles, TEM and SAED were performed, and the results are depicted in Fig. 3. In the TEM analysis, CeO_2 nanoparticles were observed to have a well-defined spherical morphology. The average diameter of the nanoparticles was found to be 21.3 nm with a relatively narrow size distribution (standard deviation ± 1.2 nm). The nanoparticles were uniformly dispersed throughout the $GSCeO_2$ hydrogel nanocomposite, and there were no signs of aggregation. The high-resolution TEM image, as shown in Fig. 3b, reveals the individual nanoparticles with a clear boundary and a uniform electron-dense appearance, consistent with the expected characteristics. The SAED analysis unequivocally verified the crystalline nature of the CeO_2 nanoparticles. By focusing an electron beam on a selected area of the sample, Fig. 3c, d reveals a distinct diffraction pattern with well-defined rings. These diffraction rings were precisely

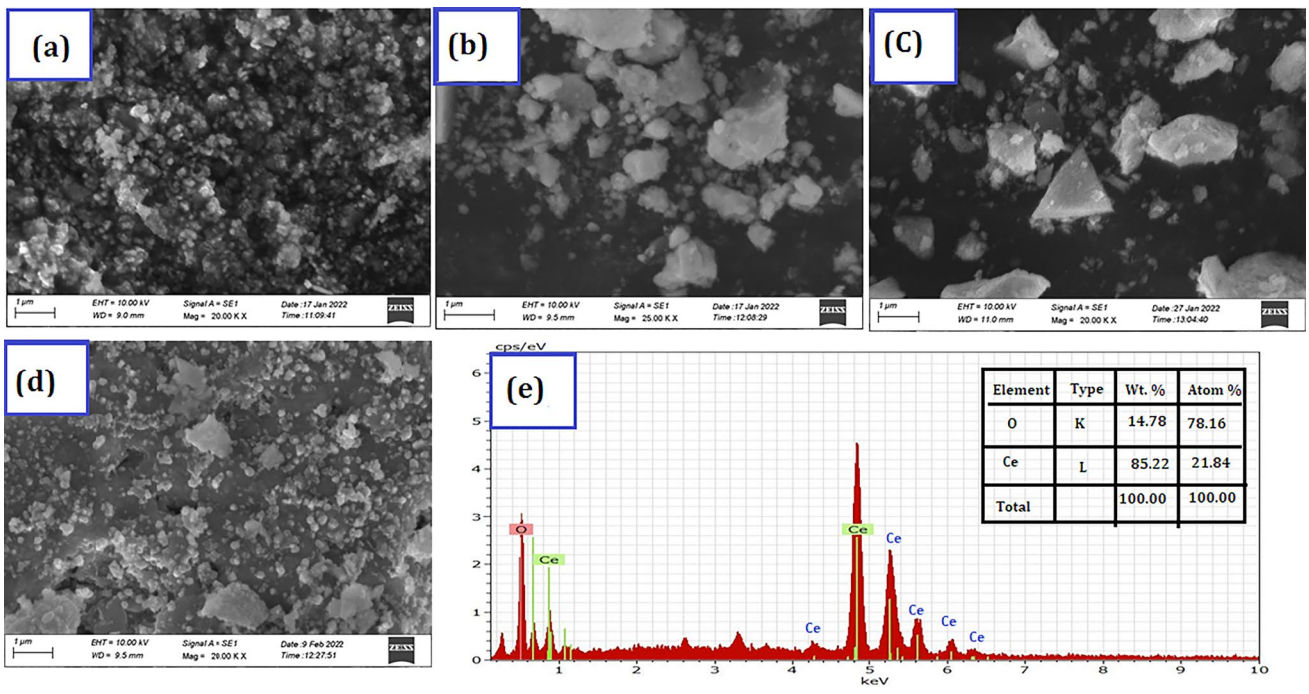

Fig. 2 SEM images for **a** 0.1 M CeO_2, **b** 0.3 M CeO_2, **c** 0.5 M CeO_2, and **d** $GSCeO_2$ nanocomposite; **e** EDAX spectra of 0.1 M CeO_2 nanoparticles

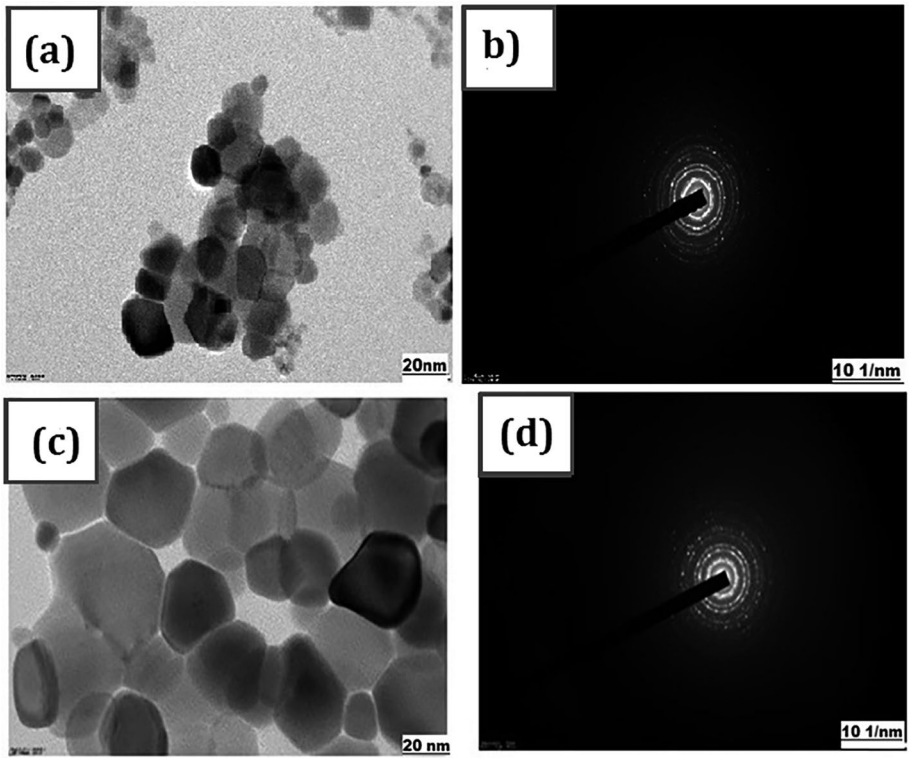

Fig. 3 TEM images of **a** CeO_2, **c** $GSCeO_2$; the SAED pattern of **b** CeO_2, **d** $GSCeO_2$

aligned with the crystallographic planes of (111), (200), (220), and (311), all characteristic of the face-centered cubic (FCC) structure of CeO_2. Importantly, the observed diffraction pattern closely mirrored the FCC crystal structure obtained from the XRD results, providing robust evidence for the crystallinity of both the synthesized CeO_2 nanoparticles and the $GSCeO_2$ composites.

FT-IR analysis

Fourier-Transform Infrared analysis was conducted to unveil the functional groups associated with the production of CeO_2 in the OU plant extract. The FT-IR spectrum, as shown in Fig. 4, disclosed distinctive absorption bands at specific wavenumbers for both CeO_2 nanoparticles and $GSCeO_2$ nanocomposites. The dominant absorption peak at 3434 cm^{-1} pointed to the presence of phenolic compounds, characterized by the O–H stretch vibration. This implies the inclusion of antioxidant and bioactive phenolic compounds in the synthesized materials. Additionally, the absorption band at 1644 cm^{-1} indicated an amine N–H bending vibration bond, signifying the presence of proteins and amino acids (Vijayan et al. 2018). Aromatic compounds were recognized at 1351 cm^{-1} and 1384 cm^{-1}. Furthermore, a robust peak at 1036 cm^{-1} correlated with phenolic and alcoholic groups and their C-N stretching vibrations. The FT-IR results corroborate the presence of CeO_2 and various organic compounds, highlighting the diverse functional

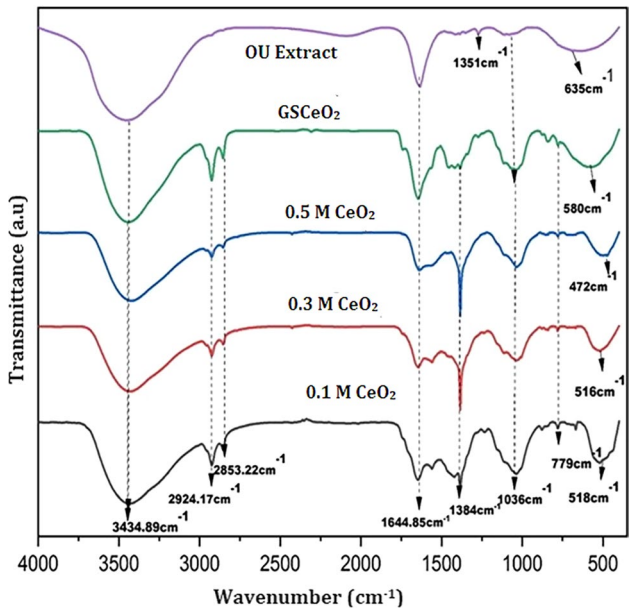

Fig. 4 FT-IR spectra of 0.1 M CeO_2, 0.3 M CeO_2, 0.5 M CeO_2, $GSCeO_2$ nanocomposite, and OU plant extract

groups within the CeO_2 nanoparticles and $GSCeO_2$ nanocomposites, with potential applications spanning nanotechnology and biomedicine.

UV–visible spectroscopy analysis

The UV–visible spectrum analysis reveals crucial insights into the composition of the $GSCeO_2$ hydrogel nanocomposite. Figure 5 illustrates the UV–visible spectrum of the CeO_2 and $GSCeO_2$ hydrogel nanocomposite. Within this spectrum, two prominent absorbance peaks were observed. At 314 nm and 343 nm, the broad maximum absorbance is indicative of specific constituents within the OU plant extract. These particular peaks are associated with components inherent to the plant extract. Furthermore, the presence of peaks at 346 nm and 361 nm aligns with well-documented electronic transitions or absorption bands characterizing CeO_2 nanoparticles. This finding serves as compelling evidence for the successful integration of CeO_2 into the hydrogel matrix. The $GSCeO_2$ nanocomposite exhibited a noticeable red-shift in its absorption edges compared to pure CeO_2 NPs. The bandgap values for CeO_2 were determined using Tauc's method (Mary et al. 2022), yielding extrapolated intercept values of 3.10 eV, 2.90 eV, 2.83 eV, and 2.65 eV for CeO_2 concentrations of 0.1 M, 0.3 M, 0.5 M, and $GSCeO_2$ composites, respectively. This red-shift in the absorption edges indicates a significant alteration in the optical properties of the nanocomposite when contrasted with pristine CeO_2 nanoparticles. This change is attributed to the inevitable interaction of oxygen atoms in CeO_2 with GS during the composite's preparation process. The chemical bonding between CeO_2 and GS creates a confinement effect on electrons within the O-2*p* orbitals, resulting in a reduction in the bandgap values observed in the $GSCeO_2$ composites.

DLS analysis

The DLS method is used for analyzing particles with sizes ranging from 72.5 nm to 103.6 mm (Fig. 6). It was determined that the biosynthesized $GSCeO_2$ hydrogel nanocomposites had an average particle size of 88.5 nm. The diameter values of 93.7 nm, 84.2 nm, 103.6 nm, and 72.5 nm correspond to 0.1 M CeO_2, 0.3 M CeO_2, 0.5 M CeO_2 nanoparticles, and $GSCeO_2$ nanocomposite, respectively. Several variables, including the size of surface structures, the size of the particle core, and the particle concentration, can influence the estimation of particle size.

Photocatalytic activity analysis

The photocatalytic activity of the $GSCeO_2$ nanocomposite hydrogel was assessed through the removal of methyl red dye under UV light irradiation. Initially, the suspensions were agitated for 30 min in the absence of light. For the photocatalytic degradation experiment, MR dye and 50 mg of $GSCeO_2$ were employed. As the methyl red dye gradually degraded over the course of one hour, UV–visible spectra were collected at various intervals. Figure 7 clearly illustrates how the concentration of methyl red dye decreased over time when exposed to UV–visible light in the presence of the $GSCeO_2$ nanocomposite. The photocatalytic degradation efficiency was calculated using the standard formula (Durairasan et al. 2021):

$$\text{Photo catalytic degradatin}\,(\%) = \frac{(C_0 - C)}{C} \times 100$$

To determine the optimal catalyst concentration, the investigation was expanded to include various

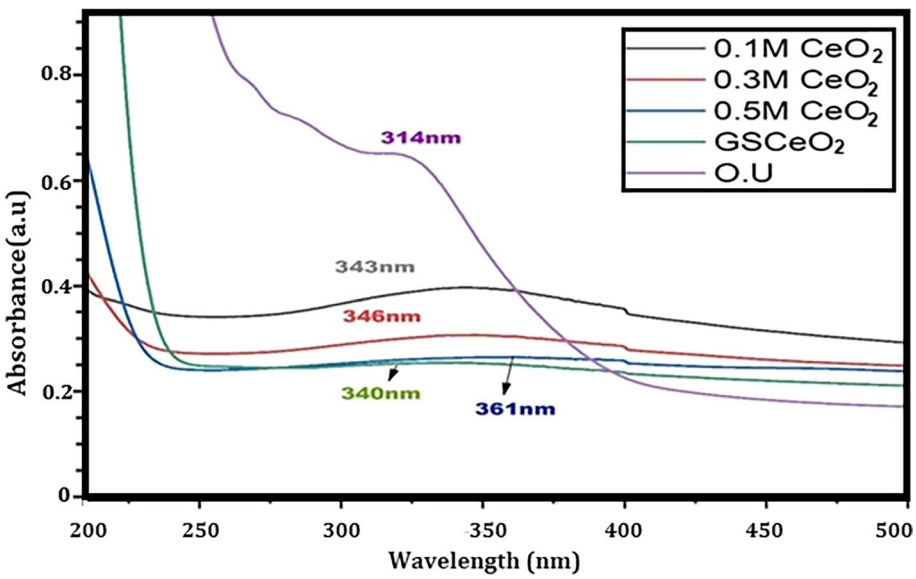

Fig. 5 UV–visible spectrum for 0.1 M CeO_2, 0.3 M CeO_2, 0.5 M CeO_2, $GSCeO_2$ nanocomposite, and OU plant extract

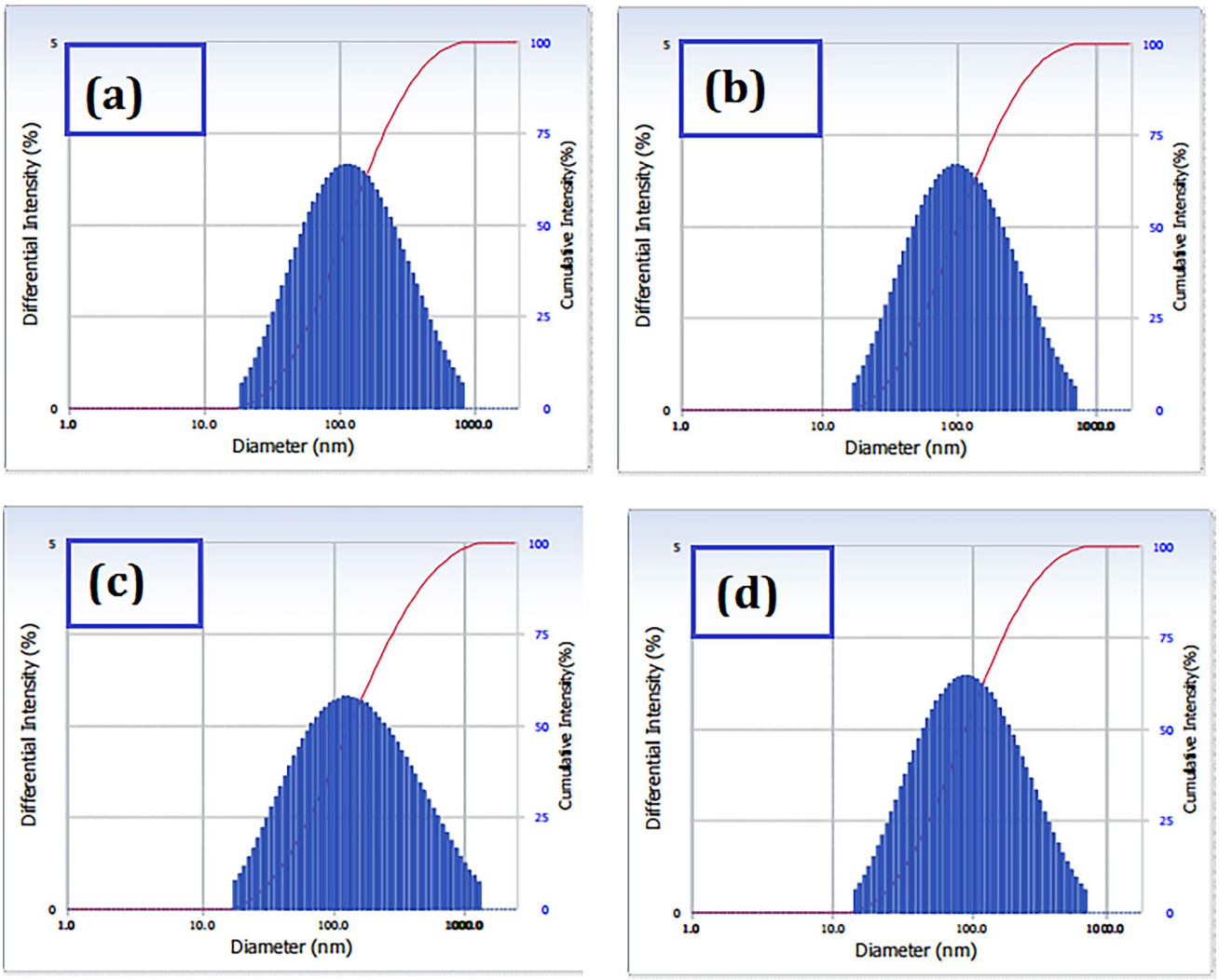

Fig. 6 DLS analysis for **a** 0.1 M CeO_2, **b** 0.3 M CeO_2, **c** 0.5 M CeO_2, and **d** $GSCeO_2$ nanocomposite

Fig. 7 Percentage of photocatalytic degradation efficiency of $GSCeO_2$ nanocomposite at different time intervals

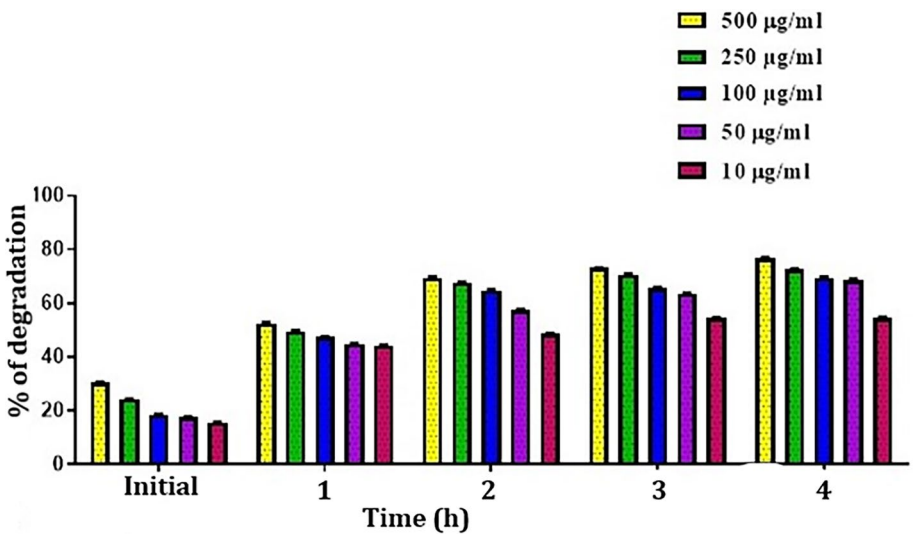

Table 1 Percentage of different concentrations of $GSCeO_2$ nanocomposite

S. no.	% of different time interval (hours)	% photoremoval efficiency (µg/ml)				
		500 µg/ml	250 µg/ml	100 µg/ml	50 µg/ml	10 µg/ml
1	Initial	30.373	24.333	18.472	17.584	15.275
2	1 h	52.930	49.911	47.424	44.937	44.404
3	2 h	69.094	67.495	64.298	57.726	48.845
4	3 h	73.001	70.159	65.719	63.765	54.174
5	4 h	76.198	72.824	69.804	68.916	54.706

Table 2 OD value for different concentrations of $GSCeO_2$ nanocomposite

S. no.	Tested sample concentration (µg/ml)	OD value at 517 nm (in triplicates)		
1	Control	1.050	0.964	1.194
2	500 µg/ml	0.378	0.513	0.525
3	250 µg/ml	0.528	0.532	0.547
4	100 µg/ml	0.552	0.573	0.579
5	50 µg/ml	0.597	0.610	0.649
6	10 µg/ml	0.650	0.682	0.690
7	Ascorbic acid	0.08	0.11	0.12

Table 3 Percentage of inhibition for $GSCeO_2$ nanocomposite

S. no.	Tested sample concentration (µg/ml)	Percentage of inhibition (in triplicates)			Mean value (%)
1.	Ascorbic acid	92.51	89.71	88.77	90.33
2.	500 µg/ml	64.63	52.01	50.88	55.84
3.	250 µg/ml	50.60	50.23	48.83	49.89
4.	100 µg/ml	48.36	46.39	45.83	46.86
5.	50 µg/ml	44.15	42.93	39.28	42.12
6.	10 µg/ml	39.19	36.20	35.45	36.95

concentrations, and the results are presented in Table 1. The table clearly indicates that a concentration of 250 µg/mL is suitable for MR dye removal.

Antioxidant activity analysis

The 2,2-diphenyl-picrylhydrazyl (DPPH) test was employed to evaluate the antioxidant activity of $GSCeO_2$ nanocomposites with ascorbic acid serving as the reference substance. The DPPH assay solution was added to the $GSCeO_2$ nanocomposite within a range of 10–500 µg/mL. The scavenging activity of the $GSCeO_2$ nanocomposites is elaborated in Tables 2 and 3. The findings reveal that at the lowest concentration of $GSCeO_2$ nanocomposite (10 µg/mL), the percentage of inhibition was measured at 36.95, and this value increased to 55.84 as the concentration was raised to 500 µg/mL. With the progressive increase in the concentration of $GSCeO_2$, the percentage of inhibition also increased. Notably, the IC50 value of the $GSCeO_2$ nanocomposite (at 500 µg/mL) was determined to be 102.1 µg/mL. The improved antioxidant activity of $GSCeO_2$ has been linked to functional groups associated with plant extracts and the reduced size of the nanocomposite. The results are presented in Fig. 8. It demonstrates the significant antiradical effect of $GSCeO_2$ hydrogel nanocomposites, particularly at a concentration of 500 µg/mL. These results suggest that $GSCeO_2$ nanocomposites possess notable antioxidant properties, with their efficiency increasing as the concentration rises. The effective antiradical effect observed in the nanocomposite at 500 µg/mL concentration underscores its potential for antioxidant applications and highlights the role of functional groups and reduced size in enhancing its activity.

Antifungal activity analysis

The antifungal activity of the $GSCeO_2$ nanocomposite was assessed, and the results are presented in Table 4. In the case of the $GSCeO_2$ nanocomposite, the inhibition zones for Candida albicans were as follows: 500 µg/mL (9.5 ± 0.7), 250 µg/mL (8.25 ± 0.35), 100 µg/mL, and 50 µg/mL (0), while the positive control exhibited an inhibition zone of (11.5 ± 0.7). As for *Aspergillus flavus*, the inhibition zones were observed as follows: 500 µg/mL (6.5 ± 0.7) and 250 µg/mL (4.25 ± 0.35), and the positive control showed an inhibition zone of (30.5 ± 0.7). It was evident that as the concentration decreased, the inhibition activity also decreased, and at the lowest concentrations, no inhibition was observed. Conversely, higher concentrations led to the formation of inhibition zones. Notably, *Candida albicans* displayed the largest inhibition zone, with a zone diameter of 9.5 ± 0.7 at 500 µg/mL. This outcome aligns with previous studies (Mohamed et al. 2020) and indicates that an increase in concentration is associated with enhanced antifungal activity. These results highlight the concentration-dependent antifungal effectiveness of the $GSCeO_2$ nanocomposite.

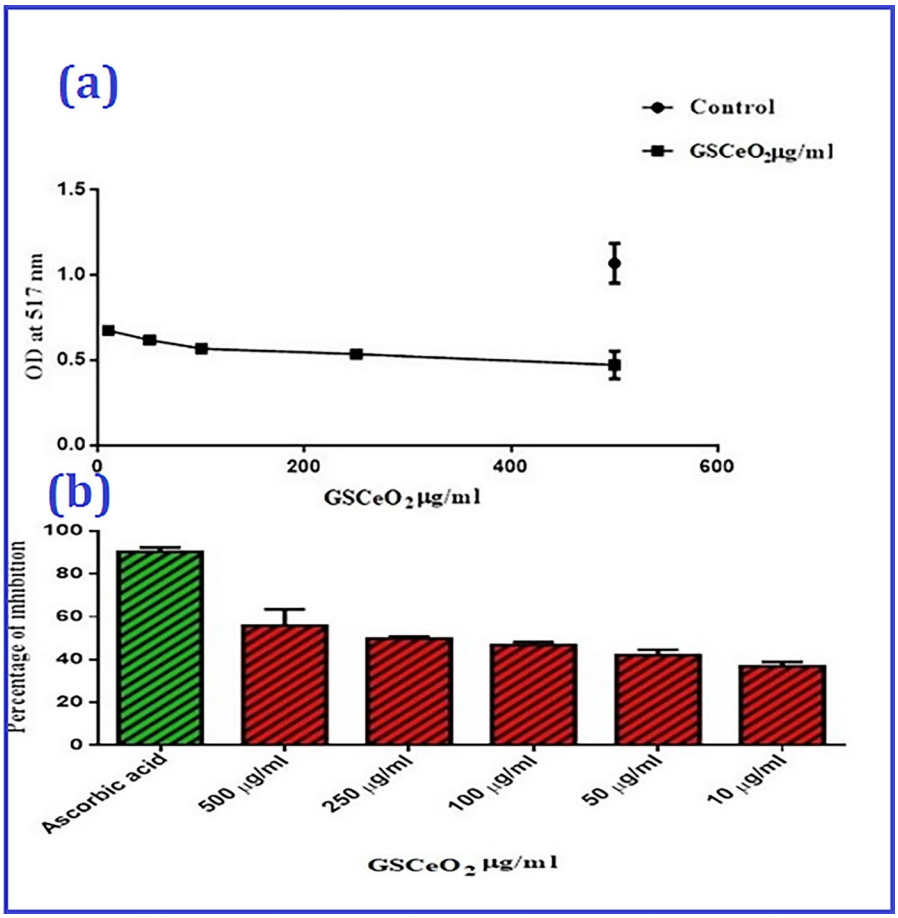

Fig. 8 **a** Graphical representation of OD value at different concentrations of $GSCeO_2$ nanocomposite, **b** graphical representation of the percentage of inhibition for $GSCeO_2$

Table 4 SD ± means of the zone of inhibition obtained by $GSCeO_2$ against *Candida albicans and Aspergillus flavus*

S. no.	Name of the test organism	Name of the sample	Zone of inhibition (mm) SD ± Mean				
			500 µg/ml	250 µg/ml	100 µg/ml	50 µg/ml	PC
1	*Candida albicans*	$GSCeO_2$	9.5 ± 0.7	8.25 ± 0.35	(less than LOQ)	(less than LOQ)	11.5 ± 0.7
2	*Aspergillus flavus*		6.5 ± 0.7	4.25 ± 0.35	(less than LOQ)	(less than LOQ)	30.5 ± 0.7

In vitro cytotoxicity

The $GSCeO_2$ nanocomposite's cytotoxicity was assessed in vitro using MDA-MB 231, a human breast cancer cell line. These cells were initially plated in a 96-well tissue culture plate at a concentration of 1 × 105 cells/mL (200 µL) in DMEM medium enriched with 10% FBS and 1% antibiotic solution. Over a 48-h period, the cell cultures were regularly observed for any signs of cytotoxic effects, including alterations in cell morphology and cell death (Raj et al. 2014; Sabouri et al. 2022). The optical density of each well at 570 nm was measured with a microplate reader, and the outcomes are summarized in Table 5. The $GSCeO_2$ nanocomposites were tested at ten different concentrations. At concentrations of 1, 5, 10, 15, and 50 µg/mL, cell death decreased, while

Table 5 Percentage of cell viability

S. no.	Tested sample concentration (µg/mL)	Cell viability (%) (in triplicates)			Mean value (%)
	Control	100	100	100	100
	1 µg/ml	95.3247	97.486	98.3516	97.054119
	5 µg/ml	79.7403	56.7039	57.1429	64.529009
	10 µg/ml	55.3247	67.3184	56.3187	59.653931
	15 µg/ml	73.2468	49.4413	43.4066	55.364896
	50 µg/ml	60.5195	37.9888	37.6374	45.38189
	100 µg/ml	30.3896	30.1676	30.7692	30.442146
	200 µg/ml	27.5325	26.5363	31.5934	28.554062
	300 µg/ml	22.3377	26.8156	29.3956	26.18297
	400 µg/ml	12.4675	16.4804	17.033	15.326982
	500 µg/ml	6.23377	8.93855	4.12088	6.4310643

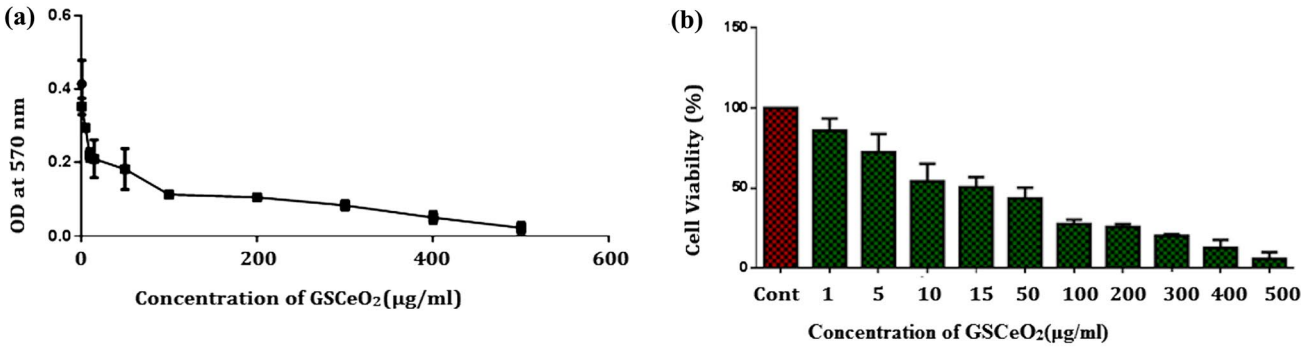

Fig. 9 **a** OD at 570 nm and $GSCeO_2$ nanocomposites, **b** graphical representation of percentage of cell viability for $GSCeO_2$ nanocomposite

it increased at concentrations exceeding 100 µg/mL. The control group, which was not exposed to the nanocomposites, displayed no cell death, and all cells remained viable. The percentage of viable cells decreased to only 6.43% at the highest concentration of 500 µg/ml. This indicates that cell mortality in human MDA-MB 231 (breast cancer cells) exhibited a dose-dependent response when exposed to various concentrations of $GSCeO_2$ nanocomposites. Notably, the control group remained entirely unaffected, with 100% cell viability. The $GSCeO_2$ nanocomposite exhibited an IC50 value of 28.69 µg/mL, as shown in Figs. 9 and 10. This indicates that the concentration at which the nanocomposite causes a 50% reduction in cell viability is 28.69 µg/mL. The lower the IC50 value, the higher the cytotoxicity of the nanocomposite. Therefore, these results suggest that the $GSCeO_2$ nanocomposite has a significant cytotoxic effect on MDA-MB 231 breast cancer cells, particularly at higher concentrations, while showing no toxicity to normal cells (control group). The dose-dependent response observed underscores the potential of this nanocomposite as an anticancer agent.

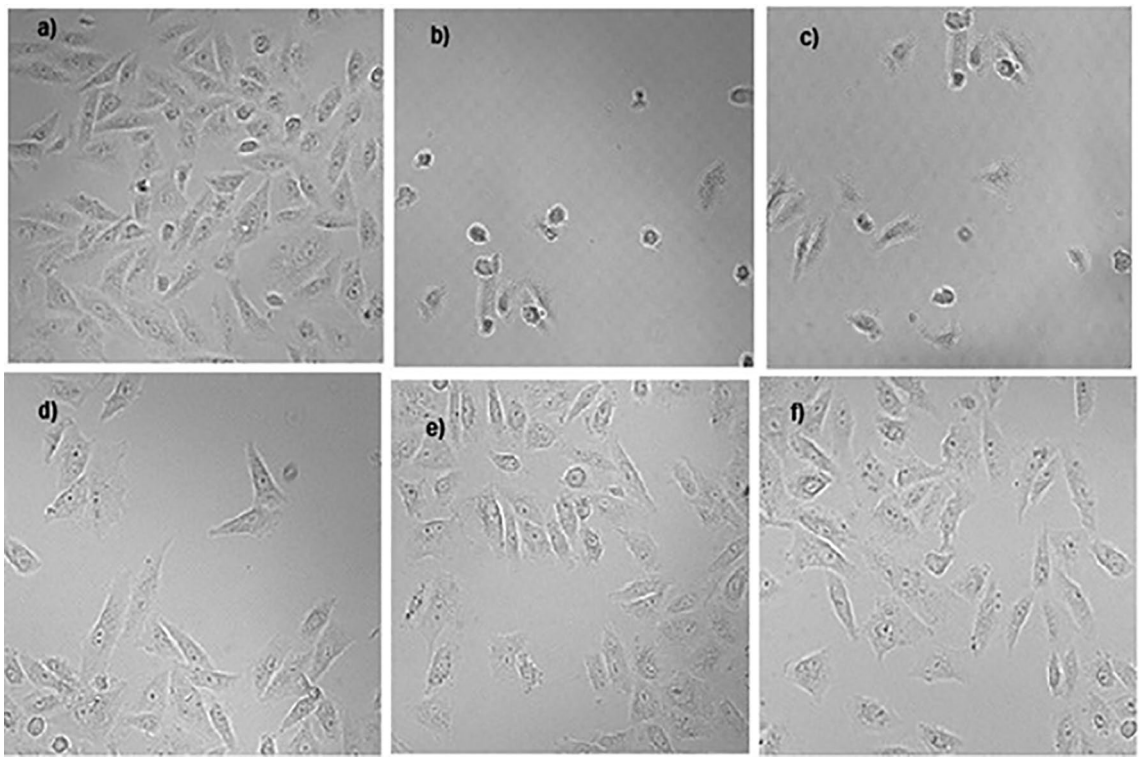

Fig. 10 Cytotoxicity of control cells and $GSCeO_2$ nanocomposite-treated cells **a** control cells, **b** 500 µg/mL, **c** 300 µg/mL, **d** 100 µg/ml, **e** 50 µg/mL, **f** 10 µg/mL

Conclusions

In summary, this study successfully synthesized non-toxic and environmentally friendly CeO_2 nanoparticles using *O. umbellata* plant extract. These nanoparticles were prepared in three different concentrations, with 0.1 M CeO_2 NPs selected for the formation of the $GSCeO_2$ nanocomposite hydrogel. The UV–visible spectrum analysis confirmed the presence of CeO_2 nanoparticles, while FT-IR spectra identified various functional groups in both the $GSCeO_2$ nanocomposite hydrogel and CeO_2 NPs. SEM investigations revealed the cubic structure and shape of CeO_2 NPs and $GSCeO_2$ nanocomposites, with DLS confirming their respective particle sizes. The $GSCeO_2$ nanocomposite exhibited excellent antioxidant properties with an IC50 value of 102.1 µg/mL. Additionally, it demonstrated superior photocatalytic activity against methyl red dye under visible light, with an IC50 value of 28.69 g/mL in the context of anticancer activity. These findings suggest that the $GSCeO_2$ nanocomposite holds promise for effective applications in photocatalysis, antifungal activities, and potential cancer therapy.

Acknowledgments We thank St. Joseph's College (Autonomous), affiliated to Bharathidasan University, Tiruchirappalli-620 002, Tamil Nadu, for providing laboratory facilities to perform the studies.

Author contributions ASSS performed experimental work, designed the work, and data collection. LS co-ordinated the research activity planning and writing the initial draft. Dr. PR performed interpretation of data for the article. Dr. RT performed validation of data, reviewing, and editing the script. Dr. SK provided funding for the project. Dr. PSK conducted manuscript revisions and final editing process.

Data availability All data generated/analyzed during the current study are included in this article, and data sharing is not applicable.

Declarations

Conflict of interest The authors declare they have no conflicts of interest.

References

Ahmad T, Iqbal J, Bustam MA, Zulfiqar M, Muhammad N, Al Hajeri BM et al (2020) Phytosynthesis of cerium oxide nanoparticles and investigation of their photocatalytic potential for degradation of phenol under visible light. J Mol Struct 1217:128292. https://doi.org/10.1016/j.molstruc.2020.128292

Altaf M, Manoharadas S, Zeyad MT (2021) Green synthesis of cerium oxide nanoparticles using *Acorus calamus* extract and their antibiofilm activity against bacterial pathogens. Microsc Res Tech 84(8):1638–1648. https://doi.org/10.1002/jemt.23724

Arumugam A, Karthikeyan C, Hameed ASH, Gopinath K, Gowri S, Karthika V (2015) Synthesis of cerium oxide nanoparticles using *Gloriosa superba* L. leaf extract and their structural, optical and antibacterial properties. Mater Sci Eng C 49:408–415. https://doi.org/10.1016/j.msec.2015.01.042

Balavi H, Samadanian-Isfahani S, Mehrabani-Zeinabad M, Edrissi M (2013) Preparation and optimization of CeO_2 nanoparticles and its application in photocatalytic degradation of Reactive Orange 16 dye. Powder Technol 249:549–555. https://doi.org/10.1016/j.powtec.2013.09.021

Behera SK, Rajasekaran C, Payas S, Fulzele DP, Doss CGP, Siva R (2018) In vitro flowering in *Oldenlandia umbellata* L. J Ayurveda Integr Med 9(2):99–103. https://doi.org/10.1016/j.jaim.2017.02.011

Bumajdad A, Eastoe J, Mathew A (2009) Cerium oxide nanoparticles prepared in self-assembled systems. Adv Coll Interface Sci 147:56–66. https://doi.org/10.1016/j.cis.2008.10.004

Caputo F, Mameli M, Sienkiewicz A, Licoccia S, Stellacci F, Ghibelli L, Traversa E (2017) A novel synthetic approach of cerium oxide nanoparticles with improved biomedical activity. Sci Rep 7(1):4636. https://doi.org/10.1038/s41598-017-04098-6

Durairasan M, Karthik PS, Balaji J, Rajeshkanna B (2021) Enhanced visible light photocatalytic performance of WSe2/CNT hybrid photocatalysts that were synthesized by a facile hydrothermal route. Ionics 27(5):2151–2158. https://doi.org/10.1007/s11581-021-03976-4

Kalaiselvi V, Mathammal R, Vijayakumar S, Vaseeharan B (2018) Microwave assisted green synthesis of hydroxyapatite nanorods using *Moringa oleifera* flower extract and its antimicrobial applications. Int J Vet Sci Med 6(2):286–295. https://doi.org/10.1016/j.ijvsm.2018.08.003

Lian Z, Shan W, Wang M, He H, Feng Q (2019) The balance of acidity and redox capability over modified CeO_2 catalyst for the selective catalytic reduction of NO with NH3. J Environ Sci 79:273–279. https://doi.org/10.1016/j.jes.2018.11.018

Maqbool Q, Nazar M, Naz S, Hussain T, Jabeen N, Kausar R, Jan T (2016) Antimicrobial potential of green synthesized CeO2 nanoparticles from *Olea europaea* leaf extract. Int J Nanomed. https://doi.org/10.2147/ijn.s113508

Mary KL, Manonmoni JV, Balan AMR, Karthik PS, Malliappan SP (2022) Phytochemical assisted synthesis of Ni doped ZnO nanoparticles using aloe vera extract for enhanced photocatalytic and antibacterial activities. Digest J Nanomater Biostruct 17(2):634–648. https://doi.org/10.15251/DJNB.2022.172.634

Mohamed HEA, Afridi S, Khalil AT, Ali M, Zohra T, Akhtar R, Ikram A, Shinwari ZK, Maaza M (2020) Promising antiviral, antimicrobial and therapeutic properties of green nanoceria. Nanomedicine 15(05):467–488. https://doi.org/10.2217/nnm-2019-0368

Muthuvel A, Jothibas M, Manoharan C (2020a) Synthesis of copper oxide nanoparticles by chemical and biogenic methods: photocatalytic degradation and in vitro antioxidant activity. Nanotechnol Environ Eng 5:1–19. https://doi.org/10.1007/s41204-020-00078-w

Muthuvel A, Jothibas M, Manoharan C, Jayakumar SJ (2020b) Synthesis of CeO_2-NPs by chemical and biological methods and their photocatalytic, antibacterial and in vitro antioxidant activity. Res Chem Intermed 46:2705–2729. https://doi.org/10.1007/s11164-020-04115-w

Nisha UM, Meeran MN, Sethupathi R, Subha V, Rajeswaran P, Sivakarthik P (2023) Studies on chitosan modified ZrO_2–CeO_2 metal oxide and their photo catalytic activity under solar light irradiation for water remediation. J Indian Chem Soc 100(8):101061. https://doi.org/10.1016/j.jics.2023.101061

Pujar MS, Hunagund SM, Desai VR, Patil S, Sidarai AH (2018) One-step synthesis and characterizations of cerium oxide nanoparticles in an ambient temperature via co-precipitation method. AIP Conf Proc. https://doi.org/10.1063/1.5028657

Qamar SA, Asgher M, Khalid N, Sadaf M (2019) Nanobiotechnology in health sciences: current applications and future perspectives. Biocatal Agric Biotechnol 22:101388. https://doi.org/10.1016/j.bcab.2019.101388

Raj KP, Sivakarthik P, Uthirakumar A, Thangaraj V (2014) Cytotoxicity assessment of synthesized nickel oxide nanoparticles on MCF-7 and A-549 cancer cell lines. J Chem Pharm Sci 974:2115

Rajeshkumar S, Naik P (2018) Synthesis and biomedical applications of cerium oxide nanoparticles: a review. Biotechnol Rep 17:1–5. https://doi.org/10.1016/j.btre.2017.11.008

Reddy BM (2021) Pharmacognostical and phytochemical evaluation of an important medicinal plant *Oldenlandia umbellata* L. J Pharmacognosy Phytochem 10(6):288–291. https://doi.org/10.22271/phyto.2021.v10.i6d.14302

Reddy Yadav LS, Manjunath K, Archana B, Madhu C, Raja Naika H, Nagabhushana H, Nagaraju G (2016) Fruit juice extract mediated synthesis of CeO_2 nanoparticles for antibacterial and photocatalytic activities. Eur Phys J plus 131:1–10. https://doi.org/10.1140/epjp/i2016-16154-y

Sabouri Z, Sabouri M, Amiri MS, Khatami M, Darroudi M (2022) Plant-based synthesis of cerium oxide nanoparticles using *Rheum turkestanicum* extract and evaluation of their cytotoxicity and photocatalytic properties. Mater Technol 37(8):555–568. https://doi.org/10.1080/10667857.2020.1863573

Senthilkumar RP, Bhuvaneshwari V, Ranjithkumar R, Sathiyavimal S, Malayaman V, Chandarshekar B (2017) Synthesis, characterization and antibacterial activity of hybrid chitosan-cerium oxide nanoparticles: as a bionanomaterials. Int J Biol Macromol 104:1746–1752. https://doi.org/10.1016/j.ijbiomac.2017.03.139

Sharma V, Eberhardt KM, Sharma R, Adams JB, Crozier PA (2010) A spray drying system for synthesis of rare-earth doped cerium oxide nanoparticles. Chem Phys Lett 495(4–6):280–286. https://doi.org/10.1016/j.cplett.2010.06.060

Sharma JK, Srivastava P, Ameen S, Akhtar MS, Sengupta SK, Singh G (2017) Phytoconstituents assisted green synthesis of cerium oxide nanoparticles for thermal decomposition and dye remediation. Mater Res Bull 91:98–107. https://doi.org/10.1016/j.materresbull.2017.03.034

Subramanian P et al (2019) Synthesis of *Oldenlandia umbellata* stabilized silver nanoparticles and their antioxidant effect, antibacterial activity, and bio-compatibility using human lung fibroblast cell line WI-38. Process Biochem 86:196–204. https://doi.org/10.1016/j.procbio.2019.08.002

Thamizhazhagan P, Sivakarthik P, Balaji J (2021) Photocatalytic reduction of CO_2 into solar fuels using M-BTC metal organic frameworks for environmental protection and energy applications. Digest J Nanomater Biostruct (DJNB) 16(4):12. https://doi.org/10.15251/djnb.2021.164.1263

Thovhogi N, Diallo A, Gurib-Fakim A, Maaza M (2015) Nanoparticles green synthesis by *Hibiscus sabdariffa* flower extract: main physical properties. J Alloy Compd 647:392–396. https://doi.org/10.1016/j.jallcom.2015.06.076

Vijayan R, Joseph S, Mathew B (2018) Green synthesis of silver nanoparticles using *Nervalia zeylanica* leaf extract and evaluation of their antioxidant, catalytic, and antimicrobial potentials. Part Sci Technol. https://doi.org/10.1080/02726351.2018.1450312

Wang H, Zhu JJ, Zhu JM, Liao XH, Xu S, Ding T, Chen HY (2002) Preparation of nanocrystalline ceria particles by sonochemical and microwave assisted heating methods. Phys Chem Chem Phys 4(15):3794–3799. https://doi.org/10.1039/B201394K

Zhang F, Chan SW, Spanier JE, Apak E, Jin Q, Robinson RD, Herman IP (2002) Cerium oxide nanoparticles: size-selective formation and structure analysis. Appl Phys Lett 80(1):127–129. https://doi.org/10.1063/1.1430502

Structural, morphological, and optical properties of praseodymium and aluminium codoped ZnO nanoparticles

M. S. Viswaksenan[a,b], A. Simi[c*], A. Panneeraselvam[d]
[a] *Research Scholar, PG & Research Department of Chemistry, St.Josephs college (Autonomous), Affiliated to Bharathidasan university, Tiruchirappalli-620 002, Tamilnadu, India*
[b] *Department of Chemistry, Vivekanandha college of Engineering for women (Autonomous), Tiruchengode-637205, Tamilnadu, India*
[c] *PG & Research Department of Chemistry, St.Josephs college (Autonomous), Tiruchirapalli-620002, Tamilnadu, India*
[d] *Department of Physics, Vivekanandha college of Engineering for women (Autonomous), Tiruchengode-637205, Tamilnadu, India*

Using a soft chemical process that involves nitrates and heat annealing, nanoparticles of undoped ZnO and praseodymium, aluminum-codoped ZnO may be produced. XRD, SEM with EDS, and FTIR analysis determine nanocatalyst structures, morphologies, and chemical bonding. PL and UV spectroscopy examines optical characteristics. The peak in the FTIR spectral line at 714 cm^{-1} in the study indicates M-O stretching in the samples and ZnO's interaction with the Pr and Al matrix. XRD patterns indicated prepared nanoparticles with nanosizes ranging from 40.07 to 38.65 to 36.84 to 38.87 to 39.91 nm. SEM analyzed nanoparticle size, shape, and interaction with the Pr and Al matrix. EDS determined NPs purity. UV-vis spectra of ZnO-Pr/Al nanocomposites showed UV absorption similar to ZnO nanoparticles. Doping ZnO with Pr and Al shrinks the bandgap and slows photogenerated electron-hole pair recombination without changing its crystalline structure.

(Received March 15, 2023; Accepted July 4, 2023)

Keywords: Zinc, Praseodymium, Aluminium, Photoluminescence

1. Introduction

Zinc oxide is widely considered to be one of the most important semiconductor materials. The most significant contributors to this phenomenon were the enormous excitonic binding energy of 60 meV and the significant direct band gap of 3.37 eV. The most frequent form of Wurtzite may be found in crystal structures containing zinc oxide [1,2]. ZnO has become a compelling material as a result of its many useful properties and impressive applications in fields as diverse as optoelectronics, reflection coatings, solar cells, anode-materials, gas-sensors, light-emitting diodes (LED), impact on biological activities, antibacterial actions, and drug delivery, and so on [3,4]. In terms of UV transmission and thermal stability at room temperature, zinc oxide surpassed both GaN and phosphorus[5]. Zinc oxide also fared better than GaN. In order to enhance surface acoustic wave filters, also known as SAW filters, which are often employed in audio and video frequency circuits, zinc oxide nanoparticles have been put to use[6]. Nanostructures made of zinc oxide have been fabricated by researchers, and they have shown exceptional light emission capabilities. In addition, zinc oxide was a chemical that had been well characterised and has obvious attraction to biological systems [7,8]. The majority of the time, the inclusion of rare earth metal ions results in an improvement of the properties like electrical and optical characteristics. Rare earth metals such as europium (Eu), gadolinium (Gd), yttrium (Yi), neodymium (Nd), samarium (Sm), and praseodymium (Pr) are co-doped with the ZnO to achieve even greater enhancements in the film's opto-electrical properties. In addition, the absorption of light at shorter wavelengths and the emission of light at longer wavelengths may be used by rare-earth metals to increase the

* Corresponding author: viswaksenan2u@gmail.com
https://doi.org/10.15251/JOR.2023.194.351

transparency of a material[9]. Pr is an important rare earth element because it can be readily incorporated into the ZnO structure to increase electrical conductivity. This is due to the fact that doped rare earth ions can be employed as down shifting layers within the electronic band structure to enhance their electrical behaviour[10]. As a result, Pr can be readily incorporated into the ZnO structure to increase electrical conductivity. Due to the fact that the ionic radius of Pr^{3+}(1.01) is greater than the ionic radii of Al^{3+}(0.54) and Zn^{2+}(0.54), it is possible for Pr ions to quickly replace the Al and Zn ions with just a little amount of alteration to the structure of the host ZnO(0.74). The creation of nanomaterials may be accomplished using a variety of processes, including thermal decomposition, hydrothermal synthesis, co-precipitation, chemical vapour deposition, spin coating technique, and others. The soft chemical technique was chosen for the synthesis of NPs because of its cheap cost and stability throughout a broad variety of environmental conditions (including swings in temperature and pressure)[11]. The synthesised NPs demonstrated a remarkable alteration in size, shape, and even optical features as a result of these characteristics[12]. The aforementioned characteristics may also be improved upon in nano-Zinc structures, nanoparticles, and nanowires, hence opening the way for an enhancement in the quality of exciton oscillators and an increase in quantum efficiency[13,14]. In this paper, Al and Pr codoped ZnO samples are synthesised via a soft chemical method and in order to examine the materials and establish their characteristics, X-ray diffraction (XRD), scanning electron microscopy (SEM) with energy dispersive x-ray emission spectroscopy (EDS), and Fourier transform infrared spectroscopy (FTIR) were all used. In order to evaluate the optical features, spectroscopic techniques such as photoluminescence (PL) and ultraviolet-visible (UV-vis) are used. The output from the synthesised NPs might be used in a wide variety of fields, including luminescence, optoelectronics, and displays.

2. Preparation of praseodymium and Aluminium codoped ZnO NPs

Zinc nitrate (0.98M), praseodymium nitrate hexahydrate (0.01), and aluminium nonahydrate (0.01M) were individually diluted in 100 cc of distilled water while vigorously swirling the solution. After that, the primary mixture was added to 25 mL of 2M NaOH in a drop-by-drop manner while the container was continually stirred. When the mixture is stirred continuously, a white precipitate forms. When the precipitate had been separated from the rest of the mixture, it was washed repeatedly in double-distilled water and ethanol. After that, the completed item was annealed for three hours at 450 degrees and dried in the oven for one hour at 100 degrees. Powder was made out of the obtained nanoparticles, and then the jar containing the powder was put away for safekeeping. The procedure was the same regardless of whether we were working with $Pr_{0.02}Al_{0.02}Zn_{0.96}O$, $Pr_{0.03}Al_{0.03}Zn_{0.94}O$ and $Pr_{0.04}Al_{0.04}Zn_{0.92}O$. The undoped ZnO NPs were produced using zinc nitrate at a concentration of 0.1M and sodium hydroxide at a concentration of 2.0M [15,16].

3. Result and discussion

3.1. X-ray diffraction analysis (XRD)

The XRD patterns of pure ZnO and Pr, Al-doped ZnO semi-conductor nanoparticles are shown in Figure 1. As shown by the existence of diffraction peaks corresponding to the (100), (002), and (101) planes, the nanocomposite material that was produced had a polycrystalline structure (Zincite, JCPDS: 36-1451). Indicating that wurtzite, which has its c-axis favoured to be perpendicular to the surface, was the primary component in the nanocomposite that developed, the strongest peak was detected at 34.5 degrees. In addition, there were no peaks created for PrO and AlO, which suggests that the only metal oxides that were present were Pr, Al codoped ZnO NPs and not any other types of metal oxides. For the purpose of determining the typical crystallite size of pure ZnO, $Pr_{0.02}Al_{0.02}Zn_{0.96}O$, $Pr_{0.03}Al_{0.03}Zn_{0.94}O$ and $Pr_{0.04}Al_{0.04}Zn_{0.92}O$ NPs, the Scherrer equation (1) was used,

$$D=K\lambda / (\beta \cos \theta) \quad (1)$$

The crystals that were grown had average nanosizes of 40.07, 38.65, 36.84, 38.87 and 39.91 nm when they were prepared. The reduction in size of Pr, Al codoped ZnO crystallites was attributed to the incorporation of Pr^{2+} and Al^{3+} into the ZnO matrix. On the other hand, the increased size of Pr, Al codoped ZnO NPs was attributed to a high number of defects brought about by the increased concentration of Pr^{2+} ions in the Al-ZnO structure.

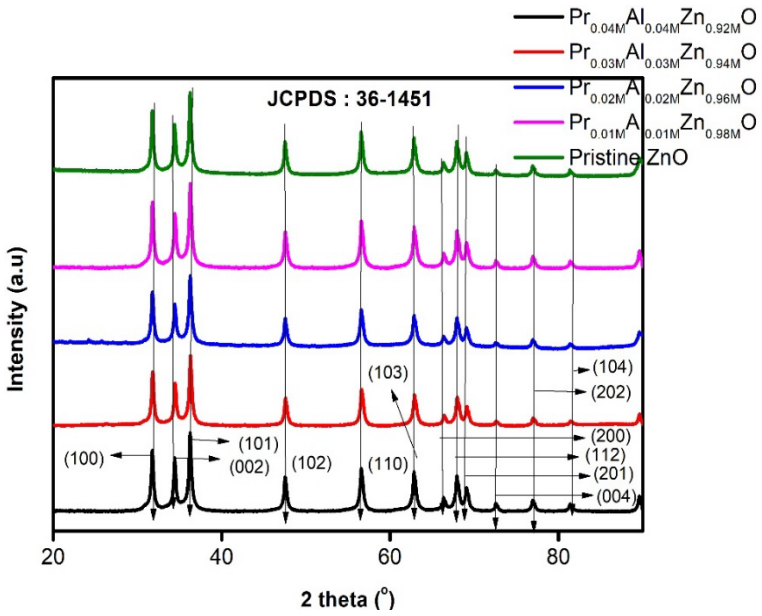

Fig. 1. XRD image of prepared nanoparticles.

3.2. Scanning Electron Microscope (SEM) and Energy Dispersive Studies (EDS)

In contrast to the undoped system, the nanoparticles formed by the Pr, Al codoping of ZnO are found to have a different shape in the SEM and EDAX photographs that are shown in Figure 2. The nanoparticles had an average size of fifty nanometers (nm). The nanoparticles that were produced were erratic in terms of both their size and their form[17]. EDAX analysis revealed that the atoms of aluminium, zinc, and oxygen were really present in the Pr, Al-ZnO nanoparticles. The EDAX scan did not reveal any oxygen-atom peaks that were distinct from those of the ZnO system, which is evidence that no additional metal oxides had formed. The results of the XRD examination supported the validity of this information as well.

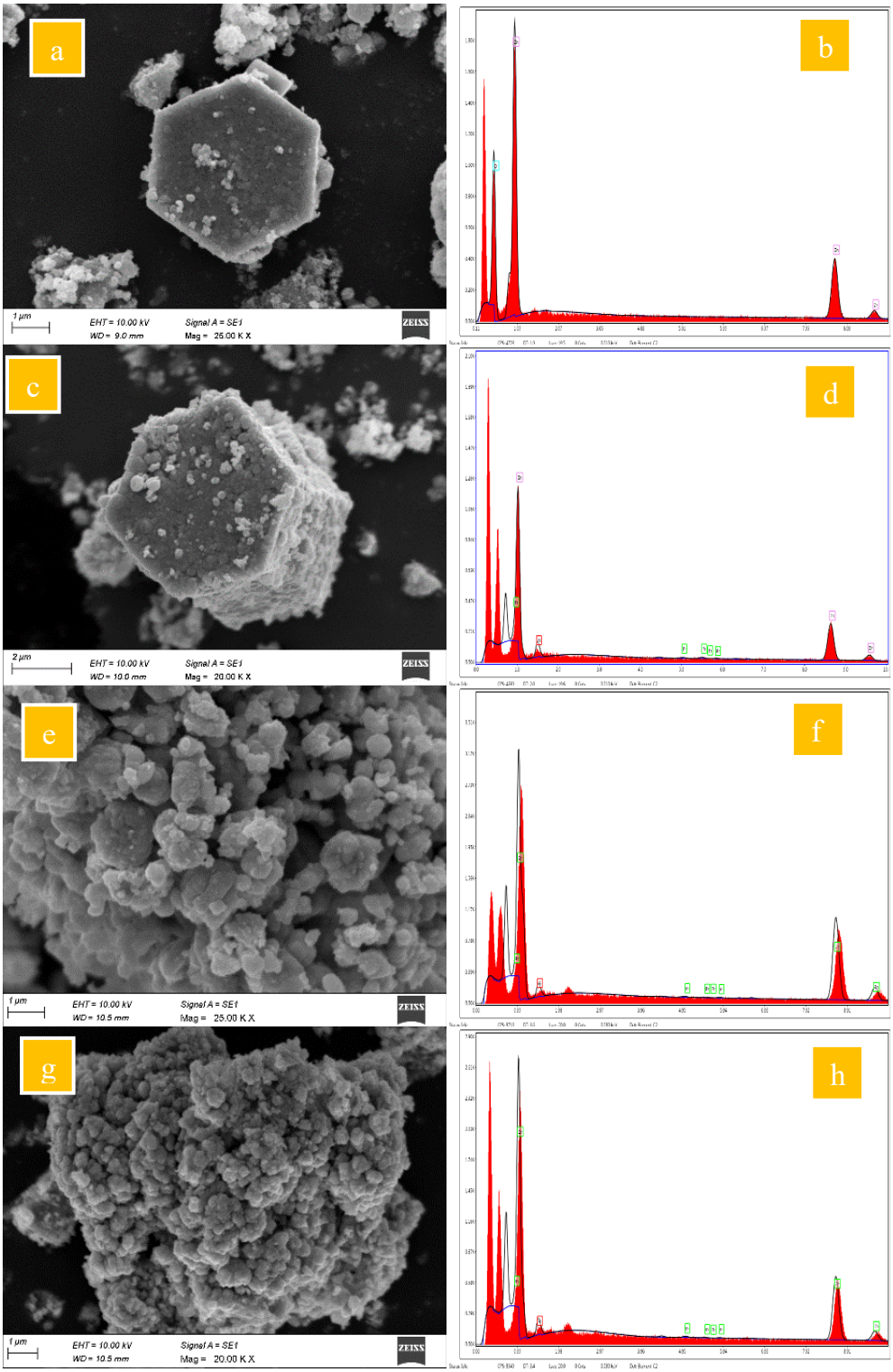
a
1 µm
EHT = 10.00 kV
WD = 9.0 mm
Signal A = SE1
Mag = 25.00 K X
ZEISS
b
c
2 µm
EHT = 10.00 kV
WD = 10.0 mm
Signal A = SE1
Mag = 20.00 K X
ZEISS
d
e
1 µm
EHT = 10.00 kV
WD = 10.5 mm
Signal A = SE1
Mag = 25.00 K X
ZEISS
f
g
1 µm
EHT = 10.00 kV
WD = 10.5 mm
Signal A = SE1
Mag = 20.00 K X
ZEISS
h

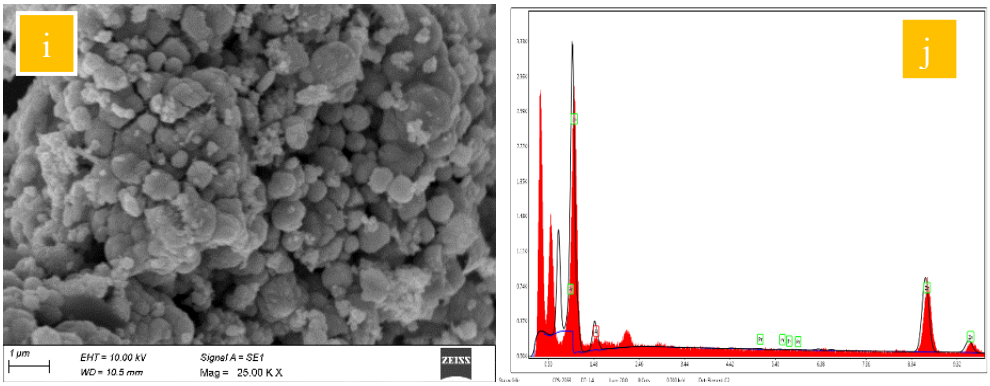

Fig. 2. SEM & EDS images of:
a)b) Pristine ZnO; c) d) $Pr_{0.01}Al_{0.01}Zn_{0.98}O$; e) f) $Pr_{0.02}Al_{0.02}Zn_{0.96}O$;
g) h) $Pr_{0.03}Al_{0.03}Zn_{0.94}O$; i) j) $Pr_{0.04}Al_{0.04}Zn_{0.92}O$.

3.3. Fourier Transform Infrared Spectroscopy (FTIR)

The method of FTIR spectroscopy was used in order to determine the functional groups that were present in the particles of generated mixed metal oxides. These particles included pure ZnO as well as ZnO NPs that had been doped with various quantities of Pr and Al. A fingerprint region of metal oxide nanoparticles was found, and its bandwidth was 716.17 cm^{-1}. The sharp peak at 1531 cm^{-1} demonstrates that the C=O molecule is vibrating symmetrically. Both of these peaks were caused by water adsorption on the surface of zinc oxide nanoparticles, which resulted in the Zn-O stretching vibration at 3723 cm^{-1} and the OH stretching bond vibration at 716.17 cm^{-1}. The wide peak at 3723 cm^{-1} was attributed to the Zn-O stretching vibration, while the peak at 716.17 cm^{-1} was caused by the OH stretching bond vibration. This is because of the vibration of the Pr,Al,Zn-O bonds, which was identified as a peak at a frequency of 716.17 cm^{-1} over a range of Pr/Al codoped ZnO concentrations[18]. The reason for this is due to the fact that ZnO may be doped with varying amounts of Pr and Al. Differences in the peak shifts are what provide conclusive evidence of the existence of Pr and Al ions in the ZnO lattice at varied concentrations. These discrepancies can be observed up top. Mixed metal oxides are produced when two dopants, Pr and Al, are introduced into ZnO. This process causes the dopants to switch places with Zn atoms in the crystal lattice, which results in the development of mixed metal oxides.

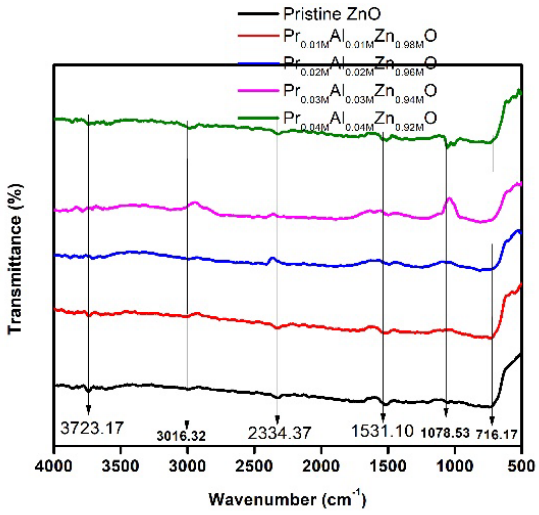

Fig. 3. FTIR spectra of Pristine ZnO and Various concentrations of Pr and Al codoped ZnO.

3.4. Ultraviolet-visible spectroscopy and bandgap calculation

The UV spectra of pure ZnO and Pr, Al-doped ZnO nanoparticles of various concentrations were determined with the use of ultraviolet spectroscopy (Figure 4). When the spectra of Pr, Al codoped ZnO nanoparticles are compared to those of pure ZnO, it is evident that the presence of these ions produces a blue shift in the absorption edge at shorter wavelengths. This can be seen clearly when comparing the two sets of spectra. The maximum absorbance of pure ZnO, as well as varying concentrations of Pr, Al-codoped ZnO NPs, can be found at 344, 344, 339, 342, and 344, respectively. When Al^{3+} and Pr^{2+} ions are introduced into ZnO NPs, the intensity of the peaks that are caused by the different ratios of Pr, Al-ZnO NPs is changed. Using the formula (hv)n =A(hv-Eg), the bandgap (fig 5) of pure ZnO and Pr, Al-doped ZnO NPs at varying concentrations was determined to be 3.10, 2.95, 2.81, 2.73, and 2.60 eV, respectively. The lower band gap values in Pr, Al codoped ZnO NPs were due to the higher concentration of Pr^{2+} ions in the ZnO system[19]. The aforementioned viewpoints demonstrate that Pr^{2+} ions and Al^{3+} are successfully incorporated into the ZnO lattice.

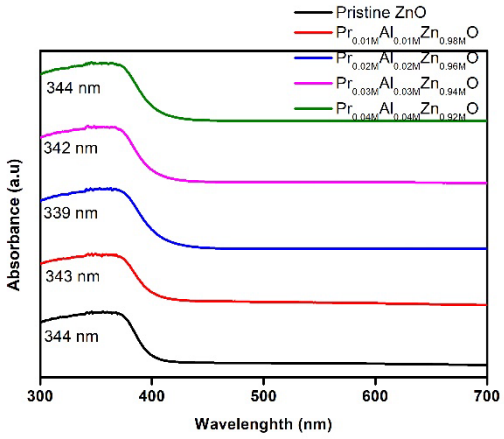

Fig. 4. UV-Visible Spectra and bandgap for Pristine ZnO and different concentrations of Pr and Al codoped ZnO.

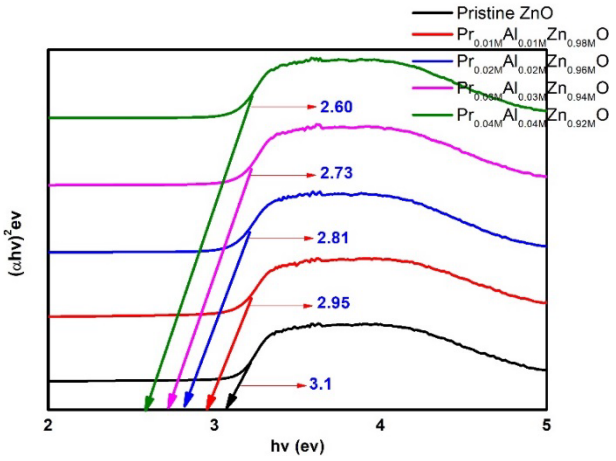

Fig. 5. Bandgap for Pristine ZnO and different concentrations of Pr and Al codoped ZnO NPs.

3.5. Photoluminescence spectra of Pr, Al-ZnO NPs

In Figure 6, the luminescence spectrum of pure ZnO as well as various concentrations of Pr, Al-doped ZnO NPs are shown. The spectrum displays four peaks that are comparable to the luminescence spectrum of pristine ZnO NPs. The first two peaks, located at 485 nm and 498 nm, are

the result of recombination between $e^-_{(CB)}$ and $h^+_{(VB)}$, while the peaks located at 470 nm and 452 nm are the result of recombination between e- (CB) and h+ (VB). The intensity shift demonstrates that Pr^{2+} and Al^{3+} have been introduced into the ZnO system, and the wide peaks demonstrate that the synthesised Pr, Al-doped ZnO NPs contain less defects.

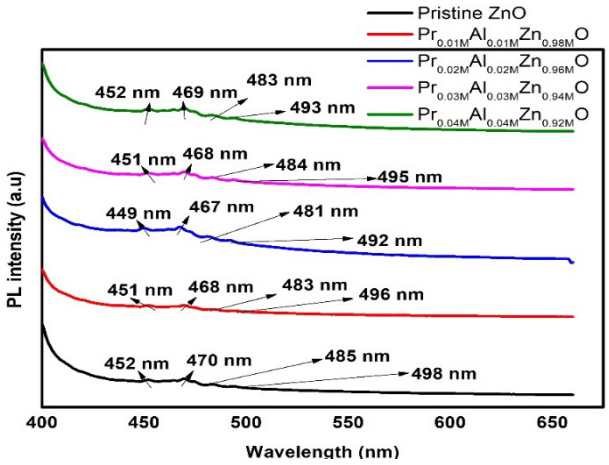

Fig. 6. Photoluminescence image of Pristine ZnO and different concentrations of Pr and Al codoped ZnO NPs.

4. Conclusion

Investigations using SEM-EDAX, FTIR, XRD, PL, and UV-Vis were carried out on the synthesized nanoparticles. The FTIR spectra of the ZnO nanocomposites in order to confirm that the Pr and Al included in the nanocomposites perform the functions for which they were designed. The absorption peak related to the ZnO stretching vibration (714 cm^{-1}). In the XRD patterns, a significant peak located at 34.5° indicated the presence of Pr and Al. This finding is consistent with the hypothesis that the ZnO NPs were in a polycrystalline phase and had a Wurtzite structure. In addition, the discovery of several ZnO crystal planes offered conclusive evidence that the NPs due to the interaction with the Pr and Al matrix. The bandgap values of pure zinc oxide, Pr and Al codoped zinc oxide with various amounts were found to be 3.10, 2.95, 2.81, 2.73, and 2.60 eV, respectively. It was discovered that the sizes of the particles were as 40.07, 38.65, 36.84, 38.87, and 39.91 nm. The nanosized ZnO particles were confirmed to have aggregated and distributed themselves across the whole Pr and Al nanosystem by scanning electron microscopy. In addition, the EDAX analysis demonstrated the sample's lack of impurities. According to the results of a UV-vis spectral investigation, the absorbance of pure ZnO and various concentrations of Pr and Al contained zinc oxide nanocomposites was increased and decreased, respectively. As shown by the concomitant intensity shift, PL spectroscopy provides conclusive evidence for the existence of Pr^{2+} and Al^{3+} in the ZnO system.

Acknowledgments

This work was supported by the King Khalid University through a grant RCAMS/KKU/04-22 under the Research Center for Advance Materials (RCAMS) at King Khalid University, Saudi Arabia

References

[1] Sharma, Dhirendra Kumar, Sweta Shukla, Kapil Kumar Sharma, and Vipin Kumar, Materials Today: Proceedings **49**, 3028-3035 (2022); https://doi.org/10.1016/j.matpr.2020.10.238
[2] Joesna.G, Saravanan.P, Zema.R, Ferin, Gunachitra.T, Sankar.D,Tamilselvan, Meena.M, Senthilkannan, Vimalan.M, and Gulam Mohamed, Journal of Materials Science: Materials in Electronics **33** (17) 14144-14158 (2022); https://doi.org/10.1007/s10854-022-08344-0
[3] Linghu, Jiajun, Tingting Song, Tong Yang, Jun Zhou, Kimyong Lim, Chornghaur Sow, Ming Yang, Yuanping Feng, and Xuezhi Wang, Materials Science in Semiconductor Processing **155,** 107237 (2023); https://doi.org/10.1016/j.mssp.2022.107237
[4] He, Haiping, Solution Processed Metal Oxide Thin Films for Electronic Applications, 7-30, (2020); https://doi.org/10.1016/B978-0-12-814930-0.00002-5
[5] Jeevanantham V, Tamilselvi D, Bavaji SR and Mohan S, Bulletin of Materials Science, 46 (1), 32 (2023); https://doi.org/10.1007/s12034-022-02868-1
[6] Shukla, Vipul J and Amit Patel, Molecular Crystals and Liquid Crystals, **712 (**1), 62-75, (2020); https://doi.org/10.1080/15421406.2020.1856505
[7] Guziewicz, Elzbieta, Tomasz Aleksander Krajewski, Ewa Przezdziecka, Krzysztof. P, Korona, Nikodem Czechowski, Lukasz Klopotowski, and Penka Terziyska. Physica Status Solidi B **257** (2), 1900472 (2020); https://doi.org/10.1002/pssb.201900472
[8] Narayana, Ashwath, Sachin Bhat, Almas Fathima, Lokesh.S.V, Sandeep.G. Surya, and Yelamaggad. C.V, RSC advances **10(23)**, 13532-13542 (2020); https://doi.org/10.1039/D0RA00478B
[9] Vinitha, Viswanathan, Mani Preeyanghaa, Vasudevan Vinesh, Ravikumar Dhanalakshmi, Bernaurdshaw Neppolian, and Vajiravelu Sivamurugan, Emergent Materials **4**,1093-1124 (2021); https://doi.org/10.1007/s42247-021-00262-x
[10] Jeevanantham V, Tamilselvi D, Rathidevi K and Bavaji SR, P Neelakandan, Biomass Conversion and Biorefinery, 1-10, https://doi.org/10.1007/s13399-023-04179-9
[11] Malhotra, Nemi, Hua-Shu Hsu, Sung-Tzu Liang, Marri Jmelou M. Roldan, Jiann-Shing Lee, Tzong-Rong Ger, and Chung-Der Hsiao, Animals **10(**9), 1663 (2020); https://doi.org/10.3390/ani10091663
[12] Manojkumar MS, Jeyajothi K, Jagadeesan A and Jeevanantham V, Journal of the Indian Chemical Society 99 (8), 100559 https://doi.org/10.1016/j.jics.2022.100559
[13] Dushyantha, Nimila, Nadeera Batapola, I. M. S. K. Ilankoon, Sudath Rohitha, Ranjith Premasiri, Bandara Abeysinghe, Nalin Ratnayake, and Kithsiri Dissanayake, Ore Geology Reviews, **122**, 103521 (2020); https://doi.org/10.1016/j.oregeorev.2020.103521
[14] Samrot, Antony.V, Chamarthy Sai Sahithya, Jenifer Selvarani, Sajna Keeyari Purayil, and Paulraj Ponnaiah, Current Research in Green and Sustainable Chemistry **4,**100042 (2021); https://doi.org/10.1016/j.crgsc.2020.100042
[15] Jeevanantham V, Tamilselvi D, Rathidevi K and Bavaji SR, Journal of Materials Research 38 (7), 1909-1918 https://doi.org/10.1557/s43578-023-00965-3
[16] Sreekanth.M, Ghosh.S, Mehta.SK, Ganguli AK, and Menaka Jha, CrystEngComm **19(**16), 2264-2270 (2017); https://doi.org/10.1039/C7CE00073A
[17] Madkour, Loutfy.H. Nanoelectronic materials: fundamentals and applications **116** (2019); https://doi.org/10.1007/978-3-030-21621-4_1
[18] Sathya V, Jagatheesan R, Jeevanantham V, Gopi D and Baby Shakila P, Journal of Applied Electrochemistry, 1-8 https://doi.org/10.1007/s10800-023-01890-3
[19] Madkour, Loutfy H., and Loutfy H. Madkour. Nanoelectronic Materials: Fundamentals and Applications 701-759 (2019); https://doi.org/10.1007/978-3-030-21621-4_17

Chemical Physics Impact 6 (2023) 100246

Contents lists available at ScienceDirect

Chemical Physics Impact

journal homepage: www.sciencedirect.com/journal/chemical-physics-impact

Highly photoactive rGO-MnO_2/CuO nanocomposite photocatalyst for the removal of metanil yellow dye and bacterial resistance against *Pseudomonas Aeruginosa*

A. Ceril Jeoffrey [a,b], S. Jothi Ramalingam [a], K. Murugaiah [a], A.R. Balu [c,*]

[a] Chemistry Department, AVVM Sri Pushpam College (Affiliated to Bharathidasan University, Tiruchirappalli), Poondi, Tamilnadu, India
[b] Chemistry Department, St. Joseph's College, Tiruchirappalli, Tamilnadu, India
[c] Physics Department, AVVM Sri Pushpam College, Poondi, Tamilnadu, India

ARTICLE INFO

Keywords:
Chemical precipitation
nanocomposite
energy band gap
photodegradation
reduced graphene oxide

ABSTRACT

The superior photocatalytic, biological, and electrochemical properties of metal oxide nanocomposites have made them an important part of contemporary nanotechnology research. Nanocomposite involving MnO_2 and CuO has been widely utilized for catalytic and electrochemical applications. However, the different oxidation states of MnO_2 and lower band gap of CuO limits the efficiency of the devices involving the composite of these two semiconductors. As a result, reduced graphene oxide (rGO) is integrated into the MnO_2/CuO matrix. rGO-MnO_2/CuO and MnO_2/CuO nanocomposites (NCs) were synthesized using one-pot green synthesis and chemical precipitation respectively. rGO decorated MnO_2/CuO NC was green synthesized from graphene oxide using *Alternanthera sessilis* leaf extract. XRD detected peaks related to orthorhombic structured MnO_2 and monoclinic structured CuO for both the composites. Star shaped nanostructures are observed for rGO incorporated MnO_2/CuO nanocomposite. MC and rMC composites have band gaps of 2.16 and 2.04 eV, respectively. FTIR spectrum showed the characteristic peaks for MnO_2 and CuO in the rGO-MnO_2/ CuO composite. Raman active A_g and B_g CuO modes occur at 270 and 450 cm^{-1} and Mn-O symmetric vibrations at 590 and 540 cm^{-1}. The incorporation of rGO into the MnO_2/CuO composite increased its photocatalytic activity from 87 % to 96 % against the degradation of metanil yellow dye by increasing its electron conductivity, adsorption capacity, and light absorption capacity. The MnO_2/CuO nanocomposite with rGO demonstrated enhanced antibacterial activity, with a zone of inhibition of 24 mm compared to 13 mm for the control and 18 mm for the MnO_2/CuO composite.

1. Introduction

The surrounding ecosystem and human health are seriously threatened by the growing amount of waste water carrying dangerous organic contaminants from diverse enterprises [1]. Water pollution is exacerbated by dyes, which are poisonous and often produced in industrial settings. The removal of organic contaminants from water has been attempted using advanced oxidation processes (AOPs). Photocatalysis, which may be carried out with just a catalyst and light, is the most efficient AOP for cleaning pollutants out of water [2]. Metal oxide semiconductors have become popular for environmental pollution cleanup due to their photosensitivity and non-toxicity [3]. With the application of photocatalytic semiconductors, water and air can be purified in a scientifically sound manner. Furthermore, it is used for the regulation of odor, the production of hydrogen, and the inactivation of bacteria and cancer cells. Metal oxide semiconductors like ZnO [4], TiO_2 [5], NiO [6], SnO_2 [7], etc. are often used in catalytic applications. In addition to these wide band oxides, lower band gap oxides such as CdO [8], Cu_2O [9], MnO [10], $BiVO_4$ [11] are also used for catalytic applications. However, using a single semiconductor has problems such as sluggish photocatalyst deactivation, low visible light harvest, poor selective adsorption, and quick electron-hole pair recombination. Combining two distinct types of metal oxides to produce a composite material that enables the effective mutual movement of charge carriers from one semiconductor to another is the strategy that has proven to be the most successful in meeting the requirements of these problems. Two semiconductors MnO_2 and CuO were coupled to form composite in this work.

* Corresponding author:
E-mail address: arbalu757@gmail.com (A.R. Balu).

https://doi.org/10.1016/j.chphi.2023.100246
Received 12 April 2023; Received in revised form 4 June 2023; Accepted 6 June 2023
Available online 7 June 2023

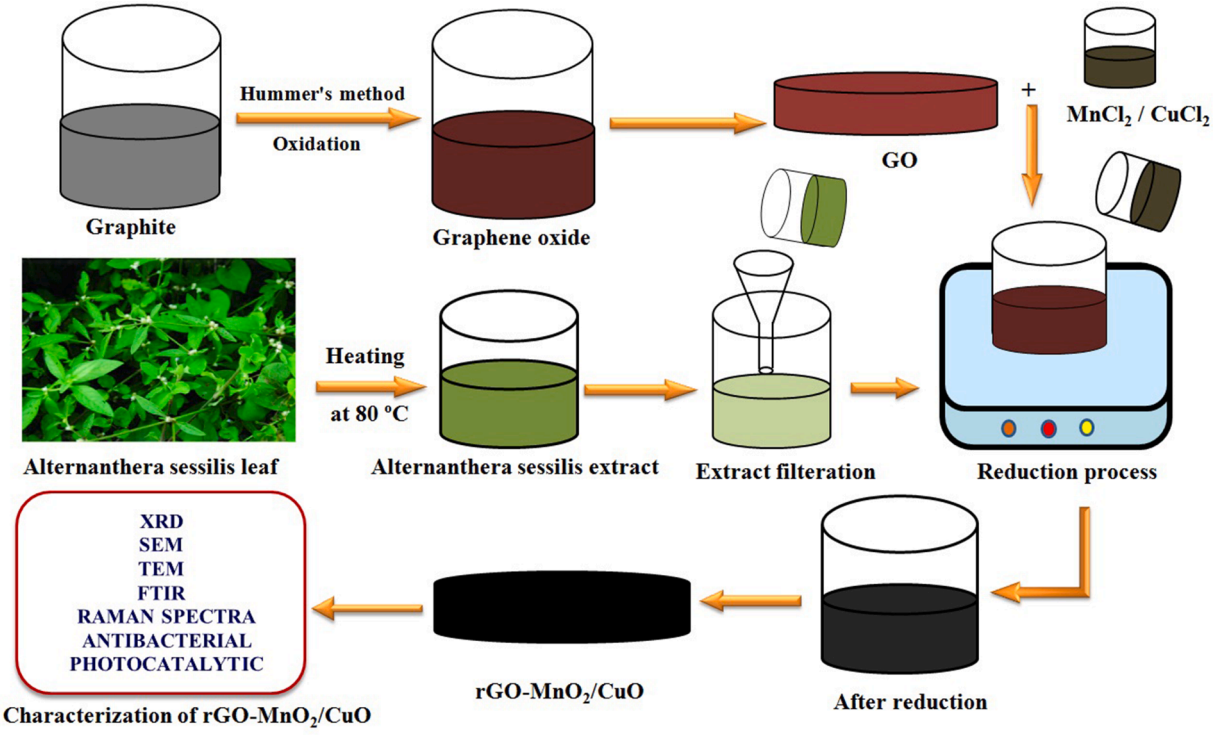

Fig. 1. Synthesizing procedure of rMC composite

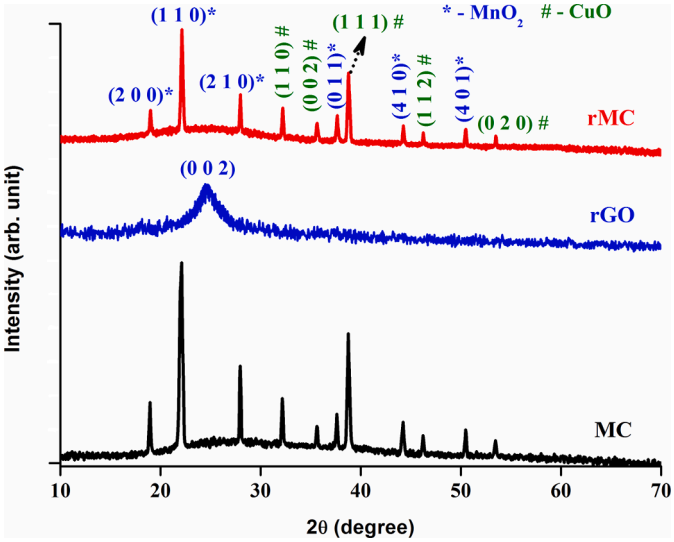

Fig. 2. Diffraction patterns of MC and rMC composites

The stable oxide manganese dioxide (MnO_2) has a high surface area, strong chemical resistance, and catalytic behavior [12]. MnO_2 is a possible pseudo-capacitive oxide with a capacitance of up to 1370 F/g [13]. MnO_2 nanostructures suited for catalytic activities have been controlled synthesized by Sun et al. [14]. Catalytic combustion of toluene using hierarchical MnO_2 via H_2O_2 selectively reducing $KMnO_4$ has been reported by Chen et al. [15]. Two dimensional MnO_2 nanosheets has been reported to promote ultra-sensitive pH-triggered theranostics of cancer by Chen et al. [16]. MnO_2 NPs with biomedical properties has been synthesized by Chen et al. [17]. However, poor electron conductivity and instability are drawbacks that limit MnO_2's use in pseudo-capacitors and catalytic applications.

Among the applications of CuO, a p-type semiconductor with a narrow band gap, are high temperature superconductors, photovoltaic materials, field emission, and catalysis [18]. The anticancer, antibacterial, and antioxidant properties of CuO nanoparticles make them an attractive biomedical material [19]. Green CuO nanoparticles possess antibacterial activity against urinary tract pathogens [20]. Singh et al. [21] bio-synthesised CuO NPs suitable for electrochemical sensing and remediation of 4-nitrophenol. Photocatalytic and antibacterial properties of CuO NPs biosynthesized using *Verbascum thapsus* leaf extract has been reported by Getu et al. [22]. In a study by Azam et al. [23], CuO NPs were reported to exhibit antimicrobial properties that depend on their size. Antioxidant and DNA cleavage properties have been reported for green synthesized CuO NPs by Duman et al. [24].

There are several reasons why CuO is preferred over MnO_2 loading, including its large specific surface area, chemical stability, non-toxicity, high conductivity, and remarkable electrochemical properties [25]. Because of the synergistic effects and morphological structures of MnO_2 and CuO, the MnO_2/CuO nanocomposite seems to be ideal material for catalysis and antimicrobial applications. With CuO introduction into MnO_2 matrix as reinforcing element, the MnO_2/CuO NC exhibited improved capacitive performance [26]. Researchers Zhang et al. [27] and GuO et al. [28] have developed CuO@MnO_2 core-shell nanostructures with high supercapacitive performance. MnO_2/CuO catalyst for co oxidation has been synthesized by Qian et al. [29]. Supercritical oxidative degradation of ethyl acetate in water has been reported by Martin et al. [30]. Lithium-ion batteries with CuO@MnO_2 core-shell nanosheet arrays synthesized by Qing et al. [31] have been found to exhibit high performance.

In spite of the good synergistic effects between MnO_2 and CuO, the photodegradation efficiency is somewhat reduced due to the different oxidation states of MnO_2 and the low band gap value of CuO. To overcome this limitation, rGO is incorporated into the MnO_2/CuO matrix. The surface of the sp^2-C atoms in rGO is adorned with oxygenated functional groups and defect sites, giving it a distinctive 2D honeycomb structure. With its variable band gap and exceptional mechanical, chemical, and thermal capabilities, rGO is well suited for composite functioning [32]. Therefore, rGO incorporation is expected to

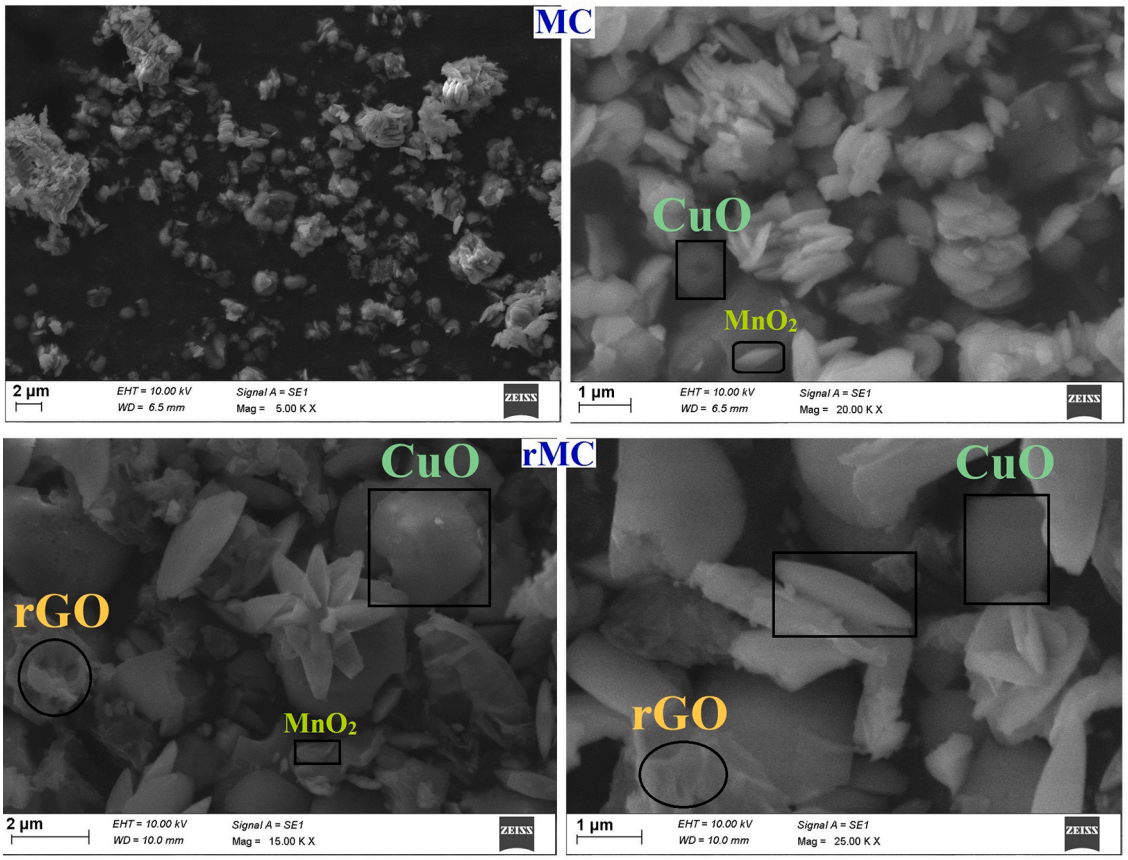

Fig. 3. SEM images of MC and rMC composites

significantly improve the catalytic and antibacterial properties of MnO_2/CuO nanocomposite. Studies on the electrochemical, catalytic and antibacterial properties of rGO embedded MnO_2/CuO is very scarce in the literature and the results obtained for the rGO incorporated MnO_2/CuO NC in this work will address the current research gaps or challenges that arise while utilizing this composite.

2. Experimental

2.1. Materials Used

The materials used included graphite powder (purity 98%), sulfuric acid (purity 98.5%), potassium permanganate (purity 99%), phosphoric acid (purity 99%), hydrochloric acid (purity 98%), hydrogen peroxide (purity 99%), manganese chloride (purity 99.6%), cupric chloride (purity 99.2%). An extract of Alternanthera sessilis leaf was used to reduce graphene oxide to rGO.

2.2. Synthesis of MnO_2/CuO (MC) composite

280 mL of demineralized water and 5 mL of weak hydrochloric acid were added to a 500 ml beaker with 0.1 M manganese (II) chloride and cupric chloride. The mixture was stirred rapidly until the salts were dissolved. After adding 15 mL of liquid NH_3, the solution's pH was neutralised and allowed to mature for 12 hours. Finally, MC nanocomposite was obtained by crushing the precipitates after they had been rinsed and calcined at 400°C for 2 hours.

2.3. Synthesis of graphene oxide (GO)

In a 500 mL beaker containing a 9:1 volume mixture of phosphoric acid and sulphuric acid, graphite powder (1 g) was gradually added and thoroughly mixed while on ice. A constant stirring was performed while potassium permanganate (6 g) was gradually added. For 12 hours, the solution's temperature was raised steadily to 50°C while being vigorously stirred. 800 mL of frozen water and 1 mL of 30% hydrogen peroxide progressively diluted the mixture. Three rounds of washing with deionized water and 10% HCl neutralized the pH. By washing with ethanol and drying for 12 hours at 60°C, brown GO powder was obtained.

2.4. Leaf extract preparation

At 95°C, 10 g of cleaned *Alternanthera sessilis* leaves were cooked for 45 minutes in 200 mL of water. After filtering the solution, the obtained extract was kept at 4°C in the fridge.

2.5. Synthesis of rMC composite

A mixture of 100 mL distilled water and 100 mg (optimized value) of GO powder was mixed before ultrasonically treating for 30 minutes. Thirty minutes after adding MnO_2/CuO precipitates, the mixture was stirred. Afterwards, 25 mL of extract was added and mixed for five hours at 95°C. The concoction was filtered as soon as it reached ambient temperature. After being cleaned and dried for five hours at 80°C, rGO-MnO_2/CuO (rMC) nanocomposite was created. Fig. 1 illustrates the entire synthesizing process.

2.6. Characterization

The chemical structure, morphology, optical nature and luminescence properties were studied using X-ray diffractometer (PRO Analytical X' pert), scanning electron microscope (S-3000H HITACHI), spectrophotometers (Lambda-35) and Varian Cary Eclipse. Functional

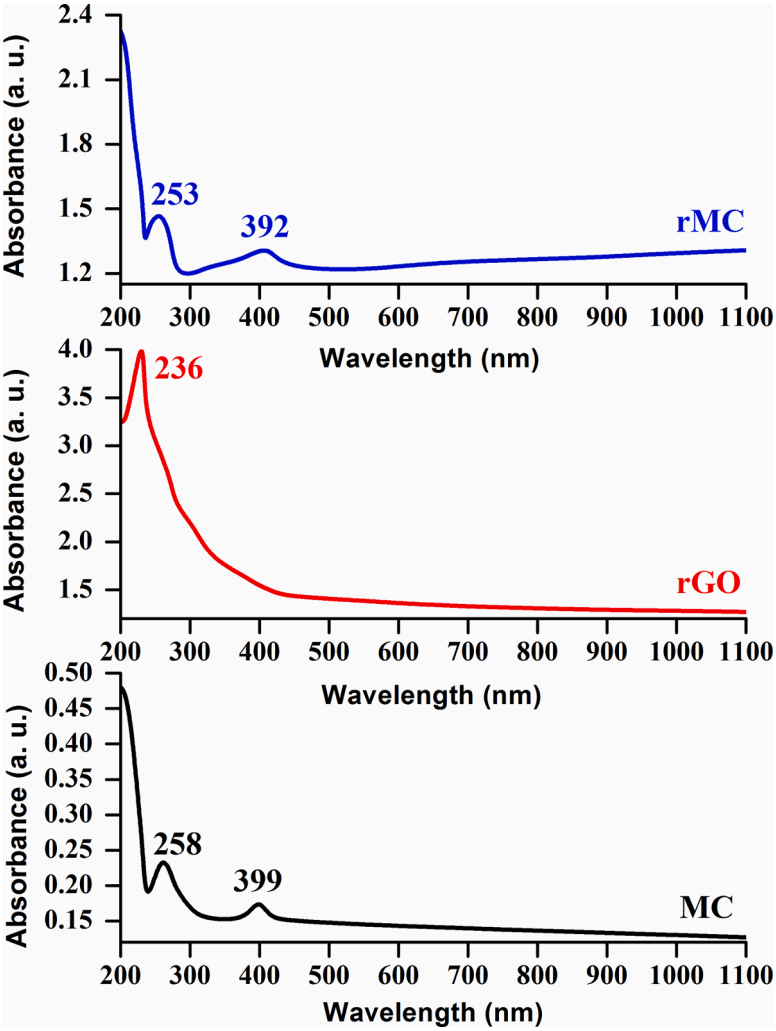

Fig. 4. Absorbance spectra of MC and rMC composites

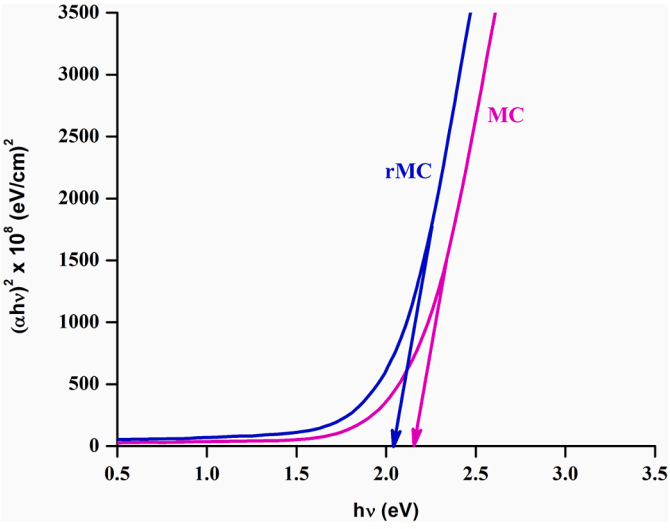

Fig. 5. $(\alpha h\nu)^2$ vs. hν plots of MC and rMC composites

groups and Raman analyses were performed using spectrophotometers (Perkin Elmer RX-1 and Renishaw Invia Laser).

2.7. Photocatalytic test

MC and rMC catalysts were evaluated for their ability to degrade metanil yellow dye under visible light. In 100 mL water, 0.05 g of MY dye was dissolved and swirled for 30 minutes with and without the catalysts of 6 mg concentration. As visible source, incandescent bulb with a power output of 100 W was used. For every 15 min, absorption spectra was recorded for the dye solution at $\lambda = 435$ nm.

2.8. Antibacterial activity

MC and rMC NCs were tested against *Pseudomonas Aeruginosa* (*P. aeruginosa*) bacteria using agar well diffusion method. Bacterial culture was spread over the petriplates containing freshly prepared Muller – Hinton agar medium. Two mg each of the control (Amikacin), MC and rMC NPs were dissolved in 25 μL DMSO and incubated at 37° C for 24 hours.

3. Outcomes of the findings

3.1. X-ray diffraction studies

The orthorhombic structure of MnO_2 [JCPDS No. 82-2169] was

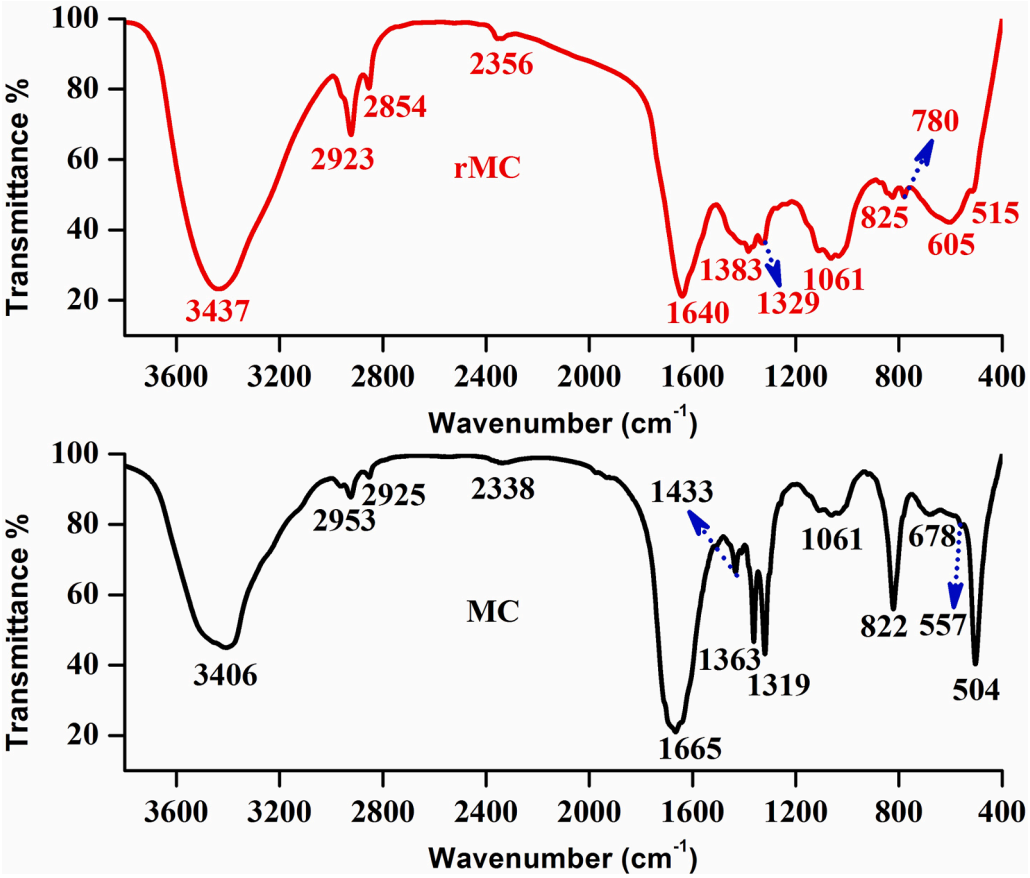

Fig. 6. FTIR spectra of MC and rMC composites

coincident with the peaks (2 0 0), (1 1 0), (2 1 0), (0 1 1), and (4 1 0) denoted by * (Fig. 2). The monoclinic structure of CuO [JCPDS No. 41-0254] was coincident with the diffraction peaks (1 1 0), (0 0 2), (1 1 1), (1 1 2), and (0 2 0) denoted by the symbol # (Fig. 2). The observed peaks for both composites clearly show MnO_2 and CuO coexistence. rGO exhibited a broad (0 0 2) peak at around 24.8° (Fig. 2). However, no peaks related to rGO were observed in the rMC composite due to its weaker intensity than that of MnO_2 and CuO [33]. The average crystallite size of MC and rMC composites was 42 and 33 nm, respectively, according to Scherrer's equation. Consistent with previous findings [34], the rMC composite was shown to have smaller crystallites. Malik et al. [35] observed a similar reduction in crystallite size for rGO-ZnO composite, which they attributed to ZnO crystal nucleation disturbances. With decreased crystallite size, the rMC composite exhibits a high surface-to-volume ratio, which could have enhanced its photocatalytic activity (Section 3.6).

3.2. SEM analysis

Fig. 3 shows the SEM images with two different magnifications of MC and rMC nanocomposites. Clustered tiny nanorods with different sizes are seen for the MC composite. Star shaped nanostructures are seen for the rMC composite. Thus, with rGO incorporation morphology of the MC composite changes significantly. Observed star-shaped structure for the rMC composite inhibits self-aggregation, as well as the creation of a larger surface area and more active sites, increasing the production of reactive oxygen species and enhancing its catalytic and antibacterial properties.

3.3. UV-Vis analysis

The absorbance peaks at 258 and 399 nm observed for the MC composite got shifted to 253 and 392 nm with rGO incorporation which exhibited absorbance peak at 236 nm (Fig. 4). Similar shifting of absorbance peaks towards smaller wavelengths with rGO incorporation has been reported earlier [36]. Since rGO has a non-zero visible absorption, rMC composites containing rGO have increased absorption in the visible range. The band gap energies (E_g) of the MC and rMC nanocomposites was calculated using absorption coefficient (α) and photon energy (hν) via Tauc plot method with the equation:

$$(\alpha h\nu)^2 = (h\nu - E_g) \quad (1)$$

The calculated E_g values are 2.16 and 2.04 eV, respectively for the MC and rMC composites (Fig. 5). Oxygen vacancies and strong interfacial interaction between rGO and MnO_2/CuO nanoparticles may be responsible for the synergistic impact reported in the rMC composite, resulting in a smaller band gap [37]. RMC composite's reduced band gap can also be attributed to surface charge and electronic coupling between MnO_2/CuO and rGO [38]. Due to decreased band gap, antibacterial activity of the rMC composite is enhanced due to more ROS generation (Section 3.7).

3.4. Functional group analysis

In FT-IR spectra of MC and rMC (Fig. 6) O-H bending occurs at 3406 and 3437 [39]. C-H stretching occurs at 2953 and 2925 cm^{-1} for MC and at 2923 and 2854 cm^{-1} for rMC [40]. The 2338 and 2356 peaks correspond to HC≡H stretching. The absorption that occurs at a frequency of 1665 cm^{-1} in MC can be traced back to the bending vibration of O-H atoms that are connected with Mn atoms [41]. Adding rGO

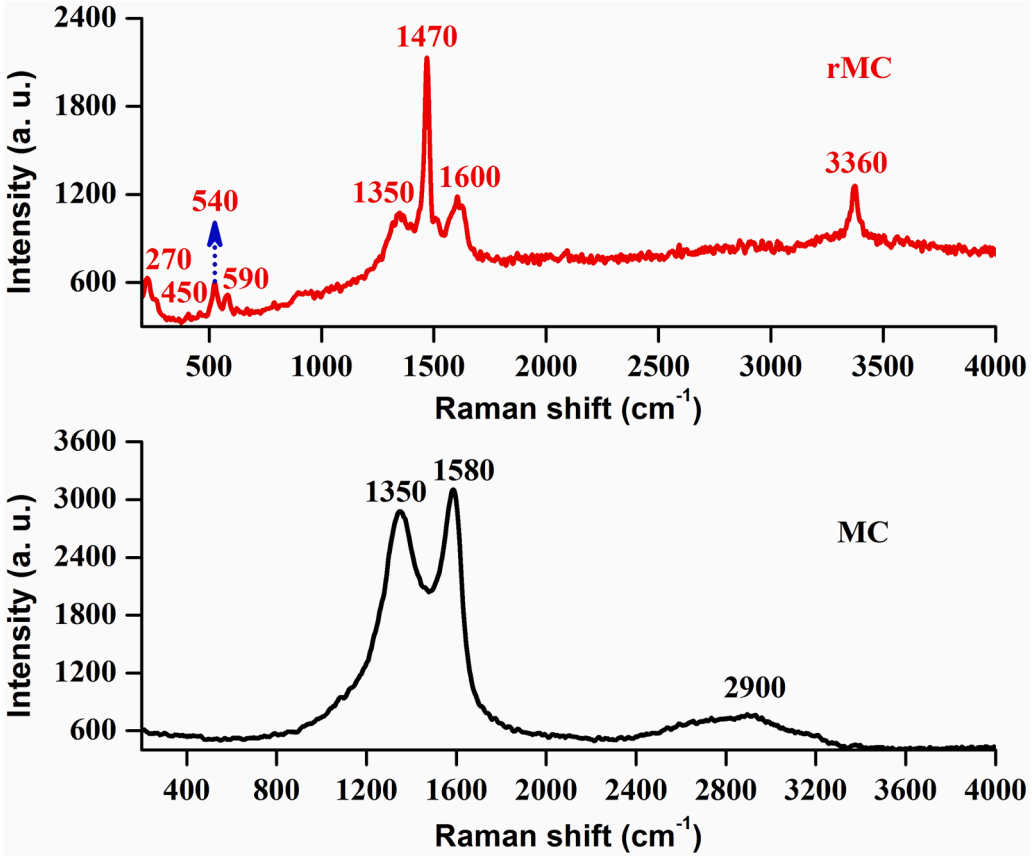

Fig. 7. Raman spectrum of rMC nanocomposite

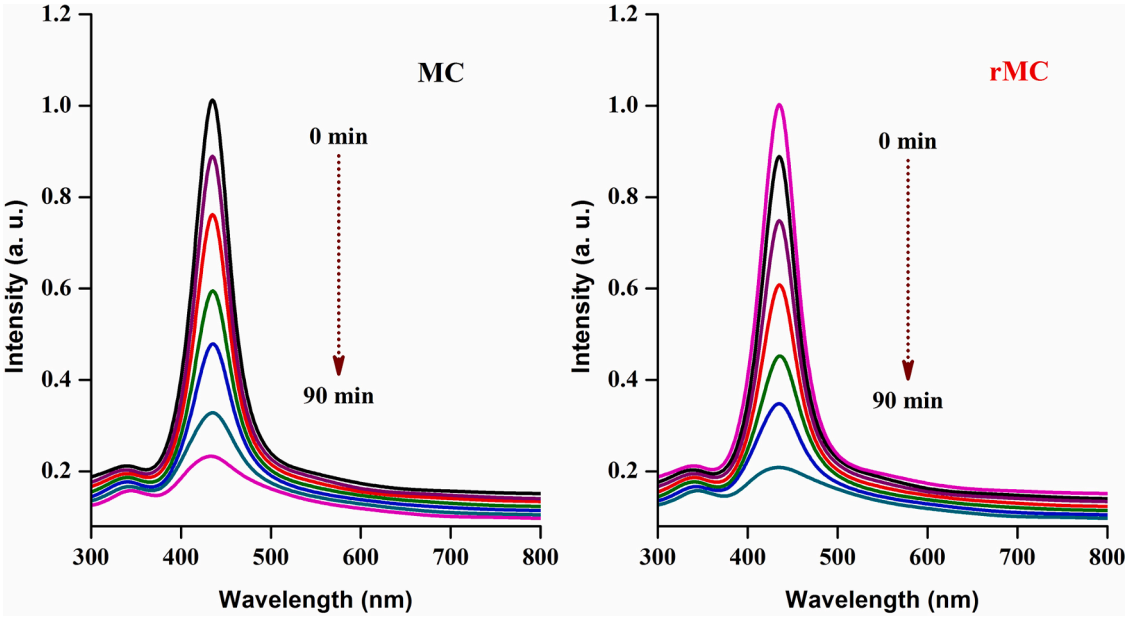

Fig. 8. Absorption spectra of MC and rMC catalysts

caused this peak to move to 1640 cm^{-1}. A band at 1433 was detected for the MC composite, and it was shown to be due to the anti-symmetric vibration of adsorbed CO_2 [42]. C–OH vibration occurs at 1363, 1319 cm^{-1} for MC and at 1383, 1329 cm^{-1} for rMC composites. C–O bond occurs at 1061 cm^{-1} [40]. The MC peak at 822 cm^{-1} correlates with Mn-O vibrations, which shift to 825 cm^{-1} in the rMC [43]. The O-Mn-O vibrational mode occurs at 780 cm^{-1} in the rMC composite [44]. The MC composite has a CuO-related peak at 678, 557 and the rMC composite at 605 cm^{-1} [45]. The MC composite's peak at 504 cm^{-1} caused by Mn-O-Mn symmetric stretching vibration shifted to 515 cm^{-1} for rMC [46].

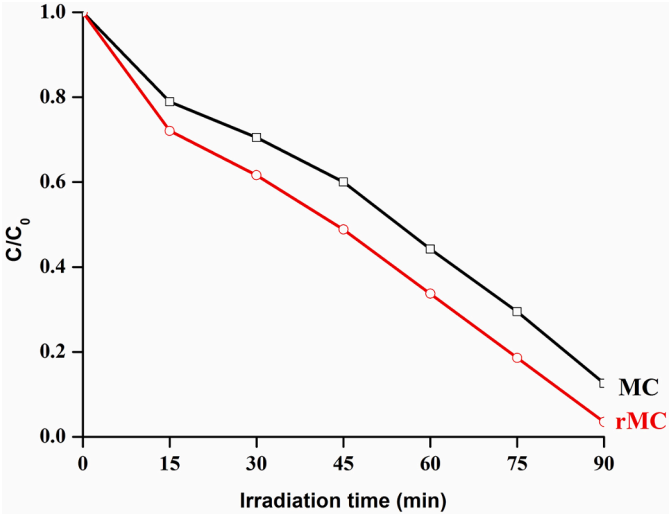

Fig. 9. C/C_0 vs. irradiation time plots of MC and rMC catalysts

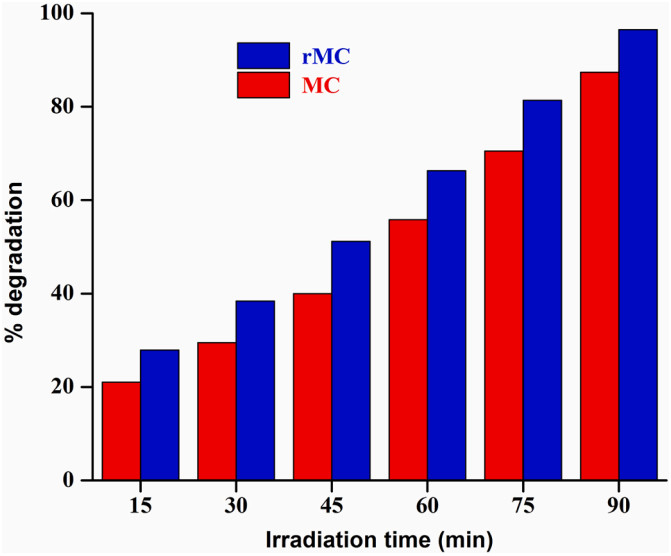

Fig. 10. Photodegradation efficiencies of MC and rMC catalysts

3.5. Raman studies

A prominent peak at 3360 appears in the Raman spectrum of rMC NC (Fig. 7) resulting from the OH stretching vibrations of moisture and rGO [47]. rGO D and G bands are represented by the 1350 and 1600 cm^{-1} peaks, respectively [48]. The D band is an indication that there are faults in the atomic layers that make up the graphite, whereas the G band is the result of the stretching of in-plane bonds between sp^2 C atoms [49]. The C-O stretching vibration of rGO causes the peak at 1470 [50]. Peaks at 590 and 540 [51] are due to Mn-O symmetric vibrations. Raman active A_g and B_g CuO modes occur at 270 and 450 cm^{-1} [52]. Thus, the rMC nanocomposite contains the Raman characteristic bands of rGO, MnO_2 and CuO materials.

3.6. Photocatalytic test

The UV-Vis spectra of MY with MC and rMC catalysts are depicted in Fig. 8. It is discovered that MY's 435 nm distinctive absorption rapidly declines with exposure to visible light and nearly vanishes after 90 minutes. The spectral absorption peak is eliminated by additional exposure, demonstrating complete decay of MY. Y^{3+} and Sm^{3+} co-doped NiO nanocomposite reported by Kannan et al. [53] are consistent with this. Fig. 9 shows the results of MY degradation under the condition of MC and rMC catalysts. Without the catalyst, the MY concentration drops very slightly when subjected to irradiation in a blank test.

Table 1
Comparison on the photodegradation efficiencies of rMC catalyst with other rGO based composites

Composite	Dye	Light Source	Irradiation time	Degradation efficiency	Reference
CdO/ CeO_2/ RGO	MO	Ultrasonic irradiation	150 min	85 %	[56]
PANI/ rGO/ MnO_2	MB	Visible	120 min	91%	[57]
TiO_2/ RGO/Ag	MB	UV	90 min	81%	[58]
ZnO/ CdO/ rGO	MO, RhB	Ultrasonic irradiation	120 min	84, 80 %	[59]
rGO/ CdO/ SnO_2	CR, MG	Visible	120 min	82%, 94%	[60]
WO_3/ CuO/ rGO	RhB	Visible	90 min	93%	[61]
rGO-MnO_2/ CuO	MY	Visible	90 min	96%	This work

The degradation percentage of MY solutions using MC and rMC catalysts for 90 min is 87 and 96 %, respectively (Fig. 10). This clearly indicates that with rGO incorporation, the photodegradation ability of MC nanocomposite is enhanced substantially. The introduction of rGO into the MC catalyst enhanced the surface area, which led to a greater degrading efficiency. rGO's higher surface area and more active areas lower electron and hole recombination [34]. rGO addition enhances the MC catalyst's light absorption via the π-π stacking interface and increased degradation efficiency [42]. The reduced band gap and star morphology of the rMC catalyst also contributed to its degradation efficiency [55]. A comparison on the degradation efficiency of the rMC catalyst with previously reported rGO decorated nanocomposites is compiled in Table 1.

The E_{CB} and E_{VB} potentials of MnO_2 and CuO computed using the following relations can be used to explore the photocatalytic mechanism involved in the rMC catalyst:

$$E_{VB} = X - E^e + 0.5\ E_g \tag{2}$$

$$E_{CB} = E_{VB} - E_g \tag{3}$$

MnO_2 and CuO have E_{CB} values of -0.757 and 0.24 eV and E_{VB} values of 1.563 and 2.05 eV, respectively, according to calculations. The higher positive edge potential of CuO contributes to its stronger oxidative ability, thus dominating the photocatalytic activity of MnO_2/CuO. The photocatalytic mechanism of the rMC catalyst is illustrated in Fig. 11. As the CB potential of MnO_2 is negative, electrons diffuse from the CB of MnO_2 to CuO through rGO under visible light exposure. Similarly, holes diffuse from the VB of CuO to MnO_2 through rGO. As a result, charge carriers are effectively segregated, lengthening their life time and improving interfacial charge transfer efficiency. Complete mineralization of MY occurred when photogenerated electrons were neutralised by dissolved oxygen molecules in water, creating O_2^{*-} radicals, and photogenerated holes interacted directly with H_2O to create OH* radicals [54].

The photodegradation rate constants (k) of MC and rMC catalysts were investigated usiong the relation:

$$k = \frac{\ln(C_0/C)}{t} \tag{4}$$

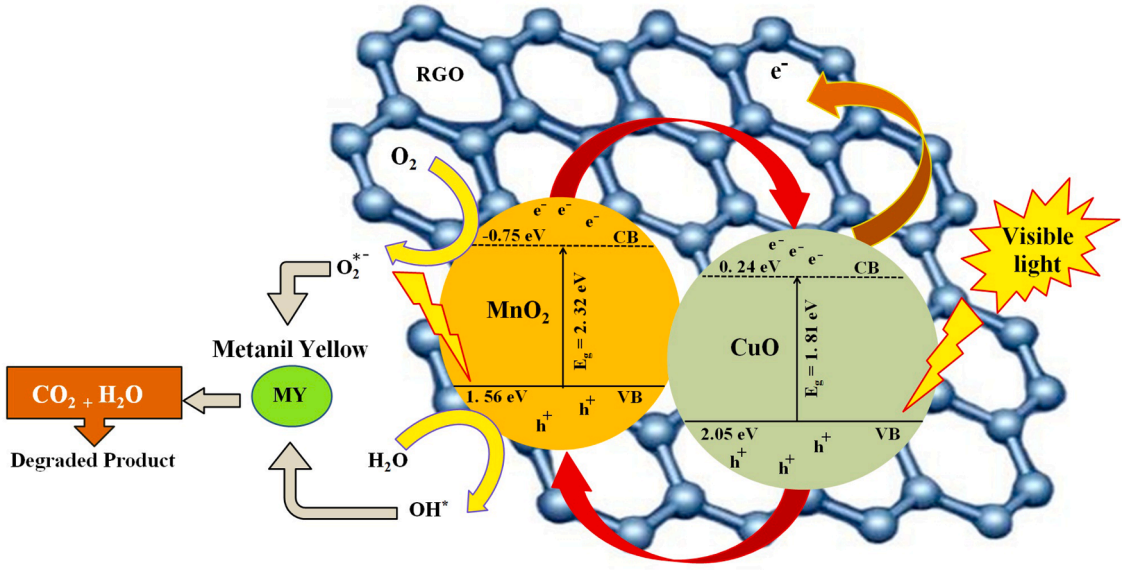

Fig. 11. Photocatalytic mechanism of rMC catalyst

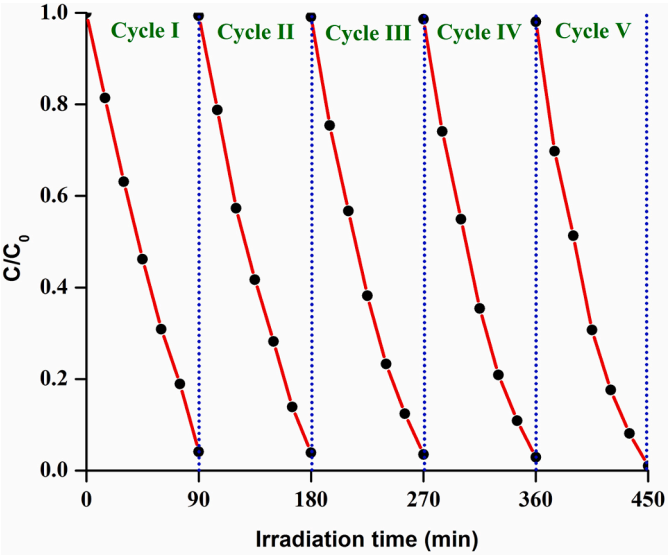

Fig. 12. Recycle test of rMC catalyst

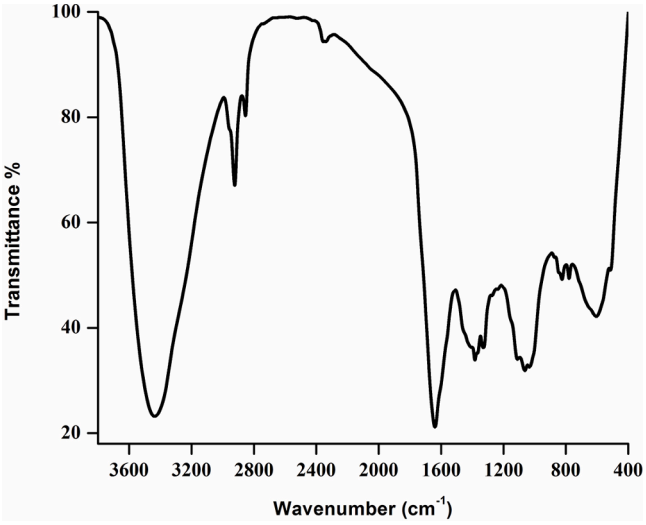

Fig. 13. FTIR spectrum of recycled rMC catalyst

where C_0 and C are the dye concentration under dark and light conditions. The k values estimated from the plots between $ln\left(\frac{C_0}{C}\right)$ vs. irradiant time were 0.0157 and 0.0284 min^{-1} for the MC and rMC catalysts, respectively. rMC catalyst's high k value confirmed its higher degradation capability.

The recyclability of the rMC catalyst was examined by doing the degradation experiment five times. Recycle experiments of the rMC catalyst with MY are shown in Fig. 12. No discernible efficiency loss was seen for the first four cycles, but an abnormal efficiency decline was seen for the fifth. The acquired results validated the photocatalyst's remarkable stability, which is further substantiated by the FTIR spectrum (Fig. 13) of the recovered photocatalyst.

3.7. Antibacterial activities

MC and rMC nanocomposites were tested for their antibacterial activity against *P. aeruginosa* bacteria. The antibacterial activity was studied with an optimum concentration of the composites (25μL). The measured ZOI values (Fig. 14) are 13, 18 and 24 mm for the control (Amikacin), MC and rMC nanocomposites. As shown in Table 2, rMC NC has superior antibacterial performance when compared with previously reported rGO nanocomposites.

The MC and rMC composites resisted the bacterial growth effectively better than the control. The highest ZOI observed for the rGO-MnO_2/CuO nanocomposite confirmed its best potentiality against the tested bacteria. Metal ion release (Mn^{2+}, Cu^{2+}), reactive oxygen species production (H_2O_2, OH*, O_2^{*-}), and the surface area of the composites were all cited as contributing to the composites' antibacterial activity [66]. O_2^{*-} is one type of ROS that is harmful to numerous cellular components like nucleic acid, lipids, proteins, DNA, and carbohydrates [67]. The bacterial cell is extremely sensitive to the severe oxidative effects of both H_2O_2 and OH* radicals. As a result, several crucial biological functions of the cell are harmed, which may prevent cell division and growth [68]. According to Kannan et al. [69], lipid peroxidation, DNA damage, and protein oxidation all cause bacteria to die, but not nonbacterial cells. Freed metal ions are attracted by the thiol groups (-SH) on the outer

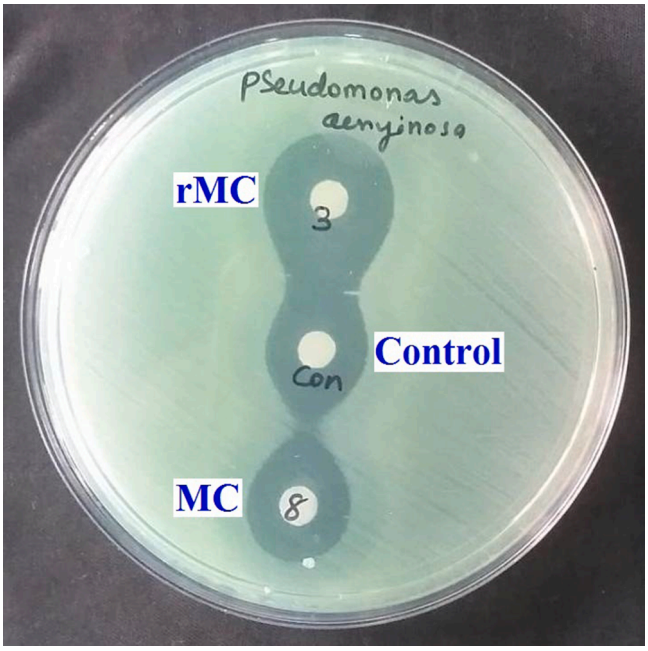

Fig. 14. Antibacterial activity of control, MC and rMC nanocomposites

Table 2
Comparison on the antibacterial performance of rMC NC with previously reported rGO based nanocomposites

Composite	Bacteria	ZOI (mm)	Reference
rGO-WO_3/CuO	Klebsiella pneumoniae	2	[61]
Palladium-rGO/ZnO	*Pseudomonas aeruginosa*	16	[62]
RGO-Ag/ZnO	*Escherichia coli*	16	[63]
rGO-SnO_2-NiO-CuO	*Staphylococcus aureus*	16	[64]
La_2CuO_4/ CeO_2/rGO	*Escherichia coli*	16	[65]
rGO-MnO_2/CuO	*Pseudomonas aeruginosa*	24	This work

surface proteins of the cell membrane, which damages the membrane by denaturement of the proteins [70]. Differences in antibacterial activity between MC and rMC NCs are due to their size or ROS generation capacity. More ROS were generated due to the smaller crystallite size and band gap found for the rMC nanocomposite, leading to improved antibacterial activity. In addition, the rGO in the MC composite triggers a chain reaction of biological processes that ultimately kills the bacteria. When bacteria come into touch with rGO, they frequently experience a loss of cell membrane integrity. Graphene-based nanoparticles can lower mitochondrial membrane potential, resulting in increased ROS generation and death through activation of the mitochondrial pathway [71]. A graphene-based nanomaterial's interactions with genetic material are usually caused by DNA intercalation and breakage. Therefore, nanoparticles made of graphene interact directly with certain genes that code for important enzymes and proteins [72]. The antibacterial activity of the rMC nanocomposite is represented in Fig. 15.

4. Conclusion

NCs of MnO_2/CuO and rGO-MnO_2CuO were prepared through chemical precipitation and one-pot green synthesis. Leaf extract from the plant *Alternanthera sessilis* was used to transform graphene oxide made using Hummer's technique into rGO. Comparison on the structural, optical, photocatalytic and antibacterial properties of MnO_2/CuO composite with that of rGO-decorated MnO_2/CuO composite is very scarce and this work presented the comparative results obtained. The rMC composite exhibited smaller crystallites. Within 90 minutes, the MC and rMC nanocomposites destroyed roughly 87 and 96% of the metanil yellow dye, respectively. rGO-MnO_2/CuO nanocomposite showed improved antibacterial activity. Thus, MnO_2/CuO nanocomposite incorporated with rGO showed good antimicrobial properties and efficiently degraded toxic metanil yellow dye.

Statements and Declarations

Funding

No funding was received to assist with the preparation of this manuscript.

Authors' contributions

Conceptualization - Dr. S. Jothi Ramalingam; **Methodology** – Mr. A. Ceril Jeoffrey; **Formal analysis and investigation** – Dr. A.R. Balu; **Writing – original draft preparation** - K. Murugaiah; **Writing – review and editing** – Dr. A.R. Balu; **Funding acquisition** - Dr. Ceril

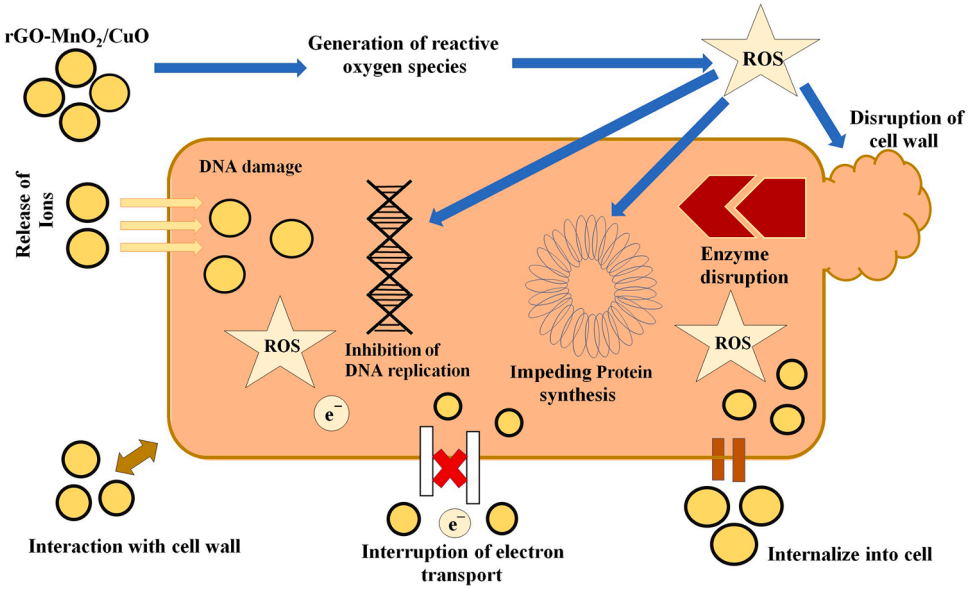

Fig. 15. Schematic representation of antibacterial resistance of rMC composite

Jeoffrey; **Interpretation of data** - Dr. S. Jothi Ramalingam.

The final manuscript was read and approved by all authors.

Research Data availability

The raw/processed data required to reproduce these findings cannot be shared at this time due to legal or ethical reasons.

Declaration of Competing Interest

The authors declare that they have no known competing financial interests or personal relationships that could have appeared to influence the work reported in this paper.

Acknowledgements

For Raman studies, we are very thankful to Alagaappa University, Karaikudi.

References

[1] Z. Cai, Y. Sun, W. Liu, F. Pan, P. Sun, J. Fu, An overview of nanomaterials applied for removing dyes from wastewater, Environ. Sci. Pollut. Res. Int. 24 (2017) 15882–15904, https://doi.org/10.1007/s11356-017-9003-8.

[2] N. Ahmad, S. Sultana, S. Sabir, M.Z. Khan, Exploring the visible light driven photocatalysis by reduced graphene oxide supported Ppy/CdS nanocomposites for the degradation of organic pollutants, J. Photochem. Photobiol. A. Chem. 386 (2020), 112129, https://doi.org/10.1016/j.jphotochem.2019.112129.

[3] R. Nallendran, G. Selvan, A.R. Balu, CdO-Fe_3O_4 nanocomposite with enhanced magnetic and photocatalytic properties, Mater. Sci. Poland 37 (2019) 100–107, https://doi.org/10.2478/msp-2019-0012.

[4] K. Tantubay, P. Das, M. Baskey Sen, Ternary reduced graphene oxide-CuO/ZnO nanocomposite as a recyclable catalyst with enhanced reducing capability, J. Environ. Chem. Eng. 8 (2020), 103818, https://doi.org/10.1016/j.jece.2020.103818.

[5] Z.M. Shammi, A.H. Kianfar, M.M. Momeni, Hydrothermal synthesis and characterization of CuO-CoO/TiO_2 for photocatalytic degradation of methylene blue under visible light and catalytic reduction of p-nitrophenol, J. Mater. Sci. Mater. Electron. 31 (2020) 14810–14822, https://doi.org/10.1007/s10854-020-04044-9.

[6] K. Kannan, D. Radhika, A.S. Nesaraj, K.K. Sadasivuni, L.S. Krishna, Facile synthesis of NiO-CYSO nanocomposite for photocatalytic and antibacterial applications, Inorg. Chem. Commun. 122 (2021), 108307, https://doi.org/10.1016/j.inoche.2020.108307.

[7] N. Manjula, G. Selvan, A.R. Balu, Photocatalytic Performance of SnO_2:Mo nanopowders against the degradation of methyl orange and rhodamine B dyes under visible light irradiation, J. Electron. Mater. 48 (2019) 401–408, https://doi.org/10.1007/s11664-018-6720-9.

[8] G. Shanmugavel, A.R. Balu, V.S. Nagarethinam, S. Ravishankar, M. Suganya, S. Balamurugan, K. USharani, C. Kayathiri, M. Karthika, CdO:Ag thin films with enhanced visible light photocatalytic activity against metanil yellow, SN Appl. Sci. 1 (2019) 1203, https://doi.org/10.1007/s42452-019-1237-2.

[9] H. Xu, W. Wang, W. Zhu, Shape evolution and size-controllable synthesis of Cu_2O octahedra and their morphology-dependent photocatalytic properties, J. Phys. Chem. B 110 (2006) 13829–13834, https://doi.org/10.1021/jp061934y.

[10] K. Ramesh, L. Chen, F. Chen, Y. Liu, Z. Wang, Y.F. Han, Re-investigating the co oxidation mechanism over unsupported MnO, Mn_2O_3 and MnO_2 catalysts, Catal. Today 131 (2008) 477–482, https://doi.org/10.1016/j.cattod.2007.10.061.

[11] L. Chen, R. Huang, Y.J. Ma, S.L. Luo, C.T. Au, S.F. Yin, Controllable synthesis of hollow and porous Ag/$BiVO_4$ composites with enhanced visible-light photocatalytic performance, RSC Adv 3 (2013) 24354–24361, https://doi.org/10.1039/C3RA43691H.

[12] M. Huang, F. Li, F. Dong, Y.X. Zhang, L.I. Zhang, MnO_2-based nanostructures for high performance supercapacitors, J. Mater. Chem. 3 (2015) 21380–21423, https://doi.org/10.1039/C5TA05523G.

[13] L. Liu, Y. Luo, W. Tan, Y. Zhang, F. Liu, G. Qiu, Facile synthesis of birnessite-type manganese oxide nanoparticles as supercapacitor electrode materials, J. Colloid Interface sci. 482 (2016) 183–192, https://doi.org/10.1016/j.jcis.2016.07.077.

[14] M. Sun, B. Lan, T. Lin, G. Cheng, F. Ye, L. Yu, Controlled synthesis of nanostructured manganese oxide: crystalline evolution and catalytic activities, CrystEngComm 15 (2013) 7010–7018, https://doi.org/10.1039/C3CE40603B.

[15] J. Chen, X. Chen, Z. Xu, W.J. Xu, J.J. Li, H.P. Jia, J. Chen, Syntheses of hierarchical MnO_2 via H_2O_2 selectively reducing $KMnO_4$ for catalytic combustion of toluene, Chemistry 1 (2016) 4052–4056, https://doi.org/10.1002/slct.201600921.

[16] Y. Chen, D. Ye, M. Wu, H. Chen, L. Zhang, J. Shi, L. Wang, Break-up of two-dimensional MnO_2 nanosheets promotes ultrasensitive ph-triggered theranostics of cancer, Adv. Mater 26 (2014) 7019–7026, https://doi.org/10.1002/adma.201402572.

[17] Y. Chen, H. Cong, Y. Shen, B. Yu, Biomedical application of manganese dioxide nanomaterials, Nanotechnol 31 (2020), 202001, https://doi.org/10.1088/1361-6528/ab6fe1.

[18] A. Nezamzadsh-Ejhieh, M. Amiri, CuO supported clinoptilolite towards solar photocatalytic degradation of p-aminophenol, Powder Technol 235 (2015) 279–288, https://doi.org/10.1016/j.powtec.2012.10.017.

[19] S.A. Akintelu, A.S. Folorunso, F.A. Folorunso, A.K. Oyebamiji, 2020. Green synthesis of copper oxide nanoparticles for biomedical application and environmental remediation. Heliyon. 6, e04508. doi:10.1016/j.heliyon.2020.e04508.

[20] S. Rajeswari, K.S.M.R. Pattanathu, R. Rajiv, A.S. Hasna, R. Venkatesh, Biogenic copper oxide nanoparticles synthesis using *Tabernaemontana divaricate* leaf extract and its antibacterial activity against urinary tract pathogen, Spectrochim. Acta Mol. Biomol. Spectrosc. 133 (2014) 178–181, https://doi.org/10.1016/j.saa.2014.05.048.

[21] S. Singh, N. Kumar, M. Kumar, J.A. Agarwal, B. Mizaikoff, Electrochemical sensing and remediation of 4-nitrophenol using bio-synthesized copper oxide nanoparticles, Chem. Eng. J. 313 (2017) 283–292, https://doi.org/10.1016/j.cej.2016.12.049.

[22] K.W. Getu, Photocatalytic and antibacterial activity of CuO nanoparticles biosynthesized using *Verbascum thapsus* leaves extract, Optik 204 (2020), 164230, https://doi.org/10.1016/j.ijleo.2020.164230.

[23] A. Azam, A.S. Ahmed, M. Oves, M.S. Khan, A. Memic, Size-dependent antimicrobial properties of CuO nanoparticles against Gram-positive and -negative bacterial strains, Int. J. Nanomed. 7 (2012) 3527–3535, https://doi.org/10.2147/IJN.S29020.

[24] F. Duman, I. Ocsoy, F.O. Kup, Chamomile flower extract-directed CuO nanoparticle formation for its antioxidant and DNA cleavage properties, Mater. Sci. Eng. C. 60 (2016) 333–338, https://doi.org/10.1016/j.msec.2015.11.052.

[25] A.K. Mishra, A.K. Nayak, A.K. Das, D. Pradhan, Microwave-assisted solvothermal synthesis of cupric oxide nanostructures for high-performance supercapacitor, J. Phys. Chem. C 122 (2018) 11249–11261, https://doi.org/10.1021/acs.jpcc.8b02210.

[26] B. Padmadevi, A. Pugazhendhi, A.S. Khalifa, R. Shanmugaantham, T. Kalaivani, Novel MnO_2-CuO-BaO metal oxide nanocomposite for high performance supercapacitors, Proc. Biochem. 110 (2021) 176–180, https://doi.org/10.1016/j.procbio.2021.08.017.

[27] Y.X. Zhang, F. Li, M. Huang, One-step hydrothermal synthesis of hierarchical MnO_2-coated CuO flower-like nanostructures with enhanced electrochemical properties for supercapacitor, Mater. Lett. 112 (2013) 203–206, https://doi.org/10.1016/j.matlet.2013.09.032.

[28] X.L. Guo, G. Li, M. Kuang, Y.X.Zhang L.Yu, Tailoring Kirkendall effect of the KCu7S4 microwires towards CuO@MnO_2 core-shell nanostructures for supercapacitors, Electrochim. Acta 174 (2015) 87–92, https://doi.org/10.1016/j.electacta.2015.05.157.

[29] K. Qian, Z. Qian, Q. Hua, Z. Jiang, W. Huang, Structure–activity relationship of CuO/MnO_2 catalysts in CO oxidation, Appl. Surf. Sci. 273 (2013) 357–363, https://doi.org/10.1016/j.apsusc.2013.02.043.

[30] A. Martin, U. Armbruster, M. Schncider, J. Radnik, M.M. Pohl, Structural transformation of an alumina-supported MnO_2-CuO oxidation catalyst by hydrothermal impact of sub and supercritical water, J. Mater. Chem. 12 (2002) 639–645, https://doi.org/10.1039/B107982B.

[31] C. Qing, B. Heng, H. Wang, D. Sun, B. Wang, M. Sun, S. Guan, R. Fu, Y. Tang, Controlled facile synthesis of hierarchical CuO@MnO_2 core-shell nanosheet arrays for high performance lithium-ion battery, J. Alloys Compnd. 641 (2015) 80–86, https://doi.org/10.1016/j.jallcom.2015.03.234.

[32] S. Korkmaz, A. Kariper, Graphene and graphene oxide based aerogels: Synthesis, characteristics and supercapacitor applications, J. Energy Storage. 27 (2020), 101038, https://doi.org/10.1016/j.est.2019.101038.

[33] D. Zhang, H. Chang, P. Li, R. Liu, Characterization of nickel oxide decorated-reduced graphene oxide nanocomposite and its sensing properties toward methane gas detection, J. Mater. Sci. Mater. Electron. 27 (2016) 3723–3730, https://doi.org/10.1007/s10854-015-4214-6.

[34] A. Irshad, F. Farooq, M.F. Warsi, N. Shabeen, A.Y. Elnaggar, E.E. Hussein, Z.M. El-Bahy, M. Shahid, Ag-doped $FeCo_2O_4$ nanoparticles and their composite with flat 2D reduced graphene oxide sheets for photocatalytic degradation of colored and colorless compounds, Flatchem 31 (2022), 100325, https://doi.org/10.1016/j.flatc.2021.100325.

[35] A.R. Malik, S. Sharif, F. Shaheen, M. Khalid, Y. Iqbal, A. Faisal, M.H. Aziz, M. Atif, S. Ahmad, M.F. Alam, N. Hossain, H. Ahmad, T. Botmart, Green synthesis of rGO-ZnO mediated *Ocimim basilicum* leaves extract nanocomposite for antioxidant, antibacterial, antidiabetic and photocatalytic activity, J. Saudi Chem. Soc. 26 (2022), 101438, https://doi.org/10.1016/j.jscs.2022.101438.

[36] I. Tanisik, O. Uguz, D. Akyuz, R.M.Z. Ayaz, C. Sarioglu, F. Karaca, A.R. Ozkaya, A. Koca, Solar-hydrogen production with reduced graphene oxide supported $Cd_xZn_{1-x}S$ photocatalysts, Int. J. Hyd. Energy 45 (2020) 34845–34856, https://doi.org/10.1016/j.ijhydene.2020.04.035.

[37] R.M. Obodo, H.E. Nsude, C.U. Eze, B.O. Okereke, S.C. Ezugwee, I. Ahmed, M. Maaza, F.I. Ezema, Optimization of MnO_2, NiO and MnO_2@ NiO electrodes using graphene oxide for supercapacitor applications, Current Res. Green Sust. Chem. 5 (2020), 100345, https://doi.org/10.1016/j.crgsc.2022.100345.

[38] X.X. Liu, X. Li, X.X. Liu, S. He, J. Jin, H. Meng, Green preparation of Ag-ZnO-rGO nanoparticles for efficient adsorption and photodegradation activity, Coll. Surf. A Physicochem. Eng. Asp. 584 (2020), 124011, https://doi.org/10.1016/j.colsurfa.2019.124011.

[39] D.L. Zhao, X. Gao, C.N. Wu, R. Xic, S.J. Feng, C.L. Chen, Facile preparation of amino functionalized graphene oxide decorated with Fe_3O_4 nanoparticles for the adsorption of Cr (VI), Appl. Surf. Sci. 384 (2016) 1–9, https://doi.org/10.1016/j.apsusc.2016.05.022.
[40] K. Rahimi, H. Zafarkish, A. Yazdani, Reduced graphene oxide can activate the sunlight-induced photocatalytic effect of NiO nanowires, Mater. Design. 144 (2018) 214–221, https://doi.org/10.1016/j.matdes.2018.02.030.
[41] K.Mohamed Racik, A. Manikandan, M. Mahendiran, P. Prabakaran, J. Madhavan, M. Victor Antony Raj, Fabrication of manganese oxide decorated copper oxide (MnO_2/CuO) nanocomposite electrodes for energy storage supercapacitor devices, Physica E 119 (2020), 114033, https://doi.org/10.1016/j.physe.2020.114033.
[42] S. Sadhukan, A. Battacharya, D. Rana, T.K. Ghosh, J.T. Orasugh, S. Khatua, K. Acharya, D. Chattopadhyay, Synthesis of rGO/NiO nanocomposites adopting a green approach and its photocatalytic and antibacterial properties, Mater. Chem. Phys. 247 (2020), 122906, https://doi.org/10.1016/j.matchemphys.2020.122906.
[43] C. Wallar, D. Luo, R. Poon, I. Zhitomirsky, Manganese dioxide–carbon nanotube composite electrodes with high active mass loading for electrochemical supercapacitors, J. Mater. Sci. 52 (2017) 3687–3696, https://doi.org/10.1007/s10853-016-0711-0.
[44] P. Sengodan, R. Govindan, G. Arumugam, B. Chettiannan, M. Navaneethan, M. R. Pallavolu, M. Hussien, M. Selvaraj, R. Rajendran, A rational design of MnO_2/CuO/r-GO hybrid and biomass-derived activated carbon for asymmetric supercapacitors, J. Energy Storage 50 (2022), 104625, https://doi.org/10.1016/j.est.2022.104625.
[45] A.M. Zardkhoshowi, S.S.H. Davarani, Flexible asymmetric supercapacitors based on CuO @ MnO_2-rGO and MoS_2-rGO with ultrahigh energy density, J. Electroanal. Chem. 827 (2018) 221–229, https://doi.org/10.1016/j.jelechem.2018.08.023.
[46] M. Jayasree, M. Parthibavaraman, R. Boopathi Raja, S. Prabhu, R. Ramesh, Ultrafine MnO_2/graphene based hybrid nanoframeworks as high-performance flexible electrode for energy storage applications, J. Mater. Sci. Mater. Electron. 31 (2020) 6910–6918, https://doi.org/10.1007/s10854-020-03254-5.
[47] L.C. Sim, K.H. Leong, S. Ibrahim, P. Saravanan, Graphene oxide and Ag engulfed TiO_2 nanotube arrays for enhanced electron mobility and visible-light-driven photocatalytic performance, J. Mater. Chem. A 2 (2014) 5315–5322, https://doi.org/10.1039/C3TA14857B.
[48] R. Kumar, S.M. Youssry, H.M. Soe, M.M. Abdel-Galeil, G. Kawamura, Honeycomb-like open-edged reduced-graphene-oxide-enclosed transition metal oxides (NiO/Co_3O_4) as improved electrode materials for high-performance supercapacitor, J. Energy Storage. 30 (2020), 101539, https://doi.org/10.1016/j.est.2020.101539.
[49] R. Kumar, M.M. Abdel-Galeil, K.Z. Ya, K. Fujita, W.K. Tan, A. Matsuda, Facile and fast microwave-assisted formation of reduced graphene oxide-wrapped manganese cobaltite ternary hybrids as improved supercapacitor electrode material, Appl. Surf. Sci. 481 (2019) 296–306, https://doi.org/10.1016/j.apsusc.2019.03.085.
[50] A.M. Abdelkader, C. Valles, A.J. Cooper, I.A. Kinloch, R.A.W. Dryfe, Alkali reduction of graphene oxide in molten halide salts: production of corrugated graphene derivatives for high-performance supercapacitors, ACS Nano 8 (2014) 11225–11233, https://doi.org/10.1021/nn505700x.
[51] R.R. Palem, S. Ramesh, C. Bathula, V. Kakani, G.D. Saratale, H.M. Yadav, J.H. Kim, H.S. Kim, S.H. Lee, Enhanced supercapacitive behavior by CuO@MnO_2/carboxymethyl cellulose composites, Ceram. Int. 47 (2021) 26738–26747, https://doi.org/10.1016/j.ceramint.2021.06.081.
[52] F. Boran, Encapsulation of CuO nanoparticles inside the channels of the multi-walled carbon nanotubes functionalized with thermal stress, Diamond Related Mater 114 (2021), 108306, https://doi.org/10.1016/j.diamond.2021.108306.
[53] K. Kannan, D. Radhika, D. Gnanasangeetha, L. Sivarama Krishna, K. Gurushankar, Y^{3+} and Sm^{3+} co-doped mixed metal oxide nanocomposite: Structural, electrochemical, photocatalytic and antibacterial properties, Appl. Surf. Sci. Adv. 4 (2021), 100085, https://doi.org/10.1016/j.apsadv.2021.100085.
[54] S. Nachimuthu, S. Thangavel, K. Kannan, V. Selvakumar, K. Muthusamy, M. R. Siddiqui, S.Mohammad Wabaidur, C. Parvathiraja, Lawsoniainermis mediated synthesis of ZnO/Fe_2O_3 nanorods for photocatalysis – Biological treatment for the enhanced effluent treatment, antibacterial and antioxidant activities, Chem. Phys. Lett. 804 (2022), 139907, https://doi.org/10.1016/j.cplett.2022.139907.
[55] N. Suganth, S. Thangavel, K. Kannan, Hibiscus subdariffa leaf extract mediated 2-D fern-like ZnO/TiO_2 hierarchical nanoleaf for photocatalytic degradation, Flatchem 24 (2020), 100197, https://doi.org/10.1016/j.flatc.2020.100197.
[56] H Mirzazadeh, M Lashanizadegan, Binary semiconductor oxide nanoparticles on graphene oxide (CdO/CeO_2/RGO) for the treatment of hazardous organic water pollutants, Kor. J. Chem. Eng. 34 (2018) 1–10, https://doi.org/10.1007/s11814-017-0299-3.
[57] Y. Park, A. Numar, N. Ponomarev, J. Eqbal, M. Khalid, Enhanced photocatalytic performance of PANI-rGO-MnO_2 ternary composite for degradation of organic contaminants under visible light, J. Environ. Chem. Eng. 9 (2021), 106006, https://doi.org/10.1016/j.jece.2021.106006.
[58] L. Fu, Y. Zheng, Z. Fu, W. Cai, J. Yu, Synthesis of Ag decorated graphene-hierarchical TiO_2 nanocomposite with enhanced photocatalytic activity, Funct. Mater. Lett. 8 (2015), 1550036, https://doi.org/10.1142/S1793604715500368.
[59] H. Mirzazadeh, M. Lashanizadegan, ZnO/CdO/reduced graphene oxide and its high catalytic performance towards degradation of the organic pollutants, J. Serb. Chem. Soc. 82 (2017) 1–16, https://doi.org/10.2298/JSC170630097M.
[60] K. Sirohi, S. Kumar, V. Singh, N. Chauhan, A. Vohra, Synthesis, characterization and photocatalytic properties of graphene-CdO/SnO_2 ternary nanocomposites in visible light, Mater. Res. Express. 6 (2019), 075901, https://doi.org/10.1088/2053-1591/ab122c.
[61] I.A. Alsafari, K. Chaudhary, M.F. Warsi, A. Warsi, M. Waqas, M. Hasan, A. Jamil, M. Shahid, A facile strategy to fabricate ternary WO_3/CuO/rGO nano-composite for the enhanced photocatalytic degradation of multiple organic pollutants and antimicrobial activity, J. Alloy. Compnd. 938 (2023), 168537, https://doi.org/10.1016/j.jallcom.2022.168537.
[62] R. Rakkappan, G.P. Halliah, Palladium-Decorated reduced graphene oxide/zinc oxide nanocomposite for enhanced antimicrobial, antioxidant and cytotoxicity activities, Process Biochem 93 (2020) 36–47, https://doi.org/10.1016/j.procbio.2020.03.010.
[63] N. Belachew, M.H. Kahsay, A. Tadesse, K. Basavaiah, Green synthesis of reduced graphene oxide grafted Ag/ZnO for photocatalytic abatement of methylene blue and antibacterial activities, J. Environ. Chem. Eng. 8 (2020), 104106, https://doi.org/10.1016/j.jece.2020.104106.
[64] S. Haq, M. Rashid, F. Menaa, N. Shahzad, M.I. Shahzad, S.Y.M. Alfaifi, O. Madkhali, M.D. Aljabri, M. Ashravi, R.A. Tayeb, M.M. Rahman, Antibacterial and antioxidant screening applications of reduced –graphene oxide modified ternary SnO_2-NiO-CuO nanocomposites, Arab. J. Chem. 16 (2023), 104917, https://doi.org/10.1016/j.arabjc.2023.104917.
[65] S. Shanavas, A. Priyadarsan, V. Vasanthakumar, A. Arunkumar, P.M. anbarasan, S. Bharathkumar, Mechanistic investigation of visible light driven novel La_2CuO_4/CeO_2/rGO ternary hybrid nanocomposites for enhanced photocatalytic performance and antibacterial activity, J. Photochem. Photobiol A. Chem. 340 (2017) 96–108, https://doi.org/10.1016/j.jphotochem.2017.03.002.
[66] V. Revathi, K. Karthik, Microwave assisted CdO-ZnO-MgO nanocomposite and its photocatalytic and antibacterial studies, J. Mater. Electron. 29 (2018) 18519–18530, https://doi.org/10.1007/s10854-018-9968-1.
[67] K. Karthik, S. Dhanuskodi, C. Gopinath, S. Prabukumar, S. Sivaramakrishnan, Nanostructured CdO-NiO composite for multifunctional applications, J. Phys. Chem. Sol. 112 (2018) 106–118, https://doi.org/10.1016/j.jpcs.2017.09.016.
[68] A.A. Ali Ahmed, Asma A.A. Al-Mushki, Bandar Ali Al-Ashahi, A.M. Abdulwahab, J. M.A. Abduljalil, F.A.A Saad, S.M.H. Qaid, H.M. Ghaithan, W.A. Farooq, A.H. Omar, Effect of ethylene glycol concentration on the structural and optical properties of multimetal oxide CdO-NiO-Fe_2O_3 nanocomposites for antibacterial activity, J. Phys. Chem. Sol. 155 (2021), 110113, https://doi.org/10.1016/j.jpcs.2021.110113.
[69] K. Kannan, D. Radhika, R.D. Kasai, D. Gnanasangeetha, G. Palani, K. Gurushankar, R. Koutavarapu, D.Y. Lee, J. Shim, Facile fabrication of novel ceria-based nanocomposite (CYO-CSO) via co-precipitation: Electrochemical, photocatalytic and antibacterial performances, J. Mol. Struct. 1256 (2022), 132519, https://doi.org/10.1016/j.molstruc.2022.132519.
[70] M. Suganya, A.R. Balu, D. Prabha, S. Anitha, S. Balamurugan, PbS-SnO_2 nanocomposite with enhanced magnetic, photocatalytic and antifungal properties, J. Mater. Sci. Mater. Electron. 29 (2018) 1065–1074, https://doi.org/10.1007/s10854-017-8007-y.
[71] A. Jarosz, M. Skoda, I. Dudek, D. Szukiewicz, Oxidative stress and mitochondrial activation as the main mechanisms underlying graphene toxicity against human cancer cells, Oxidative Med. Cell. Longev. 2016 (2015), 5851035, https://doi.org/10.1155/2016/5851035.
[72] Y. Liu, Y. Luo, J. Wu, Y. Wang, X. Yang, R. Yang, B. Wang, J. Yang, N. Zhang, Towards ultrahigh volumetric capacitance: graphene derived highly dense but porous carbons for supercapacitors, Sci. Rep. 3 (2013) 2975, https://doi.org/10.1038/srep02975.

doi.org/10.1002/cbdv.202301392 Research Article CHEMISTRY & BIODIVERSITY

www.cb.wiley.com

Indolyl-4*H*-Chromene Derivatives as Antibacterial Agents: Synthesis, *in Vitro* and *in Silico* Studies

Parthiban Anaikutti,[a] Priyanka Adhikari,[a] Sambath Baskaran,[b] Mangalaraj Selvaraj,[c] Mohd Afzal,[d] and Parameshwar Makam*[e]

In this study, indolyl-4*H*-chromene derivatives are designed and synthesised using an eco-friendly multicomponent one-pot synthesis using benzaldehydes, nitroketene *N*, *S*-acetals, and indoles combine with $InCl_3$, a Lewis acid catalyst, and ethanol, an environmentally acceptable solvent. Due to antibiotic resistance, assessed these Indolyl-4*H*-chromene derivatives for their *in vitro* antibacterial activity against Gram-positive and Gram-negative bacteria, including *Streptococcus pyogenes*, *Staphylococcus aureus*, *Clostridium pyrogenes*, *Bacillus subtilis*, *Escherichia coli*, and *Pseudomonas aeruginosa*, using the agar well diffusion method and Minimum Inhibition Concentration (MIC) assay. Three compounds, 4-(1*H*-indol-3-yl)-6-methoxy-*N*-methyl-3-nitro-4*H*-chromen-2-amine, 4-(1*H*-indol-3-yl)-3-nitro-*N*-phenyl-4*H*-chromen-2-amine and 4-(6-Fluoro-1*H*-Indol-3-yl)-*N*-methyl-3-nitro-4*H*-chromen-2-amine showed better zone of inhibition (mm) and Minimum Inhibition Concentration (MIC) values of 10 μg/mL to 25 μg/mL against all bacterial types. The K*i* values of 278.60 nM and 2.21 nM for compound 4-(1*H*-indol-3-yl)-3-nitro-*N*-phenyl-4*H*-chromen-2-amine showed improved interactions with DNA gyrase B and topoIV ParE's ATP binding sites in *in silico* studies.

Introduction

The World Health Organization (WHO) has released a prioritization list for emerging and established treatments targeting antibiotic resistance. This list aims to highlight the need for research and development efforts in the field of novel antibiotics, with a particular focus on pathogens that exhibit resistance to multiple antibiotics and are associated with severe and potentially fatal infections. The rise of bacterial strains that exhibit antimicrobial resistance (AMR), coupled with a restricted range of effective treatments, and poses a significant risk of reverting the contemporary society to a time prior to the advent of antibiotics, wherein even minor infections had lethal consequences.[1] *S. pyogenes* causes 700 million infections worldwide each year, and over 650,000 cases include severe toxic shock syndrome, scarlet fever, and rheumatic fever, which incur 25% mortality due to invasive infections and diagnostic failure that led to sepsis and death. *S. aureus* is also a deadly bacterium that can cause superficial skin infections to devastating invasive infections. Target protein alteration, efflux, lower antibiotic penetration, enzymatic drug degradation, and plasmids can help *S. aureus* avoid antibacterial drugs. Because bacteria with resistance genes, like methicillin-resistant *S. aureus* (MRSA), can spread between humans, animals, and the environment, drug-resistant illnesses threaten public health but have few effective treatments. New vancomycin-completely resistant MRSA isolates have highlighted the need for new antibacterial drug classes. Hence, it is imperative to identify a novel category of antibiotics that possess substantial therapeutic efficacy against both Gram-positive and Gram-negative bacteria.[2]

In the range of heterocyclic compounds, the oxygen-containing 4*H*-Chromene (4*H*-1-benzopyran) heterocyclic compounds have attracted particular interest because of their medicinal uses.[3–6] In Figure 1, a few 4*H*-chromene compounds having antibacterial importance are shown. The 4*H*-chromene derivatives, including 2-imino-4*H*-chromene,[7] 2-hydroxy-1,4-naphthoquinone-4*H*-chromene conjugates,[8] 2-carboxamides-4*H*-chromene,[9] naphthlamine substituted 4*H*-chromenes,[10] indole substituted 4*H*-chromenes,[11] and 3-carboxamides-4*H*-chromene,[7] showed potential antibacterial activities. Another naturally occurring 4*H*-chromene compound, Uvafzlelin, which was isolated from the stems of Uvaria Afzelii, had notable antibacterial action against gram-positive and acid-fast bacteria.[12] In addition, 4*H*-chromene derivatives are known for their spectrum of applications *Viz.* are anticancer,[13] antioxidant,[14] anti-fungal,[15] anti-malarial,[16] anti-coagulant.[17]

Similarly, the captivating atomic configuration of the indole ring renders it a suitable candidate for drug development. The indole moiety is a highly prevalent heterocycle observed in various natural products and biological systems. Indoles possess

[a] *Dr. P. Anaikutti, Dr. P. Adhikari*
Centre for GMP Extraction Facility, National Institute of Pharmaceutical Education and Research (NIPER-G), Guwahati-781101, Assam, India

[b] *Dr. S. Baskaran*
Department of Chemistry, University of Ulsan, Ulsan-44776, Republic of Korea

[c] *Dr. M. Selvaraj*
Department of Chemistry, St. Joseph's College (Autonomous), Tiruchirappalli-620002, India

[d] *Dr. M. Afzal*
Department of Chemistry, College of Science, King Saud University, Riyadh 11451, Saudi Arabia

[e] *Dr. P. Makam*
Department of Chemistry, School of Applied and Life Sciences, Uttaranchal University, Arcadia Grant, P.O. Chandanwari, Premnagar, Dehradun, Uttarakhand-248007, India
E-mail: makamchem@gmail.com

Supporting information for this article is available on the WWW under https://doi.org/10.1002/cbdv.202301392

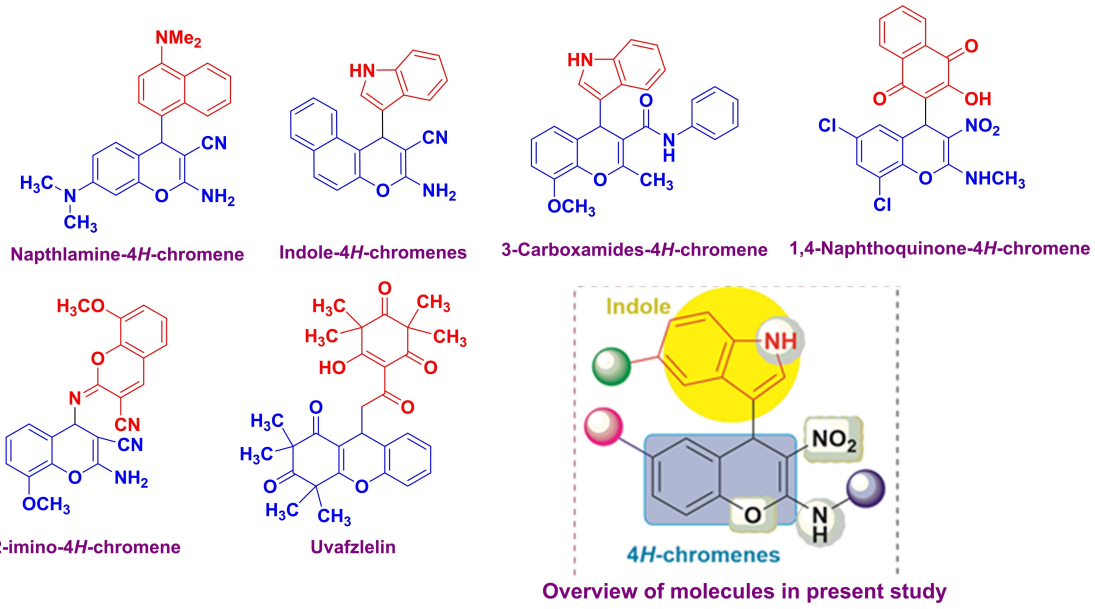

Figure 1. Structures of some important 4*H*-chromene antibacterial agents.

significant biological functionalities, encompassing anticancer, antioxidant, anti-inflammatory, antifungal, anticholinesterase, and antibacterial attributes. Within the realm of drug discovery and development, researchers exhibit a keen interest in the synthesis of indole-based hybrids that possess biological activity.[18] The primary objective behind this pursuit is to enhance the efficacy and specificity of these compounds, while simultaneously minimising any potential adverse effects. Indole and 4*H*-chromene hybrid molecules have garnered attention in organic and medicinal chemistry due to their intriguing biomedical applications.[19] In continuation of our search for anti-infective agents,[13,20] and considering the hybrid indolyl-4*H*-chromene derivatives,[21] this study aimed to design, develop a green synthesis of Indolyl-4*H*-Chromene derivatives with structural and functional modifications and to evaluate their antibacterial activity.

Results and Discussion

Design and Evaluation of Physico-Chemical Properties

The efficacy of compounds with lower molecular weight and lipophilicity in enhancing paracellular and transcellular absorption has been demonstrated.[22] Additionally, it is anticipated that they will exert a substantial impact on clearance, resulting in enhanced renal excretion[23] and a moderate level of toxicity.[24] A molecule acquires the property of being a drug-like molecule (DLM) when it meets the requirements set out by the "rule of 5" (Ro5). The Ro5 criterion encompasses molecules with a molecular mass below 500, a log P value below 5, and a count of hydrogen bond donors and acceptors below 5 and 10, respectively.[25] Based on the Veber rule, molecules exhibiting a polar surface area, number of hydrogen bond donors, and number of hydrogen bond acceptors that are equal to or less than 140, 10, and 12, respectively, demonstrate enhanced oral bioavailability.[26] Furthermore, Leeson *et al.* discovered that new chemical entities that received approval from 1983 to 2002 exhibited a notable increase of 16% to 23% in terms of molecular mass, rings, rotatable bonds, and hydrogen bonding groups.[27] These characteristics additionally facilitate the development of molecules with enhanced absorption, distribution, metabolism, excretion, and toxicity (ADMET) properties.[28] The assessment of a molecule's potential as a therapeutic candidate and its efficacy during key stages of drug development has become increasingly dependent on the careful management of its physicochemical properties.[28]

Taking into account the aforementioned factors, the hybridisation of Indole and 4*H*-chromene pharmacophores has been achieved with a covalent linker with diverse modifications in terms of both structure and functionality, as depicted in Figure 2. The evaluation of physicochemical and structural properties through computational methods entails the determination of various essential parameters. These parameters encompass heavy atoms (HA), heavy aromatic atoms (HAA), rotatable bonds (RB), hydrogen bond acceptors (HBA), hydrogen bond donors (HBD), molar refractivity (MR), and total polar surface area (TPSA). The SwissADME tool is employed for this purpose. The results of this analysis have been summarised in Table 1, and the observations are consistent with the established criteria for "drug-likeness" as outlined by the Lipinski, Ghose, Veber, Egan, and Muegge rules. The pharmacokinetic characteristics of indolyl-4*H*-chromene derivatives, such as gastrointestinal absorption (GIA) and brain-blood barrier (BBB) permeability, have also been projected. By calculating the lipophilicity (WLOGP versus TPSA), the Brain Or IntestinaL EstimateD Permeation method (BOILEDEgg) has been visually shown.[29] It is projected that all molecules that fall inside the

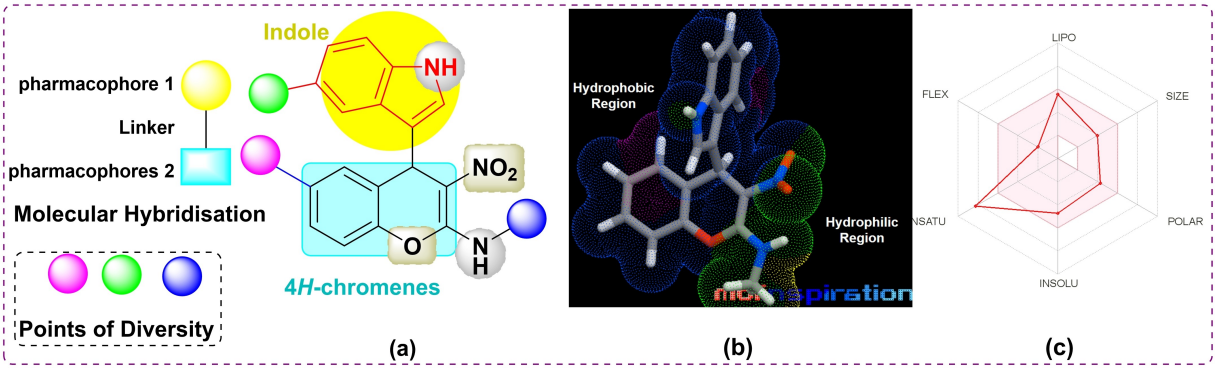

Figure 2. (**a**) Design of the molecules (**b**) MLP 3D representation of the molecule, **4 a** (**c**) Web representation of the physico-chemical properties of molecule, **4 a**.

Table 1. Physico-chemical and pharmacokinetic properties of indolyl-4*H*-chromene derivatives.

Molecule	Physico-chemical properties										Pharmacokinetic Properties		
	MW	HA	AHA	RBs	HBA	HBD	MR	TPSA	*i*LOGP	Violation	GI absorption	BBB permeant	Pgp substrate
4 a	321.33	24	15	3	3	2	92.18	82.87	2.37	0	High	No	No
4 b	355.78	25	15	3	3	2	97.19	82.87	2.66	0	High	No	No
4 c	400.23	25	15	3	3	2	99.88	82.87	2.78	0	High	No	No
4 d	351.36	26	15	4	4	2	98.67	92.1	2.63	0	High	No	No
4 e	383.4	29	21	4	3	2	113.39	82.87	2.85	0	High	No	No
4 f	397.43	30	21	5	3	2	116.66	82.87	3.01	0	High	No	No
4 g	363.41	27	15	6	3	2	106.6	82.87	3.16	0	High	No	No
4 h	339.32	25	15	3	4	2	92.13	82.87	2.48	0	High	No	No
4 i	355.78	25	15	3	3	2	97.19	82.87	2.59	0	High	No	No
4 j	400.23	25	15	3	3	2	99.88	82.87	2.71	0	High	No	No
4 k	351.36	26	15	4	4	2	98.67	92.1	2.61	0	High	No	No
4 l	346.34	26	15	3	4	2	96.89	106.66	2.36	0	High	No	No

white ellipse and none fall inside the yellow ellipse and grey region. This indicates that molecules could exhibit superior GIA but poorer BBB properties. All substances whose efflux activity in the Central Nervous System (CNS) was predicted by the P-glycoprotein (PGP) (see supporting information).

Chemistry

In contemporary times, there has been a notable surge in the interest of researchers towards investigating the effectiveness of indium (III) Lewis acids in the realm of organic synthesis. This heightened attention can be attributed to their relatively low toxicity and their ability to maintain stability in the presence of air and water at normal room temperature. The development of the indolyl-4*H*-chromene compounds' synthesis has been inspired by previously documented methodologies,[30] while incorporating enhancements that prioritise environmentally friendly and straightforward reaction procedures utilising cost-effective chemicals.[13] The experiment commenced by conducting the reaction using the starting materials nitroketene *N*,*S*-acetals (NMSM) (**1 a**), salicylaldehyde (**2 a**), and indole (**3 a**) in the absence of a catalyst. Despite subjecting the reaction to reflux conditions in ethanol as the solvent for a duration of ten hours, no product was observed (entry 1, Table 2).

The experiments were conducted using different Lewis acids as catalysts, including ferric chloride ($FeCl_3$), strontium chloride ($SnCl_2 \cdot 2H_2O$), iodine (I_2), aluminium chloride ($AlCl_3$), cupric chloride ($CuCl_2$), and *p*-toluenesulfonic acid (PTSA), under conditions of ethanol reflux. Among these reactions, it has been observed that PTSA and I_2 mediated reactions have yielded a 50% output. In contrast, other Lewis acids have proven ineffective in facilitating the reaction, even after extended periods of reaction time (entries 2–7, Table 2). Under reflux conditions in the presence of 10 mol% indium chloride ($InCl_3$) dissolved in ethanol, the reaction yields a highly favourable amount of product **4 a**, with a 98% yield as reported in Table 2, entry 8. As a result, various other solvent systems, including methanol, acetonitrile, water, and toluene, were employed in the presence of 10 mole% $InCl_3$ under reflux conditions resulting in moderate product yield of **4 a**, as indicated in entries 9–12 of Table 2.

Table 2. Optimization of reaction conditions.[a]

Entry	Catalyst (10 mol %)	Solvent	Time (h)	Yield[b] (%)
1	No catalyst	Ethanol	10	–
2	$PTSA \cdot H_2O$	Ethanol	10	45
3	$FeCl_3$	Ethanol	10	–
4	$SnCl_2 \cdot 2H_2O$	Ethanol	10	–
5	I_2	Ethanol	5	50
6	$AlCl_3$	Ethanol	10	–
7	$CuCl_2$	Ethanol	10	–
8	**$InCl_3$**	**Ethanol**	**5**	**98**
9	$InCl_3$	Methanol	7	70
10	$InCl_3$	Acetonitrile	10	41
11	$InCl_3$	Water	10	60
12	$InCl_3$	Toluene	10	35

[a]General conditions: **1a** (1 eq.), **2a** (1 eq.), **3a** (1 eq.) and catalyst (0.1 eq.) under reflux conditions; [b]Isolated yield after washing with ethanol.

This method has the advantages of high yields, rapid reaction times, ease of setup, non-chromatographic product purification, and cleaner reactions. NMSM, **1a** is an easily accessible, adaptable intermediate because it has three functional groups on the ethylene motif, an effective nitro group that efficiently draws electrons, and a strong Michael acceptor in its nitro-ethylene substructure. The methylsulfanyl group is an excellent leaving group and an electron donor. Spectral studies have been used to characterize the structure of all the synthesized compounds (**4a–l**) using the developed synthetic methodology.

A plausible reaction mechanism was proposed based on the optimisation reaction conditions outlined in Scheme 1 and Table 2, as depicted in Scheme 2. Initially, the compound 2-hydroxy benzaldehyde (**2a**) undergoes a reaction with **1a** *via* Michael addition in the presence of an $InCl_3$ catalyst. This is subsequently followed by a nitro-aldol condensation process, resulting in the formation of an unstable intermediate pyran ring intermediate (**A**). The intermediate (**A**) undergoes a dethiomethylation process, resulting in the formation of another intermediate benzopyrylium cation (**B**). The thiomethyl anion (SMe) is found in the solution and undergoes a reaction

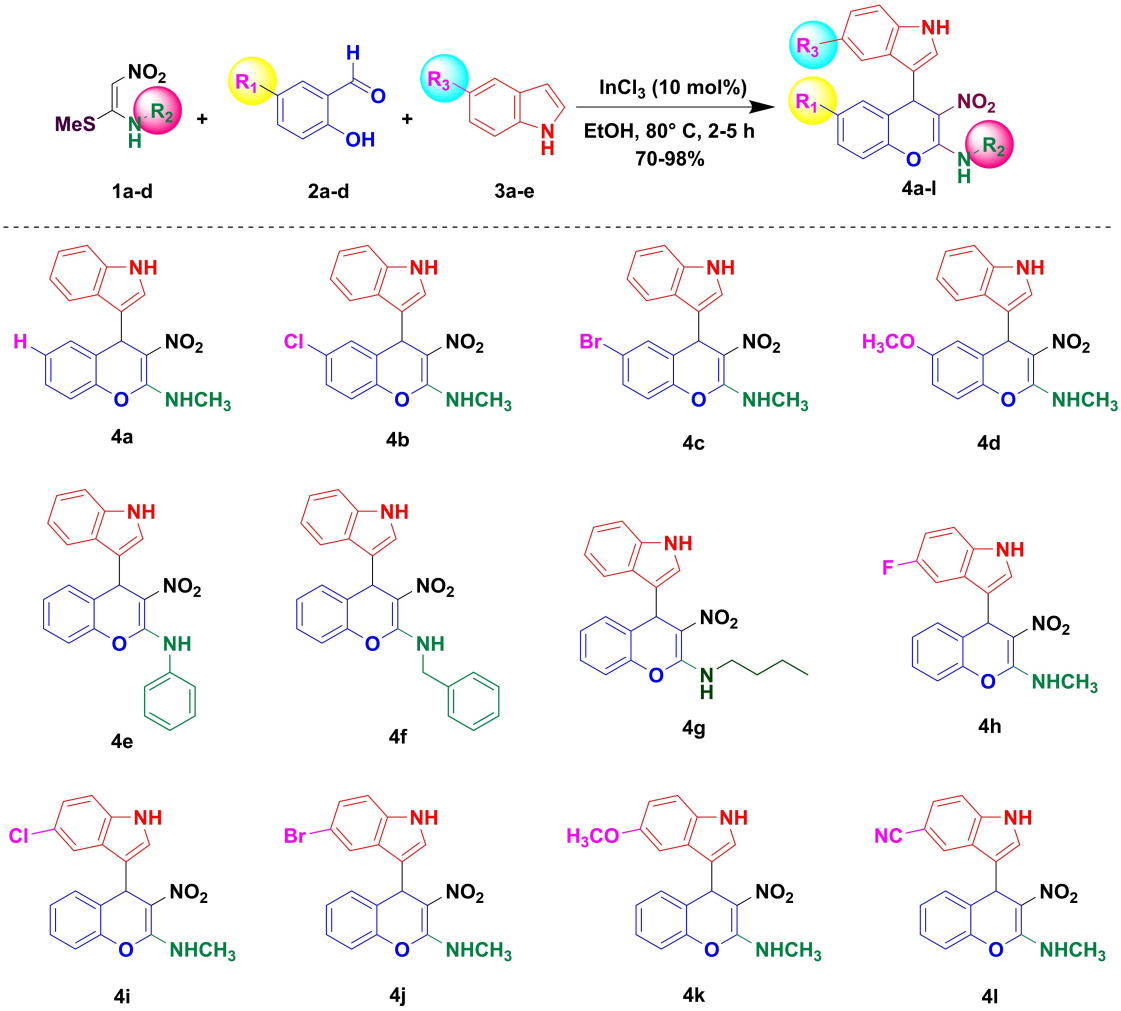

Scheme 1. One pot synthesis and library of indolyl-4*H*-chromene derivatives (**4a–l**).

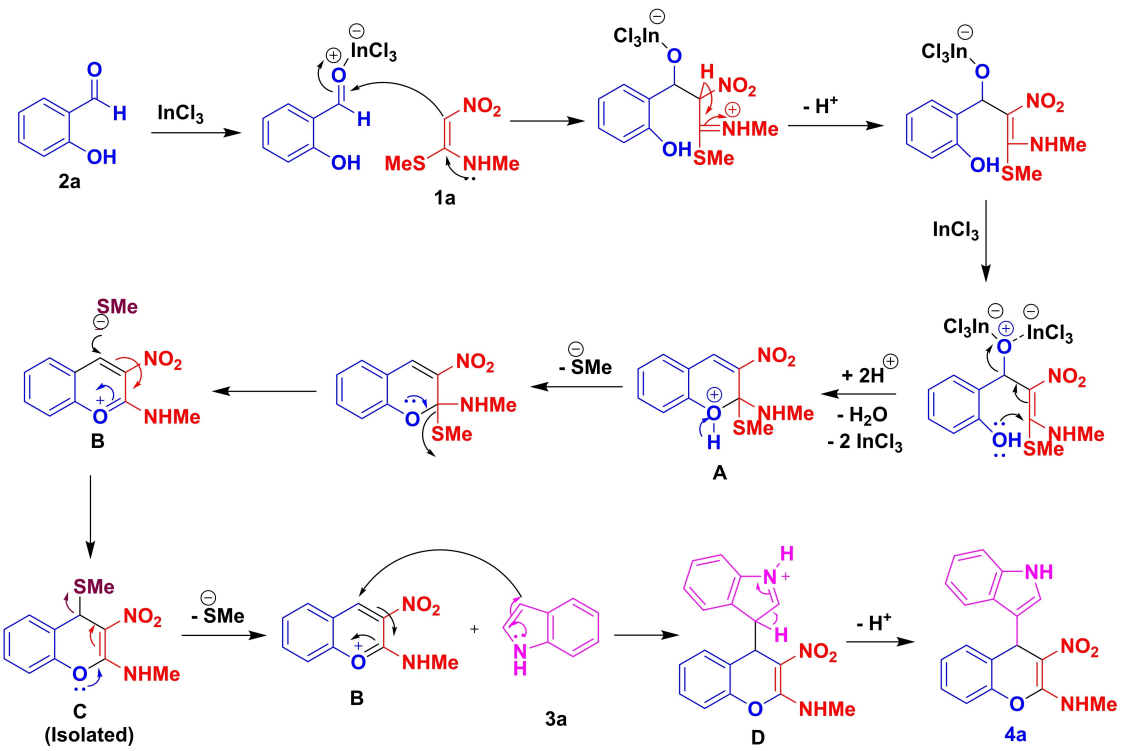

Scheme 2. A plausible mechanism for the formation of **4a.**

with the benzpyrilium cation, resulting in the formation of a stable intermediate, 4-sulfanyl-3-nitro-4H-chromene (**C**). This intermediate was subsequently isolated and characterised,[31] as detailed in the supporting information. The benzopyrylium cation (**B**), which exhibits instability, gets in reaction by the electron-rich C3 centre of indole (**3a**) *via* an aromatic electrophilic substitution mechanism, resulting in the formation of intermediate (**D**). The indole ring is intramolecularly aromatized to produce the indolyl-4*H*-chromene molecule (**4a**). This reaction takes place in the presence of an $InCl_3$ catalyst and is carried out in an ethanol reflux medium using a one-pot multicomponent reaction (MCR) pathway.

In vitro Anti-Bacterial Studies

Qualitative Test (Zone of Inhibition)

All the synthesized compounds can be classified into three categories and were subjected to their *in vitro* antibacterial activity against four Gram-positive bacteria *Viz. Streptococcus pyogenes*, *Staphylococcus aureus Clostridium pyrogenes*, *Bacillus subtilis* and two Gram-negative bacteria *Viz. Escherichia coli and Pseudomonas aeruginosa* by the agar well diffusion method by measuring the zone of inhibition. The results were shown in Figure 3. The first category (**4a–d**) involves the intact scaffold but substitution variations on the 6th position from H, Cl, Br to OCH_3. Among these molecules only **4d** has shown activity against all the tested bacteria, further **4d** displayed maximum activity against *S. Aureus* and *E. Coli* with the zone of inhibition values of 16.33 ± 0.72 mm and 16.06 ± 0.94 mm respectively.

The second category (**4e–g**) involves the variations in the substitutions on the secondary amine with variations of phenyl, benzyl and *n*-butyl. The **4f** and **4g** have selective antibacterial activity. **4g** only has antibacterial activity against *S. pyrogenes*, likewise, **4f** did not show any antibacterial activity against *C. sporogenes* and *B. subtilis*. Moreover, compound **4e** was found to be the molecule with high potent and comparable antibacterial activity against all the tested Gram +ve and Gram −ve bacteria to that of the standard drugs in clinical practice, ampicillin and vancomycin. The compound **4e** has shown significant activity against *S. pyogenes* with a zone of inhibition value of 28.35 ± 0.72 mm, which is greater than ampicillin and vancomycin. Against the *C. sporogenes*, **4e** has shown moderate activity with the zone of inhibition value of 10.08 ± 0.41 mm. In the case of *B. subtilis*, it has shown almost similar activity to that of ampicillin with a 16.33 ± 0.69 mm zone of inhibition value but lesser than the vancomycin. Whereas against *S. aureus* **4e** has shown inhibition of 18.06 ± 0.47 mm, which is more than and equivalent to vancomycin and ampicillin respectively. Similar results were obtained against *E. Coli* with a zone of inhibition value of 18.18 ± 0.45 mm.

The third category (**4h–l**) involves the functional group variations *Viz.* F, Cl, Br, OCH_3 and CN respectively on the 6th position of indole group. Among this group of molecules except **4h–4j** and **4l** has shown activity against all the tested group, but **4k** has selective antibacterial activity, it does not have activity against *S. pyogenes, B. subtilis* and *P. aeruginosa*. The compound, **4h** have higher antibacterial inhibition against

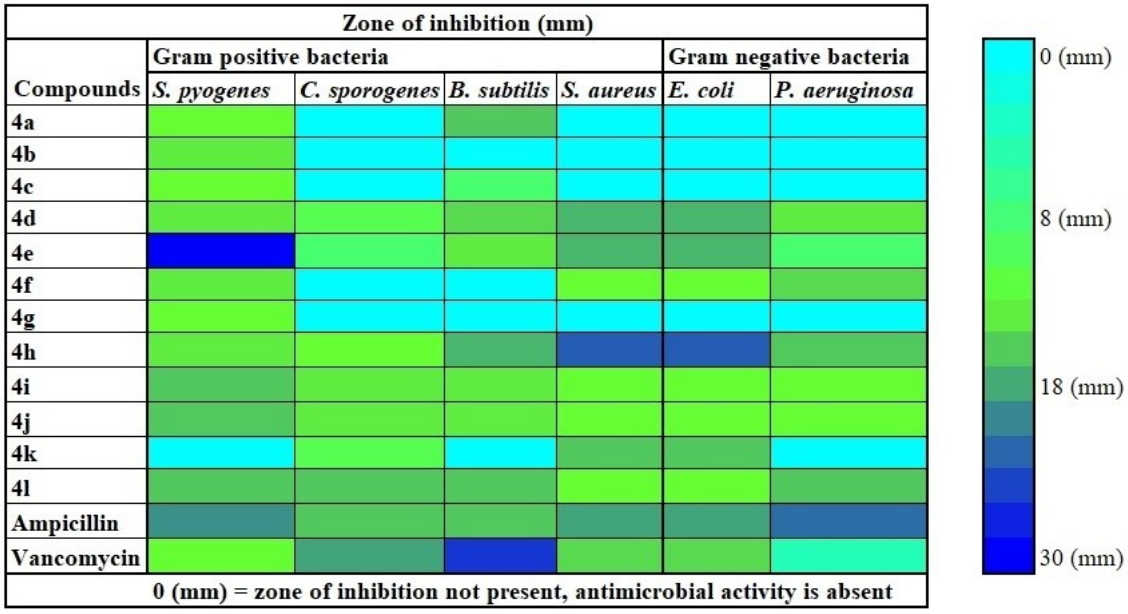

Figure 3. Heatmap showing antibacterial activity of biologically important indole substituted 4*H*-Chromenes (**4a–l**).

S. aureous (23.69 ± 0.63 mm) and *E. coli* (23.19 ± 0.75 mm) in comparison to standard tested antibiotics. Summary of results has been shown in Figure 3.

Quantitative Estimation (MIC)

After qualitative test by well diffusion methods, quantification of *in vitro* antimicrobial activity was done by estimation of MIC. The MIC is the minimum concentration of any compound which is obligatory to kill a specific category of microorganism. All the compounds dissolved in dimethylsulfoxide (DMSO) solvents with different concentrations at 10 μg, 15 μg, 20 μg, 25 μg, 30 μg, 35 μg, 40 μg and 50 μg and standard drugs used as ampicillin and vancomycin at 10 μg. **4d**, **4e** and **4h** has shown potential antibacterial activity by having MIC range between 10–25 μg/mL followed by **4i** and **4l** having MIC range between 25–50 μg/mL against all tested group. Overall, each compound has a MIC range between 10–50 μg/mL. Results in detail are given in Table 3.

Table 3. MIC of indole substituted 4*H*-Chromenes (**4a–l**).

Compound	Minimum inhibitory concentration (MIC, μg/mL)					
	Gram-positive				Gram-negative	
	S. pyogenes	*C. sporogeneses*	*B. subtilis*	*S. Aureus*	*E. coli*	*P. aeruginosa*
4a	50	–	40	–	–	–
4b	50	–	–	–	–	–
4c	45	–	50	–	–	–
4d	**15**	**20**	**25**	**15**	**15**	**25**
4e	**10**	**20**	**15**	**15**	**15**	**25**
4f	50	–	–	30	25	25
4g	50	–	–	–	–	–
4h	**20**	**25**	**15**	**20**	**15**	**20**
4i	25	50	25	25	25	50
4j	45	–	35	40	40	45
4k	–	50	–	40	40	–
4l	25	50	25	25	25	50
Ampicillin	10	15	15	10	10	10
Vancomycin	15	10	10	15	15	20

–: No antibacterial activity.

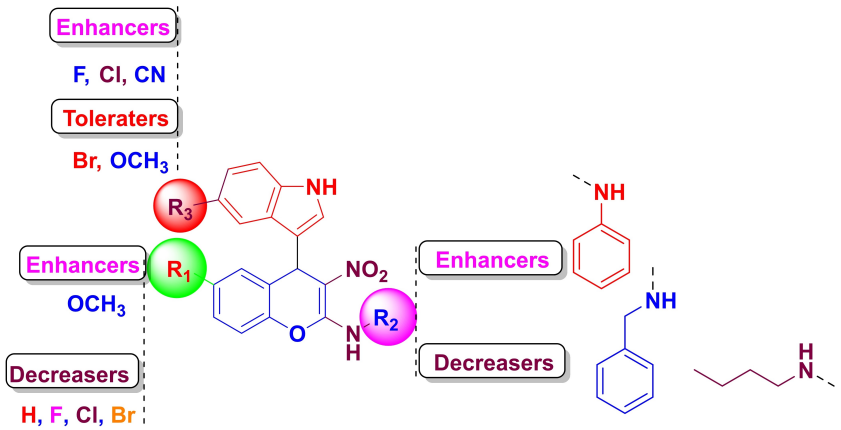

Figure 4. SAR studies of 4H-chromenes antibacterial agents.

Hence the compounds **4d**, **4e**, **4h**, **4i** and **4l** are strongly considered antibacterial agents against all the tested bacterial species. But against *S. pyogenes*, all tested compounds have potential antibacterial activity. In addition, the observations indicate that further variations with the functional groups similar to substituted aniline NH phenyl derivatives and -OCH_3 on the 6th positions of 4*H*-chromene and fluorine-related groups at the 5th position of indole could lead to the potential molecules as described in Figure 4.

Molecular docking with DNA Gyrase B and TopoIV ParE of E. Coli

Docking results of selected indolyl-4*H*-chromenes derivatives (**4a**–**4l**) in the ATP binding pocket of the DNA gyrase B and topoIV ParE from *E. coli* are shown in Table 4. We noticed that all the compounds effectively fit into the ATP binding pocket of both enzymes. The detailed interaction of the most potent compound **4e** with both proteins was displayed in Figure 5. Docking of **4e** with DNA Gryase B site of the selected protein exhibited two hydrogen bonds with binding energy = −8.94 kcal/mol and Ki = 278.60 nM, two are formed between the Chromene-O with THR165 with bond distance (2.04 Å) and indol-NH group with ASN46 (2.23 Å) amino acid residues. Similarly, compound **4e** with topoIV ParE site forms one hydrogen bond between the Indol-NH groups with ASP2045 (2.19 Å) amino acid residue with binding energy = −7.72 kcal/mol and Ki = 2.21 uM. Nevertheless, increasing inhibition constant (Ki) was predicted for compound **4e** with NH–Ph substituents at the chromene-NH, relative to *N*-Methyl substituted compounds. The presence of NH–Ph moiety in compound **4e** makes several other interactions (Pi-Sigma, Pi-Anion, and Pi-Alkyl) with the ATP-binding pocket of the proteins, which might be the reason for exhibiting better MIC activity.

Table 4. *In silico* docking of indole substituted 4*H*-Chromenes (**4a**–**l**).

Compound	*E. Coli* DNA Gryase B(1AJ6)		*E. coli* topoIV ParE (1S14)	
	FEB (kcal/mol)	Ki (*u*M)	FEB (kcal/mol)	Ki (*u*M)
4a	−727	4.71	−6.74	11.56
4b	−7.83	1.83	−7.18	5.46
4c	−7.99	1.38	−7.37	5.46
4d	−7.73	2.16	−6.91	8.63
4e	−8.94	278.6	−7.72	2.21
4f	−8.06	1.23	−7.61	2.62
4g	−8.34	770.79	−6.26	25.91
4h	−7.09	6.3	−6.57	15.4
4i	−7.23	5.02	−7.1	6.23
4j	−7.46	3.43	−7.36	4.04
4k	−6.99	7.49	−6.56	15.52
4l	−7.38	3.86	−7.25	4.83

Conclusions

In summary, diversely functionalized indolyl-4*H*-chromene has been designed and a simple, greener and economical MCR protocol has been developed from readily available starting materials involving 2-hydroxy benzaldehyde, NMSM and indole in the presence of $InCl_3$ as a catalyst in ethanol medium. The analyses of the anti-bacterial properties of the newly prepared indole-4*H*-chromenes were evaluated against four gram-positive and two negative pathogens and compounds **4d**, **4e**, **4h** and **4i** showed potential antibacterial activity, which is in comparison to standard drugs. In addition, functional groups variations similar to substituted aniline derivatives and –OCH_3 on the 2nd and 6th positions of 4*H*-chromene respectively and fluorine-related groups at the 6th position of indole could pave the way to identify the potential molecules to overcome the anti-microbial resistance. By the *in-silico* studies, the binding interaction with ATP binding pocket of the DNA gyrase B and topoIV ParE of the proteins have been evaluated and concurred with *in vitro* studies. The *in vitro* and *silico* results taken together indicate that the C2-*N*-phenyl substituted indolyl-4*H*-chromene **4d**, **4e**, **4h** and **4i** is the promising lead for the further development of more potent anti-microbial agents.

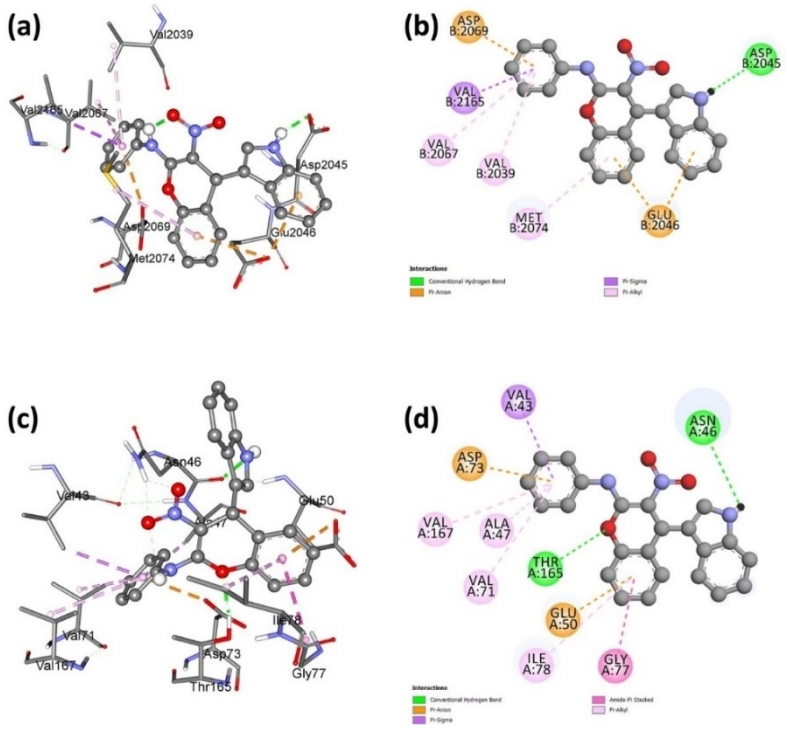

Figure 5. 2D and 2D binding pose of **4e** at the ATP binding site of DNA Topoisomerase IV ParE (**a** and **b**) and DNA gyrase B (**c** and **d**).

Experiment Section

Materials and methods

Evaluation of Physico-Chemical Properties

The process of generating SMILES representations for all the designed compounds has been successfully concluded. The SMILES representations of the compounds were entered into SwissADME, an online tool freely available on the web (http://www.swissadme.ch/index.php),[29,32] along with their respective molecular codes. After the submission process is finished, the programme includes a "run" button feature that aids in the computation of the parameters. The gathered results were obtained in both PDF and csv formats and subsequently underwent data analysis.

Chemistry

Oven-dried glassware was used to carry out all the reactions and the progression of reactions was monitored by thin-layer chromatography (TLC). VEEGO VMP-DS melting point apparatus was used to determine melting points. Melting points were uncorrected and determined in open-end capillaries. Nicolet-6700 spectrometer was used to record IR spectra using KBr. ^{1}H, ^{13}C and DEPT-135 NMR spectra were recorded on Bruker Advance 400 spectrometer using DMSO-d_6 and CCl_4 in a 1:1 ratio as solvent. DEPT spectral data were used to ascertain the number of hydrogen atoms on each carbon atom. The chemical shift value (δ) is expressed in parts per million units and is measured relative to $SiMe_4$ ($\delta = 0.00$) as the internal standard. Coupling constants (J) are measured in Hz. Multiplicities are expressed as *s* (singlet), *d* (doublet), *t* (triplet), *q* (quartet), *m* (multiplet) or broad (br). UV spectra were recorded using a Shimadzu UV-2450 double-beam spectrometer. HPLC analyses were carried out by using the SCL-10ATVP SHIMADZU instrument.

General Procedure for the Preparation of Indolyl-4H-Chromene Derivatives (4a-l)

A mixture of a solution containing 2-hydroxy benzaldehydes (1.0 eq.), NMSM and its derivatives (1.0 eq.) and indole derivatives (1.0 eq.) in ethanol (5 mL) was stirred at ethanol reflux conditions with temperature 80 °C for about 2–5 hours in the presence of $InCl_3$ (0.1 eq.) as a catalyst. The solid formation was observed. The TLC with a mobile phase of hexane: EtOAc mixture has been used to monitor the completion of the reaction. The resulting solid was cooled to 0–5 °C and filtered under a vacuum. The crude products were recrystallized from a dichloromethane and hexane mixture (9:1, v/v) to obtain analytically pure products (**4a-l**).[13]

4-(1H-indol-3-yl)-N-methyl-3-nitro-4H-1-benzopyran-2-amine (***4a***). Detailed structure is given in Figure 6. Yield 98%. mp 199 °C; IR (KBr) 3422 (NH), 1638 (C–N), 1607 (C–O), 1546, 1466, 1362, 1237, 1206, 1167, 1059, 797, 736, 692, 610 cm^{-1}; ^{1}H-NMR (400 MHz, DMSO-d_6) δ_H 10.90 (br s, 1H, Indole NH), 10.34 (d, $J = 4.4$ Hz, 1H, NH aliphatic), 7.32 (d, $J = 7.6$ Hz, 1H, H-14), 7.29 (d, $J = 5.6$ Hz, 1H, H-11), 7.26 (m,

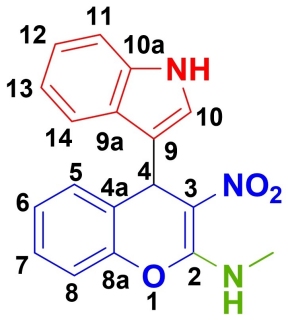

Figure 6. Structure of *4-(1H-indol-3-yl)-N-methyl-3-nitro-4H-1-benzopyran-2-amine* (**4a**)

3H, H-5, H-7&H-8), 7.11 (t, J=7.2 Hz, 1H, H-12), 6.98 (t, J=7.2 Hz, 1H, H-6), 6.88 (t, J=7.2 Hz, 1H, H-13), 5.65 (s, 1H, H-4), 3.21 (d, J=4.4 Hz, 3H, NMe); ^{13}C NMR (100 MHz, DMSO-D_6) δ_C 159.0 (C, C-2), 147.5 (C, C-8a), 136.4 (C, C-10a), 129.3 (C, C-9a), 127.9 (CH, C-5), 125.6 (CH, C-7), 125.4 (CH, C-6), 125.2 (CH, C-12), 123.2 (C. C-9), 120.9 (CH, C-14), 118.7 (CH, C-13), 118.0 (CH, C-10), 117.2 (CH, C-8), 116.0 (CH, C-11), 111.7 (C, C-4a), 107.6 (C, C-3), 33.2 (CH, C-4), 28.1 (Me). HRMS (ESI) Calcd for $C_{18}H_{15}N_3O_3$ [M+H] 322.1178 amu, found 322.1179 amu.

6-Chloro-4-(1H-indol-3-yl)-N-methyl-3-nitro-4H-chromen-2-amine (***4b***). Yield 89%; mp 198 °C; IR (KBr) 3403 (NH), 1637 (C–N), 1608 (C–O), 1468, 1399, 1356, 1167, 1097, 1055, 877, 791 cm^{-1}; ^{1}H-NMR (400 MHz, DMSO-d_6) δ 10.96 (s, 1H, Indole NH), 10.33 (d, J=4.8 Hz, 1H, NH aliphatic), 7.43 (d, J=2 Hz, 1H, H-14), 7.38-7.28 (m, 5H, H-11, H-6, H-7, H-12&H-10),7.03 (t, J=7.6 Hz, 1H, H-13), 6.93 (t, J=7.4 Hz, 1H, H-8), 5.69 (s, 1H, H-4), 3.22 (d, J=4.8 Hz, 3H, NMe); ^{13}C NMR (100 MH_z, DMSO-d_6) 158.6 (C, C-2), 146.3 (C, C-8a), 136.3 (C, C-10a), 129.0 (C, C-6), 128.7 (CH, C-5), 127.8 (CH, C-7), 127.8 (C, C-9a), 124.9 (CH, C-12), 123.5 (CH, C-14), 120.9 (C, C-9), 118.8 (CH, C-13), 118.2 (CH, C-10), 117.8 (CH, C-11), 116.7 (C, C-4a), 111.8 (CH, C-8), 107.0 (C, C-3), 33.0 (CH, C-4), 28.2 (NHMe) ppm. HRMS (ESI) Calcd for $C_{18}H_{14}ClN_3O_3$ [M+H] 356.0713 amu, found 356.0714 amu.

6-Bromo-4-(1H-indol-3-yl)-N-methyl-3-nitro-4H-chromen-2-amine (***4c***)**.** Yield 82%; mp 195 °C; IR (KBr) 3726 (NH), 1638 (C–N), 1604 (C–O), 1468, 1400, 1364, 1218, 1166, 1066, 790 cm^{-1}; ^{1}H-NMR (400 MHz, DMSO-d_6+CCl_4, 1:1) δ 10.89 (s, 1H, Indole NH), 10.24 (d, J=4.8 Hz, 1H, aliphatic NH), 7.65 (d, J=2 Hz, 1H, H-14),7.49 (s, 1H, H-11), 7 .45 (d, J=2.4 Hz, 1H, H-5), 7.39 (d, J=7.8 Hz, 1H, H-7), 7.39 (q, J=3.6 Hz, 1H, H-10), 7.32–7.20 (m, 1H, H-12), 6.10 (t, J=7.6 Hz, 1H, H-13), 6.89 (t, J=8 Hz, 1H, H-8), 5.64 (d, J=4.8 Hz, 1H, H-4), 3.21 (d, J=5.2 Hz, 3H, NMe) ; ^{13}C (100 MH_z, DMSO-d_6+CCl_4, 1;1) 158.5 (C, C-2), 146.8 (C, C-8a), 136.5 (C, 10a), 131.6 (CH, C-14), 131.5 (CH, C-7), 131.2 (C, C-9a), 130.8 (CH, C-10), 128.1 (C, C-9), 125.0 (C, C-6), 123.4 (CH, C-12), 120.9 (CH, C-14), 118.3 (CH, C-13), 117.7 (CH, C-8), 117.2 (C, C-4a), 116.6 (C, C-5), 111.8 (CH, C-11), 107.2 (C, C-3), 33.1 (CH, C-4), 28.2 (NHMe) ppm. HRMS (ESI) Calcd for $C_{18}H_{14}BrN_3O_3$ [M+H] 400.0212 amu, found 400.0213 amu.

4-(1H-indol-3-yl)-6-methoxy-N-methyl-3-nitro-4H-chromen-2-amine (***4d***). Yield 86%; mp 202 °C; IR (KBr) 3333 (NH), 3188, 2944 (C–H), 1639 (C–N), 1610 (C–O), 1464, 1499, 1400, 1363, 1242, 1203, 1174, 1062, 811, 739 cm^{-1}; ^{1}H-NMR (400 MHz, DMSO-d_6+CCl_4, 1:1) δ 10.82 (s, 1H, Indole NH), 10.29 (d, J=4.8 Hz, 1H, aliphatic NH), 7.30 (t, J=7.2 Hz, 2H, H-11&H-14), 7.19 (q, J=5.3 Hz, 2H, H-5&H-10), 6.99 (t, J=7.6 Hz, 1H, H-12), 6.88 (t, J=7.5 Hz, 1H, H-13), 6.82-6.78 (m, 2H, H-7&H-8), 5.60 (s, 1H, H-4), 3.64 (s, 3H, OMe), 3.21 (d, J=4.8 Hz, 3H, NMe); ^{13}C NMR (100 MHz, DMSO-d_6+CCl_4, 1:1) 159.2 (C, C-2), 156.5 (C, C-6), 141.7 (C, C-8a), 136.5 (C, C-10a), 126.6 (C, C-9a), 125.2 (C, C-9), 123.2 (CH, C-13), 120.9 (CH, C-14), 118.8 (CH, C-12), 118.1 (CH, C-10), 117 (CH, C-8), 116.9 (C, C-4a), 113.6 (CH, C-5), 113.5 (CH, C-7), 111.8 (CH, C-11), 107.6 (C, C-3), 55.5 (OMe), 33.7 (CH, C-4), 28.1 (NMe) ppm. HRMS (ESI) Calcd for $C_{19}H_{17}N_3O_4$ [M+H] 352.1283 amu, found 352.1284 amu.

4-(1H-indol-3-yl)-3-nitro-N-phenyl-4H-chromen-2-amine (***4e***). Yield 70%; mp. 163 °C; IR (KBr) 3400 (NH), 1681(C–N), 1634 (C–O), 1582, 1458, 1416, 1370, 1207, 1249, 1145, 1108, 1061, 753, 741 cm^{-1}; ^{1}H-NMR (400 MHz, DMSO-d_6+CCl_4, 1:1) δ 11.95 (s, 1H, Indole NH), 10.89 (d, J=1.2 Hz, 1H, aliphatic NH), 7.56 (d, J=7.6 Hz, 2H, H-14&H-11), 7.49 (t, J=7.8 Hz, 2H, H-5&H-7), 7.36 (d, J=7.6 Hz, 2H, H-8&H-10), 7.31 (t, J=7.2 Hz, 2H, H-17&17′, NHPh), 7.27–7.22 (m, 2H, H-6&H-8), 7.11 (d, J=7.2 Hz, 1H, H-12), 7.00 (t, J=7 Hz, 1H, H-13), 6.9 (t, J=3.6 Hz 1H, H-18, NHPh), 6.8 (t, J=5.2 Hz, 2H, H-16&H-16′, NHPh, ; ^{13}C NMR (100 MHz, DMSO-d_6+CCl_4, 1:1) 156.04 (C, C-2), 147.4 (C, C-8), 136.5 (C, C-10a), 135.4 (C, C-15), 129.3 (CH, C-17&17′), 129.2 (CH, C-5), 128.0 (CH, C-7), 126.10 (CH, C-6), 125.8 (CH, C-18), 125.4 (C, C-9a), 125.1 (CH, C-16&C-16′), 123.5 (CH, C-12), 123.5 (CH, C-14), 123.4 (CH, C-13), 120.9 (CH, C-10), 118.8 (CH, C-8), 117.9 (CH, C-11), 116.7 (C, C-9), 115.8 (C, C-4a), 109.3 (C, C-3), 33.2 (CH, C-4) ppm. HRMS (ESI) Calcd for $C_{23}H_{17}N_3O_3$ [M+H] 384.2133 amu, found 384.2134 amu.

N-Benzyl-4-(1H-indol-3-yl)-3-nitro-4H-chromen-2-amine (***4f***). Yield 75%; mp. 221 °C; IR (KBr) 3452 (NH), 2920 (C–H), 1657 (C–N), 1626 (C–O), 1599, 1453, 1415, 1344, 1236, 1203, 1177, 1144, 1047, 974, 852, 793, 754, 700 ;cm$^{-1.}$ ^{1}H-NMR (400 MHz, DMSO-d_6+CCl_4, 1:1) δ 10.86 (s, 1H, Indole NH), 10.79 (t, J=6.2 Hz, 1H, aliphatic NH), 7.44 (d, J=7.6 Hz, 2H, H-14, H-11), 7.31 (t, J=7.4 Hz, 2H, H-17&17′), 7.33–7.28 (m, 3H, H-16&18′&H-18), 7.23-7.19 (m, 3H, H-5, H-7&H-8), 7.22-7.04 (m, 2H, H-10&H-12), 7.97 (t, J=7.4 Hz, 1H, H-13), 6.74 (q, J=3.8 Hz 1H, H-6), 5.62 (s,1H, H-4), 4.85 (d, J=6.4 Hz, 2H, CH_2) ;^{13}C NMR (100 MHz, DMSO-d_6+CCl_4, 1:1) 158.9 (C, C-2), 147.4 (C, C-8a), 138.2 (C, C-15), 136.5 (C, C-11a), 129.4 (CH, C-5), 128.6 (CH, C-17&17′), 127.9 (CH, C-16&16′), 127.7 (CH, H-18), 127.6 (CH, H-7), 127.4 (CH, H-6), 125.5 (C, C-11a), 125.4 (CH, C-10), 124.1 (C, C-9), 120.8 (CH, C-12), 118.6 (CH, C-13), 117.9 (CH, C-14), 116.8 (C, C-4a), 115.8 (CH, C-8), 111.7 (CH, C-11), 107.9 (C, C-3), 44.7 (CH_2), 33.3 (CH, C-4) ppm. HRMS (ESI) Calcd for $C_{24}H_{19}N_3O_3$ [M+H] 398.1401 amu, found 398.1402 amu.

N-Butyl-4-(1H-indol-3-yl)-3-nitro-4H-chromen-2-amine (***4g***). Yield 85%; mp.171 °C; IR (KBr) 3416 (NH), 3326 (NH aliphatic), 2958 (CH), 1636 (CN), 1609 (C–O), 1543, 1458, 1367, 1240, 1207, 1181, 1158, 1097, 823, 793, 702 ;cm^{-1}; ^{1}H-NMR (400 MHz, DMSO-d_6+CCl_4, 1:1) δ 10.86 (s, 1H, Indole NH), 10.45 (s, 1H, aliphatic NH), 7.36–7.22 (m, 6H, H-14, H-11, H-5, H-7, H-8&H-10) 7.12 (t, J=3.8 Hz, 1H, H-8), 6.99 (t, J=7.2 Hz, 1H, H-12), 6.88 (d, J=7.2 Hz, 2H, H-13&H-6), 5.66 (s, 1H, H-4), 3.69 (dd, J=6.4 Hz, J=12.6 Hz, 2H, CH_2), 1.72 (t, J=7 Hz, 2H, CH_2), 1.49 (q, J=7.0 Hz, 2H, CH_2), 1.00 (d, J=14 Hz, 3H, Me); ^{13}C NMR (100 MHz, DMSO-d_6+CCl_4, 1:1) 158.4 (C, C-2), 147.4 (C, C-8a), 136.2 (C, C-10a), 133.3 (C, C-9a), 129.2 (CH, C-5), 127.8 (CH, C-6), 125.4 (C, C-10), 125.3 (CH, C-7), 124.9 (C, C-4a), 123.1 (CH, C-12), 120.6 (CH, C-13), 118.4 (CH, C-14), 117.8 (CH, C-8), 117.8 (CH, C-11), 107.4 (C, C-3), 40.7 (CH_2), 33.1 (CH, C-4), 31.6 (CH_2), 19.4 (CH_2), 13.5 (Me) ppm. HRMS (ESI) Calcd for $C_{21}H_{21}N_3O_3$ [M+H] 364.2164 amu, found 364.2165 amu.

4-(6-Fluoro-1H-Indol-3-yl)-N-methyl-3-nitro-4H-chromen-2-amine (***4h***). Yield 88%; mp 198 °C; IR (KBr) 3417 (NH), 1706 (C–N), 1603 (C–O) 1602, 1578, 1458, 1359, 1210, 1167, 1060, 875, 828, 766, 730, ;cm^{-1}; ^{1}H-NMR (400 MHz, DMSO-d_6+CCl_4, 1:1) δ 10.95 (s, 1H, Indole NH), 10.31 (d, J=5.2 Hz, 1H, aliphatic NH), 7.33 (d, J=7.6 Hz, 1H, H-11), 7.28 (q, J=5.8 Hz, 3H, H-14, H-5&H-7), 7.02 (dd, J=2 Hz, J=10.4 Hz, 1H, H-10), 6.81 (tt, J=8 Hz, J=8.8 Hz, 1H, H-12), 6.72 (d, J=5.2 Hz, 2H, H-6&H-8), 5.60 (d, J=8 Hz, 1H, H-4), 3.10 (d, J=5.2 Hz, 3H, NMe); ^{13}C NMR (100 MHz, DMSO-d_6+CCl_4, 1:1) 158.8 (C, C-2), 157.8 (C, C-13), 147.5 (C, C-10a), 132.9 (C, C-9a), 129.1 (CH, C-5), 127.9 (C, C-9), 125.4 (CH, C-7), 125.1 (CH, C-6), 117.4 (C, C-4a), 115.9 (CH, C-8), 112.5 (CH, C-11), 112.4 (CH, C-12), 109.0 (CH, C-14), 102.5 (C, C-3), 32.9 (CH, C-4), 28.0 (NHMe) ppm. HRMS (ESI) Calcd for $C_{18}H_{14}FN_3O_3$ [M+H] 340.5101 amu, found 340.5102 amu.

4-(6-Chloro-1H-indol-3-yl)-N-methyl-3-nitro-4H-chromen-2-amine (***4i***). Yield 75%; mp 226 °C; IR (KBr) 3373 (NH), 1705 (C–N), 1639 (C–O), 1610, 1455, 1475, 1427, 1263, 1235, 1171, 1058, 1031, 944, 894, 800, 827, 765 cm^{-1}; ^{1}H-NMR (400 MHz, DMSO-d_6) δ 11.13 (d, J=1. 6 Hz, 1H, Indole NH), 10.35 (d, J=4.8 Hz, 1H, aliphatic NH), 7.38 (d, J=2 Hz, 1H, H-14), 7.35 (q, J=2.1 Hz, 1H, H-5) 7.33-7.29 (m, 3H, H-11, H-12&H-6), 7.27 (d, J=6.8 Hz, 1H, H-10), 7.18 (td, J=23.6 Hz, J=7.4 Hz, 1H, H-7), 7.02 (dd, J=2.1 Hz, 1H, H-8), 5.69 (s, 1H, H-4), 3.22 (d, J=4.8 Hz, 3H, NMe); ^{13}C NMR (100 MHz, DMSO-d_6) 158.9 (C, C-2), 147.5 (C, C-8a), 138.2 (C, C-10a), 134.7 (C, C-9a), 129.7 (CH, C-5), 128.1 (CH, C-7), 126.9 (C, C-13), 125.6 (CH, H-6), 125.4 (C, C-9), 125.0

(CH, C-12), 120.4 (CH, C-14), 117.5 (C, C-4a), 117.4 (CH, C-8), 116.1 (CH, C-13)113.2 (CH, C-11),107.5 (C, C-3), 32.7 (CH, C-4), 28.1 (NMe) ppm. HRMS (ESI) Calcd for $C_{18}H_{14}ClN_3O_3$ [M+H] 356.1076 amu, found 356.1078 amu.

*4-(6-bromo-1H-indol-3-yl)-N-methyl-3-nitro-4H-chromen-2-amine (**4j**).* Yield 82%; mp 226 °C; IR (KBr) 3373 (NH), 1705 (C–N), 1639 (C–O), 1610, 1455, 1475, 1427, 1263, 1235, 1171, 1058, 1031, 944, 894, 800, 827, 765 cm^{-1}; ^{1}H-NMR (400 MHz, DMSO-d_6) δ 11.13 (d, *J*=1. 6 Hz, 1H, Indole NH), 10.35 (d, *J*=4.8 Hz, 1H, aliphatic NH), 7.38 (d, *J*= 2 Hz, 1H, H-14), 7.35 (q, *J*=2.1 Hz, 1H, H-12) 7.33-7.29 (m, 3H, H-11, H-5&H-8), 7.27 (d, *J*=6.8 Hz, 1H, H-6), 7.18 (td, *J*=23.6 Hz, *J*= 7.4 Hz, 1H, H-7), 7.02 (dd, *J*=2.1 Hz, 1H, H-10), 5.64 (s, 1H, H-4), 3.22 (d, *J*=4.8 Hz, 3H, NMe); ^{13}C NMR (100 MHz, DMSO-d_6) 158.9 (C, C-2), 147.5 (C, C-8a), 138.2 (C, C-10a), 134.7 (C, C-9a), 129.7 (CH, C-5), 128.1 (CH, C-6), 126.9 (C, C-7), 125.6 (CH, C-12), 125.4 (C, C-9), 125.0 (CH, C-14), 123.4 (C, C-13), 120.4 (CH, C-11), 117.5 (C), 117.4 (CH, C-10), 116.1 (CH, C-8), 107.5 (C, C-3), 32.7 (CH, C-4), 28.1 (NMe) ppm. HRMS (ESI) Calcd for $C_{18}H_{14}BrN_3O_3$ [M+H] 400.0212 amu, found 400.0213 amu.

*4-(6-methoxy-1H-indol-3-yl)-N-methyl-3-nitro-4H-chromen-2-amine (**4k**).* Yield 90%; mp 205 °C; IR (KBr) 3333 (NH), 3056 (C–H), 1639 (C–O), 1610 (C–C), 1464, 1499, 1400, 1363, 1242, 1203, 1174, 1062, 811, 739 cm^{-1}; ^{1}H-NMR (400 MHz, DMSO-d_6+CCl_4, 1:1) δ 10.82 (s, 1H, Indole NH), 10.29 (d, *J*=4.8 Hz, 1H, aliphatic NH), 7.30 (t, *J*= 7.2 Hz, 2H, H-11&H-14), 7.19 (q, *J*=5.3 Hz, 2H, H-5&H-7), 6.99 (t, *J*= 7.6 Hz, 1H, H-8), 6.88 (t, *J*=7.5 Hz, 1H, H-10), 6.82–6.78 (m, 2H, H-12&H-6), 5.60 (s, 1H, H-4), 3.64 (s, 3H, OMe), 3.21 (d, *J*=4.8 Hz, 3H, NMe); ^{13}C NMR (100 MHz, DMSO-d_6+CCl_4, 1:1) 159.2 (C, C-2), 156.5 (C,C-8a), 141.7 (C, C-13), 136.5 (C, C-4a), 126.6 (C, C-10a), 125.2 (C, C-9a), 123.2 (CH, H-5), 120.9 (CH, H-6), 118.8 (CH, H-8), 118.1 (CH, H-7), 117 (CH, H-12), 113.6 (CH, H-10), 107.6 (C, H-3), 55.5 (OMe), 33.7 (CH, C-4), 28.1 (NMe) ppm. HRMS (ESI) Calcd for $C_{19}H_{17}N_3O_4$ [M+H] 352.1283 amu, found 352.1284 amu.

*3-(2-(methylamino)-3-nitro-4H-chromen-4-yl)-1H-indole-6-carbonitrile (**4l**).* Yield 73%; mp 250 °C; IR (KBr) 3373 (NH), 2260 (CH), 2210 (CN group), 1705, 1639 (C–O), 1610 (C–O), 1455, 1475, 1427, 1263, 1235, 1171, 1058, 1031, 944, 894, 800, 827, 765 cm^{-1}; ^{1}H-NMR (400 MHz, DMSO-d_6) δ 11.13 (d, *J*=1. 6 Hz, 1H, Indole NH), 10.35 (d, *J*=4.8 Hz, 1H, aliphatic NH), 7.38 (d, *J*=2 Hz, 1H, H-14), 7.35 (q, *J*=2.1 Hz, 1H, H-11) 7.33–7.29 (m, 3H, H-12, H-5&H-8), 7.27 (d, *J*=6.8 Hz, 1H, H-7), 7.18 (td, *J*=23.6 Hz, *J*=7.4 Hz, 1H, H-10), 7.02 (dd, *J*=2.1 Hz, 1H, H-6), 5.64 (s, 1H, H-4), 3.22 (d, *J*=4.8 Hz, 3H, NMe); ^{13}C NMR (100 MHz, DMSO-d_6) 158.9 (C, C-2), 148. 6 (CN), 147.5 (C, C-8a), 138.2 (C, C-10a), 134.7 (C, C-9a), 129.7 (CH, C-5), 128.1 (CH, C-12), 126.9 (C, C-10), 125.6 (CH, C-14), 125.4 (C, C-9), 125.0 (CH, C-11), 123.4 (C, C-6), 120.4 (CH, C-7), 117.5 (C, C-13), 116.1 (CH, C-7), 115.6 (C, C-4a), 113.2 (CH, C-8), 107.5 (C, C-3), 32.7 (CH, C-4), 28.1 (NMe) ppm. HRMS (ESI) Calcd for $C_{19}H_{14}N_4O_3$ [M+H] 347.1071 amu, found 347.1072 amu.

Biological Evaluation

Qualitative Test (Agar Well Diffusion Method)

The bacterial cultures, Gram-positive i.e., Streptococcus pyogenes, Clostridium pyrogenes, Bacillus subtilis, Staphylococcus aureus and Gram-negative namely Escherichia coli and Pseudomonas aeruginosa were used in this investigation. The media used for the antibacterial test was Muller Hinton Agar. The antibacterial activity was carried out by employing 24 h of cultures.[33] The activity of the indole 4H-chromene series of compounds was screened for its antibacterial activity and was tested separately using agar well diffusion method. About 30 mL of the agar medium with respective strains of bacteria was transferred aseptically into each sterilized Petri plate. A well of 6 mm diameter was made using a sterile cork borer. The standard drug Ampicillin (10 μg) and vancomycin (10 μg) was used and the compounds were placed in a 6 mm diameter well. Antibacterial assay plates were incubated at 37 °C for 24–48 h and the diameter of the zone of inhibition was measured.

Quantitative Estimation (MIC)

MIC was determined following the Clinical and Laboratory Standard Institute methodology.[34] Bacterial culture suspensions were prepared in Muller Hinton broth. For determination of MIC, 0.500 mL standard compound solution of different concentrations ranging from 10 to 50 μg/mL was diluted using, 0.500 mL test organism and 4 mL Muller Hinton broth in the sterile test tube, and then incubated at 37 °C for 24–48 h. Control was prepared in two sets, one containing broth medium and test organism while the other containing broth medium and extract. After 24 h, the MIC values were recorded based on the lowest concentration showing an absence of growth in the tubes. The test was further confirmed by plating on Muller Hinton agar.

Docking Study

The in-*silico* molecular docking calculation was performed using AutoDock 4.2 software[35] to understand the docking location and binding mode of ligands towards the ATP binding pocket of the DNA gyrase B and topoIV ParE from *E. coli* (PDB ID: 1AJ6 and 1S14, respectively). The X-ray coordinates of the DNA gyrase B and topoIV ParE were obtained from Protein Data Bank (www.rcsb.org). The protein preparation step includes the removal of native ligand and water molecules and the addition of polar hydrogens, merging of non-polar hydrogens, the addition of Gasteiger charges and finally saving into PDBQT file format. Then the 2D structure of Indolyl-4*H*-chromenes derivatives was energy minimized using a 6-31G*[36] basis set and the B3LYP[37] functional were employed in Gaussian 16 code. ENREF 71[38] Furthermore, the Auto Dock Tolls suite is used to add polar hydrogens, merge non-polar hydrogens, and the adding of Gasteiger charges to finally save into PDBQT format. After this, the grid box was formed around the entire protein model. The finest docking complex was selected based on the lower ΔG value and the higher number of docking orientations present in the binding site. Finally, the molecular docking results of DNA gyrase B and topoIV ParE with Indolyl-4*H*-chromenes derivatives were analysed using Discovery Studio 2020 Client software.

Author Contributions

Parthiban. A. and Makan. P designed the study, Perfomed the experiment, and wrote the manuscript. Adhikari, P. performed the antimicrobial experiments and wrote manuscript. Selvaraj M, performed the molecular docking and wrote manuscript. Afzal M. editing of manuscript. Parthiban. A. and Makan. P edited, revised the article critically and all authors finally gave approval of the final version.

Acknowledgements

We also thank to Dr. USN Murty, the Director of the National Institute of Pharmaceutical Education and Research Guwahati (NIPER-G) for excellent support. The author, Mohd Afzal extend his appreciation to the Researchers Supporting Project number (RSPD2023R979), King Saud University, Riyadh, Saudi Arabia.

Conflict of Interests

The authors declare no conflict of interest.

Data Availability Statement

The data that support the findings of this study are available in the supplementary material of this article.

Keywords: antibacterial · 4*H*-chromene · indole · *in vitro* · *in silico* studies

[1] a) E. Christaki, M. Marcou, A. Tofarides, *J. Mol. Evol.* **2020**, *88*, 26–40; b) L. Morrison, T. R. Zembower, *Gastrointest. Endosc. Clin. N.* **2020**, *30*, 619–635.
[2] a) E. J. Septimus, *Med. Clin. N. Am.* **2018**, *102*, 819–829; b) WHO., World Health Organization, **2022**.
[3] a) A. A. Abu-Hashem, M. A. Gouda, F. A. Badria, *Med. Chem. Res.* **2018**, *27*, 2297–2311; b) A. A. Abu-Hashem, S. A. Al-Hussain, *Molecules* **2022**, *27*, 835; c) M. N. M. Yousif, R. M. Abdelhameed, A. A. Abu-Hashem, N. M. Yousif, *Egypt. J. Chem.* **2023**, *66*, 113–120; d) A. A. Abu-Hashem, M. E. A. Zaki, *J. Heterocycl. Chem.* **2019**, *56*, 886–894; e) A. A. Abu-Hashem, M. A. Gouda, *J. Heterocycl. Chem.* **2017**, *54*, 850–858; f) A. A. Abu-Hashem, M. El-Shazly, *Eur. J. Med. Chem.* **2015**, *90*, 633–665; g) A. A. Abu-Hashem, M. A. Gouda, *Arch. Pharm.* **2011**, *344*, 543–551; h) V. Raj, J. Lee, *Front. Chem.* **2020**, *8*; i) M. Costa, T. A. Dias, A. Brito, F. Proença, *Eur. J. Med. Chem.* **2016**, *123*, 487–507.
[4] A. Parthiban, M. Kumaravel, J. Muthukumaran, R. Rukkumani, R. Krishna, H. S. P. Rao, *Med. Chem. Res.* **2016**, *25*, 1308–1315.
[5] A. Parthiban, M. Kumaravel, J. Muthukumaran, R. Rukkumani, R. Krishna, H. Surya Prakash Rao, *Med. Chem. Res.* **2015**, *24*, 1226–1240.
[6] A. Parthiban, J. Muthukumaran, A. Moushumi Priya, S. Jayachandran, R. Krishna, H. Surya Prakash Rao, *Med. Chem. Res.* **2014**, *23*, 642–659.
[7] L. Abrunhosa, M. Costa, F. Areias, A. Venâncio, F. Proença, *J. Ind. Microbiol. Biotechnol.* **2007**, *34*, 787–792.
[8] H. S. P. Rao, V. S. Tangeti, L. N. Adigopula, *Res. Chem. Intermed.* **2016**, *42*, 7285–7303.
[9] C. V. Subbareddy, S. Sumathi, *New J. Chem.* **2017**, *41*, 9388–9396.
[10] M. Kidwai, S. Saxena, M. K. Rahman Khan, S. S. Thukral, *Bioorg. Med. Chem. Lett.* **2005**, *15*, 4295–4298.
[11] R. Hossein nia, M. Mamaghani, K. Tabatabaeian, F. Shirini, M. Rassa, *Bioorg. Med. Chem. Lett.* **2012**, *22*, 5956–5960.
[12] C. D. Hufford, B. Oguntimein, M. Martin, J. Clardy, *Tetrahedron Lett.* **1984**, *25*, 371–374.
[13] P. Anaikutti, M. Selvaraj, J. Prabhakaran, T. Pooventhiran, T. C. Jeyakumar, R. Thomas, P. Makam, *J. Mol. Struct.* **2022**, 133464.
[14] S. V. Chitreddy, S. Shanmugam, *J. Mol. Liq.* **2017**, *243*, 494–502.
[15] K. Y. Mohamed Salah, O. A. Ahmed Abdou, I. E.-E. Talaat, *Heterocycl. Commun.* **2017**, *23*, 55–64.
[16] a) A. Parthiban, J. Muthukumaran, A. Manhas, K. Srivastava, R. Krishna, H. S. P. Rao, *Bioorg. Med. Chem. Lett.* **2015**, *25*, 4657–4663; b) R. Devakaram, D. S. Black, K. T. Andrews, G. M. Fisher, R. A. Davis, N. Kumar, *Bioorg. Med. Chem.* **2011**, *19*, 5199–5206.
[17] I. Zghab, B. Trimeche, M. B. Mansour, M. Hassine, D. Touboul, H. B. Jannet, *Arab. J. Chem.* **2017**, *10*, S2651–S2658.
[18] E. Mahmoud, A. M. Hayallah, S. Kovacic, D. Abdelhamid, M. Abdel-Aziz, *Pharmacol. Rep.* **2022**, *74*, 570–582.
[19] a) C. V. Subbareddy, S. Sundarrajan, A. Mohanapriya, R. Subashini, S. Shanmugam, *J. Mol. Liq.* **2018**, *251*, 296–307; b) H. T. Afifi, M. R. Okasha, H. Alsherif, E. A. H. Ahmed, S. A. Abd-El-Aziz, *Curr. Org. Synth.* **2017**, *14*, 1036–1051; c) M. S. Shaik, M. R. Nadiveedhi, M. Gundluru, A. K. R. Narreddy, K. R. Thathireddy, R. Ramakrishna, S. R. Cirandur, *J. Heterocycl. Chem.* **2021**, *58*, 137–152.
[20] a) L. Saswata, V. Lakshmana Rao, S. Swamy, B. Verra Narayana, M. Parameshwar, M. Seshadri Rao, D. Debashish, WO Patent WO/2010/035283 A2, **2010**; b) S. Lahiri, L. R. Vadali, S. Saidugari, V. N. Bandlamudi, P. Makam, S. R. Manukonda, D. Datta, Google Patents, **2013**; c) P. Makam, R. Kankanala, A. Prakash, T. Kannan, *Eur. J. Med. Chem.* **2013**, *69*, 564–576; d) P. Makam, T. Kannan, *Eur. J. Med. Chem.* **2014**, *87*, 643–656; e) P. Makam, P. K. Thakur, T. Kannan, *Eur. J. Pharm. Sci.* **2014**, *52*, 138–145; f) P. Makam, M. Samipillai, H. G. Kruger, T. Govender, T. Naicker, *Z. fur Krist. - New Cryst. Struct.* **2017**, *232*, 577–578; g) R. Matsa, P. Makam, M. Kaushik, S. Hoti, T. Kannan, *Eur. J. Pharm. Sci.* **2019**, *137*, 104986; h) N. Thota, P. Makam, K. K. Rajbongshi, S. Nagiah, N. S. Abdul, A. A. Chuturgoon, A. Kaushik, G. Lamichhane, A. M. Somboro, H. G. Kruger, *ACS Med. Chem. Lett.* **2019**, *10*, 1457–1461; i) P. Anaikutti, P. Makam, *Bioorg. Chem.* **2020**, *105*, 104379; j) M. Hublikar, V. Kadu, J. K. Dublad, D. Raut, S. Shirame, P. Makam, R. Bhosale, *Arch. Pharm.* **2020**, *353*, 2000003; k) S. Chinnam, P. Bobbala, B. Chandrasekaran, K. Potla, S. Chigurupati, K. Khatana, P. Makam, S. Rathore, S. S. Kondakkagari, K. S. R., AP Patent 2,021,105,627, **2021**; l) P. Makam, R. Matsa, *Curr. Top. Med. Chem.* **2021**, *21*, 2779–2799; m) M. Hublikar, V. Kadu, D. Raut, S. Shirame, S. Anbarasu, M. K. Al-Muhanna, P. Makam, R. Bhosale, *J. Mol. Struct.* **2022**, *1261*, 132903; n) R. Matsa, P. Makam, G. Sethi, A. A. Thottasseri, A. R. Kizhakkandiyil, K. Ramadas, V. Mariappan, A. B. Pillai, T. Kannan, *RSC Adv.* **2022**, *12*, 18333–18346.
[21] a) E. Ruijter, R. Orru, *Drug Discovery Today Technol.* **2018**, *29*, 1–2; b) B. B. Touré, D. G. Hall, *Chem. Rev.* **2009**, *109*, 4439–4486.
[22] a) J. Huuskonen, D. J. Livingstone, D. T. Manallack, *SAR QSAR Environ. Res.* **2008**, *19*, 191–212; b) M. Yazdanian, S. L. Glynn, J. L. Wright, A. Hawi, *Pharm. Res.* **1998**, *15*, 1490–1494; c) P. Artursson, A.-L. Ungell, J.-E. Löfroth, *Pharm. Res.* **1993**, *10*, 1123–1129.
[23] a) M. Sharifi, T. Ghafourian, *AAPS J.* **2014**, *16*, 65–78; b) M. V. Varma, Y. Lai, A. F. El-Kattan, *Adv. Drug Delivery Rev.* **2017**, *116*, 92–99.
[24] S. Struck, U. Schmidt, B. Gruening, I. S. Jaeger, J. Hossbach, R. Preissner, in *Genome Informatics 2008*, Imperial College Press, **2008**, pp. 231–242.
[25] a) C. A. Lipinski, F. Lombardo, B. W. Dominy, P. J. Feeney, *Adv. Drug Delivery Rev.* **1997**, *23*, 3–25; b) C. A. Lipinski, F. Lombardo, B. W. Dominy, P. J. Feeney, *Adv. Drug Delivery Rev.* **2001**, *46*, 3–26; c) I. Kola, J. Landis, *Nat. Rev. Drug Discovery* **2004**, *3*, 711–716.
[26] D. F. Veber, S. R. Johnson, H.-Y. Cheng, B. R. Smith, K. W. Ward, K. D. Kopple, *J. Med. Chem.* **2002**, *45*, 2615–2623.
[27] P. D. Leeson, A. M. Davis, *J. Med. Chem.* **2004**, *47*, 6338–6348.
[28] a) M. P. Gleeson, A. Hersey, D. Montanari, J. Overington, *Nat. Rev. Drug Discovery* **2011**, *10*, 197–208; b) S. Khojasteh, H. Wong, C. C. A. Hop, in *Drug metabolism and pharmacokinetics quick guide*, Springer New York, **2011**, pp. 165–181.
[29] A. Daina, O. Michielin, V. Zoete, *Sci. Rep.* **2017**, *7*, 42717.
[30] M. Gampa, P. Padmaja, S. Aravind, P. N. Reddy, *Chem. Heterocycl. Compd.* **2021**, *57*, 1176–1180.
[31] H. S. P. Rao, K. Geetha, *Tetrahedron Lett.* **2009**, *50*, 3836–3839.
[32] B. Bakchi, A. D. Krishna, E. Sreecharan, V. B. J. Ganesh, M. Niharika, S. Maharshi, S. B. Puttagunta, D. K. Sigalapalli, R. R. Bhandare, A. B. Shaik, *J. Mol. Struct.* **2022**, *1259*, 132712.
[33] P. Lalitha, A. Parthiban, V. Sachithanandam, R. Purvaja, R. Ramesh, *S. Afr. J. Bot.* **2021**, *142*, 149–155.
[34] J. H. Rex, *Clinical* **2008**, *28*, 1–25.
[35] G. M. Morris, R. Huey, W. Lindstrom, M. F. Sanner, R. K. Belew, D. S. Goodsell, A. J. Olson, **2009**, *30*, 2785–2791.
[36] a) R. Ditchfield, W. J. Hehre, J. A. Pople, *J. Chem. Phys.* **1971**, *54*, 724–728; b) P. C. Hariharan, J. A. Pople, *Theor. Chim. Acta.* **1973**, *28*, 213–222; c) W. J. Hehre, R. Ditchfield, J. A. Pople, *J. Chem. Phys.* **1972**, *56*, 2257–2261.
[37] a) A. D. Becke, *J. Chem. Phys.* **1993**, *98*, 5648–5652; b) A. D. Becke, *J. Chem. Phys.* **1993**, *98*, 1372–1377; c) C. Lee, W. Yang, R. G. Parr, *Phys. Rev. B* **1988**, *37*, 785–789; d) A. D. Becke, *Phys. Rev. A* **1988**, *38*, 3098–3100; e) P. J. Stephens, F. J. Devlin, C. F. Chabalowski, M. J. Frisch, *J. Phys. Chem.* **1994**, *98*, 11623–11627.
[38] M. J. Frisch, G. W. Trucks, H. B. Schlegel, G. E. Scuseria, M. A. Robb, J. R. Cheeseman, G. Scalmani, V. Barone, G. A. Petersson, H. Nakatsuji, X. Li,

M. Caricato, A. V. Marenich, J. Bloino, B. G. Janesko, R. Gomperts, B. Mennucci, H. P. Hratchian, J. V. Ortiz, A. F. Izmaylov, J. L. Sonnenberg, Williams, F. Ding, F. Lipparini, F. Egidi, J. Goings, B. Peng, A. Petrone, T. Henderson, D. Ranasinghe, V. G. Zakrzewski, J. Gao, N. Rega, G. Zheng, W. Liang, M. Hada, M. Ehara, K. Toyota, R. Fukuda, J. Hasegawa, M. Ishida, T. Nakajima, Y. Honda, O. Kitao, H. Nakai, T. Vreven, K. Throssell, J. A. Montgomery Jr., J. E. Peralta, F. Ogliaro, M. J. Bearpark, J. J. Heyd, E. N. Brothers, K. N. Kudin, V. N. Staroverov, T. A. Keith, R. Kobayashi, J. Normand, K. Raghavachari, A. P. Rendell, J. C. Burant, S. S. Iyengar, J. Tomasi, M. Cossi, J. M. Millam, M. Klene, C. Adamo, R. Cammi, J. W. Ochterski, R. L. Martin, K. Morokuma, O. Farkas, J. B. Foresman, D. J. Fox, Wallingford, CT, **2016**.

Manuscript received: September 9, 2023
Accepted manuscript online: December 5, 2023
Version of record online: ■■, ■■

Journal of Biomolecular Structure and Dynamics

ISSN: (Print) (Online) Journal homepage: https://www.tandfonline.com/loi/tbsd20

Antimicrobial activity prediction, inter- and intramolecular charge transfer investigation, reactivity analysis and molecular docking studies of adenine derivatives

C. Geetha Priya, B. R. Venkatraman, I. Arockiaraj, S. Sowrirajan, N. Elangovan, Mohammad Shahidul Islam & Sakkarapalayam M. Mahalingam

To cite this article: C. Geetha Priya, B. R. Venkatraman, I. Arockiaraj, S. Sowrirajan, N. Elangovan, Mohammad Shahidul Islam & Sakkarapalayam M. Mahalingam (18 Nov 2023): Antimicrobial activity prediction, inter- and intramolecular charge transfer investigation, reactivity analysis and molecular docking studies of adenine derivatives , Journal of Biomolecular Structure and Dynamics, DOI: 10.1080/07391102.2023.2281636

To link to this article: https://doi.org/10.1080/07391102.2023.2281636

JOURNAL OF BIOMOLECULAR STRUCTURE AND DYNAMICS
https://doi.org/10.1080/07391102.2023.2281636

Antimicrobial activity prediction, inter- and intramolecular charge transfer investigation, reactivity analysis and molecular docking studies of adenine derivatives

C. Geetha Priya[a], B. R. Venkatraman[a], I. Arockiaraj[b], S. Sowrirajan[c], N. Elangovan[c], Mohammad Shahidul Islam[d] and Sakkarapalayam M. Mahalingam[e]

[a]Department of Chemistry, Thanthai Periyar Government Arts and Science College (Autonomous), Affiliated to Bharathidasan University, Tiruchirappalli, Tamil Nadu, India; [b]Department of Chemistry, St. Joseph's College (Autonomous), Affiliated to Bharathidasan University, Tiruchirappalli, Tamil Nadu, India; [c]Research Centre for Computational and Theoretical Chemistry, Tiruchirappalli, Tamil Nadu, India; [d]Department of Chemistry, College of Science, King Saud University, Riyadh, Saudi Arabia; [e]Department of Chemistry, Purdue University, West Lafayette, IN, USA

Communicated by Ramaswamy H. Sarma

ABSTRACT

The utilization of the density functional theory (DFT) methodology has developed as a highly efficient method for investigating molecular structure and vibrational spectra, and it is increasingly being employed in various applications relating to biological systems. This study focuses on conducting investigations, both experimental and computed, to analyze the molecular structure, electronic properties and features of (E)-4-(((9H-purin-6-yl)imino)methyl)-2-methoxyphenol (ANVA). The expression ANVA should be rewritten as follows: the compound is a derivative of adenine (primary amine), specifically a vanillin (aldehyde). The present study reports the synthesis, characterization, DFT, docking and antimicrobial activity of ANVA. The optimization of the molecular structure was conducted, and the determination of its structural features was performed using DFT with the B3LYP/cc-pVDZ method. The vibrational assignments were determined in detail by analyzing the potential energy distribution. A strong correlation was observed between the spectra that were observed and the spectra that were calculated. The calculation of intramolecular charge transfer was performed using natural bond orbital analysis. In addition, several computational methods were employed, including highest occupied molecular orbital–least unoccupied molecular orbital analysis, molecular electrostatic potential calculations, non-linear optical, reduced density gradient, localization orbital locator and electron localization function analysis. This paper examines the present use of adenine derivatives in combatting bacterial and fungal infections, as well as the inclusion of spectral and quantum chemical calculations in the discussion.

ARTICLE HISTORY
Received 21 August 2023
Accepted 4 November 2023

KEYWORDS
Synthesis; DFT; inter- and intramolecular interactions; topology; docking; antimicrobial activity

Introduction

Schiff base is mainly used in dyes, pigments, catalysts, intermediates in chemical synthesis and polymer stabilizers. These chemicals are also antifungal, antibacterial, anti-malarial, anti-proliferative, anti-inflammatory, anti-viral and antipyretic. Schiff bases are carbonyl-substituted aldehydes or ketones. The double bond between carbon and nitrogen bonds the nitrogen atom to an aryl or alkyl group, excluding hydrogen (Jayachitra et al., 2023). Schiff bases possess a general chemical formula of $R_1N=CR_2R_3$, whereby R_1 represents a phenyl or alkyl moiety that imparts stability to the Schiff base. The numerical value provided by the user is insufficient to determine the context or subject matter for a Despite the reversible nature of Schiff base production, wherein imine hydrolysis can occur under specific conditions, the reaction remains very uncomplicated and is likely to proceed successfully (Thilagavathi et al., 2022). The stability of different types of Schiff bases in the presence of water, particularly under acidic conditions, remains uncertain. While certain Schiff bases exhibit sensitivity to water and readily undergo hydrolysis, reverting to aldehyde, the specific type of Schiff base that remains stable in the presence of water is yet to be determined. To moderate the risk of hydrolysis, it is advisable to conduct the Schiff base reaction in a solvent environment devoid of moisture or employ supplementary techniques to eliminate the byproduct, water, during the imine production process (Abu Ali et al., 2022). The presence of a lone pair on the nitrogen atom in the imine moiety facilitates the donation of electrons, hence facilitating the establishment of a suitable donor bond with a metal ion, leading to the occurrence of complexation. Several Schiff bases possess an additional functional group, typically hydroxyl (OH) and thiol (SH) groups, or another nitrogen (N) atom, near the imine group (Sowrirajan et al., 2022). The presence of these functional groups facilitates the development of chelate rings consisting of five or six members upon coordination with various metal ions. The focus of this thesis is the synthesis of

CONTACT N. Elangovan drelangovanchem@gmail.com

Supplemental data for this article can be accessed online at https://doi.org/10.1080/07391102.2023.2281636.

novel Schiff base ligands containing various functional groups, such as phenol OH and N from pyridine ring ligands.

The principal understanding of the process of Schiff base production is that it involves nucleophilic addition to the carbonyl group. The primary amine serves as the nucleophile in the process of Schiff base production (Elangovan & Sowrirajan, 2021). During the initial step of the reaction, the amine nitrogen lone pair of electrons undergo an attack on the aldehyde or ketone, resulting in the formation of a carbinolamine. This additional product is characterized by its essential instability. Due to its classification as an alcohol, the carbinolamine experiences dehydration under the influence of acid catalysis (Rajimon et al., 2023).

In the Literature survey, the author Sugandha Singhal et al. recently synthesized and studied DNA-based Schiff bases such as 2-(1-aminobenzyl)benzimidazole compound. They studied density functional theory (DFT), molecular docking, electronic properties (UV-visible and fluorescence) and antimicrobial properties (Singhal et al., 2019). Kaushal k. Joshi et al synthesized a new pyridine-based Schiff base and studied antimicrobial activities (Joshi, 2022). Susmitha Kasula et al., previously studied DFT and molecular docking studies of 4-amino indane derived from Schiff base (Kasula & Dandu, 2023). Based on these research surveys we plan to synthesize a new series of Schiff bases with condensation of adenine and vanillin. The resulting product ANVA was characterized, by FTIR, ^{1}H–^{13}C-NMR and UV-visible analysis. The DFT study was used to analyze the titled compound structural analysis. The antimicrobial study also examined using six different microorganisms for four antibacterial and two fungal strains.

Experimental

Materials and methods

The adenine and vanillin utilized in this study were provided by Sigma-Aldrich. Upon procuring the solvents from a local provider, they were directly utilized. The FTIR spectrum was recorded using the KBr pellet model in the range of 4000–400 cm^{-1}. The absorption spectrum was examined using the Lambda-35 instrument and dimethyl sulfoxide (DMSO) as a solvent. The Bruker equipment was utilized for the record of the ^{1}H and ^{13}C-NMR spectra.

Synthesis of (E)-4-(((9H-purin-6-yl)imino)methyl)-2-methoxyphenol (ANVA)

Following dissolution in a minimal amount of ethanol, adenine (1.35 mg, 0.01 mmol) and vanillin (1.52 mg, 0.01 mmol) were combined for 30 min. Following the transfer of the mixture into a 100 mL round-bottom flask, the subsequent step involves subjecting the flask to reflux under a water bath for 5 h. Following reflux, the resulting product was filtered and subsequently dried at room temperature. The ANVA product is re-crystallized in DMSO (Elangovan et al., 2021; Sowrirajan et al., 2022). The schematic representation of the synthesized scheme is depicted in Figure 1.

Pharmacology

The agar well diffusion method was utilized to evaluate the antibacterial and antifungal activity of ANVA derived from adenine and vanillin. Amoxicillin was employed as the positive control, whereas DMSO was designated as the negative control (PrabhuKumar et al., 2022). A total of six microorganisms were pricked (four antibacterial and two antifungal) in the Petri plate. Following the loading of the microorganisms, the plates were enveloped with paraffin tape and subsequently positioned in an incubator set at a temperature of 37 °C (Yiğit et al., 2022). The plates were left in an inverted orientation for 24 h. The measurement of the zone of inhibition surrounding the wells was conducted using a ruler and the results were recorded in millimeters (mm; Pillai et al., 2020). The efficacy of the crude plant medications over time was assessed by measuring the zone of inhibition once more after 48 h.

Computational methods

Gaussian, Inc. was used for theoretical computations with a conventional split valence double-zeta polarized basis set of cc-pVDZ (Frisch et al., 2009). The DFT was used with B3LYP hybrid functional theory. The reduced mass, force constant and infrared intensity frequencies are achieved without scaling (Tomita et al., 2022). To match theoretical and experimental frequencies, B3LYP rescales vibrational frequencies by 0.9651. Scaling the experiment difference makes it more significant. Vibrational assignments were calculated theoretically. The VEDA4.0 computed the potential energy distribution (PED) and assigned vibrational frequencies (Demircioğlu et al., 2015). After Gaussian, Inc. processing, the time-dependent density functional theory (TD-DFT) technique determined the electronic spectrum, which was merged with experimental data (Elangovan et al., 2021). The NMR structural optimization at GIAO uses the same basis set. An NBO 3.1 calculation was utilized to identify the intramolecular interactions, using DFT/B3LYP and cc-pVDZ (Domínguez-

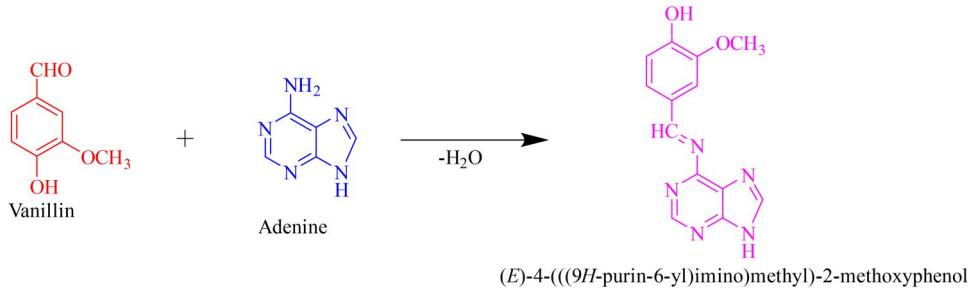

Figure 1. Synthesis of (E)-4-(((9H-purin-6-yl)imino)methyl)-2-methoxyphenol (ANVA).

Flores & Melander, 2022). The molecular electrostatic potential (MEP) surface map, total density, highest occupied molecular orbital–least unoccupied molecular orbital (HOMO–LUMO), localization orbital locator (LOL), electron localization function (ELF), average local ionization energy (ALIE) and reduced density gradient (RDG) method of the optimized geometric structure of the ANVA molecule were calculated. For the topological analysis calculations, we used Multiwfn software (Lu & Chen, 2012). AutoDock software was utilized in molecular docking studies (Goodsell et al., 2021).

Results and discussion

Structural geometry analysis

The ANVA compound was optimized using the B3LYP/cc-pVDZ basis set (Elkaeed et al., 2022). The optimized structure is depicted in Figure 1, the optimized structure developed by Chemcraft software. This study focuses on the calculation of the bond length, bond angle and dihedral angle of the named compound (Soltani et al., 2019). Specifically, the bond length between O19 and C20 is determined to be a bond length of 1.4297 Å. Additionally, the bond angle between C6-C5-N8 is found to be 132.213 Å, while the dihedral angle between C4-N9-C10-H23 is measured at 179.998 Å. The above-mentioned bond properties are highest in the ANVA structure (Gonçalves et al., 2022). Additionally, the other characteristics of the bond are displayed in Table 1. The ANVA structure was optimized in the gas phase (Manivel et al., 2022). The thermal energy of the optimized structures is measured to be 156.432 kcal/mol in the gas phase.

Vibrational analysis

The FTIR analysis was made at the same basis set level as previously mentioned. The FTIR spectra, both experimental and computed, are presented in Figure 2. The ANVA combination consists of a total of 31 atoms and belongs to the C1 point group (Alam et al., 2019). It exhibits 30 stretching mode vibrations, 29 bending mode vibrations, 28 torsion mode vibrations and 27 CH mode vibrations (Arjunan et al., 2011). The scale factor for this analysis is 0.9651. Table 2 presents a complete examination of the distribution of vibration energy, as measured by the PED analysis. The subsequent paragraphs will examine several important vibration frequencies.

CN vibration

The C = N stretching vibration was present in the region of 1700–1600 cm^{-1} (Elangovan et al., 2021). The ANVA molecule CN str, frequency (experimental) is 1672 cm^{-1}, and simulated frequencies of 1587 and 1579 cm^{-1}, respectively. These simulated frequencies correspond to the vibrational mode νCN and are influenced by the PED effect of 32% and 49%. The values obtained for simulated bending and torsion vibrations are 1407, 1391, 1374, 1361, 1281, 1228 cm^{-1} and 933, 922, 838, 644 cm^{-1}, respectively. These values are associated with the influence of PED, which is calculated to be 24%, 51%, 20%, 14%, 23%, 20% and 74%, 65%, 74%, 13%, respectively. These values can be considered equivalent to βHCN and τHCNC. The observed frequencies obtained from the experiment align with the predicted frequencies based on theoretical calculations.

OH vibration

The FTIR analysis of the synthesized compound ANVA reveals a characteristic OH stretching vibration at a wavenumber of 3355 cm^{-1} (Ali et al., 2022). The simulated stretching wavenumber for this functional group is determined to be 3509 cm^{-1}. Furthermore, the influence of the PED on the OH stretching vibration is found to be a perfect match, with a 100% correlation to the νOH mode. The simulated vibrational frequencies for bending and torsion are 1406, 1252, 1213 cm^{-1} and 1550, 1467, 1165 and 1137 cm^{-1}, with a PED contribution of 17%, 14%, 21% and 21%, 17%, 48%, 38% in relative to βHOC and τHCOC, respectively.

CH vibration

The infrared spectrum exhibits a characteristic CH stretching vibration at a wavenumber of 2939 cm^{-1}. The simulated infrared spectrum stretching frequencies of 2964, 3123, 3112, 3095, 3071, 3050, 3035 and 2979 cm^{-1}, respectively (Elangovan et al., 2023; Thilagavathi et al., 2023). The relative contributions of these vibrations to the PED were determined to be 100%, 99%, 90%, 91%, 100%, 95%, 95% and 100% for the νCH mode. The bending vibration as

Table 1. HOMO–LUMO energy contribution and wavelength of ANVA with different solvents.

Media	Wavelength (nm)	Band gap (eV)	Energy (cm^{-1})	Oscillator strength	Contribution
	351.94543		28413.4957	0.8231	HOMO->LUMO (98%)
Gas	328.39788	2.481	30450.8662	0.0006	H-4->LUMO (67%), H-2->LUMO (31%)
	325.16808		30753.3262	0.0002	H-4->LUMO (30%), H-2->LUMO (66%)
	369.53693		27060.8946	0.9449	HOMO->LUMO (99%)
Chloroform	322.33605	2.481	31023.5238	0.0009	H-4->LUMO (54%), H-3->LUMO (43%)
	318.90359		31357.4397	0.0012	H-4->LUMO (43%), H-3->LUMO (52%)
	370.80792		26968.1402	0.9191	HOMO->LUMO (99%)
DMSO	320.0809	2.481	31242.1016	0.0105	H-4->LUMO (28%), H-3->LUMO (63%), H-1->LUMO (7%)
	319.43765		31305.0133	0.1317	H-1->LUMO (86%), H-3->LUMO (6%), H-2->LUMO (4%)
	369.07492		27094.7701	0.8933	HOMO->LUMO (99%)
Water	319.94874	2.481	31255.0066	0.0081	H-4->LUMO (28%), H-3->LUMO (65%), H-1->LUMO (5%)
	319.21559		31326.7904	0.1399	H-1->LUMO (87%), H-3->LUMO (5%), H-2->LUMO (4%)

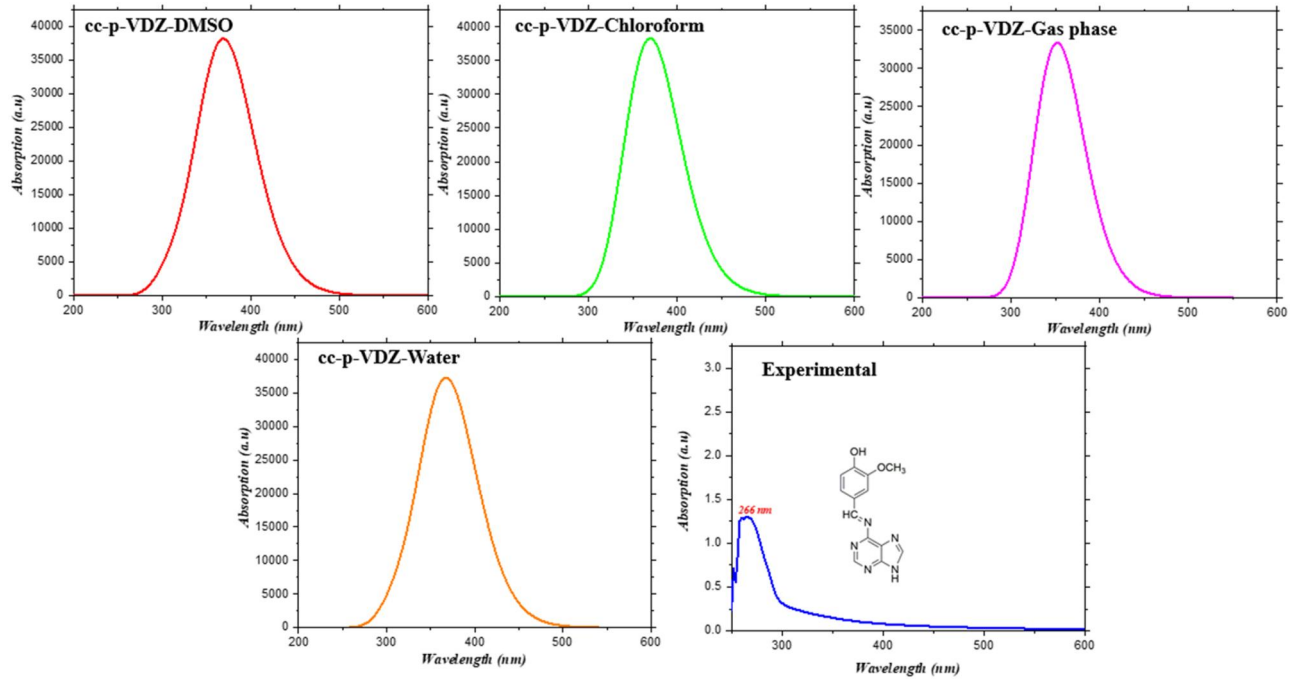

Figure 2. Comparison UV-visible spectrum of ANVA in gas phase and different solvent phase.

Table 2. FMO properties of ANVA in gas phase and different solvent phase.

Property	Values
εHOMO	−5.7364
εLUMO	−2.0153
Energy gap (ΔE)	3.7211
Ionisation energy ($I = \varepsilon HOMO = -HOMO$)	5.7364
Electron affinity ($A = \varepsilon LUMO = -LUMO$)	2.0153
Global hardness ($\Pi = (I - A)/2$)	1.8605
Global softness ($S = 1/\Pi$)	0.5374
Chemical potential ($\mu = -(I + A)/2$)	−3.8758
Electronegativity ($\chi = -\mu$)	3.8758
Electrophilicity index ($\omega = \mu^2/2\Pi$)	3.7382
Nucleophilicity index ($N = 1/\omega$)	0.2675
Electron accepting power ($\omega + = A2/2\ (I - A)$	0.2707
Electron donating power ($\omega + = I2/2\ (I - A)$	0.7707

determined through calculations, is seen at 1438, 1417, 1374, 1361, 1310, 1285, 1262, 1213, 1143 and 1118 cm^{-1}. These frequencies are associated with the respective PED contributions of 16%, 14%, 14%, 25%, 22%, 10%, 13%, 10%, 10%, 13% and 39% corresponding to βHCC. The torsion vibrations seen in this study exhibit wavenumbers of 1550, 1467, 1165, 1143, 1137, 560, 261 and 176 cm^{-1}. These vibrations are associated with respective percentages of PED participation of 21%, 17%, 48%, 15%, 38%, 92%, 11% and 30%. These PED percentages are attributed to the torsional mode involving the τHCOC moiety.

NMR spectral analysis

Figure 3 displays the chemical shifts of the ^{1}HNMR spectrum. The ^{1}HNMR spectrum provides information regarding the number of hydrogen isotopes present within a molecule and its instant locality. The chemical shift of the molecule -HC = N- has been determined to be 10.38 (s, 1H) ppm, and it has been DFT to be 10.33 (24H) ppm, respectively (Manoj et al., 2022). The hydrogen atom peak of the azomethine group is observed to lie downfield due to the presence of the electronegative nitrogen atom (Elangovan et al., 2022). The hydroxyl group (-OH) proton chemical shift is observed at 3.79 (s, 1H) ppm (experimental), and the related simulated proton chemical shift is 6.24 (28H) ppm. The methoxy group (-OCH_3) experimentally observed proton chemical shift is 3.47 (s, 3H) ppm, with corresponding calculated proton chemical shift is 4.63 (29H), 4.33 (30H), 4.37 (31H) ppm, respectively. In the ANVA compound observed experimental singlet proton shifts are 7.10 (s, 1H), 8.41 (s, 1H), 8.09 (s, 1H) and 7.12 (s, 1H) ppm, the corresponding simulated shifts are 8.52 (25H), 9.27 (21H), 8.30 (23H) and 9.09 (22H) ppm, respectively (Muthukumar et al., 2022). The doublet chemical shifts are 7.12 (s, 1H) and 7.10 (s, 1H) ppm in experimental and calculated 7.33 (26H) and 7.76 (27H) ppm, respectively.

The structural characteristics of a compound can be determined by the examination of the chemical shifts of various carbon isotopes in ^{13}CNMR absorption spectra. Figure 4 illustrates the chemical shifts seen in the ^{13}CNMR analysis (Jayachitra et al., 2023). The chemical shift of ketone and aldehyde functional groups is approximately 200 ppm, whereas aromatic carbons often exhibit chemical shifts ranging from 110 to 160 ppm. The chemical shift range typically observed for double-bonded carbon atoms is between 100 and 50 ppm. The chemical shifts for the -HC = N- part of this molecule were determined experimental at 152.68 ppm and calculated to be 151.77 ppm, respectively (Latha et al., 2022). Chemical changes in the carbon atom of a methyl group range from 10 to 50 ppm. The experimental carbon chemical shift is 57.70 ppm, which is confirmed by the methoxy group (-OCH_3) with the corresponding calculated shift is 44.31 (20 C) ppm. The other simulated chemical shifts are 141.60, 136.16, 98.00, 118.45, 119.95, 102.22, 145.72, 118.38, 141.15 and 127.82 ppm, with corresponding experimental carbon

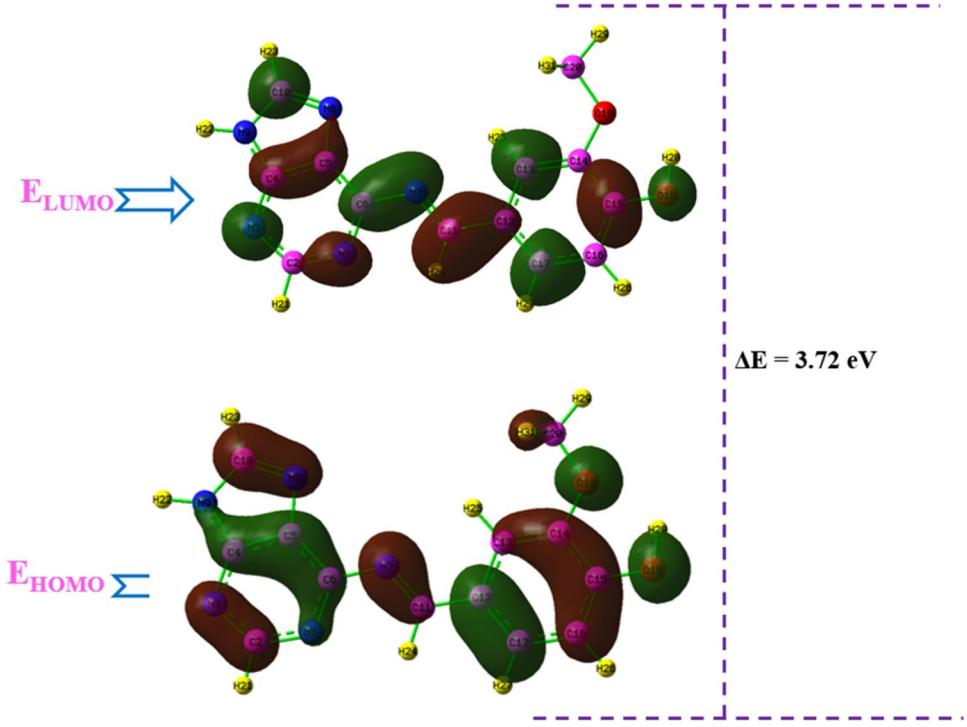

Figure 3. HOMO and LUMO energy diagram of ANVA.

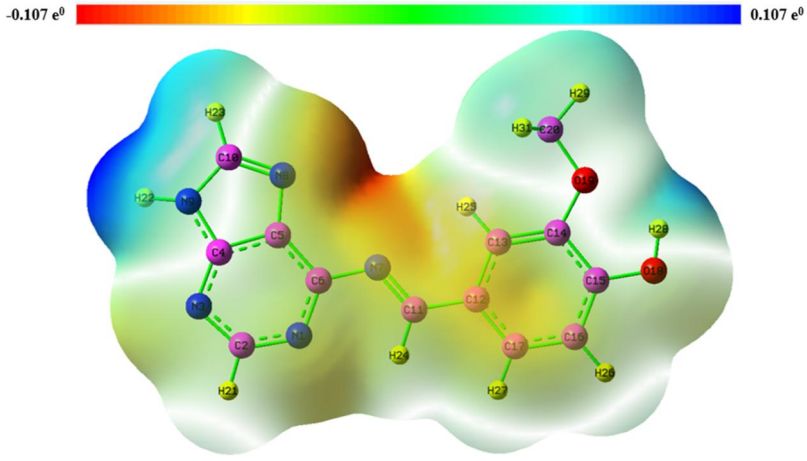

Figure 4. MEP surface map of ANVA.

shifts are 139.87, 131.11, 96.57, 112.58, 114.66, 109.28, 149.55, 119.40, 133.59, 14.17 and 125.27 ppm, respectively.

Absorption spectrum

The titled compound experimentally observed UV-visible wavelength is 266 nm. Figure 2 displays the absorption spectrum, both experimental and theoretical (Dikmen & Kani, 2020). In the theoretical section, we employed both the gas phase and other solvent phases, including chloroform, DMSO and water. The computed wavelengths for the DMSO solvent are 370, 320 and 319 nm, with corresponding oscillator strengths of 0.9191, 0.0105 and 0.1317, respectively. The absorption energies of DMSO were determined to be 26,968.14,016, 31,242.1016 and 31,305.01328 cm^{-1}, respectively (Manjunatha et al., 2021). The wavelengths obtained through calculation are 369, 322 and 318 nm, respectively, as determined in the medium of chloroform. The predicted wavelengths for the gas phase and water are as follows: 351, 328, 325 and 369 nm, 319 nm and 319 nm, respectively. The contribution of the HOMO and LUMO in the DMSO solvent was computed (Manhas et al., 2022). The HOMO to LUMO contribution was found to be 99%, with a corresponding wavelength of 370 nm. Additionally, the HOMO–LUMO contributions for specific molecular orbitals were determined as follows: H-4 to LUMO (28%), H-3 to LUMO (63%) and H-1 to LUMO (7%). Moreover, the primary contribution of the HOMO to the LUMO was determined to be H-1->LUMO, accounting for 86% of the total contribution. The wavelength associated with this transition is measured to be 319 nm. Additional information regarding the contributions of various solvents and the gas phase highest occupied molecular orbital (HOMO) and LUMO, including their respective

wavelengths, energies and energy gaps, may be found in the accompanying Table 1.

HOMO–LUMO analysis

The Gaussian, Inc. software package was employed to conduct the frontier molecular orbital (FMO) theory. In a general context, the FMO theory designates the HOMO as an electron-donating unit. The LUMO is commonly referred to as the electron acceptor (John et al., 2022). The electrons underwent a transition from the HOMO to the LUMO (Nakakuki et al., 2022). The HOMO energy, computed from the gas phase, is determined to be −5.74 eV, while the LUMO energy is found to be −2.02 eV. The determined energy difference between the HOMO and the LUMO is found to be 3.72 (eV). The molecule exhibits a significantly low band gap value, indicating a high degree of stability and notable biological activity. Figure 3 displays the FMO surface map (Kateris et al., 2023). The HOMO is observed across the total of the molecule, whereas the LUMO is likewise observed throughout the molecule, except the methoxy group (-OCH_3) and the two nitrogen atoms from the purine five-member ring. The color green is used to represent the positive phase, whereas the color red is used to represent the negative phase. The properties of the FMO are presented in Table 2.

Molecular electrostatic potential

The MEP has been determined using the B3LYP/cc-pVDZ basis set. The nucleophilic and electrophilic attacking sites are determined. Figure 4 displays the color-filled surface maps of the molecule's electrostatic potential (Ramesh & Reddy, 2023). The surface map prominently displays negative potential regions in red and positive potential regions in green. The color yellow is associated with a state of zero potential. In the MEP map, the color progression follows an ascending order from red to blue (Ghosh et al., 2021). The color red was found to correspond to the highest level of repulsion, whereas the color blue was associated with the greatest degree of attraction. At the ANVA molecule, the presence of blue color is observed at the -OH group and -NH site of the purine ring (Elangovan et al., 2022). According to the data, the locations containing –OH and –NH functional groups exhibit the highest degree of attraction. The red color is observed at two nitrogen atoms. The first nitrogen atom is located at the connecting bridge between the benzene ring and the purine heterocyclic ring, while the second nitrogen atom is found in the five-member ring of the purine heterocyclic ring (Silvarajoo et al., 2020). The red color signifies the presence of the strongest repulsion. In the context of chemical reactions, it is commonly understood that the negative potential corresponds to nucleophilic behavior, whereas the positive potential is associated with electrophilic behavior. The color is determined within the range of −0.107 e^0 to 0.107 e^0, and this calculation is performed based on the gas phase.

Mulliken population analysis (MPA) and natural population analysis (NPA)

The understanding of compound chemical reactivity, electrostatic interaction and electrostatic potential charge dispersion holds significant utility. The NPA and MPA methods are utilized to observe the electron dispersion occurring between atoms within molecules (Demircioğlu et al., 2015). Atoms undergo electron gain or loss to acquire a negative or positive charge, respectively. This study uses the Mulliken and NPA methods to elucidate the electrophilic and nucleophilic characteristics of the molecules under investigation. Table 3 presents the results of the NPA, whereas Table 4 displays the Mulliken atomic charges (Téllez Soto et al., 2013). The MPA analysis reveals the identification of the atom with the highest positive and negative charges as C11 (0.184412) and O19 (−0.327436), respectively. The graphical representation of the MPA analysis of atom charges, both positive and negative, is depicted in Figure 5. Atoms of element carbon possess both positive and negative charges in the context of both MPA and NPA, respectively (Arivazhagan & Kavitha, 2012). The hydrogen atom possesses exclusively a positive charge, while the electronegative atoms nitrogen (N) and oxygen (O) exhibit exclusively negative charges in both the MPA and NPA analyses. According to the examination conducted by the NPA, the largest charge is seen at position H28 with a value of 0.48709. Additionally, the highest negative charge is found at position O18 with a value of −0.67282. The graphical representation illustrating the NPA analysis is presented in Figure 6.

Table 3. Natural population analysis of ANVA calculated from B3LYP/cc-pVDZ basis set.

Atom No.	Natural Charge	Natural population			
		Core	Valance	Rydberg	Total
N 1	−0.57894	1.99932	5.55918	0.02044	7.57894
C 2	0.30607	1.99927	3.66233	0.03233	5.69393
N 3	−0.55271	1.99935	5.53097	0.0224	7.55271
C 4	0.4121	1.99886	3.5589	0.03013	5.5879
C 5	0.06086	1.99872	3.91521	0.02521	5.93914
C 6	0.44933	1.99888	3.52116	0.03062	5.55067
N 7	−0.53687	1.9993	5.52007	0.01751	7.53687
N 8	−0.51064	1.99943	5.48775	0.02347	7.51064
N 9	−0.61538	1.9992	5.60606	0.01012	7.61538
C 10	0.27255	1.99924	3.69967	0.02855	5.72745
C 11	0.17553	1.99907	3.80009	0.02531	5.82447
C 12	−0.12644	1.99889	4.11139	0.01616	6.12644
C 13	−0.26321	1.99886	4.24765	0.0167	6.26321
C 14	0.26897	1.99859	3.70948	0.02296	5.73103
C 15	0.34734	1.99864	3.62796	0.02605	5.65266
C 16	−0.28262	1.99892	4.26795	0.01574	6.28262
C 17	−0.18993	1.99894	4.17684	0.01415	6.18993
O 18	−0.67282	1.99977	6.663	0.01005	8.67282
O 19	−0.5771	1.99972	6.56763	0.00975	8.5771
C 20	−0.25317	1.99935	4.24007	0.01375	6.25317
H 21	0.20039	0	0.79734	0.00226	0.79961
H 22	0.43109	0	0.56399	0.00492	0.56891
H 23	0.21242	0	0.78565	0.00193	0.78758
H 24	0.19868	0	0.79371	0.00762	0.80132
H 25	0.25915	0	0.73635	0.00449	0.74085
H 26	0.24176	0	0.75494	0.00331	0.75824
H 27	0.23241	0	0.76451	0.00308	0.76759
H 28	0.48709	0	0.50475	0.00817	0.51291
H 29	0.21206	0	0.78595	0.00199	0.78794
H 30	0.19604	0	0.80024	0.00373	0.80396
H 31	0.196	0	0.80027	0.00373	0.804

Analysis of natural bond orbital (NBO)

The NBO analysis suggests a valuable background for the investigation of the presence of conjugative interaction or charge transfer inside molecular systems through the evaluation of inter and intramolecular bond interactions. The application of second-order perturbation theory allows for the prediction of energies associated with bonding, anti-bonding and donor–acceptor delocalization (Lin et al., 2013). In the context of electron transfer between a donor and an acceptor, it can be observed that the E (2) value is significantly elevated, suggesting a higher degree of conjugation within the system. Stabilization interactions between acceptor and donor species result in the delocalization of electron density for both Lewis and non-Lewis NBOs (Ajayi & Shapi, 2020). According to the concept of NBO theory, Lewis NBOs are associated with bonding interactions, while non-Lewis NBOs correspond to anti-bonding interactions. The structure proposed by Lewis provides evidence of significant electron delocalization through donor–acceptor interactions. Table 3 presents the outcomes of the NBO analysis, along with the corresponding values for the stabilization energies (Kargar et al., 2021). The NBO analysis yielded a total of 135.46438 (96.760% of 140) Lewis structures, which encompass both the core and valence Lewis structures. Additionally, a total of 4.53562 (3.240% of 140) non-Lewis

Table 4. Mulliken population analysis of ANVA calculated from B3LYP/cc-pVDZ basis set.

Atom	Charge	Atom	Charge	Atom	Charge	Atom	Charge
1 N	−0.234336	9 N	−0.096566	17 C	0.03777	25 H	−0.023744
2 C	0.127409	10 C	0.14302	18 O	−0.158059	26 H	−0.022292
3 N	−0.213657	11 C	0.184412	19 O	−0.327436	27 H	−0.039073
4 C	0.167765	12 C	−0.059164	20 C	0.127881	28 H	0.150715
5 C	0.036102	13 C	0.020696	21 H	−0.001394	29 H	0.037116
6 C	0.149951	14 C	0.159156	22 H	0.09653	30 H	0.042211
7 N	−0.208524	15 C	0.028723	23 H	0.00685	31 H	0.04217
8 N	−0.203698	16 C	0.054185	24 H	−0.024718		

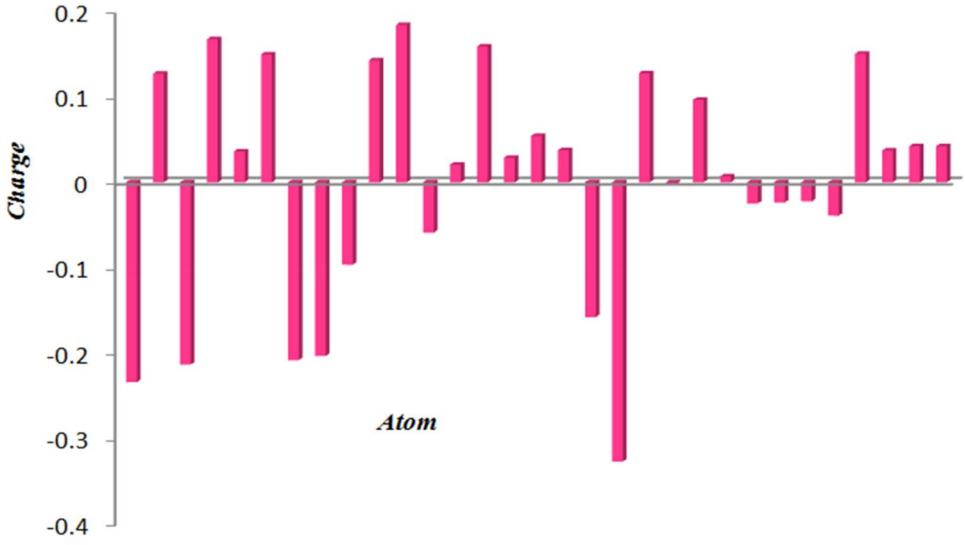

Figure 5. Mulliken population analysis graphical representation of ANVA.

Figure 6. Natural population analysis graphical diagram of ANVA.

structures, consisting of valence and Rydberg structures, were estimated.

The highest stabilization energies were reported for the lone pair interactions LP (1)–N9, LP (1)–N9 and LP (2)–O19 with the anti-bonding orbitals π*(N8–C10), π*(C4–C5) and π*(C13–C14), respectively (Sarojini et al., 2012). The corresponding stabilization energies were measured to be 44.64, 37.75 and 27.08 kcal/mol, with occupancies of 1.60562, 1.60562 and 1.85808, respectively. Moreover, the bond pairs with the highest stabilization energies were observed in the bonding orbitals π(N1–C6), π(C4–C5), π(C2–N3) and π(N7–C11) for the corresponding anti-bonding orbitals π*(C2–N3), π*(N1–C6), π*(C4–C5) and π*(N1–C6). The calculated energies for these interactions were found to be 36.75, 32.58, 28.7 and 22.35 kcal/mol, respectively. Additionally, the occupancy values for these orbitals were determined to be 1.69852, 1.55932, 1.74732 and 1.8535, respectively. The formation of the s(N1–C2) bond involved the interaction between the hybrid orbital of nitrogen, namely $sp^{1.73}$ (with 63.23% p-character), and the hybrid orbital of carbon, specifically $sp^{1.88}$ (with 65.27% p-character; Kanchana et al., 2023). The carbon hybrid orbital, characterized as $sp^{1.92}$ with 65.65% p-character, suffered interaction with the nitrogen hybrid orbital, characterized as $sp^{1.87}$ with 64.98% p-character, resulting in the creation of the s(C2–N3) bond.

Topology analysis

The utilization of the ELF and the LOL is imperative in conducting investigations to topological analysis. These aforementioned techniques were employed for topological analysis (SangeethaMargreat et al., 2021). The ELF and LOL are highly significant electrons in molecular space due to their ability to engage in covalent bonding, contributing to the establishment of a fundamental reference point (Sanakarganesan et al., 2023). The representation of maximum localized orbital overlaps is commonly denoted as LOL, whereas the electron pair density that corresponds to orbital gradients is referred to as ELF. The software tool Multiwfn was employed for the analysis of ELF and LOL. Figure 7 presents the surface maps of ELF and LOL, with a color gradient ranging from blue to red. The ELF function is measured on a scale ranging from 0.000 to 1.000, while the LOL scale extends from 0.000 to 0.800. There are variations in hue ranges seen between localized and delocalized orbitals (Kazachenko et al., 2022). The color spectrum below 0.5 signifies the presence of a delocalized orbital zone, whereas over 0.5 suggests a localized orbital region. The ELF and LOL orbitals exhibit variations in color intensity. In both the ELF and LOL surface maps, the regions indicating the highest concentration of bonding and non-bonding electrons are visually represented as red at hydrogen (H) atoms and blue at carbon (C) atoms.

Non-covalent interaction (NCI)

The utilization of RDG has proven important in the assessment and analysis of covalent, intramolecular and intermolecular interactions. Figure 8 illustrates the representation of the RDG surface map, showcasing potential hydrogen bond interactions (Pramila et al., 2023). The potential biological activity of the chemical ANVA was assessed through the use of NCIs (Elangovan et al., 2023). The surface map provided by NCI illustrates the presence of enhanced interactive

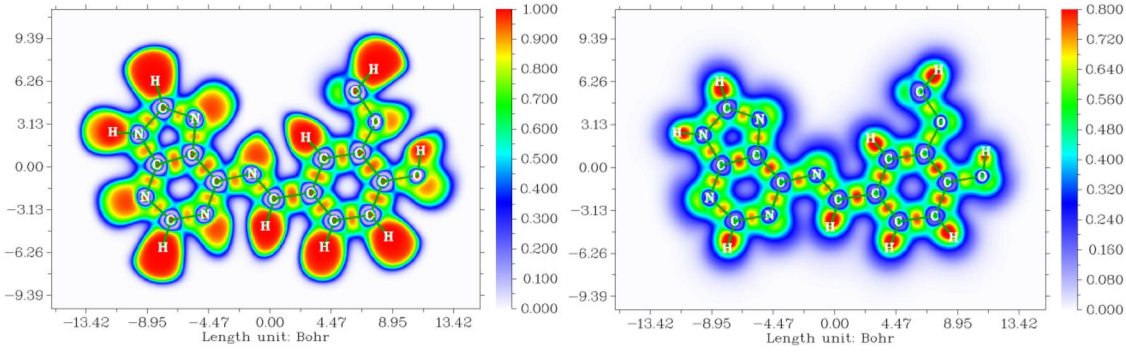

Figure 7. ELF and LOL color-filled surface map of ANVA.

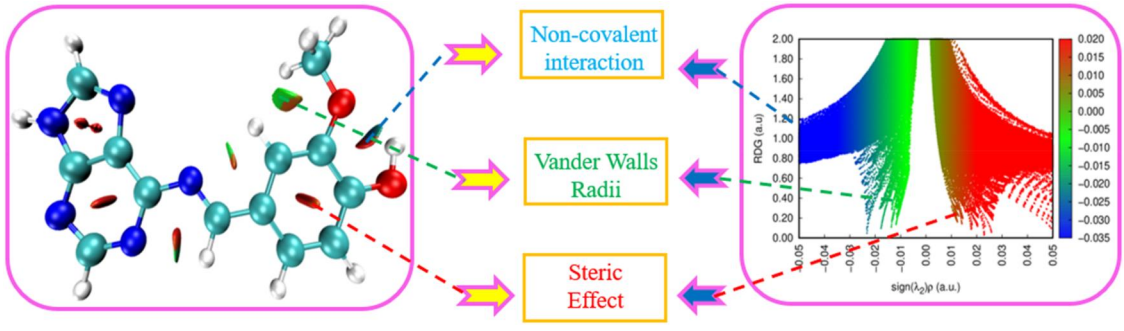

Figure 8. Non-covalent interaction of ANVA with water.

hydrogen bonding, pronounced repulsion and van der Waals interactions attributed to the chemical compound denoted by the colors blue, red and green, respectively (Arulaabaranam et al., 2021). The NCI analysis can be utilized to identify several types of intermolecular interactions, including hydrogen bonding, ion–dipole interaction, dipole–dipole interaction, hydrophobic interaction, pi-stacking and van der Waals forces.

Antibacterial activity

The disc diffusion assay was employed to evaluate the antibacterial efficacy of the synthetic compounds that were synthesized, targeting both Gram-negative and Gram-positive bacterial strains (Shntaif et al., 2021). Bacterial cultures were procured from the diagnostic laboratory in Pune. The process involved transferring isolated pure associations of bacteria that were obtained from freshly produced cultures into sterile normal saline solution (Essghaier et al., 2021). These colonies were then subjected to vertexing to create uniform suspensions of the bacterial cells. Subsequently, the turbidity was calibrated to a value of 0.5 Mc Farland standard units, and the suspensions were subsequently applied onto Mueller–Hinton agar (MHA) plates. The experiment involved the placement of sterile filter paper discs with a diameter of 6 mm onto the plates (Gulbagca et al., 2019). The sterile discs were saturated with a volume of 20 µL of the compounds under investigation, which were prepared at a concentration of 25 mg/mL, 50 mg/mL, 75 mg/mL and 100 mg/mL, it is dissolved in DMSO. The experimental setup included the utilization of a positive control, specifically ciprofloxacin, and a negative control, which consisted of sterile distilled water. Subsequently, the plates were subjected to incubation at a temperature of 37 °C for 24 h. The measurement of the inhibitory zones was conducted in millimeters (Pillai et al., 2020). We used four different bacterial strains namely *Escherichia coli*, *Klebsiella aerogenes*, *Bacillus subtilis* and *Staphylococcus aureus*. The antibacterial activity and Inhibition zone are presented in Table 5 and Figure 9. When compared to standard ciprofloxacin, our synthesized compound ANVA has less activity. But compared to other bacterial strains, *Bacillus subtilis* has the highest activity, this activity showed in 100 mg/mL concentration with a measured inhibition constant is 32 mg/mL.

Table 5. Antimicrobial activity inhibition zone of ANVA.

Compound	Name of the microorganism	25 µm	50 µm	75 µm	100 µm	Standard
ANVA	*Escherichia coli*	9	11	15	30	38
	Klebsiella aerogenes	10	13	17	26	30
	Bacillus subtilis	15	17	21	32	40
	Staphylococcus aureus	17	20	24	29	35
	Aspergillus niger	8	11	16	28	35
	Candida albicans	11	13	17	26	32

Antifungal activity

The fungal strains were cultivated on the disc well diffusion method and subjected to incubation at a temperature of

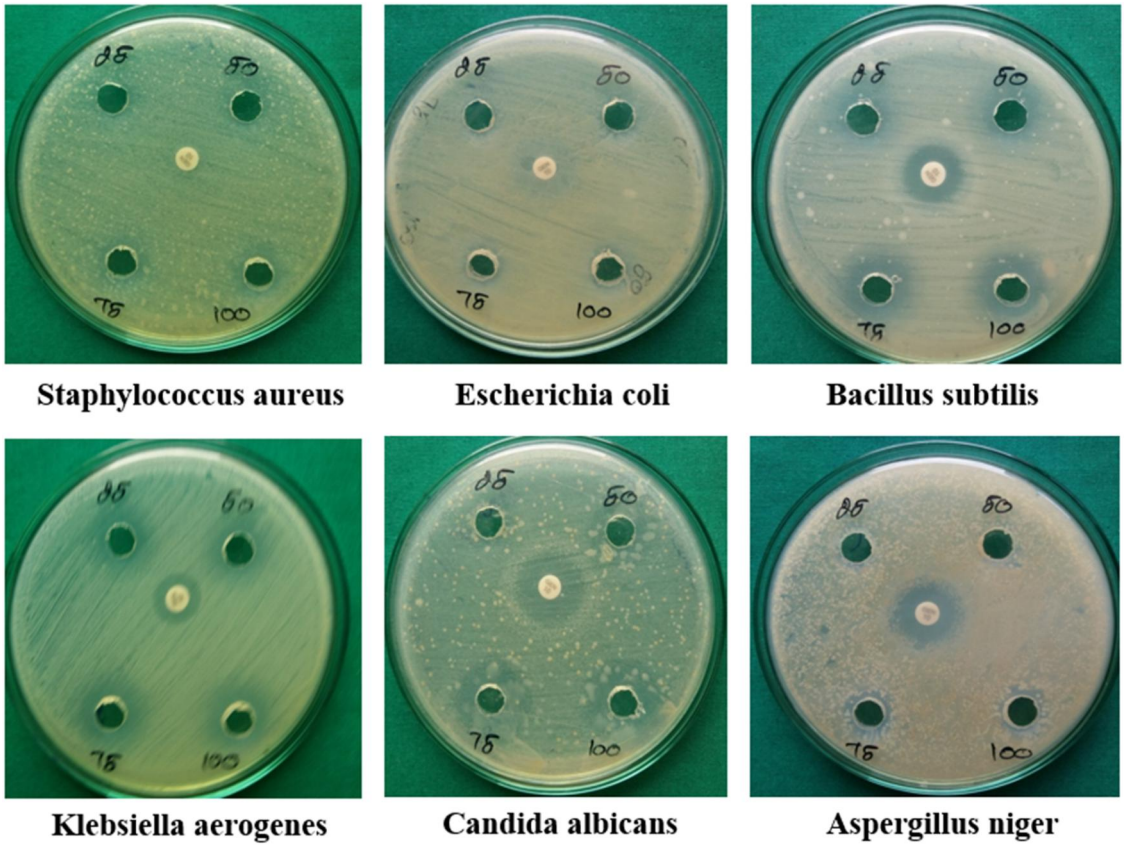

Figure 9. Antimicrobial activity of ANVA.

Table 6. Protein–ligand interaction binding energies of ANVA with 3DRA, 1KS5, 3I41, 6LL6, 6GP7, and 8SBW proteins.

Protein	Rank	Run	Binding energy	Cluster RMSD	Reference RMSD
	1	2	−5.17	0	68.77
	2	6	−4.61	0	37.56
	2	9	−4.13	0.75	37.66
	3	3	−4.28	0	61.52
3DRA	4	8	−3.96	0	61.02
	5	4	−3.85	0	51.98
	6	1	−3.72	0	37.86
	6	10	−3.59	1.63	38.6
	7	7	−3.72	0	38.9
	8	5	−3.14	0	21.65
	1	1	−4.24	0	123.11
	1	5	−4.09	0.96	123.89
	1	9	−4.03	1.7	124.6
	2	3	−3.93	0	125.17
1KS5	3	2	−3.71	0	126.58
	3	4	−3.55	0.78	126.86
	4	6	−3.62	0	114.96
	5	7	−3.59	0	117.45
	6	8	−3.4	0	110.95
	7	10	−2.97	0	124.29
	1	1	−4.05	0	44.09
	2	6	−3.95	0	43.6
	3	2	−3.92	0	8.84
	4	9	−3.75	0	29.69
3I41	5	7	−3.73	0	40.9
	6	4	−3.45	0	39.27
	7	3	−3.42	0	30.88
	8	8	−3.38	0	40.35
	9	5	−3.32	0	32.76
	10	10	−3.3	0	38.77
	1	3	−3.81	0	19.88
	2	5	−3.52	0	24.32
	3	10	−3.44	0	23.74
	4	7	−3.39	0	24.07
6LL6	5	4	−3.36	0	14.77
	6	1	−3.35	0	18.67
	7	2	−3.27	0	15.68
	8	9	−3.24	0	24.37
	9	6	−3.17	0	14.14
	10	8	−2.93	0	14.65
	1	2	−4.51	0	17.02
	1	3	−4.17	1.5	16.79
	2	1	−4.23	0	13.72
	3	5	−4.11	0	14.19
6GP7	3	7	−4.1	0.74	14.46
	3	4	−4.08	1.05	14.35
	3	9	−4.06	1.35	14.14
	3	10	−4.04	1	14.17
	3	6	−3.98	1.35	13.89
	4	8	−4.02	0	12.78
	1	7	−5.07	0	26.24
	2	2	−4.29	0	33.21
	3	9	−4.23	0	31.94
	4	6	−4.16	0	27.04
8SBW	5	1	−3.88	0	32.14
	6	10	−3.84	0	42.37
	6	4	−3.53	1.42	42.19
	7	8	−3.84	0	31.84
	7	5	−3.75	1.38	31.96
	8	3	−3.15	0	12.68

35 °C for 24 h. For the mold fungi, a period of 5 days was allotted for incubation on a slant of potato dextrose agar (Yiğit et al., 2022). The *Candida albicans* and *Aspergillus niger* species were transferred into a tube containing sterile normal saline using a sterile loop. The microorganisms were prepared in four different concentrations such as 25 mg/mL, 50 mg/mL, 75 mg/mL and 100 mg/mL, respectively. The suspension was subsequently diluted at a ratio of 1:10 to get the final working inoculums with the above-mentioned concentration (Abdou, 2022). The inocula were put onto MHA that was treated. The positive control in this study involved the utilization of the widely accepted antifungal medicine Nystatin, while the negative control consisted of sterile distilled water (Dhonnar et al., 2022). Both the positive and negative controls were subjected to incubation at a temperature of 35 °C for 48 h. The diameter of the zone of inhibition was measured in millimeters. In our compound moderate activity against *Candida albicans* and *Aspergillus niger* microorganisms. But compared to *Candida albicans* the *Aspergillus niger* is the highest antifungal activity. Both strains have 100 mg/mL concentration only the highest antifungal activity, with measured inhibition activity being 28 mg/mL and 26 mg/mL for *Aspergillus niger* and *Candida albicans*, respectively. Table 5 and Figure 9 present the antifungal activity and Inhibition zone of the titled compound.

Molecular docking

The software tool AutoDock is widely employed in the field of computational chemistry and drug development to perform molecular docking simulations. The primary objective of this computational tool is to predict the binding orientations and affinities of small molecules, commonly referred to as ligands, to protein or nucleic acid targets, which are commonly known as receptors (Kumar et al., 2023). The AutoDock software employs several algorithms and scoring systems to systematically explore the conformational space of ligands within the binding site of a receptor. This study aims to forecast the most energetically beneficial binding positions precisely (Youssef et al., 2020).

The ANVA molecule analyzes physicochemical and drug-like properties, yielding substantial insights (Izuchukwu et al., 2022). The Lipinski rule five was employed as a physicochemical approach. Compound physicochemical and biological active site analysis is a valuable tool for scientific investigation (Elangovan et al., 2022). According to Lipinski's fifth rule, a compound is considered to have favorable drug-like properties if it meets the following criteria: (i) its molecular mass is below 500, (ii) its logarithm of the partition coefficient ($\log_p$) is <5, (iii) it has fewer than 5 hydrogen bond donors, (iv) it has fewer than 10 hydrogen bond acceptors and (v) its molar refractivity falls between the range of 40 and 130. Table 4 presents the physicochemical activity of the substance mentioned in the title molecule (Hamed et al., 2023). This activity was determined using the Swiss ADME online tool. Under the antimicrobial investigation, we have selected six different proteins for analysis, namely 3DRA (*Candida albicans*), 1KS5 (*Aspergillus niger*), 3I41 (*Staphylococcus aureus*), 6LL6 (*Escherichia coli*), 6GP7 (*Bacillus subtilis*) and 8SBW (*Klebsiella aerogenes*), respectively. The crystal structures of the proteins were obtained by downloading them from the RCSB PDB database. To prepare for docking, it is necessary to align the protein structure, remove water molecules, introduce polar hydrogen atoms and apply Kollman charges. These steps can be performed using the Discovery Studio Visualizer software. Table 6 displays the binding affinity of the entire protein. Table 5 presents the amino acid

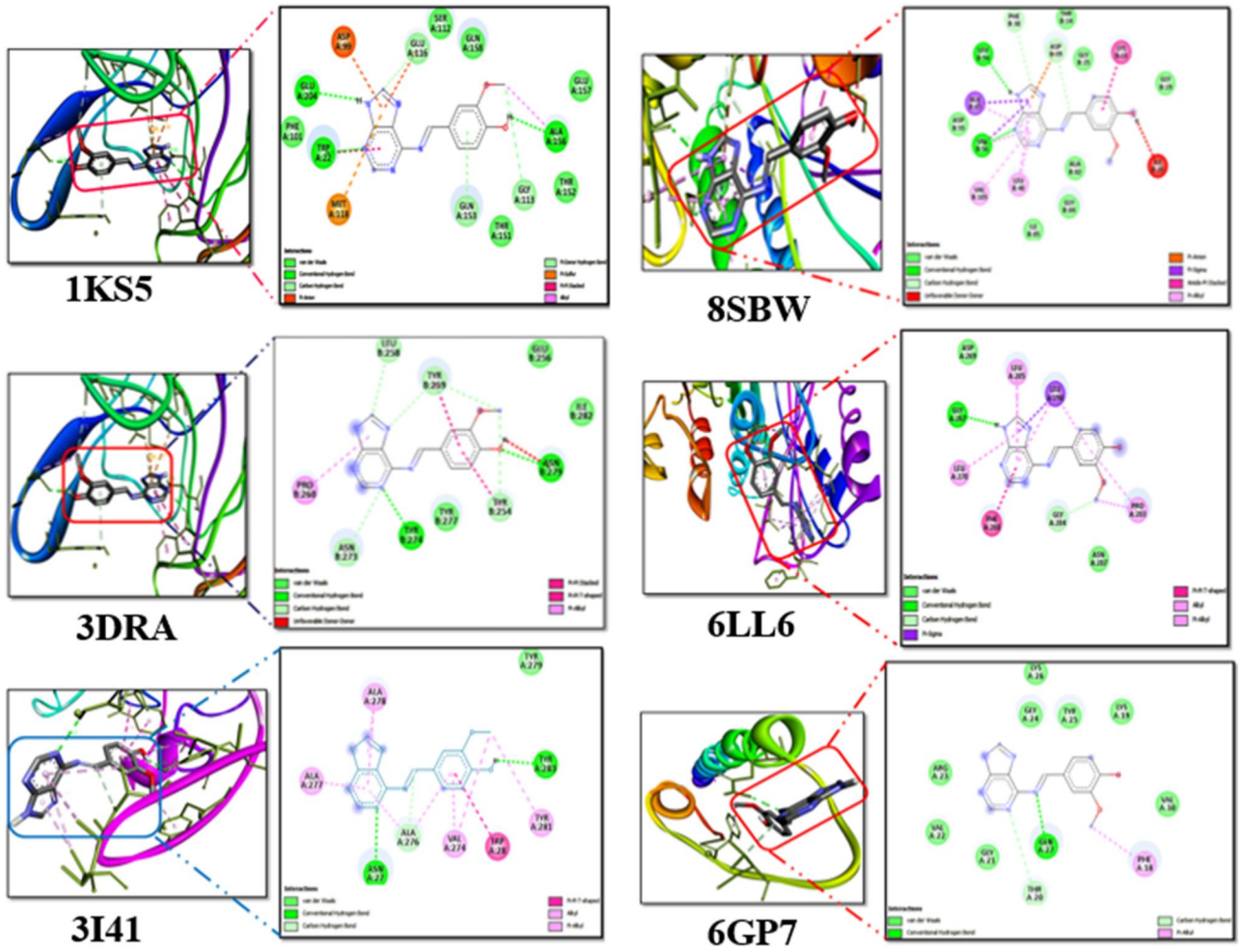

Figure 10. Protein–ligand interaction of ANVA with 1KS5, 6GP7, 6LL6, 3DRA, 3I41and 8SBW proteins.

interactions of the entire protein with the ANVA compound. The protein 1KS5 exhibits interactions with ANVA, through three non-covalent hydrogen bonds are shown in Figure 10. These interactions involve Trp22, Glu204 and Ala156, with bond distances measuring 2.8, 2.35 and 2.14 Å, respectively. Then there are two hydrogen bonds seen in the 3DRA, 3I41 and 8SBW proteins, which are shown in Figure 10, respectively. These connections involve the amino acid residues Tyr274, Asn279, Asn27, Tyr283, Val56 and Leu54. The bond distances for these interactions are measured to be 2.14, 2.3, 2.6, 2.23, 2.5 and 2.21 Å, respectively. Subsequently, two other proteins, namely 6LL6 and 6GP7, were found to bind with specific amino acids, Gly267 and Gln27, are shown in Figure 10, respectively. The bond distances for these interactions were measured to be 2.2 and 2.3 Å, respectively.

Conclusion

The experimental data exhibit a high degree of concordance with the computational methods using the DFT/B3LYP/cc-pVDZ method. In the examination of FMO, a minimal energy gap value was observed, indicating that the named molecule has great stability. The UV-visible values obtained using TD-DFT calculations for the appropriate chemical exhibit a high degree of agreement with the observed UV-visible spectrum values. The investigation conducted by the MEP demonstrates the occurrence of electrophilic and nucleophilic attacks on the synthesized molecule. The compound (ANVA) has a favorable dipole moment and polarizability characteristics. The results of a pharmacological assessment evaluating drug-likeness and toxicity indicate that the tested chemical exhibits potential for medicinal application. In the antimicrobial study, our synthesized compound showed moderate antibacterial and antifungal activity. The highest binding affinity score was identified by a molecular docking study. The protein 3DRA has the highest binding affinity score, which is −5.17 kcal/mol.

Acknowledgment

The authors extend their appreciation to the Deputyship for Research and Innovation, "Ministry of Education," in Saudi Arabia for funding this research (IFKSOR3-575-1).

Disclosure statement

No potential conflict of interest was reported by the authors.

Funding

The author(s) reported there is no funding associated with the work featured in this article.

References

Abdou, A. (2022). Synthesis, structural, molecular docking, DFT, vibrational spectroscopy, HOMO-LUMO, MEP exploration, antibacterial and antifungal activity of new Fe(III), Co(II) and Ni(II) hetero-ligand complexes. *Journal of Molecular Structure*, *1262*, 132911. https://doi.org/10.1016/j.molstruc.2022.132911

Abu Ali, O. A., Elangovan, N., Mahmoud, S. F., El-Bahy, S. M., El-Bahy, Z. M., & Thomas, R. (2022). Synthesis, structural features, excited state properties, fluorescence spectra, and quantum chemical modeling of (E)-2-hydroxy-5-(((4-sulfamoylphenyl)imino) methyl)benzoic acid. *Journal of Molecular Liquids*, *360*, 119557. https://doi.org/10.1016/j.molliq.2022.119557

Ajayi, T. J., & Shapi, M. (2020). Solvent-free mechanochemical synthesis, Hirshfeld surface analysis, crystal structure, spectroscopic characterization and NBO analysis of Bis(ammonium) Bis((4-methoxyphenyl) phosphonodithioato)-nickel (II) dihydrate with DFT studies. *Journal of Molecular Structure*, *1202*, 127254. https://doi.org/10.1016/j.molstruc.2019.127254

Alam, M. J., Khan, A. U., Alam, M., & Ahmad, S. (2019). Spectroscopic (FTIR, FT-Raman, ^{1}H NMR and UV–Vis) and DFT/TD-DFT studies on cholesteno [4,6-b,c]-2′,5′-dihydro-1′,5′-benzothiazepine. *Journal of Molecular Structure*, *1178*, 570–582. https://doi.org/10.1016/j.molstruc.2018.10.063

Ali, O. A. A., Elangovan, N., Mahmoud, S. F., El-Gendey, M. S., Elbasheer, H. Z. E., El-Bahy, S. M., & Thomas, R. (2022). Synthesis, characterization, vibrational analysis and computational studies of a new Schiff base from pentafluoro benzaldehyde and sulfanilamide. *Journal of Molecular Structure*, *1265*, 133445. https://doi.org/10.1016/j.molstruc.2022.133445

Arivazhagan, M., & Kavitha, R. (2012). Molecular structure, vibrational spectroscopic, NBO, HOMO–LUMO and Mulliken analysis of 4-methyl-3-nitro benzyl chloride. *Journal of Molecular Structure*, *1011*, 111–120. https://doi.org/10.1016/j.molstruc.2011.12.006

Arjunan, V., Ravindran, P., Rani, T., & Mohan, S. (2011). FTIR, FT-Raman, FT-NMR, *ab initio* and DFT electronic structure investigation on 8-chloroquinoline and 8-nitroquinoline. *Journal of Molecular Structure*, *988*(1–3), 91–101. https://doi.org/10.1016/j.molstruc.2010.12.032

Arulaabaranam, K., Muthu, S., Mani, G., & Ben Geoffrey, A. S. (2021). Speculative assessment, molecular composition, PDOS, topology exploration (ELF, LOL, RDG), ligand-protein interactions, on 5-bromo-3-nitropyridine-2-carbonitrile. *Heliyon*, *7*(5), e07061. https://doi.org/10.1016/j.heliyon.2021.e07061

Demircioğlu, Z., Albayrak Kaştaş, Ç., & Büyükgüngör, O. (2015). The spectroscopic (FT-IR, UV–vis), Fukui function, NLO, NBO, NPA and tautomerism effect analysis of (E)-2-[(2-hydroxy-6-methoxybenzylidene) amino]benzonitrile. *Spectrochimica Acta Part A: Molecular and Biomolecular Spectroscopy*, *139*, 539–548. https://doi.org/10.1016/j.saa.2014.11.078

Demircioğlu, Z., Kaştaş, Ç. A., & Büyükgüngör, O. (2015). Theoretical analysis (NBO, NPA, Mulliken population method) and molecular orbital studies (hardness, chemical potential, electrophilicity and Fukui function analysis) of (E)-2-((4-hydroxy-2-methylphenylimino)methyl)-3-methoxyphenol. *Journal of Molecular Structure*, *1091*, 183–195. https://doi.org/10.1016/j.molstruc.2015.02.076

Dhonnar, S. L., More, R. A., Adole, V. A., Jagdale, B. S., Sadgir, N. V., & Chobe, S. S. (2022). Synthesis, spectral analysis, antibacterial, antifungal, antioxidant and hemolytic activity studies of some new 2,5-disubstituted-1,3,4-oxadiazoles. *Journal of Molecular Structure*, *1253*, 132216. https://doi.org/10.1016/j.molstruc.2021.132216

Dikmen, G., & Kani, İ. (2020). Synthesis, spectroscopic characterization (FT-IR, Raman, UV-VIS, XRD), DFT studies and DNA binding properties of $[Ni(C_6H_5CH_2COO)(C_{12}H_8N_2)_2](ClO_4)(CH_3OH)$ compound. *Journal of Molecular Structure*, *1209*, 127955. https://doi.org/10.1016/j.molstruc.2020.127955

Domínguez-Flores, F., & Melander, M. M. (2022). Electrocatalytic rate constants from DFT simulations and theoretical models: Learning from each other. *Current Opinion in Electrochemistry*, *36*, 101110. https://doi.org/10.1016/j.coelec.2022.101110

Elangovan, N., & Sowrirajan, S. (2021). Synthesis, single crystal (XRD), Hirshfeld surface analysis, computational study (DFT) and molecular docking studies of (E)-4-((2-hydroxy-3,5-diiodobenzylidene)amino)-N-(pyrimidine)-2-yl) benzenesulfonamide. *Heliyon*, *7*(8), e07724. https://doi.org/10.1016/j.heliyon.2021.e07724

Elangovan, N., Alomar, S. Y., Sowrirajan, S., Rajeswari, B., Nawaz, A., & Kalanthoden, A. N. (2023). Photoluminescence property and solvation studies on sulfonamide: Synthesis, structural, topological analysis, antimicrobial activity and molecular docking studies. *Inorganic Chemistry Communications*, *155*, 111019. https://doi.org/10.1016/j.inoche.2023.111019

Elangovan, N., Gangadharappa, B., Thomas, R., & Irfan, A. (2022). Synthesis of a versatile Schiff base 4-((2-hydroxy-3,5-diiodobenzylidene) amino) benzenesulfonamide from 3,5-diiodosalicylaldehyde and sulfanilamide, structure, electronic properties, biological activity prediction and experimental antimicrobial properties. *Journal of Molecular Structure*, *1250*, 131700. https://doi.org/10.1016/j.molstruc.2021.131700

Elangovan, N., Sangeetha, R., Sowrirajan, S., Sarala, S., & Muthu, S. (2022). Computational investigation on structural and reactive sites (HOMO-LUMO, MEP, NBO, NPA, ELF, LOL, RDG) identification, pharmacokinetic (ADME) properties and molecular docking investigation of (E)-4-((4-chlorobenzylidene)amino) benzene sulfonamide compound. *Analytical Chemistry Letters*, *12*(1), 58–76. https://doi.org/10.1080/22297928.2021.1933588

Elangovan, N., Sowrirajan, S., Alzahrani, A. Y. A., Rajendran Nair, D. S., & Thomas, R. (2023). Fluorescent azomethine by the condensation of sulfadiazine and 4-chlorobenzaldehyde in solution: Synthesis, characterization, solvent interactions, electronic structure, and biological activity prediction. *Polycyclic Aromatic Compounds*, 1–22. https://doi.org/10.1080/10406638.2023.2216833

Elangovan, N., Sowrirajan, S., Manoj, K. P., & Kumar, A. M. (2021). Synthesis, structural investigation, computational study, antimicrobial activity and molecular docking studies of novel synthesized (E)-4-((pyridine-4-ylmethylene)amino)-N-(pyrimidin-2-yl)benzenesulfonamide from pyridine-4-carboxaldehyde and sulfadiazine. *Journal of Molecular Structure*, *1241*, 130544. https://doi.org/10.1016/j.molstruc.2021.130544

Elangovan, N., Thomas, R., & Sowrirajan, S. (2022). Synthesis of Schiff base (E)-4-((2-hydroxy-3,5-diiodobenzylidene)amino)-N-thiazole-2-yl) benzenesulfonamide with antimicrobial potential, structural features, experimental biological screening and quantum mechanical studies. *Journal of Molecular Structure*, *1250*, 131762. https://doi.org/10.1016/j.molstruc.2021.131762

Elangovan, N., Thomas, R., Sowrirajan, S., & Irfan, A. (2021). Synthesis, spectral and quantum mechanical studies and molecular docking studies of Schiff base (E)2-hydroxy-5-(((4-(N-pyrimidin-2-yl)sulfamoyl)-phenyl)imino)methyl benzoic acid from 5-formyl salicylic acid and sulfadiazine. *Journal of the Indian Chemical Society*, *98*(10), 100144. https://doi.org/10.1016/j.jics.2021.100144

Elangovan, N., Thomas, R., Sowrirajan, S., Manoj, K. P., & Irfan, A. (2021). Synthesis, spectral characterization, electronic structure and biological activity screening of the Schiff base 4-((4-hydroxy-3-methoxy-5-nitrobenzylidene)amino)-n-(pyrimidin-2-yl)benzene sulfonamide from 5-nitrovaniline and sulphadiazine. *Polycyclic Aromatic Compounds*, *42*(10), 6818–6835. https://doi.org/10.1080/10406638.2021.1991392

Elkaeed, E. B., Mughal, E. U., Kausar, S., Al-Ghulikah, H. A., Naeem, N., Altaf, A. A., & Sadiq, A. (2022). Theoretical vibrational spectroscopy (FT-IR), PED and DFT calculations of chromones and thiochromones. *Journal of Molecular Structure*, *1270*, 133972. https://doi.org/10.1016/j.molstruc.2022.133972

Essghaier, B., Dridi, R., Arouri, A., & Zid, M. F. (2021). Synthesis, structural characterization and prospects for a new tris (5-methylbenzimidazole) tris (oxalato) ferrate(III) trihydrate complex as a promising

antibacterial and antifungal agent. *Polyhedron*, *208*, 115420. https://doi.org/10.1016/j.poly.2021.115420

Frisch, M. J., Trucks, G. W., Schlegel, H. B., Scuseria, G. E., Robb, M. A., Cheeseman, J. R., Scalmani, G., Barone, V., Mennucci, B., Petersson, G. A., Nakatsuji, H., Caricato, M., Li, X., Hratchian, H. P., Izmaylov, A. F., Bloino, J., Zheng, G., Sonnenberg, J. L., Hada, M., … Fox, D. J. (2009). *Gaussian 09, Revision B.01*. Gaussian, Inc. (pp. 1–20). citeulike-article-id:9096580.

Ghosh, B., Roy, N., Roy, D., Mandal, S., Ali, S., Bomzan, P., Roy, K., & Nath Roy, M. (2021). An extensive investigation on supramolecular assembly of a drug (MEP) with βCD for innovative applications. *Journal of Molecular Liquids*, *344*, 117977. https://doi.org/10.1016/j.molliq.2021.117977

Gonçalves, R. F. B., Kuznetsov, A., Rocco, B. T., Rocco, L., & Rocco, J. A. F. F. (2022). Reactive molecular dynamics and DFT simulations of FTDO explosive. *Computational and Theoretical Chemistry*, *1212*, 113723. https://doi.org/10.1016/j.comptc.2022.113723

Goodsell, D. S., Sanner, M. F., Olson, A. J., & Forli, S. (2021). The AutoDock suite at 30. *Protein Science: A Publication of the Protein Society*, *30*(1), 31–43. https://doi.org/10.1002/pro.3934

Gulbagca, F., Ozdemir, S., Gulcan, M., & Sen, F. (2019). Synthesis and characterization of Rosa canina-mediated biogenic silver nanoparticles for anti-oxidant, antibacterial, antifungal, and DNA cleavage activities. *Heliyon*, *5*(12), e02980. https://doi.org/10.1016/j.heliyon.2019.e02980

Hamed, M. M., Sayed, M., Abdel-Mohsen, S. A., Saddik, A. A., Ibrahim, O. A., El-Dean, A. M. K., & Tolba, S. (2023). Synthesis, biological evaluation, and molecular docking studies of novel diclofenac derivatives as antibacterial agents. *Journal of Molecular Structure*, *1273*, 134371. https://doi.org/10.1016/j.molstruc.2022.134371

Izuchukwu, U. D., Asogwa, F. C., Louis, H., Uchenna, E. F., Gber, T. E., Chinasa, U. M., Chinedum, N. J., Eze, B. O., Adeyinka, A. S., & Chris, O. U. (2022). Synthesis, vibrational analysis, molecular property investigation, and molecular docking of new benzenesulphonamide-based carboxamide derivatives against *Plasmodium falciparum*. *Journal of Molecular Structure*, *1269*, 133796. https://doi.org/10.1016/j.molstruc.2022.133796

Jayachitra, R., Padmavathy, M., Kanagavalli, A., Thilagavathi, G., Elangovan, N., Sowrirajan, S., & Thomas, R. (2023). Synthesis, computational, experimental antimicrobial activities and theoretical molecular docking studies of (E)-4-((4-hydroxy-3-methoxy-5-nitrobenzylidene) amino)-N-(thiazole-2-yl) benzenesulfonamide. *Journal of the Indian Chemical Society*, *100*(1), 100824. https://doi.org/10.1016/j.jics.2022.100824

Jayachitra, R., Thilagavathi, G., Kanagavalli, A., Elangovan, N., Sirajunnisa, A., Sowrirajan, S., & Thomas, R. (2023). Synthesis, computational, electronic spectra, and molecular docking studies of 4-((diphenylmethylene)amino)-N-(pyrimidin-2-yl)benzenesulfonamide. *Journal of the Indian Chemical Society*, *100*(1), 100836. https://doi.org/10.1016/j.jics.2022.100836

John, N. L., Abraham, S., George, J., Karuppasamy, P., Senthilpandian, M., Ramasamy, P., & Vinitha, G. (2022). Synthesis, structure, NBO, Hirshfeld surface, NMR, HOMO-LUMO, UV, photoluminescence, z scan, vibrational and thermal analysis of piperazinedi-ium tetrakis (μ2-chloro)-diaqua-dichloro-di-cadmium single crystal. *Journal of Molecular Structure*, *1258*, 132685. https://doi.org/10.1016/j.molstruc.2022.132685

Joshi, K. K. (2022). Chemistry with Schiff bases of pyridine derivatives: Their potential as bioactive ligands and chemosensors. In S. Pal (Ed.), *Exploring chemistry with pyridine derivatives*. IntechOpen, *7*, 7585–7594. https://doi.org/10.5772/intechopen.106749

Kanchana, S., Kaviya, T., Rajkumar, P., Kumar, M. D., Elangovan, N., & Sowrirajan, S. (2023). Computational investigation of solvent interaction (TD-DFT, MEP, HOMO-LUMO), wavefunction studies and molecular docking studies of 3-(1-(3-(5-((1-methylpiperidin-4-yl)methoxy)pyrimidin-2-yl)benzyl)-6-oxo-1,6-dihydropyridazin-3-yl)benzonitrile. *Chemical Physics Impact*, *7*, 100263. https://doi.org/10.1016/j.chphi.2023.100263

Kargar, H., Fallah-Mehrjardi, M., Behjatmanesh-Ardakani, R., & Munawar, K. S. (2021). Synthesis, spectra (FT-IR, NMR) investigations, DFT, FMO, MEP, NBO analysis and catalytic activity of MoO2(VI) complex with ONO tridentate hydrazone Schiff base ligand. *Journal of Molecular Structure*, *1245*, 131259. https://doi.org/10.1016/j.molstruc.2021.131259

Kasula, S., & Dandu, S. (2023). Green synthesis, DFT and molecular docking studies of 4-amino indane derived Schiff bases. *Materials Today: Proceedings*, *08*, 119. https://doi.org/10.1016/j.matpr.2023.08.119

Kateris, N., Jayaraman, A. S., & Wang, H. (2023). HOMO-LUMO gaps of large polycyclic aromatic hydrocarbons and their implication on the quantum confinement behavior of flame-formed carbon nanoparticles. *Proceedings of the Combustion Institute*, *39*, 1069–1077. https://doi.org/10.1016/j.proci.2022.07.168

Kazachenko, A. S., Issaoui, N., Sagaama, A., Malyar, Y. N., Al-Dossary, O., Bousiakou, L. G., Kazachenko, A. S., Miroshnokova, A. V., & Xiang, Z. (2022). Hydrogen bonds interactions in biuret-water clusters: FTIR, X-ray diffraction, AIM, DFT, RDG, ELF, NLO analysis. *Journal of King Saud University – Science*, *34*(8), 102350. https://doi.org/10.1016/j.jksus.2022.102350

Kumar, H., Dhameja, M., Kurella, S., Uma, A., & Gupta, P. (2023). Synthesis, in-vitro α-glucosidase inhibition and molecular docking studies of 1,3,4-thiadiazole-5,6-diphenyl-1,2,4-triazine hybrids: Potential leads in the search of new antidiabetic drugs. *Journal of Molecular Structure*, *1273*, 134339. https://doi.org/10.1016/j.molstruc.2022.134339

Latha, A., Elangovan, N., Manoj, K. P., Keerthi, M., Balasubramani, K., Sowrirajan, S., Chandrasekar, S., & Thomas, R. (2022). Synthesis, XRD, spectral, structural, quantum mechanical and anticancer studies of di(*p*-chlorobenzyl) (dibromo) (1,10-phenanthroline) tin (IV) complex. *Journal of the Indian Chemical Society*, *99*(7), 100540. https://doi.org/10.1016/j.jics.2022.100540

Lin, H., Zhu, S.-G., Li, H.-Z., & Peng, X.-H. (2013). Synthesis, characterization, AIM and NBO analysis of HMX/DMI cocrystal explosive. *Journal of Molecular Structure*, *1048*, 339–348. https://doi.org/10.1016/j.molstruc.2013.06.013

Lu, T., & Chen, F. (2012). Multiwfn: A multifunctional wavefunction analyzer. *Journal of Computational Chemistry*, *33*(5), 580–592. https://doi.org/10.1002/jcc.22885

Manhas, F. M., Fatima, A., Verma, I., Siddiqui, N., Muthu, S., AlSalem, H. S., Savita, S., Singh, M., & Javed, S. (2022). Quantum computational, spectroscopic (FT-IR, NMR and UV–Vis) profiling, Hirshfeld surface, molecular docking and dynamics simulation studies on pyridine-2,6-dicarbonyl dichloride. *Journal of Molecular Structure*, *1265*, 133374. https://doi.org/10.1016/j.molstruc.2022.133374

Manivel, S., S Gangadharappa, B., Elangovan, N., Thomas, R., Abu Ali, O. A., & Saleh, D. I. (2022). Schiff base (Z)-4-((furan-2-ylmethylene)amino) benzenesulfonamide: Synthesis, solvent interactions through hydrogen bond, structural and spectral properties, quantum chemical modeling and biological studies. *Journal of Molecular Liquids*, *350*, 118531. https://doi.org/10.1016/j.molliq.2022.118531

Manjunatha, B., Bodke, Y. D., Sandeep Kumar Jain, R., Lohith, T. N., & Sridhar, M. A. (2021). Novel isoxazolone based azo dyes: Synthesis, characterization, computational, solvatochromic UV-Vis absorption and biological studies. *Journal of Molecular Structure*, *1244*, 130933. https://doi.org/10.1016/j.molstruc.2021.130933

Manoj, K. P., Elangovan, N., & Chandrasekar, S. (2022). Synthesis, XRD, Hirshfeld surface analysis, ESP, HOMO-LUMO, quantum chemical modeling and anticancer activity of di(*p*-methyl benzyl)(dibromo)(1,10-phenanthroline) tin(IV) complex. *Inorganic Chemistry Communications*, *139*, 109324. https://doi.org/10.1016/j.inoche.2022.109324

Muthukumar, R., Karnan, M., Elangovan, N., Karunanidhi, M., Sankarapandian, V., & Venkateswaran, K. (2022). Synthesis, experimental antimicrobial activity, theoretical vibrational analysis, quantum chemical modeling and molecular docking studies of (E)-4-(benzylideneamino)benzenesulfonamide. *Journal of Molecular Structure*, *1263*, 133187. https://doi.org/10.1016/j.molstruc.2022.133187

Nakakuki, Y., Hirose, T., & Matsuda, K. (2022). Logical design of small HOMO–LUMO gap: Tetrabenzo[*f,jk,mn,r*][7]helicene as a small-molecule near-infrared emitter. *Organic Letters*, *24*(2), 648–652. https://doi.org/10.1021/acs.orglett.1c04095

Pillai, A. M., Sivasankarapillai, V. S., Rahdar, A., Joseph, J., Sadeghfar, F., Anuf A, R., Rajesh, K., & Kyzas, G. Z. (2020). Green synthesis and characterization of zinc oxide nanoparticles with antibacterial and

antifungal activity. *Journal of Molecular Structure*, *1211*, 128107. https://doi.org/10.1016/j.molstruc.2020.128107

PrabhuKumar, K. M., Satheesh, C. E., RaghavendraKumar, P., Kumar, M. N. S., Lingaraju, K., Suchetan, P. A., & Rajanaika, H. (2022). Synthesis, characterization, antibacterial, antifungal and antithrombotic activity studies of new chiral selenated Schiff bases and their Pd complexes. *Journal of Molecular Structure*, *1264*, 133172. https://doi.org/10.1016/j.molstruc.2022.133172

Pramila, M. J., Dhas, D. A., Joe, I. H., Balachandran, S., & Vinitha, G. (2023). Structural insights, spectral, fluorescence, Z-scan, C-H … O/N-H … O hydrogen bonding and AIM, RDG, ELF, LOL, FUKUI analysis, NLO activity of N-2(methoxy phenyl) acetamide. *Journal of Molecular Structure*, *1272*, 134140. https://doi.org/10.1016/j.molstruc.2022.134140

Rajimon, K. J., Elangovan, N., Amir, A., & Thomas, R. (2023). Schiff bases from chlorine substituted anilines and salicylaldehyde: Synthesis, characterization, fluorescence, thermal features, biological studies and electronic structure investigations. *Journal of Molecular Liquids*, *370*, 121055. https://doi.org/10.1016/j.molliq.2022.121055

Ramesh, G., & Reddy, B. V. (2023). Investigation of barrier potential, structure (monomer & dimer), chemical reactivity, NLO, MEP, and NPA analysis of pyrrole-2-carboxaldehyde using quantum chemical calculations. *Polycyclic Aromatic Compounds*, *43*(5), 4216–4230. https://doi.org/10.1080/10406638.2022.2086889

Sanakarganesan, T., Elangovan, N., Chandrasekar, S., Ganesan, E., Balachandran, V., Sowrirajan, S., Balasubramani, K., & Thomas, R. (2023). Synthesis, Hirshfeld surface analysis, computational, wave function properties, anticancer and cytotoxicity activity of di[(p-chlorobenzyl) (dibromo)] (4,7-dimethyl-1,10-phenanthroline)tin (IV) complex. *Inorganica Chimica Acta Synthesis*, *547*, 121361. https://doi.org/10.1016/j.ica.2022.121361

SangeethaMargreat, S., Ramalingam, S., Al-Maqtari, H. M., Jamalis, J., Sebastian, S., Periandy, S., & Xavier, S. (2021). Synthesis, spectroscopic, quantum computation, electronic, AIM, wavefunction (ELF, LOL) and molecular docking investigation on (*E*)-1-(2,5-dichlorothiophen-3-yl)-3-(thiophen-2-yl)-2-propen-1-one. *Chemical Data Collections*, *33*, 100701. https://doi.org/10.1016/j.cdc.2021.100701

Sarojini, K., Krishnan, H., Kanakam, C. C., & Muthu, S. (2012). Synthesis, X-ray structural, characterization, NBO and HOMO–LUMO analysis using DFT study of 4-methyl-N-(naphthalene-1-yl)benzene sulfonamide. *Spectrochimica Acta Part A: Molecular and Biomolecular Spectroscopy*, *96*, 657–667. https://doi.org/10.1016/j.saa.2012.07.037

Shntaif, A. H., Khan, S., Tapadiya, G., Chettupalli, A., Saboo, S., Shaikh, M. S., Siddiqui, F., & Amara, R. R. (2021). Rational drug design, synthesis, and biological evaluation of novel N-(2-arylaminophenyl)-2,3-diphenylquinoxaline-6-sulfonamides as potential antimalarial, antifungal, and antibacterial agents. *Digital Chinese Medicine*, *4*(4), 290–304. https://doi.org/10.1016/j.dcmed.2021.12.004

Silvarajoo, S., Osman, U. M., Kamarudin, K. H., Razali, M. H., Yusoff, H. M., Bhat, I. U. H., Rozaini, M. Z. H., & Juahir, Y. (2020). Dataset of theoretical molecular electrostatic potential (MEP), highest occupied molecular orbital-lowest unoccupied molecular orbital (HOMO-LUMO) band gap and experimental cole-cole plot of 4-(*ortho*-, *meta*- and *para*-fluorophenyl)thiosemicarbazide isomers. *Data in Brief*, *32*, 106299. https://doi.org/10.1016/j.dib.2020.106299

Singhal, S., Khanna, P., & Khanna, L. (2019). Synthesis, DFT studies, molecular docking, antimicrobial screening and UV fluorescence studies on ct-DNA for novel Schiff bases of 2-(1-aminobenzyl) benzimidazole. *Heliyon*, *5*(10), e02596. https://doi.org/10.1016/j.heliyon.2019.e02596

Soltani, S., Magri, P., Rogalski, M., & Kadri, M. (2019). Charge-transfer complexes of hypoglycemic sulfonamide with π-acceptors: Experimental and DFT-TDDFT studies. *Journal of Molecular Structure*, *1175*, 105–116. https://doi.org/10.1016/j.molstruc.2018.07.074

Sowrirajan, S., Elangovan, N., Ajithkumar, G., & Manoj, K. P. (2022). (E)-4-((4-bromobenzylidene) amino)-N-(pyrimidin-2-yl) benzenesulfonamide from 4-bromobenzaldehyde and sulfadiazine, synthesis, spectral (FTIR, UV–Vis), computational (DFT, HOMO–LUMO, MEP, NBO, NPA, ELF, LOL, RDG) and molecular docking studies. *Polycyclic Aromatic Compounds*, *42*(10), 7616–7631. https://doi.org/10.1080/10406638.2021.2006245

Sowrirajan, S., Elangovan, N., Ajithkumar, G., Sirajunnisa, A., Venkatraman, B. R., Ibrahim, M. M., Mersal, G. A. M., & Thomas, R. (2022). Synthesis, spectral, structural features, electronic properties, biological activities, computational, wave function properties, and molecular docking studies of (E)-4-(((pentafluorophenyl) methylene) amino)-N-(pyrimidin2-yl)benzenesulfonamide. *Journal of Molecular Structure*, *1265*, 133472. https://doi.org/10.1016/j.molstruc.2022.133472

Téllez Soto, C. A., Costa, A. C., Ramos, J. M., Versiane, O., Ondar, G. F., Ferreira, G. B., Fávero, P. P., Rangel, J. L., Raniero, L., Bueno Costa, G., Bussi, G. G. A., & Martin, A. A. (2013). Surface enhanced Raman scattering, electronic spectrum and Mulliken charge distribution in the normal modes of bis(diethyldithiocarbamate)zinc(II) complex. *Spectrochimica Acta Part A: Molecular and Biomolecular Spectroscopy*, *110*, 443–449. https://doi.org/10.1016/j.saa.2013.03.039

Thilagavathi, G., Jayachitra, R., Kanagavalli, A., Elangovan, N., Sirajunnisa, A., Sowrirajan, S., & Thomas, R. (2023). Synthesis, computational, molecular docking studies and photophysical properties of (Z)-N-(pyrimidin-2-yl)-4-(thiophen-2-ylmethylene)amino) benzenesulfonamide. *Journal of the Indian Chemical Society*, *100*(1), 100835. https://doi.org/10.1016/j.jics.2022.100835

Thilagavathi, G., Kanagavalli, A., Jayachitra, R., Padmavathy, M., Elangovan, N., & Thomas, R. (2022). Synthesis, structural, computational, electronic spectra, wave function properties and molecular docking studies of (Z)-4-(((5-methylfuran-2-yl)methylene)amino)-N-(thiazol-2-yl)benzenesulfonamide. *Journal of the Indian Chemical Society*, *99*(12), 100786. https://doi.org/10.1016/j.jics.2022.100786

Tomita, K., Tsutake, C., Takahashi, K., & Fujii, T. (2022). Denoising multi-view images by soft thresholding: A short-time DFT approach. *Signal Processing: Image Communication*, *105*, 116710. https://doi.org/10.1016/j.image.2022.116710

Yiğit, M., Şireci, N., Günal, S., Önderci, M., Özdemir, N., Arınç, A., Yiğit, B., & Özdemir, İ. (2022). Synthesis, spectroscopic characterization and antimicrobial properties of silyl-tethered benzimidazolium salts. *Journal of Molecular Structure*, *1264*, 133308. https://doi.org/10.1016/j.molstruc.2022.133308

Youssef, E., El-Moneim, M. A., Fathalla, W., & Nafie, M. S. (2020). Design, synthesis and antiproliferative activity of new amine, amino acid and dipeptide-coupled benzamides as potential sigma-1 receptor. *Journal of the Iranian Chemical Society*, *17*(10), 2515–2532. https://doi.org/10.1007/s13738-020-01947-6

Chemistry Europe
European Chemical Societies Publishing

WILEY VCH

Excellence in Chemistry Research

Announcing our new flagship journal

- Gold Open Access
- Publishing charges waived
- Preprints welcome
- Edited by active scientists

Meet the Editors of *ChemistryEurope*

Luisa De Cola
Università degli Studi di Milano Statale, Italy

Ive Hermans
University of Wisconsin-Madison, USA

Ken Tanaka
Tokyo Institute of Technology, Japan

ChemistrySelect

Research Article
doi.org/10.1002/slct.202301277

Chemistry Europe
European Chemical Societies Publishing

www.chemistryselect.org

Cytotoxicity of copper(I) complexes containing indole-based thiosemicarbazones and triphenylphosphine

Periyanayagam Arockia Doss,[a, b] Jebiti Haribabu,[c] Nithya Balakrishnan,[a] Srividya Swaminathan,[d] Jose A. Pino,[e] Nattamai Bhuvanesh,[f] and Ramasamy Karvembu*[a]

The research and development department continues searching for effective and definite anticancer medications that would help eradicate cancer. The thiosemicarbazone ligands with indole fragment were utilized to create four new copper(I) complexes. Several spectral examinations and elemental analyses validated the formation of the complexes (**1**–**4**). Single crystal X-ray diffraction (XRD) also proved that complex **4** had the expected tetrahedral structure. Complexes **1**–**4** were assessed for their cytotoxic property on different cell lines such as immortalized human vascular endothelial (EAhy.926), hepatocellular carcinoma (HepG-2), and bladder cancer (T24), and kidney epithelial normal cells extracted from an African green monkey (Vero). The complexes showed reduced toxicity towards healthy Vero cells while being active in cancer cell lines. While the standard cisplatin revealed IC_{50} values of 26.60 and 49.90 μM, the N-phenyl substituted complex **3** displayed a superior cytotoxic effect with IC_{50} values of 13.82 and 24.93 μM towards EAhy.926 and HepG-2 cells, respectively.

Introduction

It is important to develop effective anticancer drugs with minimal toxicity and maximal selectivity to treat tumours.[1–3] Thiosemicarbazones (TSCs) [$R_1R_2C{=}NNHC(=S)NR_3R_4$] are widely utilized in this regard owing to their wide variety of biological actions, including antibacterial, anticancer, antimalarial, antiviral, and antifungal effects.[4–12] Metal complexes resulting from the coordination of TSCs which are N, S-donor ligands, have increased biological activity compared to the respective ligand.[13] The anticancer activity of TSCs has been established in the literature for exhibiting various modes of action against cancer cell lines.[14–22] The binding of TSC ligands to several essential proteins, including ribonucleotide reductase (RR) and vascular endothelial growth factor receptor 2 (VEGFR2) that are involved in invasive cancers, was linked to their anticancer properties.[23–28] Numerous TSC chelators targeting DNA production[28–34] and cell cycle markers[24,35,36] have also demonstrated promising anticancer efficacy. The TSC derivatives such as amithiozone, marboran and cutisone were proven to possess antituberculosis, antiviral and antifungal activities, indicating their biological significance.[37] Multiple TSC ligands have been discovered and studied in clinical trials in light of their crucial role in drug discovery[38] (Figure 1).

Copper, a vital trace element, is essential for many cellular functions. It is commonly recognized that copper metabolism is drastically disrupted in neoplastic disorders. The difference between cancerous and normal cells in their response to copper has contributed to the development of anticancer copper complexes. Several copper complexes containing distinct kinds of ligands were created for this purpose and have shown notable *in vitro* cytotoxicity.[39–43]

Bicyclic heterocycles such as indoles are often found in microbes, plants and animals. Indole-based chemicals, both natural and synthetic, have a long history of usage for anticancer, antihistaminic, anti-inflammatory, antifungal and antibacterial medications.[44,45] The non-steroidal anti-inflammatory medication indomethacin and antiviral delavirdine are two examples of such substances that are now used in clinical settings.[46,47] Various indole-based substances were developed to inhibit sirtuins (involved in gene expression), histone deacetylase, tubulin formation (essential for cellular division), DNA topoisomerase (responsible for DNA transcription), or to directly affect DNA by forming inter- and intra-strand cross-links.[48–51] Some prominent examples are vincristine, a well-known antimitotic drug used to treat various tumors, and vinblastine which is involved in treating lymphocytic leukemia, and lung and breast carcinoma.[52–54]

There have been previous reports on indole-based TSCs conjugated with various metal ions as anticancer agents targeting numerous cancer cell lines, effectively inhibiting the proliferation and migration of cancer cells[55–59] but the ones with copper(I) are pretty scarce.[60–65] The copper(I) complexes with indole-based TSCs attracted our attention due to their

[a] *P. Arockia Doss, Dr. N. Balakrishnan, Prof. R. Karvembu*
Department of Chemistry, National Institute of Technology, Tiruchirappalli 620015, India
E-mail: kar@nitt.edu

[b] *P. Arockia Doss*
Department of Chemistry, St. Joseph's College (Autonomous), Tiruchirappalli 620002, India

[c] *Dr. J. Haribabu*
Faculty of Medicine, University of Atacama, Copayapu 485, Copiapó, Chile

[d] *Dr. S. Swaminathan*
Chennai Institute of Technology (CIT), Chennai 600069, India

[e] *Dr. J. A. Pino*
Department of Medicine, School of Medicine, University of Atacama, Copiapó, Chile

[f] *Dr. N. Bhuvanesh*
Department of Chemistry, Texas A & M University, College Station, Texas 77842, United States

Supporting information for this article is available on the WWW under https://doi.org/10.1002/slct.202301277

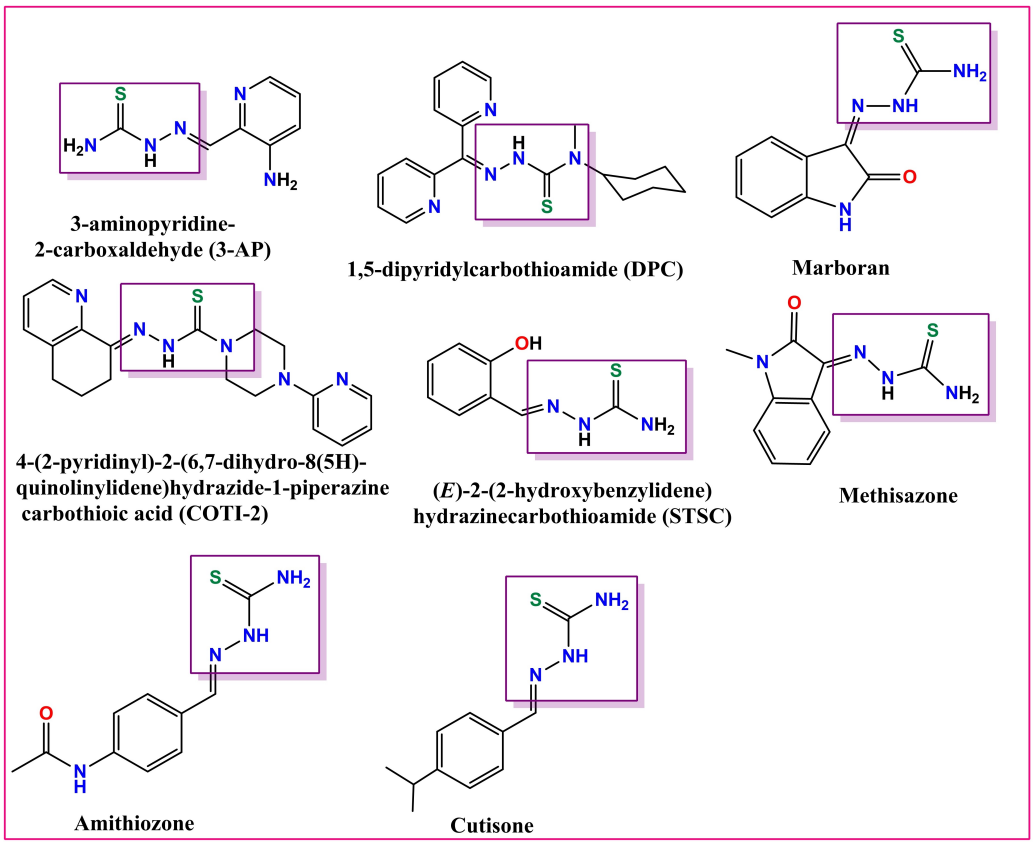

Figure 1. Compounds with TSC assembly in drug discovery.

possible anticancer action owing to their biologically active constituents. Herein, we used TSC derivatives that included indole fragment to develop copper(I) complexes for anticancer applications.

Results and discussion

Synthesis

Typical condensation of the appropriate thiosemicarbazide and 3-indole carboxaldehyde in the presence of glacial acetic acid yielded the indole-based TSC ligands (L1–L4) (Scheme 1). The copper(I) complexes (**1**–**4**) were obtained by heating the resultant ligands with $[(PPh_3)_2Cu(Cl)_2Cu(PPh_3)]$ (Scheme 2). The complexes were subjected to elemental analyses and spectroscopic examinations to analyze their structure. The geometry of

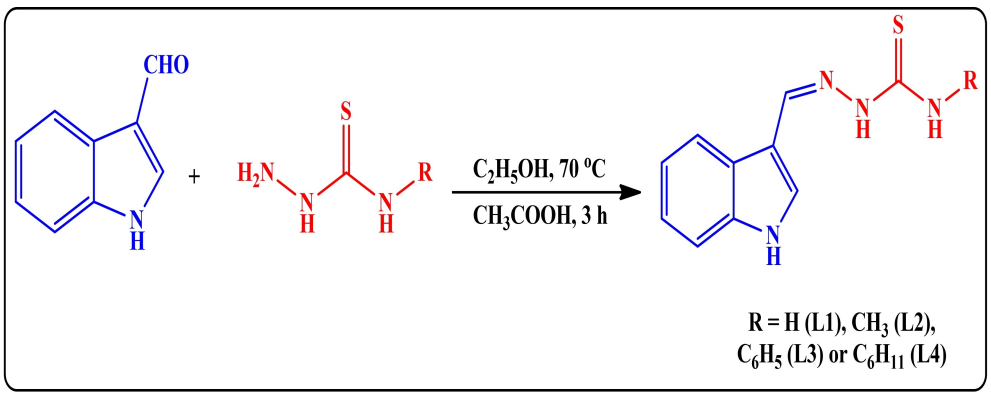

Scheme 1. Preparation of the ligands (L1–L4).

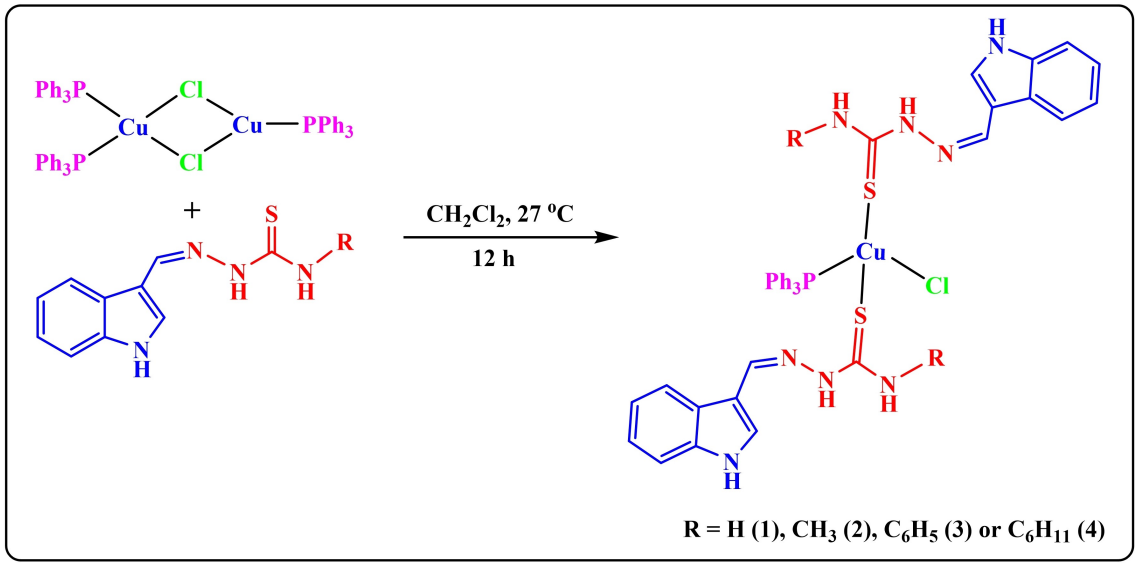

Scheme 2. Preparation of the copper(I) complexes (**1**–**4**).

complex **4** was validated through single crystal XRD. The complexes were soluble in organic solvents such as methanol, ethanol, acetonitrile, DMF, *etc.*, but insoluble in water.

Spectroscopy

The ligands' UV-Vis spectra showed two bands in the regions 262–265 and 329–341 nm, associated with $\pi\rightarrow\pi^*$ and $n\rightarrow\pi^*$ transitions, respectively. Three bands were seen in the UV-Vis spectra of the complexes in DMF. The intra-ligand transitions in the complexes were seen at 274–278 and 245–258 nm. The complex formation was corroborated by a band in the 332–341 nm region ascribed to the ligand-to-metal charge transfer (LMCT) transition (Figures S1–S4).[66–71]

The ligands' FT-IR spectra showed three bands; at 3409–3448 cm^{-1} for indole N–H, 3300–3343 cm^{-1} for N–H coupled to azomethine and 3169–3238 cm^{-1} for N–H linked to thiocarbonyl. The peaks at 1548–1567 and 1261–1299 cm^{-1} were attributed to azomethine (C=N) and thiocarbonyl (C=S) moieties, respectively. The TSC ligands coordinated to the copper(I) ion through the thiocarbonyl sulphur, which was suggested by a decrease in the thiocarbonyl stretching frequency (1244–1249 cm^{-1}) in the spectra of the complexes. Further, the appearance of new bands at 1433–1434, 1048–1074, and 742–746 cm^{-1} (Figures S5–S8) in their FT-IR spectra confirmed the presence of coordinated triphenylphosphine.

The indole N–H proton signal was seen at 11.92–11.72 ppm in the ^{1}H NMR spectra of the complexes, and at 11.85–11.72 ppm in those of the ligands. ^{1}H NMR spectra of the ligands displayed the N–H proton (attached to imine) resonance in the region 11.63–11.19 ppm;[57] only a small fluctuation in this chemical shift was observed for the complexes (**1**–**4**) (11.74–11.67 ppm), demonstrating the neutral coordination of the ligand to the metal center. In the spectra of the complexes (**2**–**4**) and ligands (L2–L4), the terminal N–H proton signal was found between 9.78 and 4.55 ppm. The ligands' ^{1}H NMR spectra showed signals characteristic of azomethine C–H protons (8.31–8.05 ppm) and pyrrole C–H protons (7.81–7.61 ppm). In the spectra of the complexes, the azomethine C–H and pyrrole C–H signals could be seen at 8.16–7.88 and 8.48–8.39 ppm, respectively. Two broad singlets, corresponding to NH_2 protons, were detected at 8.02 and 7.80 ppm in the spectrum of ligand L1, whereas these were seen at 9.68 and 7.16 ppm in the spectrum of complex **1**. The CH_3 protons accounted for the appearance of a doublet at 3.10 and 3.09 ppm in the spectra of complex **2** and ligand L2, respectively. Further, cyclohexyl protons were observed at 1.91–1.16 and 1.80–1.28 ppm in the spectra of complex **4** and ligand L4, respectively (Figures S9–S20).

In the ^{13}C NMR spectra of the ligands, signals were generated at 177.1–174.1 and 140.9–139.3 ppm due to the C=S and C=N carbons, respectively, which persisted at 173.9–172.8 and 144.3–142.5 ppm, respectively in the spectra of the complexes (**1**–**4**). Other expected proton and carbon chemical shifts were observed[72] (Figures S9–S20). A signal for coordinated triphenylphosphine was seen in the ^{31}P NMR spectra of the complexes (**1**–**4**) at 25.73–25.64 ppm. HR-MS spectra of the complexes (**1**–**4**) displayed characteristic peaks at molecular weights that agreed well with those determined by calculation. These peaks appeared at *m/z* 543.0854, 557.1031, 651.1202 and 625.1768, respectively for complexes **1**, **2**, **3** and **4** (Figures S21-S24).

Crystal structure

After the slow evaporation of a solution of complex **4** in a mixture of DMF-CH_2Cl_2 (1:2), suitable crystals (reddish-brown colour) were obtained for XRD. Figure 2 shows an atomically

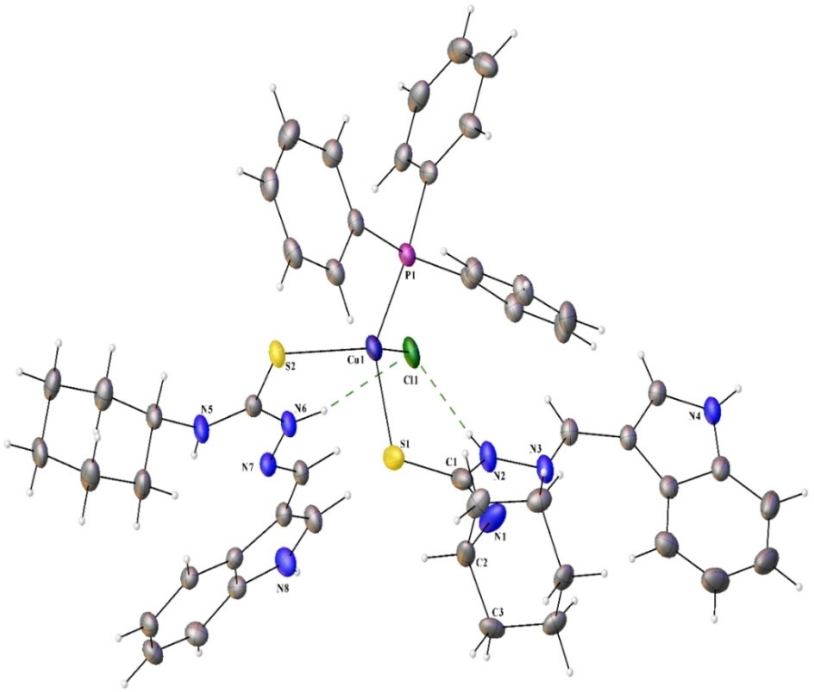

Figure 2. Thermal ellipsoidal plot of complex **4** (50 % probability level).

labelled thermal ellipsoidal plot of complex **4**. Crystallographic data and specific values for interatomic bond lengths and angles can be found in Tables S1 and S2, respectively. A monoclinic crystal system (*P21/n* space group) was found for complex **4**, and the number of complex units per unit cell (*Z*) was found to be 4. Complex **4** has a perfect tetrahedral form, with the copper(I) ion coordinated to the TSC, triphenylphosphine, and chlorido ligands. The N(6)H···Cl(1) and N(8)H···Cl(1) intramolecular hydrogen bonds had 2.354 and 2.446 Å bond lengths, respectively. The S(1)–Cu(1)–Cl(1) and P(1)–Cu(1)–S(2) angles, both around 109.5°, indicated the tetrahedral geometry of complex **4**. Since the C=S bond length increased in complex **4** in relation to ligand L4, it was clear that the ligand linked to the copper(I) ion *via* the thiocarbonyl S atom. The length of the Cu(1)–S(1) bond (2.3404 Å) was greater than that of the Cu(1)–P(1) bond (2.2278 Å) and less than that of the Cu(1)–Cl(1) bond (2.4192 Å). The Cu(1)–S(2)–C(17)–N(5), Cu(1)–P-(1)–C(33)–C(34) and Cu(1)–P(1)–C(39)–C(40) torsional angles were 170.83(14), 56.97(15), and 26.54(16)°, respectively. As mentioned earlier, the reports on copper(I) TSC complexes are quite rare.[60–65,73] Even in the presence of excess triphenylphosphine (as can be seen in Scheme 2), the copper(I) ion preferred to bind to two TSC ligands as observed by Dorairaj *et al.*[73]

Stability

The efficacy of a metallodrug is highly dependent on its stability and solubility in water. Since many biological studies are performed in a 1 % water-DMSO combination, it is necessary to comprehend the complexes' stability in this medium for 24 h. Figures S25–S28 show the UV-Vis spectra of the complexes (**1**–**4**), recorded over 24 h, which revealed minor shift in band positions or intensities, indicating the hydrolysis of labile chlorido ligand.[74–77]

Cytotoxicity assessment

The complexes (**1**–**4**), $CuCl_2 \cdot 2H_2O$ and $[(PPh_3)_2Cu(\mu\text{-}Cl)_2Cu(PPh_3)]$ were evaluated for their cytotoxicity against immortalized human vascular endothelial (EAhy.926), hepatocellular carcinoma (HepG-2), and bladder cancer (T24) cell lines, along with Vero normal cells, through the MTT test.[78] As a positive control, cisplatin was employed. The selection of cancer cells was made at random as an initial test of the complexes' cytotoxic nature. Table 1 displays the IC_{50} values of the complexes, $CuCl_2 \cdot 2H_2O$ and $[(PPh_3)_2Cu(\mu\text{-}Cl)_2Cu(PPh_3)]$ (Figure S29). According to the IC_{50} values, complexes **3** and **4** had more cytotoxicity than

Table 1. Cytotoxicity of the copper(I) complexes (**1**–**4**)

Compound	IC_{50} value (μM)			
	EAhy.926	HepG-2	T24	Vero
1	49.31 ± 0.06	64.21 ± 0.20	70.63 ± 0.15	98.79 ± 0.10
2	66.95 ± 0.10	50.70 ± 0.13	99.93 ± 0.11	> 100
3	13.82 ± 0.09	24.93 ± 0.08	60.25 ± 0.18	48.91 ± 0.07
4	25.03 ± 0.16	61.67 ± 0.12	26.30 ± 0.06	89.26 ± 0.14
$CuCl_2 \cdot 2H_2O$	> 100	> 100	> 100	> 100
$[(PPh_3)_2Cu(\mu\text{-}Cl)_2Cu(PPh_3)]$	> 100	> 100	> 100	97.12 ± 0.21
Cisplatin	26.60[a]	49.90[a]	> 50[a]	29.50[a]

[a] Ref. [78]

cisplatin. Furthermore, the higher IC_{50} values (48.91 to >100 μM) towards Vero cells showed that all the complexes were less hazardous to normal healthy cells (Figure 3). Complex **3** outperformed cisplatin in terms of its effectiveness against EAhy.926 and HepG-2 cancer cells, probably due to the lipophilic and bulky phenyl terminal substituent. In contrast, the ones with less bulky/non-aromatic substituent did not show encouraging cytotoxicity.

Conclusions

In the present study, the TSC ligands comprising of an indole nucleus were used and four unique copper(I) complexes (**1**–**4**) were synthesized. The complexes' structures were verified using the information derived from the spectroscopic and crystallographic methods. Using MTT assay, cytotoxicity of the complexes towards three cancer cells (EAhy.926, HepG-2, and T24) and toxicity towards Vero normal cells were screened. The complexes displayed moderate cytotoxicity to cancer cells but were less harmful to Vero cells. Complex **3** was more efficient than cisplatin, with IC_{50} values of 13.82 and 24.93 μM towards EAhy.926 and HepG-2 cell lines, as compared to 26.60 and 49.90 μM, respectively, for cisplatin. The initial findings from these biological screening efforts point to a promising framework of complexes that may result in effective anticancer medicines in the future.

Experimental

Materials and methods

From Sigma Aldrich/Merck, we obtained all the necessary solvents and chemicals. The melting points were determined utilizing Lab India equipment and are uncorrected. A Nicolet-iS5 spectrophotometer was employed to produce FT-IR spectra of the complexes. A Shimadzu-2600 spectrophotometer was utilized to capture the UV-Visible (UV-Vis) spectra. A Bruker 400 MHz spectrometer was employed to document the NMR spectra of the complexes (DMSO-d_6). On an Agilent high-resolution mass spectrometer, mass spectra were captured. The procedure for synthesizing indole-based TSCs (L1–L4) is available in the literature.[57] The copper(I) precursor was synthesized using a method reported in the literature.[73] UV-Vis spectra of the complexes (**1**–**4**) in water (with 1% DMSO) were recorded over 24 h to assess their stability. The cytotoxicity of the complexes (**1**–**4**) was assessed through MTT assay.[78]

Synthesis of the copper(I) complexes (1–4)

The dichloromethane solutions (15 mL) of $[(PPh_3)_2Cu(\mu\text{-}Cl)_2Cu(PPh_3)]$ (0.500 g, 0.75 mmol) and corresponding indole-based TSC (0.451–0.327 g, 1.5 mmol) were mixed, and the reaction mixture was stirred using a magnetic stirrer at ambient temperature over 12 h. Then, dichloromethane was removed at a decreased pressure, that produced an oily product. A pale-yellow precipitate was obtained after adding a 9:1 *n*-hexane-ethyl acetate mixture to the oily product which was filtered, washed using petroleum ether, and dried.

$[Cu(L1)_2Cl(PPh_3)]$ (1)

L1 (1.5 mmol, 0.327 g) was utilized. Pale yellow solid. M.p.: 242 °C. Yield: 92%. UV-Vis (λ_{max}, DMF, nm): 332 (LMCT), 278 (n→π*), 245

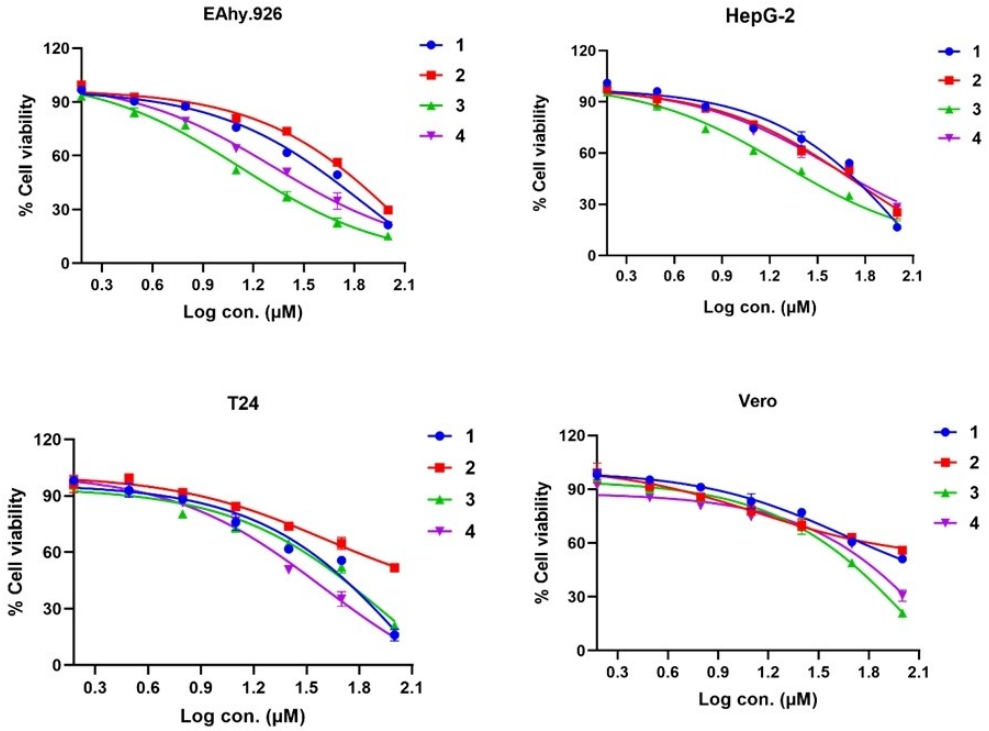

Figure 3. Cytotoxicity of complexes **1**–**4**.

($\pi\rightarrow\pi^*$). FT-IR (cm^{-1}, KBr): 3142 (N–H), 1593 (C=N), 1249 (C=S), 1433, 1048, 746 (PPh_3). ^{1}H NMR (DMSO-d_6, 400 MHz, ppm): δ, 11.76 (2H, s, indole N–H), 11.71 (2H, s, imine attached N–H), 8.73 (2H, s, terminal NH_2), 8.41 (2H, s, pyrrole ring C–H), 8.36 (2H, d, $J=7.8$ Hz, Ar–H), 8.05 (2H, s, imine C–H), 7.91 (2H, d, $J=7.5$ Hz, Ar–H), 7.42–7.45 (17H, m, phenyl H of PPh_3), 7.15–7.13 (4H, m, terminal NH_2 and Ar–H). ^{13}C NMR (DMSO-d_6, 100 MHz, ppm): δ, 172.8 (C=S), 144.3 (C=N), 137.5, 133.9, 132.6, 132.0, 131.9, 130.6, 129.3, 129.2, 124.3, 123.3, 121.3, 112.2, 111.1 (Ar–C). ^{31}P NMR (DMSO-d_6, 162 MHz, ppm): δ, 25.68. ESI mass {[Cu(L1)(PPh_3)]$^+$}, Calcd. (Found): m/z 543.0833 (543.0854). Anal. Calcd. for $C_{38}H_{35}ClCuN_8PS_2$: C, 57.21; H, 4.42; N, 14.04; S, 8.04; Found: C, 57.18; H, 4.39; N, 14.01; S, 8.06.

[Cu(L2)$_2$Cl(PPh_3)] (2)

L2 (1.5 mmol, 0.348 g) was utilized. Pale yellow solid. M.p.: 240 °C. Yield: 91 %. UV-Vis (λ_{max}, DMF, nm): 333 (LMCT), 276 ($n\rightarrow\pi^*$), 253 ($\pi\rightarrow\pi^*$). FT-IR (cm^{-1}, KBr): 3213 (N–H), 1576 (C=N), 1244 (C=S), 1434, 1074, 745 (PPh_3). ^{1}H NMR (DMSO-d_6, 400 MHz, ppm): δ, 11.75 (2H, s, indole N–H), 11.69 (2H, s, imine attached N–H), 8.40 (2H, s, pyrrole ring C–H), 8.34 (2H, d, $J=7.3$ Hz, Ar–H), 8.16 (2H, s, imine C–H), 7.89 (2H, q, $J=5.0$ Hz, terminal N–H), 7.48-7.37 (17H, m, phenyl H of PPh_3 and Ar–H), 7.23 (2H, t, $J=7.0$ Hz, Ar–H), 7.17 (2H, t, $J=7.2$ Hz, Ar–H), 3.10 (6H, d, $J=4.1$ Hz, CH_3). ^{13}C NMR (DMSO-d_6, 100 MHz, ppm): δ, 173.9 (C=S), 143.0 (C=N), 137.5, 133.9, 133.7, 132.3, 132.0, 131.9, 130.5, 129.2, 129.2, 123.2, 121.1, 112.2 (Ar–C), 31.5 (CH_3). ^{31}P NMR (DMSO-d_6, 162 MHz, ppm): δ, 25.73. ESI mass {[Cu(L2)(PPh_3)]$^+$}, Calcd. (Found): m/z 557.1002 (557.1031); Anal. Calcd. for $C_{40}H_{39}ClCuN_8PS_2$: C, 58.17; H, 4.76; N, 13.57; S, 7.76; Found: C, 58.15; H, 4.73; N, 13.54; S, 7.73.

[Cu(L3)$_2$Cl(PPh_3)] (3)

L3 (1.5 mmol, 0.442 g) was utilized. Pale yellow solid. M.p.: 246 °C. Yield: 83 %. UV-Vis (λ_{max}, DMF, nm): 341 (LMCT), 276 ($n\rightarrow\pi^*$), 255 ($\pi\rightarrow\pi^*$). FT-IR (cm^{-1}, KBr): 3122 (N–H), 1549 (C=N), 1244 (C=S), 1433, 1064, 744 (PPh_3). ^{1}H NMR (DMSO-d_6, 400 MHz, ppm): δ, 11.92 (2H, s, indole N–H), 11.74 (2H, s, imine attached N–H), 9.78 (2H, s, terminal N–H), 8.48 (2H, s, pyrrole ring C–H), 8.29 (2H, d, $J=7.2$ Hz, Ar–H), 7.95 (2H, s, imine C–H), 7.48 (4H, d, $J=7.0$ Hz, Ar–H), 7.45–7.39 (21H, m, phenyl H of PPh_3 and Ar–H), 7.16 (4H, t, $J=7.2$ Hz, Ar–H), 7.09 (2H, d, $J=7.0$ Hz, Ar–H). ^{13}C NMR (DMSO-d_6, 100 MHz, ppm): δ, 173.0 (C=S), 142.9 (C=N), 139.3, 137.5, 133.8, 132.3, 130.4, 130.4, 129.1, 128.7, 126.1, 125.9, 123.2, 122.5, 121.2, 113.5, 112.3 (Ar–C). ^{31}P NMR (DMSO-d_6, 162 MHz, ppm): δ, 25.64. ESI mass {[Cu(L3)$_2$]$^+$}, Calcd. (Found): m/z 651.1174 (651.1202). Anal. Calcd. for $C_{50}H_{43}ClCuN_8PS_2$: C, 63.21; H, 4.56; N, 11.79; S, 6.75; Found: C, 63.19; H, 4.55; N, 11.74; S, 6.79.

[Cu(L4)$_2$Cl(PPh_3)] (4)

L4 (1.5 mmol, 0.451 g) was utilized. Pale yellow solid. M.p.: 228 °C. Yield: 89 %. UV-Vis (λ_{max}, DMF, nm): 334 (LMCT), 274 ($n\rightarrow\pi^*$), 258 ($\pi\rightarrow\pi^*$). FT-IR (cm^{-1}, KBr): 3142 (N–H), 1550 (C=N), 1245 (C=S), 1434, 1067, 742 (PPh_3). ^{1}H NMR (DMSO-d_6, 400 MHz, ppm): δ, 11.72 (4H, s, indole and imine N–H), 8.39 (2H, s, pyrrole ring C–H), 8.08 (2H, d, $J=6.6$ Hz, Ar–H), 7.92 (2H, s, imine C–H), 7.78–7.50 (2H, m, Ar–H), 7.61–7.24 (17H, m, phenyl H of PPh_3 and Ar–H), 7.24–7.13 (4H, m, Ar–H), 4.55 (2H, d, $J=7.1$ Hz, terminal N–H), 1.91 (4H, d, $J=9.5$ Hz, Cyclohexyl-H), 1.71 (4H, d, $J=11.6$ Hz, Cyclohexyl-H), 1.58 (2H, d, $J=11.3$ Hz, Cyclohexyl-H), 1.47 (4H, d, $J=10.3$ Hz, Cyclohexyl-H), 1.40–1.16 (6H, m, Cyclohexyl-H). ^{13}C NMR (DMSO-d_6, 100 MHz, ppm): δ, 172.8 (C=S), 142.5 (C=N), 137.5, 133.9, 133.7, 133.3, 132.1, 130.4, 129.2, 123.2, 121.8, 121.2, 112.5, 111.1 (Ar–C), 52.5, 32.3, 25.4, 24.8 (Cyclohexyl-C). ^{31}P NMR (DMSO-d_6, 162 MHz, ppm): δ, 25.64. ESI mass {[Cu(L4)(PPh_3)]$^+$}, Calcd. (Found): m/z 625.1616 (625.1768). Anal. Calcd. for $C_{50}H_{55}ClCuN_8PS_2$: C, 62.42; H, 5.76; N, 11.65; S, 6.67; Found: C, 62.37; H, 5.75; N, 11.59; S, 6.63.

Single crystal X-ray diffraction

A Bruker Quest X-ray diffractometer was utilized to gather the X-ray diffraction (XRD) information for complex **4**. The Mo-Iμs X-ray tube (K = 0.71073 Å) produced X-ray radiation. The goniometer was managed *via* the APEX3 software,[79,80] which was also utilized to collect integrated intensity data for each reflection. Utilizing the absorption correction tool SADABS, the collected data were adjusted for absorption effects. The PLATON (ADDSYM) software was used to establish no additional symmetry.[81] The structure was finally strategized using the programme Olex2.[82] Deposition Number 2225797 (for **4**) contains the supplementary crystallographic data for this paper. These data are provided free of charge by the joint Cambridge Crystallographic Data Centre and Fachinformationszentrum Karlsruhe Access Structures service.

Supporting information summary

Detailed crystallographic information and spectra of all types (UV-Vis, FT-IR, NMR, mass) are provided. The structure of complex **4** presented here has been deposited in the Cambridge Crystallographic Data Centre (CCDC 2225797).

Acknowledgements

J.H. thanks the Fondo Nacional de Ciencia y Tecnologia (FONDECYT, Project No. 3200391) for the postdoctoral fellowship. S.S. thanks the Center for Computational Modeling, Chennai Institute of Technology (CIT), India for funding (CIT/CCM/2023/RP-021). J.A.P. thanks the Fondo Nacional de Ciencia y Tecnologia (FONDECYT, Project No. 11191049) for funding.

Conflict of Interests

The authors declare no competing financial interest.

Data Availability Statement

The data that support the findings of this study are available with the corresponding author.

Keywords: Copper(I) complexes · Cytotoxicity · Indole · Thiosemicarbazones · Triphenylphosphine

[1] K. J. Kilpin, P. J. Dyson, *Chem. Sci.* **2013**, *4*, 1410–1419.
[2] S. Swaminathan, J. Haribabu, N. Balakrishnan, P. Vasanthakumar, R. Karvembu, *Coord. Chem. Rev.* **2022**, *459*, 214403.
[3] R. G. Kenny, C. J. Marmion, *Chem. Rev.* **2019**, *119*, 1058–1137.
[4] N. A. Mohamed, R. R. Mohamed, R. S. Seoudi, *Int. J. Biol. Macromol.* **2014**, *63*, 163–169.
[5] M. M. Aly, Y. A. Mohamed, K. A. M. El-Bayouki, W. M. Basyouni, S. Y. Abbas, *Eur. J. Med. Chem.* **2010**, *45*, 3365–3373.

[6] U. Kulandaivelu, V. G. Padmini, K. Suneetha, *Arch. Pharm.* **2011**, *344*, 84–90.
[7] Y. Yu, D. S. Kalinowski, Z. Kovacevic, *J. Med. Chem.* **2009**, *52*, 5271–5294.
[8] R. K. Agarwal, L. Singh, D. K. Sharma, *Bioinorg. Chem. Appl.* **2006**, *59509*, 1–10.
[9] V. Pósa, A. Stefanelli, J. H. B. Nunes, S. Hager, M. Mathuber, N. V. May, W. Berger, B. K. Keppler, C. R. Kowol, É. A. Enyedy, P. Heffeter, *Cancers* **2022**, *14*, 4455.
[10] K. C. Park, L. Fouani, P. J. Jansson, D. Wooi, S. Sahni, D. J. R. Lane, D. Palanimuthu, H. C. Lok, Z. Kovačević, M. L. H. Huang, D. S. Kalinowski, D. R. Richardson, *Metallomics* **2016**, *8*, 874–886.
[11] Z. A. Kaplancikli, M. D. Altintop, B. Sever, Z. Cantürk, A. Özdemir, *J. Chem.* **2016**, *2016*, 1692540.
[12] F. R. Pavan, P. I. da S. Maia, S. R. A. Leite, V. M. Deflon, A. A. Batista, D. N. Sato, S. G. Franzblau, C. Q. F. Leite, *Eur. J. Med. Chem.* **2010**, *45*, 1898–1905.
[13] T. S. Lobana, R. Sharma, G. Bawa, S. Khanna, *Coord. Chem. Rev.* **2009**, *253*, 977–1055.
[14] B. Šarkanj, M. Molnar, M. Čačić, L. Gille, *Food Chem.* **2013**, *139*, 488–495.
[15] P. Padmanabhan, S. Khaleefathullah, K. Kaveri, G. Palani, G. Ramanathan, S. Thennarasu, U. T. Sivagnanam, *J. Med. Virol.* **2017**, *89*, 546–552.
[16] P. Chellan, N. Shunmoogam-Gounden, D. T. Hendricks, J. Gut, P. J. Rosenthal, C. Lategan, P. J. Smith, K. Chibale, G. S. Smith, *Eur. J. Inorg. Chem.* **2010**, *2010*, 3520–3528.
[17] M. G. Temraz, P. A. Elzahhar, A. E. D. A. Bekhit, A. A. Bekhit, H. F. Labib, A. S. Belal, *Eur. J. Med. Chem.* **2018**, *151*, 585–600.
[18] J. L. R. de Melos, E. C. Torres-Santos, V. D. S. Faiões, C. D. N. Del Cistia, C. M. R. Sant'Anna, C. E. Rodrigues-Santos, A. Echevarria, *Eur. J. Med. Chem.* **2015**, *103*, 409–417.
[19] M. D. Hall, K. R. Brimacombe, M. S. Varonka, K. M. Pluchino, J. K. Monda, J. Li, M. J. Walsh, M. B. Boxer, T. H. Warren, H. M. Fales, M. M. Gottesman, *J. Med. Chem.* **2011**, *54*, 5878–5889.
[20] M. L. Pati, M. Niso, D. Spitzer, F. Berardi, M. Contino, C. Riganti, W. G. Hawkins, C. Abate, *Eur. J. Med. Chem.* **2018**, *144*, 359–371.
[21] J. F. de Oliveira, T. S. Lima, D. B. Vendramini-Costa, S. C. B. de Lacerda Pedrosa, E. A. Lafayette, R. M. F. da Silva, S. M. V. de Almeida, R. O. de Moura, A. L. T. G. Ruiz, J. E. de Carvalho, M. D. C. A. de Lima, *Eur. J. Med. Chem.* **2017**, *136*, 305–314.
[22] F. Vandresen, H. Falzirolli, S. A. A. Batista, A. P. B. da Silva-Giardini, D. N. de Oliveira, R. R. Catharino, A. L. T. Ruiz, J. E. de Carvalho, M. A. Foglio, C. C. da Silva, *Eur. J. Med. Chem.* **2014**, *79*, 110–116.
[23] Y. Yu, J. Wong, D. B. Lovejoy, D. S. Kalinowski, D. R. Richardson, *Clin. Cancer Res.* **2006**, *12*, 6876–6883.
[24] D. S. Kalinowski, P. C. Sharpe, P. V. Bernhardt, D. R. Richardson, *J. Med. Chem.* **2007**, *50*, 6212–6225.
[25] Y. Yu, D. S. Kalinowski, Z. Kovacevic, A. R. Siafakas, P. J. Jansson, C. Stefani, D. B. Lovejoy, P. C. Sharpe, P. V. Bernhardt, D. R. Richardson, *J. Med. Chem.* **2009**, *52*, 5271–5294.
[26] B. M. Zeglis, V. Divilov, J. S. Lewis, *J. Med. Chem.* **2011**, *54*, 2391–2398.
[27] D. B. Lovejoy, D. M. Sharp, N. Seebacher, P. Obeidy, T. Prichard, C. Stefani, M. T. Basha, P. C. Sharpe, P. J. Jansson, D. S. Kalinowski, P. V. Bernhardt, *J. Med. Chem.* **2012**, *55*, 7230–7244.
[28] D. R. Richardson, P. C. Sharpe, D. B. Lovejoy, D. Senaratne, D. S. Kalinowski, M. Islam, P. V. Bernhardt, *J. Med. Chem.* **2006**, *49*, 6510–6521.
[29] Z. G. Jiang, M. S. Lebowitz, H. A. Ghanbari, *CNS Drug Rev.* **2006**, *12*, 77–90.
[30] H. E. Elsayed, H. Y. Ebrahim, E. G. Haggag, A. M. Kamal, K. A. El Sayed, *Bioorg. Med. Chem.* **2017**, *25*, 6297–6312.
[31] C. Guo, L. Wang, X. Li, S. Wang, X. Yu, K. Xu, Y. Zhao, J. Luo, X. Li, B. Jiang, D. Shi, *J. Med. Chem.* **2019**, *62*, 3051–3067.
[32] S. Y. Abbas, R. A. Al-Harbi, M. A. S. El-Sharief, *Eur. J. Med. Chem.* **2020**, *198*, 112363.
[33] A. G. Ribeiro, S. M. V. de Almeida, J. F. de Oliveira, T. R. C. de Lima Souza, K. L. Dos Santos, A. P. de Barros Albuquerque, M. C. D. B. L. Nogueira, L. B. de Carvalho Junior, R. O. de Moura, A. C. da Silva, V. R. A. Pereira, *Eur. J. Med. Chem.* **2019**, *182*, 111592.
[34] A. Lindemann, A. A. Patel, N. L. Silver, L. Tang, Z. Liu, L. Wang, N. Tanaka, X. Rao, H. Takahashi, N. K. Maduka, M. Zhao, *Clin. Cancer Res.* **2019**, *25*, 5650–5662.
[35] A. Mrozek-Wilczkiewicz, K. Malarz, M. Rejmund, J. Polanski, R. Musiol, *Eur. J. Med. Chem.* **2019**, *171*, 180–194.
[36] J. F. de Oliveira, A. L. da Silva, D. B. Vendramini-Costa, C. A. da Cruz Amorim, J. F. Campos, A. G. Ribeiro, R. O. de Moura, J. L. Neves, A. L. T. G. Ruiz, J. E. de Carvalho, M. D. C. A. de Lima, *Eur. J. Med. Chem.* **2015**, *104*, 148–156.
[37] M. H. Khalilian, S. Mirzaei, A. A. Taherpour, *New J. Chem.* **2015**, *39*, 9313–9324.
[38] N. Balakrishnan, J. Haribabu, A. K. Dhanabalan, S. Swaminathan, S. Sun, D. F. Dibwe, N. Bhuvanesh, S. Awale, R. Karvembu, *Dalton Trans.* **2020**, *49*, 9411–9424.
[39] F. Tisato, C. Marzano, M. Porchia, M. Pellei, C. Santini, *Med. Res. Rev.* **2010**, *30*, 708–749.
[40] M. Usman, M. Zaki, R. A. Khan, A. Alsalme, M. Ahmad, S. Tabassum, *RSC Adv.* **2017**, *7*, 36056–36071.
[41] S. Tabassum, R. A. Ahmad Khan, Z. Hussain, S. Srivastav, S. Srikrishna, F. Arjmand, *Dalton Trans.* **2013**, *42*, 16749–16761.
[42] R. A. Khan, A. De Almeida, K. Al-Farhan, A. Alsalme, A. Casini, M. Ghazzali, J. Reedijk, *J. Inorg. Biochem.* **2016**, *165*, 128–135.
[43] N. K. Wee, D. C. Weinstein, S. T. Fraser, S. J. Assinder, *Int. J. Biochem. Cell Biol.* **2013**, *45*, 960–963.
[44] Y. Wan, Y. Li, C. Yan, M. Yan, Z. Tang, *Eur. J. Med. Chem.* **2019**, *183*, 111691.
[45] S. Dadashpour, S. Emami, *Eur. J. Med. Chem.* **2018**, *150*, 9–29.
[46] X. Hui, L. Min, *Curr. Pharm. Des.* **2009**, *15*, 2120–2148.
[47] S. Lal, T. J. Snape, *Curr. Med. Chem.* **2012**, *19*, 4828–4837.
[48] Y. L. Sang, W. M. Zhang, P. C. Lv, H. L. Zhu, *Curr. Top. Med. Chem.* **2017**, *17*, 120–137.
[49] A. D. Napper, J. Hixon, T. McDonagh, K. Keavey, J. F. Pons, J. Barker, W. T. Yau, P. Amouzegh, A. Flegg, E. Hamelin, R. J. Thomas, *J. Med. Chem.* **2005**, *48*, 8045–8054.
[50] S. Grant, C. Easley, P. Kirkpatrick, *Nat. Rev. Drug Discovery* **2007**, *6*, 21–22.
[51] R. Furumai, A. Matsuyama, N. Kobashi, K. H. Lee, M. Nishiyama, H. Nakajima, A. Tanaka, Y. Komatsu, N. Nishino, M. Yoshida, S. Horinouchi, *Cancer Res.* **2002**, *62*, 4916–4921.
[52] W. T. Bradner, *Cancer Treat. Rev.* **2001**, *27*, 35–50.
[53] M. A. Jordan, R. H. Himes, L. Wilson, *Cancer Res.* **1985**, *45*, 2741–2747.
[54] L. Almagro, F. Fernández-Pérez, M. A. Pedreño, *Molecules* **2015**, *20*, 2973–3000.
[55] N. Balakrishnan, J. Haribabu, D. A. Krishnan, S. Swaminathan, D. Mahendiran, N. S. P. Bhuvanesh, R. Karvembu, *Polyhedron* **2019**, *170*, 188–201.
[56] N. Balakrishnan, J. Haribabu, R. E. Malekshah, S. Swaminathan, C. Balachandran, N. Bhuvanesh, S. Aoki, R. Karvembu, *Inorg. Chim. Acta* **2022**, *534*, 120805.
[57] J. Haribabu, K. Jeyalakshmi, Y. Arun, N. S. P. Bhuvanesh, P. T. Perumal, R. Karvembu, *J. Biol. Inorg. Chem.* **2017**, *22*, 461–480.
[58] J. Haribabu, S. Priyarega, N. S. P. Bhuvanesh, R. Karvembu, *J. Struct. Chem.* **2020**, *61*, 66–72.
[59] J. Haribabu, N. Balakrishnan, S. Swaminathan, J. Peter, D. Gayathri, C. Echeverria, N. Bhuvanesh, R. Karvembu, *Inorg. Chem. Commun.* **2021**, *134*, 109029.
[60] A. Khan, J. P. Jasinski, V. A. Smolenski, E. P. Hotchkiss, P. T. Kelley, Z. A. Shalit, M. Kaur, K. Paul, R. Sharma, *Bioorg. Chem.* **2018**, *80*, 303–318.
[61] A. B. M. Ibrahim, M. K. Farh, P. Mayer, *Inorg. Chem. Commun.* **2018**, *94*, 127–132.
[62] A. Saswati, S. P. Chakraborty, A. K. Dash, R. Panda, A. Acharyya, S. Biswas, S. K. Mukhopadhyay, A. Bhutia, Y. P. Crochet, M. Patil, R. Nethaji, R. Dinda, *Dalton Trans.* **2015**, *44*, 6140–6157.
[63] A. R. Cowley, J. R. Dilworth, P. S. Donnelly, E. Labisbal, A. Sousa, *J. Am. Chem. Soc.* **2002**, *124*, 5270–5271.
[64] L. J. Ashfield, A. R. Cowley, J. R. Dilworth, P. S. Donnelly, *Inorg. Chem.* **2004**, *43*, 4121–4123.
[65] J. F. Machado, F. Marques, T. Pinheiro, M. J. Villa de Brito, G. Scalese, L. Pérez-Díaz, L. Otero, J. P. M. António, D. Gambino, T. S. Morais, *ChemMedChem* **2023**, *18*, e202300074.
[66] P. Kalaivani, R. Prabhakaran, E. Ramachandran, F. Dallemer, G. Paramaguru, R. Renganathan, P. Poornima, V. V. Padma, K. Natarajan, *Dalton Trans.* **2012**, *41*, 2486–2499.
[67] J. X. Li, T. Zhang, H. J. Chen, Z. X. Du, *Z Kristallogr. Cryst. Mater.* **2021**, *236*, 251–259.
[68] Y. J. Liang, G. Feng, X. Zhang, J. X. Li, Y. Jiang, *J. Struct. Chem.* **2021**, *62*, 300–308.
[69] J. X. Li, Z. X. Du, *J. Cluster Sci.* **2020**, *31*, 507–511.
[70] H. Hu, J. Quan, Z. Tan, J. H. Fu, Y. J. Liang, J. X. Li, *Russ. J. Gen. Chem.* **2021**, *91*, 910–914.
[71] J. X. Li, Z. X. Du, J. Wang, X. Feng, *Z. Naturforsch. B* **2019**, *74*, 839–845.
[72] R. Prabhakaran, R. Karvembu, T. Hashimoto, K. Shimizu, K. Natarajan, *Inorg. Chim. Acta* **2005**, *358*, 2093–2096.

[73] D. P. Dorairaj, J. Haribabu, D. Mahendiran, R. E. Malekshah, S. C. N. Hsu, R. Karvembu, *Appl. Organomet. Chem.* **2023**, *37*, e7087.
[74] S. Keinan, D. Avnir, *J. Chem. Soc. Dalton Trans.* **2001**, *6*, 941–947.
[75] J. Haribabu, S. Srividya, R. Umapathi, D. Gayathri, P. Venkatesu, N. Bhuvanesh, R. Karvembu, *Inorg. Chem. Commun.* **2020**, *119*, 108054.
[76] S. Swaminathan, J. Haribabu, N. K. Kalagatur, R. Konakanchi, N. Balakrishnan, N. Bhuvanesh, R. Karvembu, *ACS Omega* **2019**, *4*, 6245–6256.
[77] J. Haribabu, C. Balachandran, M. M. Tamizh, Y. Arun, N. S. P. Bhuvanesh, S. Aoki, R. Karvembu, *J. Inorg. Biochem.* **2020**, *205*, 110988.
[78] J. Haribabu, V. Garisetti, R. E. Malekshah, S. Srividya, D. Gayathri, N. Bhuvanesh, R. V. Mangalaraja, C. Echeverria, R. Karvembu, *J. Mol. Struct.* **2022**, *1250*, 131782.
[79] G. M. Sheldrick, *Acta Crystallogr. Sect. C Struct. Chem.* **2015**, *71*, 3–8.
[80] G. M. Sheldrick, *Acta Crystallogr. Sect. A Found. Crystallogr.* **2008**, *64*, 112–122.
[81] A. L. J. Spek, *J. Appl. Crystallogr.* **2003**, *36*, 7–13.
[82] O. V. Dolomanov, L. J. Bourhis, R. J. Gildea, J. A. Howard, H. Puschmann, *J. Appl. Crystallogr.* **2009**, *42*, 339–341.

Manuscript received: April 2, 2023

Biomass Conversion and Biorefinery
https://doi.org/10.1007/s13399-023-04589-9

ORIGINAL ARTICLE

Enriched biological activity of copper oxide nanoparticles derived from *Aloe vera* extract

Mahesh Narayanan[1] · Ramesh Kannan Natarajan[2] · Dayana Jeyaleela Gnana Sekar[3] · Rojamalar Paramasivan[1] · Balakumar Srinivasan[1] · Zubair Ahmad[4,5] · Farhat S. Khan[4,5,6]

Received: 28 December 2022 / Revised: 18 May 2023 / Accepted: 2 June 2023

Abstract
Nanotechnology is an expanding field with significant potential to benefit society. This study focuses on the environmentally friendly synthesis of copper oxide nanoparticles (CuONPs) using *Aloe vera* leaf extract and explores their applications in the field of biomedicine. *Aloe vera* extracts were carefully evaluated and analyzed both qualitatively and quantitatively. The synthesized CuONPs derived from *Aloe vera* were thoroughly characterized using various techniques, including UV–Vis spectroscopy, FTIR microscopy, SEM, TEM, zeta potential, and histogram analysis with EDX. Furthermore, the biomedical applications of CuONPs were extensively examined. This involved assessing their efficacy against respiratory tract-causing microbes, evaluating in vitro antioxidant, antidiabetic, and anti-inflammatory activities, conducting MTT assays against L929 cell lines, and utilizing the AO/EtBr staining method. The results unequivocally demonstrated the exceptional potential of environmentally friendly CuONPs in various biomedical activities.

Keywords Plant-mediated nanoparticles · CuONPs · *Aloe vera* · Biomedical applications

1 Introduction

Nanotechnology encompasses translational research and focuses on particles ranging from 1 to 100 nm [1]. The development of environmentally friendly metallic nanoparticles employs organic materials [2]. This interdisciplinary field includes various scientific domains, such as physical science [3]. Nanomaterials are synthesized through chemical, biological, and material processes, resulting in diverse morphologies like platelets, cylinders, and tubes. Noble metals, including Cu, Ag, Ti, Pt, Au, and Pd, are commonly used for nanoparticle production. Synthesized nanoparticles find applications in cosmetics, detergents, shampoos, shoes, soaps, and toothpaste [4]. Nanoparticles can be categorized as organic or inorganic, with inorganic nanoparticles comprising magnets, noble metals (such as copper, gold, and silver), and semiconductors (e.g., gallium nitride) [5]. Due to their size, structure, and shape, inorganic nanoparticles exhibit compatibility advantages. Moreover, inorganic nanoparticles hold potential as drug candidates [6]. Metallic nanomaterials possess flexibility, usefulness, and similarities to drug delivery systems.

Metallic nanoparticles are synthesized physically, chemically, and biologically. The natural process was cheaper, non-toxic, and more effective in antibacterial, antifungal, anti-inflammatory, anticancer, and antioxidant activities [7]. Bioreduction and biosorption methods synthesize metallic nanoparticles from plant leaf extract. Unlike chemical synthesis, it is safe. Plants contain more phytochemical activity because they reduce and cap [8]. Copper oxide nanoparticles are a common,

✉ Balakumar Srinivasan
balakumarmicro@gmail.com

1 Department of Chemistry and Biosciences, SASTRA Deemed University, Kumbakonam 612001, Tamil Nadu, India

2 PG and Research Department of Biochemistry, Srimad Andavan Arts and Science College (Autonomous), Affiliated to Bharathidasan University, Tiruchirappalli 620005, Tamil Nadu, India

3 PG & Research Department of Chemistry, St. Joseph's College (Autonomous), Affiliated to Bharathidasan University, Tiruchirappalli 620002, Tamil Nadu, India

4 Unit of Bee Research and Honey Production, Faculty of Science, King Khalid University, P.O. Box 62527, Abha, Saudi Arabia

5 Applied College, Mahala Campus, King Khalid University, P.O. Box 62527, Abha, Saudi Arabia

6 College of Arts and Sciences, Dehran Aljunoub, King Khalid University, P.O. Box 62527, Abha, Saudi Arabia

Published online: 24 July 2023

inexpensive, and non-toxic starting material. Copper is a plant-growing microelement in block D of the periodic table [9]. CuONPs in various materials harm human health (Bai and Tang, 2020). The previous report on CuONPs harmed protozoa, crustaceans, algae, and zebrafish [11]. Biological processes produce effective antimicrobial nanoparticles.

Aloe vera (Asphodelaceae), used in social remedies, is 18 inches long and 2 inches wide at the base. Aloe has 3-foot-tall yellow blossoms in winter and spring [12]. The real *A. vera* has yellow flowers, but many clones have orange. *A. vera* has 20 healthy minerals and 22 amino acids. Eight are "essential" because the body cannot make them. *A. vera* contains eight "essential" amino acids and 11 secondary ones. Rosca-Casian et al. *A. vera* has A, B1, B2, B6, B12, C, and E [13]. The burn plant's positive effects on the skin are believed to help sustain youth in India [14].

This article describes a "rapid and green" method for synthesizing copper oxide nanoparticles (CuONPs) using *A. vera*. It also screens and estimates the phytochemical constituents in the plant extract. *A. vera* was used to produce copper oxide nanoparticles and evaluate their biomedical applications and photocatalytic activity.

2 Results and discussion

2.1 Qualitative analysis of secondary metabolites

This work analyzes methanol and aqueous extracts of *A. vera* for phytochemicals. Both methanol and aqueous extracts are rich in tannin, saponin, flavonoids, steroids, terpenoids, triterpenoids, antroquinone polyphenol, glycoside, and coumarins. The extract details are shown in Table 1. Both extracts lacked alkaloids. Previous research using *A. vera* extracts had a similar result [15–19].

Table 1 Qualitative analysis of phytochemicals in *Aloe vera* leaves extract

S. no	Phytochemicals	Extracts	
		Methanol	Aqueous
1	Tannin	++	+
2	Saponin	++	++
3	Flavonoids	++	++
4	Steroids	++	+
5	Terpenoids	++	++
6	Triterpenoids	++	+
7	Alkaloids	-	-
8	Anthraquinone	++	+
9	Polyphenol	++	++
10	Glycoside	++	+
11	Coumarins	++	++

(-) Absence; (+) presence; (++) high concentration

2.2 Quantitative analysis of secondary metabolites

The secondary metabolites in the plants are a key part of figuring out what kind of drug is being used. Quantifying phytochemicals is important for finding compounds like flavonoids, terpenoids, and phenolics for medicine and industry. The quantitative analysis of critical organic components is recorded in Fig. 1a. Flavonoids are polyphenolic chemicals that scavenge free radicals, inhibit hydrolytic and oxidative enzymes, and reduce inflammation (Pourmorad et al., 2006). Flavonoids scavenge hydroxyl radicals, lipid peroxy radicals, and superoxide anion radicals, promoting human health and preventing oxidative damage to membrane proteins and DNA [21]; 40 mg/g dry-weight total flavonoids were found in the *A. vera* extract. Flavonoids fight cell-damaging free radicals. Systematic epidemiological studies link flavonoids to a reduced risk of immunological insufficiency, cardiovascular disease, and cancer [22].

Phenols are widespread plant secondary metabolites with antioxidant, antimutagenic, antimicrobial, and gene-expression-altering effects [23]. Leaf extracts contained 185.71 mg/g phenolics. Phenolics can scavenge free radicals. Phenolics protect against bacterial and fungal infections, as studies show. High phenolic content aids antioxidant activity (Tian et al., 2020). Terpenoids are crucial secondary metabolites in plants. Natural molecules are the most abundant. Terpenoids affect plant growth, development, environmental response, and physiology. Terpenoids are used in the pharmaceutical, culinary, and cosmetics industries (Li et al., 2020). Terpenoids enhance transdermal absorption, prevent and treat cardiovascular diseases, and have hypoglycemic effects (Yang et al., 2020). Terpenoids have been linked to microbial resistance, immunoregulation, antioxidation, antiaging, and neuroprotection. This study's quantitative analysis produced comparable results to previous research [27–31].

2.3 Synthesis of copper oxide nanoparticles from A. vera leaves extract

Figure 1b illustrates the leaf powder's color shift during $Cu(C_2H_3O_2)_2 \bullet H_2O$ reduction. The rate of CuONP synthesis can be seen by the color change from blue to green. After 10 min, a brown precipitate sank at ambient temperature, indicating the creation of copper oxide nanoparticles. CuONPs were synthesized using a green synthesis strategy with *A. vera* aqueous extract, which is more cost-effective and ecologically friendly than earlier methods. The green production of CuONPs may be attributed to *A. vera* aqueous leaf extract exposure. Color change shows CuONPs

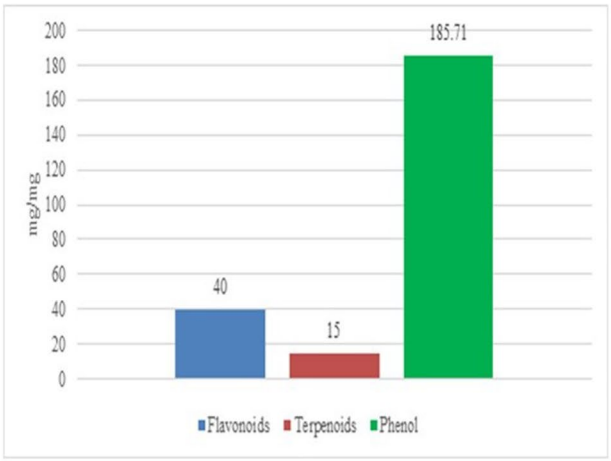

(a)

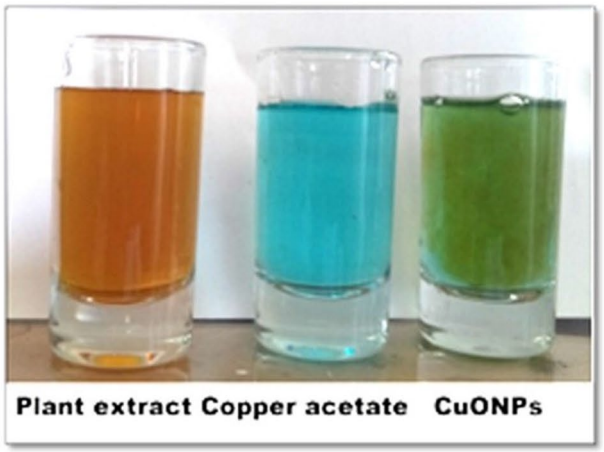

(b)

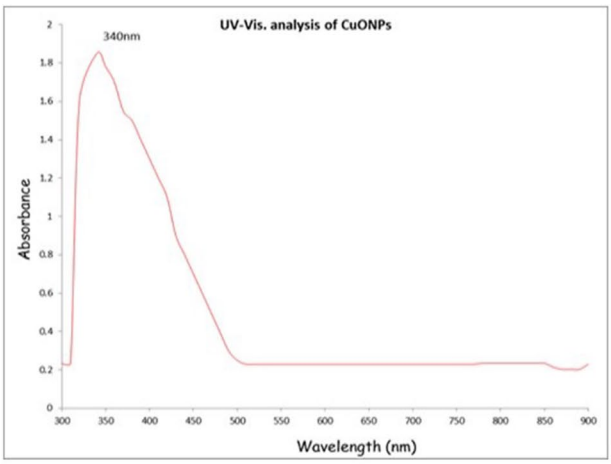

(c)

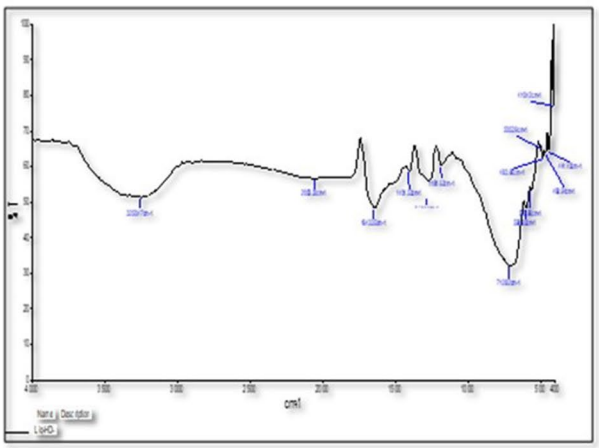

(d)

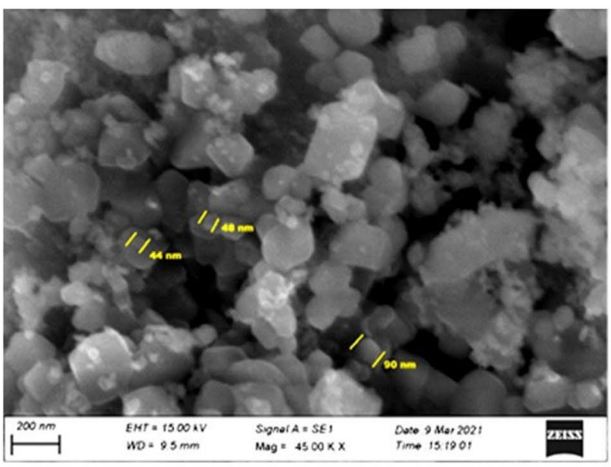

(e)

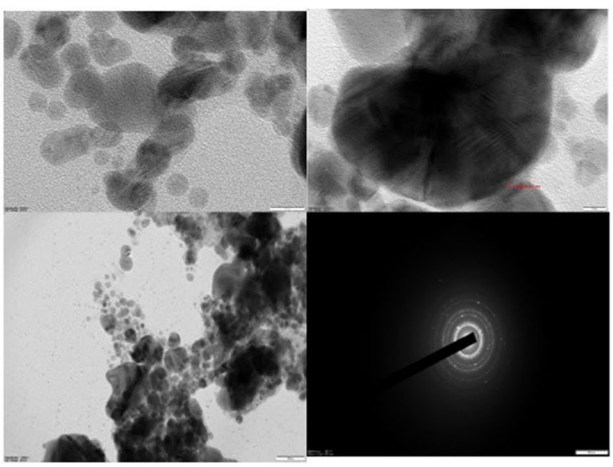

(f)

Fig. 1 **a** Quantitative analysis of secondary metabolites from *Aloe vera* leaf extract; (**b**) color changes of *Aloe vera* extract; (**c**) UV–Vis absorption spectra of CuONPs using *Aloe vera* aqueous extract; (**d**) Fourier transform infrared spectra; (**e**) SEM analysis; and (**f**) transmission electron microscopy (TEM) analysis of CuONPs

reduction from copper ions, which may be analyzed by UV–Vis spectroscopy [32, 33]. The synthesized CuONPs are green in an aqueous solution due to surface plasmon vibration excitation [32–34]. The characteristics of synthesized CuONPs were evaluated by UV–vis, FTIR, and SEM with EDX. UV–Vis spectra of *A. vera* extract in copper acetate solution peaked at 340 nm. CuONPs are created by reducing copper acetate monohydrate for 10 min at room temperature. This outcome is consistent with earlier investigations using plant extracts other than *A. vera* [33, 35–38].

2.4 Characterization of CuONPs

Figure 1c shows a UV spectrophotometer examination of CuONPs. The peaks of CuONPs were discovered using a Perkin Elmer Spectrophotometer at 380–800 nm. Figure 1c displays *Aloe vera*-synthesized CuONPs absorption spectra. CuONPs have 340-nm absorption peaks; 664 nm was the sample's peak UV absorption. An aqueous solution with CuONPs degraded the same sample better early on and increased with time and wavelength; however, MB dissolved in water degraded less over time. CuONPs accelerated MB deterioration at the same wavelength and period. The CuONP-free sample did not deteriorate. Reactive radicals break down organic pollutants into CO_2 and H_2O [39]. CuONPs photo-catalytically destroy MB at 78% efficiency, according to this study. Crystallite size, shape, and surface morphology may explain the difference [40]. CuONPs may degrade organic pollutants photo-catalytically. Both studies agree. UV absorption declines with degradation.

Spectrophotometric Fourier transforms infrared analysis. It measures 400–4000 cm^{-1} peaks and functional groups around nanoparticles. Figure 1d confirms every characterization result twice. Functional groups or biomolecules may help synthesize and stabilize CuONP. This method's IR spectrum is useful for identifying a molecule's chemical bonds, like a molecular fingerprint [41]. FTIR analysis was used to minimize 400–4000 cm^{-1}. Figure 1d exhibits CuONPs utilizing chemical co-precipitation at 3250.47 cm^{-1}, 1276.63 cm^{-1}, 1401.53 cm^{-1}, 1181.62 cm^{-1}, and 712.82 cm^{-1}.

FTIR analysis was utilized to examine the plant extract's dual action as a reducing and capping agent and to identify functional groups in CuONPs. FTIR analysis was used to identify biomolecules involved in capping and stabilizing CuONPs with *A. vera* leaf extract [33]. Alcohols and phenols with hydrogen-bonded O–H groups and amide amines N–H cause a prominent peak at 3250.47 cm^{-1}. A qualitative phytochemical study confirms that *A. vera* leaf extract contains polyphenols, flavonoids, and other O–H and N–H phytochemicals. *A. vera* leaf extract's shoulder peak at 1643.35 cm^{-1} may be due to C = C stretching, C = O amide vibrations, and conjugated C = O of proteins involved in capping CuONPs. The 1276.63 cm^{-1} peak is due to aromatic amine C–N band stretching. The aromatic extension of the alkene group (C = C) is 1401.53 cm^{-1}. The 1118.62 cm^{-1} absorption peak is due to primary and secondary alcohols' C–O stretching vibration. Firm peaks in the 712.82 cm^{-1} range have been given to phenolic groups, C–C stretching vibrations of alkene, and the aromatic bending beat of the C–H group. Lesser peaks in the 900–700 cm^{-1} region have also been allocated to the C-H group's aromatic bending beat. Carbonyl and NH groups stabilize nanoparticles [42]. The doublet of electrons in both groups can help electrostatically stabilize CuONP nanoparticles [43].

SEM analysis is used to identify the dimensions and form of the solid surface of CuONPs. Joel JSM-6480 LV SEM machine was utilized in this study. The voltage is kept in between the range of 10–20 kV. The SEM result of synthesized CuONPs is shown in Fig. 1e. The morphological features of biosynthesised CuONPs were shown in the SEM image (Fig. 1e). The nanoparticles are spherical and size 44 nm, 48 nm, and 90 nm. TEM has been used to investigate the morphology of the newly synthesized CuONPs. As shown in Fig. 1f using TEM, the CuONPs morphology and particle size distribution were also examined. The TEM data indicate that the particles are round and irregularly shaped.

Figure 1f showed (i) a view of CuONPs from *Aloe vera*, (ii) *an enlarged view of* CuONPs, (iii) the dispersion CuONPs in solution, and (iv) the SAED pattern of CuONPs. For CuONPs, a spherical shape was observed. Figure 1f shows that CuONPs have an average size of around 0.29 nm. The lack of surface-protecting ligands causes the picture of nanoscale CuONPs to seem slightly aggregated. The high-magnification TEM image of the nanoparticles showed that the particles were crystalline, and the copper lattice could be observed [44]. A direct comparison of the TEM pictures shows that the uncapped CuONPs are more likely to aggregate than the thiol-capped nanoparticles. Observe that the size distribution of CuONPs modified by thiol is narrower than that of fundamental particles [45].

TEM results showed that CuONPs are well spread and have hexagonal shapes, and the size of the CuONPs that were made was between 30 and 50 nm. Using *A. vera* extract, the average size of the CuONPs that was made was about 34 nm [46]. In TEM micrographs, many primarily hexagonal CuONPs between 50 nm were seen [47]. An earlier study agreed that TEM analysis revealed CuO with a thiol cap has mean particle sizes of around 12 nm, while CuO without a thiol cap has about 47 nm. It was discovered that the particles were almost spherical [48].

Zeta potential analysis was performed to find the surface charges CuONPs gained, which can be utilized to find out more about the stability of the colloidal CuONPs. Zeta potential analyses were also used to determine the hydrodynamic size and strength of CuONPs. Particle stability, which

ultimately dictates NPs' varied applicability, is determined by the size of the zeta potential. Particles with a high zeta potential are often very stable nanoparticles. This tendency caused some nanoparticles to the group, decreasing their surface area. CuONPs need to be thoroughly ultrasonically treated for at least 15 min in a water bath to solve this issue. The outcome also indicates that the produced CuONPs exhibit repellent electrostatic forces, which cause the particles to monodispersity. The zeta potential of CuONPs was found to be − 35.7 mV.

The strength of the zeta potential, which ranges from 30 to + 30 mV, suggests that the colloidal system may be stable [49]. The zeta potential influences the stability of the nanoparticles in the solution. The more significant zeta potential values indicate less aggregation, which increases nanoparticle stability and results in smaller z-averaged hydrodynamic diameters. The strength of the nano-suspension decreases at lower zeta values because the nanoparticles flocculate more quickly [50]. The produced nanoparticles were moderately stable, which resulted in their monodispersity, according to the zeta potential of CuONPs in the current investigation, which was − 24.0 mV (Fig. 2a). The outcome was consistent with the zeta potential, which was 5.36 mV [51].

Additionally, It was observed that CuONPs with a zeta potential of 9 mV exhibited a strong antibacterial effect and enhanced toxicity [52]. It is well known that certain nanoparticles tend to aggregate, resulting in a smaller surface area for the remaining nanoparticles. Ultrasonication CuONPs can only fix this problem in a water bath for at least 15 min.

Figure 2b shows the average particle size for nanoparticles spanning from 39 to 150 nm: 71.62 ± 31.05 nm. Overall, CuONPs particle size was highly distributed between 40 and 80 nm, indicating they were synthesized at less than 100 nm. The nanoparticle size distribution spanned from 40 to 150 nm, and the average particle size was 71.62 ± 31.05 nm (Fig. 2b). Overall, CuONPs particle size was highly dispersed between 40 and 80 nm, indicating NPs were less than 100 nm (NPs 100 nm). The average diameter of CuONPs nanoparticles was 6.50 ± 1.50 nm. EDX analysis determines

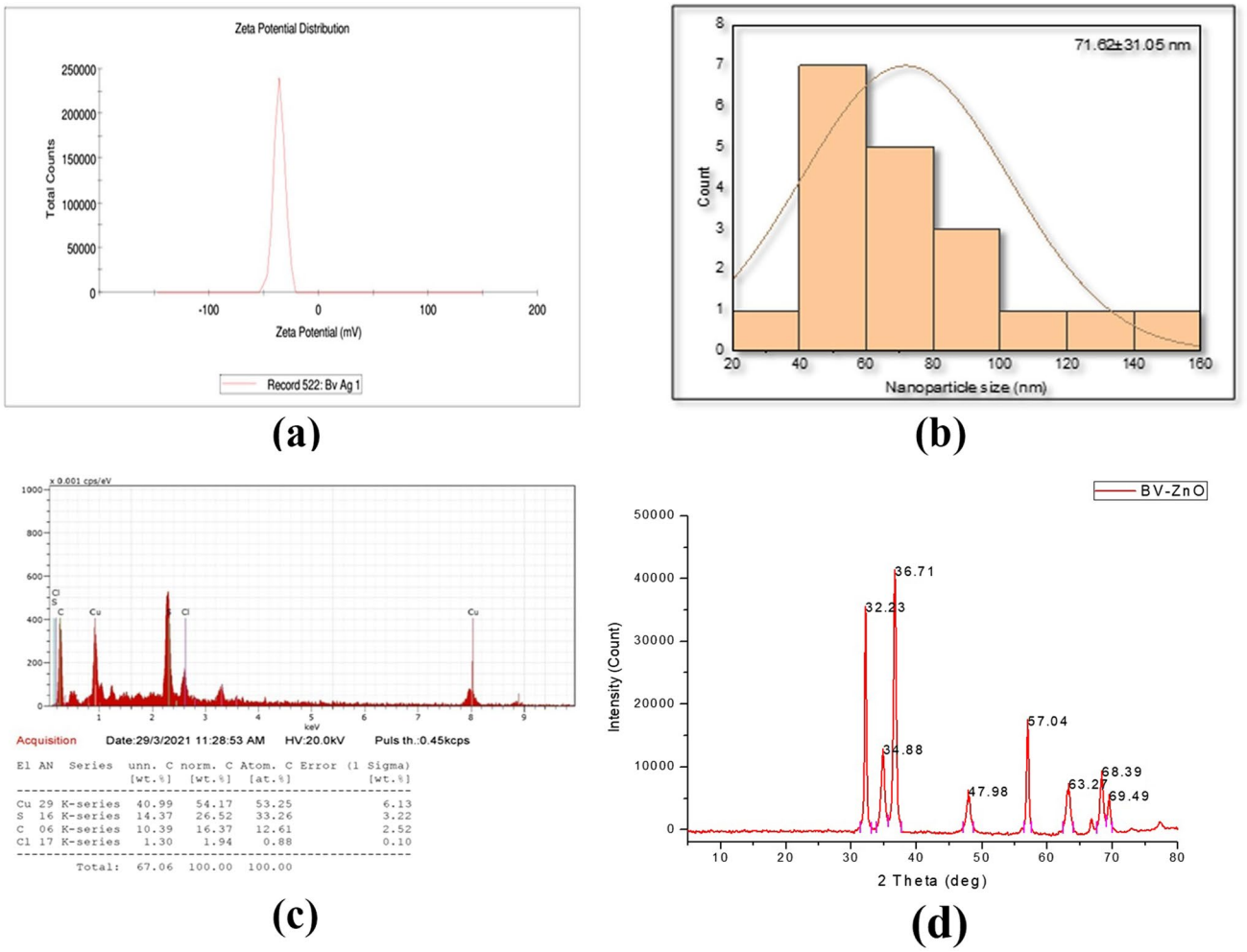

Fig. 2 **a** Surface zeta potential, (**b**) histogram analysis, (**c**) energy dispersive spectroscopy (EDS), and (**d**) X-ray diffraction analysis of CuONPs

the elemental composition of CuONPs. For example, it can detect metals and pollutants (Fig. 2c). Figure 2c shows an EDX signal in the copper region, validating the production of CuONPs. Copper nanocrystals have a 20 keV optical absorption peak due to surface plasmon resonance (SPR). Cu has a high EDX signal. EDAX showed the sample included copper oxide and other impurities (Fig. 2c). EDX determined the reaction mixture's elemental makeup. EDS of CuONPs showed pure copper (53.25%) and very little chloride (0.88%). But copper is the key component element in CuONPs (Fig. 2c). XRD pattern analysis of synthesized CuONPs revealed the crystalline nature (Fig. 2) which showed various small distinct diffraction peaks at 32.2, 34.8, 36.7, 47.9, 57.0, 63.2, 68.3, and 69.4. This represents (110), (− 111), (111), (− 112), (202), (− 113), (− 311), and (220) of the monoclinic phase structure of copper oxide nanoparticles, respectively. XRD pattern of CuONPs was exactly matched to the JCPDS database (80–0076). The mean grain size of CuONPs formed in the bioreduction process was measured using the Debye–Scherrer formula $D = k\lambda/\beta\cos\theta$, where D is the average crystalline size (Å), k is a constant 1, "λ" is the wavelength of X-ray source (0.1541 nm), β is the angular line full width at half maximum (FWHM) intensity in radians, and "θ" is the Bragg's angle. The average particle size of the synthesized CuONPs was calculated as 25.92 nm from the obtained XRD patterns. The *A. vera* CuONPs study concurred with the green CuONPs synthesis. [53–57].

2.5 Determination of MIC of CuONPs against respiratory tract-causing microbes

To examine liquid-cultured microorganisms, lower MIC detects the lowest growth-inhibiting medication, which showed good antibacterial activity. This study examined the MIC of CuONPs against respiratory tract microorganisms such as *S. aureus*, *P. aeruginosa*, *S. pyogen,* and *Candidarial* strains and *C. albicans* and *A. niger* for fungus strains. *S. aureus* strains have a lower CuONPs MIC (12 g/ml or 4 g/ml) than *P. aeruginosa* and *S. pyogenes*. *C. albicans* exhibited a lower MIC (12 g/ml) than *A. niger*. CuONPs' antibacterial activity was determined by plate microdilution. MIC antimicrobial concentrations hinder bacterial development. Table 2 shows that all microorganisms synthesized CuONPs with MICs against respiratory tract pathogens. *S. aureus* 2 g/mL or 4 g/mL, *P. aeruginosa* and *S. pyogenes* 4 g/mL or 8 g/mL, *C. albicans* 8 g/mL or 12 g/mL, and *A. niger* 12 g/mL or 16 g/mL. The results of experiments suggested CuONPs killed tested bacteria by producing ROS when they adhered to them. However, ROS species can be cleaned by antioxidants like enzymes or molecules like ascorbic acid when subjected to intracellular oxidative stress. [58].

2.6 Antimicrobial activity against respiratory tract-causing microbes

To synthesize and characterize CuONPs from *A. vera* leaf extract and evaluate antimicrobial activity against respiratory tract infection-causing microbes such as *P. aeruginosa*, *S. aureus*, and *S. pyogenes* for bacterial strains and *C. albicans* and *A. niger* for fungal strains. Herbal remedies were used. This study aims to determine the green synthesis of CuONPs using *A. vera* and evaluate antimicrobial activity against respiratory tract-causing microbes like *P. aeruginosa*, *S. aureus*, and *S. pyogenes* for bacterial strains and *C. albicans* and *A. niger* for fungal strains. This work investigated the antibacterial activity of copper acetate, plant extract, and CuONPs; CuONPs were more active than copper acetate and plant extract in all microbiological strains. CuONPs inhibited *Staphylococcus aureus* significantly more than *Pseudomonas aeruginosa*, *S. pyogenes*, *C. albicans*, and *A. niger* (Table 3 and Fig. 3a). Nanoparticles have a high surface area-to-volume ratio, are tiny, and disperse well to interact with microbial surfaces. CuONPs have a large surface area; thus, they interact with bacteria and perform antimicrobial actions [59]. Few findings on CuONP antibacterial research demonstrate they can destroy a wide spectrum of pathogens [60]. Also, they create hydroxyl radicals that bind to DNA and dismantle proteins by combining with their amino, sulfhydryl, and carboxyl groups, blocking enzymes from operating [61]. Inactive surface proteins are rendered

Table 2 Determination of MIC of CuONPs against respiratory tract infection-causing microbes (turbidity in broth)

Concentration (µg/ml)	Microbial strains				
	P. aeruginosa	*S. aureus*	*S. pyogenes*	*C. albicans*	*A. niger*
2 (µg/ml)	+	+	+	+	+
4 (µg/ml)	+	-	+	+	+
8 (µg/ml)	-	-	-	+	+
12 (µg/ml)	-	-	-	-	+
16 (µg/ml)	-	-	-	-	-
20 (µg/ml)	-	-	-	-	-
MIC (µg/ml)	4 or < 8	2 or < 4	4 or < 8	8 or < 12	12 or < 16

+, growth; -, no growth

Table 3 Evaluation of the antimicrobial activity of copper acetate, plant extract, and CuONPs against respiratory tract-causing microbes

Microbial strains	(50 µl)			Std. (30 µl)
	Copper acetate (mm)	Plant extract (mm)	CuONPs (mm)	
Bacteria strains				
P. aerugi-nosa	7.50	10.50	11.50	12.50
S. aureus	9.00	11.00	12.00	12.70
S. pyogenes	7.00	9.50	10.00	13.00
Fungal strains				
C. albicans	6.10	7.60	9.80	11.70
A. niger	6.00	7.40	9.00	11.00

Bacterial standard: chloramphenicol; fungal standard: fluconazole

less selective transporters by CuONPs, which prevent them from passing through cytoplasmic membranes. Marine actinomycetes recently showed how CuONPs are generated and used to attack bacteria [62].

2.6.1 In vitro antioxidant activity

DPPH is a stable-free radical containing hydrogen and exhibits a distinctive absorption peak at 517 nm. The ability of the CuONPS and *A. vera* extract to scavenge free radicals is illustrated in Fig. 3c. CuONPS was produced with plant exhibited strong free radical scavenging activity; *A. vera* extract was also examined for antioxidant activity and evaluated at concentrations of 10 µg/ml, 50 µg/ml, 100 µg/ml, 250 µg/ml, and 500 µg/ml that demonstrated an increase in free radical scavenging activity. The scavenging effect of CuONPS (85.89 ± 0.73%) was higher than that of *A. vera* extract (72.43 ± 1.58%) at 500 µg/ml. The scavenging activity of biosynthesised CuONPs was higher than that of fungal filtrate and slightly below that of ascorbic acid, the standard. Copper acetate did not have any ability to scavenge free radicals [63]. Compared to ascorbic acid, biosynthesized CuONPs of *A. vera* has potential antioxidant action.

Specific metabolites in plants are known to do a variety of valuable things. By changing the color of DPPH from purple to yellow, spectrophotometry was used to measure how much CuO nanoparticles were made with both a chemical and a green method reduced [64]. Biologically produced nanoparticles were better at eliminating free radicals than chemically made ones. This may be because of the capping substances found in plant extracts and on the surface of metals [65].

Potential antioxidant action against 2, 2'-diphenyl-1-picrylhydrazyl and H_2O_2 radicals were observed in *Pestalotiopsis microspora* of CuONPs [66]. The antioxidants in the plant extract react with DPPH to form 1,1-diphenyl-2-picryl hydrazine. As the concentration of *A. vera* extract in the test samples increases, the proportion of DPPH scavenged increases. Additionally, the change in color from dark purple to bright yellow is proportionate to the hydrogen atoms absorbed by the DPPH extract [67]. Numerous antioxidants in the extract may work in conjunction with one another [68]. During the manufacturing process of CuONPs, these metabolites are integrated. They adsorb on the surface of the CuONPs [69]. These CuONPs appear to have a high affinity for interacting with and decreasing DPPH due to their high surface area-to-volume ratio (Fig. 3c). Additionally, the data obtained suggested that the IC_{50} value for CuONPs was 5.21 g ml^{-1}.

2.6.2 In vitro anti-diabetic activity

Chronically elevated blood sugar levels are a hallmark of diabetes mellitus (DM), a metabolic disorder. The inability of body cells to respond normally to insulin is at the root of diabetes [70]. According to a study by the International Diabetes Federation (IDF) (2017), 425 million persons have diabetes, and this figure is anticipated to increase to 629 million by 2045 [71]. The amount of amylase inhibition that biosynthesised CuONPs and *A. vera* extracts was used to estimate its anti-diabetic effectiveness. At various concentrations, such as 10 µg/ml, 50 µg/ml, 100 µg/ml, 250 µg/ml, and 500 µg/ml, biosynthesized CuONPs significantly inhibit amylase. In all of the examined samples, it was found that the percentage of inhibition was lowest at a concentration of 10 µg/ml and maximum at a concentration of 500 µg/ml.

The α-amylase-inhibiting action of CuONPs and *A. vera* extracts was investigated, and the findings are shown in Fig. 4a. The anti-diabetic effect of CuONPs (95.46 ± 0.88%) was higher than *A. vera* extracts (68.34 ± 1.54%) at 500 µg/ml. Comparing the inhibitory activity of CuONPs and *A. vera* extracts against the α-amylase enzyme to that of acarbose, the results demonstrated that these biosynthesized CuONPs possess a considerable level of inhibitory action. Among the most important clinical approaches to treating diabetes is decreasing postprandial hyperglycemia. The two most important carbohydrate-hydrolyzing digestive enzymes, alpha-amylase and alpha-glucosidase, can be inhibited to accomplish this [72]. Stopping α-amylase and α-glucosidase from doing their jobs, which are in charge of breaking down carbohydrates, the blood glucose level can be kept within a safe range. Starch digestion is slowed by stopping these enzymes from working [73]. This is a key part of keeping diabetes under control. In this study, CuONPs made from extracts of roots and leaves showed different effects than crude extracts. Consistent with earlier studies [74], our results indicate that CuONPs have a modest inhibitory effect on α-amylase activity. During CuONPs treatment of cell lines, insulin mimic and insulin sensitization activity were found, and the resulting decrease in glucose concentration in cells was confirmed.

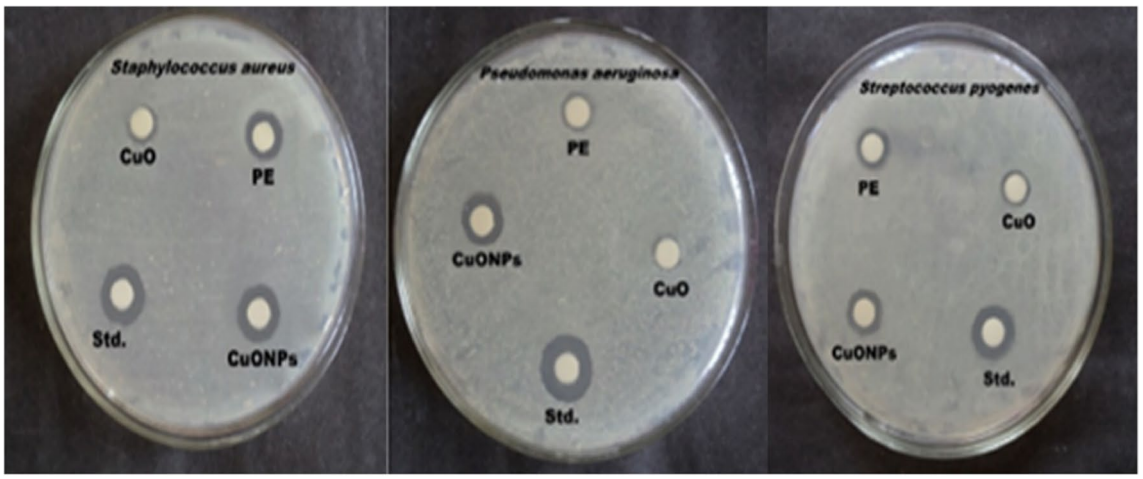

(a)

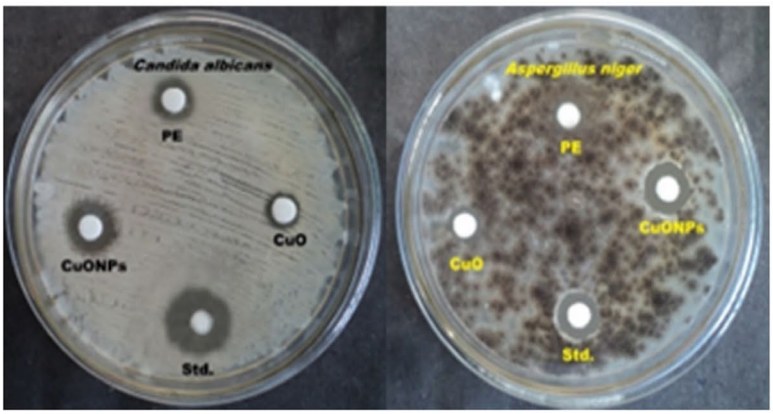

(b)

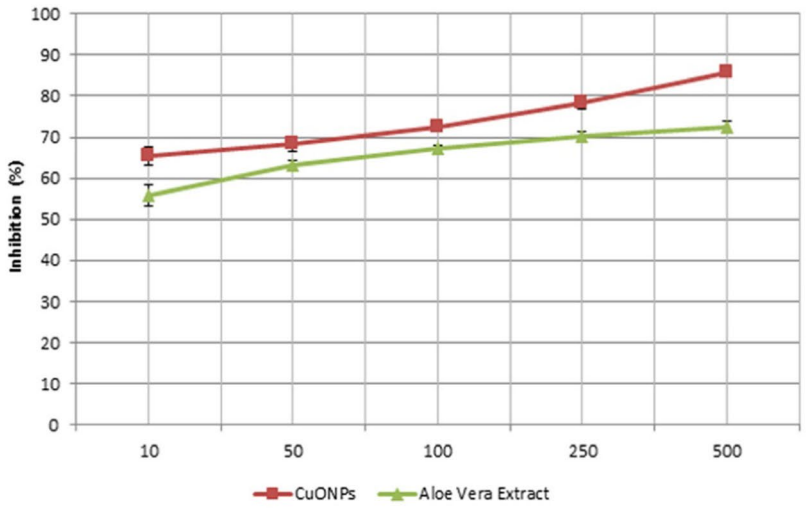

(c)

Fig. 3 **a** Bacterial strains, (**b**) fungal strains, and (**c**) free radical scavenging activity of CuONPs against DPPH

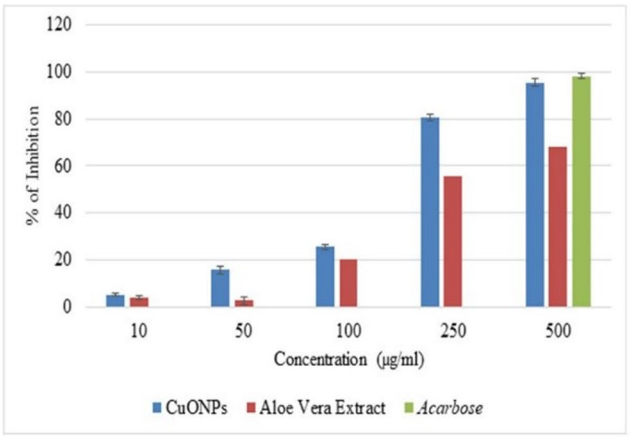

(a)

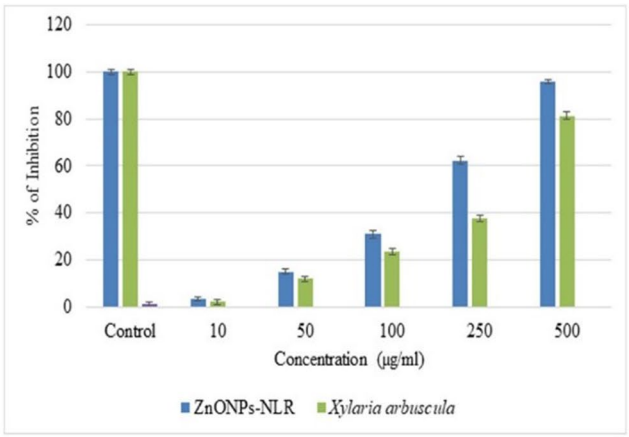

(b)

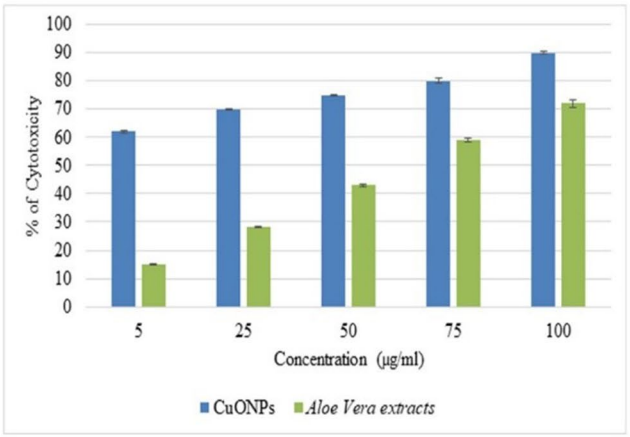

(c)

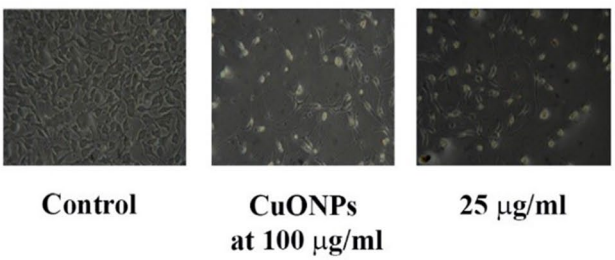

(d)

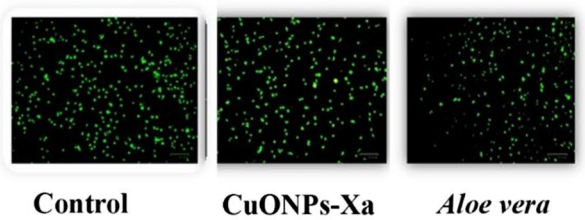

(e)

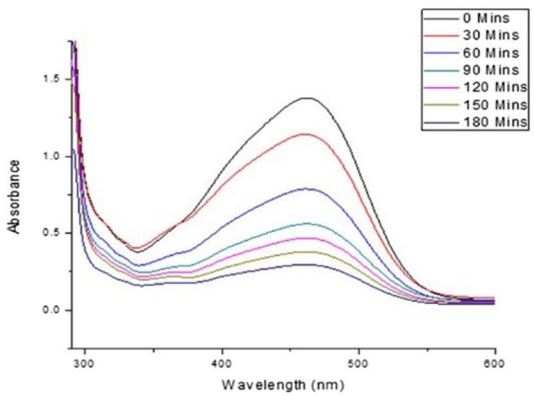

(f)

Fig. 4 **a** Antidiabetic (α amylase) activity. (**b**) Albumin denaturation inhibition activity. (**c**) MTT assay. (**d**) MTT assay of CuONPs and *A. vera* extracts on L929 cell lines at 100 µg/ml; (**e**) In vitro cytotoxic evaluation of L929 cell treated with CuONPs and *A. vera* extracts by acridine orange and ethidium bromide staining assay using fluorescent microscopy and (**f**) UV spectra of degradation of methylene blue dye using CuONPs

2.6.3 In vitro anti-inflammatory activity

Inflammation is the automatic response of the body's immune system to numerous pathogens, irritants, damaged cells, and harmful stimuli. Albumin denaturation is another way to test how well CuONPs work as an active anti-inflammatory agent. Proteins lose their secondary and tertiary structures and biological functions when stressed from the outside. This process is called denaturation. Inflammation is also known to be caused by the breakdown of proteins [75] to evaluate the anti-inflammatory potential of CuONPs and *A. vera* extracts by albumin denaturation assay.

The current study demonstrated the in vitro anti-inflammatory effect of biosynthesized CuONPs and *A. vera* extracts by preventing protein denaturation. Our biosynthesized CuONPs were discovered to be capable of controlling the denaturation of proteins implicated in the inflammatory process by reducing heat-induced albumin denaturation in a concentration-dependent way. The in vitro anti-inflammatory activity of CuONPs and *A. vera* extracts was investigated, and the findings are shown in Fig. 4b. The in vitro anti-inflammatory activity of CuONPS ($95.84 \pm 0.86\%$) was higher than that of *A. vera* extracts ($81.28 \pm 1.58\%$) at 500 µg/ml.

The in vitro anti-inflammatory effects of numerous metallic NPs and secondary metabolites have been demonstrated. Flavonoids are effectively capped, as shown by HPLC analysis of CuONPs. These flavonoids can reduce the production of inflammatory mediators like leukotrienes and prostanoids by inhibiting enzymes like cyclooxygenase (often selectively on COX-1 vs. COX-2), phospholipase A2, and lipoxygenases (enzymes producing eicosanoids) [76]. Evidence suggests CuO nanoparticles increase TNF levels in acute and chronic inflammatory conditions. Treatments for inflammatory diseases have included TNF, IL-1, and IL-6, which coordinate inflammatory responses in immune cells [77].

CuONPs worked to reduce inflammation in another way by keeping proteins (albumins) from losing their shape. When a protein is used, its secondary and tertiary structures change. This means the protein can no longer do its job [78]. Proteins and nucleic acids undergo denaturation when subjected to conditions that cause them to lose their native quaternary, tertiary, and secondary structures. A strong acid- or base-concentrated inorganic salt, organic solvents like alcohol or chloroform, radiation, or heat can all cause this [79]. The amount of albumin denaturation inhibition greatly increased with increasing concentrations of both CuONPs and aspirin. Therefore, CuONP might heal skin wounds brought on by inflammation.

It is difficult, if not impossible, to cure certain inflammatory diseases with the currently available medicines because of their inability to reduce inflammation and its symptoms [80]. For example, we know that CuONPs can pass through microbial membranes, so we can solve this issue by increasing drug penetration into the site of active microbial infection. Recent research into the development of CuONPs aims to prevent and regulate polluted and inflammatory sites for identification [81].

2.7 Cell line studies

2.7.1 MTT assay

The MTT assay depends on the enzyme mitochondrial dehydrogenase's capacity to convert a yellow tetrazolium dye into a formazan crystal. 3-(4,5-Dimethylthiazol-2-yl)-2,5-diphenyl tetrazolium bromide is a colorimetric assay measuring the impact on cell growth (MTT). The formation rate of formazan crystals is proportional to the total number of viable cells. The untreated group is a "positive control," with a 100% success rate [82]. Murine fibroblast L929 cells were used to examine the effects of both untreated and treated CuONPs on cell death in a petri dish. Mice fibroblast L929 cells are commonly used to assess cytotoxicity and could serve as a suitable in vitro skin formulation model. Most cytotoxicity testing uses L929 mouse fibroblast cells, which may be adequate as an in vitro screening model for topical skin formulations [83]. Figure 4c shows that the proportion of viable L929 cells decreased as the dose increased. As a result, it appears that both CuONPs and *A. vera* extracts have a potent cytotoxic effect (Fig. 4c). The MTT assay results of CuONPS ($90 \pm 0.36\%$) were higher than *A. vera* extracts ($72 \pm 1.42\%$) at 100 µg/ml. The biosynthesized CuONPs and *A. vera* extracts of different concentrations, 5 µg/ml, 25 µg/ml, 50 µg/ml, 75 µg/ml, and 100 µg/ml, were treated against L929 (murine fibroblast) cancer cell line. The result indicates that on using different concentrations of the CuONPs and *A. vera* extracts ranging from 5 to 100 µg/ml, cytotoxicity was more when 100 µlg/ml of the sample was used. The cell viability decreased by increasing concentrations.

Figures 4c and 3d show that MTT results showed that higher CuONPs caused more severe cytotoxicity. All tested types of nanoparticles significantly reduced the cells' ability to live when used at the highest concentration (100 g/ml). Fibroblasts L929 were especially sensitive to both unmodified and modified CuONPs. Nano-CuO toxicity was shown to be concentration dependent, as demonstrated [84]. The significance was reached for all treatments at 25 g/ml. Even though the amount of CuONPs used is very important, the size of the nanoparticles should also be considered. Many studies have shown

that the size of nanoCuO affects how dangerous it is. It is intriguing to speculate that the surface deposit could alter the interaction between cells and NPs, thus the future use of nanoparticles in biomedical settings [85]. The number of viable cells was significantly decreased at the highest measured concentration of CuONPs.

2.7.2 Acridine orange and ethidium bromide staining

Cell death was found with the AO/EB double staining assay. Acridine orange was taken up by living cells, which gave off a green glow. Ethidium bromide was only taken up by no longer alive cells, making damaged DNA glow red [86]. The acridine orange (AO)/ethidium bromide (EB) double staining concept takes into account both the shape of chromatin in a stained nucleus and how the fluorescent DNA-binding dyes acridine orange and ethidium bromide are taken up differently [87]. Based on their ability to destabilize cell membranes, CuONPs and other tested samples can be tested using the AO/EB assay [88]. Compared to the control, cultures exposed to CuONPs and *A. vera* extracts (Fig. 4e) revealed a reduction in the number of viable cells and an increase in the quantity of early apoptotic cells. Cells treated to a different concentration demonstrated that necrotic and late apoptotic cells increasingly predominated [89].

AO/EB analysis was used to examine how the shape of the nucleus of the treated L929 cell line changed. Damage to the DNA showed which cells were dying. Dual staining with AO/EB was used to look for different signs of apoptosis in nucleate alternations. Cells that were still alive and not dying looked green, while cells that were dying looked orange or red. As shown in Fig. 4e, when cells were exposed to CuONPs, the membranes broke down, and more lysosome vacuoles were made than in untreated control cells. Nanoparticles can get through the cellular membrane and affect the mRNA expression of suppression genes, which causes the production of reactive oxygen species (ROS) to rise in the cell [90]. This means that nanoparticles have a high ability to kill cells. When there is more ROS and oxidative stress, CuONPs negatively affect the cell's lipids, proteins, and nucleic acids [91]. Increased ROS can damage membranes through lipid peroxidation and protein denaturation, leading to cell death through necrosis and damage to DNA strands, which leads to cell death through apoptosis [92].

2.8 Photocatalytic degradation of methylene blue

Figure 4f and Table 4 show the effect of varying CuONPs concentrations on the degradation of methylene blue azo dye under 664-nm light (Fig. 4f and Table 4). CuONPs' photocatalytic and antibacterial potential has been studied extensively. The photocatalytic activity of the synthesized CuONPs was tested using MB dye degradation. After 30 min under sunlight, the dye's absorbance (at 664 nm) dropped. Changes in MB color from deep to light blue indicated deterioration. CuONPs degraded MB dye concentration dependently. CuONPs with methylene blue azo dye reduced nanocomposites' visual discomfort. CuONPs concentrations rise, increasing the degradation percentage. Keep the dye solution and photocatalyst sample in the dark for 30 min to maintain adsorption–desorption equilibrium. CuONPs were calculated using degradation efficiency (1 − C/C0)*100. Different (percent) amounts of methylene blue dye degrade organic compounds by photocatalysis.

Table 4 UV spectra depicting degradation of methylene blue

S. no	Time (min)	Initial absorbance (blank)	Sample absorbance	Percentage of degradation
1	0	1.379	1.379	0
2	30	1.379	1.143	17.11385062
3	60	1.379	0.788	42.85714286
4	90	1.379	0.561	59.31834663
5	120	1.379	0.468	66.06236403
6	150	1.379	0.3789	72.5235678
7	180	1.379	0.29614	78.52501813

3 Experimental

3.1 Collection of samples

The *A. vera* leaves sample was collected in February 2021 at Kumbakonam, Thanjavur district, Tamil Nadu, India.

3.2 Preparation of *A. vera* leaves extract

The collected leaves were washed with distilled water, dehydrated, and powdered for use. We prepared aqueous and methanolic leaf extracts. The aqueous and methanolic extracts each contain 50 ml. Both conical flasks received 1 g of *A. vera* powder. Mix for 30 min, then incubate overnight. Then, Whatman's No. 1 filter paper. The extract was then analyzed further.[93].

3.3 Qualitative analysis for phytochemical studies

From the crude methanol extracts of different species, secondary metabolites such as saponin, tannin, flavonoids, terpenoids, steroids, alkaloids, triterpenoids, polyphenol, anthraquinone, coumarins, and glycoside were screened using their respective tests [18, 94].

3.4 Quantitative analysis

3.4.1 Estimation of total phenols

Take 0.25 g of powdered leaves dissolved in 10 ml of ether and leave to sit for 15 min; 2.5 ml of extract was mixed with 5 ml of water, and then 1 ml of NH4OH and 2.5 ml of concentrated amyl alcohol were added. Incubate for 30 min for shading improvement. Measure the OD value at 505 nm [95].

3.4.2 Estimation of flavonoid

Take 0.25 g of leaves powder mixed with 10 ml of methanol and incubate for 30 min. Then separated, the extraction was done by utilizing Whatman No.1 filter paper. After separating, the extraction is transferred into a China dish. It is placed in the oven and allowed to evaporate. We weighed the flavonoid amount compared to an empty China dish [96].

3.4.3 Estimation of total terpenoids

Take 0.25 g of plant powder that was taken separately and soaked in alcohol (10 ml) for 24 h. After filtration, the extract was added to a 1:3 ratio of petroleum ether and transferred into a China dish. It is placed in the oven and allowed to evaporate. We weighed the terpenoid amount compared to an empty China dish [97].

3.5 Synthesis of copper oxide nanoparticles

Take 200 ml of deionized water mixed with 5 g of *A. vera* leaves powder; heat for 10 min and cool. The leaf extract was filtered by utilizing Whatman No.1 filter paper. After filtration, the leaf extract was used in nanoparticle synthesis. Take 0.56 g copper acetate monohydrate that was dissolved into deionized water (500 ml) and stirred magnetically for 5 min. Afterward, dropwise *A. vera* aqueous extract was added to the copper acetate solution under mixed conditions. The *A. vera* extract phytochemicals in contact with copper ions rapidly change the blue color into a green color solution. After 10 min, the brown color precipitate was sediment at room temperature, indicating the synthesis of copper oxide nanoparticles [98, 99]

3.6 Characterization of copper oxide nanoparticles [100]

The prepared CuONPs were characterized using UV–VIS spectrometer, Fourier transform infrared spectroscopy (FTIR), scanning electron microscopy (SEM), transmission electron microscopy (TEM), zeta potential, histogram, and EDX analysis.

3.7 Assessment of minimum inhibitory concentration (MIC) and turbidity

Take a conical flask with distilled water and 2.8 g nutrient media. The flask was well stirred; 1 ml of bacteria culture was added to 5 ml of nutrients, 1×106 cells/ml. A control contained 5 ml of nutrient media; 1 ml of 10 g/ml sample was added to inoculated nutrient media at 0 min. Each test tube received 1 ml of 2 g/ml, 4 g/ml, 8 g/ml, 12 g/ml, 16 g/ml, and 20 g/ml. The procedure was repeated twice at 30-min intervals. All sample concentrations were tested. Shaker rotated the tube at 250 rpm. A lab kept a sample and inoculums at 35 °C for 24 h. No visible bacterial growth at the lowest MIC level took 24 h [101].

3.8 Determination of antimicrobial activity

The disc diffusion method performed the antimicrobial activity [102]. In a boiling bath, take 28.0 g of nutrient media and dissolve it in 1 L of distilled water; 15 min at 15 Ibs (121 c) sterilizes the press. Pour the medium into sterile Petri dishes. Dissolve 39.0 g of PDA in 1 L of distilled water in a boiling water bath for a few minutes; 15 min at 15 Ibs (121 c) sterilizes the press. Then, acidify the media to pH 3.5 with sterile 10% tartaric acid. Never heat acid-added medium. Pour medium into sterile Petri plates. [103].

Respiratory tract infection-causing microbes were collected from microbial type culture collection (MTCC) at the Institute of Microbial Technology (IMTECH), Chandigarh, India. The respiratory tract infections causing microbes are *Staphylococcus aureus* (MTCC 3160), *Pseudomonas aeruginosa* (MTCC 358), and *Streptococcus pyogenes* (MTCC 102) for bacterial strains and *Candida albicans* (MTCC 183) and *Aspergillus niger* (MTCC 232) for fungal strains. A loop full of each microorganism was inoculated in proper culture slants and then incubated for 24 h for bacteria at 37 °C and 48 h for fungi at 25 °C. After incubation, growth was detected. Finally, the sample was kept at 2–8 °C for further use.

3.9 Preparation of leaf extract, CuONPs, and standard solutions for the experiment

We prepared the leaves to extract the utilized *A. vera* powder mixed into deionized water, and then CuONPs were designed using copper acetate and leaves extract. Standard solutions are chloramphenicol for bacterial strains and fluconazole for fungal strains. This is used in antimicrobial activities. The four-disc was prepared 6 mm in diameter using Whatman No.1 filter paper and put in hot air for sterilization. After sterilizing the disc, the 30 µl of leaf extract, CuONPs and standard solution was loaded. At last, the plates were kept under refrigeration for 24 h.

Disc diffusion technique utilizing tests finished antibiogram. Petri plates were set up by pouring 30 ml of nutrient agar (NA) medium for microorganisms and potato dextrose agar (PDA) for fungi. The twisted glass rod is disinfected and spreads the organism-containing fluid consistently on the plates utilizing 24-h culture of individual microbes. For the time being, bacterial inoculums were placed on nutrient agar plates, and fungal strains were placed on potato dextrose agar. Clean filter sheets (6 mm wide) containing each 30 l of plant concentrate, CuONPs, and standard were placed outside the vaccine agar plate using sterilized forceps. Bacterial strains were incubated for 24 h at 37 °C, while fungal strains were incubated for 48 h. A millimeter scale assesses the area of inhibition surrounding the disc.

3.9.1 In vitro antioxidant activity

DPPH was used to determine how well CuONPs and *A. vera* extracts eliminated free radicals. In 95% methanol, a 0.04%W/V DPPH solution was made. From the stock solution, 0.2 to 1.0 ml were put in the five test tubes and diluted to make 10 µg/ml, 50 µg/ml, 100 µg/ml, 250 µg/ml, and 500 µg/ml concentrations. A 0.5-ml solution of freshly made DPPH was mixed with the test drug. After 10 min, the absorbance at 517 nm was measured with a spectrophotometer. The reference was ascorbic acid.

3.9.2 Calculation

% scavenging of the DPPH free radical was measured using the following equation:

$$\text{DPPH Scavenging activity (\%)} = \frac{A_{\text{Control}} - A_{\text{Test}}}{A_{\text{Control}}} \times 100$$

The antioxidant activity of the leaf extracts was expressed as IC_{50} and compared with the standard. The IC_{50} value was defined as the extract concentration that inhibits the formation of DPPH radicals by 50% [104].

3.9.3 In vitro anti-diabetic activity

The ability to stop α-amylase from working was measured using a method described by Jini and Sharmila [105], with some changes. In short, test samples (CuONPs and *A. vera* extracts) with concentrations of 500 µg/ml, 250 µg/ml, 100 µg/ml, 50 µg/ml, and 10 µg/ml were mixed with 200 µl of an α-amylase solution (1.0 U/ml in phosphate buffer pH 6.9) and left at 25 °C for 30 min. After the pre-incubation, each tube got 400 µl of a 0.25% starch solution in a phosphate buffer (pH 6.9) to start the reaction. After 5 min at 37 °C, 1.0 ml of the DNS reagent (1% 3,5-dinitro salicylic acid and 12% sodium potassium tartrate in 0.4 M NaOH) was added to stop the reaction. The test tubes were then put in a bath of boiling water for 10 min, leaving them to cool to room temperature. The reaction mixture was then diluted by adding enough distilled water to bring the total volume to 10 ml. The absorbent (A) was then measured at 540 nm. By putting buffers in place of the extracts, 100% enzyme activity was shown in control incubations. The enzyme solution was replaced with buffer solution for blank incubation, and absorbance was measured. This was done so that the extracts could make absorbance. The amylase-blocking ability was given as a percentage and was calculated as follows:

$$\%\ \text{Inhibition} = \frac{A_{\text{control}} - \left(A_{\text{test}} - A_{\text{background}}\right)}{\text{Control}} \times 100$$

where A_{control}, A_{test}, and $A_{\text{background}}$ represented the absorbance of 100% enzyme activity, the test sample with and without the enzyme, respectively.

3.9.4 In vitro anti-inflammatory activity

Proteins becoming less stable are the main cause of inflammation. The effect of stopping proteins from breaking down was examined with a few changes. CuONPs were mixed with 500 µl of 1% bovine serum albumin, and *A. vera* extracts (500 µg/ml, 250 µg/ml, 100 µg/ml, 50 µg/ml, and 10 µg/ml) were added to a test sample. After 10 min at room temperature, this mixture was heated at 51 °C for 20 min. The solution was cooled to room temperature, and absorbance was measured at 660 nm. As a good control, acetylsalicylic acid was used. The experiment was done three times, and the percent inhibition for protein denaturation was figured out using the following: % Inhibition = 100 − (A2 − A1)*100/A0, where A_1 is the control's absorbance, A_2 is the test sample's absorbance, and A_0 is the positive control's absorbance. To find the IC_{50} values, a dose–response curve was made. IC_{50} is the concentration needed to get 50% of the maximum ability to eliminate something. All tests and analyses were done three times each, and the average was taken.

3.10 Cell line analysis

3.10.1 L929 cell line

Human dermal fibroblasts and L929 murine fibroblasts differed significantly in cell size and division rate. L929 murine fibroblasts could go through osteogenic and adipogenic differentiation using the conditions utilized in this study. In contrast, human dermal fibroblasts could only be made to go through osteogenic differentiation. The findings of Jääger and Neuman assert that it is challenging to stimulate human fibroblasts to undergo adipogenic differentiation because

these cells delay the induction of genes associated with adipogenesis [106]. The recent findings demonstrated that L929 murine fibroblasts could differentiate into osteogenic and adipogenic cells when cultivated in the medium with the supplements described in the methods. Another study shows the flexibility of L929 murine fibroblasts, which can be successfully coaxed to undergo differentiation under various culture conditions. The L929 mouse fibroblast cell line has benefited multiple experiment elements thanks to their demonstrated efficacy [107].

3.10.2 MTT assay

The monolayer cell culture was treated with trypsin, and the number of cells was changed to 1×10^6 cells/ml by adding 10% FBS to DMEM. Each well of the 96 healthy microtitre plates got 0.1 ml of the diluted cell suspension, which comprised about 10,000 cells. After 24 h, when a partial monolayer had formed, the supernatant was flicked off and washed once with medium, and 100 µl of different test concentrations of CuONPs and *A. vera* extracts were added to the partial monolayer in microtitre plates. The plates were kept at 37 °C for 3 days in an atmosphere with 5% CO_2. Every 24 h, a microscopic examination was done, and observations were made. After 72 h, the drug solutions in the wells were thrown away, and 50 µl of MTT in PBS was added to each well. The plates were gently shaken and kept at 37 °C with 5% CO_2 in the air for 3 h. The supernatant was removed, 100 µl of propanol was added, and the plates were gently shaken to dissolve the formed formazan. At 540 nm, a microplate reader was used to measure the absorbance. The following formula was used to figure out how much growth was stopped. The dose–response curves for each cell line determine the concentration of the test drug needed to slow cell growth by 50% (CTC50).

$$\%\ \text{of Growth Inhibiton} = \frac{\text{Mean OD of Individual test group}}{\text{Mean OD of Control group}} \times 100$$

3.10.3 EtBr/AO staining

L929 cells were put in a 24-well plate (1×10^5 cells ml^{-1}) and treated with CuONPs and *A. vera* extracts for 48 h at 37 °C. The CuONPs and *A. vera* extract-treated test samples for L929 were taken and washed with phosphate-buffered saline (PBS; pH 7.2). For staining, 1 µl of the AO/EtBr dye mixture, which has 10 mg/ml of acridine orange (AO) and 10 mg/ml of ethidium bromide (EtBr) in PBS, was added to 9 µl of a cell suspension (1×10^5 cells ml1) on a clean microscope coverslip. After letting the cells sit for a few minutes, they were looked at with a fluorescence microscope (Nikon Eclipse, Inc., Japan) at 40× magnification with an excitation filter set to 510–590 nm [108]. The number of apoptotic cells was worked out by using the formula below:

$$\textit{Percentage of apoptotic cells} = \frac{\textit{Total Number of apoptotic cells}}{\textit{Total Number of Normal and Apoptotic Cells}} \times 100$$

3.11 Photocatalytic activity

Nagaraju et al. [109] investigated the photocatalytic activity of CuONPs by decomposing MB dye. To attain adsorption equilibrium, successive additions of CuONPs powder, weighing 20 mg, 40 mg, 60 mg, 80 mg, and 100 mg, were made to a 100-ml aqueous solution of MB (10 mg/1) while constantly stirring for 1 h in the dark. After 20 min of exposure to room temperature sunlight, 5 ml of CuONPs-dye mixture was centrifuged, and the absorbance at 664 nm was measured. A control experiment was conducted without the presence of nanoparticles [110]. The degradation efficiency reached 85% within 180 min.

4 Conclusions

CuONPs can be synthesized using an aqueous extract of *A. vera L.*, offering a simple, low-cost, and environmentally friendly method. This discovery holds promise for exploring additional biomedical applications for nanoparticles, as they are expected to become an integral component of medical technology. In this particular study, the extract from *A. vera* was utilized to synthesize CuONPs. The study's findings emphasize the remarkable biological activity of these green nanoparticles, including antibacterial, antifungal, antioxidant, anti-diabetic, anti-inflammatory, cytotoxic, and wound-healing properties. The prepared CuONPs exhibit degradation efficiency reached 85% within 180 min. Consequently, the proposed procedure is efficient, simple, safe, and non-toxic, requiring no specialized equipment, organic solvents, or surfactants. Based on the outcomes, the green synthesized prepared materials exhibit excellent candidates for environmental application.

Acknowledgements The authors from King Khalid University extend their appreciation to the Deanship of Scientific Research at King Khalid University for funding this work through the Research Groups Program under Grant No. R.G.P.2/443/44.

Author contribution **Mahesh Narayanan:** conceptualization, methodology, experiments, formal analysis, writing – review and editing**. Ramesh Kannan Natarajan:** software, methodology**. Dayana Jeyaleela Gnana Sekar:** methodology, formal analysis**. Rojamalar Paramasivan:** methodology, formal analysis. **Balakumar Srinivasan:** conceptualization, funding acquisition, writing – review and editing**. I.M. Ashraf:** methodology, formal analysis**. Mohd. Shkir:** methodology, formal analysis**.**

Data availability Data will be made available upon request.

Declarations

Ethics approval and consent to participate Not applicable.

Consent for publication Not applicable.

Competing interests The authors declare no competing interests.

References

1. Park K (2007) Nanotechnology: what it can do for drug delivery. J Control Release Off J Control Release Soc 120:1
2. Iravani S (2011) Green synthesis of metal nanoparticles using plants. Green Chem 13:2638–2650
3. Bowker GC, Baker K, Millerand F, Ribes D (2009) Toward information infrastructure studies: ways of knowing in a networked environment. In: Hunsinger J, Klastrup L, Allen M (eds) International handbook of internet research. Springer, Dordrecht. https://doi.org/10.1007/978-1-4020-9789-8_5
4. Djahaniani H, Rahimi-Nasrabadi M, Saiedpour M et al (2017) Facile synthesis of silver nanoparticles using Tribulus longipetalus extract and their antioxidant and antibacterial activities. Int J Food Prop 20:922–930
5. Yang K, Zhang S, He J, Nie Z (2021) Polymers and inorganic nanoparticles: a winning combination towards assembled nanostructures for cancer imaging and therapy. Nano Today 36:101046. https://doi.org/10.1016/j.nantod.2020.101046
6. Yang K, Zhang S, He J, Nie Z (2021) Polymers and inorganic nanoparticles: a winning combination towards assembled nanostructures for cancer imaging and therapy. Nano Today 36:101046
7. Vijayakumar S, Malaikozhundan B, Saravanakumar K et al (2019) Garlic clove extract assisted silver nanoparticle – antibacterial, antibiofilm, antihelminthic, anti-inflammatory, anticancer and ecotoxicity assessment. J Photochem Photobiol B Biol 198:111558
8. Soni V, Raizada P, Singh P et al (2021) Sustainable and green trends in using plant extracts for the synthesis of biogenic metal nanoparticles toward environmental and pharmaceutical advances: a review. Environ Res 202:111622
9. Singh A, Singh NB, Hussain I et al (2017) Synthesis and characterization of copper oxide nanoparticles and its impact on germination of Vigna radiata (L.) R. Wilczek Trop Plant Res 4:246–253
10. Bai C, Tang M (2020) Toxicological study of metal and metal oxide nanoparticles in zebrafish. J Appl Toxicol 40:37–63
11. Nair PMG, Chung IM (2014) Impact of copper oxide nanoparticles exposure on Arabidopsis thaliana growth, root system development, root lignificaion, and molecular level changes. Environ Sci Pollut Res 21:12709–12722
12. Klein AD, Penneys NS (1988) Aloe vera. J Am Acad Dermatol 18:714–720
13. Rosca-Casian O, Parvu M, Vlase L, Tamas M (2007) Antifungal activity of Aloe vera leaves. Fitoterapia 78:219–222
14. Surjushe A, Vasani R, Saple DG (2008) Aloe vera: a short review. Indian J Dermatol 53:163
15. Joseph B, Raj SJ (2010) Pharmacognostic and phytochemical properties of Aloe vera linn an overview. Int J Pharm Sci Rev Res 4:106–110
16. Kumar S, Yadav A, Yadav M, Yadav JP (2017) Effect of climate change on phytochemical diversity, total phenolic content and in vitro antioxidant activity of Aloe vera (L.) Burm. f. BMC Res Notes 10:1–12
17. Nalimu F, Oloro J, Kahwa I, Ogwang PE (2021) Review on the phytochemistry and toxicological profiles of Aloe vera and Aloe ferox. Futur J Pharm Sci 7:1–21
18. Dharajiya D, Pagi N, Jasani H, Patel P (2017) Antimicrobial activity and phytochemical screening of Aloe vera (Aloe barbadensis Miller). Int J Curr Microbiol App Sci 6:2152–2162
19. Gorsi FI, Kausar T, Murtaza MA (2019) 27. Evaluation of antibacterial and antioxidant activity of Aloe vera (Aloe barbadensis Miller) gel powder using different solvents. Pure Appl Biol 8:1265–1270
20. Pourmorad F, Hosseinimehr SJ, Shahabimajd N (2006) Antioxidant activity, phenol and flavonoid contents of some selected Iranian medicinal plants. African J Biotechnol 5 (11):1142–1145
21. Pisoschi AM, Pop A (2015) The role of antioxidants in the chemistry of oxidative stress: a review. Eur J Med Chem 97:55–74
22. Durazzo A, Lucarini M, Souto EB et al (2019) Polyphenols: a concise overview on the chemistry, occurrence, and human health. Phyther Res 33:2221–2243
23. Karak P (2019) Biological activities of flavonoids: an overview. Int J Pharm Sci Res 10:1567–1574
24. Tian S, Sun Y, Chen Z, Zhao R (2020) Bioavailability and bioactivity of alkylresorcinols from different cereal products. J Food Qual. https://doi.org/10.1155/2020/5781356
25. Li Y, Kong D, Fu Y et al (2020) The effect of developmental and environmental factors on secondary metabolites in medicinal plants. Plant Physiol Biochem 148:80–89
26. Yang W, Chen X, Li Y et al (2020) Advances in pharmacological activities of terpenoids. Nat Prod Commun 15:1934578X20903555
27. Girreser U, Ugolini T, Çiçek SS (2019) Quality control of Aloe vera (Aloe barbadensis) and Aloe ferox using band-selective quantitative heteronuclear single quantum correlation spectroscopy (bs-qHSQC). Talanta 205:120109
28. Kaparakou EH, Kanakis CD, Gerogianni M et al (2021) Quantitative determination of aloin, antioxidant activity, and toxicity of Aloe vera leaf gel products from Greece. J Sci Food Agric 101:414–423
29. Thakur NS, Jilariya DJ, Gunaga RP, Singh S (2018) Positive allelospoly of Melia dubia Cav. spatial geometry improve quantitative and qualitative attributes of Aloe vera L. Ind Crops Prod 119:162–171
30. Usman RB, Adamu M, Isyaku IM, Bala HA (2020) Quantitative and qualitative phytochemicals and proximate analysis of Aloe vera (Aloe barbadensis miller). Int J Adv Acad Res 6(1):95–109
31. Kim MK, Choi YC, Cho SH et al (2021) The antioxidant effect of small extracellular vesicles derived from aloe vera peels for wound healing. Tissue Eng Regen Med 18:561–571
32. Rajendran A, Siva E, Dhanraj C, Senthilkumar S (2018) A green and facile approach for the synthesis copper oxide nanoparticles using Hibiscus rosa-sinensis flower extracts and it's antibacterial activities. J Bioprocess Biotech 8:324
33. Gebremedhn K, Kahsay MH, Aklilu M (2019) Green synthesis of CuO nanoparticles using leaf extract of catha edulis and its antibacterial activity. J Pharm Pharmacol 7:327–342
34. Vidovix TB, Quesada HB, Januário EFD et al (2019) Green synthesis of copper oxide nanoparticles using Punica granatum leaf extract applied to the removal of methylene blue. Mater Lett 257:126685
35. Nordin NR, Shamsuddin M (2019) Biosynthesis of copper (II) oxide nanoparticles using Murayya koeniggi aqueous leaf extract

and its catalytic activity in 4-nitrophenol reduction. Malaysian J Fundam Appl Sci 15:218–224
36. Pakzad K, Alinezhad H, Nasrollahzadeh M (2019) Green synthesis of Ni@ Fe3O4 and CuO nanoparticles using Euphorbia maculata extract as photocatalysts for the degradation of organic pollutants under UV-irradiation. Ceram Int 45:17173–17182
37. John MS, Nagoth JA, Zannotti M et al (2021) Biogenic synthesis of copper nanoparticles using bacterial strains isolated from an antarctic consortium associated to a psychrophilic marine ciliate: characterization and potential application as antimicrobial agents. Mar Drugs 19:263
38. Akter J, Sapkota KP, Hanif MA et al (2021) Kinetically controlled selective synthesis of Cu2O and CuO nanoparticles toward enhanced degradation of methylene blue using ultraviolet and sun light. Mater Sci Semicond Process 123:105570
39. Wang D, Xing G, Gao M et al (2011) Defects-mediated energy transfer in red-light-emitting Eu-doped ZnO nanowire arrays. J Phys Chem C 115:22729–22735
40. Lang J, Wang J, Zhang Q et al (2014) Rapid synthesis and photoluminescence properties of Eu-doped ZnO nanoneedles via facile hydrothermal method. Chem Res Chinese Univ 30:538–542
41. Lucarini M, Durazzo A, Kiefer J et al (2019) Grape seeds: chromatographic profile of fatty acids and phenolic compounds and qualitative analysis by FTIR-ATR spectroscopy. Foods 9:10
42. Achary LSK, Nayak PS, Barik B et al (2020) Ultrasonic-assisted green synthesis of β-amino carbonyl compounds by copper oxide nanoparticles decorated phosphate functionalized graphene oxide via Mannich reaction. Catal Today 348:137–147
43. Jovanović Ž, Radosavljević A, Šiljegović M et al (2012) Structural and optical characteristics of silver/poly (N-vinyl-2-pyrrolidone) nanosystems synthesized by γ-irradiation. Radiat Phys Chem 81:1720–1728
44. Sathiyaraj E, Thirumaran S (2020) Structural, morphological and optical properties of iron sulfide, cobalt sulfide, copper sulfide, zinc sulfide and copper-iron sulfide nanoparticles synthesized from single source precursors. Chem Phys Lett 739:136972
45. Woźniak-Budych MJ, Maciejewska B, Przysiecka Ł et al (2020) Comprehensive study of stability of copper oxide nanoparticles in complex biological media. J Mol Liq 319:114086
46. Faisal S, Jan H, Abdullah et al (2022) In vivo analgesic, anti-inflammatory, and anti-diabetic screening of Bacopa monnieri-synthesized copper oxide nanoparticles. ACS Omega 7:4071–4082
47. Alam MW, Aamir M, Farhan M et al (2021) Green synthesis of Ni-Cu-Zn based nanosized metal oxides for photocatalytic and sensor applications. Crystals 11:1467
48. Ribeiro AI, Dias AM, Zille A (2022) Synergistic effects between metal nanoparticles and commercial antimicrobial agents: a review. ACS Appl Nano Mater 5:3030–3064
49. Cacua K, Ordoñez F, Zapata C et al (2019) Surfactant concentration and pH effects on the zeta potential values of alumina nanofluids to inspect stability. Colloids Surf A Physicochem Eng Asp 583:123960
50. Kamble S, Agrawal S, Cherumukkil S et al (2022) Revisiting zeta potential, the key feature of interfacial phenomena, with applications and recent advancements. ChemistrySelect 7:e202103084
51. Divya M, Govindarajan M, Karthikeyan S et al (2020) Anti-biofilm and anticancer potential of β-glucan-binding protein-encrusted zinc oxide nanoparticles. Microb Pathog 141:103992
52 Halbus AF, Horozov TS, Paunov VN (2019) Strongly enhanced antibacterial action of copper oxide nanoparticles with boronic acid surface functionality. ACS Appl Mater \ Interfaces 11:12232–12243
53. Karunakaran G, Jagathambal M, Kumar GS, Kolesnikov E (2020) Hylotelephium telephium flower extract-mediated biosynthesis of CuO and ZnO nanoparticles with promising antioxidant and antibacterial properties for healthcare applications. JOM 72:1264–1272
54. Moon SA, Salunke BK, Saha P et al (2018) Comparison of dye degradation potential of biosynthesized copper oxide, manganese dioxide, and silver nanoparticles using Kalopanax pictus plant extract. Korean J Chem Eng 35:702–708
55. Rafique M, Shafiq F, Gillani SSA et al (2020) Eco-friendly green and biosynthesis of copper oxide nanoparticles using Citrofortunella microcarpa leaves extract for efficient photocatalytic degradation of Rhodamin B dye form textile wastewater. Optik (Stuttg) 208:164053
56. Fazlzadeh M, Rahmani K, Zarei A et al (2017) A novel green synthesis of zero valent iron nanoparticles (NZVI) using three plant extracts and their efficient application for removal of Cr (VI) from aqueous solutions. Adv Powder Technol 28:122–130
57. Gnanavel V, Palanichamy V, Roopan SM (2017) Biosynthesis and characterization of copper oxide nanoparticles and its anticancer activity on human colon cancer cell lines (HCT-116). J Photochem Photobiol B Biol 171:133–138
58. Applerot G, Lellouche J, Lipovsky A et al (2012) Understanding the antibacterial mechanism of CuO nanoparticles: revealing the route of induced oxidative stress. Small 8:3326–3337
59. Shende S, Ingle AP, Gade A, Rai M (2015) Green synthesis of copper nanoparticles by Citrus medica Linn. (Idilimbu) juice and its antimicrobial activity. World J Microbiol Biotechnol 31:865–873
60. Hassanien R, Husein DZ, Al-Hakkani MF (2018) Biosynthesis of copper nanoparticles using aqueous Tilia extract: antimicrobial and anticancer activities. Heliyon 4:e01077
61. Yoon K-Y, Byeon JH, Park J-H, Hwang J (2007) Susceptibility constants of Escherichia coli and Bacillus subtilis to silver and copper nanoparticles. Sci Total Environ 373:572–575
62. Rasool U, Hemalatha S (2017) Marine endophytic actinomycetes assisted synthesis of copper nanoparticles (CuNPs): characterization and antibacterial efficacy against human pathogens. Mater Lett 194:176–180
63. Ameena S, Rajesh N, Anjum SM et al (2022) Antioxidant, antibacterial, and anti-diabetic activity of green synthesized copper nanoparticles of Cocculus hirsutus (Menispermaceae). Appl Biochem Biotechnol 194:4424–4438. https://doi.org/10.1007/s12010-022-03899-4
64. Yasin A, Fatima U, Shahid S et al (2022) Fabrication of copper oxide nanoparticles using Passiflora edulis extract for the estimation of antioxidant potential and photocatalytic methylene blue dye degradation. Agronomy 12:2315
65. El Shafey AM (2020) Green synthesis of metal and metal oxide nanoparticles from plant leaf extracts and their applications: a review. Green Process Synth 9:304–339
66. da Silva PB, Machado RTA, Pironi AM et al (2019) Recent advances in the use of metallic nanoparticles with antitumoral action-review. Curr Med Chem 26:2108–2146
67. Jafarirad S, Mehrabi M, Divband B, Kosari-Nasab M (2016) Biofabrication of zinc oxide nanoparticles using fruit extract of Rosa canina and their toxic potential against bacteria: a mechanistic approach. Mater Sci Eng C 59:296–302
68. Do QD, Angkawijaya AE, Tran-Nguyen PL et al (2014) Effect of extraction solvent on total phenol content, total flavonoid content, and antioxidant activity of Limnophila aromatica. J Food Drug Anal 22:296–302
69. Nair PMG, Chung IM (2014) A mechanistic study on the toxic effect of copper oxide nanoparticles in soybean (Glycine max L.) root development and lignification of root cells. Biol Trace Elem Res 162:342–352
70. Muoio DM, Newgard CB (2008) Molecular and metabolic mechanisms of insulin resistance and β-cell failure in type 2 diabetes. Nat Rev Mol cell Biol 9:193–205

71. Simeni Njonnou SR, Boombhi J, Etoa Etoga MC et al (2020) Prevalence of diabetes and associated risk factors among a group of prisoners in the Yaoundé central prison. J Diabetes Res. 2020:5016327
72. Modh PG, Patel LJ (2022) In vitro screening on Alpha amylase and Alpha glucosidase inhibitory activities of some novel Quinazolinone derivatives. Res J Pharm Technol 15:4226–4229
73. Lu P, Li X, Janaswamy S et al (2020) Insights on the structure and digestibility of sweet potato starch: effect of postharvest storage of sweet potato roots. Int J Biol Macromol 145:694–700
74. Sarkar J, Chakraborty N, Chatterjee A et al (2020) Green synthesized copper oxide nanoparticles ameliorate defence and antioxidant enzymes in Lens culinaris. Nanomaterials 10:312
75. Gupta A, Kumar R, Ganguly R et al (2021) Antioxidant, anti-inflammatory and hepatoprotective activities of Terminalia bellirica and its bioactive component ellagic acid against diclofenac induced oxidative stress and hepatotoxicity. Toxicol Rep 8:44–52
76. Meshram MA, Bhise UO, Makhal PN, Kaki VR (2021) Synthetically-tailored and nature-derived dual COX-2/5-LOX inhibitors: structural aspects and SAR. Eur J Med Chem 225:113804
77. Tazi J, Begon-Pescia C, Campos N et al (2021) Specific and selective induction of miR-124 in immune cells by the quinoline ABX464: a transformative therapy for inflammatory diseases. Drug Discov Today 26:1030–1039
78. Mishra S, Looger LL, Porter LL (2019) Inaccurate secondary structure predictions often indicate protein fold switching. Protein Sci 28:1487–1493
79. El Knidri H, Belaabed R, Addaou A et al (2018) Extraction, chemical modification and characterization of chitin and chitosan. Int J Biol Macromol 120:1181–1189
80. Hassanzadeh K, Rahimmi A (2019) Oxidative stress and neuroinflammation in the story of Parkinson's disease: could targeting these pathways write a good ending? J Cell Physiol 234:23–32
81. Ishida T (2018) Antiviral activities of Cu2+ ions in viral prevention, replication, RNA degradation, and for antiviral efficacies of lytic virus, ROS-mediated virus, copper chelation. World Sci News 99:148–168
82. Velayutham M, Haridevamuthu B, Priya PS et al (2022) Serine O-acetyltransferase derived NV14 peptide reduces cytotoxicity in H2O2 induced MDCK cells and inhibits MCF-7 cell proliferation through caspase gene expression. Mol Biol Rep 49:9205–9215
83. Jamadar AT, Peram MR, Chandrasekhar N et al (2022) Formulation, optimization, and evaluation of ultradeformable nanovesicles for effective topical delivery of hydroquinone. J Pharm Innov. https://doi.org/10.1007/s12247-022-09657-7
84. Baskar V, Safia N, Sree Preethy K et al (2021) A comparative study of phytotoxic effects of metal oxide (CuO, ZnO and NiO) nanoparticles on in-vitro grown Abelmoschus esculentus. Plant Biosyst Int J Deal with all Asp Plant Biol 155:374–383
85. Rana A, Yadav K, Jagadevan S (2020) A comprehensive review on green synthesis of nature-inspired metal nanoparticles: mechanism, application and toxicity. J Clean Prod 272:122880
86. Tülüce Y, Hussein AI, Koyuncu I et al (2022) The effect of a bis-structured Schiff base on apoptosis, cytotoxicity, and DNA damage of breast cancer cells. J Biochem Mol Toxicol 36(10):e23148
87. Usman M, Khan RA, Khan MR et al (2021) A novel biocompatible formate bridged 1D-Cu (ii) coordination polymer induces apoptosis selectively in human lung adenocarcinoma (A549) cells. Dalt Trans 50:2253–2267
88. Chandrasekar A, Vasantharaj S, Jagadeesan NL et al (2021) Studies on phytomolecules mediated synthesis of copper oxide nanoparticles for biomedical and environmental applications. Biocatal Agric Biotechnol 33:101994
89. Lone SA, Wani MY, Fru P, Ahmad A (2020) Cellular apoptosis and necrosis as therapeutic targets for novel eugenol tosylate congeners against Candida albicans. Sci Rep 10:1–15
90. Makhdoumi P, Karimi H, Khazaei M (2020) Review on metal-based nanoparticles: role of reactive oxygen species in renal toxicity. Chem Res Toxicol 33:2503–2514
91. Yahya RAM, Azab AE, El Karema MS (2019) Effects of copper oxide and/or zinc oxide nanoparticles on oxidative damage and antioxidant defense system in male albino rats. EASJ Pharm Pharmacol 1:135–144
92. D'Arcy MS (2019) Cell death: a review of the major forms of apoptosis, necrosis and autophagy. Cell Biol Int 43:582–592
93. Tippayawat P, Phromviyo N, Boueroy P, Chompoosor A (2016) Green synthesis of silver nanoparticles in aloe vera plant extract prepared by a hydrothermal method and their synergistic antibacterial activity. PeerJ 2016:1–15. https://doi.org/10.7717/peerj.2589
94. Kumar A, Mahajan A, Begum Z (2020) Phytochemical screening and in vitro study of free radical scavenging activity of flavonoids of aloe vera. Res J Pharm Technol 13:593–598
95. Edeoga HO, Okwu DE, Mbaebie BO (2005) Phytochemical constituents of some Nigerian medicinal plants. African J Biotechnol 4:685–688
96. Mir MA, Parihar K, Tabasum U, Kumari E (2016) Estimation of alkaloid, saponin and flavonoid, content in various extracts of Crocus sativa. J Med Plants Stud 4:171–174
97. Indumathi C, Durgadevi G, Nithyavani S, Gayathri PK (2014) Estimation of terpenoid content and its antimicrobial property in Enicostemma litorrale. Int J ChemTech Res 6:4264–4267
98. Kumar PPNV, Shameem U, Kollu P et al (2015) Green synthesis of copper oxide nanoparticles using aloe vera leaf extract and its antibacterial activity against fish bacterial pathogens. Bionanoscience 5:135–139. https://doi.org/10.1007/s12668-015-0171-z
99. Kerour A, Boudjadar S, Bourzami R, Allouche B (2018) Eco-friendly synthesis of cuprous oxide (Cu2O) nanoparticles and improvement of their solar photocatalytic activities. J Solid State Chem 263:79–83
100. Rajeshkumar S, Tharani M, Jeevitha M, Santhoshkumar J (2019) Anticariogenic activity of fresh aloe vera gel mediated copper oxide nanoparticles. Indian J Public Heal Res & Dev 10(11):3664
101. Varghese A, Babu HM, Kukkera PN (2018) Comparative evaluation of efficacy of Murraya koenigii and chlorhexidine gluconate in the treatment of gingivitis: a randomized controlled clinical trial. J Indian Soc Periodontol 22:427
102. Prabakaran AS, Mani N (2018) Evaluation of antimicrobial activity of silver nanoparticle using Eichhornia crassipes leaves extract. J Pharmacogn Phytochem 7:1308–1311
103. Chatterjee AK, Chakraborty R, Basu T (2014) Mechanism of antibacterial activity of copper nanoparticles. Nanotechnology 25:135101
104. Bharathi D, Bhuvaneshwari V (2019) Synthesis of zinc oxide nanoparticles (ZnO NPs) using pure bioflavonoid rutin and their biomedical applications: antibacterial, antioxidant and cytotoxic activities. Res Chem Intermed 45:2065–2078
105. Jini D, Sharmila S (2020) Green synthesis of silver nanoparticles from Allium cepa and its in vitro antidiabetic activity. Mater Today Proc 22:432–438
106. Arseniy L, Anna M (2022) Osteogenic differentiation: a universal cell program of heterogeneous mesenchymal cells or a similar extracellular matrix mineralizing phenotype? Biol Commun 67:32–48

107. Liu M, Tao J, Guo H et al (2021) Efficacy of water-soluble pearl powder components extracted by a CO2 supercritical extraction system in promoting wound healing. Materials (Basel) 14:4458
108. Yuan C, Sun P, Ge X et al (2022) Rehmanniae radix leaves stimulates ROS-induced apoptosis on human mammary cancer cells through suppressing PI3K/AKT/mTOR and GSK3$β$ signaling pathway. Pharmacogn Mag 18:281
109. Nagaraju G, Nagabhushana H, Basavaraj RB et al (2016) Green, nonchemical route for the synthesis of ZnO superstructures, evaluation of its applications toward photocatalysis, photoluminescence, and biosensing. Cryst Growth Des 16:6828–6840
110. Abdelhakim HK, El-Sayed ER, Rashidi FB (2020) Biosynthesis of zinc oxide nanoparticles with antimicrobial, anticancer, antioxidant and photocatalytic activities by the endophytic Alternaria tenuissima. J Appl Microbiol 128:1634–1646

St. Joseph's College (Autonomous)
Tiruchirappalli - 620 002

DEPARTMENT OF COMMERCE

GRAND OPENING

TAX FILING

PROFESSOR IN-CHARGE

DR.A.FRANCIS VIJAYAKUMAR
ASSISTANT PROFESSOR
DEPARTMENT OF COMMERCE

STUDENTS IN-CHARGES

STANLY VIJAY R
VINOTH V

ST. JOSEPH'S INSTITUTE OF TALLY EDUCATION (J I T E)

ST. JOSEPH'S COLLEGE (AUTONOMOUS)

Accredited at A++ Grade (4th Cycle) by NAAC *Special Heritage Status awarded by UGC*
College with Potential for Excellence by UGC *DBT-STAR & DST-FIST sponsored College*

TIRUCHIRAPPALLI - 620 002.

Cell : 73730 20866 E-mail : jitesjctry@gmail.com Website : www.sjctni.edu

Dr. G. John
Centre Head

Rev. Dr. Arockiasamy Xavier SJ
Principal & Director

Certificate of Appreciation

This is to acknowledge the services rendered as a Resource Person by Dr.J.Vinoth Kumar, Assistant Professor in Commerce, St. Joseph's College, Trichy-2, for the Certificate Course in Tally Essentials during the year 2023-2024.

St.Joseph's Institute of Tally Education (JITE) appreciates his expertise and contribution in imparting computerized accounting skills to the student community.

19/2/24

Centre Head- JITE

Dr. G. JOHN, Ph.D.,
Centre Head - JITE
St. Joseph's College (Autonomous)
Tiruchirappalli-620 002

ST. JOSEPH'S INSTITUTE OF TALLY EDUCATION (J I T E)

ST. JOSEPH'S COLLEGE (AUTONOMOUS)

Accredited at A++ Grade (4th Cycle) by NAAC *Special Heritage Status awarded by UGC*
College with Potential for Excellence by UGC *DBT-STAR & DST-FIST sponsored College*

TIRUCHIRAPPALLI - 620 002.

Cell : 73730 20866 E-mail : jitesjctry@gmail.com Website : www.sjctni.edu

Dr. G. John
Centre Head

Rev. Dr. Arockiasamy Xavier SJ
Principal & Director

Certificate Appreciation

This is to acknowledge the services rendered as a Resource Person by Dr.M.Antony Jesuraja, Assistant Professor in Commerce, St. Joseph's College, Trichy-2, for the Certificate Course in Tally Essentials during the year 2023-2024.

St.Joseph's Institute of Tally Education (JITE) appreciates his expertise and contribution in imparting computerized accounting skills to the student community.

19/2/24

Centre Head- JITE

Dr. G. JOHN, Ph.D.,
Centre Head - JITE
St. Joseph's College (Autonomous)
Tiruchirappalli-620 002

ST. JOSEPH'S INSTITUTE OF TALLY EDUCATION (J I T E)

ST. JOSEPH'S COLLEGE (AUTONOMOUS)

Accredited at A++ Grade (4th Cycle) by NAAC *Special Heritage Status awarded by UGC*

College with Potential for Excellence by UGC *DBT-STAR & DST-FIST sponsored College*

TIRUCHIRAPPALLI - 620 002.

Cell : 73730 20866 E-mail : jitesjctry@gmail.com Website : www.sjctni.edu

Dr. G. John
Centre Head

Rev. Dr. Arockiasamy Xavier SJ
Principal & Director

Certificate of Appreciation

This is to acknowledge with gratitude the services of Dr. J.Vinoth Kumar, Assistant Professor, Department of Commerce who served as a Resource Person during the "14-Day Faculty Development Programme on TallyPrime" (virtual mode), jointly conducted by JITE and the Department of Commerce in the months of December 2023 and January 2024.

Principal

Pondicherry University (Central University)

&

The Society of St. Joseph's College

Tiruchirappalli - 620 002

PU-SJC MBA Twinning Programme

Dr. M. Antony Jesuraja,
M.Com., M.Phil., Ph.D.
Coordinator

Rev. Fr. M. Berchmans, SJ,
M.Com., M.Phil., NET, SET.
Asst. Coordinator

Date: 20th February 2024

Certificate of Appreciation

This is to certify that **Dr. Dennis Edward Fernando,** Assistant Professor, Department of Commerce, St. Joseph's College (Autonomous), Tiruchirappalli has been the Resource Person of Pondicherry University & St. Joseph's College MBA Twinning Programme for the year 2023-2024.

We thank and appreciate **Dr. Dennis Edward Fernando** for his enriching and informative lectures on **Business Law and Global Marketing.**

Dr. M. Antony Jesuraja
Coordinator
MBA Twinning Programme
St. Joseph's College (Autonomous)
Trichy-02.

College Seal

Pondicherry University (Central University)

&

The Society of St. Joseph's College

Tiruchirappalli - 620 002

PU-SJC MBA Twinning Programme

Dr. M. Antony Jesuraja,
M.Com., M.Phil., Ph.D.
Coordinator

Rev. Fr. M. Berchmans, SJ,
M.Com., M.Phil., NET, SET.
Asst. Coordinator

Date: 20th February 2024

Certificate of Appreciation

This is to certify that **Dr. J. Vinothkumar,** Assistant Professor, Department of Commerce, St. Joseph's College (Autonomous), Tiruchirappalli has been the Resource Person of Pondicherry University & St. Joseph's College MBA Twinning Programme for the year 2023-2024.

We thank and appreciate **Dr. J. Vinothkumar** for his enriching and informative lectures on **Business Environment and Information Technology & E-Business.**

Dr. M. Antony Jesuraja
Coordinator
MBA Twinning Programme
St. Joseph's College (Autonomous)
Trichy-02.

College Seal

Pondicherry University (Central University)

&

The Society of St. Joseph's College

Tiruchirappalli - 620 002

PU-SJC MBA Twinning Programme

Dr. M. Antony Jesuraja,
M.Com., M.Phil., Ph.D.
Coordinator

Rev. Fr. M. Berchmans, SJ,
M.Com., M.Phil., NET, SET.
Asst. Coordinator

Date: 20th February 2024

Certificate of Appreciation

This is to certify that **Dr. S. Kirubakaran,** Assistant Professor, Department of Commerce, St. Joseph's College (Autonomous), Tiruchirappalli has been the Resource Person of Pondicherry University & St. Joseph's College MBA Twinning Programme for the year 2023-2024.

We thank and appreciate **Dr. S. Kirubakaran** for his enriching and informative lectures on **International Trade and Finance.**

Dr. M. Antony Jesuraja
Coordinator
MBA Twinning Programme
St. Joseph's College (Autonomous)
Trichy-02.

College Seal

Pondicherry University (Central University)

&

The Society of St. Joseph's College

Tiruchirappalli - 620 002

PU-SJC MBA Twinning Programme

Dr. M. Antony Jesuraja,
M.Com., M.Phil., Ph.D.
Coordinator

Rev. Fr. M. Berchmans, SJ,
M.Com., M.Phil., NET, SET.
Asst. Coordinator

Date: 20th February 2024

Certificate of Appreciation

This is to certify that **Dr. A. Sahayaraj Alexander,** Assistant Professor, Department of Commerce, St. Joseph's College (Autonomous), Tiruchirappalli has been the Resource Person of Pondicherry University & St. Joseph's College MBA Twinning Programme for the year 2023-2024.

We thank and appreciate **Dr. A. Sahayaraj Alexander** for his enriching and informative lectures on **Marketing Management.**

Dr. M. Antony Jesuraja
Coordinator
MBA Twinning Programme
St. Joseph's College (Autonomous)
Trichy-02.

College Seal

ST.JOSEPH'S CA ACADEMY

(ICAI ACCREDITED COACHING CENTER FOR FOUNDATION COURSE)

ST.JOSEPH'S COLLEGE (AUTONOMOUS)

Accredited at A++ (4th Cycle) by NAAC
Special Heritage Status Awarded by UGC
Tiruchirappalli – 620 002, Tamil Nadu.

Date: 15th February 2024

Certificate of Appreciation

This is to acknowledge the services rendered as a Resource Person by Dr. B .Augustine Arockiaraj, Assistant Professor in Commerce, St. Joseph's College, Trichy-2, for CA Foundation Course during the year 2023-2024.

We thank and appreciate Dr. B. Augustine Arockiaraj, for his enriching and informative lectures on Business Environment and BCK.

Dr. B. Augustine Arockiaraj
Coordinator
St. Joseph's CA Academy
Trichy-02.

ICAI Accredited Centre
Foundation Course
St. Joseph's College (Autonomous),
Tiruchirappalli - 2, TN

PG & RESEARCH DEPARTMENT OF ENGLISH
ST. JOSEPH'S COLLEGE (AUTONOMOUS)
TIRUCHIRAPPALLI, TAMIL NADU

Certificate
OF APPRECIATION

awarded to

Dr Dennis Edward Fernando

Assistant Professor

Department of Commerce

for handling Bridge Course classes

for the first-year undergraduate students

from July to August 2023.

Dr. V. Francis Coordinator, Bridge Course	Rev. Dr. S. Paul Pragash SJ Coordinator, Bridge Course Advisory Committee	Rev. Dr. M. Arockiasamy Xavier SJ Principal St. Joseph's College

PG Dept. of Counselling Psychology & Counselling Centre

St. Joseph's College (Autonomous), Trichy - 02

A seminar on

Maintaining Healthy Relationships

for the Department of

B.COM Honours

I UG

Resource Persons

Ms. Christeeba
Counsellor

Ms. Christeela
Counsellor

DATE: 14.09.2023 - 11.45 A.M.

VENUE: SAIL HALL

Organizing committee

Ms. Shylin

Ms. Christeela

PG DEPARTMENT OF COUNSELLING PSYCHOLOGY &

COUNSELLING CENTER

ST. JOSEPH'S COLLEGE (Autonomous)

Tiruchirappalli-620 002

Report on 'Maintaining Healthy Relationship' – Seminar

Date: 14th September 2023

Audience: Students of I B.Com Honours

Introduction

A seminar series on topics like "Rising above Addiction," "Maintaining Healthy Relationships," and "Managing negative Emotions" is being organised by the PG Department of Counselling Psychology and the Counselling Centre. Members of the organising committee were Ms. Christeela and Ms. Shylin. 56 students from the Department of I B.Com Honours attended the seminar.

About the theme

Relationships are essential to happiness and leading fulfilling lives. This is due to the wide range of benefits they offer. Relationships give us access to friends and family who we can share our lives with as well as individuals who can support us when we need it. They frequently make us laugh a lot, which fills us with joy. Healthy relationships include communication, openness, respect, limits, affection, and mutual giving and taking. There is no power disparity.

At 11:45 am, the session began with a hymn of prayer at SAIL HALL. The seminar's master of ceremonies was **Ms. Shylin**. **Ms. Christeeba, Counsellor,** the first speaker. Ms. Christeeba discussed the value of relationship. She also emphasised the signs and major factors that make relationships successful and

healthy. And also she explained the factors in unhealthy relationships. She stressed the advantages of having healthy relationships. She also emphasised to the students about having good and healthy intrapersonal relationship.

At 12.30 p.m. **Ms. Christeela**, **Counsellor**, the second speaker talked about the importance of counselling and mental health. She explained the myths and misconceptions about counselling lingering in our society. She also conducted a mind game called cube personality test. This test helped the students to know their subconscious desires and goals.

This seminar covered a wide range of topics, such as:

- The value of open communication, mutual trust, support, congruence, boundaries and respect in relationships.
- The components of successful relationships
- How to set boundaries and say no
- How to handle conflict in a healthy way
- How to recognize the signs of an unhealthy relationship
- How to solve problems in relationships?
- Signs of Emotional Immaturity
- Personality
- Where to go for help if you are in such a relationship.
- Importance of counselling and mental health
- Myths and misconceptions about counselling
- Relevance of counselling
- The role of counsellor and client
- Who can come for counselling?
- Ethical issues in counselling
- Benefits of counselling
- Cube Personality Test

Conclusion

At 1:15 PM, the session came to a close. Ms. Christeela also offered help with the technology as a sign of support. The attendees in this seminar on "Maintaining Healthy Relationships" learned how to spot relationship toxicity and how to treat others with respect and compassion.

Dr. EMMANUEL AROCKIAM, S.J., Ph.D.
DIRECTOR - DEPT OF COUNSELLING PSYCHOLOGY
ST. JOSEPH'S COLLEGE (AUTONOMOUS)
TRICHY-620 002


GPS MAP CAMERA
Dept. of Counselling Psychology &
Counselling Centre, St. Joseph's
Latitude: 10.8284625
Longitude: 78.6904613
Date: 14 Sep 2023
Time: 11:56 AM
Google


GPS MAP CAMERA
Dept. of Counselling Psychology &
Counselling Centre, St. Joseph's
Latitude: 10.8284625
Longitude: 78.6904613
Date: 14 Sep 2023
Time: 11:56 AM
Google


GPS MAP CAMERA
Dept. of Counselling Psychology &
Counselling Centre, St. Joseph's
Latitude: 10.8284625
Longitude: 78.6904613
Date: 14 Sep 2023
Time: 11:56 AM
Google


GPS MAP CAMERA
Dept. of Counselling Psychology &
Counselling Centre, St. Joseph's
Latitude: 10.8284625
Longitude: 78.6904613
Date: 14 Sep 2023
Time: 11:46 AM
Google


GPS MAP CAMERA
Dept. of Counselling Psychology &
Counselling Centre, St. Joseph's
Latitude: 10.8284625
Longitude: 78.6904613
Date: 14 Sep 2023
Time: 11:56 AM
Google


GPS MAP CAMERA
Dept. of Counselling Psychology &
Counselling Centre, St. Joseph's
Latitude: 10.8284625
Longitude: 78.6904613
Date: 14 Sep 2023
Time: 11:46 AM
Google


GPS MAP CAMERA
Dept. of Counselling Psychology &
Counselling Centre, St. Joseph's
Latitude: 10.8284625
Longitude: 78.6904613
Date: 14 Sep 2023
Time: 11:46 AM
Google


GPS MAP CAMERA
Dept. of Counselling Psychology &
Counselling Centre, St. Joseph's
Latitude: 10.8284625
Longitude: 78.6904613
Date: 14 Sep 2023
Time: 11:56 AM


GPS MAP CAMERA
Dept. of Counselling Psychology &
Counselling Centre, St. Joseph's
Latitude: 10.8284625
Longitude: 78.6904613
Date: 14 Sep 2023
Time: 11:56 AM
Google


GPS MAP CAMERA
Dept. of Counselling Psychology & Counselling Centre, St. Joseph's
Latitude: 10.8284625
Longitude: 78.6904613
Date: 14 Sep 2023
Time: 11:56 AM
CRY OF THE EARTH
Google

ST. JOSEPH'S COLLEGE, TRICHY

PG DEPARTMENT OF COUNSELLING PSYCHOLOGY & COUNSELLING CENTRE

SEMINAR SERIES – ATTENDANCE LIST

DEPARTMENT: B.Com Honours

DATE: 14.09.23 TIME: 11.45 A.M. VENUE: SAIL AUDITORIUM

S.NO	NAME	D.NO	CLASS	SIGN
1.	K. Haridharshini	23UCR515	B.com (Honours)	
2.	S. Pooja Shri	23UCR521	B. com (Honours)	
3.	M. Jeyasri	23UCR523	B.Com(Honours)	M. Jeyasri.
4.	P. Parkavi rohini	23UCR547	B.Com(Honours)	
5.	M. Nithyasri	23UCR504	B.Com (Honours)	M. Nithyasri
6.	G. Josheka	23UCR503	B.com(Honours)	
7.	MEERA. K	23UCR506	B.com (H)	
8.	Nithya Rubiga. PR	23UCR553	B.com [Hons]	
9.	J. Jensiba Sharon	23UCR539	B.com (Hons)	
10.	S. Aparna	23UCR561	B.com(hons)	S. Aparna
11.	S. Fathima Juwairiyya	23UCR501	B.com (hons)	
12.	I. RITHANYA	23UCR555	B.com (hons)	
13.	D. Monica Nevis	23UCR530	B.Com (hons)	
14.	Ajitha Christy. J	23UCR517	B.com (hons)	
15.	S. Yuvapriya	23UCR534	B.Com(hons)	S. Yuvapriya
16.	V. Sai Rakshambika	23UCR505	B.Com(hon	V. Sai Raksha
17.	J. Mercy Ponica	23UCR533	B.com(hons)	
18.	M. Achutha	23UCR522	B.Com[hons]	Achutha
19.	Srinithi S	23UCR512	B.com(hons)	S. Srinithi
20.	Christo. J	23UCR502	B.com(hons)	J. Christo
21.	Savitha. M	23UCR531	B.Com(Hons)	Savitha
22.	Mathumetha. S	23UCR545	B.Com (Hons)	Sathu
23.	M. Roshini	23UCR552	B.com Hons	RR
24.	C. Vincy Baptisca	23UCR514	B.com(Hons)	C Vincy
25.	V. Bavithra Paulin Beney	23UCR532	B.com (Hons)	V.Bavi

DATE: TIME: VENUE:

S.NO	NAME	D.NO	CLASS	SIGN
1.	S Pragadeesh Waran	23UCR546	B.Com(Hons)	S. Pragadeesh Waran
2.	D. Naveen Kumar	23UCR529	I. B.Com Honours	D. Naveen Kumar
3.	A. Lobus Peter	23UCR538	I B.com Honours	A. Lobus Peter
4.	C. Darwin Isac	23UCR540	I B.com Honours	C. Darwin Isac
5.	A Vishnu pandian	23UCR511	I-B.Com Honours	A. Vishnupandian
6.	V.S. Aswin Karthick	23UCR556	I. B.com honours	V.S. Aswin Karthick
7.	S. AAKASH	23UCR525	I-B.com honours	S. Aakash
8.	R Sabari vasan	23UCR557	I. B.com honours	Sabari. R
9.	P Karthick	23UCR562	I Bcom Honours	P Karthick
10.	J.S. Rijo Godwin	23UCR536	I Bcom Hons	J.S. Rijo Godwin
11.	S. Dishi Kumar	23UCR541	Bcom Hons	S. Dishi Kumar
12.	R. Kishore	23UCR524	B.Com (Hons)	R. Kishore
13.	A. Suriya Ragavan	23UCR554	B.Com Hons	A. Suriya Ragavan
14.	S.T. Bhuvan Prasath	23UCR520	B.Com(Hons)	S.T. Bhuvan Prasath
15.	G. Patrick	23UCR526	B.Com(Hons)	G. Patrick
16.	S. Siva Ananth	23UCR550	B.Com(Hons)	S. Siva Ananth
17.	Nirmal. R	23UCR527	B.Com(Hons)	R. Nirmal
18.	Rahul. R	23UCR510	B.Com Honours	Rahul
19.	Roshan Paul H	23UCR507	B.Com(Hons)	R. Roshan Paul H
20.	DHANUSH KODI M	23UCR565	BCOM (HONS)	Dhanush
21.	JayaPrakash R	23UCR513	BComhons	J. Jaya Prakash R
22.	Srivasanth	23UCR549	B.com(Hons)	Srivasanth
23.	Aafiya Thameem	23UCR502	BCom (Hons)	Aafiya Thameem
24.	P. Reshma Banu	23UCR543	B.com(Hons)	P. Reshma Banu
25.	V. Shruthi	23UCR509	I.B.com(Hons)	V. Shruthi

S.NO	NAME	D.NO	CLASS	SIGN
1.	V. Akitha	23UCR559	B.com(Hons)	V. Akitha
2.	V. Pavithra	23UCR544	B.com(Hons)	V Pavithra
3.	M. Santhiya	23UCR564	BCOM(HONS)	A sandy
4.	R. Tejaswini	23UCR518	Bcom hons	R Tejaswini
5.	V. NilaSri	23UCR548	Bcom(Hons)	V. N.
6.	SM Ranganayaki	23UCR558	BCom Hons	S Ranga
7.				
8.				
9.				

PG Dept. of Counselling Psychology & Counselling Centre

St. Joseph's College (Autonomous), Trichy - 02

A seminar on

Maintaining Healthy Relationships

for the Department of

B. Voc.

Software Development & System Administration

Resource Person

Dr. A. Vimal Jerald., M.C.A., (NET), M.B.A., M.Phil., PGDBI., Ph.D

Assistant Professor in Computer Science

DATE: 12.09.2023 - 9.30 A.M.

VENUE: SAIL HALL

Organizing committee

Ms. Shylin

Ms. Christeela

PG DEPARTMENT OF COUNSELLING PSYCHOLOGY

& COUNSELLING CENTRE

ST. JOSEPH'S COLLEGE (Autonomous)

Tiruchirappalli-620 002

Report on Maintaining Healthy relationships – seminar

Date: 12.09.23

Audience: I, II & III B.Voc (SD & SA)

Introduction

The PG Department of Counselling Psychology and the Counselling Centre are hosting series of seminar on the topics "Managing Negative Emotions," "Rising above Addiction," and "Maintaining Healthy Relationships." Members of the organizing committee are Ms. Christeela and Ms. Shylin. 98 students from the Department of I, II & III B.Voc (SD & SA) attended the seminar on the topic 'Maintaining Healthy Relationships'.

About the theme

Building and maintaining healthy relationships is an important part of looking after our mental health. Humans are social being and relationships are essential to happiness and leading fulfilling life.. Relationships give us access to friends and family who we can share our lives with as well as individuals who can support us when we need. Healthy relationships include communication, openness, respect, limits, affection, and mutual giving and taking. There is no power disparity.

At 9:45 AM at Sail Hall, the session began with a prayer song. The seminar was hosted by Ms. Shylin. She introduced the topic and the resource person, Dr. A. Vimal Jerald to the gathering and requested him to take over the session. Healthy relationships are essential for living a meaningful and fulfilled life.

The quality of our relationships with others affects our personal and professional lives and our sense of belonging to a wider community and humanity. The more positive effort you put into a relationship, the healthier it should be. People in healthy relationships love and support each other. They help each other practically as well as emotionally. They are there for each other in the good times and the bad times. Healthy relationships are commonly based on respect, trust, open communication, equality, both shared and individual interests, understanding, honesty, care, emotional support, shared values around finances, child raising and other important matters.

Conclusion

At 11:15 AM, the session came to an end. The students provided their feedback about the session and thanked the counsellors for organizing the seminar. Ms. Christeela offered help with the technology as a sign of support. The attendees in this seminar on "Maintaining Healthy Relationships" learned how to spot relationship toxicity and how to treat others with respect and compassion.

Dr. EMMANUEL AROCKIAM, S.J., Ph.D.
DIRECTOR - DEPT OF COUNSELLING PSYCHOLOGY
ST. JOSEPH'S COLLEGE (AUTONOMOUS)
TRICHY-620 002


GPS MAP CAMERA
Dept. of Counselling Psychology &
Counselling Centre, St. Joseph's
Latitude: 10.8284625
Longitude: 78.6904613
Date: 12 Sep 2023
Time: 9:47 AM
Google


GPS MAP CAMERA
Dept. of Counselling Psychology &
Counselling Centre, St. Joseph's
Latitude: 10.8284625
Longitude: 78.6904613
Date: 12 Sep 2023
Time: 9:47 AM
Google

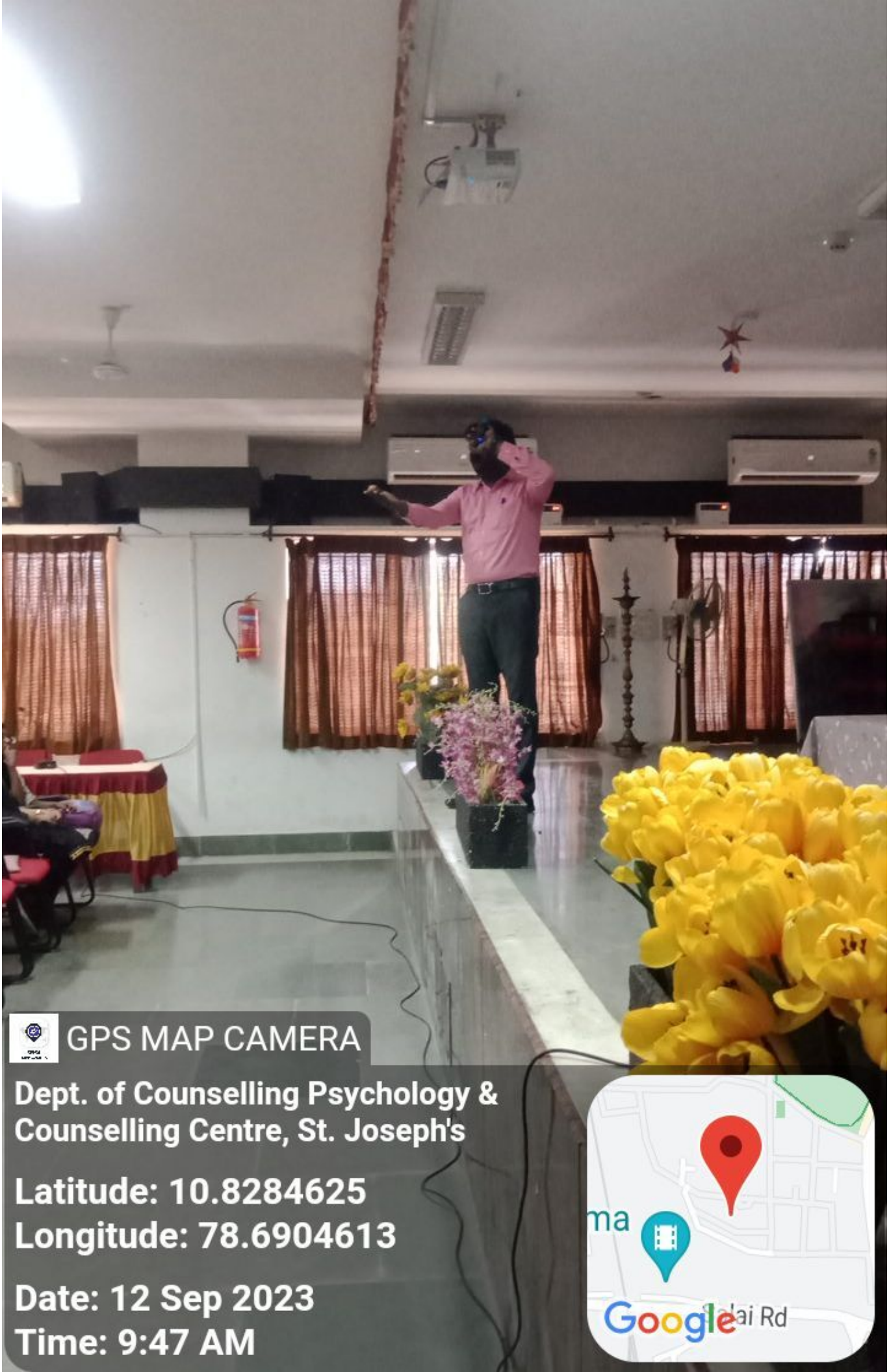
GPS MAP CAMERA
Dept. of Counselling Psychology &
Counselling Centre, St. Joseph's
Latitude: 10.8284625
Longitude: 78.6904613
Date: 12 Sep 2023
Time: 9:47 AM
Google


GPS MAP CAMERA
Dept. of Counselling Psychology &
Counselling Centre, St. Joseph's
Latitude: 10.8284625
Longitude: 78.6904613
Date: 12 Sep 2023
Time: 9:46 AM
Google

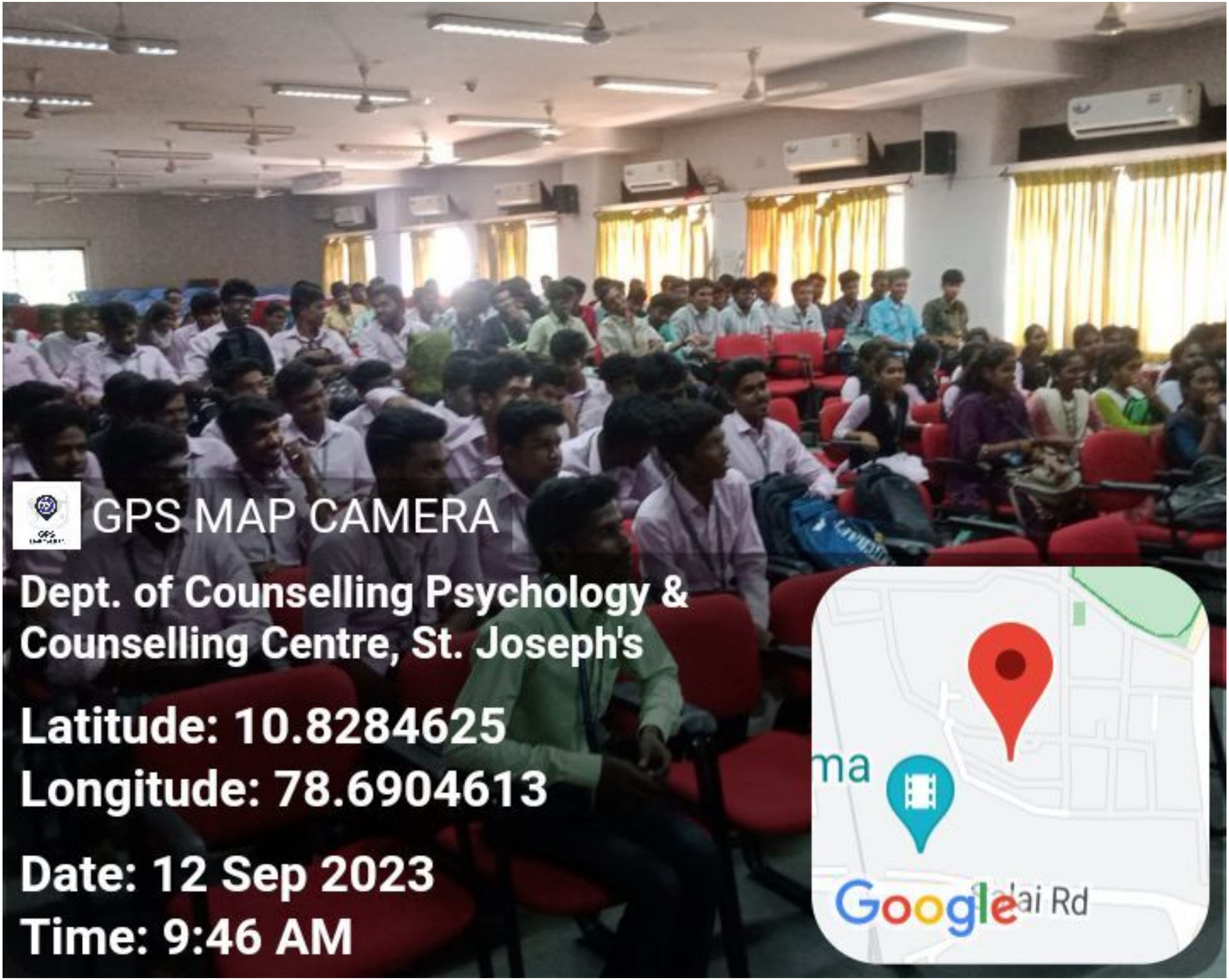
GPS MAP CAMERA
Dept. of Counselling Psychology &
Counselling Centre, St. Joseph's
Latitude: 10.8284625
Longitude: 78.6904613
Date: 12 Sep 2023
Time: 9:46 AM
Google


GPS MAP CAMERA
Dept. of Counselling Psychology &
Counselling Centre, St. Joseph's
Latitude: 10.8284625
Longitude: 78.6904613
Date: 12 Sep 2023
Time: 9:42 AM
Google


GPS MAP CAMERA
Dept. of Counselling Psychology &
Counselling Centre, St. Joseph's
Latitude: 10.8284625
Longitude: 78.6904613
Date: 12 Sep 2023
Time: 9:46 AM
Google


GPS MAP CAMERA
Dept. of Counselling Psychology &
Counselling Centre, St. Joseph's
Latitude: 10.8284625
Longitude: 78.6904613
Date: 12 Sep 2023
Time: 9:41 AM
Google


GPS MAP CAMERA
Dept. of Counselling Psychology &
Counselling Centre, St. Joseph's
Latitude: 10.8284625
Longitude: 78.6904613
Date: 12 Sep 2023
Time: 9:41 AM
Google

ST. JOSEPH'S COLLEGE, TRICHY

PG DEPARTMENT OF COUNSELLING PSYCHOLOGY & COUNSELLING CENTRE

SEMINAR SERIES – ATTENDANCE LIST

DEPARTMENT: B.Voc SD & SA

DATE: 12.09.23 TIME: 9.30 A.M. VENUE: SAIL HALL

S.NO	NAME	D.NO	CLASS	SIGN
1.	M. MOHANA PRIYA	22USS134	II B.VOC	M.Mohanapriya
2.	M DIVYA SRI	22USS105	II B.VOC	
3.	N. NIGARIGA	22USS112	II B.VOC	
4.	D Monica Mary Sheldon	22USS131	II B.VOC	
5.	V. Yuga roy	22USS130	II B.VOC	
6.	Chitra.C	22US3153	II B.VOC	
7.	Rithanya.R	22USS119	II B.VOC	
8.	S Dharani	22USS107	II B.VOC	
9.	R. Sowmiya	22USS108	II B.VOC	
10.	S. Bhavadharani	22USS115	II B.VOC	S.Bhavadharani
11.	R. Sobiya	22USS155	II B.VOC	
12.	J. Priyathershini	22USS154	II B.VOC	
13.	S. Denil Jones	23USS104	I-B.VOC	
14.	K. RUPA	23USS135	I-B.VOC	
15.	A. Ranjani	21USS106	III. B.VOC	
16.	S. Amala Delphine	21USS103	III. B.VOC	
17.	S. Janani	21USS129	III. B.VOC	
18.	A Manjula	21USS148	III. B.VOC	
19.	P. Parkavi	21USS109	III B.VOC	
20.	V. Dharmitha	21USS102	III B.VOC	
21.	S Monika	21USS134	III B.VOC	
22.	B. Faheema	21USS119	III B.VOC	
23.	S. Vidhya Sakthi	21USS117	III B.VOC	
24.				
25.				

ST. JOSEPH'S COLLEGE, TRICHY

PG DEPARTMENT OF COUNSELLING PSYCHOLOGY & COUNSELLING CENTRE

SEMINAR SERIES – ATTENDANCE LIST

DEPARTMENT: II B VOC (SD & SA)

DATE: 12.09.2023 TIME: 9.30 AM VENUE: Sail Hall

S.NO	NAME	D.NO	CLASS	SIGN
1.	Chella Sonathi.V	22USS139	B.Voc 'II'	
2.	Srinesh Srinivasan	22USS150	II B Voc	
3.	Karanraj.R	22USS140	"	
4.	Susai Antony Rosan A	22USS103	"	
5.	Vimala Santhosh	22USS142	"	
6.	Arnold Anand	22USS101	"	
7.	Janis Israel	22USS143	"	
8.	VISHAL	22USS102	"	
9.	S. Rishikaran	22USS118	"	
10.	F Renin Jose	22USS127	"	
11.	N. KESAVAN	22USS151	"	
12.	R. Locius Celestin	22USS123	"	
13.	A. INFANT WILKINGS	22USS145	"	
14.	NAVEEN.T	22USS114	"	
15.	Hari Prasanna.S	22USS120	"	
16.	Muthamizhselvan.S	22USS110	"	
17.	Muthu Palani .B	22USS144	"	
18.	Francis xavier.A	22USS146	"	
19.	Vincent Albert.C	22USS113	"	
20.	Shakthi.R	22USS132	"	
21.	Jo Harinesh	22USS135	"	
22.	SRINITHIKKUMARAN.S	22USS133	"	
23.				
24.				
25.				

S.NO	NAME	D.NO	CLASS	SIGN
1.	P. Kishore Dhilipkan	21USS112	III B.Voc(SDSM)	Kis
2.	Kishanth . B	21USS146	III B.Voc(SDSM)	K. Kishanth
3.	Riyas Aravinth . J	21USS107	III. BVOC	Riyas Aravinth
4.	Dhanushraj . S	21USS136	III - B.VOC	S Dhanush
5.	Sanjai . K	21USS121	III - B.VOC	Sanjai. K
6.	A. thilosavan . P	21USS122	III B.VOC	A.thilosavan.P
7.	Arunkumar . A	21USS137	III B.VOC	A. Arunkumar
8.	Dhinesh . J	21USS108	III B.VOC	J. Dhinesh
9.	S. Sree Ranganathan	21USS149	III. B.VOC	S. Sree Ranganathan
10.	Y. RAGUL GANDHI	21USS132	III - B.Voc	Ragul
11.	Nimalan . A	21USS116	III B.VOC	Amj
12.	Reegan . S	21USS138	III B.VOC	Reegan
13.	A Jerome Mang'	21USS111	III B.VOC SDSM	A Jerome
14.	MUGUNTHAN . K	21USS125	III . B. Voc (SDSM)	Mugunthan
15.	AKASH . C	21USS131	III . B. Voc (SDSM)	Akash
16.	RIO VIL JONSE	21USS124	III . B. Voc (SDSM)	Rio Vil Jonse
17.	ROSHAN NIVAS .	21USS101	III . B Voc (SDSM)	Roshan
18.	GOKULRAM T.K	21USS155	III B. Voc (SDSM)	Gokul
19.	JEEVA S	21USS152	III . B. Voc (SDSM)	S Jeeva
20.	PENTAL BHARATHI S	21USS123	III . B. Voc (SDSM)	
21.	Bino xavier Roy . k	21USS105	III . B. Voc (SDSM)	K Bino
22.	RAJESH KANNAN . P	21USS115	III . B. Voc (SDSM)	P Rajesh
23.	SELVA . P	21USS154	III . B. Voc (SDSM)	P Selva
24.	Karan . N	21USS127	III . B. Voc (SDSM)	N. Karan
25.	Ashok kumar . k	21USS113	III B.Voc (SDSM)	K. Ashok

26. M. Irudhaya Shalin Christ	21USS1141	III B.VOC	
27. James Irai anbu	21USS1114	III B.VOC	
28. Manikandan. R	21US21151	III B.VOC	
29. Manikandan. D	21USS1140	III B.VOC	
30.			

S.NO	NAME	D.NO	CLASS	SIGN
1.	J. Nicholas	22USS117	II B.Voc(SA&SS)	J. Nicholas
2.	S. Shyamsundar	22USS128	II B.Voc(SA&SS)	S. Shyamsundar
3.	T. Mohan gopu	22USS121	II B.Voc	T. Mohan gopu
4.	K. Sujya	22USS129	II B.Voc	K. Sujya
5.	N. Manoj	22USS125	II B.Voc	N. Manoj
6.	A. Girinath	22USS116	II B.Voc	A. Girinath
7.	P. Maruthu Pandiyan	22USS152	II B.Voc	P. Maruthu Pandiyan
8.	A. Leo joseph	22USS104	II B.Voc	A. Leo joseph
9.	Testy Benesha	23USS151	I B.Voc	Testy Benesha
10.	J. Rahamathunnisha	23USS109	I B.Voc	J. Rahamathunnisha
11.	P. Shapnila	23USS102	I B.Voc	P. Shapnila
12.	A. Almas	23USS131	I B.Voc	A. Almas
13.	Sowndharya V	23USS107	I B.Voc	Sowndharya V
14.	Harini C	23USS143	I B.Voc	Harini C
15.	Jeniliya J	23USS120	I B.Voc	Jeniliya J
16.	Esther vinoraja S	23USS122	I B.Voc	Esther vinoraja S
17.	KAUSALYA D	23USS153	I B.Voc	D. Kausalya
18.	Soumitha Jasmine C	23USS112	I B.Voc	Soumitha Jasmine C
19.	Mahalakshmi P	23USS139	I B.Voc	Mahalakshmi P
20.	Jeniliya G	23USS149	I B.Voc	G Jeniliya
21.	Amala Benita A	23USS121	I B.Voc	A Amala Benita
22.	Delsa A	23USS110	I B.Voc	A Delsa
23.	G. Arunthathi Askar	23USS147	I B.Voc	G. Arunthathi Askar
24.	S. Joys Dayana	23USS111	I B.Voc	S. Joys Dayana
25.				

PG Dept. of Counselling Psychology & Counselling Centre

St. Joseph's College (Autonomous), Trichy - 02

A seminar on
Maintaining Healthy Relationships

for the Department of

BOTANY

III UG, I & II PG

Resource Person

Ms. Christeeba
Counsellor

Ms. Shylin
Counsellor

DATE: 08.09.2023 - 11.45 A.M.
VENUE: AV HALL

Organizing committee

Ms. Shylin
Ms. Christeela

PG DEPARTMENT OF COUNSELLING PSYCHOLOGY

& COUNSELLING CENTRE

ST. JOSEPH'S COLLEGE (Autonomous)

Tiruchirappalli-620 002

Report on Maintaining Healthy relationships – seminar

Date: 08.09.23

Audience: III B.Sc Botany, I & II M.Sc Botany

Introduction

The PG Department of Counselling Psychology and the Counselling Centre are hosting series of seminar on the topics "Managing Negative Emotions," "Rising above Addiction," and "Maintaining Healthy Relationships." Members of the organizing committee are Ms. Christeela and Ms. Shylin. 94 students from the Department of III UG and I & II PG Botany attended the seminar on the topic 'Maintaining Healthy Relationships'.

About the theme

Building and maintaining healthy relationships is an important part of looking after our mental health. Humans are social being and relationships are essential to happiness and leading fulfilling life.. Relationships give us access to friends and family who we can share our lives with as well as individuals who can support us when we need. Healthy relationships include communication, openness, respect, limits, affection, and mutual giving and taking. There is no power disparity.

At 11:45 AM at AV Hall, the session began with a prayer song. The seminar was hosted by Ms. Shylin. She introduced the topic and the resource person, Ms. F.M Christeeba to the gathering and requested her to take over the session. She discussed the value of having wholesome connections and also emphasized that healthy relationships with partner and family members can

enhance life and make everyone feel good about themselves. They don't just happen though; healthy relationships take time to build and need work to keep them healthy. The more positive effort you put into a relationship, the healthier it should be. People in healthy relationships love and support each other. They help each other practically as well as emotionally. They are there for each other in the good times and the bad times. Healthy relationships are commonly based on respect, trust, open communication, equality, both shared and individual interests, understanding, honesty, care, emotional support, shared values around finances, child raising and other important matters.

Ms. Shylin summarized the session with the four aspects that a person must have for a healthy relationship: Relationship with self, Relationship with others, Relationship with Environment and Relationship with God. She also said that a features of a good relationship. A good relationship will accept you, love you, allow you to grow, gives you joy and meaning and live fully.

Conclusion

At 1:15 PM, the session came to an end. The students provided their feedback about the session and thanked the counsellors for organizing such a needful seminar. Ms. Shylin offered help with the technology as a sign of support. The attendees in this seminar on "Maintaining Healthy Relationships" learned how to spot relationship toxicity and how to treat others with respect and compassion.

Dr. EMMANUEL AROCKIAM, S.J., Ph.D.
DIRECTOR - DEPT OF COUNSELLING PSYCHOLOGY
ST. JOSEPH'S COLLEGE (AUTONOMOUS)
TRICHY-620 002

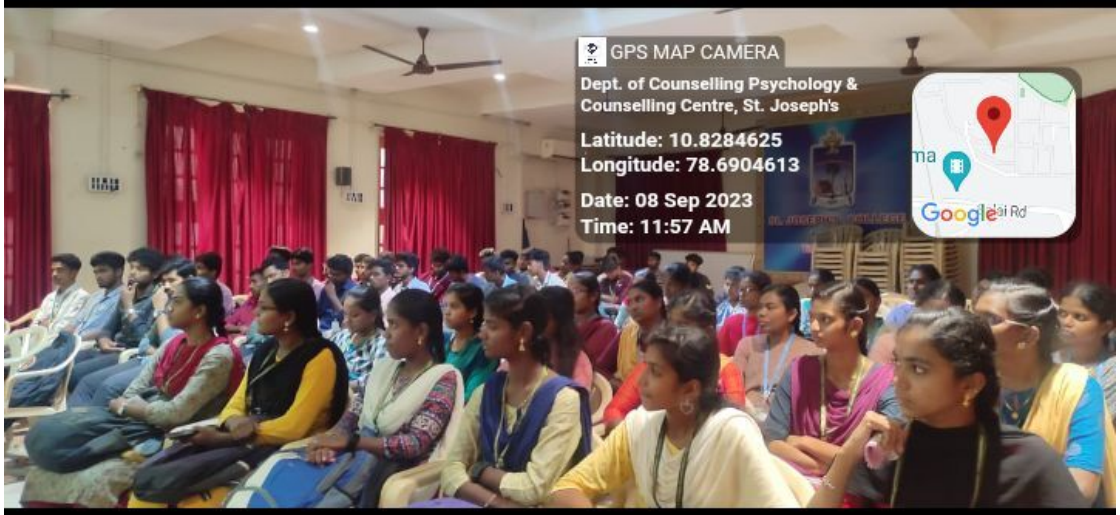
GPS MAP CAMERA
Dept. of Counselling Psychology &
Counselling Centre, St. Joseph's
Latitude: 10.8284625
Longitude: 78.6904613
Date: 08 Sep 2023
Time: 11:57 AM
Google


GPS MAP CAMERA
Dept. of Counselling Psychology & Counselling Centre, St. Joseph's
Latitude: 10.8284625
Longitude: 78.6904613
Date: 08 Sep 2023
Time: 11:57 AM
Google
ST. JOSEPH'S COLLEGE


GPS MAP CAMERA
Dept. of Counselling Psychology &
Counselling Centre, St. Joseph's
Latitude: 10.8284625
Longitude: 78.6904613
Date: 08 Sep 2023
Time: 11:57 AM
Google


GPS MAP CAMERA
Dept. of Counselling Psychology &
Counselling Centre, St. Joseph's
Latitude: 10.8284625
Longitude: 78.6904613
Date: 08 Sep 2023
Time: 11:57 AM
Google


GPS MAP CAMERA
Dept. of Counselling Psychology &
Counselling Centre, St. Joseph's
Latitude: 10.8284625
Longitude: 78.6904613
Date: 08 Sep 2023
Time: 11:57 AM
Google

ST. JOSEPH'S COLLEGE, TRICHY

PG DEPARTMENT OF COUNSELLING PSYCHOLOGY & COUNSELLING CENTRE

ATTENDANCE LIST

DEPARTMENT: Botany Pg - I, II UG - III AV HALL

DATE: 08/09/23 TIME: 11.45 AM TOPIC: Maintaining Healthy Relationship

S.NO	NAME	D.NO	CLASS	SIGN
1.	T. Jones Vinod	21UB0117	III B.Sc	
2.	Apradeesh	21UB0135	III B.Sc	
3.	anthiraban. R	21UB0133	III B.Sc	
4.	Abdulsha Beck. A	21UB0116	III. B.Sc	
5.	Karthickraj	22PB0102	II - M.Sc	
6.	V. Hemalazar	22PB0103	II. M.Sc	V. Hemalazar
7.	Adityan S.T.	21UB0124	III. B.Sc	
8.	T. Agaramuthalvan	21UB0143	III. B.Sc	T. Agathalvan
9.	Gnana manikandan. D.S	22PB0115	II. M.Sc	D.S
10.	AKILESH KANNA. S.T	21UB0122	III BSc.	
11.	Akash Banerjeeman	21UB0139	III. Bsc Botany	
12.	Naveen kumar. S	21UB0132	III Bsc Botany	
13.	Manikal. R	21UB0147	III Bsc Botany	
14.	V. Priyanka	23PB0108	I st MSc Botany	V. Priyanka
15.	A. Prakash	23PB0109	I M.Sc Botany	A. Prakash
16.	N. Pradeep	23PB0101	I M.Sc Botany	N. Pradeep
17.	A. Dimbiga devi	23PB0106	I M.Sc Botany	A. Dimbiga
18.	J. Angela Agnes	23PB0113	I M.Sc Botany	J. Angela Agnes
19.	M. Arun	23PB0107	I M.Sc Botany	M. Arun
20.	K. G. Selva Ganesh	21UB0109	III Bsc Botany	
21.	Kevin Deepak. P	21UB0102	III Bsc Botany	
22.	KEIN. Y.	22PB0113	II M.Sc Botany	Y. Kein
23.	Hariharan. S. M	21UB0152	III Bsc Botany	
24.	Rajarathinam. M	21UB0136	III B.Sc Botany	M.
25.	Dhanush. J	21UB0155	III-B.Sc Botany	

26.	Y. Aroan raj	21UB0129	III BSc	Y.
27.	AROCKIARAJ. A	21UB0154	III Bsc	Anto vinc
28.	Nandha kumar. S	21UB0188	III BSC	S.
29.	HARISH. R	21UB0131	III B Sc	
30.	R. SATHARNATH	21UB0123	III B Sc	R.
31.	V. Mohandass	21UB0125	III B.Sc	V. Mohan
32.	V. Vivian Lutin Ponson	21UB0103	III. B.Sc.	V.
33.	Shrithyaneni	21UB0134	III B.Sc.	S. Srini
34.	M. Dominick Raj	21UB0106	III B.Sc	M.
35.	A. Karthikeyan	21UB0144	III B.Sc	A. Karthikeya
36.	M. Karthikeyan	21UB0146	III BSC	M. Kartho.
37.	K. Lakshman	22PB0120	II M.Sc	K. Lakshm
38.	N. ANANDHAKUMARS	22PB0110	II M.Sc	N. Anand
39.	D. Samson Daniel	22PB0118	II M.Sc	D. Samson Dan
40.	R. Murali	22PB0119	II-M.Sc	R. Murali
41.	HARIHARAN. U	22PB0111	II- M.Sc	U. Hari
42.	Arun Surya. L.	23PB0107	I - M.Sc	Surya
43.	JEEVA. S	23PB0112	II M Sc	S.

S.NO	NAME	D.NO	CLASS	SIGN
1	P. JENAVA	21UB0111	III BSc, Botany	P Jenava
2	S. ABINAYASRI	21UB0126	III B.Sc Botany	S. Abinaya
3.	D. SHEEBA JESNI	21UB0114	III B.Sc Botany	D. Sheeba.
4	P. Jonefai Arc.	21UB0101	III BSc Botany	P. Jonefai
5	G. Stephy Axokiya mary	21UB0105	III BSC Botany	G. Stephy
6.	A R. Pradeepa	21UB0115	III Bsc Botany	A.R.
7.	M. NIVETHA.	21UB0140	III Bsc Botany	M. Nivetha
8.	K. MEENAKSHI	21UB0153	III BSc Botany	K. Meenakshi
9.	B. PRABAVATHY	21UB0145	III BSc Botany	B. Prabavathy
10.	J. SOWMIYA	21UB0121	III B.Sc Botany	J. Sowmiya
11	S Vishnupriya	21UB0130	III B.Sc Botany	S. Vishnupriya
12.	J. Margaret Sofiya	21UB0108	III B.Sc Botany	Margaret Sofiya
13.	S. Sarathi	23PB0117	I M.Sc Botany	S. Sarathi
14.	Sr. Josphin Daisin Amali.	23PB0104.	I M.Sc Botany	Sr. Amali.
15.	Joseph Irene Beulah. I	23PB0103	I M.Sc Botany	Irene
16.	S. Sandhiya	23PB0115	I M.Sc Botany	S. Sandhiya
17	B Raveena	23PB0116	I M.Sc Botany	B. Raveena
18	ASwini. P	23PB0112	I M.Sc BOTANY	Aswini P
19	Ambigadevi. R	23PB0106	I M.Sc Botany	Ambigadevi R
20	MONISHA. G	22PB0108	II M.Sc, BOTANY	G. Monisha
21	NISHA NANDHINI S	22PB0109	II M.Sc. Botany	S. Nisha
22	Sherlin Denis M	22PB0106	II M.Sc. Botany	Sherlin M.
23	Vinisha. K	22PB0101	II Msc Botany	Vinisha K
24	Jershia Hadrin J.	22PB0117	II MSc Botany	
25.	Thasma Jenifer.	22PB0114	II Msc Botany	
26.	Gloxy Mary	23PB0114	I MSc Botany	A. Gloxy Mary
27.	Savari Vinsiya	23PB0110	I MSc Botany	J. Savari Vinsiya
28.	Hameela	23PB0105	I MSc Botany	A Hameela

S.NO	NAME	D.NO	CLASS	SIGN
1.	MELYARASU IRUTHAYA NATHAN.P	23UBO136	I Year	
2.	Sachin. M	23UBO130	I year	
3.	Santhosh. A	23UBO121	I year	
4.	STANLEY. A	23UBO154	I year	
5.	S. Bodlean raju	23UBO127	I year	
6.	R. Bharath raj roi	23UBO118	I year	
7.	M. Bhuvaneshwaran	23UBO131	I year	
8.	V. JOE CRISPIN	22UBO102	II year	
9.	D. Sheyam	22UBO134	II year	
10.	R. vignesh	22UBO114	II year	
11.	A. Peter Alexander	22UBO119	II year	
12.	V. Allwin dinakar	22UBO118	II year	
13.	S. Karthikeyan	22UBO128	II Year	
14.	R. Ramish	22UBO151	II year	
15.	V. ENOCH	22UBO146	II year	
16.	G. Siva	22UBO133	II year	
17.	S. Rahul	22UBO101	II year	
18.	M. Britto	22UBO122	II year	
19.	D. PETERSON	22UBO130	IInd year	
20.	M. Subash	22UBO116	IInd year	
21.	C. KISHORE	22UBO124	IInd year	
22.	S. Antony	22UBO105	IInd year	
23.	S. JAYASEELAN	22UBO147	IInd Year	
24.				
25.				

PG Dept. of Counselling Psychology & Counselling Centre

St. Joseph's College (Autonomous), Trichy - 02

A seminar on

Maintaining Healthy Relationships

for the Department of

BOTANY

I & II UG

Resource Person

Rev. Dr. Emmanuel Arockiam, SJ

Head, Dept. of Counselling Psychology

DATE: 08.09.2023 - 9.30 A.M.

VENUE: AV HALL

Organizing committee

Ms. Shylin

Ms. Christeela

PG DEPARTMENT OF COUNSELLING PSYCHOLOGY &

COUNSELLING CENTER

ST. JOSEPH'S COLLEGE (Autonomous)

Tiruchirappalli-620 002

Report on 'Maintaining Healthy Relationship' – Seminar

Date: 08.09.2023

Audience: Students of I & II UG Botany, St. Joseph's College

Introduction

PG Department of Counselling Psychology & Counselling Centre are collaboratively conducting a seminar series on various theme like "Rising above Addiction," "Maintaining Healthy Relationship" & "Managing negative Emotions." **Ms. Shylin** and **Ms. Christeela** were the members in the organizing committee. There were 62 students from the Dept. of Botany participated in the seminar.

About the theme

Relationships are a cornerstone of happiness and living a full life. This is because they come with a wide array of rewards. Relationships provide us with friends and family to share our lives with and people who can help us out in tough times. They tend to bring us plenty of laughs and as a result lots of joy. Healthy relationships involve trust, openness, boundaries, respect, affection, communication, and mutual give-and-take. There is no imbalance of power.

Session started at 9.30 a.m. with a prayer song at AV HALL. Ms. Christeela was the master of ceremony of that seminar. **Ms. Christeela** introduced the resource person, **Rev. Dr. Emmanuel Arockiam, SJ** to take over the session. Fr. Emmanuel talked about the significance of having healthy relationships. In

addition to that, he highlighted the six success elements in relationships. He emphasized the benefits of being in good relationships. He also stressed the values behind the motto of Jesuits, 'making men and women for others' to the participants.

This seminar covered a variety of topics, including:

- The importance of communication, trust, and respect in relationships
- Elements of successful relationships
- How to set boundaries and say no
- How to deal with conflict in a healthy way
- How to recognize the signs of an unhealthy relationship
- Qualities of a healthy relationship and healthy people
- Where to get help if you are in an unhealthy relationship.

Conclusion

The seminar came to an end at 11.00 A.M. **Ms. Christeela** also showed her support by offering assistance with the technology. This seminar, '**Maintaining Healthy Relationship,'** helped the participants to recognize the signs of toxicity in relationships and how to approach other people with kindness and compassion.

Dr. EMMANUEL AROCKIAM, S.J., Ph.D.
DIRECTOR - DEPT OF COUNSELLING PSYCHOLOGY
ST. JOSEPH'S COLLEGE (AUTONOMOUS)
TRICHY-620 002


INTERPERSONAL RELATION
GPS MAP CAMERA
Dept. of Counselling Psychology &
Counselling Centre, St. Joseph's
Latitude: 10.8284625
Longitude: 78.6904613
Date: 08 Sep 2023
Time: 9:50 AM
Google


INTERPERSONAL RELATIONSHIPS
GPS MAP CAMERA
Dept. of Counselling Psychology &
Counselling Centre, St. Joseph's
Latitude: 10.8284625
Longitude: 78.6904613
Date: 08 Sep 2023
Time: 9:49 AM
Google


INTERPERSONAL RELATIONSHIPS
GPS MAP CAMERA
Dept. of Counselling Psychology &
Counselling Centre, St. Joseph's
Latitude: 10.8284625
Longitude: 78.6904613
Date: 08 Sep 2023
Time: 9:50 AM
Google


INTERPERSONAL RELATIONSHIPS
GPS MAP CAMERA
Dept. of Counselling Psychology &
Counselling Centre, St. Joseph's
Latitude: 10.8284625
Longitude: 78.6904613
Date: 08 Sep 2023
Time: 9:49 AM
Google


INTERPERSONAL RELATIONSHIPS
GPS MAP CAMERA
Dept. of Counselling Psychology &
Counselling Centre, St. Joseph's
Latitude: 10.8284625
Longitude: 78.6904613
Date: 08 Sep 2023
Time: 9:50 AM
Google


GPS MAP CAMERA
Dept. of Counselling Psychology &
Counselling Centre, St. Joseph's
Latitude: 10.8284625
Longitude: 78.6904613
Date: 08 Sep 2023
Time: 9:49 AM
Google


INTERPERSONAL RELATIONSHIPS
GPS MAP CAMERA
Dept. of Counselling Psychology &
Counselling Centre, St. Joseph's
Latitude: 10.8284625
Longitude: 78.6904613
Date: 08 Sep 2023
Time: 9:49 AM
Google


INTERPERSONAL RELATIONSHIPS
GPS MAP CAMERA
Dept. of Counselling Psychology &
Counselling Centre, St. Joseph's
Latitude: 10.8284625
Longitude: 78.6904613
Date: 08 Sep 2023
Time: 9:49 AM
Google


INTERPERSONAL RELATI
GPS MAP CAMERA
Dept. of Counselling Psychology &
Counselling Centre, St. Joseph's
Latitude: 10.8284625
Longitude: 78.6904613
Date: 08 Sep 2023
Time: 9:51 AM
Google


GPS MAP CAMERA
Dept. of Counselling Psychology &
Counselling Centre, St. Joseph's
Latitude: 10.8284625
Longitude: 78.6904613
Date: 08 Sep 2023
Time: 9:49 AM
Google

ST. JOSEPH'S COLLEGE, TRICHY

PG DEPARTMENT OF COUNSELLING PSYCHOLOGY & COUNSELLING CENTRE

SEMINAR SERIES – ATTENDANCE LIST

DEPARTMENT: BOTANY

DATE: 08/09/23 TIME: 9.30 AM VENUE: AV HALL

S.NO	NAME	D.NO	CLASS	SIGN
1.	REMO VINU . K	22UBO104	II B.Sc Botany	
2.	JONO GLADYS . D	22UBO141	II B.Sc Botany	
3.	VELVIZHE . A	22UBO113	II B. Sc. Botany	
4.	Neerajaa . R.	22UBO143	II BSc Bot	
5.	Mandkari . J	22UBO111	//	
6.	PThamarai Poriyenatchi	23UBO149	I BS Botany	
7.	J. Shophiya Mery	23UBO112	I BSC Botany	
8.	R. Dharshini	23UBO146	I BSc Botany	
9.	A. Anu Divya	23UBO147	I BSC Botany	
10.	M. Nithya Sri	23UBO111	I B Sc Botany	
11.	R. Dafni Angel	23UBO115	I st B.Sc Botany	
12.	M Vincelet catherina	23UBO 103	1st BSC Botany	
13.	M. Dhanusha	23UBO124	1st BSC Botany	
14.	A. CARMEL ROSITTA	23UBO133	1st BSC Botany	
15.	F. Ramya	23UBO105	1st BSC Botany	
16.	D. Vanika.	23UBO109	I st BSc Botany.	
17.	I. Rihana	23UBO150	I st B3 Botany	
18.	A. Jency	23UBO112	I st B.Sc Botany	
19.	M. Esvamiyal	23UBO117	I st B Sc Botany	
20.	L. Lavie Angelin	23UBO156	I st B.Sc Botany	
21.	A. Asvin Christiya	23UBO122	I st B.Sc. Botany	
22.	G. Saravanathi	23UBO114	I st B.Sc. Botany	
23.	R. Vani Sri	23UBO104	I st BSC Botany	
24.	B. Laksheetha	23UBO137	I st B.Sc. Botany	
25.	R. Nithyashree	23UBO102	I st B.Sc Botany	

S.NO	NAME	D.NO	CLASS	SIGN
1.	22UB0156 J. Jayclish	22UB0156	II-BSC	J. Jayclish
2.	S. Gilson Brenith	22UB0150	II. BSc Botany	
3.	B. Saranlin joy	22UB0112	II BSC Botany	
4.	S M. Prasanna	22UB0158	II B.Sc Botany	
5.	C. MANIKANDAN	23UB0139	I.B.SC BOTANY	C. Mani
6.	M. Arun kumar.	23UB0162	I B.Sc. Botany	M. Arun
7.	P. Sabarish	23UB0143	I B Sc Botany	P. Sabarish
8.	I Pearson	23UB0128	I. B.Sc Botany	
9.	I. Joshua Vincent	23UB0141	I. B.Sc botany	
10.	J. Pirajith	23UB0148	I. B.SC botany	
11.	R Jesus Stewalk	23UB0126	I B Sc Botany	R Stewalk
12.	M. Sundar	23UB0135	I B.Sc Botany	M. Sundar
13.	G. Anantha Kumar.	23UB0145	I B.Sc Botany	G. Anantha Kumar
14.	A. Patriseluan	23UB0153	I. B.Sc Botany	
15.	N. Nantha Kumar	23UB0126	I st B.Sc Botany	N. Nantha Kumar
16.	N. Thirupathi	23UB0108	I st BSc Bot	N. Th
17.	C. Saran.	23UB0113	I st B.Sc. Bot	C. Saran
18.	I Jominic Roshan	23UB0129	I st B Sc Botany	J. R
19.	C. Kabilan	23UB0120	I st B.Sc Botany	C. Kabilan
20.	G. Balasubbiramani	23UB0138	I st B Sc Botany	
21.	S. Sakthi Subbiah	23UB0110	I st B.Sc Botany	S. Sakthi
22.	S. BRUTHAYA RAJA	23UB0134	I st B.Sc Botany	S. BRUTHAYA RAJA.
23.	M. Subash	23UB0144	I st B Sc Botany	
24.	V. ALBERT	23UB0151	I st B.Sc Botany	V. Albert
25.				

S.NO	NAME	D.NO	CLASS	SIGN
1.	S. Priyadharshini	22UB0125	II - BSC. Botany	S Priyadharshini
2.	M Harini	22UB0132	II B.Sc Botany	Harini
3.	E. Pavithra	22UB0135	II Bsc Botany	E Pavithra.
4.	E. Sowmiya	22UB0160	II BSC Botany	E Sowmiya.
5.	S. Deepika	22UB0161	II Bsc Botany.	S. Deepika
6.	R. Dhanalakshmi	22UB0153	II. BSC Botany	R. Dhanalakshmi
7.	S. Jayalakshmi	22UB0158	II. BSC Botany	S Jayalakshmi
8.	P. Sarala	22UB0117	II. B.Sc Botany	P. Sarala
9.	P. Asleena Sagi	22UB0111	II B.Sc Botany	P Asleena
10.	B. Jayashree	22UB0157	II B.Sc Botany	B Jayashree
11.	B.S. Vayathri shri	22UB0159	II. BSC Botany	B.S Vayathri shri
12.	K. Valarmathi	22UB0155	II B.Sc Botany.	K Valarmathi
13.	J. Avaira John Kiruba	22UB0127	II B.Sc Botany	J. Avaira John Kiruba
14.				
15.				
16.				
17.				
18.				
19.				

PG Dept. of Counselling Psychology & Counselling Centre

St. Joseph's College (Autonomous), Trichy - 02

A SEMINAR ON

Maintaining Healthy Relationships

for the Department of

ECONOMICS

Shift I

I & II UG

Resource Person

Rev. Dr. Emmanuel Arockiam, SJ

Head, Dept. of Counselling Psychology

Organizing committee

MS. SHYLIN

MS. CHRISTEELA

DATE: 29 August 2023
12.00 P.M.

VENUE: AV HALL

PG DEPARTMENT OF COUNSELLING PSYCHOLOGY &

COUNSELLING CENTER

ST. JOSEPH'S COLLEGE (Autonomous)

Tiruchirappalli-620 002

Report on 'Maintaining Healthy Relationship' – Seminar

Date: 29th August 2023

Audience: Students of I & II UG Economics, St. Joseph's College

Introduction

PG Department of Counselling Psychology & Counselling Centre are collaboratively conducting a seminar series on various theme like "Rising above Addiction," "Maintaining Healthy Relationship" & "Managing negative Emotions." **Ms. Shylin** and **Ms. Christeela** were the members in the organizing committee. There were 68 students from the Dept. of Economics participated in the seminar.

About the theme

Relationships are a cornerstone of happiness and living a full life. This is because they come with a wide array of rewards. Relationships provide us with friends and family to share our lives with and people who can help us out in tough times. They tend to bring us plenty of laughs and as a result lots of joy. Healthy relationships involve trust, openness, boundaries, respect, affection, communication, and mutual give-and-take. There is no imbalance of power.

Session started at 12.00 p.m. with a prayer song at AV HALL. Ms. Christeela was the master of ceremony of that seminar. **Ms. Christeela** introduced the resource person, **Rev. Dr. Emmanuel Arockiam, SJ** to take over the session. Fr. Emmanuel talked about the significance of having healthy relationships. In

addition to that, he highlighted the six success elements in relationships. He emphasized the benefits of being in good relationships. He also stressed the values behind the motto of Jesuits, 'making men and women for others' to the participants.

This seminar covered a variety of topics, including:

- The importance of communication, trust, and respect in relationships
- Elements of successful relationships
- How to set boundaries and say no
- How to deal with conflict in a healthy way
- How to recognize the signs of an unhealthy relationship
- Qualities of a healthy relationship and healthy people
- Where to get help if you are in an unhealthy relationship.

Conclusion

The seminar came to an end at 1:30 P.M. **Ms. Shylin** showed her support by offering assistance with the technology. This seminar, '**Maintaining Healthy Relationship,'** helped the participants to recognize the signs of toxicity in relationships and how to approach other people with kindness and compassion.

Dr. EMMANUEL AROCKIAM, S.J., Ph.D.
DIRECTOR - DEPT OF COUNSELLING PSYCHOLOGY
ST. JOSEPH'S COLLEGE (AUTONOMOUS)
TRICHY-620 002


GPS MAP CAMERA
Dept. of Counselling Psychology &
Counselling Centre, St. Joseph's
Latitude: 10.8284625
Longitude: 78.6904613
Date: 29 Aug 2023
Time: 12:21 PM
Google


GPS MAP CAMERA
Dept. of Counselling Psychology &
Counselling Centre, St. Joseph's
Latitude: 10.8284625
Longitude: 78.6904613
Date: 29 Aug 2023
Time: 12:21 PM
Google


GPS MAP CAMERA
Dept. of Counselling Psychology &
Counselling Centre, St. Joseph's
Latitude: 10.8284625
Longitude: 78.6904613
Date: 29 Aug 2023
Time: 12:22 PM
Google

GPS MAP CAMERA

Dept. of Counselling Psychology & Counselling Centre, St. Joseph's

Latitude: 10.8284625
Longitude: 78.6904613

Date: 29 Aug 2023
Time: 12:21 PM


GPS MAP CAMERA
Dept. of Counselling Psychology &
Counselling Centre, St. Joseph's
Latitude: 10.8284625
Longitude: 78.6904613
Date: 29 Aug 2023
Time: 12:21 PM
Google


GPS MAP CAMERA
Dept. of Counselling Psychology &
Counselling Centre, St. Joseph's
Latitude: 10.8284625
Longitude: 78.6904613
Date: 29 Aug 2023
Time: 12:22 PM
Google


GPS MAP CAMERA
Dept. of Counselling Psychology &
Counselling Centre, St. Joseph's
Latitude: 10.8284625
Longitude: 78.6904613
Date: 29 Aug 2023
Time: 12:21 PM
Google

ST. JOSEPH'S COLLEGE, TRICHY

PG DEPARTMENT OF COUNSELLING PSYCHOLOGY & COUNSELLING CENTRE

SEMINAR SERIES – ATTENDANCE LIST

DEPARTMENT: Economics

DATE: 29.08.2023 TIME: 12.00 P.M. VENUE: AV HALL

S.NO	NAME	D.NO	CLASS	SIGN
1.	N. Vithya	22UEC166	II - BA Economics	N Vithya
2.	M. priyadharsini	22UEC115	II - B.A	M priya
3.	T. Nalini	22UEC113	II - B.A	T N
4.	Jency princess	22UEC101	II - B.A	Jency
5.	Dorayani V	22UEC117	II - B A	Dorayani
6.	Sahaya Cathrin Serena V	22UEC162	II - B A	
7.	K. Rajeswari	22UEC114	II - BA	K. Rajeswari
8.	Kausalya	22UEC160	II BA	
9.	T. Priyanka	22UEC103	II - BA	
10.	A. Ezhil Oviya	22UEC104	II - BA	
11.	D. Samyuktha	22UEC141	II - BA	
12.	Juliet princess. J	22UEC102	II - BA	
13.	Subhasri. D	22UEC143	II - BA	
14.	Abisha. L	22UEC164	II - BA	
15.	M. Kiruba Shri	22UEC111	II - BA ECO	
16.	Kiranshiya. S	22UEC109	II - BA ECO	
17.	Godwin	22UEC105	II - ECO	
18.	Sanjey	22UEC116	"	
19.	Suronthiran	22UEC153	"	
20.	Mohan	22UEC154	"	
21.	Roshan Adhithya S.S	22UEC168	II - BA - Eco	S.S. Roshan
22.	Kavithick Roshan. L	23UEC112	I - BA - ECO	
23.	Jenat Jeslen. I	23UEC119	I - BA - Eco	
24.	K. Ronald vasanth	23UEC107	I. B.A. Eco	
25.	A. Martin wilson	23UEC103	I BA ECO	A martin wilson

ST. JOSEPH'S COLLEGE, TRICHY

PG DEPARTMENT OF COUNSELLING PSYCHOLOGY & COUNSELLING CENTRE

SEMINAR SERIES – ATTENDANCE LIST

DEPARTMENT: Economics

DATE: 29.08.23 TIME: 12.00 P.M. VENUE: AV HALL

S.NO	NAME	D.NO	CLASS	SIGN
1.	R. Suriya	23UEC127	BA. Economics	R. Suriya
2.	A Mariya Salvan.	23UEC106	I BA. Economics	A Mariya
3.	A Edigon	23UEC141	BA Economics	A. Edigon
4.	A.V. Manoj kumar	23UEC125	B.A Economics	Manoj
5.	S. Infant Alwin Raj	22UEC107	II BA Economics	S. Infant Alwin
6.	C.T ASHOK ALWIN	23UEC121	I.BA Economics	Ashok
7.	P. Niranjan	23UEC150	I B.A Economics	Niranjan
8.	K. Kiruba Karan	23UEC115	I.BA Economics	Kiruba
9.	L Sanjay	23UEC137	I BA Economics	L Sanjay
10.	S. ANBUSELVAN	23UEC154	I. bA. Economics	S Anbuselvan
11.	M. PRAKASH	23UEC158	I BA ECONOMK	M. Prakash
12.	C. SAKTHIVEL	23UEC159	I. BA. ECONOMICS	C. Sakthivel
13.	P. Pradeep	23UEC160	I.B.A ECONOMICS	P Pradeep
14.	Durai Duraiyam	23UEC118	I BA Economics	Durai
15.	MAADESH K B	23UEC131	I B.A ECONOMICS	K B Maadesh
16.	P.K. DINESH	23UEC105	I. B.A. Economics	P.K. Dinesh
17.	EMANUEL KAVIRAJ. D	23UEC123	I BA. ECONOMICS	E. Kaviraj
18.	S. Pandi Thurai	23UEC155	I. BA Economics	Pandi Thurai
19.	M. Harini	23UEC163	I. BA Economics	M. Harini
20.	V. Vanitha	23UEC143	I BA Economics	Vanitha
21.	V. Santhiya	23UEC145	I BA Economics	V. Santhiya
22.	S. Jamuna devi	23UEC144	I BA Economics	S. Jamuna
23.	C. Mariyammal	23UEC111	I (BA) Economics	C. Mariyammal
24.	G Jannathul Firdose	23UEC104	I BA Economics	G Jannathul Firdose
25.	S. Vishnulakshmi	23UEC133	I BA Economics	S. Vishnulakshmi

ST. JOSEPH'S COLLEGE, TRICHY

PG DEPARTMENT OF COUNSELLING PSYCHOLOGY & COUNSELLING CENTRE

SEMINAR SERIES – ATTENDANCE LIST

DEPARTMENT: Economics

DATE: 29.08.23 TIME: 12.00 P.M. VENUE: AV HALL

S.NO	NAME	D.NO	CLASS	SIGN
1.	M. Arul Anand	23UEC108	I. B.A	M. Arulanand
2.	P. Maria thomas lesly	23UEC113	I. B.A.	P. Thomas
3.	R. ABILASH	23UEC102	I B.A.	R. Albin
4.	D. Sabari Gowtham	23UEC151	I BA	Do
5.	K. venkatesh	23UEC139	I B.A	K. venkatesh
6.	M. Thirumoorthi	23UEC130	I B.A	M. Thirumoorthi
7.	J. Reegan	23UEC124	I B.A	
8.	V. Divyaprasanth	23UEC135	I B.A.	V.
9.	K. Tony Manoj	23UEC120	I. B. A	
10.	N. ARUN KUMAR	23UEC124	I B.A	
11.	A. Mohamed Mansur Ali	23UEC122	I B.A	
12.	S. Sunil	23UEC116	I B.A	
13.	T. Hari vignesh	23UEC161	I B A	T. Hari vignesh
14.	P. Vishvas	23UEC147	I BA	Vishvas
15.	D. Balakrishnan	23UEC148	I BA	
16.	A. Sivanathan	23UEC152	I BA	A. Sivanathan
17.	J. Giridharan	23UEC142	I BA	J. Giridharan
18.	M. MOHAMMED RASOOL KHAN	22UEC106	II BA	
19.				
20.				
21.				
22.				

PG Dept. of Counselling Psychology & Counselling Centre

St. Joseph's College (Autonomous), Trichy - 02

A seminar on

Maintaining Healthy Relationships

for the Department of

History

Resource Person

Rev. Dr. Emmanuel Arockiam, SJ

Head, Dept. of Counselling Psychology

DATE: 04.09.2023 - 11.45 A.M.

VENUE: JUBILEE HALL

Organizing committee

Ms. Shylin

Ms. Christeela

PG DEPARTMENT OF COUNSELLING PSYCHOLOGY

& COUNSELLING CENTRE

ST. JOSEPH'S COLLEGE (Autonomous)

Tiruchirappalli-620 002

Report on Maintaining Healthy relationships – seminar

Date: 04.09.23

Audience: I, II & III BA History

Introduction

The PG Department of Counselling Psychology and the Counselling Centre are hosting series of seminar on the topics "Managing Negative Emotions," "Rising above Addiction," and "Maintaining Healthy Relationships." Members of the organizing committee are Ms. Christeela and Ms. Shylin. 122 students from the Department of History attended the seminar on the topic 'Maintaining Healthy Relationships'.

About the theme

Humans are social being and relationships are essential to happiness and leading fulfilling life. This is due to the wide range of benefits they offer. Relationships give us access to friends and family who we can share our lives with as well as individuals who can support us when we need. Building and maintaining healthy relationships is an important part of looking after our mental health. Healthy relationships include communication, openness, respect, limits, affection, and mutual giving and taking. There is no power disparity.

At 11:45 am at Jubilee Hall, the session began with a prayer song. The seminar was hosted by Ms. Shylin. She introduced the resource person, Rev. Dr. Emmanuel Arockiam, SJ, to the gathering and requested him to take over the session. Fr. Emmanuel discussed the value of having wholesome connections. He also emphasized the factors that make relationships successful. He stressed on the advantages of having healthy relationships. He mentioned the four aspects that a person must have for a healthy relationship. They are:

i. Relationship with self
ii. Relationship with others
iii. Relationship with Environment
iv. Relationship with God

He also emphasized to the attendees the principles that underlie the Jesuits' motto, "making men and women for others." This seminar covered a wide range of topics, such as: The value of open communication, mutual trust, and respect in relationships, the components of successful relationships, how to set boundaries and say no, how to handle conflict in a healthy way, how to recognize the signs of an unhealthy relationship and, where to go for help if you are in such a relationship.

Conclusion

At 1:15 PM, the session was concluded by raising number of questions regarding relationship issues and Fr. Emmanuel answered them all. The students conveyed their feedback about the session and thanked Fr. Emmanuel and the counsellors for organizing such a useful seminar. Ms. Shylin offered help with the technology as a sign of support. The attendees in this seminar on "Maintaining Healthy Relationships" learned how to spot relationship toxicity and how to treat others with respect and compassion.

Dr. EMMANUEL AROCKIAM, S.J., Ph.D.
DIRECTOR - DEPT OF COUNSELLING PSYCHOLOGY
ST. JOSEPH'S COLLEGE (AUTONOMOUS)
TRICHY-620 002


GPS MAP CAMERA
Dept. of Counselling Psychology &
Counselling Centre, St. Joseph's
Latitude: 10.8284625
Longitude: 78.6904613
Date: 04 Sep 2023
Time: 11:57 PM
Google


GPS MAP CAMERA
Dept. of Counselling Psychology &
Counselling Centre, St. Joseph's
Latitude: 10.8284625
Longitude: 78.6904613
Date: 04 Sep 2023
Time: 11:57 PM
Google


GPS MAP CAMERA
Dept. of Counselling Psychology &
Counselling Centre, St. Joseph's
Latitude: 10.8284625
Longitude: 78.6904613
Date: 04 Sep 2023
Time: 11:57 PM
Google


GPS MAP CAMERA
Dept. of Counselling Psychology &
Counselling Centre, St. Joseph's
Latitude: 10.8284625
Longitude: 78.6904613
Date: 04 Sep 2023
Time: 11:57 PM
Google


GPS MAP CAMERA
Dept. of Counselling Psychology &
Counselling Centre, St. Joseph's
Latitude: 10.8284625
Longitude: 78.6904613
Date: 04 Sep 2023
Time: 11:57 PM
Google

ST. JOSEPH'S COLLEGE, TRICHY

PG DEPARTMENT OF COUNSELLING PSYCHOLOGY & COUNSELLING CENTRE

SEMINAR SERIES – ATTENDANCE LIST

DEPARTMENT: History

DATE: 04.09.23 TIME: 11:45 AM VENUE: Jubilee Hall

S.NO	NAME	D.NO	CLASS	SIGN
1.	A. Augustin	22UHS121	History II	
2.	A. Kishok	22UHS101	History II	
3.	J. VALAN	22UHS106	History II	
4.	R. Stalin	22UHS164	History III	
5.	G. Jayamalan	21UHS119	History III	
6.	N. Asan	22chs176	History II	
7.	R. David Raj	22UHS125	History II	
8.	S. Lukas	22UHS122	History II	
9.	Sam Samuel Ekka	23UHS115	History I	
10.	Chikka Sasimoneesha Raju	22UHS124	History-II	
11.	A. Jeyapathi Antony	22UHS110	History-II	
12.	S.S. Yaman Roy	22UHS119	History-II	
13.	Manikandan. C.	22UHS162	History-II	
14.	A. Sheik Mohammed Ali.	23UHS153	History I	
15.	G. Sanjay	23UHS119	History-I	
16.	J. John Xavier raj	23UHS111	History-I	
17.	S. Arunachalam	23UHS173	History-I	
18.	S. Arul vishva	23UHS102	History-I	
19.	S. Alwin	23UHS124	History-I	
20.	P. Dinesh kumar	22UHS168	History II	
21.	A. Daniyel smith	22UHS169	History II	
22.				
23.				
24.				
25.				

S.NO	NAME	D.NO	CLASS	SIGN
1.	A. Samuvel	21UHS105	III rd year	A Samuvel
2.	T. Praveen Kumar	21UHS118	III rd Year	T Praveen Kumar
3.	S. Kellevalavan	21UHS128	III rd Year	
4.	V. MUGESH KANNAN	21UHS175	III rd YEAR	
5.	S. SALAI ARUN RAJU	21UHS125	III rd YEAR	S. Salai Arun Raju
6.	Fernando Marweiss	21UHS108	III rd year	
7.	R. Poranesh	21UHS114	III rd year	
8.	K. Sabarish.	21UHS157	III rd year	
9.	T. Aravinthan	21UHS165	III rd year	T. Anith
10.	[illegible]	23UHS149	I st year	K. Sathash
11.	M. Rashik Ahamed	23UHS159	I st year	
12.	G. Jaarat	23UHS160	I 2nd year	G. Jaarat
13.	L. Sebastian Anto	22UHS164	II nd year	
14.	C. Charan Shan Kirthiyayan	22UHS155	II nd year	
15.	S. Arokia Snehan	23UHS137	I st Year	
16.	S. Saboreesh	23UHS135	I st year	
17.	A. Sugumar Jose	23UHS114	I year	A Sjoseej
18.	E. Deepak	23UHS127	I year	E. Deepak
19.	A. Sahaya Jerome	23UHS126	I. Year	A. Sahaya Jerome
20.	G. vignesh	23UHS152	I year	G. vignesh
21.	S. Jeron Raja	23UHS129	I Year	S. Jeron
22.	J. Jerin Joseph Raj	23UHS104	I Year	J. Jerin
23.	Thomas Alva Edison. J	25UHS108	I year.	
24.				
25.				

S.NO	NAME	D.NO	CLASS	SIGN
1)	J. KEERTHI VENGATESH	21UHS127	III UG HISTORY	J. Venkatesh.
2)	J. Issac Jones	21UHS138	III UG History	
3)	A. Mekwin prasad	21UHS101	III B A History	
4)	P. Raja Selva	21UHS120	III B A History	
5.	KAVINKUMAR. R	21UHS113	III BA History	
6	PRABAKAR. S	21UHS126	III BA HISTORY	
7.	Dheepakraja. T	21UHS104	II B.A History	
8.	Nabin. T	21UHS176	III B.A. History	
9	K. Mukilan	22UHS127	II BA. History	
10	Arun Terrance	22UHS113	II BA History	
11.	J. CHRISTOPHER	22UHS123	II BA History	
12.	S GILBERT ROSHAN	22UHS114	II BA History	
13.	S. E. Haroon	23UHS172	I BA History	
14.	M. Vijaya Marudhan	23UHS121	I UG history	
15	S.G. Harish Kumar	23UHS139	I UG History	
16.	V Dhanasekar	23UHS166	(I UG) History	
17	R. GOPINATH	23UHS171	(I BA) History	
18	N. Ginesh	23UHS150	I BA History	

ST. JOSEPH'S COLLEGE, TRICHY

PG DEPARTMENT OF COUNSELLING PSYCHOLOGY & COUNSELLING CENTRE

SEMINAR SERIES – ATTENDANCE LIST

History

04.09.23 11.45 AM Jubilee Hall.

S.NO	NAME	D.NO	CLASS	SIGN
1.	K. Raghul	22UHS163	II UG	K. Raghul
2.	Barathwaj. D	22UHS151	II UG	Barathwaj
3.	Bharanidharan B	22UHS104	II UG	Bharani
4.	M. Madhesh	22UHS117	II UG	Madhesh
5.	D. Joshua	22UHS111	II UG	Joshua
6.	V. Gnanaprasin	23UHS133	I UG	V. Gnana
7.	V. Durai Samy.	23UHS143	I UG	V. Durai Samy
8.	K. Tharun.	23UHS142	I UG.	K. Tharun.
9.	F. Vincent Raj	23UHS112	I UG	F. Vincent
10.	B. Robin Niranjan	23UHS134	I UG	B. Robin
11.	R. Dhanush Kadi	23UHS130	I UG	R. Dhanush
12.	K. James Babu.	23UHS103	I UG	K. James Babu
13.	S. Kamal	22UHS158	II U.G.	S. Kamal
14.	K. Vishnupriyan	22UHS116	II U.G	K. Vishnupriyan
15.	J. BESIL JENNY	22UHS159	II U.G	Besil
16.	V. Agnel Wilfred	22UHS132	II U.G	Agnel
17.	A. Alwin	22UHS130	II U.G	A. Alwin
18.	D. Josua	22UHS111	II U.G	Josua
19.	M. Madesh	22UHS117	II U.G	Madesh
20.	P. Giriraj	22UHS144	II U.G	P. Giriraj
21.				
22.				
23.				
24.				
25.				
26.				

DEPARTMENT: History

DATE: 04.09.23 TIME: 11:45 AM VENUE: Jubilee Hall

S.NO	NAME	D.NO	CLASS	SIGN
1.	Maria Rabin	22UH118	B.A History - II	
2.	M. Anbuselvan	22UHS161	B.A History - II	
3.	Vishvaa. K	21UHS170	III B.A History	Vishvaa K
4.	Dinesh kumar	21UHS106	II - B.A History	
5.	Sham Daniel. A	21UHS116	III - BA History	
6.	M. Siddhan	21UHS171	III - BA History	M. Siddhan
7.	A. HARIHARAN	21UHS174	III BA History	
8.	M Sai Vasanthan	21UHS134	III B.A History	
9.	V. Harish Jayaraj.	21UHS121	III B.A History	
10.	I. BENADICT MARIYAN	22UHS108	II. BA History	
11.	S. Jeya Prakash	23UHS167	I - BA History	
12.	R. Bharathi	23UHS125	I - BA history	
13.	S. Akash	23UHS123	I - BA history	
14.				
15.				
16.				
17.				
18.				

ST. JOSEPH'S COLLEGE, TRICHY

PG DEPARTMENT OF COUNSELLING PSYCHOLOGY & COUNSELLING CENTRE

SEMINAR SERIES – ATTENDANCE LIST

S.NO	NAME	D.NO	CLASS	SIGN
1.	M. kalaiselvi	23UHS1146	1st B.A(History)	M. Kalaiselvi
2.	A. kanishka	23UHS1161	1st BA(History)	A. Kanishka.
3.	S. Nirainathi	23UHS1163	1st B.A(History)	S. Nirainathi
4.	K. pavithra	23UHS1169	1st (B.A History)	K. Pavithra.
5.	C. AbithaRose	22UHS1103	2nd BA HISTORY	Abitha 04/09
6.	S. Kalpana	21UHS1102	3rd B.A History	S. Kalpana
7.	S. Divya	21UHS1166	3rd B.A History	S. Divya
8.	S. Evangeline Teba	21UHS1129	3rd BA History	S. Evangeline Teba
9.	V. Preetha	21UHS1150	3rd BA. HISTORY	V. Preetha
10.	J. Pabithra	22UHS1131	2nd BA History	J. Pabithra
11.	S. Rexci Dona	23UHS1160	1st BA History	S. Rexci Dona
12.	A. Nilofar Nisha	23UHS1128	1st BA History	A. Nilofar Nisha
13.	V. Varsha	23UHS1122	1st BA History	V. Varsha.
14.	R. Pyinthamil Selvi	23UHS1174	1st BA History	R. Pyinthamil Selvi.
15.	M. Kavya.	23UHS1144	1st BA History	M. Kavya.
16.	ARLEAN VINCY. P	23UHS109	1st BA History	Arlean Vincy. P
17.	L. Preethi Monica	23UHS1138	1st BA History	L. Preethi Monica
18.	J. Reshmi	23UHS1136	1st BA History	J. Reshmi
19.	V. Reni	23UHS105	1st BA History	V. Reni.
20.	K. TamilaT	23UHS170	1st B.A History	K. TamilaT.
21.	J.K. Dowadharshini	23UHS110	1st BA history	J.K. Dowadharshini
22.	S. Nithya Sri	23UHS1168	1st B.A. History	S. Nithya Sri
23.	A. Susan.	22UHS1118	2nd B.A. History	A. Susan.
24.	SURIYA AS.	22UHS165	2nd BA. HISTORY	A. Suriya
25.	Varshini. V	22UHS102	2nd BA History	V. Varshini
26.	Sheela. C	22UHS1141	2nd BA History	C. Sheela.
27.	Praveena. A	22UHS175	2nd BA History	A. Praveena.
28.				
29.				

PG Dept. of Counselling Psychology & Counselling Centre

St. Joseph's College (Autonomous), Trichy - 02

A seminar on

Maintaining Healthy Relationships

for the Department of

MCA

Resource Person

Rev. Dr. V. Gilburt Camillus, SJ

Additional Vice Principal (Shift II)

DATE: 12.09.2023 - 11.45 A.M.

VENUE: SAIL HALL

Organizing committee

Ms. Shylin

Ms. Christeela

PG DEPARTMENT OF COUNSELLING PSYCHOLOGY

& COUNSELLING CENTRE

ST. JOSEPH'S COLLEGE (Autonomous)

Tiruchirappalli-620 002

Report on Maintaining Healthy relationships – seminar

Date: 12.09.23

Audience: I & II MCA

Introduction

The PG Department of Counselling Psychology and the Counselling Centre are hosting series of seminar on the topics "Managing Negative Emotions," "Rising above Addiction," and "Maintaining Healthy Relationships." Members of the organizing committee are Ms. Christeela and Ms. Shylin. 123 students from the Department of MCA attended the seminar on the topic 'Maintaining Healthy Relationships'.

About the theme

Healthy relationships are those that connect us to those in our lives in meaningful and safe ways. They contribute to our mental health and well-being in positive ways. Humans are social being and relationships are essential to happiness and leading fulfilling life. This is due to the wide range of benefits they offer. Relationships give us access to friends and family who we can share our lives with as well as individuals who can support us when we need. While every relationship is unique, healthy relationships often have the same key components for their core. A few of those components are Trust and Respect, Boundaries and Equality/Equity

Learning how to improve communication, especially with regard to conflicts within your relationship, is one of the easiest ways to grow and enhance a healthy relationship.

At 11:45AM at Sail Hall, the session began with a prayer song. The seminar was hosted by Ms. Shylin. She introduced the resource person, Rev. Dr. V. Gilburt Camillus SJ, Additional Vice-Principal. He mentioned the four aspects that a person must have for a healthy relationship. They are:

i. Relationship with self
ii. Relationship with others
iii. Relationship with Environment
iv. Relationship with God

People in healthy relationships love and support each other. They help each other practically as well as emotionally. They are there for each other in the good times and the bad times. Ms. Shylin summarized the session with the features of a good relationship. A good relationship will accept you, love you, allow you to grow, gives you joy and meaning and live fully.

Conclusion

At 1:15 PM, the session was concluded by answering the doubts raised by the students. Ms. Shylin offered help with the technology as a sign of support. The attendees in this seminar on "Maintaining Healthy Relationships" learned how to spot relationship toxicity and how to treat others with respect and compassion.

Dr. EMMANUEL AROCKIAM, S.J., Ph.D.
DIRECTOR - DEPT OF COUNSELLING PSYCHOLOGY
ST. JOSEPH'S COLLEGE (AUTONOMOUS)
TRICHY-620 002


GPS MAP CAMERA
Dept. of Counselling Psychology &
Counselling Centre, St. Joseph's
Latitude: 10.8284625
Longitude: 78.6904613
Date: 12 Sep 2023
Time: 11:55 AM
Google

GPS MAP CAMERA

Dept. of Counselling Psychology &
Counselling Centre, St. Joseph's

Latitude: 10.8284625
Longitude: 78.6904613

Date: 12 Sep 2023
Time: 11:55 AM


GPS MAP CAMERA
Dept. of Counselling Psychology &
Counselling Centre, St. Joseph's
Latitude: 10.8284625
Longitude: 78.6904613
Date: 12 Sep 2023
Time: 11:55 AM
Google


GPS MAP CAMERA
Dept. of Counselling Psychology &
Counselling Centre, St. Joseph's
Latitude: 10.8284625
Longitude: 78.6904613
Date: 12 Sep 2023
Time: 11:54 AM
Google


GPS MAP CAMERA
Dept. of Counselling Psychology &
Counselling Centre, St. Joseph's
Latitude: 10.8284625
Longitude: 78.6904613
Date: 12 Sep 2023
Time: 11:55 AM
Google


MAINTAINING
RELATIONS
GPS MAP CAMERA
Dept. of Counselling Psychology &
Counselling Centre, St. Joseph's
Latitude: 10.8284625
Longitude: 78.6904613
Date: 12 Sep 2023
Time: 11:54 AM
Google

ST. JOSEPH'S COLLEGE, TRICHY

PG DEPARTMENT OF COUNSELLING PSYCHOLOGY & COUNSELLING CENTRE

SEMINAR SERIES – ATTENDANCE LIST

DEPARTMENT: I MCA

DATE: 12/09/23 TIME: 11.45 - 12.45 VENUE: Sail Auditorium

S.NO	NAME	D.NO	CLASS	SIGN
1.	R. Ranjanath	23PCA115	I MCA	R. Ranjanath
2.	C. SANJAY	23PCA147	I MCA	C. Sanjay
3.	M. ASIL STEPHEN	23PCA112	I MCA	M. Asil Stephen
4.	D. IRFHAN JOE	23PCA129	I MCA	D. Irfhan Joe
5.	A. VINCENTPEO	23PCA104	I MCA	A. Vincentpeo
6.	M. Krishna Kishore	23PCA154	I MCA	M. Krishna Kishore
7.	B. Surya Aswin	23PCA153	I MCA	B. Surya Aswin
8.	K. SAKTHI VELAN	23PCA148	I-MCA	K. Sakthi Velan
9.	JEROM SUNDAR	23PCA126	I-MCA	Jerom
10.	Revaldo	23PCA127	I-MCA	Revaldo
11.	Anthoniraj. R	23PCA106	I-MCA	Anthoniraj
12.	A. Jaya Prabhu	23PCA119	I-MCA	A. Jaya Prabhu
13.	C. Siva	23PCA140	I-MCA	C. Siva
14.	Issac R	23PCA139	I-MCA	R. Issac
15.	Rivaldo A	23PCA127	I MCA	Rivaldo A
16.	Harsha. R	23PCA120	I-MCA	Harsha R
17.	Jushlin Anitha	23PCA121	I MCA	J. Jushlin
18.				
19.				
20.				

ST. JOSEPH'S COLLEGE, TRICHY

PG DEPARTMENT OF COUNSELLING PSYCHOLOGY & COUNSELLING CENTRE

SEMINAR SERIES – ATTENDANCE LIST

DEPARTMENT: I MCA

DATE: 12.09.2023 TIME: 11:45 AM VENUE: SAIL HALL

S.NO	NAME	D.NO	CLASS	SIGN
1.	AJAY JAMES	23PCA101	I MCA	J. Ajay
2.	JEBIN J	23PCA152	I MCA	J. Jebin
3.	AATHITHYAN.S.R	23PCA158	I MCA	
4.	ANTONY SYMON.A	23PCA125	I MCA	
5.	I SRIRAM	23PCA149	I MCA	I. Sriram
6.	S. THAMIZHTHENDRAL	23PCA150	I MCA	
7.	S. VISHWA	23PCA146	I MCA	
8.	S. Swanthiranraj	23PCA149	IMCA	
9.	ARCKIA INFANT RAJ M	23PCA136	IMCA	
10.	A.T. Daniel Benni	23PCA102	I MCA	
11.	G. Silvester	23PCA133	I MCA	
12.	A GEORGE	23PCA103	IMCA	A George
13.	M. BASTINRAJA	23PCA114	I MCA	
14.	M. MALAVIKA	23PCA162	I MCA	
15.	S. POOJA	23PCA138	IMCA	
16.	S. JANANI	23PCA141	IMCA	
17.	G. Monisika	23PCA137	I MCA	
18.				
19.				
20.				

S.NO	NAME	D.NO	CLASS	SIGN
1.	S Santhosh Kumar	pg22pca140	II - MCA	S Santhosh Kumar
2.	Jerry Jose	Pg22PCA133	II - MCA	Jerry
3.	Pavalan .S	Pg22PCA131	II - MCA	Pavalan
4.	S.Nova Ronald	Pg22PCA134	II - MCA	S. Nova Ronald
5.	S.SADMESH	Pg22PCA161	II - MCA	S Sadmesh
6.	PETER THAMIYAN I	22PCA132	II - MCA	P. Peter Thamiyan
7	THAINESH STEVAK G	22PCA121	II - MCA	Stevak
8.	JOM JOSE	22PCA137	II - MCA	Jom Jose
9.	S. Alwin Raja	22PCA136	II - MCA	S. Alwin Raja
10.	A. Ignatius	22PCA135	II - MCA	A. Ignatius
11	Collince Gracian M	22PCA106	II - MCA	Collince
12	P. Susai Fernandas	22PCA145	II - MCA	P. Susai Fernandas
13	P. Loyola.	22PCA113	II MCA	P. Loyola
14.	Alan Edward Raja J.	22PCA108	II MCA	Alan Edward Raja J.
15.	Immanuvel Rohith D	22PCA112	II MCA	D. Rohith
16	SANJAY V	22PCA148	II MCA	V. Sanjay
17	R Anand	22PCA163	II MCA	R. Anand
18	P. Prathyush	22PCA154	II MCA	P. Prathyush
19	S. Saravanakar	22pca9159	II - MCA	S. Saravanakar
20	HASHWAR. E	22PCA138	II MCA	E. Hashwar
21	Mukesh. R	22PCA156	II MCA	R. Mukesh

S.NO	NAME	D.NO	CLASS	SIGN
1.	SIMON RAJA . M	22PCA104	II nd MCA	
2.	PRINCE ROSHAN . P	22PCA128	II - MCA	
3.	SUDHARSAN . S	22PCA147	II - MCA	
4.	I . JOSHUA	22PCA117	II - MCA	
5.	Bagyo . P	22PCA155	II - MCA	
6.	GAINS . A	22PCA122	II - MCA	
7.	Lakshmanan . P	22PCA107	II . MCA	
8.	V. Vikram	22PCA141	II . MCA	
9.	X . DRAVID	22PCA139	II . MCA	
10.	M . Antony Diwan	22PCA110	II . MCA	
11.	P . Peo Francis	22PCA115	II - MCA	
12.	A . Johnson Selvakumar	22PCA118	II - MCA	
13.	Rahul . P	22PCA109	II - MCA	
14.	SHYAM GANESH R	22PCA146	II MCA	
15.	A . Sreenath	22PCA152	II MCA	
16.	MANIKANDAN . T	22PCA162	II MCA	
17.	PRABAKARAN . F	22PCA124	II MCA .	
18.	A Sanjay Rohith	22PCA127	II MCA	
19.	A . ARMSTRONG SELES	22PCA103	II - MCA	
20.	Martin Raj A	22PCA111	II MCA	M . R
21.	J . Prince Raja	22PCA119	II MCA	
22.	M . Johnson Maria Tony	22PCA125	II - MCA	
23.				
24.				

S.NO	NAME	D.NO	CLASS	SIGN
1.	SIMON RAJA.M	22PCA104	II MCA	
2.	PRINCE ROSHAN.P	22PCA128	II - MCA	
3.	SUDHARSAN.S	22PCA147	II - MCA	
4.	I. JOSHUA	22PCA117	II - MCA	
5.	Bagyo.P	22PCA155	II - MCA	
6.	GAINS.A	22PCA122	II - MCA	
7.	Lakshmanan.P	22PCA107	II MCA	
8.	V. Vikram	22PCA141	II. MCA	
9.	X. DRAVID	22PCA139	II MCA	
10.	M. Antony Diwan	22PCA140	II. MCA	
11.	P. Peo Francis	22PCA115	II-MCA	
12.	A. Johnson Selvakumar	22PCA118	II-MCA	
13.	Rahul.P	22PCA109	II-MCA	
14.	SHYAM GANESH R	22PCA146	II MCA	
15.	A. Shreenath	22PCA152	II MCA	
16.	MANIKANDAN.T	22PCA162	II MCA	
17.	PRABAKARAN.F	22PCA124	II MCA	
18.	A Sanjay Rohith	22PCA127	II MCA	
19.	A. ARMSTRONG SELES	22PCA103	II-MCA	
20.	Martin Raj A	22PCA111	II MCA	M.R
21.	J. Prince Raja	22PCA119	II MCA	
22.	M. Johnson Maria Tony	22PCA125	II - MCA	
23.				
24.				

PG DE

ST. JOSEPH'S COLLEGE, TRICHY

PG DEPARTMENT OF COUNSELLING PSYCHOLOGY & COUNSELLING CENTRE

SEMINAR SERIES - ATTENDANCE LIST

DEPARTMENT: MCA

DATE: 12/09/23 TIME: 11:45 to 12:45 TOPIC: Healthy Relationship

S.NO	NAME	D.NO	CLASS	SIGN
01	G. Nisha	23PCA132	MCA-I	G.Nisha
02	M. Philo Helena	23PCA131	MCA-I	
03	B. Aarika	23PCA107	I-MCA	B. Aarika
04	Jenifer Caslin	23PCA143	I-MCA	Jenifer caslin
5	Rincy Michele J	23PCA134	I.MCA	Rincy Michele J
6	J.M Tisha Evangeline	23PCA123	I. MCA	J.M Tisha Evangeline
7.	S. Arockiya Filoni Resia	23PCA122	I MCA	S. Arockiya
8.	BERYL. A	23PCA130	I MCA	Beryl. A
9.	Shiney Mary L	23PCA108	I MCA	
10.	Santhiya Praveena. V	23PCA117	I MCA	V Santhiya Praveena.
11	Joy Ribeena. A	23PCA109	I MCA	A Joy
12.	A. Jasmine Sumitha	23PCA124	I MCA	A Jasmine Sumitha.
13.	I Antony Steffy	23PCA116	I MCA	I. Antony Steffy
14.	Jellin Hebsiba. A	23PCA105	I MCA	
15.	Athiban. C	23PCA161	I MCA	C. Athiban
16.	DANIEL FERNANDO D	23PCA157	I MCA	D. Daniel FN
17	JOHN BRITTO M	23PCA156	I MCA	

S.NO	NAME	D.NO	CLASS	SIGN
1.	A. Jessica Mary	22PCA116	II - MCA	A. Jessicamary
2.	R. J. Selva Deeshani	22PCA130	II MCA	Selvadeeshani.
3.	S. Reeba	22PCA102	II MCA	S. Reeba
4.	Amala P	22PCA105	II - MCA	
5.	Rashini. J	22PCA129	II - MCA	
6.	Divika. P	22PCA149	II - MCA	
7.	J. Mary Agnes	22PCA126	II - MCA	
8.				
9.				

PG Dept. of Counselling Psychology & Counselling Centre

St. Joseph's College (Autonomous), Trichy - 02

A seminar on

Maintaining Healthy Relationships

for the Department of

English - Shift I

III UG & All PG

Resource Persons

Rev. Dr. Emmanuel Arockiam, SJ
Head, Dept. of Counselling Psychology

MS. SHYLIN
Counsellor

MS. CHRISTEELA
Counsellor

DATE: 07.12.2023 - 11.30 A.M.
VENUE: SAIL HALL

Organizing committee

Ms. Shylin
Ms. Christeela

PG DEPARTMENT OF COUNSELLING PSYCHOLOGY

& COUNSELLING CENTRE

ST. JOSEPH'S COLLEGE (Autonomous)

Tiruchirappalli-620 002

Report on Maintaining Healthy relationships – seminar

Date: 07.12.23

Audience: III UG all PG students of English Dept. (Shift I)

Introduction Centre

The Student Counsellors and the PG Department of Counselling Psychology are hosting series of seminar on the topics "Managing Negative Emotions," "Rising above Addiction," and "Maintaining Healthy Relationships." Members of the organizing committee are Ms. Christeela and Ms. Shylin. 95 students from the Department of English (Shift I) attended the seminar on the topic 'Maintaining Healthy Relationships'.

About the theme

Taking care of our mental health includes establishing and preserving healthy connections. Since humans are social creatures, having relationships is crucial to happiness and living a full life. Through relationships, we can connect with people who can help us in times of need as well as friends and family with whom we can share our lives. Mutual giving and receiving, boundaries, openness, respect, communication, and affection are all components of healthy relationships. There is not an imbalance of power.

At 11:30 AM at Sail Hall, the session began with a prayer song. Resource Person was Ms. Christeela. Unfortunately, Rev. Dr. Emmanuel Arockiam, SJ couldn't join the session due to an emergency. Ms. Christeela introduced the topic and took over the session. Healthy relationships are essential for living a meaningful and fulfilled life.

The quality of our relationships with others affects our personal and professional lives and our sense of belonging to a wider community and humanity. The more positive effort you put into a relationship, the healthier it should be. People in healthy relationships love and support each other. They help each other practically as well as emotionally. They are there for each other in the good times and the bad times. Healthy relationships are commonly based on respect, trust, open communication, equality, both shared and individual interests, understanding, honesty, care, emotional support, shared values around finances, child rising and other important matters.

Conclusion

At 1.00 PM, the session came to an end. The students provided their feedback about the session and thanked the counsellors for organizing the seminar. The attendees in this seminar on "Maintaining Healthy Relationships" learned how to spot relationship toxicity and how to treat others with respect and compassion.

Dr. EMMANUEL AROCKIAM, S.J., Ph.D.
DIRECTOR - DEPT OF COUNSELLING PSYCHOLOGY
ST. JOSEPH'S COLLEGE (AUTONOMOUS)
TRICHY-620 002


GPS MAP CAMERA
Counselling Centre & DEPT OF
Counselling Psychology, St. Joseph's
Latitude: 10.828479
Longitude: 78.6904903
Date: 07 Dec 2023
Time: 12:38 PM
Google


GPS MAP CAMERA
Counselling Centre & DEPT OF
Counselling Psychology, St. Joseph's
Latitude: 10.828479
Longitude: 78.6904903
Date: 07 Dec 2023
Time: 12:38 PM
Google


GPS MAP CAMERA
Counselling Centre & DEPT OF Counselling Psychology, St. Joseph's
Latitude: 10.828479
Longitude: 78.6904903
Date: 07 Dec 2023
Time: 12:38 PM
Google


GPS MAP CAMERA
Counselling Centre & DEPT OF
Counselling Psychology, St. Joseph's
Latitude: 10.828479
Longitude: 78.6904903
Date: 07 Dec 2023
Time: 12:41 PM
Google

ST. JOSEPH'S COLLEGE, TRICHY

PG DEPARTMENT OF COUNSELLING PSYCHOLOGY & COUNSELLING CENTRE

SEMINAR SERIES – ATTENDANCE LIST

DEPARTMENT: English (Shift I) TOPIC: Maintaining Healthy Relationships

DATE: 7.12.23 TIME: 11.30 AM VENUE: Sail Hall

S.NO	NAME	D.NO	CLASS	SIGN
1.	ARUNA . M	23PEN123	I - MA ENGLISH	
2.	PAVITHRA B.S	23PEN133	I M.A ENGLISH	
3.	ANTHONY SHILPA. J	23PEN128	I. M.A. ENGLISH	
4.	SHINEY. J	23PEN122	I. M.A. ENGLISH	
5.	ANNIE D	23PEN113	I MA ENGLISH	
6.	PRINCY A.	23PEN114	I M.A ENGLISH	A. Princy.
7.	Jeeva Alice N R	23PEN136	I MA English	
8.	Maheshwari. M	23PEN137	I MA English	
9.	Annie Lumina . A	23PEN102	I MA English	
10.	Selva Shega . P	23PEN106	I MA Eng	
11.	Trinita Vinola J	23PEN138	I MA Eng	
12.	Shiny Christina A.S	23PEN142	I MA Eng.	
13.	Abinaya . C	23PEN141	I M A Eng	
14.	Silviya Mary. I	23PEN143	I. MA. Eng.	
15.	Vindiya Recielin. W	23PEN132	I. MA. Eng	
16.	Nivya C	23PEN119	I. M A Eng	
17.	Gurudev V	23PEN116	I MA Eng	
18.	Kumuthra. R	23PEN139	I MA Eng	
19.	Ananda kumar P	23PEN124	I MA Eng	
20.	Rohith. R	23PEN134	I MA Eng	
21.	Kevin Samuel J	23PEN126	I MA Eng	
22.	Nivya Peter .	23PEN117	I MA Eng.	
23.	Praveen J	23PEN118	I MA English	
24.	KIRUTHISH - S	23PEN121	I MA ENGLISH	
25.	Rahul Kumar M.K	23PEN105	I MA English	

ST. JOSEPH'S COLLEGE, TRICHY

PG DEPARTMENT OF COUNSELLING PSYCHOLOGY & COUNSELLING CENTRE

SEMINAR SERIES – ATTENDANCE LIST

DEPARTMENT: TOPIC:

DATE: TIME: VENUE:

S.NO	NAME	D.NO	CLASS	SIGN
1.	C. Sugumar	23PEN112	I M.A ENG	
2.	R. David Jeeva	23PEN104	I MA ENGLISH	07.12.23
3.	Naveen Infant P	23 PEN 115	I MA Eng	
4.	B Ebinesar	23 PEN101	I MA Eng	
5.	J. Aaron	23PEN109	I M.A Eng	
6.	J. M. Rajith Raja	23PEN130	I M.A Eng	
7.	M Ponik	23PEN129	I M.A English	M Ponik
8.	Sebastin Gilbert. P	23 PEN 120	I MA ENG	
9.	Prakash Roy. G	22PEN130	II MA Eng	
10.	Praveen S	22PEN104	II M.A Eng	
11.	Agni Vinoth S	22 PEN 124	II M.A Eng	
12.	A. Abhishek Jesuraj	22PEN109	II-M.A Eng	
13.	Dhinanth V	22PEN129	II M.A Eng	
14.	J. Bharathidasan	22PEN111	II MA Eng	
15.	R. Marshlene	22PEN108	II M.A Eng	
16.	N. Radha Krishnan	22PEN134	II M.A Eng	
17.				
18.				
19.				
20.				
21.				
22.				
23.				
24.				
25.				

ST. JOSEPH'S COLLEGE, TRICHY

PG DEPARTMENT OF COUNSELLING PSYCHOLOGY & COUNSELLING CENTRE

SEMINAR SERIES – ATTENDANCE LIST

DEPARTMENT: ENGLISH TOPIC:

DATE: 07.12.2023 TIME: 11.30 AM VENUE:

S.NO	NAME	D.NO	CLASS	SIGN
1.	Wanjingshai	21UEN123	III B.A	
2.	K.S. Gilo Sugaraj	21UEN102	II BA English	K.S. Gilo
3.	Rantam Baliyarsingh	21UEN129	III BA English	
4.	Brendip Barla	21UEN141	III BA English	
5.	G. Karthik	21UEN134	III BA English	
6.	K. Jithendra	21UEN142	III BA English	
7.	Ch. Jeevan Sadhwik	21UEN130	III BA English	
8.	G. John Babu	21UEN133	III BA English	
9.	A. Anthony Samy	21UEN111	III BA English	
10.	Robert Jaslin. S	21UEN148	III BA English	
11.	Poling Richard. P	21UEN149	III BA English	P. Richard
12.	A ARNOLD	21UEN114	III B.A Eng	A Arnold
13.				
14.				
15.				
16.				
17.				
18.				
19.				
20.				
21.				
22.				
23.				
24.				
25.				

ST. JOSEPH'S COLLEGE, TRICHY

PG DEPARTMENT OF COUNSELLING PSYCHOLOGY & COUNSELLING CENTRE

SEMINAR SERIES – ATTENDANCE LIST

DEPARTMENT: ENGLISH TOPIC:

DATE: 07.12.2023 TIME: 11.30 AM VENUE: Sail Audirium

S.NO	NAME	D.NO	CLASS	SIGN
1.	S. XAVIER EMMANUVEL	21UEN121	III - B.A Eng	S. Xavier
2.	S. VISHNU	21UEN140	III - BA Eng	S. Vishnu
3.	T. NALIN	21UEN143	III BA Eng	T. Nalin
4.	F. SYED MOHAMED	21UEN	III	F. Syed
5.	J. Praveen	167	BA Eng	
6.	Delphin Sankumar	147	III BA	Delphin
7.	Ajith.S	151	III BA	
8.	Jeffrey Joseph	126	III BA	Jeffrey
9.	Dhivin	162	III BA	Dhivin
10.	R. Hepzon	136	III B.A	
11.	P. Samjoovy	115	III BA	
12.	D. Robinson	135	III BA	
13.	P RENOLD ROJAN	109	III BA	
14.	S Malaimadhan Christopher	101	III BA	
15.	Rahul Antony	110	III BA	
16.	Nikkis Franklin	119	III BA	
17.	Abel S Abraham	117	III BA	
18.	Paul Leons	160	III BA	
19.	J Rayston	107	III BA	
20.	Maniya Antony .J	118	III BA	
21.	Nandhabalan. S	171	III - BA	
22.	Nithin Roy. S	103	III - BA	
23.	Sikakollu Pavan Kumar	132	III - B.A	
24.	Pyosbeinlang Wanniang	21UEN120	III - B.A	
25.	Gundugobbu Raviteja	21UEN127	III - B.A	

ST. JOSEPH'S COLLEGE, TRICHY

PG DEPARTMENT OF COUNSELLING PSYCHOLOGY & COUNSELLING CENTRE

SEMINAR SERIES – ATTENDANCE LIST

DEPARTMENT: II MA ENGLISH TOPIC:

DATE: 07.12.2023 TIME: VENUE:

S.NO	NAME	D.NO	CLASS	SIGN
1.	Felixa . E	22PEN139	II MA Eng	Felixa·E
2.	Sri Sivabagya · A	22PEN142	II MA Eng	Sri Sivabagya
3.	Mahisha · S	22PEN136	II·MA·Eng	S·Mahisha
4.	Prabha	22PEN141	II·MA·Eng	Prabha
5.	S. Sherlif	22 PEN107	II MA Eng	S Sherlif
6.	Lathika Sherine D S	22 PEN140	II MA Eng	Lathika
7.	Sohila M.	22 PEN127	II M.A.Eng.	M Sohila
8.	LINNET A	22PEN126	II MA·Eng.	Linnet. A
9.	Rufina Sharon · D	22PEN120	II·M.A·Eng	D. Rufina Sharon
10.	Belinda Asia · Y	22PEN131	II M.A Eng	Y. Belinda Asia.
11.	Praveen Raj · V	22PEN114	II M.A.Eng	Praveen
12.	Boomanathan k	22 PEN126	II M.A.Eng	K Boomanathan
13.	WILSON AROKIA TONY·C	22PEN122	II MA·Eng	C Wilson
14.	Arul Godwin . S	22PEN110	II M.A Eng	S Arul Godwin
15.	Sugavaneshwaran G	22PEN118	II MA Eng	G. Sugavaneshwaran
16.	S. Arul Kavi	22PEN132	II MA ENG	S. Arul Kavi
17.	X. Franklin	22PEN116	II MA Engl.	X. Franklin
18.				
19.				
20.				
21.				
22.				
23.				
24.				
25.				

PG Dept. of Counselling Psychology & Counselling Centre

St. Joseph's College (Autonomous), Trichy - 02

A seminar on

Maintaining Healthy Relationships

for the Department of HRM

Resource Persons

Rev. Dr. Emmanuel Arockiam, SJ
Head, Dept. of Counselling Psychology

MS. CHRISTEELA
Counsellor

DATE: 08.12.2023 - 11.30 A.M.
VENUE: JUBILEE HALL

Organizing committee
Ms. Shylin
Ms. Christeela

PG DEPARTMENT OF COUNSELLING PSYCHOLOGY

& COUNSELLING CENTRE

ST. JOSEPH'S COLLEGE (Autonomous)

Tiruchirappalli-620 002

Report on Maintaining Healthy relationships – seminar

Date: 08.12.23

Audience: Students of the Dept. of HRM

Introduction Centre

The Student Counsellors and the PG Department of Counselling Psychology are hosting series of seminar on the topics "Managing Negative Emotions," "Rising above Addiction," and "Maintaining Healthy Relationships." Members of the organizing committee are Ms. Christeela and Ms. Shylin. 62 students from the Department of HRM attended the seminar on the topic 'Maintaining Healthy Relationships'.

About the theme

Building and maintaining healthy relationships is an important part of looking after our mental health. Humans are social being and relationships are essential to happiness and leading fulfilling life. Relationships give us access to friends and family who we can share our lives with as well as individuals who can support us when we need. Healthy relationships include communication, openness, respect, limits, affection, and mutual giving and taking. There is no power disparity.

At 11:30 AM at Sail Hall, the session began with a prayer song. Resource Persons were Ms. Christeela and Rev. Dr. Emmanuel Arockiam, SJ. Ms. Christeela introduced the topic and took over the session. Healthy relationships are essential for living a meaningful and fulfilled life.

The quality of our relationships with others affects our personal and professional lives and our sense of belonging to a wider community and humanity. The more positive effort you put into a

relationship, the healthier it should be. People in healthy relationships love and support each other. They help each other practically as well as emotionally. They are there for each other in the good times and the bad times. Healthy relationships are commonly based on respect, trust, open communication, equality, both shared and individual interests, understanding, honesty, care, emotional support, shared values around finances, child rising and other important matters. She gave tips on figuring out toxicity in people and body cues. Fr. Emmanuel talked about how to deal with tough people in the working place. He also highlighted the importance of intrapersonal relationship, relationship with God and the World.

Conclusion

The session concluded at 1:00 PM. The students thanked the counsellors for setting up the seminar and gave their opinions about the meeting. This seminar on "Maintaining Healthy Relationships" taught participants how to recognize relationship toxicity and how to show empathy and respect to others.

Dr. EMMANUEL AROCKIAM, S.J., Ph.D.
DIRECTOR - DEPT OF COUNSELLING PSYCHOLOGY
ST. JOSEPH'S COLLEGE (AUTONOMOUS)
TRICHY-620 002

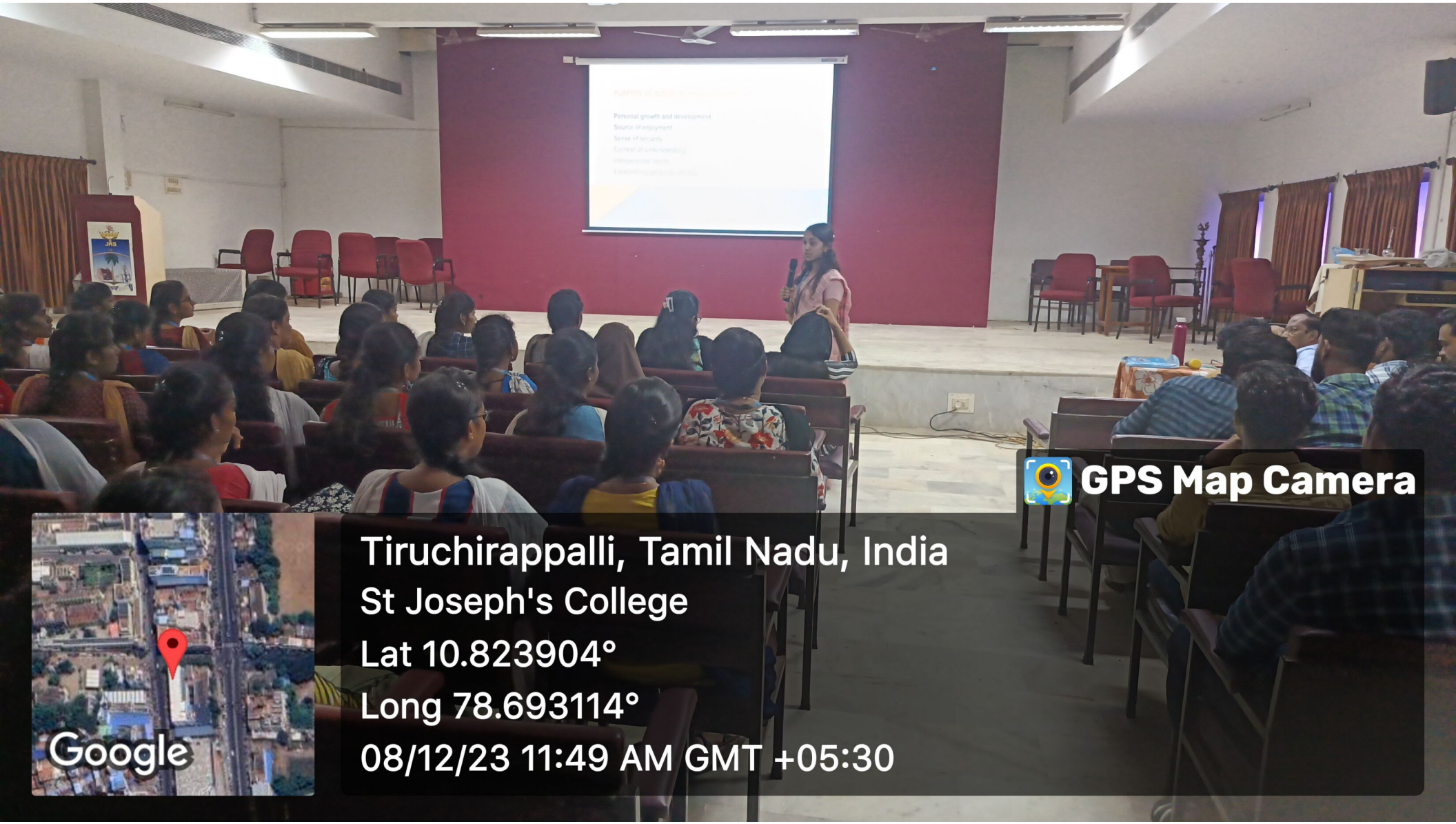
Personal growth and development
Source of enjoyment
Sense of security
GPS Map Camera
Tiruchirappalli, Tamil Nadu, India
St Joseph's College
Lat 10.823904°
Long 78.693114°
08/12/23 11:49 AM GMT +05:30
Google


GPS Map Camera
Tiruchirappalli, Tamil Nadu, India
St Joseph's College
Lat 10.823904°
Long 78.693114°
08/12/23 11:51 AM GMT +05:30
Google


GPS Map Camera
Tiruchirappalli, Tamil Nadu, India
St Joseph's College
Lat 10.823904°
Long 78.693114°
08/12/23 11:51 AM GMT +05:30
Google

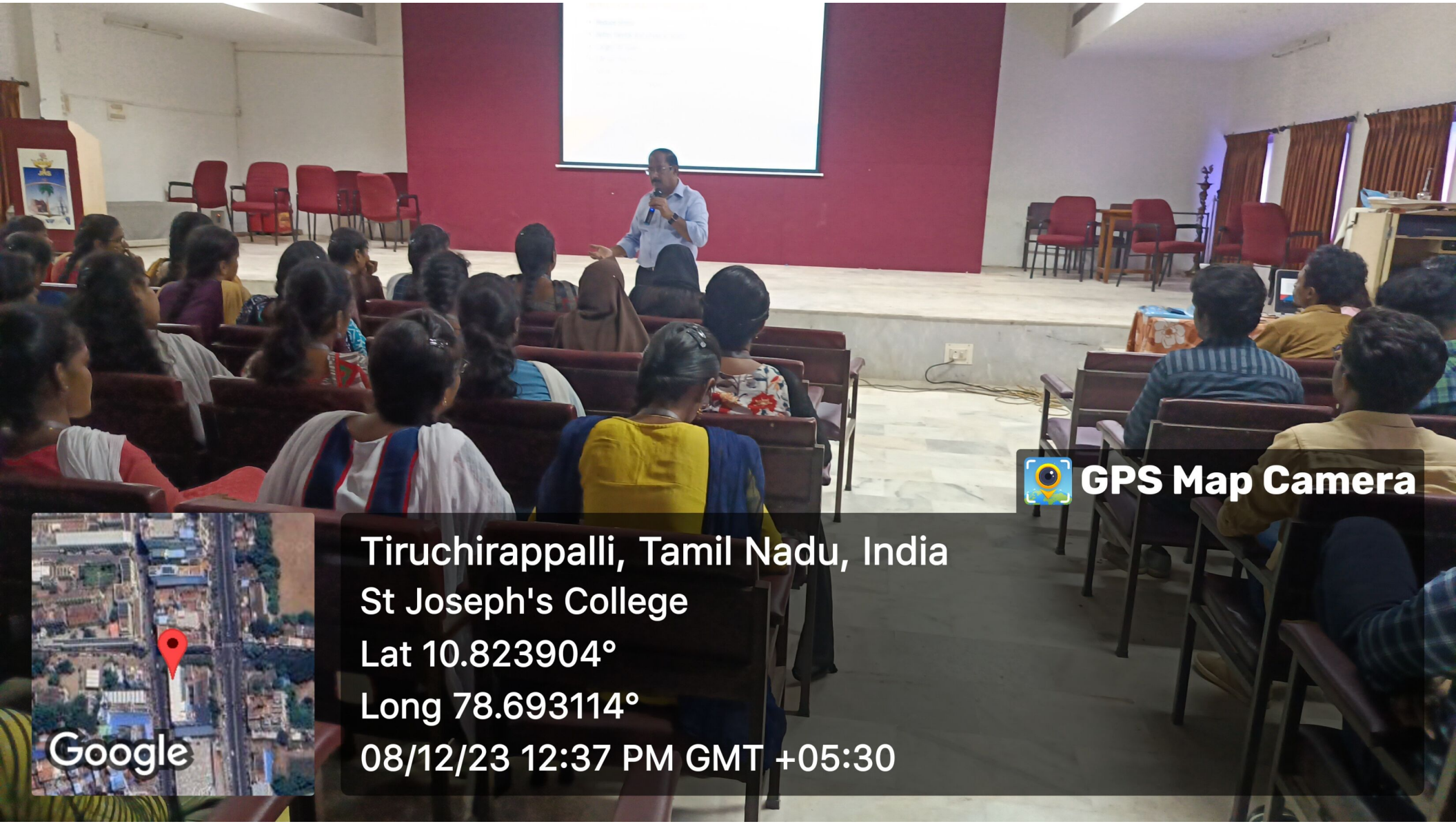
GPS Map Camera
Tiruchirappalli, Tamil Nadu, India
St Joseph's College
Lat 10.823904°
Long 78.693114°
08/12/23 12:37 PM GMT +05:30
Google

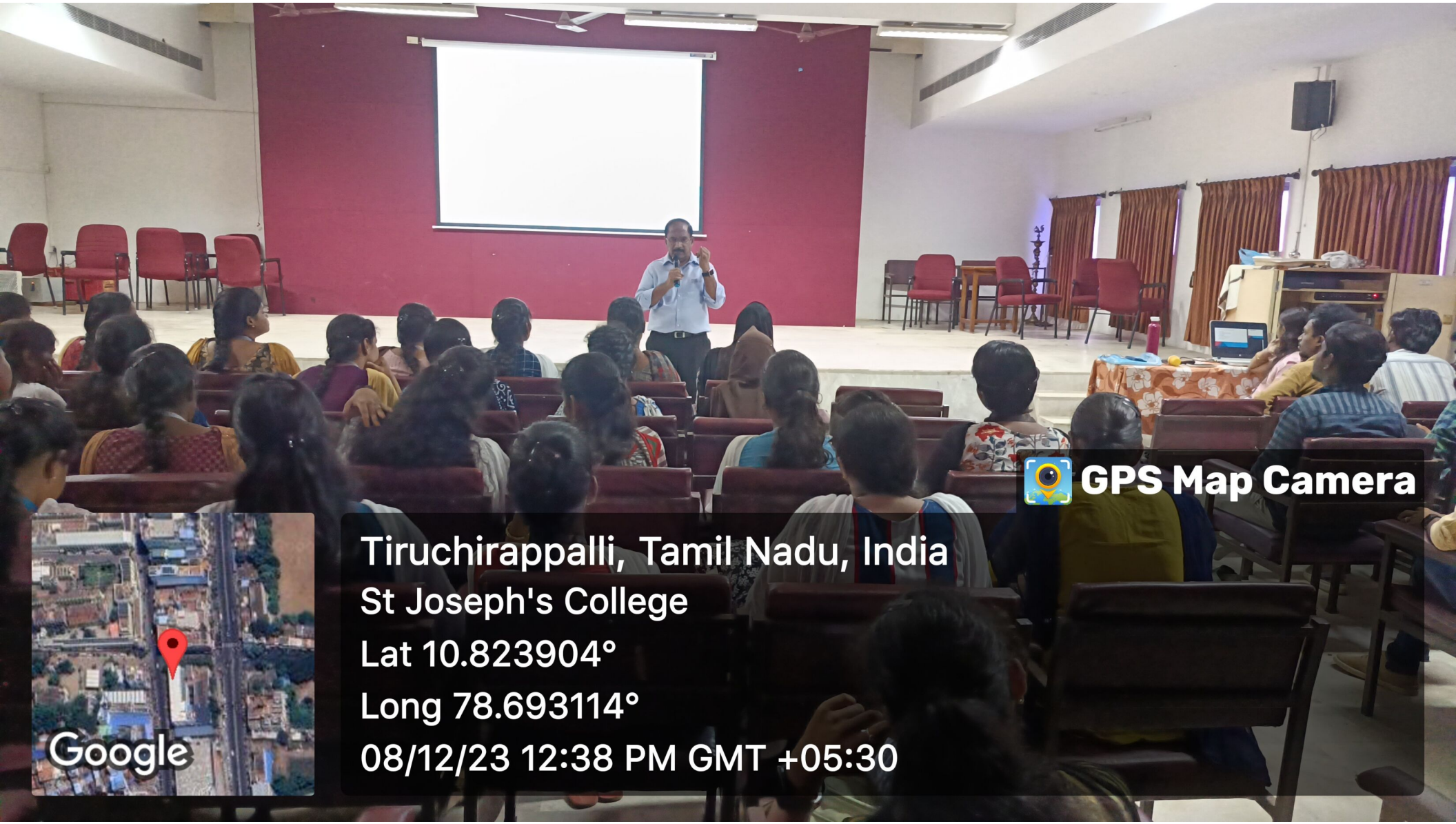
GPS Map Camera
Tiruchirappalli, Tamil Nadu, India
St Joseph's College
Lat 10.823904°
Long 78.693114°
08/12/23 12:38 PM GMT +05:30
Google

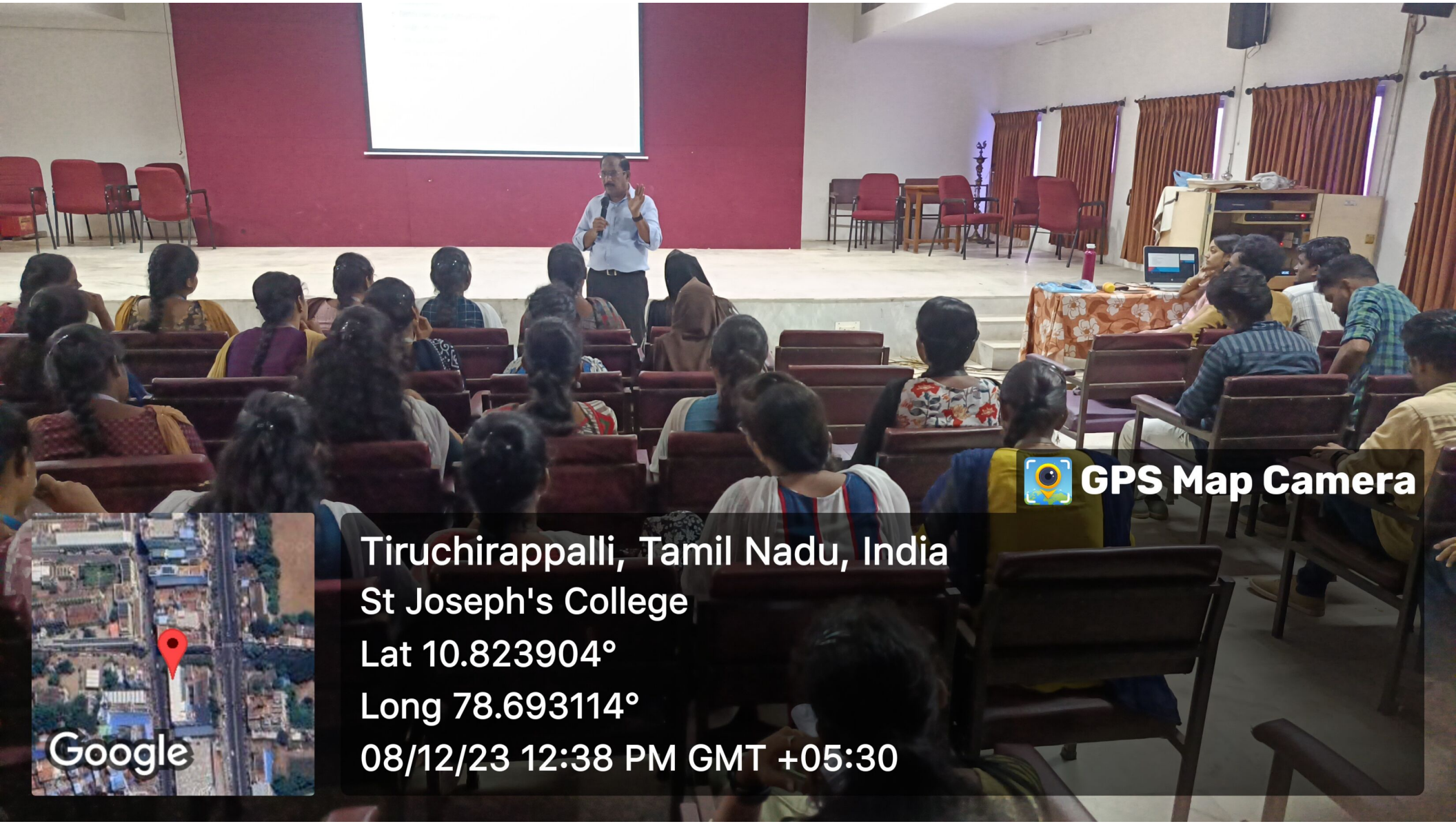
GPS Map Camera
Tiruchirappalli, Tamil Nadu, India
St Joseph's College
Lat 10.823904°
Long 78.693114°
08/12/23 12:38 PM GMT +05:30
Google

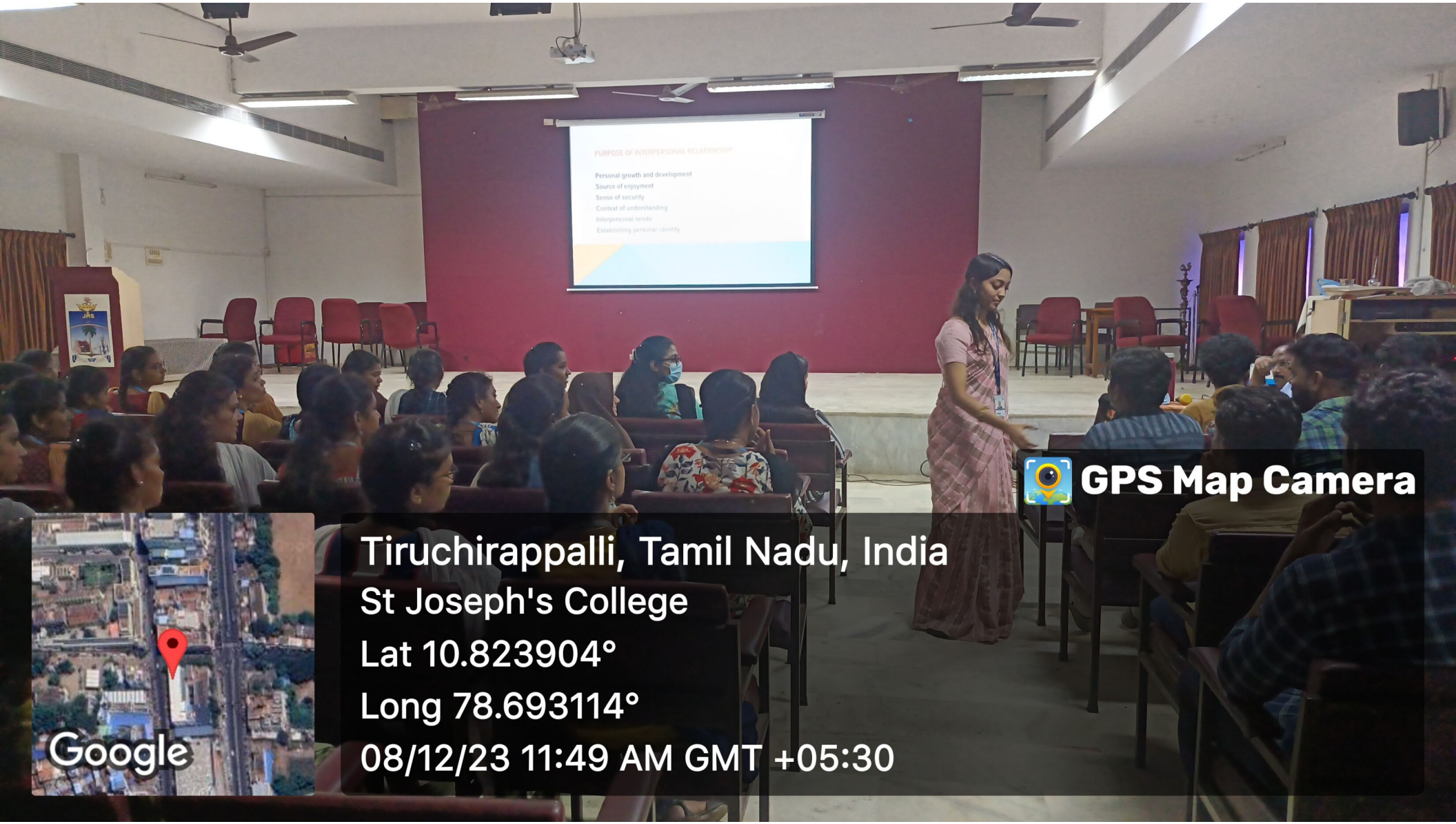
PURPOSE OF INTERPERSONAL RELATIONSHIP
Personal growth and development
Source of enjoyment
Sense of security
Context of understanding
Interpersonal needs
Establishing personal identity
GPS Map Camera
Tiruchirappalli, Tamil Nadu, India
St Joseph's College
Lat 10.823904°
Long 78.693114°
08/12/23 11:49 AM GMT +05:30
Google


GPS Map Camera
Tiruchirappalli, Tamil Nadu, India
St Joseph's College
Lat 10.823904°
Long 78.693114°
08/12/23 11:51 AM GMT +05:30
Google

ST. JOSEPH'S COLLEGE, TRICHY

PG DEPARTMENT OF COUNSELLING PSYCHOLOGY & COUNSELLING CENTRE

SEMINAR SERIES – ATTENDANCE LIST

DEPARTMENT: MA.HRM TOPIC:

DATE: 8-12-2023 TIME: 11:30 VENUE: Jubilee Hall

S.NO	NAME	D.NO	CLASS	SIGN
1.	K. Dani Kenedy	22PHR152	II. MA.HRM	
2.	S. Arockia David	23PHR104	I.M.A.HRM	
3.	L Karunkaran	22PHR117	II MA HRM	
4.	JOHN K	22PHR135	II MA HRM	
5.	A. EDISON IGNESH	22PHR134	II. MA. HRM	
6.	J. mohamed Ashik	23PHR116	I.M.A.HRM	
7.	A. Lathi vendhan	22PHR141	II MA HRM	
8.	Tsudari David	23PHR120	I MA. HRM	
9.	J. Jogaya praba	22 PHR115	II MA. HRM	
10.	B. Nelson Devaraj	22PHR125	II MA HRM	
11.	S. MURUGHESAN	22PHR138	II MA HRM	
12.	R.K. Gracela leennon	22PHR131	II MA HRM	
13.	BASKAR	22PHR103	II MA HRM	
14.	KARISHMA A	22PHR124	II. MA. HRM	
15.	Rinthiya Layonie	22PHR119	II. MA HRM	
16.	S. Dhivaiya	22pHR139	II. M.A HRM	
17.	A. Soosan Fiona.	22pHR104	II. M.A HRM	
18.	P. KEERTHANA	22PHR114	II M.A. HRM	
19.	R. Seelia Jenifer	22PHR116	II MA (HRM)	
20.	M. Shyamala	22PHR128	II MA HRM	
21.	SOFIYA JASMINE J	22PHR129	II MA HRM	
22.	SINDHUJA R	22PHR137	II. MA HRM	
23.	JENCY DEVA PRIYA. J.	22PHR101	II MA HRM	
24.	Arockia Varsha. J	22PHR136	II. MA HRM	
25.	S. Joansina.	22PHR105	II M.A. HRM	
26.	Theres Roselin	22PHR121	II M.A. HRM	
27.	P. Jasmine Anantha	22PHR123	II MA. HRM	
28.	F.R. Jenifer catharine	22PHR122	II MA HRM	
29.	S. Tallarine	22PHR118	II MA HRM	S. Tallarine.

ST. JOSEPH'S COLLEGE, TRICHY

PG DEPARTMENT OF COUNSELLING PSYCHOLOGY & COUNSELLING CENTRE

SEMINAR SERIES – ATTENDANCE LIST

DEPARTMENT: I MA HRM TOPIC:

DATE: 8/12/23 TIME: 11.30 AM VENUE:

S.NO	NAME	D.NO	CLASS	SIGN
1.	A. Deepak	23PHR135	HRM	A.D.
2.	Maria Edward Francis. J	23PHR111	HRM	Francis. J
3.	X. PRAVEEN	23PHR114	HRM	X. Praveen
4.	M. Alocious Jokin	23PHR127	HRM	M. Alocious
5.	P Nesamani	23PHR126	HRM	P Nesamani
6.	T. Asik ussain	23PHR107	HRM	T. Asik Hus
7.	D. Pasupathi Raja	23PHR133	HRM	Pasupathi Raja D
8.	R. Jeeva	23PHR119	HRM	R. Jeeva
9.	A.K. ARUNSHANKAR IYYAPAN	23PHR106	HRM	Aiyyapan
10.	S. Arakia David	23PHR104	I.M.A.HRM	S. Arakia David
11.	T. SURYA	23PHR140	I. M A. HRM	T. Surya
12.	M. Karthik	23PHR105	I. MAHRM	M. Karthik
13.	J. Samuel Daniel	23PHR103	I. MAHRM	J. Samuel Daniel
14.	A. SHEEBA	23PHR112	HRM	A. Sheeba
15.	M. Ramila Catherin	23PHR141	I MA HRM	M. Ramila
16.	J. Mary Jebisha	23PHR137	I.MA+IRm	Jebisha.
17.	R. Preethi	23PHR116	IM.A.HRM	R. Preethi
18.	S. Yamuna	23PHR117	I MA HRM	S. Yamuna
19.	D. Baithi Sasa	23PHR121	I MAHRM	Baithi
20.	S B Nitthiya Sri	23PHR122	I MA HRM	Nitthiya
21.	L Monika Mayseat	23PHR124	I MA HRM	L Monika
22.	Susan Alfida. J	23PHR108	I MA HRM	Susan Alfida
23.	Nisma Begum. Z	23PHR102	I MAHRM	Nisma
24.				
25.				

ST. JOSEPH'S COLLEGE, TRICHY

PG DEPARTMENT OF COUNSELLING PSYCHOLOGY & COUNSELLING CENTRE

SEMINAR SERIES – ATTENDANCE LIST

DEPARTMENT: I. MA HRM TOPIC:

DATE: 8/12/23 TIME: 11.30 AM VENUE:

S.NO	NAME	D.NO	CLASS	SIGN
1.	K. Valliammai	23PHR130	I MA HRM	K. valli
2.	Jenna christy. S	23PHR109	I MA HRM	Jenna
3.	Dhivitha M	23PHR123	I MA HRM	
4.	G. Soundariya	23PHR132	I MA HRM	G. S
5.	Padma Priya. R	23PHR101	I MA HRM	
6.	M. Fatima Beevi.	23PHR128	I MA HRM.	M. F
7.	S. Banithra	23PHR125	I MA HRM	S. Banithra
8.	A. Infant Flora	23PHR115	I MA HRM	
9.	G. Gokila	23PHR110	I MA HRM	Gokila
10.	M. Keerthi	23PHR131	I MA HRM	
11.				
12.				
13.				
14.				
15.				
16.				
17.				
18.				
19.				
20.				
21.				
22.				
23.				
24.				
25.				

ST. JOSEPH'S COLLEGE (AUTONOMOUS), TRICHY – 02

PG Dept. of Counselling Psychology & Counselling Centre

A seminar on

MAINTAINING HEALTHY RELATIONSHIPS

for the Department of

Mathematics

Shift I

III UG, I & II PG

Resource Person

Rev. Dr. Emmanuel Arockiam, SJ

Head, Dept. of Counselling Psychology

24 August 2023

11.45 A.M.

SAIL HALL

Organizing committee

Ms. Shylin

Ms. Christeela

PG DEPARTMENT OF COUNSELLING PSYCHOLOGY &

COUNSELLING CENTER

ST. JOSEPH'S COLLEGE (Autonomous)

Tiruchirappalli-620 002

Report on 'Maintaining Healthy Relationship' – Seminar

Date: 24th August 2023

Audience: Students of III UG, I & II PG Mathematics, St. Joseph's College

Introduction

PG Department of Counselling Psychology & Counselling Centre are collaboratively conducting a seminar series on various theme like "Rising above Addiction," "Maintaining Healthy Relationship" & "Managing negative Emotions." **Ms. Shylin** and **Ms. Christeela** were the members in the organizing committee. There were 112 students from the Dept. of Mathematics participated in the seminar.

About the theme

Relationships are a cornerstone of happiness and living a full life. This is because they come with a wide array of rewards. Relationships provide us with friends and family to share our lives with and people who can help us out in tough times. They tend to bring us plenty of laughs and as a result lots of joy. Healthy relationships involve trust, openness, boundaries, respect, affection, communication, and mutual give-and-take. There is no imbalance of power.

Session started at 11.45 p.m. with a prayer song. Ms. Christeela was the master of ceremony of that seminar. Ms. Christeela introduced the resource person, Rev. Dr. Emmanuel Arockiam, SJ to take over the session. Fr. Emmanuel talked about the significance of having healthy relationships. In addition to that, he highlighted the six success elements in relationships. He emphasized the benefits of being in good relationships. He also stressed the values behind the motto of Jesuits, 'making men and women for others' to the participants.

This seminar covered a variety of topics, including:

- The importance of communication, trust, and respect in relationships

- Elements of successful relationships
- How to set boundaries and say no
- How to deal with conflict in a healthy way
- How to recognize the signs of an unhealthy relationship
- Where to get help if you are in an unhealthy relationship.

Conclusion

The seminar came to an end at 1:15 P.M. thanked the speakers and attendees for their contributions. **Ms. Shylin** showed her support by offering assistance with the technology. This seminar, '**Maintaining Healthy Relationship,'** helped the participants to recognize the signs of toxicity in relationships and how to approach other people with kindness and compassion.

Dr. EMMANUEL AROCKIAM, S.J., Ph.D.
DIRECTOR - DEPT OF COUNSELLING PSYCHOLOGY
ST. JOSEPH'S COLLEGE (AUTONOMOUS)
TRICHY-620 002


GPS MAP CAMERA
Dept. of Counselling Psychology &
Counselling Centre, St. Joseph's
Latitude: 10.8284625
Longitude: 78.6904613
Date: 24 Aug 2023
Time: 11:51 AM
Google


GPS MAP CAMERA
Dept. of Counselling Psychology &
Counselling Centre, St. Joseph's
Latitude: 10.8284625
Longitude: 78.6904613
Date: 24 Aug 2023
Time: 11:51 AM
Google

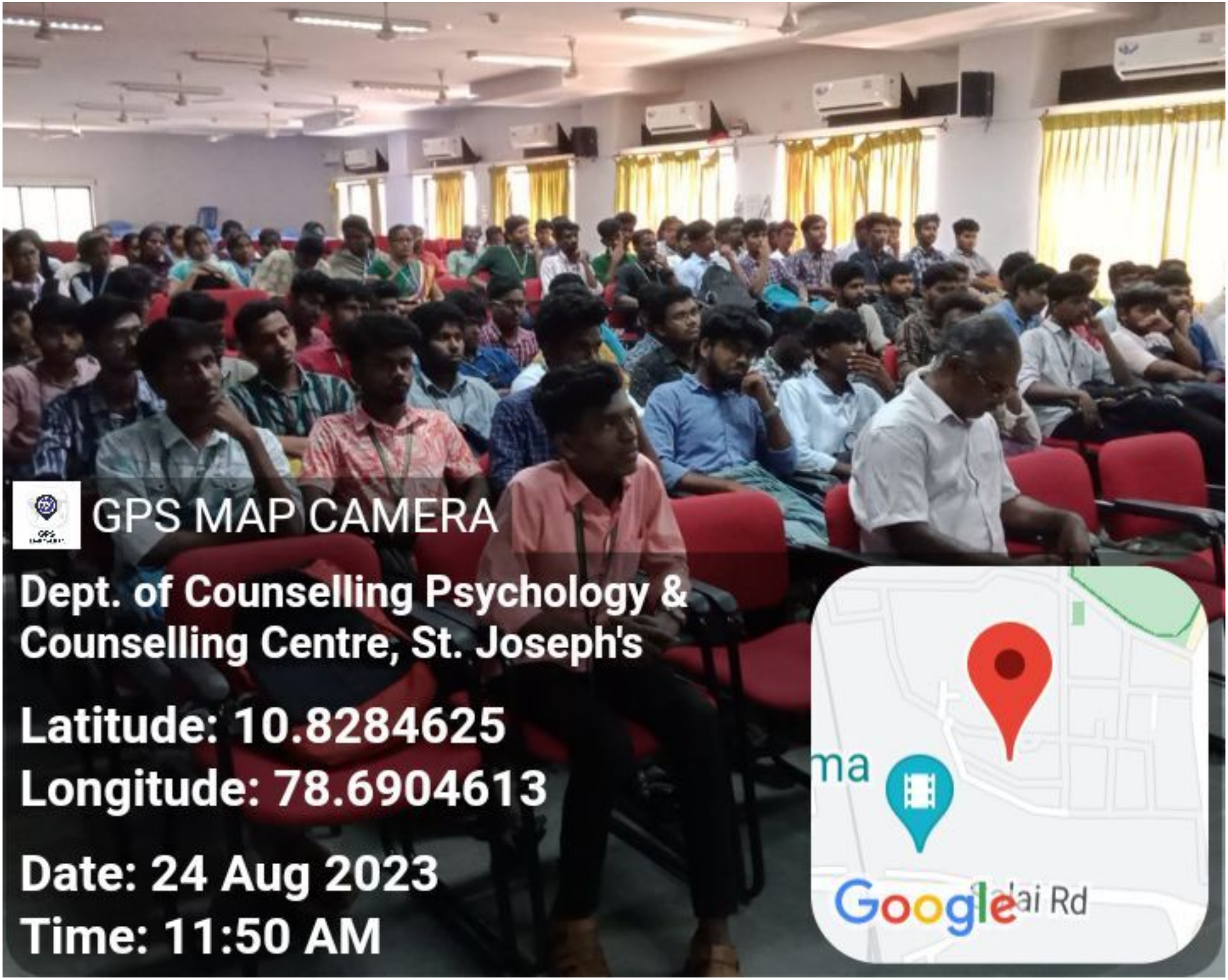
GPS MAP CAMERA
Dept. of Counselling Psychology &
Counselling Centre, St. Joseph's
Latitude: 10.8284625
Longitude: 78.6904613
Date: 24 Aug 2023
Time: 11:50 AM
Google


GPS MAP CAMERA
Dept. of Counselling Psychology &
Counselling Centre, St. Joseph's
Latitude: 10.8284625
Longitude: 78.6904613
Date: 24 Aug 2023
Time: 11:50 AM
Google


GPS MAP CAMERA
Dept. of Counselling Psychology &
Counselling Centre, St. Joseph's
Latitude: 10.8284625
Longitude: 78.6904613
Date: 24 Aug 2023
Time: 11:51 AM
Google

ST. JOSEPH'S COLLEGE, TRICHY

PG DEPARTMENT OF COUNSELLING PSYCHOLOGY & COUNSELLING CENTRE

SEMINAR SERIES – ATTENDANCE LIST

DEPARTMENT: Mathematics

DATE: 24.08.2023 TIME: 11.30 to 1.20 PM VENUE: Sail Auditorium

S.NO	NAME	D.NO	CLASS	SIGN
1.	Agastin Deva Sagayam J	21UMA102	II BSc Maths "A"	
2.	Harish G	21UMA143	A	
3.	Vijay S	21UMA111	A	
4.	Abishek T	21UMA130	A	
5.	Paul clament S	21UMA109	A	
6.	Amal edwin rohan G	21UMA158	A	
7.	Dony infant edison M	21UMA107	A	
8.	Jestin Vino S	21UMA131	A	
9.	Karthikeyan P	21UMA137	A	
10.	Moganapriyan S	21UMA121	A	
11.	Bhararitharan E	21UMA104	A	
12.	Bhavathi G	21UMA144	A	
13.	Francis Benito	21UMA105	A	Benito
14.	Jananthan	21UMA138	A	
15.	Kevin Bedric	21UMA113	A	
16.	Valan Jeremiah	21UMA106	A	
17.	Arun Kumar	21UMA116	A	
18.	Stanley deepak	21UMA132	A	
19.	Kishore . D	21UMA148	A	
20.	Sakthivel . R	21UMA157	A	
21.	Mahesh Kirubhanidhi	21UMA155	A	
22.	Mukesh Kumar	21UMA134	A	
23.	Ranjith	21UMA151	A	
24.	Ruban	21UMA150	A	
25.	Arun Kumar J	21UMA159	A	

ST. JOSEPH'S COLLEGE, TRICHY

PG DEPARTMENT OF COUNSELLING PSYCHOLOGY & COUNSELLING CENTRE

SEMINAR SERIES – ATTENDANCE LIST

DEPARTMENT: MATHEMATICS

DATE: 24-08-2023 TIME: 11:30 AM VENUE: SAIL AUDITORIUM

S.NO	NAME	D.NO	CLASS	SIGN
1.	SHAM LOGESH. B	21UMA202	III B.Sc 'B' MATHS	
2.	JOVIN FRANCIS. G	21UMA203	"	
3.	KISHORE KALVIN. A	21UMA204	"	
4.	SANTHOSH DORRIEN. P.J	21UMA205	"	
5.	BIJU VIJONSON. N	21UMA206	"	
6.	ROSHAN. M	21UMA207	"	
7.	ALBERT REEGAN. S	21UMA208	"	
8.	RUSHWALD RICHARD. A	21UMA209	"	
9.	CHELUSTIN KUMAR. A	21UMA210	"	
10.	MARTIN JOSHUA. B	21UMA212	"	
11.	ROBERT. J	21UMA213	"	
12.	LOUNGH MINGH SAKAL. J	21UMA214	"	
13.	PRABU. S.	21UMA216	"	
14.	SIBISELVAN. D	21UMA217	"	
15.	VENKATESH. A	21UMA220	"	
16.	SURYA. R	21UMA221	"	
17.	ADITYA. D	21UMA223	"	
18.	SHIVASUBRAMANIAN. K. V.	21UMA224	"	
19.	SARATHI. S	21UMA225	"	
20.	LOGESWARAN. S	21UMA228	"	
21.	HANEESH. J	21UMA230	"	
22.	DINESH BABIYAN. R	21UMA234	"	
23.	DHINESH. P	21UMA236	"	
24.	MANISHANKAR. K. C.	21UMA240	"	
25.	PRIYADHARSHAN. P	21UMA241	"	

ST. JOSEPH'S COLLEGE, TRICHY

PG DEPARTMENT OF COUNSELLING PSYCHOLOGY & COUNSELLING CENTRE

SEMINAR SERIES – ATTENDANCE LIST

DEPARTMENT: MATHEMATICS

DATE: 24-08-2023 TIME: 11:30 AM VENUE: SAIL AUDITORIUM

S.NO	NAME	D.NO	CLASS	SIGN
1.	LOGEASWARAN. K	21UMA245	III B.Sc 'B'	K.Logea
2.	~~KOUSICK~~ VINOTH. J	21UMA249	III B.Sc 'B'	J. Vinoth
3.	VASAN. V	21UMA254	"	
4.	SHIVAM. S	21UMA255	"	S. Shiva
5.	GIRIVASAN. M	21UMA257	"	G
6.	JOSHUA REGIT. D	21UMA259	"	D.
7.				
8.				
9.				

ST. JOSEPH'S COLLEGE, TRICHY

PG DEPARTMENT OF COUNSELLING PSYCHOLOGY & COUNSELLING CENTRE

SEMINAR SERIES – ATTENDANCE LIST

DEPARTMENT: Mathematics

DATE: 24.08.23 TIME: 11.30 to 1.20 P.M VENUE: Sail Auditorium

S.NO	NAME	D.NO	CLASS	SIGN
1.	Jeron	21UMA127	A	M Ruba
2.	Dhanush ragupathi	21UMA154	A	m. Dhanush
3.	Naveen	21UMA117	A	K. Naveen
4.	Timy clinton	21UMA108	A	U. Timy
5.	Pravin	21UMA115	A	A. Pravin
6.				
7.				
8.				
9.				
10.				

ST. JOSEPH'S COLLEGE, TRICHY

PG DEPARTMENT OF COUNSELLING PSYCHOLOGY & COUNSELLING CENTRE

SEMINAR SERIES – ATTENDANCE LIST

DEPARTMENT: Mathematics

DATE: 24.08.2023 TIME: 11.30am VENUE: Sail Auditorium

S.NO	NAME	D.NO	CLASS	SIGN
1.	A. Sandhya Mangaal Jeya	22PMA139	II Msc. maths	
2.				
3.	ARUN KUMAR	22PMA126	II. Msc. Maths	
4.	ROHAN CRUZ M	22PMA138	II M.Sc. Maths	
5.	Sunida Jenifer A	23PMA133	I M.Sc Maths	
6.	Hemalatha . C	23PMA113	I . MSc Maths	
7.	Mekaniya . P	23PMA127	I. MSc Maths	
8.	Mariya Ponciya . S	23PMA102	I. Msc Maths	
9.	Jenifer E	23PMA107	I M.Sc Maths	
10.	Arockia Arthi . S	23PMA137	I.M.Sc Maths	
11.	Angelin . L	23PMA117	I M.Sc Maths	
12.	J. JENSY THERASA	23PMA109	I. M.Sc MATHS	
13.	J. Jobitha	23PMA111	I M.Sc MATHS	
14.	V. JERINE SILVIYA	23PMA136	I MSC MATHS	
15.	S. Liney Raja Mary	23PMA126	I M.S.C Maths	
16.	A . Madona	23PMA125	I M.Sc. Maths	
17.	A Arul Reeta	23PMA129	I M.Sc Maths	
18.	A Pushparani	23PMA132	I M.Sc Maths	
19.	A Palica Nancy	23PMA112	I M.Sc Maths	
20.	V. Vishnu	23PMA103	I M.Sc Maths	
21.	A. Elayaraja	23PMA120	I MSC MATHS	
22.	L. Thirukumaran	23PMA119	I Msc Maths	
23.	A. VIJAY	23pma108	I M.Sc maths	
24.	P Sabael.	23Pma123	I M.Sc maths	
25.	GIRISHWAR . T	23PMA110	I M Sc Maths	
26.	Jesrin M	23PMA122	I M.Sc Maths	
27.	MILADIN JOEL . R	23PMA141	I M.Sc maths	

ST. JOSEPH'S COLLEGE, TRICHY

PG DEPARTMENT OF COUNSELLING PSYCHOLOGY & COUNSELLING CENTRE

SEMINAR SERIES – ATTENDANCE LIST

DEPARTMENT: Mathematics

DATE: 24.08.2023 TIME: 11.30a.m VENUE: Sail Auditorium

S.NO	NAME	D.NO	CLASS	SIGN
1.	K AKASAMENAN	22PMA101	II M.Sc	
2.	Arockia koruba R	22PMA102	II - M.Sc	
3.	Deepak. R	22PMA104	II - M.Sc	
4.	S. Mathu kumar	22PMA105	II - M.Sc	
5.	J. kishore	22PMA106	II M.Sc	
6.	Arun V S	22PMA108	II M.Sc	
7.	J. Ibiya Infanta	22PMA109	II M.Sc	
8.	Jeneya Chrishpin. G	22PMA110	II M.Sc	
9.	Vijayeshwaran T	22PMA111	II M.Sc	
10.	KOSMA SARAN KUMAR. A	22PMA112	II M.Sc	
11.	Rajatharan T	22PMA113	II M.Sc	
12.	S. Anali	22PMA115	II - M.Sc	
13.	Joselin Infanta. J	22PMA116	II - M.Sc	
14.	Manisha Maron J	22PMA117	II - M.Sc	
15.	Jaruniya Christy. L	22PMA 122	II - M.Sc	
16.	S Sriram	22PMA124	II - M.Sc	
17.	Alwin denish. D	22PMA127	II - M.Sc	
18.	J Monica Bibiana	22PMA131	II - M.Sc	
19.	R. BINO	22PMA132	II - M.Sc	
20.	B. Dona	22PMA133	II M.Sc	
21.	P. Sangeetha Roveena	22PMA134	II M.Sc	
22.	Praveena. J	22PMA135	II M.Sc	
23.	Jenifer. H	22PMA136	II M.Sc	
24.	ROGER S	22PMA137	II M.Sc	
~~25.~~		~~138~~		
~~26.~~	ALBERT A	22PMA114	II M.Sc	

ST. JOSEPH'S COLLEGE (AUTONOMOUS), TRICHY - 02

PG Dept. of Counselling Psychology & Counselling Centre

A SEMINAR ON

Maintaining Healthy Relationships

for the Department of

B.VOC.
Viscom Technology

RESOURCE PERSON

REV. DR. EMMANUEL AROCKIAM, SJ

Head, Dept. of Counselling Psychology

14.09.2023
9.30 A.M.

SAIL HALL

Organizing committee

Ms. Shylin
Ms. Christeela

PG DEPARTMENT OF COUNSELLING PSYCHOLOGY &

COUNSELLING CENTER

ST. JOSEPH'S COLLEGE (Autonomous)

Tiruchirappalli-620 002

Report on 'Maintaining Healthy Relationship' – Seminar

Date: 14.09.2023

Audience: Students of B.Voc. Viscom Technology

Introduction

PG Department of Counselling Psychology & Counselling Centre are collaboratively conducting a seminar series on various theme like "Rising above Addiction," "Maintaining Healthy Relationship" & "Managing negative Emotions." **Ms. Shylin** and **Ms. Christeela** were the members in the organizing committee. There were 71 students from the Dept. of B.Voc. Viscom Technology participated in the seminar.

About the theme

Relationships are a cornerstone of happiness and living a full life. This is because they come with a wide array of rewards. Relationships provide us with friends and family to share our lives with and people who can help us out in tough times. They tend to bring us plenty of laughs and as a result lots of joy. Healthy relationships involve trust, openness, boundaries, respect, affection, communication, and mutual give-and-take. There is no imbalance of power.

Session started at 9.30 a.m. with a prayer song at SAIL HALL. Ms. Christeela was the master of ceremony of that seminar. **Ms. Christeela** introduced the resource

person, **Rev. Dr. Emmanuel Arockiam, SJ** to take over the session. Fr. Emmanuel talked about the significance of having healthy relationships. In addition to that, he highlighted the six success elements in relationships. He emphasized the benefits of being in good relationships. He also stressed the values behind the motto of Jesuits, 'making men and women for others' to the participants.

This seminar covered a variety of topics, including:

- The importance of communication, trust, and respect in relationships
- Elements of successful relationships
- How to set boundaries and say no
- How to deal with conflict in a healthy way
- How to recognize the signs of an unhealthy relationship
- Qualities of a healthy relationship and healthy people
- Where to get help if you are in an unhealthy relationship.

Conclusion

The seminar came to an end at 11.00 A.M. This seminar, '**Maintaining Healthy Relationship,'** helped the participants to recognize the signs of toxicity in relationships and how to approach other people with kindness and compassion.

Dr. EMMANUEL AROCKIAM, S.J., Ph.D.
DIRECTOR - DEPT OF COUNSELLING PSYCHOLOGY
ST. JOSEPH'S COLLEGE (AUTONOMOUS)
TRICHY-620 002


GPS MAP CAMERA
Dept. of Counselling Psychology &
Counselling Centre, St. Joseph's
Latitude: 10.8284625
Longitude: 78.6904613
Date: 14 Sep 2023
Time: 10:01 AM
Google


GPS MAP CAMERA
Dept. of Counselling Psychology &
Counselling Centre, St. Joseph's
Latitude: 10.8284625
Longitude: 78.6904613
Date: 14 Sep 2023
Time: 10:01 AM
Google


GPS MAP CAMERA
Dept. of Counselling Psychology &
Counselling Centre, St. Joseph's
Latitude: 10.8284625
Longitude: 78.6904613
Date: 14 Sep 2023
Time: 10:01 AM
Google

ST. JOSEPH'S COLLEGE, TRICHY

PG DEPARTMENT OF COUNSELLING PSYCHOLOGY & COUNSELLING CENTRE

SEMINAR SERIES – ATTENDANCE LIST

DEPARTMENT: B.VOC. VISCOM TECHNOLOGY

DATE: 14.09.23 TIME: 10:00AM VENUE: SAIL AUDITORIUM

S.NO	NAME	D.NO	CLASS	SIGN
1.	N. Nithiya Mary	22UVT101	II B.Voc viscom	Nithiya.
2.	G. Dhanushiya	22UVT115	II B.Voc viscom	G.Dhanushiya
3.	S.S. Nazneen Khatoon	22UVT127	II. B.Voc vis com	Nazneen
4.	N. Madhumitha.	22UVT140	II. B.Vo visco m Tech.	N.Madhumitha
5.	A. Aneetta	23UVT120	I. B.voc Viscom Tech	A. Aneetta
6.	M. Pelchiammal	23UVT111	I B.voc viscom Tech	M. Pelchiammal.
7.	B. CARON MEIBA	23UVT134	I B.VOC Viscom Tech	B.CARON MEIBA
8.	K. Thivyasri	21UVT104	III B.voc visco Tech	K.Thivyasri
9.	Pooranic	21UVT142	III B.VOC.Vis Tech	C.Pooranic.
10.	D. Haribaskar	22UVT118	II B.VOC. Viscom	Haribaskar.D
11.	R. Praveen kumar.	22UVT195.	II B.VOC viscom	R.Praveen kumar
12.	M. Divagar	22UVT133	II B.VOC. VISCOM	Divagar
13.	C. Balakrishnan	22UVT103	II B.VOC. VISCOM	C.Balakrishnan
14.	R. Nithishkamar	23UVT109.	I B.VOC. Viscom	R.Nithishkamar
15.	R. Ajay	23UVT143	I B.VOC. Visco	R.Ajay.
16.	K. Prakash	23UVT121	I B.VOC. VISCOM	K.Prakash
17.	J. Felix	23UVT144	I B.VOC. Viscom	J. Felix
18.	A. NIKIL	23UVT139	I B.VO C VISC	A.NIKIL
19.	M. Hariharan	23UVT116	I B.VOC. VISCOM	M. Hariharan
20.	S. Bhavan Easwer	23UVT124	I B.Voc. viscom	S. Bhavan Easwer.
21.	S. Paranjothi.	23UVT135	I B.Voc. VIS.com	S. Paranjothi.
22.	V. Bhavath.	23UVT122	I B.VOC VISCOM	V.Bhavath
23.	A. Lohith	22UVT145	II. nd B. Voc. Vis com. Tech.	A.Lohith.
24.	T. Alex	22UVT149	I nd B. VOC viscom Tech	T.Alex.
25.	R. Sri Ram	21UVT120	III B. VOC VISCOM TECH	R.Sri Ram.

S.NO	NAME	D.NO	CLASS	SIGN
1.	V Aravind	21UVT114	III BVoc VCT	
2.	S. Manojkumar	21UVT115	III B.Voc V.C.T.	
3.	D. Subash	21UVT141	III B.Voc V.C.T	
4.	D. Sasvin Raj	22UVT146	II B.Voc V.C.T	
5.	K. Madhan	22UVT123	II B.Voc V.C.T	
6.	R. JoeBastin	22UVT144	II B.Voc viscom	
7.	J. Dilson	22UVT153	II B.Voc. VIS	
8.	R. Yogesh	22UVT114	II B.voc.viscom	
9.	A Maria Clinton	22UVT107	II B.Voc	
10.	SARAN. M	22UVT117	II-B.VOC.VCT	
11.	Silvaraj. P	22UVT136	II. B. voc. vct	
12.	Jeyandheran S	22UVT112	II B. Voc VCT	
13.	Sivabalan R	22UVT111	II B.Voc. VCT	
14.	Dineshkumar. S	22UVT120	II B.Voc VCT	
15.	Mukesh Kannan. A	23UVT150	I B.voc V.C.T	
16.	R. ARUN RAJ	23UVT141	I B.voc VCT	
17.	Dinesh Kanna M	23UVT142	I B.Voc VCT	
18.	S. ARUN RAJ	23UVT114	I. B. VOC VIS	
19.	J. Naveen kumar	23UVT105	I B.voc. vis	
20.	K. Dastin Nelson	21UVT130	III B.Voc vis	
21.	A Thilak	21UVT145	III B.Voc VIS	
22.	Krishna. R	21UVT144	III B.Voc VIS	
23.	Naresh kumar K	21UVT122	III B.Voc VIS	
24.	Ramsamy J	21UVT125	III B.Voc VIS	
25.	Josh Mathew P.J.	21UVT116	III B.Voc vis	

ST. JOSEPH'S COLLEGE, TRICHY

PG DEPARTMENT OF COUNSELLING PSYCHOLOGY & COUNSELLING CENTRE

SEMINAR SERIES – ATTENDANCE LIST

DEPARTMENT: B.VOC. VISCOM TECHNOLOGY

DATE: 14/09/2023 TIME: 10:00 A.M VENUE: Seminar Hall Auditorium.

S.NO	NAME	D.NO	CLASS	SIGN
1.	P. N. SURYA	21UVT132	III B.VOC. VISCOM Tech	
2.	Nikhil Krishna SR	23UVT138	I st B.VOC	
3.	A AARON	22UVT104	I B.VOC	
4.	Richard J	22UVT132	2 st B.VOC	
5.	Jeevan	22UVT109	2st B.VOC	
6.	Kathir	22UVT109	2st B.VOC	
7.	K. Daniel	21UVT135	III B. VOC VISCOM	
8.	S. EZHIL	21UVT129	III. B.VOC. Viscom	
9.	M. Kevin	21UVT137	III B.VOC	
10.	J. LOUIS	21UVT121	III .B.VOC.	
11.	G. Rakikesh	21UVT105	III B.VOC. VISCOM	G. Rakikesh.
12.	Anbu Selvan. V	21UVT112	III.B.VOC VISCOM	Anbuselvan.
13.	Balaji. V	21UVT131	III B.VOC VISCOM	V. Balaji
14.	Sathish. A	21UVT102	III B.VOC VISCOM	
15.	K. Dhanasekaran	21UVT110	III. B.VOC	K. Dhanasekaran
16.	G. Gugan	23UVT107	I. B.VOC	G. Gugan
17.	Ag. Ashik	23UVT124	I. B.VOC	
18.	S. RAJKUMAR	23UVT147	I B.VOC	
19.	A. AKASH SURUBAN	23UVT103	I. BVOC	AG. ASL.
20.	Shaun Sammuel Roy	23UVT126	I. BOV	
21.	Dupak Dhanotharaj	23UVT129	I. BOV	Dupak
22.				
23.				

ST. JOSEPH'S COLLEGE (AUTONOMOUS), TRICHY - 02

PG Dept. of Counselling Psychology & Counselling Centre

A SEMINAR ON

RISING ABOVE ADDICTION

FOR THE DEPARTMENT OF

B.COM HONOURS

III UG

RESOURCE PERSON

REV. DR. EMMANUEL AROCKIAM, SJ
Head, Dept. of Counselling Psychology

02 SEPT 2023
11.45 A.M.

SAIL HALL

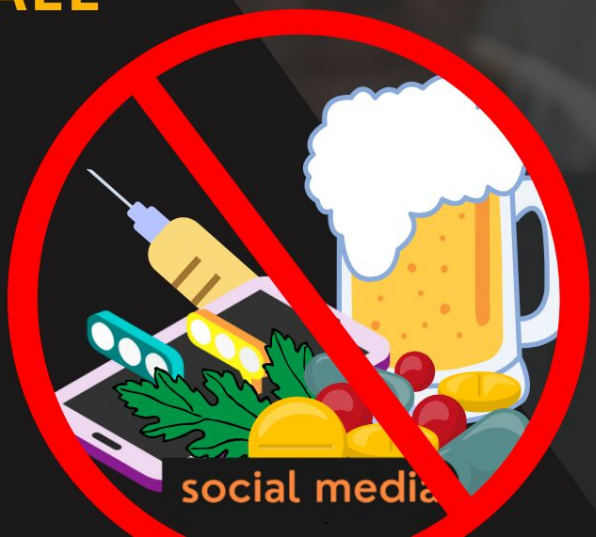

Organizing committee

Ms. Shylin
Ms. Christeela

PG DEPARTMENT OF COUNSELLING PSYCHOLOGY

& COUNSELLING CENTRE

ST. JOSEPH'S COLLEGE (Autonomous)

Tiruchirappalli-620 002

Report on Rising above Addiction – seminar

Date: 02.09.23

Audience: Students of III B.COM HONOURS

Introduction

The PG Counselling Psychology Department and the Counselling Centre are working together to host a seminar series on topics including "Managing Negative Emotions," "Rising above Addiction," and "Maintaining Healthy Relationships." Members of the organising committee were **Ms. Christeela** and **Ms. Shylin**. The lecture was attended by 58 students from the Department of B.COM Honours.

About the theme

An addiction is a persistent malfunction of the reward, motivation, and memory systems in the brain. It has to do with how your body desires a substance or behaviour, especially if it leads to an obsessional or compulsive desire for the "reward" and a lack of regard for the consequences.

Someone who has an addiction will: be unable to refrain from taking the drug or stopping the addictive behaviour; show a lack of self-control; have an increased desire for the drug or behaviour; discount the possibility that their behaviour may be harming others; and lack an emotional response.

This seminar's goal is to educate young people about addiction and provide them with strategies for overcoming it.

At SAIL HALL, the programme got underway at 11.45 a.m. A song of prayer opened the session. The master of ceremonies for the session was Ms. Christeela, a counsellor.

Rev. Dr. Emmanuel Arockiam, S.J., Head of the Department of Counselling Psychology and Director of the Arrupe Library, was introduced by Ms. Christeela as the resource person.

Rising above Addiction was the topic of Dr. Emmanuel's lecture. He explained he origin, triggers, and approaches for managing addiction. Through some thought-provoking questions and hypothetical scenario illustrations, he assisted the pupils in developing rational thought. The pupils engaged fully in that lesson.

Two people from the rehabilitation facility ARRUPE SUGALAYA were invited to the meeting. They are receiving care from the rehab facility run by Rev. Fr. Jayapathy, SJ.

Both of them used their personal stories to discuss the negative impacts of alcohol and drugs. Following their discussion, Fr. Emmanuel gave the kids advice on how to deal with addiction and cravings. The session ended with a vote of gratitude at 1.15 p.m.

Conclusion

Participants learned about the numerous elements causing addiction and how to stop it. At 1.15 P.M., the session came to a conclusion. The seminar "Rising above Addiction" taught the attendees how to spot the symptoms of addiction, how to address the subject with respect and compassion, and how to support those who are dealing with drug misuse problems.

Dr. EMMANUEL AROCKIAM, S.J., Ph.D.
DIRECTOR - DEPT OF COUNSELLING PSYCHOLOGY
ST. JOSEPH'S COLLEGE (AUTONOMOUS)
TRICHY-620 002


GPS MAP CAMERA
Dept. of Counselling Psychology &
Counselling Centre, St. Joseph's
Latitude: 10.8284625
Longitude: 78.6904613
Date: 02 Sep 2023
Time: 11:58 AM
Google


GPS MAP CAMERA
Dept. of Counselling Psychology &
Counselling Centre, St. Joseph's
Latitude: 10.8284625
Longitude: 78.6904613
Date: 02 Sep 2023
Time: 11:58 AM
Google


GPS MAP CAMERA
Dept. of Counselling Psychology &
Counselling Centre, St. Joseph's
Latitude: 10.8284625
Longitude: 78.6904613
Date: 02 Sep 2023
Time: 11:58 AM
Google


GPS MAP CAMERA
Dept. of Counselling Psychology &
Counselling Centre, St. Joseph's
Latitude: 10.8284625
Longitude: 78.6904613
Date: 02 Sep 2023
Time: 11:58 AM
Google


GPS MAP CAMERA
Dept. of Counselling Psychology &
Counselling Centre, St. Joseph's
Latitude: 10.8284625
Longitude: 78.6904613
Date: 02 Sep 2023
Time: 11:58 AM
Google


GPS MAP CAMERA
Dept. of Counselling Psychology &
Counselling Centre, St. Joseph's
Latitude: 10.8284625
Longitude: 78.6904613
Date: 02 Sep 2023
Time: 11:58 AM
Google


GPS MAP CAMERA
Dept. of Counselling Psychology &
Counselling Centre, St. Joseph's
Latitude: 10.8284625
Longitude: 78.6904613
Date: 02 Sep 2023
Time: 11:58 AM
Google

ST. JOSEPH'S COLLEGE, TRICHY

PG DEPARTMENT OF COUNSELLING PSYCHOLOGY & COUNSELLING CENTRE

SEMINAR SERIES - ATTENDANCE LIST

DEPARTMENT: B Com (Honours) SAIL HALL

DATE: 02/09/2023 TIME: 11.45 AM TOPIC: Rising above Addiction

S.NO	NAME	D.NO	CLASS	SIGN
1.	Vikram	21UCR509	III	
2.	Edison J	21UCR521	III	
3.	Balaravbabu T M	21UCR532	III	
4.	Sri Ganga Harish	21UCR517	III	
5.	R. Dinesh Shekar	21UCR511	III	
6.	A. Sachin Aadhithya	21UCR518	III	
7.	Pranav Baalaji. M	21UCR549	III	
8.	Kesavamurthy V	21UCR537	III	
9.	Vasanth Karthick	21UCR506	III B. Com (Hons)	
10.	William Anthony Raj	21UCR502	III B.Com Hons	
11.	Dharush Kanna S	21UCR534	III B.Com (Hons)	
12.	MERWIN PRAKASS L.	21UCR546	III B.COM (HONS)	
13.	A. Sunil Adhithya	21UCR529	III B.com (Hons)	
14.	Kamalathiyagarajan S	21UCR553	III. B.com (Hons)	
15.	Crotaul P	21UCR530	III B.com (Hons)	
16.	Jose Thayal Sanjeev	21UCR552	III - B.com Hons	
17.	T. Krishna Priya	21UCR510	III - B.com Hons	
18.	R. Jayasri Vishwariya	21UCR526	III - B Com Hons	
19.	A. Rishika	21UCR520	III. B.com Hons	
20.	I. Afthaab Al Nazar	21UCR515	III B com Hons	
21.	R.K. Jayashree	21UCR554	III B.com hons	
22.	S. Monnika	21UCR542	III B.com hons	
23.	V. Rishi Karthick	21UCR546	III B com hons	
24.	G. Dhananya	21UCR531	III B Com (Hons)	
25.	Kirupah Sri R.	21UCR538	III B Com (Hons)	

S.NO	NAME	D.NO	CLASS	SIGN
1.	Varsha.S	21UCR550	III rd B com (Honours)	VarshaS
2.	Thanika P.S.	21UCR548	III B Com Honours	P.S.Thanika
3.	S. Joyce	21UCR523	III rd B.com (Honours)	S. Joyce
4.	P. Sugarthi	21UCR535	III B.com Honours	Sathi
5.	S Gurus Jenifer	21UCR504	III B.com Honours	S. Jenifer
6.	G Shivalanjini	21UCR516	III B.com Honours	Shivalanjini G
7.	R.keerthana	21UCR505	B.com Honours	
8.	G Priyadharshini	21UCR536	III rd B.COM (Hons)	Priya G
9.	K.N.R. Vaayathri Vidya	21UCR545	III rd B Com Hons	Vaayathri
10.	M. VARSHINI	21UCR522	III BCOM HONS	M. Varshini
11.	S. Pavithraasri	21UCR547	III BCom (HONS)	S. Pavithra
12.	S. Akshaya	21UCR518	III BCom Honours	S. Akshaya
13.	B. Evangeline	21UCR501	III BCom Honours	B. Evangeline
14.	R Sujitha	21UCR508	III B. Com (Hons)	R. Sujitha
15.	N. Keerthana	21UCR543	III B.Com (Hons)	N. Keerthana
16.	S. Christha Evangelin	21UCR514	III B.com (Hons)	S. Christha Evangelin
17.	D. Dalphia	21UCR541	III B.Com (Honours)	D. Dalphia
18.	A. Denila Sameeen	21UCR502	III B.com (Honours)	A. Denila Sameeen
19.	Jeeviga. M	21UCR540	III - B.com (Hons)	M. Jeeviga
20.	SHIVA SAKTHI. M	21UCR519	III B.Com (Hons)	M. Shiva Sakthi
21.	Manisha. M	21UCR533	III B.com (Hons)	M. Manisha
22.	K. Charu Bala	21UCR513	III B.com (Hons)	K. Charu Bala
23.	S. Keerthi.	21UCR524	III B.com (Hons)	S. Keerthi
24.				
25.				

PG Dept. of Counselling Psychology & Counselling Centre

St. Joseph's College (Autonomous), Trichy - 02

A seminar on

Rising above Addiction

for the Department of

Commerce - Shift I

I & II UG

Resource Person

Rev. Dr. Emmanuel Arockiam, SJ

Head, Dept. of Counselling Psychology

DATE: 13.09.2023 - 9.30 A.M.

VENUE: SAIL HALL

Organizing committee

Ms. Shylin

Ms. Christeela

PG DEPARTMENT OF COUNSELLING PSYCHOLOGY

& COUNSELLING CENTRE

ST. JOSEPH'S COLLEGE (Autonomous)

Tiruchirappalli-620 002

Report on Rising above Addiction – seminar

Date: 13.09.23

Audience: Students of I & II B.COM Shift I

Introduction

The PG Counselling Psychology Department and the Counselling Centre are working together to host a seminar series on topics including "Managing Negative Emotions," "Rising above Addiction," and "Maintaining Healthy Relationships." Members of the organising committee were **Ms. Christeela** and **Ms. Shylin**. The lecture was attended by 202 students from the Department of Commerce Shift I

About the theme

An addiction is a persistent malfunction of the reward, motivation, and memory systems in the brain. It has to do with how your body desires a substance or behaviour, especially if it leads to an obsessional or compulsive desire for the "reward" and a lack of regard for the consequences.

Someone who has an addiction will: be unable to refrain from taking the drug or stopping the addictive behaviour; show a lack of self-control; have an increased desire for the drug or behaviour; discount the possibility that their behaviour may be harming others; and lack an emotional response.

This seminar's goal is to educate young people about addiction and provide them with strategies for overcoming it.

At SAIL HALL, the programme got underway at 9.30 a.m. A song of prayer opened the session. The master of ceremonies for the session was **Ms. Christeela**, a counsellor.

Rev. Dr. Emmanuel Arockiam, S.J., Head of the Department of Counselling Psychology and Director of the Arrupe Library, was introduced by Ms. Christeela as the resource person.

Rising above Addiction was the topic of Dr. Emmanuel's lecture. He explained he origin, triggers, and approaches for managing addiction. Through some thought-provoking questions and hypothetical scenario illustrations, he assisted the pupils in developing rational thought. The pupils engaged fully in that lesson.

A person from the rehabilitation facility ARRUPE SUGALAYA was invited to the meeting. He is receiving care from the rehab facility run by Rev. Fr. Jayapathy, SJ.

He used his personal stories to discuss the negative impacts of alcohol and drugs. Following his discussion, Fr. Emmanuel gave the kids advice on how to deal with addiction and cravings. The session ended with a vote of gratitude at 11.00 a.m.

Conclusion

Participants learned about the numerous elements causing addiction and how to stop it. At 11.00 A.M., the session came to a conclusion. The seminar "Rising above Addiction" taught the attendees how to spot the symptoms of addiction, how to address the subject with respect and compassion, and how to support those who are dealing with drug misuse problems.

Dr. EMMANUEL AROCKIAM, S.J., Ph.D.
DIRECTOR - DEPT OF COUNSELLING PSYCHOLOGY
ST. JOSEPH'S COLLEGE (AUTONOMOUS)
TRICHY-620 002


GPS MAP CAMERA
Dept. of Counselling Psychology &
Counselling Centre, St. Joseph's
Latitude: 10.8284625
Longitude: 78.6904613
Date: 13 Sep 2023
Time: 9:46 AM
Google


GPS MAP CAMERA
Dept. of Counselling Psychology &
Counselling Centre, St. Joseph's
Latitude: 10.8284625
Longitude: 78.6904613
Date: 13 Sep 2023
Time: 9:45 AM
Google


GPS MAP CAMERA
Dept. of Counselling Psychology &
Counselling Centre, St. Joseph's
Latitude: 10.8284625
Longitude: 78.6904613
Date: 13 Sep 2023
Time: 9:46 AM
Google


GPS MAP CAMERA
Dept. of Counselling Psychology &
Counselling Centre, St. Joseph's
Latitude: 10.8284625
Longitude: 78.6904613
Date: 13 Sep 2023
Time: 9:46 AM
Google


GPS MAP CAMERA
Dept. of Counselling Psychology &
Counselling Centre, St. Joseph's
Latitude: 10.8284625
Longitude: 78.6904613
Date: 13 Sep 2023
Time: 9:46 AM
Google


GPS MAP CAMERA
Dept. of Counselling Psychology &
Counselling Centre, St. Joseph's
Latitude: 10.8284625
Longitude: 78.6904613
Date: 13 Sep 2023
Time: 9:46 AM
Google


GPS MAP CAMERA
Dept. of Counselling Psychology &
Counselling Centre, St. Joseph's
Latitude: 10.8284625
Longitude: 78.6904613
Date: 13 Sep 2023
Time: 9:46 AM
Google

ST. JOSEPH'S COLLEGE, TRICHY

PG DEPARTMENT OF COUNSELLING PSYCHOLOGY & COUNSELLING CENTRE

SEMINAR SERIES – ATTENDANCE LIST

DEPARTMENT: Commerce (Shift I)

DATE: 13.09.23 TIME: 9.30 A.M. VENUE: SAIL HALL

S.NO	NAME	D.NO	CLASS	SIGN
1.	S. Deepak	22UC0249	II-B.Com-B	
2.	W. Joshi Jess	22UC0222	II-B.Com-B	
3.	S. John Infant Raj	22UC0231	II-B.Com-B	
4.	V. Keerthivasan	22UC0234	II-B.Com-B	
5.	R.M.S Vansoothasan	22UC0128	II B.Com "A"	
6.	M. Dharshan	22UC0111	II B.Com 'A'	
7.	K. Shibiraaj	22UC0157	II B.Com 'A'	
8.	A. Arul Bharath Raj	22UC0204	II Bcom 'B'	
9.	S. Ebinezer pat	22UC0202	II B.Com B	
10.	R. Reegan	22UC0135	II B.Com 'A'	
11.	I. Jerald	22UC0136	II B.Com 'A'	
12.	N. Purushothaman	23UC0157	I B.Com 'A'	
13.	S. Stephen James	23UC0128	I B.Com 'A'	
14.	X Kevin Dajan	23UC0122	I B.Com (A)	
15.	A.R. Jaison Ruswelt	23UC0136	I B.Com (A)	Jaison
16.	Shijai S	23UC0251	I B.Com (B)	
17.	SACHIO ROUBERTIA	22UC0203	II - B.COM (B)	
18.	VIGNESHR	22UC0270	II - B.COM (B)	Vignesh
19.	K. Yakash	22UC0268	II - B.Com (B)	
20.	N. AKASH	22UC0232	II - B.Com (B)	
21.	S. Adithya	22UC0240	II B.Com (B)	
22.	Sivalingam selvaraj	22UC0230	II - B.Com (B)	
23.	R Hari Krishnan	23UC0206	I - B.Com B	
24.	J. ALIN INSTAN	23UC0202	I - B.Com B	
25.	J. Jeyaprakash	23UC0215	I - B.Com (B)	

ST. JOSEPH'S COLLEGE, TRICHY

PG DEPARTMENT OF COUNSELLING PSYCHOLOGY & COUNSELLING CENTRE

SEMINAR SERIES – ATTENDANCE LIST

DEPARTMENT: Commerce (Shift-I)

DATE: 13.09.23 TIME: 9.30 A.M. VENUE: SAIL HALL

S.NO	NAME	D.NO	CLASS	SIGN
1.	Arockia Joshua J	22UC0166	II B.Com A	
2.	Abinash. K.S	22UC0229	II B.Com 'B'	
3.	Dharshan. C	22UC0253	II B.Com 'B'	
4.	Antony Devota. J.	22UC0220	II. B.Com 'B'	
5.	N. Sudharsan	22UC0108	II B.Com A	
6.	Sriharish. M	22UC0272	II B.Com 'B'	
7.	Bharathi Kannan. K	23UC0158	I B.Com 'A'	
8.	Pandi Selvam. S	23UC0268	I B.Com 'B'	
9.	Krishna prakash. P	23UC0217	I B.Com "B"	
10.	AJAY. B	23UC0265	I. B.Com B	
11.	Jeevanandharan. E	23UC0270	I. B.Com B	
12.	A. Riyas Adaikala Raj	22UC0210	II B.Com B	
13.	S. Manikanda Prabu.	22UC0260	II. B.Com. B	
14.	R. Ajay	23UC0165	I. B.Com 'A'	
15.	A. Rakesh	23UC0266	I. B.Com B	
16.	R. Saranraj	23UC0277	I. B.Com B	
17.	Rohith K	23UC0101	I B.Com 'A'	
18.	Karthik. R	23UC0234	I. B.Com-B	
19.	Raj Barath. R	23UC0241	I B.Com-B	
20.	Arvinth. M	23UC0151	I. B.Com-B	
21.	R. Saravana	23UC0205	I B.Com B	
22.	S. Prabhakaran	23UC0173	I B.Com 'A'	
23.	S. Kishore Kumar	28UC0109	I. B.Com "A"	
24.	M. Hari Haran	23UC0211	I B.Com "B"	
25.	S. Hrithick	23UC0119	I B.Com A	
26.	R. Monish	23UC0106	I B.Com A	
27.	K. Dharun.	23UC0150	I-B.Com-A	
28.	Luthin.	22UC0103	II. B.Com A	
29)	A Swith. C	22UC0158	II. B.Com 'A'	
30)	Jeevan. P	22UC0129	II B.Com 'A'	

31)	J. Andrew Rishwanth	22UC0124	II B.com(A)	J. Andrew
32)	S. VIGNESH	22UC0143	II-BCom "A"	
33)	A. Mariya Jayantha Kumar	22UC0102	II B.com "A"	A. Mariya
34)	K. R. Pranav Suriya	23UC0241	I B.com "B"	K.R. Pranav Suriya
35)	S. Ajay ram	23UC0225	I B. com B	S. Ajay
36)	R. HARIHARAN SUDHAN	23UC0275	I B.COM B	R. Hari
37)	S. Adithya	23UC0175	I-B.COM "A"	S. Adithya
38)	Jerome Immanuvel. L	23UC0129	I-B.COM "A"	Jerome Immanuvel.
39)	A. Mishale	23UC0214	I-B.com-B	A. Mishale
40)	R. Subramaniya Dharun	23UC0203	I-B.Com-'B'	R. Subramaniya Dharun
41)	R. Jeeva	23UC0130	I-B.Com-'A'	R. Jeeva
42)	X. Godwin	23UC0102	I-B.Com 'A'	X. Godwin
43)	J. Harris franklin	23UC0126	I-B.com "A"	J. Harris franklin
44)	J. Jeswin Reeves	22UC0225	II. B.com 'B'	Jeswin
45)	Jeshwin Romlod	22UC0214	II. B.com 'B'	

ST. JOSEPH'S COLLEGE, TRICHY

PG DEPARTMENT OF COUNSELLING PSYCHOLOGY & COUNSELLING CENTRE

SEMINAR SERIES – ATTENDANCE LIST

DEPARTMENT: Commerce (shift I)

DATE: 13.09.23 TIME: 9.30 A.M. VENUE: SAIL HALL

S.NO	NAME	D.NO	CLASS	SIGN
1.	Bishwin Tom Cruse, AS	22UC0263	B.Com	
2.	A. Pravinraj	23UC0233	B.Com	
3.	N.D Lawdhu Vishal	23UC0111	B-COMA	
4.	A. YUNAS	23UC0108	B.Com "A"	
5.	P. Pravin	23UC0153	B.com 'A'	
6.	G Ronald Navin Edison	23UC0135	B.Com 'A"	
7.	A. Daniel Joseph	23UC0267	B.com 'B"	
8.	J. David sirumani	23UC0227	B.Com 'B'	
9.	G. SRIKRISHNA	23UC0155	B.Com 'A'	
10.	A. Merlin Mithila	23UC0127	B.com "A"	
11.	A. Judeth	23UC0112	B.COM. 'A'	
12.	James Ranjithan	23UC0105	B.com. 'A'	
13.	P. Arockia Joshua.	23UC0134.	B.com "A"	
14.	A. Sahaya Anish	23UC0138	B.COM 'A'	
15.	W. Bright Nishwin	23UC0255	B.com 'B'	
16.	P. Arul Dinesh	23UC0135	B.com 'A'	
17.	K. Nitish	23UC0264	B.com "B"	
18.	V. Robin Nicksalson	23UC0113	B.com "A"	
19.	Johnson Paulraj. A	23UC0139	B. Com "A"	
20.	Jaya Prakash Ebenazer	23UC0145	B. Com 'A'	
21.	Karthick. D	22UC0255	II B.com 'B"	
22.	Assain Mohamed. B	22UC0172	II B. Com 'A'	
23.	Akashraj. J	23UC0207	I B Com 'B'	
24.	Gugan. T	23UC0167	I Bcom 'A'	
25.	Dharshan. K	23UC0160	I. Bcom 'A'	
26.	James Vasanth. K	23UC0117	I. Bcom 'A'	
27.	P. Pradiv.	23UC0220	I. BCOM B'	
28	K. Manojkumar	23UC0252	I Bcom 'B'	
29.	Suresh. CM	23UC0156	I B.COM(A)	

30.	NaveenRaj. S	23UC0164	I - B.com(A)	NaveenRaj
31.	Kishorekanth. D	23UC0163	I B.Com "A"	Kishorekanth
32	LOGESHWARAN.S	23UC0140	I B.Com 'A'	S. Logesh
33	Ajay J.B.T	23UC0146	I B Com "A"	Ajay
34	P. Bala	23UC0152	I BCom - A	
35.	E. JOHN SUNEJ	23UC0107	I B.com - A	E. John Sunej
36.	D. Domni	23UC0161	I B.com - A	D. Domni
37.	Nathin Jenish. N	23UC0154	I. B.com - A	Nathin
38	Bharanees. S	23UC0259	I - B.com - B	Bharanees

ST. JOSEPH'S COLLEGE, TRICHY

PG DEPARTMENT OF COUNSELLING PSYCHOLOGY & COUNSELLING CENTRE

SEMINAR SERIES – ATTENDANCE LIST

DEPARTMENT: Commerce (Shift I)

DATE: 13.09.2023 TIME: 9.30 A.M. VENUE: SAIL HALL

S.NO	NAME	D.NO	CLASS	SIGN
1.	Paul Jack . S	22UCO211	II - B.Com B	
2.	N. Immanuel.	22UCO265	II - B.Com B	
3.	B. Immanuel.	22UCO261	II - B.Com B	
4.	K. Balaji	22UCO246	II - B.Com B	
5.	F. Infant Tom	22UCO235	II - B.Com B	
6.	Bhavan Prajicca Almeida	22UCO212	II - B.Com B	
7.	P. Sherwin Joshua	22UCO101	II. B.Com (A)	
8.	M.S Teevanandham	22UCO155	II B.Com (A)	
9.	J. ALLWIN	22UCO227	II B.Com 'B'	
10.	R. Suriya Narayanan	22UCO243	II B.Com 'B'	
11.	T.R. Lakshmi Narayanan	22UCO273	II B.Com B	
12.	S. Bharanidharan	22UCO257	II B.Com 'B'	
13.	S. Jagatheesh Pandian	22UCO244	II B.Com 'B'	
14.	C. Ghogulram	22UCO228	II B.Com 'B'	
15.	E. Thomas Edison	22UCO259	II. B.Com 'B'	
16.	T. Murali Manohar.	22UCO271	II B.Com 'B'	
17.	A.J Allan George	22UCO206	II B.Com 'B'	
18.	A. Jithin Francis	22UCO209	II B.Com 'B'	
19.	A. CABOL BENEDICT	23UCO209	I B.Com B	
20.	Nugaranthan	23UCO243	I B.Com B	
21.	A. Dinesh Andrew	23UCO249	I B.Com B	
22.	C. Manish	23UCO238	I B.Com B	
23.	V. Mithilesh	22UCO119	II - B.Com - A	
24.	B. Surya	22UCO159	II - B.Com - A" B	
25.	A. Mervin Titus	22UCO217	II - B.Com B	
26.	Siva varneshwar	22UCO144	II B.Com A	
27	Janahi Raman	22UCO162	II B.Com A	
28	clifton	22UCO156	II B.Com (A)	

29)	R.T. Saravanan	23UC0174		1st B.com A
30)	S. Akash	23UC0263		I-B.com (B) Sec
31)	A. Richard	23UC0245	A. Richard	I B.Com (B)
32)	A. Reganraj	23UC0204		I-B.Com(B)
33)	R. Ramakrishnan.	23UC0250		I st B.Com (B)
34)	A Jeromedaniel	23UC0247		I B.com (B)
35)	S. Balamurugan.	23UC0257		I B.Com (B)

ST. JOSEPH'S COLLEGE, TRICHY

PG DEPARTMENT OF COUNSELLING PSYCHOLOGY & COUNSELLING CENTRE

SEMINAR SERIES – ATTENDANCE LIST

DEPARTMENT: Commerce (Shift I)

DATE: 13.09.23 TIME: 9.30 A.M. VENUE: SAIL HALL

S.NO	NAME	D.NO	CLASS	SIGN
1.	G. Thamotrai Seluan	22UC0138	II-B.com-A	G. Thamo
2.	V. Celestine Jones	22UC0161	II, B com-A	V. Jones
3.	S. Stalin Jeffrey	22UC0109	II. B.Com-A	S. Jeffrey
4.	J. Robin	22UC0127	II Bcom - A	
5.	S. Rohith	22UC0149	II. Bcom-A	Rohith S
6.	P. Paes	22UC0110	II B Com-A	Paes
7.	S. Chandrasekar	22UC0168	II B.com-A	S Sekhar
8.	J. Joel Daniel	23UC0261	I B.Com-B	J. Joel Daniel
9.	A. Ananth benoit	23UC0216	I B.Com-B	A. Ananth Benoit
10.	M. Veera Mani	23UC0260	I B.com B	M. Mani
11.	K Arun kumar	23UC0210	I B.com-B	K. Arun Kumar
12.	A. Aswin	23UC0201	I B.Com. B	A Aswin
13.	R. Joe Gnana raj	23UC0228	I B.Com B	R. Joe Gnana raj
14.	R. Gabriel	23UC0229	I B.com-B	R. Gabriel
15.	A.S. Manoj Kumar	23UC0258	I. B Com-B	A.S. Manoj
16.	R. Aaron	22UC0130	II. B.Com-A	R. Aaron
17.	P. K. Hari prasath	22UC0131	II. B Com-A	P. K. Hari
18.	J. Haritharan	22UC0146	II. B.com. A	J. Haritharan
19.	C.K. Pugazhanthi	23UC0171	I - B.com.A	
20.	T. Aro Prashanth	23UC0137	I. B.com. A	
21.	K. Harish	23UC0162	I. B.Com "A"	
22.	Roshan K	23UC0226	I.B.com "B"	R. M.
23.	B. Deebendraa	23UC0114	I B.Com "A"	B. Deebendraa
24.	S. Manojkumar	23UC0125	I. B.com A	S. Manojkumar
25.	R. Bala Kumar	23UC0276	I. B.com "B"	R. Bala Kumar

26)	Jeffrey Aroc	22UC0266	II B.Com(B)	
27)	Shri Hari Krishnan M	22UC0254	II B.Com : B	
28)	Pradhumnan. S	22UC0238	II B.Com - B	
29)	Kiruthic Raj T S	22UC0258	II B.Com - B	
30)	S. ARUNPRAKASH	22UC0207	II - B.Com 'B'	
31)	C.S. NANDHA	22UC0247	II - B.Com 'B'	
32)	A. Karthick	22UC0262	II B.Com 'B'	

ST. JOSEPH'S COLLEGE, TRICHY

PG DEPARTMENT OF COUNSELLING PSYCHOLOGY & COUNSELLING CENTRE

SEMINAR SERIES – ATTENDANCE LIST

DEPARTMENT: Commerce (Shift - II)

DATE: 13.09.23 TIME: 9.30 A.M. VENUE: SAIL HALL

S.NO	NAME	D.NO	CLASS	SIGN
1.	A. Elvin castro	22UC0156	II B.Com A	
2.	Karthik	22UC0133	II B.Com A	
3.	B. Dilipan	22UC0123.	II B.Com A	
4.	V. Mugesh Varmal	22UC0163	II - B.Com A	
5.	Jawin	22UC0134	II - B.Com A	
6.	Jekwin	22UC0164	II. B.Com	
7.	Karthik	22UC0160	II. B. Com	
8.	K. Kishore	23UC0274	I. B. Com	
9.	P Rajapandi.	23UC0271	I B.com	
10.	N. Vigneshwaran	23UC0272	I B.Com'B'	
11.	P.R. Viswanathan.	23UC0224	I B.Com'B"	
12.	R Ajay Dinakaran	22UC0122	II. B.Com-A	
13.	J. Jayasooriya	23UC0110	I B.Com-A	
14.	R. Paul Antony	23UC0123	I. B.Com-A	
15.	Srivisarga o KP	23UC0131	I. Bcom -A	
16.	A. Raja	23UC0236	I. B.Com-B	
17.	M Zebby	23UC0231	I. B. Com B	
18.	A Nigillsivam	23UC0232	I. B.Com-B	
19.	J. Sathish Kumar	23UC0147	I st B.Com-A	
20.	S. Ajay Prawin Kumar	23UC0248	I st B.Com-B	
21.	R. Aravindh	22UC0223	II B.Com B	
22.	N. UDHAYA	23UC0254	I B.Com B	
23.	N. JAYABHARATHI	23UC0212	I. B.Com-B	
24.	K. SACHITHANANDHAM	23UC0235	I. B.Com. B	
25.	M. DHARUN	23UC0219	I B.Com - B	
26.	D. Arul Jayal Vinith	23UC0172	I B.Com - A	
27.	S. Salveder Nitheen	22UC0256	II B.COM-B	

PG Dept. of Counselling Psychology & Counselling Centre

St. Joseph's College (Autonomous), Trichy - 02

A SEMINAR ON

Rising above Addiction

for the Department of

ECONOMICS

Shift I

III UG, I & II PG

Resource Person

Rev. Dr. Emmanuel Arockiam, SJ

Head, Dept. of Counselling Psychology

Organizing committee

MS. SHYLIN

MS. CHRISTEELA

DATE: 31 August 2023
11.45 A.M.

VENUE: AV HALL

PG DEPARTMENT OF COUNSELLING PSYCHOLOGY

& COUNSELLING CENTRE

ST. JOSEPH'S COLLEGE (Autonomous)

Tiruchirappalli-620 002

Report on Rising above Addiction – seminar

Date: 31 August 2023

Audience: Students of III UG, I & II PG Economics (SHIFT I), St. Joseph's College

Introduction

The PG Counselling Psychology Department and the Counselling Centre are working together to host a seminar series on topics including "Managing Negative Emotions," "Rising above Addiction," and "Maintaining Healthy Relationships." Members of the organising committee were Ms. Christeela and Ms. Shylin. 53 students from the Economics department attended the seminar.

About the theme

An addiction is a chronic dysfunction of the brain system that involves reward, motivation, and memory. It's about the way your body craves a substance or behavior, especially if it causes a compulsive or obsessive pursuit of "reward" and lack of concern over consequences.

Someone experiencing an addiction will:

- be unable stay away from the substance or stop the addictive behavior
- display a lack of self-control
- have an increased desire for the substance or behavior
- dismiss how their behavior may be causing problems
- lack an emotional response

The purpose of this seminar is to create awareness among the young minds on addiction and ways to rise above addiction.

The program started at 11.45 A.M. at AV HALL. The session was started with a prayer song. Ms. Shylin, Counsellor was the session's Master of Ceremony.

Ms. Shylin introduced the resource person, **Rev. Dr. Emmanuel Arockiam, S.J.,** Head of the Department of Counselling Psychology and Director of Arrupe Library.

Dr. Emmanuel talked about "What is addiction? causes of addiction, origin, triggers and techniques to manage addiction." He helped the students to think rationally by provoking some questions and illustrating hypothetical situations. The students actively participated in that session.

One person from ARRUPE SUGALAYA, a rehabilitation center, was invited to the session. He is taking treatment from that rehabilitation center heading by Rev. Fr. Jayapathy, SJ.

He talked about the ill effects of alcohol and drugs by narrating his life story. After his talk, **Fr. Emmanuel** taught some strategies and techniques to the students to handle addiction and cravings. Session ended at 1.30 P.M. with vote of thanks. **Ms. Christeela** showed her support by offering assistance with the technology.

Conclusion

Dr. Suvakkin, HoD, Dept. of Economics thanked the resource person. Participants became aware of the various factors contributing to addiction and ways to prevent that. The seminar came to an end at 1.30 P.M. This seminar, '**Rising above Addiction**,' helped the participants to recognize the signs of addiction and how to approach the topic with kindness and compassion and helping friends identify those struggling with substance abuse issues.

Dr. EMMANUEL AROCKIAM, S.J., Ph.D.
DIRECTOR - DEPT OF COUNSELLING PSYCHOLOGY
ST. JOSEPH'S COLLEGE (AUTONOMOUS)
TRICHY-620 002


GPS MAP CAMERA
Dept. of Counselling Psychology &
Counselling Centre, St. Joseph's
Latitude: 10.8284625
Longitude: 78.6904613
Date: 31 Aug 2023
Time: 11:58 AM
Google


GPS MAP CAMERA
Dept. of Counselling Psychology &
Counselling Centre, St. Joseph's
Latitude: 10.8284625
Longitude: 78.6904613
Date: 31 Aug 2023
Time: 11:59 AM
Google


GPS MAP CAMERA
Dept. of Counselling Psychology &
Counselling Centre, St. Joseph's
Latitude: 10.8284625
Longitude: 78.6904613
Date: 31 Aug 2023
Time: 11:59 AM
Google


JHS
PRO BONO ET VERO
GPS MAP CAMERA
Dept. of Counselling Psychology &
Counselling Centre, St. Joseph's
Latitude: 10.8284625
Longitude: 78.6904613
Date: 31 Aug 2023
Time: 12:07 PM
Google


JHS
JHS
GPS MAP CAMERA
Dept. of Counselling Psychology &
Counselling Centre, St. Joseph's
Latitude: 10.8284625
Longitude: 78.6904613
Date: 31 Aug 2023
Time: 12:07 PM
Google


GPS MAP CAMERA
Dept. of Counselling Psychology &
Counselling Centre, St. Joseph's
Latitude: 10.8284625
Longitude: 78.6904613
Date: 31 Aug 2023
Time: 11:59 AM
Google


GPS MAP CAMERA
Dept. of Counselling Psychology &
Counselling Centre, St. Joseph's
Latitude: 10.8284625
Longitude: 78.6904613
Date: 31 Aug 2023
Time: 11:59 AM
Google


GPS MAP CAMERA
Dept. of Counselling Psychology &
Counselling Centre, St. Joseph's
Latitude: 10.8284625
Longitude: 78.6904613
Date: 31 Aug 2023
Time: 11:58 AM
Google


GPS MAP CAMERA
Dept. of Counselling Psychology &
Counselling Centre, St. Joseph's
Latitude: 10.8284625
Longitude: 78.6904613
Date: 31 Aug 2023
Time: 11:59 AM
Google


GPS MAP CAMERA
Dept. of Counselling Psychology &
Counselling Centre, St. Joseph's
Latitude: 10.8284625
Longitude: 78.6904613
Date: 31 Aug 2023
Time: 11:58 AM
Google

ST. JOSEPH'S COLLEGE, TRICHY

PG DEPARTMENT OF COUNSELLING PSYCHOLOGY & COUNSELLING CENTRE

SEMINAR SERIES – ATTENDANCE LIST

DEPARTMENT: Economics

DATE: 31.08.2023 TIME: 11.45 AM VENUE: AV HALL

S.NO	NAME	D.NO	CLASS	SIGN
1.	Masaneri Nithish kumar	21UEC116	III BA	
2.	Balamasthi Mahesh	21UEC115	III B A	
3.	Alwin Riyas A	22PEC118	II MA	
4.	J Agnockia Sebastin Raja	22PEC103	II M.A	
5.	V. Gobi° krishna	23PEC102	I MA	
6.	K. Sudharsanan	21UEC163	III BA	
7.	R. Sathish kumar	23PEC126	I. MA	
8.	T. KARAN RAJ	23PEC124	I. MA	
9.	K. RAVICHANDRAN	23PEC117	I MA	
10.	G Vincent	21UEC112	III B.A	
11.	B. Akhil Kumar	21UEC114	III B. A	
12.	Bipin Basteray	23PEC121	I MA	
13.	A. Rani Prasath	21UEC174	III B.A	
14.	R. Varun	21UEC141	III-B.A	
15.	S. Pranav.	21UEC155	III B.A	
16.	D. Napiyer Jasue	23PEC104	I MA	
17.	M. Jayasibiraj	23PEC122	I-M.A	
18.	S. Jackson	23PEC113	I-M.A	
19.	B. ELAYAKAVI	23PEC111	I-M.A	
20.	D. ROOSHO INFANT	23PEC108	I-M.A	
21.	P. Saran	23PEC116	I-M.A	
22.	K. Tamil Selvan	21UEC168	III-B.A	
23.	K. DINESH	21UEC136	III BA	
24.	S. CHAFLIN GILBERT	21UEC107	III BA	
25.	ARVIN VITUSH RAJ.K	21UEC102	III BA	
26.	M.U. Thirumoorthy	21UEC157	III BA.	
27.	N. SAIJAYA NISHANTH	21UEC126	III .BA	

28.	V. Sathish	21UEC140	III B.A	V. Sathish
29.	R.G. Jaswanth Kumar	21UEC155	III B.A	R.G. Jaswanth
30.	R. Sathiyamoorthy	21UEC142	III B.A	R. Sathiyamoorthy

ST. JOSEPH'S COLLEGE, TRICHY

PG DEPARTMENT OF COUNSELLING PSYCHOLOGY & COUNSELLING CENTRE

SEMINAR SERIES – ATTENDANCE LIST

DEPARTMENT: Economics

DATE: 31.08.2023 TIME: 11.45 AM VENUE: AV HALL

S.NO	NAME	D.NO	CLASS	SIGN
1.	S. Madhumitha	21UEC161	III B.A Economics	madhumitha
2.	A.L. Seethalakshmi	21UEC129	III B.A Economics	
3.	M. Sharmila Banu	21UEC122	III B.A Economics	
4.	S.P. Jenifer rose	21UEC104	III B.A Economics	
5.	H. Devadarshini	21UEC108	III B.A Economics	
6.	Pavithra. M	21UEC121	"	
7.	Aarthi. B	21UEC101	"	
8.	Thangadharshini	21UEC143	"	
9.	Monika	21UEC138	"	
10.	D. Preethi Merlin	22PEL111	II MA ECONOMICS	D Preethi
11.	A. Shalini	22PEC110	"	
12.	M. Arthi	22PEC112	"	
13.	C. Shelshiya	23PEC105	I MA Economics	
14.	J. Anushri	23PEC101	I MA Economics	J. Anushri
15.	D. Epsheeba	23PEC118	I MA ECONOMICS	
16.	C. Jeeva	23PEC115	"	
17.	S. Vaishnavi	23PEC189	"	
18.	A. Jasmin Nivetha	23PEC110	"	
19.	R. Ramya	22PEC108	II MA ECONOMICS	R Ramya
20.	R. Ruthra	22PEC113	"	
21.	A. Indrani	22PEC107	"	
22.	A. Merlin Rose	22PEC121	II MA ECONOMICS	A. Merlin Rose
23.	J. Kiran khyati	22PEC116	II MA Economics	
24.				
25.				

PG Dept. of Counselling Psychology & Counselling Centre

St. Joseph's College (Autonomous), Trichy - 02

A seminar on

RISING ABOVE ADDICTION

for the Department of

BCA - III UG

Shift II

Resource Person

Rev. Dr. Emmanuel Arockiam, SJ

Head, Dept. of Counselling Psychology

DATE: 04.09.2023 - 2.45 P.M.

VENUE: SAIL HALL

Organizing committee

Ms. Shylin

Ms. Christeela

PG DEPARTMENT OF COUNSELLING PSYCHOLOGY

& COUNSELLING CENTRE

ST. JOSEPH'S COLLEGE (Autonomous)

Tiruchirappalli-620 002

Report on Rising above Addiction – seminar

Date: 04.09.23

Audience: Students of III BCA shift II

Introduction

The PG Counselling Psychology Department and the Counselling Centre are working together to host a seminar series on topics including "Managing Negative Emotions," "Rising above Addiction," and "Maintaining Healthy Relationships." Members of the organising committee were **Ms. Christeela** and **Ms. Shylin**. The lecture was attended by 81 students from the Department of BCA.

About the theme

An addiction is a persistent malfunction of the reward, motivation, and memory systems in the brain. It has to do with how your body desires a substance or behaviour, especially if it leads to an obsessional or compulsive desire for the "reward" and a lack of regard for the consequences.

Someone who has an addiction will be unable to refrain from taking the drug or stopping the addictive behaviour; show a lack of self-control; have an increased desire for the drug or behaviour; discount the possibility that their behaviour may be harming others; and lack an emotional response.

This seminar's goal is to educate young people about addiction and provide them with strategies for overcoming it.

At SAIL HALL, the programme got underway at 2.45 p.m. A song of prayer opened the session. The master of ceremonies for the session was Ms. Christeela, a counsellor.

Rev. Dr. Emmanuel Arockiam, S.J., Head of the Department of Counselling Psychology and Director of the Arrupe Library, was introduced by Ms. Christeela as the resource person.

Rising above Addiction was the topic of Dr. Emmanuel's lecture. He explained he origin, triggers, and approaches for managing addiction. Through some thought-provoking questions and hypothetical scenario illustrations, he assisted the pupils in developing rational thought. The pupils engaged fully in that lesson.

Two people from the rehabilitation facility ARRUPE SUGALAYA were invited to the meeting. They are receiving care from the rehab facility run by Rev. Fr. Jayapathy, SJ.

Both of them used their personal stories to discuss the negative impacts of alcohol and drugs. Following their discussion, Fr. Emmanuel gave the kids advice on how to deal with addiction and cravings. The session ended with a vote of gratitude at 4.15 p.m.

Conclusion

Participants learned about the numerous elements causing addiction and how to stop it. At 4.15 P.M., the session came to a conclusion. The seminar "Rising above Addiction" taught the attendees how to spot the symptoms of addiction, how to address the subject with respect and compassion, and how to support those who are dealing with drug misuse problems.

Dr. EMMANUEL AROCKIAM, S.J., Ph.D.
DIRECTOR - DEPT OF COUNSELLING PSYCHOLOGY
ST. JOSEPH'S COLLEGE (AUTONOMOUS)
TRICHY-620 002


GPS MAP CAMERA
Dept. of Counselling Psychology &
Counselling Centre, St. Joseph's
Latitude: 10.8284625
Longitude: 78.6904613
Date: 04 Sep 2023
Time: 3:09 PM
Google


GPS MAP CAMERA
Dept. of Counselling Psychology &
Counselling Centre, St. Joseph's
Latitude: 10.8284625
Longitude: 78.6904613
Date: 04 Sep 2023
Time: 3:09 PM
Google


GPS MAP CAMERA
Dept. of Counselling Psychology &
Counselling Centre, St. Joseph's
Latitude: 10.8284625
Longitude: 78.6904613
Date: 04 Sep 2023
Time: 3:09 PM
Google


GPS MAP CAMERA
Dept. of Counselling Psychology &
Counselling Centre, St. Joseph's
Latitude: 10.8284625
Longitude: 78.6904613
Date: 04 Sep 2023
Time: 3:09 PM
Google


GPS MAP CAMERA
Dept. of Counselling Psychology &
Counselling Centre, St. Joseph's
Latitude: 10.8284625
Longitude: 78.6904613
Date: 04 Sep 2023
Time: 3:09 PM
Google


RISING ABOVE
ADDICTION
GPS MAP CAMERA
Dept. of Counselling Psychology &
Counselling Centre, St. Joseph's
Latitude: 10.8284625
Longitude: 78.6904613
Date: 04 Sep 2023
Time: 3:08 PM
Google

ST. JOSEPH'S COLLEGE, TRICHY

PG DEPARTMENT OF COUNSELLING PSYCHOLOGY & COUNSELLING CENTRE

SEMINAR SERIES – ATTENDANCE LIST

DEPARTMENT: BCA - Shift II

DATE: 04.09.23 TIME: 2.45 P.M. VENUE: SAIL HALL

S.NO	NAME	D.NO	CLASS	SIGN
1.	JOHN WILLBERT S	21UBC616	III - BCA - B	John. S
2.	Praveen Kumar R	21UBC625	III - BCA - B	Praveen R
3.	Justin Arun Antony. R	21UBC612	III BCA - B	
4.	Ashikdeen. A	21UBC669	III BCA "D"	
5.	Kailash. S	21UBC528	III - BCA - A	S. Kailash
6.	B. Chandru	21UBC557	III - BCA - A	B. Chandru
7.	Muthukannan. E	21UBC566	III - BCA - A	E. Muthu
8.	P. Navin Raj	21UBC511	III - BCA - A	P. Navin Raj
9.	P. Ajith	21UBC561	III - BCA - A	P. Ajith
10.	B. Raja Ganapathy	21UBC560	III - BCA - A	B. Raja
11.	S. Ganesan	21UBC537	III - BCA - A	S. Ganesan
12.	F. Allwin	21UBC551	III - BCA - A	F. Allwin
13.	K. Vallarasu	21UBC568	III - BCA A	K. Vallarasu
14.	V. Vivek Kaviraman	21UBC658	III - BCA - B	V. Vivek
15.	W. Deepak Melvin	21UBC634	III - BCA - B	Deepak
16.	M. Boopathi	21UBC610	III - BCA - "B"	M. Boopathi
17.	D. Kiran	21UBC657	III - BCA - "B"	D. Kiran
18.	S. Saktiumel	21UBC553	III - BCA - A	S. Saktiumel
19.	P. Vasanth	21UBC548	III - BCA A	P. Vasanth
20.	Nithish. A	21UBC652	III - BCA - A	Nithish. A
21.	S. Stasvin	21UBC531	III - BCA A	S. Stasvin
22.	J. Evans Irodwin	21UBC545	III - BCA - A	J. Evans Irodwin
23.	M. Balaprasanna	21UBC520	III - BCA - A	M. Balaprasanna
24.	L. Ignatius Liyan	21UBC517	III - BCA - A	L. Ignatius Liyan
25.	R. Bharathwaj	21UBC570	III - BCA - A	R. Bharathwaj

ST. JOSEPH'S COLLEGE, TRICHY

PG DEPARTMENT OF COUNSELLING PSYCHOLOGY & COUNSELLING CENTRE

SEMINAR SERIES – ATTENDANCE LIST

DEPARTMENT: BCA

DATE: 04.09.23 TIME: 2.45 P.M. VENUE: SAIL HALL

S.NO	NAME	D.NO	CLASS	SIGN
1.	A. Nimalson	21UBC649	III - BCA - B	A Nimalson
2.	A. Prabhu	21UBC623	III - BCA - B	A. Prabhu
3.	F. GEORGE FERNANDES	21UBC638	III - BCA - B	F. George
4.	J. Pravin Raj	21UBC650	III - BCA - B	J. Pravin Raj
5.	Sam Prasad K	21UBC626	III BCA - B	Sam Prasad K
6.	M PRAKASH	21UBC666	III - BCA - B	M Prakash
7.	A. DHARAN	21UBC611	III - BCA - B	A. Dharan
8.	P. Dhanus kodi	21UBC659	III - BCA - B	P. Dhanus kodi
9.	Karthik Anudhan	21UBC661	III BCA B	Karthik Anudhan
10.	S. Alvin David	21UBC603	III BCA B	S. Alvin David
11.	F. Sachin Albert	21UBC667	III BCA 'B'	Sachin.
12.	Arokiya Raj	21UBC647	III BCA 'B'	Arokiya Raj
13.	M. periyanayagam	21UBC602	III - BCA 'B'	M. periyanayagam
14.	S. Vasuki	21UBC654	III - BCA 'B'	S. Vasuki
15.	S. Harish	21UBC670	III - BCA "B"	S. Harish
16.	A. Boris Jefferson	21UBC628	III - BCA 'B'	A. Boris Jefferson
17.	Nandhan J	21UBC660	III - BCA - B	J. Nandhan
18.	S Shree purushotthaman	21UBC629	III - BCA - B	S. Shree purushotthaman
19.				
20.				
21.				
22.				
23.				

S.NO	NAME	D.NO	CLASS	SIGN
1.	I. Felicks Alwin	21UBC533	III - BCA-A	Felicks Alwin
2.	M. Ari	21UBC543	III - BCA-A	M. Ari
3.	S Francis Mariya Chako	21UBC542	III - BCA-A	S Chako
4.	S. Hendry praveen	21UBC503	III - BCA-A	S. Hendry
5.	P. Ebenazar Brighten	21UBC505	III - BCA - A	P S. Brighten
6.	N. AKASH	21UBC506	III - BCA-A	Akash.N
7.	B. LIFAN	21UBC527	III - BCA-A	Lifan
8.	P. Harivignesh	21UBC536	III BCA A	P.Harivignesh
9.	A. Stevensan	21UBC514	III BCA - A	A. Stevensan
10.	N. Arjun	21UBC567	III - BCA - A	N. Arjun
11.	K. Manish yashwant	21UBC532	III - BCA - A	K. Manish
12.	Dupak Pitchaikaran. K	21UBC555	III - BCA - A	Dkp
13.	Bharath. M	21UBC564	III BCA A	Bharath. M
14.	Saboreeswar. R	21UBC538	III BCA - A	Saboreeswar. R
15.	Agestin Raj. B	21UBC504	III - BCA - A	A. Agestin Raj
16.	Thansen Ferdin	21UBC565	III - BCA A	Thansen Ferdin
17.	ARCKUPA KISHORE. F	21UBC509	III - BCA - A	F. Arockiya Kishore
18.	PARTHIV RAJ. M	21UBC510	III - BCA - A	Parthiv Raj. M
19.				
20.				
21.				
22.				
23.				

S.NO	NAME	D.NO	CLASS	SIGN
1.	A. Gopinath	21UBC622	III - BCA B	Gopinath
2.	YOGESHWARAN.M	21UBC604	III - BCA 'B'	Yogeshwaran
3.	GUHAN. M.	21UBC608	III - BCA 'B'	
4.	BALAJI.S	21UBC636	III - BCA 'B'	S Balaji
5.	LOGESH.S	21UBC637	III - BCA 'B'	S. Logesh
6.	C.P.Ruthran	21UBC652	III - BCA 'B'	
7.	M.Klindan	21UBC633	III BCA 'B'	
8.	F.Chriskevin.F	21UBC643	III BCA 'B'	
9.	A. Sudhiraj	21UBC668	"	
10.	S. Vinoj Kumar	21UBC639	III - BCA - B	
11.	G. Harikaran	21UBC642	III - BCA - B	G. Harikaran
12.	K. Gokul	21UBC644	III - BCA - B	K. Gokul
13.	R. Pragadeeshwaran	21UBC645	III BCA - B	R. Prag
14.	S. Prince Matthew	21UBC632	III BCA - B	S. Prince
15.	K. Sriram	21UBC656	III BCA B	
16.	L. Christopher	21UBC635	III - BCA - B	L. Christ
17.	S. Balakumar	21UBC605	III BCA B	S. Balakumar
18.	S. Lesly Anmo Daniel	21UBC521	III - BCA 'A'	S. Lesly Anmo Dan
19.	Jerome R	21UBC516	III BCA 'A'	
20.	R. Jeeva Rathinam	21UBC554	III - BCA 'A'	R. Jeeva
21.				
22.				
23.				
24.				

ST. JOSEPH'S COLLEGE (AUTONOMOUS), TRICHY – 02

PG Dept. of Counselling Psychology & Counselling Centre

A seminar on

RISING ABOVE ADDICTION

for the Department of

Mathematics

Shift I

I & II UG

Resource Person

Rev. Dr. Emmanuel Arockiam, SJ

Head, Dept. of Counselling Psychology

23 August 2023

9.30 A.M.

SAIL HALL

Organizing committee

Ms. Shylin

Ms. Christeela

PG DEPARTMENT OF COUNSELLING PSYCHOLOGY

& COUNSELLING CENTRE

ST. JOSEPH'S COLLEGE (Autonomous)

Tiruchirappalli-620 002

Report on Rising above Addiction – seminar

Date: 23rd August 2023

Audience: Students of I & II B.Sc. Mathematics, St. Joseph's College

Introduction

PG Department of Counselling Psychology & Counselling Centre are collaboratively conducting a seminar series on various theme like "Rising above Addiction," "Maintaining Healthy Relationship" & "Managing negative Emotions." **Ms. Shylin** and **Ms. Christeela** were the members in the organizing committee. There were 102 students from the Dept. of Mathematics participated in the seminar.

About the theme

An addiction is a chronic dysfunction of the brain system that involves reward, motivation, and memory. It's about the way your body craves a substance or behavior, especially if it causes a compulsive or obsessive pursuit of "reward" and lack of concern over consequences.

Someone experiencing an addiction will:

- be unable stay away from the substance or stop the addictive behavior
- display a lack of self-control
- have an increased desire for the substance or behavior
- dismiss how their behavior may be causing problems
- lack an emotional response

The purpose of this seminar is to create awareness among the young minds on addiction and ways to rise above addiction.

The program started at 9.30 A.M. at SAIL HALL. The session was started with a prayer song. Ms. Shylin, Counsellor was the session's Master of Ceremony.

Ms. Shylin introduced the resource person, **Rev. Dr. Emmanuel Arockiam, S.J.,** Head of the Department of Counselling Psychology and Director of Arrupe Library.

Dr. Emmanuel talked about "What is addiction? causes of addiction, origin, triggers and techniques to manage addiction." He helped the students to think rationally by provoking some questions and illustrating hypothetical situations. The students actively participated in that session.

Two persons from ARRUPE SUGALAYA, a rehabilitation center, were invited to the session. They are taking treatment from that rehabilitation center heading by Rev. Fr. Jayapathy, SJ.

Both of them talked about the ill effects of alcohol and drugs by narrating their life story. After their talk, **Fr. Emmanuel** taught some strategies and techniques to the students to handle addiction and cravings. Session ended at 11.15 A.M. with vote of thanks. **Ms. Christeela** showed her support by offering assistance with the technology.

Conclusion

Participants became aware of the various factors contributing to addiction and ways to prevent that. The seminar came to an end at 11.15 A.M. This seminar, '**Rising above Addiction**,' helped the participants to recognize the signs of addiction and how to approach the topic with kindness and compassion and helping friends identify those struggling with substance abuse issues.

Dr. EMMANUEL AROCKIAM, S.J., Ph.D.
DIRECTOR - DEPT OF COUNSELLING PSYCHOLOGY
ST. JOSEPH'S COLLEGE (AUTONOMOUS)
TRICHY-620 002


GPS MAP CAMERA
Dept. of Counselling Psychology &
Counselling Centre, St. Joseph's
Latitude: 10.8284625
Longitude: 78.6904613
Date: 23 Aug 2023
Time: 9:59 AM
Google


GPS MAP CAMERA
Dept. of Counselling Psychology &
Counselling Centre, St. Joseph's
Latitude: 10.8284625
Longitude: 78.6904613
Date: 23 Aug 2023
Time: 9:49 AM
Google


GPS MAP CAMERA
Dept. of Counselling Psychology &
Counselling Centre, St. Joseph's
Latitude: 10.8284625
Longitude: 78.6904613
Date: 23 Aug 2023
Time: 10:00 AM
Google


GPS MAP CAMERA
Dept. of Counselling Psychology &
Counselling Centre, St. Joseph's
Latitude: 10.8284625
Longitude: 78.6904613
Date: 23 Aug 2023
Time: 9:55 AM
Google


GPS MAP CAMERA
Dept. of Counselling Psychology &
Counselling Centre, St. Joseph's
Latitude: 10.8284625
Longitude: 78.6904613
Date: 23 Aug 2023
Time: 10:00 AM
Google


ADDICTION
GPS MAP CAMERA
Dept. of Counselling Psychology &
Counselling Centre, St. Joseph's
Latitude: 10.8284625
Longitude: 78.6904613
Date: 23 Aug 2023
Time: 10:01 AM
Google

ST. JOSEPH'S COLLEGE, TRICHY

PG DEPARTMENT OF COUNSELLING PSYCHOLOGY & COUNSELLING CENTRE

SEMINAR SERIES – ATTENDANCE LIST

DEPARTMENT: Mathematics

DATE: 23.08.2023 TIME: 9.30 AM VENUE: SAIL HALL

S.NO	NAME	D.NO	CLASS	SIGN
1.	V. Akilan Sebastin	22UMA236	II B.Sc Maths 'B'	Akilan
2.	A. SYLVAN	22UMA227	"	
3.	A. Fernando Immanuvel	22UMA239	"	A. Immanuvel
4.	Sibikanna "	22UMA249	"	Sibikanna
5.	A. William James	22UMA205	"	
6.	G. Sudhagar	22UMA242	"	G. Sudhagar
7.	T. Yoshppu	22UMA247	"	T. Y
8.	C. Victor Kingsilin	22UMA203	"	C. Vict
9.	kingston	22UMA206	"	King
10.	Dhareen	22UMA243	"	Dhareen
11.	Cranishkar	22UMA218	"	Cran
12.	Sudharsan	22UMA216	"	Sudh
13.	Shesashthai	22UMA250	"	Shesh
14.	S Mithul kartik	22UMA211	"	S. Mithul
15.	T. Hemilton	22UMA209	"	T. Hem
16.	M. Joshua Mathew	22UMA212	"	M.
17.	S. Nithish kumar	22UMA251	"	S. Nithish kumar
18.	R. Sujith	22UMA214	"	R. Sujith
19.	T. Renish	22UMA248	"	Renish
20.	E. KARTHIKEYAN	22UMA244	"	E. Karthi
21.	K. Mukilarasan	22UMA228	"	K. Mukil
22.	J. Kilbert Savarinathan	22UMA221	"	J. Kilbert
23.				
24.				
25.				

ST. JOSEPH'S COLLEGE, TRICHY

PG DEPARTMENT OF COUNSELLING PSYCHOLOGY & COUNSELLING CENTRE

SEMINAR SERIES – ATTENDANCE LIST

DEPARTMENT: Mathematics

DATE: 23/08/2023. TIME: 9.30 AM VENUE: SAIL HALL

S.NO	NAME	D.NO	CLASS	SIGN
1.	R. Shri Kumar	22UMA201	II-B.Sc MATHS-B	Shri Kumar
2.	A.C.Nithan	22UMA253	II-B.Sc MATHS B	A.C.Nithan
3.	R. Vasanth	22UMA246	II Bsc. Maths B	R. Vasanth
4.	R. Rahul	22UMA241	II BSC Maths B	R. Rahul
5.	P. SOKO7	22UMA226	II BSC MathsB	SOKO7
6.	S. VASUDEVAN	22UMA210	II B.Sc MATHS	S. Vasu
7.	M. Gilbert John paul.	22UMA215	II. BSC. Maths B	
8.	N. Saravana Priyan	22UMA231	II-B.Sc. maths	
9.	J. Abisenth Yohwa	22UMA225	II-Bsc. Maths	J. Abi
10.	K. Ranjith kumar	22UMA238	II-BSC.MATHS	K. Ranjith
11.	V.P. Aniruth	22UMA220	II-BSC MATHS	Aniruth
12.				
13.				
14.				
15.				

ST. JOSEPH'S COLLEGE, TRICHY

PG DEPARTMENT OF COUNSELLING PSYCHOLOGY & COUNSELLING CENTRE

SEMINAR SERIES – ATTENDANCE LIST

DEPARTMENT: MATHEMATICS

DATE: 23.08.2022 TIME: 9.30 AM VENUE: SAIL HALL

S.NO	NAME	D.NO	CLASS	SIGN
1.	D. Spencer Deva Anand	22UMA101	II BSc Maths	D Spencer
2.	U. Kaaliyappan	22UMA111		
3.	J. DEEPAK	22UMA131	II-BSC Mathematics	J. Deepak
4.	A. Samson	22UMA105	II. B.Sc. Maths	A. Samson
5.	M. Devan	22UMA138	II. BSc MATHS	M. Devan
6.	M. Baranidharan	22UMA113	II BSc Maths	M. Baranidharan
7.	K. Kanagaraj.	22UMA133	II. BSc Maths	K. Kanagaraj
8.	D Ebinayasr	22UMA109	II BSC Maths	D Ebinayasr
9.	S. Alwin Jackson	22UMA122	II BSc Maths	S. Alwin Jackson
10.	A. Reesan	22UMA115	II B.Sc Maths	A. Reesan
11.	T. Guruprakash	22UMA124	II B.Sc Mathematics	T. Guruprakash
12.	Jasper Jude	22UMA149	II - B.Sc Mathematics	Jasper Jude
13.	Tamil Selvan P	22UMA144	II - B.Sc Maths	P. Selvan
14.	Ivano Sharon E.	22UMA119	II B.Sc Maths	E. Ivano Sharon
15.	Prasanth. S	22UMA126	"	S. Prasanth
16.	A. Sowndu Diocresia Franklin	22UMA108	"	A. Sowndu Diocresia Franklin
17.	S. Pradeep	22UMA123	"	S. Pradeep
18.	V. S Devaraja.	22UMA105	"	V. S Devaraja
19.	P. Valentine Judiath	22UMA104	"	P. Valentine Judiath
20.	M. Manjai	22UMA137	"	M. Manjai
21.	R. Madhavan	22UMA135	"	R. Madhavan
22.	S. Jagnesh	22UMA131	"	S. Jagnesh
23.	Sabastinrajan. S	22UMA114	"	S. Sabastinrajan
24.	X. Selamon Raj	22UMA103	"	X. Selamon Raj
25.	R. Harihara puthiran	22UMA121	"	R. Harihara puthiran

ST. JOSEPH'S COLLEGE, TRICHY

PG DEPARTMENT OF COUNSELLING PSYCHOLOGY & COUNSELLING CENTRE

SEMINAR SERIES – ATTENDANCE LIST

DEPARTMENT: Mathematics

DATE: 2·3/08/23 TIME: 9.30 AM VENUE: SAIL HALL

S.NO	NAME	D.NO	CLASS	SIGN
1.	Janesh.P	23UMA101	I.B.Sc.Maths	Janesh.P
2.	Anbarasan.R	23UMA120	I.B.Sc.Maths	
3.	Balakrishnan.C	23UMA135	I Bsc Maths	
4.	Tony John.R	23UMA116	I B.Sc Maths	
5.	RETHINAGIRI.M	23UMA124	I.B.Sc maths	Rethingiri.
6.	J.Anto Brighten	23UMA109	I.Bsc.Maths	Anto Bright
7.	Praveen.S	23UMA137	I.Bsc..Maths	
8.	Vishwa.S	23UMA106	I.Bsc Maths	S.Vish
9.	Divine Britto.A	23UMA121	I-A-B.Sc Maths	A Divinebritto
10.	S.Jayasurya	23UMA123	I.BSC maths	
11.	L.CARMEL VINOTHINI	23UMA126	I.BSC.maths	L.C.Vinothini
12.	S.Ruban	23UMA102	I BSC maths	S.Ruban
13.	J.Antony Rajesh	23UMA133	I Bsc Maths	J.Antony Raj
14.	D.Gnanasekar.	23UMA108	I BSC Maths A	D.Gnanas
15.	S.Vishal	23UMA129	I B.SC Maths A	S.Visha
16.	Ragavan.A	23UMA110	I BSC (maths)	Ragu A
17.	S.Joshua Kishore	23UMA132	I-Bsc Maths	S.
18.	R.Jeevan	23UMA118	I.Bsc Maths	R.Jeeva
19.	E.Mohanapriyan	23UMA114	I.Bsc Maths	E.
20.	R.Dinesh	23UMA107	I.Bsc Maths	R.
21.	R.Haribabu	23UMA131	I.BSC Maths	R.
22.				
23.				
24.				
25.				

ST. JOSEPH'S COLLEGE, TRICHY

PG DEPARTMENT OF COUNSELLING PSYCHOLOGY & COUNSELLING CENTRE

SEMINAR SERIES – ATTENDANCE LIST

DEPARTMENT: MATHEMATICS

DATE: 23.08.2023 TIME: 9.30 A.M VENUE: SAIL HALL

S.NO	NAME	D.NO	CLASS	SIGN
1.	S. Surendhar	22UMA143	II BSc. Maths	S Surendhar
2.	R. Sivaram	22UMA106	II BSC. Maths	R. Sivaram
3.	P. Thangarasu	22UMA125	II BSc. Maths	P. Thangarasu
4.				
5.				
6.				
7.				

PG Dept. of Counselling Psychology & Counselling Centre

St. Joseph's College (Autonomous), Trichy - 02

A seminar on

Managing Negative Emotions

for the Department of

Commerce - Shift I

III UG, I & II PG

Resource Person

Rev. Dr. V. Gilburt Camillus, SJ

Additional Vice Principal (Shift II)

DATE: 13.09.2023 - 11.45 A.M.

VENUE: SAIL HALL

Organizing committee

Ms. Shylin

Ms. Christeela

PG DEPARTMENT OF COUNSELLING PSYCHOLOGY

& COUNSELLING CENTRE

ST. JOSEPH'S COLLEGE (Autonomous)

Tiruchirappalli-620 002

Report on Managing Negative Emotions – seminar

Date: 13.09.23

Audience: III UG, I & II PG Commerce

Introduction

The PG Department of Counselling Psychology and the Counselling Centre are hosting series of seminar on the topics "Managing Negative Emotions," "Rising above Addiction," and "Maintaining Healthy Relationships." Members of the organizing committee are Ms. Christeela and Ms. Shylin. The seminar was attended by 123 students from the Department of III UG, I & II PG Commerce on the topic 'Managing Negative emotions'.

About the theme

Negative emotions can be described as any feeling which causes you to be miserable and sad. These emotions make you dislike yourself and others, and reduce your confidence and self-esteem, and general life satisfaction.

Emotions that can become negative are hate, anger, jealousy and sadness. Yet, in the right context, these feelings are completely natural. Negative emotions can dampen our enthusiasm for life, depending on how long we let them affect us and the way we choose to express them. Negative emotions can come from a triggering event, such as an overwhelming workload.

At 11.45 AM at Sail Hall, the session began with a prayer song. The seminar's host was Ms. Shylin. The resource person for the seminar was Rev. Dr. V. Gilburt Camillus SJ, Additional Vice-Principal. Fr. Gilburt started the session by discussing the various types of emotions. He stated the importance to distinguish between what an emotion is and what a feeling is. While the two are interconnected, there's a bigger difference than one may realize. Negative emotions stop us from thinking and behaving rationally and seeing situations in their true perspective. When

this occurs, we tend to see only what we want to see and remember only what we want to remember. This only prolongs the anger or grief and prevents us from enjoying life. The longer this goes on, the more set the problem becomes.

Dealing with negative emotions inappropriately can also be harmful – for example, expressing anger with violence. So instead of trying to ignore feelings, finding ways to understand, accept, and reframe emotions is often more helpful. Making changes in our life can cut down on negative emotions, but it won't eliminate our stress triggers. As we make changes in our life to bring about less frustration, we will also need to find healthful outlets for dealing with these emotions The goal isn't to repress these feelings but to find healthier ways of regulating them. Building these coping skills can lead to greater emotional resilience and well-being.

Conclusion

At 1.10 PM, the session came to an end. The attendees in this seminar on 'Managing negative Emotions' understood how to name the emotion and reframe it in a healthier way.

Dr. EMMANUEL AROCKIAM, S.J., Ph.D.
DIRECTOR - DEPT OF COUNSELLING PSYCHOLOGY
ST. JOSEPH'S COLLEGE (AUTONOMOUS)
TRICHY-620 002


GPS MAP CAMERA
Dept. of Counselling Psychology &
Counselling Centre, St. Joseph's
Latitude: 10.8284625
Longitude: 78.6904613
Date: 13 Sep 2023
Time: 11:52 AM
Google


GPS MAP CAMERA
Dept. of Counselling Psychology &
Counselling Centre, St. Joseph's
Latitude: 10.8284625
Longitude: 78.6904613
Date: 13 Sep 2023
Time: 11:52 AM
Google


GPS MAP CAMERA
Dept. of Counselling Psychology &
Counselling Centre, St. Joseph's
Latitude: 10.8284625
Longitude: 78.6904613
Date: 13 Sep 2023
Time: 11:52 AM
Google


GPS MAP CAMERA
Dept. of Counselling Psychology &
Counselling Centre, St. Joseph's
Latitude: 10.8284625
Longitude: 78.6904613
Date: 13 Sep 2023
Time: 11:52 AM
Google


GPS MAP CAMERA
Dept. of Counselling Psychology &
Counselling Centre, St. Joseph's
Latitude: 10.8284625
Longitude: 78.6904613
Date: 13 Sep 2023
Time: 11:52 AM
Google

ST. JOSEPH'S COLLEGE, TRICHY

PG DEPARTMENT OF COUNSELLING PSYCHOLOGY & COUNSELLING CENTRE

SEMINAR SERIES – ATTENDANCE LIST

DEPARTMENT: Commerce (Shift I)

DATE: 13.09.23 TIME: 11.45 AM VENUE: SAIL HALL

S.NO	NAME	D.NO	CLASS	SIGN
1.	J. Deepak Benito	21UCO259	III, B Com-B	
2.	T. Thomas Berlin	21UCO220	III B.com 'B'	
3.	Jadline Bino Rose J	21UCO206	III B.com 'B'	
4.	J. Anselmo	21UCO268	III B.com 'B'	
5.	CYRIL SIMSOAN J	21UCO267	III B.com 'B'	
6.	R Lingeshwaran	21UCO254	III B.Com B	
7.	P Ruthreshwaran	21UCO229	III. B.Com B	
8.	N. Sanjeeth	21UCO226	III B.COM 'B'	
9.	S. Madhavan	21UCO224	III B.COM 'B'	
10.	P Jaswanth Raj	21UCO250	III B.com 'B'	
11.	S. Santhoshkumar	21UCO255	III - B.Com - B'	
12.	M. Jaison anto	21UCO258	III - B.Com - B	
13.	W. Russel Morris	21UCO230	III B.COM 'B'	
14.	M. MAHIRAJ	21UCO242	III. B.com 'B'	
15.	V Abiram Vishal	21UCO251	III B.com B"	
16.	T. Nikil Vikram Jose	21UCO211	III B.com B"	
17.	S. Alwin Vasanth	21UCO252	III B.com B"	
18.	S. Kowsic Narayana	22PCO128	II M.com	
19.	A.E. Godwin	21UCO127	III BcomA	
20.	Suchit	21UCO139	III BcomA	
21.	I. DAVIS PRabhakar.	21UCO135	III BCOM A	
22.	Andrews Kevin. R	21UCO157	III BCOM A	
23.	M. Parthasarathi	21UCO130	III BCOM A	
24.	Richard Silvestar	21UCO1M	III BcomA	
25.	Karthickeyan. P	21UCO[illegible]	III BcomA	
26.	Sam Antony Surya	21UCO132	III BcomA	
27	Louis Godwin	21UCO144	III BcomA	
28	[illegible] Chandru Sharwin	21UCO120	III BcomA	
29	Rohith P	21UCO152	III B.ComA	
30	Arockiya Jegan	21UCO146	III B.ComA	

S.NO	NAME	D.NO	CLASS	SIGN
1.	MANOJ V	23PC0115	I MCOM	V. Manoj
2.	A. SHEIK MOHAMED	23PC0136	I. M. COM	A. Sheik Mohd.
3.	S. SANTHOSH	23PC0125	I M.com	
4.	D. Paul Richard	23PC0102	I M. com	D. Richard
5.	S. SAHAYA ROBERT	23PC0133	I M. com	S. Robert
6.	R. AKash	23PC0105	I. M. COM	R. Akash.
7.	M. Vinoth Kumar	23PC0117	I. M. COM	M. Vinoth
8.	A. Hemnath.	23PC0139	I. M. Com	A. Hemnath.
9.	V. Praveen Devaraj	23PC0114	I. M. com	V. Praveen
10.	C. George Infant Raj	23PC0113	I. M. com	C. George
11.	R. Godwin Leo	23PC0116	I-M-com	R. Godwin
12.	S. Tovisan	23PC0141	I. M. com	S. Tovisan
13.	S. Gilbert Antony Raj	23PC0119	I. M. com	S. Gilbert
14.	A. JAYARAMAN	23PC0110	I. M. Com	A. Jayaraman
15.	M. Abidha Begam	23PC0129	I. M. com	M. Abidha Begam
16.	B. Pairose Bance.	23PC0124	I. M. COM.	B. Pairose Bance
17.	D. Lincy monal.	23PC0108	I M. COM	D. Lincy
18.	V. Shirly	23PC0106	I-M. com	V. Shirly
19.				
20.				

S.NO	NAME	D.NO	CLASS	SIGN
1.	M Kiruba	23PC0138	I M.COM	Kirut
2.	R. sharmila.	23PC0143	I. M.com.	Sharmj.
3.	A Abarna	23PC0112	I. M.com	Abarnaj
4.	M. Mitin Athitha	23PC01140	I .M.com	M Mitin
5.	C. Pooja	23PC0134	I. M. Com	C Pooja
6.	R. Prathiksha Lakshmi	23PC0123	I. M. COM	R. Prathiksha
7.	d. Kooparvathy	23PC0144	I M COM	d. Kooparvathy
8.	R. Annie Gladys	23PC0104	I M.COM	R. Annie Gladys.
9.	KAVIYA K	23PC0142	I M COM	K.kaviya
10.	Pavithra . M	22PC0133	II M.com	M Pavithra
11.	Aishwarya. B	22PC0139	II M.com	B. Aishwarya
12.	Hari Priya. R	22PC0131	II M.com	R Hari Priya
13.	S Queency Sabthica	22PC0119	II. M.com	S Queency Sabthica
14.	E Eshila	23PC0101	I. M.Com	E. Eshila
15.	C. Jeevithasree	23PC0118	I. M.com	C. Jeevithasree
16.	J. Jernisha	22PC0118	II - M.com	J. Jernisha
17.	G. kowsika.	23PC0127	I M.com	G. kowsika.
18.	S. Joneline	22PC0108	II M.Com	S. Joneline
19.	Shakcoy B	22PC0110	II. M.com	B Shakcoy
20.	Bastin Deno J	22PC0109	II M. com	J Bastin Deno
21.	J. Sherlin infanta	22PC0104	II M.com	J. Sherlin infanta
22.	W. Sneka	22PC0113	II M.com	W. Sneka
23.	X. Vincy Mercoona	22PC0122	II M.com	X Vincy Mercoona
24.	R. Kavyadevi	23PC0132	I. M.com	R. Kavyadevi
25.	V. Janani	23PC0131	I. M.com	V. Janani

S.NO	NAME	D.NO	CLASS	SIGN
1.	M. AUGUSTIN JOSHVA	21UC0153	III. BCOM A	
2.	Manuj Kumar. J	21UC0126	III B.com A	
3.	JELWIN ROHITH. P	21UC0124	III B.com A	
4.	Thomas Gladwin. C	21UC0133	III B.com A	
5.	MUTHURAMAN M	21UC0136	III. B.com A	
6.	Shakthi Ganeshaan. N	21UC0164	III-B.com-A	
7.	SANGAMESHWARAN. N	21UC0104	III-BCOM-A	
8.	Kavinkumar. G	21UC0249	III-B.Com 'B'	
9.	Krishnakumar. G	21UC0270	III-B.Com 'B'	
10.	S. SUVA	21UC0208	III-B.Com'B'	
11.	N Sanjay	21UC0210	III-B.COM B	
12.	P. Muthu Raja Guru	21UC0237	III-BCOM B	
13.	Vishnu Ram J	21UC0257	III-B.Com'B'	
14.	LINGESWARAN S	21UC0243	III-B.COM "B"	
15.	Karthikeyan. P	21UC0264	III-B.com'B'	
16.	EDWARD JOSHUA. J	21UC0225	III B.Com'B'	
17.	C. JOHN BRITTO	21UC0241	III B.COM'B'	
18.	J. JEBARAJ SIMSON	21UC0201	III B.Com "B"	
19.	CHELLA KUMARAN	21UC0246	III-BCom-B	
20.	S. SALAMON CHRISTOPHER	21UC0231	III BCom-B	
21.	BEJILIN. B.A	21UC0234	III-B.com 'B'	
22.	T. Andrews	21UC0217	III B.Com.B	
23.	N. Kabilan	21UC0247	III. B.com. B	
24.	Stanly Vijay R	21UC0205	III-BCom-B	
25.	Mathiyalagan. E	21UC0269	III Bcom-B	

VENUE:

S.NO	NAME	D.NO	CLASS	SIGN
1.	R Felix Antony	21UC0214	III B.com 'B'	R.Felix Antony
2.	K. Deepak Roshan	21UC0129	III B.Com(A)	K. Deepak Roshan.
3.	M. Johnpeter	21UC0209	III B.Com(B)	M. Johnpeter
4.	S. Biaerson	21UC0221	III B.com 'B'	
5.	J. George Kennedy	21UC0207	III B.com'B	J. George Kennedy
6.	Balaji R	21UC0256	III B.Com 'B'	
7.	SANJAYNATH	21UC0266	III B.Com.B	
8.	Sanjay.K	21UC0128	III B.Com A	
9.	Ronald Nassrl. R	21UC0134	III B.Com A	
10.	Sharone. R	21UC0156	III B.Com A	
11.	Raldfo. R	21UC0118	III B.Com A	
12.	Asbin. A	21UC0109	III B.Com A	
13.	Jonathan	21UC0101	III BcomA	
14.	VISHVA. A.E	21UC0108	III - B.COM(A)	
15.	Nirmalan. M	21UC0144	III B.COM 'A'	
16.	Bellarminmicheal. S	21UC0131	III B.Com 'A'	
17.	P. Arwin	21UC0146	III. B.Com 'A'	
18.	S. Deepak	21UC0165	III BCOM A	
19.	As. Felix	21UC0143	III. Bcom. A	
20.	Daniel Roche	21UC0151	III. Bcom. A	
21.	V. Dhanush kingsly	21UC0167	III. B.Com(A)	
22.	G. Hari Hara Dhanush	21UC0148	III B.Com 'A'	
23.	S. Sanju	21UC0248	III Bcom 'B'	
24.	A. Renie Christober	21UC0159	III B.COM A	
25.	G. Arun Kumar	21UC0162	III B.Com 'B'	

PG Dept. of Counselling Psychology & Counselling Centre

St. Joseph's College (Autonomous), Trichy - 02

A seminar on

MANAGING NEGATIVE EMOTIONS

for the Department of

M.Sc. Computer Science

Shift II

Resource Person

Rev. Dr. Emmanuel Arockiam, SJ

Head, Dept. of Counselling Psychology

DATE: 07.09.2023 - 2.45 P.M.

VENUE: SAIL HALL

Organizing committee

Ms. Shylin

Ms. Christeela

PG DEPARTMENT OF COUNSELLING PSYCHOLOGY &

COUNSELLING CENTER

ST. JOSEPH'S COLLEGE (Autonomous)

Tiruchirappalli-620 002

Report on 'Managing negative Emotions' – Seminar

Date: 07 September 2023

Audience: Students of I & II PG M.Sc. Computer Science

Introduction

A seminar series on topics like "Rising above Addiction," "Maintaining Healthy Relationships," and "Managing negative Emotions" is being organised by the PG Department of Counselling Psychology and the Counselling Centre. Members of the organising committee were Ms. Christeela and Ms. Shylin. 93 students from Shift II of the Department of Computer Science attended the seminar.

About the theme

Negative emotions can come from a triggering event, such as an overwhelming workload. Your thoughts surrounding an event also play a role. The way that you interpret what happened can alter how you experience the event and whether or not it causes stress.

Research has shown that tactics like suppressing your emotions are ineffective and can even be harmful. So instead of trying to ignore your feelings, finding ways to understand, accept, and reframe your emotions is often more helpful.

Making changes in our life can cut down on negative emotions, but it won't eliminate our stress triggers. As we make changes in our life to bring about less frustration, we will also need to find healthful outlets for dealing with these emotions.

Negative emotions are normal and even expected. The goal isn't to repress these feelings but to find healthier ways of regulating them. Building these coping skills can lead to greater emotional resilience and well-being.

At 2:45 pm, the session began with a hymn of prayer at SAIL AUDITORIUM. The seminar's master of ceremonies was **Ms. Shylin**. **Rev. Dr. Emmanuel Arockiam, SJ**, the resource person, was introduced by Ms. Shylin to lead the session. Fr. Emmanuel discussed the value of having wholesome connections. He also emphasised the six factors that make relationships successful. He stressed the advantages of having healthy relationships.

This seminar covered a wide range of topics, such as:

- Types of emotions
- Ruminating on emotions
- Poor coping skills
- Regions of brain
- Physiological reactions in the body
- Differences between feelings and emotions
- Healthy ways to handle negative emotions
- Components of Emotional Intelligence

Conclusion

At 4:15 PM, the session came to a close. Ms. Christeela offered help with the technology as a sign of support. . The attendees in this seminar on "Managing negative Emotions" learned how to spot relationship toxicity and how to treat others with respect and compassion.

Dr. EMMANUEL AROCKIAM, S.J., Ph.D.
DIRECTOR - DEPT OF COUNSELLING PSYCHOLOGY
ST. JOSEPH'S COLLEGE (AUTONOMOUS)
TRICHY-620 002


GPS MAP CAMERA
Dept. of Counselling Psychology &
Counselling Centre, St. Joseph's
Latitude: 10.8284625
Longitude: 78.6904613
Date: 07 Sep 2023
Time: 3:14 PM
Google


GPS MAP CAMERA
Dept. of Counselling Psychology &
Counselling Centre, St. Joseph's
Latitude: 10.8284625
Longitude: 78.6904613
Date: 07 Sep 2023
Time: 3:14 PM
Google


GPS MAP CAMERA
Dept. of Counselling Psychology &
Counselling Centre, St. Joseph's
Latitude: 10.8284625
Longitude: 78.6904613
Date: 07 Sep 2023
Time: 3:14 PM
Google


GPS MAP CAMERA
Dept. of Counselling Psychology &
Counselling Centre, St. Joseph's
Latitude: 10.8284625
Longitude: 78.6904613
Date: 07 Sep 2023
Time: 3:13 PM
Google


GPS MAP CAMERA
Dept. of Counselling Psychology &
Counselling Centre, St. Joseph's
Latitude: 10.8284625
Longitude: 78.6904613
Date: 07 Sep 2023
Time: 3:14 PM
Google


GPS MAP CAMERA
Dept. of Counselling Psychology &
Counselling Centre, St. Joseph's
Latitude: 10.8284625
Longitude: 78.6904613
Date: 07 Sep 2023
Time: 3:13 PM
Google


GPS MAP CAMERA
Dept. of Counselling Psychology &
Counselling Centre, St. Joseph's
Latitude: 10.8284625
Longitude: 78.6904613
Date: 07 Sep 2023
Time: 3:14 PM
Google


GPS MAP CAMERA
Dept. of Counselling Psychology &
Counselling Centre, St. Joseph's
Latitude: 10.8284625
Longitude: 78.6904613
Date: 07 Sep 2023
Time: 3:13 PM
Google

ST. JOSEPH'S COLLEGE, TRICHY

PG DEPARTMENT OF COUNSELLING PSYCHOLOGY & COUNSELLING CENTRE

SEMINAR SERIES – ATTENDANCE LIST

DEPARTMENT: Computer Science (Shift -II)

DATE: 7.9.2023. TIME: 2.45 P.M. VENUE: SAIL HALL

S.NO	NAME	D.NO	CLASS	SIGN
1.	M. Keerthana Sree	23PCS923	I M.Sc - CS	M. Keerthanasree
2.	R. Ronuga	23PCS931	I M Sc - CS	R.
3.	M. Yuva Bharathi	23PCS943	I M.Sc - CS	M. Yuva Bharathi
4.	M. Saumiyaa	23PCS937	I M.Sc - CS - B	M. Saumiyaa
5.	K. Sharmili	23PCS929	I. M.Sc - CS - B'	K. Sharmili
6.	R. Nandhithe	23PCS921	I M Sc CS 'B'	R.
7.	B. Jeevitha	23PCS938	I - M.Sc. CS 'B'	B. J
8.	R. Barkavi	23PCS843	I - M.Sc. CS 'A'	R. Barkavi
9.	K. Kavya	23PCS819	I - M.Sc. CS 'A'	K. Kavya
10.	A. Nancy Joshlin	23PCS805	I M.Sc CS 'A'	A
11.	D. Saumiya	23PCS823	I - M.Sc CS 'A'	D. S
12.	V. Shareegha	23PCS828	I - M.Sc CS 'A'	V. Shareegha
13.	G. Divya	23PCS910	I - M.Sc - CS 'B'	G. Divya.
14.	J. Nithilyashree	23PCS919	I - M.Sc - CS 'B'	J. Nithilyashree
15.	Manisha Soni R	23PCS944	I M.Sc CS 'B'	Manisha
16.	Kani Mozhi. M	23PCS901	I M.Sc - CS - B	K. Mozhi. M
17.	P. RAMYA	23PCS922	I M.Sc - CS - B	P. Ramya
18.	S. Vishalini	23PCS822	I M.Sc - CS - A	Vishalini
19.	M. MAHALAKSHMI	23PCS811	I M.Sc - CS - A	Mahalakshmi
20.	R. ROSHINI	23PCS815	I M.Sc - CS - A	Roshini
21.	R. ~~ARUL ANGELIN~~ Arul Angelin	23PCS838	I M.Sc - CS - A	Arul angelin
22.				
23.				
24.				
25.				

ST. JOSEPH'S COLLEGE, TRICHY

PG DEPARTMENT OF COUNSELLING PSYCHOLOGY & COUNSELLING CENTRE

SEMINAR SERIES – ATTENDANCE LIST

DEPARTMENT: M.Sc. Computer Science (Shift II)

DATE: 07.09.23 TIME: 2.45 P.M. VENUE: SAIL HALL

S.NO	NAME	D.NO	CLASS	SIGN
1.	S. Osvi Shermin	23PCS915	I-MSc CS	S osvi.
2.	L. Austing Libi	23pcs950	I-MSc CS	L. Austing
3.	R H keerthana	23pcs935	I-MSc. CS	R H keerthana.
4.	P. Jenifer Mary	22PCS841	II MSc. CS	P. Jenifer.
5.	A. Arthi	22PCS844	II. MSC. CS	A. Arthi
6.	D. Hareni	23PCS802	I. MSC. CS	D. Hareni
7.	S. Thilagavathi	22pcs905	II MSc CS	S Thila
8.	J. Alockia Sweety	22pcs928	II MSc CS	J. Alockia Sweety
9.	S. Sregadevi	22pcs935	II MSc CS	S.sregadevi
10.	J. Dhanalath	22pcs937	II MSc CS	J. Dhanalath
11.	J. Joseph Elvin Mary	22pcs904	II MSc CS	J. Joseph Elvin Mary
12.	S. Haripreetha	23PCS821	I MSc CS	S. Haripreetha
13.	N. Swathy	23PCS909	I MSC CS	N. Swathy
14.	M. Marin Missma	23PCS806	I MSc CS	M. Marin Missma
15.	R. Umamaheswari	22PCS908	II MSc CS	R. Umamaheswari
16.	M. Soumiya	22PCS942	II MSc CS	M. Soumiya
17.	K. Sakti dheeptha	22PCS846	II MSc CS	K. Sakti dheeptha
18.	K. Maidhu Bala	22PCS831	II MSc CS	K. Maidhu Bala
19.	S. Geetha	23pcs908	I MSc CS	S. Geetha
20.	R. Kowsalya	23PCS804	I MSc CS 'A'	R. Kowsi
21.	S. Priyadharshini	23PCS928	I MSc CS 'B'	S. Priyadh.
22.	N. Vidhyabharathi	22PCS815	II MSc CS 'A'	N. Vidhya
23.	Y. Sugashini	22PCS823	II MSc CS 'A'	Y. Sugashini
24.	A. Shalini	22PCS832	II M.Sc CS 'A'	A. Shalini.
25.	R. Sahaya Ara Nilopher	22PCS812	II-M.Sc CS 'A'	R. Sahaya Ara Nilopher

S.NO	NAME	D.NO	CLASS	SIGN
1.	A. Vinek	22PCS843	II-MSc-CS	A. V
2.	P. Yogesh	22PCS811	II. MSc-CS	P. Yo
3.	R. Ajay	22PCS848	II MSc. CS	R
4.	G. Gokul	22PCS833	II. MSc. CS	G
5.	E. Soriram	22PCS835	II-MSc-CS	E
6.	X. Jenis	23PCS936	I MS CS	X
7.	C. Kavin Kumar.	22PCS818	II. MSc. CS	C
8.	A. ASEER ANUVIN	23PCS801	I MSc. CS	A
9.	R. Sriram	23PCS820	I. MSc. CS	R
10.	A. Kevin Princely	22PCS901	II MSC. CS	A
11.	V. Priyanathan	22PCS906	II-MSc. CS	V
12.	D. Yovan	22PCS908	II. MSC. CS	D
13.	CHRIS N	22PCS900	II MSc CS	
14.	Mathew	22PCS813	II-MSc(CS)-A	M
15.	SAMSON PAUL R.	22PCS807	II. MSc. CS 'A'	S
16.	J. Clarison Kevin	22PCS814	II MSc. CS 'A'	J. C
17.	V. Mani Kandan	22PCS810	II. MSC. CS 'A'	V. M
18.	R. Dinesh	22PCS802	II-M.Sc., CS 'A'	R
19.	C. Rajesh.	22PCS820	II. M.Sc, CS A	C. R
20.	Gilbert Messiah. A	22PCS936	II M.Sc. CS "B"	G
21.	S. Arockia Infant Niranjan	23PCS946	I. MSc CS	S.
22.	A. YUVARANI	22PCS806	II-MSc CS 'A'	A.
23.				
24.				
25.				

S.NO	NAME	D.NO	CLASS	SIGN
1.	K. Raman	22PCS940	II M.SC. CS B	
2.	Sagaya Rakash A	23PCS948	I M.SC(CS) B	
3.	PONNAR. A	22PCS804	II - MSC - CS 'A'	
4.	ASHOKKUMAR. V	22PCS927	II - MSC - CS 'B'	
5.	Gurlan N	22PCS923	II MSC CS B	
6.	Jennis Sellan. S	23PCS848	I MSC. CS 'A'	
7.	SIVASUBRAMANI YAV M	23PC846	I MSC. CS 'A'	
8.	Aswin. D	22PCS821	II. MSC. CS 'A'	
9.	WALLOT Ricardo. J	22PCS917	II MSC CS 'B'	
10.	Farok. R	22PCS819	II MSC CS A	
11.	A. Senthil velan	23PCS812	I MSC - CS 'A'	
12.	SCOSA. S	23PCS809	I-MSC. CS 'A'	
13.	I JUSTIN SAGAYA RAS	23PCS842	I MSC, C S 'A'	
14.	N. JEEVANANTHAM	23PCS841	I - M.SC. CS 'A'	
15.	C Ram Kumar	23PCS844	I MSC CS 'A'	
16.	P. Saravana kumar P	22PCS905	II MSC CS 'B'	
17.	R. Saravana Prasath R	22PCS931	II MSC CS 'B'	
18.	S - Joshua	23PCS847	I MSC. CS 'A'	
19.	N. Akash	22PCS840	II. MSC - CS 'A'	
20.	D. Balaje	22PCS845	II MSC CS 'A'	
21.	JOTHIS J.S	22PCS809	II MSc CS 'A'	
22.	Deperson S	22PCS847	II M.SC - CS - A	
23.	Karan. S	22PCS947	II MSC. CS 'B'	
24.	W. Ronish Arockia Raj	22PCS916	II. MSC CS 'B'	
25.	B Ranugopal	22PCS920	II MSC CS 'B'	

ST. JOSEPH'S COLLEGE (AUTONOMOUS), TRICHY - 02

PG Dept. of Counselling Psychology & Counselling Centre

A SEMINAR ON

Managing Negative Emotions

for the Department of

English - Shift I

I & II UG

RESOURCE PERSONS

REV. DR. EMMANUEL AROCKIAM, SJ
Head, Dept. of Counselling Psychology

MS. SHYLIN
Counsellor

MS. CHRISTEELA
Counsellor

NOV | 28 | 2023

11.45 AM | **SAIL HALL**

Organizing committee

Ms. Shylin
Ms. Christeela

PG DEPARTMENT OF COUNSELLING PSYCHOLOGY &

COUNSELLING CENTER

ST. JOSEPH'S COLLEGE (Autonomous)

Tiruchirappalli-620 002

Report on 'Managing negative Emotions' – Seminar

Date: November 28, 2023

Audience: Students of I & II B.A. English (Shift I)

Introduction

A seminar series on topics like "Rising above Addiction," "Maintaining Healthy Relationships," and "Managing negative Emotions" is being organized by the PG Department of Counselling Psychology and the Counselling Centre. Members of the organizing committee were Ms. Christeela and Ms. Shylin. 76 students from Shift I of the Department of English attended the seminar.

Program

At 11.45 am, the session began with a hymn of prayer at SAIL AUDITORIUM. The seminar's master of ceremonies was **Ms. Christeela**. She oriented the students about the program and the theme of the seminar. **Rev. Dr. Emmanuel Arockiam, SJ**, the resource person, started with questions and explained them about the process undergo in the brain and body when we experience something. He stressed the advantages of stabilizing our emotions. He helped the students to think rationally by provoking some questions and illustrating hypothetical situations.

This seminar covered a wide range of topics, such as:

- Definition of emotions
- Types of emotions
- Ruminating on emotions
- Poor coping skills

- Regions of brain
- Physiological reactions in the body
- Differences between feelings and emotions
- Healthy ways to handle negative emotions
- Components of Emotional Intelligence

He explained that emotions are regarded as ‘lower level’ responses. They first occur in the subcortical areas of the brain such as the amygdala and the ventromedial prefrontal cortices. These areas are responsible for producing biochemical reactions that have a direct impact on your physical state.

He added that negative emotions are unpleasant and disruptive emotional reactions. Examples of negative emotions include sadness, fear, anger, or jealousy. These feelings aren't just unpleasant; they also make it hard to function in your normal daily life, and they interfere with your ability to accomplish goals.

He also educated them that no emotion, including a negative one, is inherently bad. It's perfectly normal to feel these things in certain contexts or situations. These emotions become problematic when they are persistent and interfere with your ability to live your life normally.

Everyone feels negative emotions from time to time, but in some cases, these feelings can be a sign of a mental health condition such as depression or anxiety.

Research has shown that tactics like suppressing your emotions are ineffective and can even be harmful. So instead of trying to ignore your feelings, finding ways to understand, accept, and reframe your emotions is often more helpful.

Making changes in our life can cut down on negative emotions, but it won't eliminate our stress triggers. As we make changes in our life to bring about less frustration, we will also need to find healthful outlets for dealing with these emotions.

Negative emotions are normal and even expected. The goal isn't to repress these feelings but to find healthier ways of regulating them. Building these coping skills can lead to greater emotional resilience and well-being.

Conclusion

At 1:15 PM, the session came to a close. Ms. Christeela thanked the participants. The attendees in this seminar on "Managing negative Emotions" learned how to spot negative emotions and learned to observe the physiological changes happen in our body when something happens.

Dr. EMMANUEL AROCKIAM, S.J., Ph.D.
DIRECTOR - DEPT OF COUNSELLING PSYCHOLOGY
ST. JOSEPH'S COLLEGE (AUTONOMOUS)
TRICHY-620 002


GPS MAP CAMERA
DEPT OF Counselling Psychology, St. Joseph's College, Tamil Nadu India
Latitude: 10.828479
Longitude: 78.6904903
Date: 28 Nov 2023
Time: 11:50 AM
Google


GPS MAP CAMERA
DEPT OF Counselling Psychology, St. Joseph's College, Tamil Nadu India
Latitude: 10.828479
Longitude: 78.6904903
Date: 28 Nov 2023
Time: 11:50 AM
Google


GPS MAP CAMERA
DEPT OF Counselling Psychology, St. Joseph's College, Tamil Nadu India
Latitude: 10.828479
Longitude: 78.6904903
Date: 28 Nov 2023
Time: 11:50 AM
Google


GPS MAP CAMERA
DEPT OF Counselling Psychology, St. Joseph's College, Tamil Nadu India
Latitude: 10.828479
Longitude: 78.6904903
Date: 28 Nov 2023
Time: 11:50 AM
Google


GPS MAP CAMERA
DEPT OF Counselling Psychology, St. Joseph's College, Tamil Nadu India
Latitude: 10.828479
Longitude: 78.6904903
Date: 28 Nov 2023
Time: 11:50 AM
Google

ST. JOSEPH'S COLLEGE, TRICHY

PG DEPARTMENT OF COUNSELLING PSYCHOLOGY & COUNSELLING CENTRE

SEMINAR SERIES – ATTENDANCE LIST

DEPARTMENT: English – Shift I TOPIC: Managing Negative emotions

DATE: 28/11/23 TIME: 11.30 VENUE: Seal Hall.

S.NO	NAME	D.NO	CLASS	SIGN
1.	Kothore. C	23UEN126	I.B.A English	C.
2.	Sridhar	23UEN113	I. BA. ENG	
3.	Bren JeraldL	23UEN123	I. BA. ENG	
4.	M. Jayakumar	23UEN141	I BA English	
5.	Vijay Anmol Minj	23UEN151	I B A English	
6.	John Bosco. P	23UEN153	I B.A English	
7.	K. James	23UEN150	I BA. English	James.
8.	S. Daniel	23UEN129	I B. A. English	
9.	A Michael Jabez	23UEN108	I. BA. Eng	
10.	R. Kalaivithi	23UEN161	I BA. English	
11.	Akash	23UEN128	I BA. English	
12.	T. Sam Santhosh	23UEN132	I B.A. English	
13.	R. Rohith	23UEN167	I B. A. English	
14.	Y. Muin Nikson	23UEN131	I. B.A. English	
15.	D. Prabhakaran.	23UEN127	I. B.A. English	
16.	G. Milan	23UEN160	I. B.A. English	
17.	A. Joe michael	23UEN130	I. B.A English	
18.				
19.				
20.				
21.				
22.				
23.				
24.				
25.				

ST. JOSEPH'S COLLEGE, TRICHY

PG DEPARTMENT OF COUNSELLING PSYCHOLOGY & COUNSELLING CENTRE

SEMINAR SERIES – ATTENDANCE LIST

DEPARTMENT: TOPIC:

DATE: TIME: VENUE:

S.NO	NAME	D.NO	CLASS	SIGN
1.	Sishanth mallick	23UEN138	I BA English	
2.	Prakash Dungdung	23UEN163	"	
3.	Theophil Barla	23UEN122	"	
4.	Mathew. K	23UEN114	"	K. Mathew
5.	Keerthi. K	23UEN162	"	
6.	Vishal. W	23UEN125	"	
7.	Joel	23UEN118	"	
8.	Gabriel	23UEN104	"	
9.		23UEN135	"	
10.	S. Sam	23UEN144	"	
11.	R T Kishore	23UEN120	"	
12.	X. Jonathan Darwin Rayar	23UEN147	"	
13.	M.A Rahul Christuraja	23UEN117	"	
14.				
15.				
16.				
17.				
18.				
19.				
20.				
21.				
22.				
23.				
24.				
25.				

ST. JOSEPH'S COLLEGE, TRICHY

PG DEPARTMENT OF COUNSELLING PSYCHOLOGY & COUNSELLING CENTRE

SEMINAR SERIES – ATTENDANCE LIST

DEPARTMENT: TOPIC:

DATE: TIME: VENUE:

S.NO	NAME	D.NO	CLASS	SIGN
1.	G. Raju	23UEN154	I B A English	G. Raju
2.	M. Vamsi	23UEN152	I B A English	Vamsi
3.	B. Ashath	23UEN155	I B A English	Ashath
4.	James Sro Arun	23UEN109	I BA English	
5.	M. VISHWA	23UEN133	I BA ENGLISH	M. Vishwa
6.	T. Kalaiyarasan	23UEN148	I BA English	T. Kalai
7.	K. Santhosh	23UEN139	I BA English	
8.	B. Sumanth.	23UEN136	I BA English	B. Sumanth
9.	A. Anish Jefrin	23UEN103	I. B. A English	
10.	J. NAVEEN ABINASH	23UEN115	"	
11.	P. Allen Joshua Paul	23UEN156	B A English	
12.	T. Deena	23UEN146	"	
13.	Rogith Joel	23UEN124	I B.A English	
14.	E. Ooshal.	23UEN134	I B. A English	
15.				
16.				
17.				
18.				
19.				
20.				
21.				
22.				
23.				
24.				
25.				

ST. JOSEPH'S COLLEGE, TRICHY

PG DEPARTMENT OF COUNSELLING PSYCHOLOGY & COUNSELLING CENTRE

SEMINAR SERIES – ATTENDANCE LIST

DEPARTMENT: TOPIC:

DATE: TIME: VENUE:

S.NO	NAME	D.NO	CLASS	SIGN
1.	G. Raju	23UEN154	I B A English	G. Raju
2.	M. Vamsi	23UEN152	I BA English	Vamsi
3.	B. Prakash.	23UEN155	I B. A English	Prakash
4.	James Sro Arun	23UEN109	I BA English	
5.	M. VISHWA	23UEN133	I BA ENGLISH	M. Vishwa
6.	T. Kalaiyarasan	23UEN148	I BA English	T. Kalai
7.	K. Santhosh	23UEN139	I BA English	
8.	B. Sumanth.	23UEN136	I BA English	B. Sumanth
9.	A. Anish Jefrin	23UEN103	I. B. A English	
10.	J. NAVEEN ABINASH	23UEN115	"	
11.	P Allen Joshua Paul	23UEN156	B A English	P Allen
12.	T. Deena	23UEN146	"	
13.	Rogith Joel	23UEN124	I B A English	
14.	E. Gokul.	23UEN134	I B. A English	
15.				
16.				
17.				
18.				
19.				
20.				
21.				
22.				
23.				
24.				
25.				

ST. JOSEPH'S COLLEGE, TRICHY

PG DEPARTMENT OF COUNSELLING PSYCHOLOGY & COUNSELLING CENTRE

SEMINAR SERIES – ATTENDANCE LIST

DEPARTMENT: II nd BA. English TOPIC:

DATE: TIME: VENUE:

S.NO	NAME	D.NO	CLASS	SIGN
1.	P. Sathiyaraj	22UEN131	II. BA	P. Sathiyaraj
2.	EZhilarasan. P	22UEN140	II. BA. Eng	P Ezhilarasan
3.	Santhosh Kumar SG	22UEN167	II. B.A.	Santhosh
4.	A Arul Thiyagu	22UEN119	II. BA	Thiy
5.	J. Faysal Raja	22UEN135	II. BA	J. Faysal Raja
6.	Peter Damian	22UEN126	II. B. A	Peter.
7.	Pavam Ekka	22UEN151	II	
8.	Patras Hansdah	22UEN123	II	Hansdah
9.	Khaw Kuper	22UEN125	II	Kuper
10.	A. Helin David	22UEN128	II. BA. English	Helin
11.	Cr. J. Evinesh Sharon	22UEN107	II BA. English	Evinesh
12.	A. Jayan Christopher Raj	22UEN117	II B. A English	A Jayan
13.	P. Sahaya Churchil	22UEN130	II. B.A. English	P. Churchil
14.	M. Moses Anthony	22UEN150	II. BA English	Moses
15.	Kruthi	22UEN139	II BA Englis	Kruthi
16.				
17.				
18.				
19.				
20.				
21.				
22.				
23.				
24.				
25.				

ST. JOSEPH'S COLLEGE, TRICHY

PG DEPARTMENT OF COUNSELLING PSYCHOLOGY & COUNSELLING CENTRE

SEMINAR SERIES – ATTENDANCE LIST

DEPARTMENT: TOPIC:

DATE: TIME: VENUE:

S.NO	NAME	D.NO	CLASS	SIGN
1.	JUSTIN. P	22UEN102	II BA ENGLISH	Justin
2.	SANJA Y. D.	22UEN166	II BA English	D Sanja
3.	Joswin vasantha kumar	22UEN157	II BA English	
4.	P. Saravanish	22UEN136	II - BA English	
5.	T. Sriram	22UEN103	II - BA English	
6.	S. Sivasander	22UEN111	II - B.A. English	S. Sivasander
7.	S. Gopal	22UEN142	II BA English	S. Gopal
8.	James Murmu	22UEN149	"	
9.	G.N. Shashanam	22UGN152	"	G N Shyla
10.	Naveen Barla	22UEN122	"	N Barla
11.	R.V. Rudin Joel	22UEN115	II - BA English	R.V. R J
12.	B. Dhalapathi	22UEN129	"	B
13.	T Mohan Raj	22UEN168	II BA Eng	
14.	YESUDAS	22UEN124	II BA Eng	
15.	C. Poobalan	22UEN108	II B A English	
16.	R Sanjay Kumar.	22UEN143	" " "	R. Sanjay
17.	M. Nantha kumar	22UEN137	" "	
18.				
19.				
20.				
21.				
22.				
23.				
24.				
25.				

ST. JOSEPH'S COLLEGE (AUTONOMOUS), TRICHY – 02

PG Dept. of Counselling Psychology & Counselling Centre

A seminar on

MANAGING NEGATIVE EMOTIONS

for the Department of

B.COM HONOURS

II UG

Resource Person

Dr. V. Suganthi
Asst. Professor
Dept. of Counselling Psychology

01 Sept 2023
11.45 A.M.

SAIL HALL

Organizing committee

Ms. Shylin
Ms. Christeela

PG DEPARTMENT OF COUNSELLING PSYCHOLOGY

& COUNSELLING CENTRE

ST. JOSEPH'S COLLEGE (Autonomous)

Tiruchirappalli-620 002

Report on Managing Negative Emotions – seminar

Date: 01.09.23

Audience: Students of II B.COM HONOURS

Introduction

The PG Department of Counselling Psychology and the Counselling Centre are hosting series of seminar on the topics "Managing Negative Emotions," "Rising above Addiction," and "Maintaining Healthy Relationships." Members of the organizing committee are Ms. Christeela and Ms. Shylin. The lecture was attended by 55 students from the Department of II B.COM Honours on the topic 'Managing Negative emotions'.

About the theme

Negative emotions can come from a triggering event, such as an overwhelming workload. It can be described as any feeling which causes you to be miserable and sad. These emotions make you dislike yourself and others, and reduce your confidence and self-esteem, and general life satisfaction. Emotions that can become negative are hate, anger, jealousy and sadness. Your thoughts surrounding an event also play a role. The way that you interpret what happened can alter how you experience the event and whether or not it causes stress.

At 11.45 AM at Sail Hall, the session began with a prayer song. The seminar's host was Ms. Shylin. The resource person for the seminar was Dr. Suganthi, Assistant Professor, Dept. of Counselling Psychology. She took started the session by discussing the various types of emotions we experience and the rationale behind it. She stated the importance to distinguish between what an emotion is and what a feeling is. While the two are interconnected, there's a bigger difference than one may realize. Emotions – Emotions are regarded as 'lower level' responses. They first occur in the subcortical areas of the brain such as the amygdala and the ventromedial prefrontal

cortices. Emotions are coded into our DNA and are thought to have developed as a way to help us respond quickly to different environmental threats, much like our ‘fight or flight’ response. The amygdala has also been shown to play a role in the release of neurotransmitters that are essential for memory, which is why emotional memories are often stronger and easier to recall. Feelings – Emotions are seen as preceding feelings, which tend to be our reactions to the different emotions we experience. Feelings occur in the neocortical regions of the brain and are the next step in how we respond to our emotions as an individual. She conducted activities to the students for them to understand emotions in a better way.

So instead of trying to ignore feelings, finding ways to understand, accept, and reframe emotions is often more helpful. Making changes in our life can cut down on negative emotions, but it won't eliminate our stress triggers. As we make changes in our life to bring about less frustration, we will also need to find healthful outlets for dealing with these emotions The goal isn't to repress these feelings but to find healthier ways of regulating them. Building these coping skills can lead to greater emotional resilience and well-being.

Conclusion

At 01.00 PM, the session came to an end. The attendees in this seminar on "Managing negative Emotions” understood how to name the emotion, understand it and reframe it in a healthier way possible.

Dr. EMMANUEL AROCKIAM, S.J., Ph.D.
DIRECTOR - DEPT OF COUNSELLING PSYCHOLOGY
ST. JOSEPH'S COLLEGE (AUTONOMOUS)
TRICHY-620 002


GPS MAP CAMERA
Dept. of Counselling Psychology &
Counselling Centre, St. Joseph's
Latitude: 10.8284625
Longitude: 78.6904613
Date: 01 Sep 2023
Time: 11:39 AM
Google


GPS MAP CAMERA
Dept. of Counselling Psychology &
Counselling Centre, St. Joseph's
Latitude: 10.8284625
Longitude: 78.6904613
Date: 01 Sep 2023
Time: 11:39 AM
Google


GPS MAP CAMERA
Dept. of Counselling Psychology &
Counselling Centre, St. Joseph's
Latitude: 10.8284625
Longitude: 78.6904613
Date: 01 Sep 2023
Time: 11:39 AM
Google


GPS MAP CAMERA
Dept. of Counselling Psychology &
Counselling Centre, St. Joseph's
Latitude: 10.8284625
Longitude: 78.6904613
Date: 01 Sep 2023
Time: 11:39 AM
Google


GPS MAP CAMERA
Dept. of Counselling Psychology &
Counselling Centre, St. Joseph's
Latitude: 10.8284625
Longitude: 78.6904613
Date: 01 Sep 2023
Time: 11:39 AM
Google


GPS MAP CAMERA
Dept. of Counselling Psychology &
Counselling Centre, St. Joseph's
Latitude: 10.8284625
Longitude: 78.6904613
Date: 01 Sep 2023
Time: 12:24 PM
Google

ST. JOSEPH'S COLLEGE, TRICHY

PG DEPARTMENT OF COUNSELLING PSYCHOLOGY & COUNSELLING CENTRE

SEMINAR SERIES - ATTENDANCE LIST

DEPARTMENT: II B.com Honours

DATE: 01/09/2023 TIME: 11.30 AM TOPIC: Managing Negative Emotions

S.NO	NAME	D.NO	CLASS	SIGN
1.	JAISREE S	22UCR543	II B.COM HONOURS	
2.	MUGUNITHA PRIYA	22UCR540	"	
3.	S. Sivaranjani	22UCR515	"	
4.	K.M. Swethalakshmi	22UCR541	"	
5.	Mohanapriya	22UCR532	"	
6.	Madhu Suhasini	22UCR514	"	
7.	Sulakchana. G	22UCR508	"	
8.	Srivardhini. E	22UCR526	"	
9.	Rajalakshmi B	22UCR570	"	Rajalakshmi B
10.	Shreya. R	22UCR530	"	
11.	V. Viveka	22UCR518	"	
12.	A. Jemi Sama	22UCR520	"	
13.	R. Shivani	22UCR529	"	
14.	S. Amala Rainika	22UCR522	"	
15.	K. Sarveshwari	22UCR517	"	
16.	S. Amirtha	22UCR552	"	
17.	S. Shruthimaya	22UCR561	"	
18.	M. Steffy	22UCR519	"	
19.	A. Jovita	22UCR558	"	
20.	M. Abirami	22UCR544	"	
21.	M. Shalaj	22UCR555	"	
22.	B. Maria Rexy	22UCR553	"	
23.	J. Esther	22UCR513	"	
24.	Janani	22UCR565	"	
25.	M. Monika	22UCR547	"	

ST. JOSEPH'S COLLEGE, TRICHY

PG DEPARTMENT OF COUNSELLING PSYCHOLOGY & COUNSELLING CENTRE

SEMINAR SERIES - ATTENDANCE LIST

DEPARTMENT: II B.com Honours

DATE: 01/09/2023 TIME: 11.30 AM TOPIC: Managing Negative Emotions

S.NO	NAME	D.NO	CLASS	SIGN
1.	SAMUEL J	22UCR569	II BCom (Honours)	Samuel J
2.	Thoufik.M	22UCR527	II B.Com	Thouf
3.	Praveen Kumar R	22UCR562	II B.Com (Hons)	P.R
4.	Vasanthan	22UCR564	II B Com (Hons)	Vasanthan
5.	Leo Logesh.A	22UCR546	II B Com (Hon)	A.Leo
6.	GOKULNATH.M.K	22UCR511	II B.COM(HONS)	
7.	MUKILAN .V	22UCR537	II B.COM(HONS)	
8.	Vinoth Kumar.M	22UCR504	II B.com(Hons)	
9.	Kevinn Infan Benedick.B	22UCR536	II B.Com(Hons)	B.Kevinn
10.	Aathish G	22UCR503	II B.Com(Hons)	G.Aathish
11.	Lakshmi Raj.V.J	22UCR550	II B.Com (Hons)	
12.	Siddarth Vishvaan	22UCR551	II B.com(Hons)	Siddarth
13.	Hariram	22UCR525	II B.com Hons.	Hariram
14.	Mohamed Jasim S	22UCR538	II B.com(Hons)	
15.	mohamed Jasim.m	22UCR510	II B.com (Hons)	
16.	Kevin.T	22UCR549	II B.com (Hons)	
17.	V.K.P Easwaraa Prasath	22UCR525	II B.com(Hons)	
18.	Rajesh	22UCR516	II BCOM HONS	M.RAJESH
19.	Hariharan Kaviyash DV	22UCR548	II B.COM HONS	Kaviyash
20.	DHINESH KUMAR .M	22UCR521	" "	Dhinesh
21.	S.PRATHEEP	22UCR535	II B.Com Honours	S.Pratheep
22.	N.Giridhar	22UCR563	II B.COM HONS	N.Giridhar
23.	S.Manu	22UCR556	II B COM Hons	
24.	Vasanth Kumar D	22UCR545	II B.Com Hons	Vasanth
25.				

ST. JOSEPH'S COLLEGE, TRICHY

PG DEPARTMENT OF COUNSELLING PSYCHOLOGY & COUNSELLING CENTRE

SEMINAR SERIES - ATTENDANCE LIST

DEPARTMENT: II B.com Honours

DATE: 01/09/2023 TIME: 11.30 TOPIC: Managing Negative Emotions

S.NO	NAME	D.NO	CLASS	SIGN
1.	B. ABARNA	22UCR559	II B.COM HONOURS	Abs
2.	E. RUTHRA DEVI	22UCR502	"	Ruthradevi
3.	S.V. Akshaya	22UCR505	"	Akshaya.
4.	M. Kalyani	22UCR560	"	Kalyani
5.	M. Keerthana	22UCR506	"	Keerthana.
6.	A.G. Srimuki	22UCR509	"	Srimuki
7.				
8.				
9.				
10.				
11.				

PG Dept. of Counselling Psychology & Counselling Centre

St. Joseph's College (Autonomous), Trichy - 02

A seminar on

Managing Negative Emotions

for the Department of

Statistics

Resource Person

Rev. Dr. Emmanuel Arockiam, SJ

Head, Dept. of Counselling Psychology

DATE: 01.09.2023 - 9.30 A.M.

VENUE: SAIL HALL

PG DEPARTMENT OF COUNSELLING PSYCHOLOGY &

COUNSELLING CENTER

ST. JOSEPH'S COLLEGE (Autonomous)

Tiruchirappalli-620 002

Report on 'Managing negative Emotions" – Seminar

Date: 01 September 2023

Audience: Students of Statistics Department

Introduction

A seminar series on topics like "Rising above Addiction," "Maintaining Healthy Relationships," and "Managing negative Emotions" is being organized by the PG Department of Counselling Psychology and the Counselling Centre. Members of the organizing committee were Ms. Christeela and Ms. Shylin. 152 students from Shift I of the Department of Statistics attended the seminar.

About the theme

Negative emotions can come from a triggering event, such as an overwhelming workload. Your thoughts surrounding an event also play a role. The way that you interpret what happened can alter how you experience the event and whether or not it causes stress.

Research has shown that tactics like suppressing your emotions are ineffective and can even be harmful. So instead of trying to ignore your feelings, finding ways to understand, accept, and reframe your emotions is often more helpful.

Making changes in our life can cut down on negative emotions, but it won't eliminate our stress triggers. As we make changes in our life to bring about less

frustration, we will also need to find healthful outlets for dealing with these emotions.

Negative emotions are normal and even expected. The goal isn't to repress these feelings but to find healthier ways of regulating them. Building these coping skills can lead to greater emotional resilience and well-being.

At 9.30 am, the session began with a hymn of prayer at SAIL HALL. The seminar's master of ceremonies was **Ms. Christeela**. **Rev. Dr. Emmanuel Arockiam, SJ**, the resource person, was introduced by Ms. Christeela to lead the session. Fr. Emmanuel discussed the value of having wholesome connections.

This seminar covered a wide range of topics, such as:

- Types of emotions
- Ruminating on emotions
- Poor coping skills
- Regions of brain
- Physiological reactions in the body
- Differences between feelings and emotions
- Healthy ways to handle negative emotions
- Components of Emotional Intelligence

Conclusion

At 11.00 AM, the session came to a close. The attendees in this seminar on "Managing negative Emotions" learned how to spot relationship toxicity and how to treat others with respect and compassion.

Dr. EMMANUEL AROCKIAM, S.J., Ph.D.
DIRECTOR - DEPT OF COUNSELLING PSYCHOLOGY
ST. JOSEPH'S COLLEGE (AUTONOMOUS)
TRICHY-620 002


DEALING WITH
NEGATIVE EMOTIONS
GPS MAP CAMERA
Dept. of Counselling Psychology &
Counselling Centre, St. Joseph's
Latitude: 10.8284625
Longitude: 78.6904613
Date: 01 Sep 2023
Time: 9:52 AM
Google


GPS MAP CAMERA
Dept. of Counselling Psychology &
Counselling Centre, St. Joseph's
Latitude: 10.8284625
Longitude: 78.6904613
Date: 01 Sep 2023
Time: 9:52 AM
Google


GPS MAP CAMERA
Dept. of Counselling Psychology &
Counselling Centre, St. Joseph's
Latitude: 10.8284625
Longitude: 78.6904613
Date: 01 Sep 2023
Time: 9:52 AM
Google


GPS MAP CAMERA
Dept. of Counselling Psychology &
Counselling Centre, St. Joseph's
Latitude: 10.8284625
Longitude: 78.6904613
Date: 01 Sep 2023
Time: 9:51 AM
Google


DEALING WITH
NEGATIVE EMOTIONS
GPS MAP CAMERA
Dept. of Counselling Psychology &
Counselling Centre, St. Joseph's
Latitude: 10.8284625
Longitude: 78.6904613
Date: 01 Sep 2023
Time: 9:52 AM
Google


GPS MAP CAMERA
Dept. of Counselling Psychology &
Counselling Centre, St. Joseph's
Latitude: 10.8284625
Longitude: 78.6904613
Date: 01 Sep 2023
Time: 9:51 AM
Google


GPS MAP CAMERA
Dept. of Counselling Psychology &
Counselling Centre, St. Joseph's
Latitude: 10.8284625
Longitude: 78.6904613
Date: 01 Sep 2023
Time: 9:51 AM
Google


GPS MAP CAMERA
Dept. of Counselling Psychology &
Counselling Centre, St. Joseph's
Latitude: 10.8284625
Longitude: 78.6904613
Date: 01 Sep 2023
Time: 9:51 AM
Google


GPS MAP CAMERA
Dept. of Counselling Psychology &
Counselling Centre, St. Joseph's
Latitude: 10.8284625
Longitude: 78.6904613
Date: 01 Sep 2023
Time: 9:51 AM
Google

ST. JOSEPH'S COLLEGE, TRICHY

PG DEPARTMENT OF COUNSELLING PSYCHOLOGY & COUNSELLING CENTRE

ATTENDANCE LIST

SAIL HALL

DEPARTMENT: STATISTICS

DATE: 1-09-2023 TIME: 9.30 AM TOPIC: Managing Negative Emotion

S.NO	NAME	D.NO	CLASS	SIGN
1.	Sudharsan.S	23UST150	I UG	S.Sudh
2.	Jeroen Samuel.J	23UST132	"	Jeroen
3.	Vizwa.R	23UST123	"	
4.	Ashik.S	23UST138	"	
5.	S.Dheenadharshan.	23UST147	"	
6.	M.Marshal	23UST109	"	
7.	HARIKRISHNAN.V	23UST112	"	
8.	Immanuvel Rajendran.A	23UST136	"	Immanuvel
9.	S.Bharath Mokesh	23UST113	"	S.
10.	M.S.Hari Haran	23UST160	"	M.S.Hari
11.	A.AKASH.	23UST102	"	A.
12.	R. Sanjay	23UST148	"	R.Sanjay
13.	C. Robin	22UST121	"	
14.	D. Nageshwaran	22UST115	"	
15.	D. Benadict Raj	22UST118	"	D Benadict Raj
16.	PATRICK XAVIER U	22UST140	"	Patrick Xavier
17.	G. Sudharsan	22UST144	"	G Sudharsan
18.	B. Praveen	22UST146	"	B. Praveen
19.	C. Arputha Amos	22UST133	"	
20.	S. Nishanth	22UST149	"	
21.	N. Varatharajan	22UST114	"	VARATHARAJAN
22.	G. Yashvanth	22UST134	"	G. Yash
23.	P. ARUN	22UST116	"	P.
24.	M. ANISTON	22UST120	"	M.
25.	M. GHANAGAVEL	22UST109	"	M. ghanagavel

26.	Allwin. PL	22UST119	
27.	N. Hariprasad	22UST151	N.HariPrasad
28.	S. Sugan kumar	22UST130	S. Sugan kumar
29.	N. Nitha Sravanya sastha	22UST153	N. S. Sastha
30.	S. K. Dinesh ganesha	22UST147	S.K. Dinesh ganesha
31.	Surya kumar. S	21UST144	
32.	S. Yuvaraj	21UST165	S. Yuvaraj
33.	I. Stakfion	21UST107	I. Stakfion
34.	N. Tharun	21UST121	N. Tharun
35.	S. Venkadesaperumal	21UST161	S. Venkadesaperumal
36	K. Chandru	21UST147	K. Chandru
37.	S. SERGIUS MILAN	21UST112	S. Milan
38	S. SANJAI	22UST151	S. Sanjai
39	P. Allan Tony Xavier	22UST158	P. Allan
40	Karthikeyan	22UST128	Karthikeyan
41	M. Amuthan Ruso	22UST123	M. Amuthan
42.	M. Mohamad Ismail	22UST159	Ismail
43.	AKILESH. S.	22UST142	Akilesh. S.
44.	R. Abisho George	22UST155	R. Abisho George
45.	L. Yagaresh	22UST143	L. Yagaresh
46.	A. Faheem Ajhar	22UST137	A. Faheem Ajhar
47.	A. Anil Agathiyan	21UST117	A. Anil Agathiyan
48.	M. Dharabalan	21UST166	M. Dharabalan
49.	M. Vignesh Kumar	21UST134	M. Vignesh Kumar
50.	M SANJAY	21UST140	M. Sanjay

DEPARTMENT: Statistics

DATE: 01.09.2023 TIME: 9.30 AM TOPIC: Managing Negative Emotions

S.NO	NAME	D.NO	CLASS	SIGN
1.	Radha. V	23UST168	1st (BSc. Statistics	Radha. V
2.	Shabeena Jose S	23UST143	1st BSC. Stat	Shabeena
3.	PUGAZHARASAN. A	21UST135	3rd Bsc. Stat	A. Pugazharasan
4.	SESHAN. I	21UST167	3rd B.Sc., STATISTICS	S seshan.
5.	Logeshwaran P	21UST116	3rd BSc. Statistics	Plogeshwaran
6.	Manikandaa. S	21UST148	3rd BSc statistics	Smani
7.	PL. Ram Kailash	21UST127	III. Bsc. Statistics	PL. Ram
8.	R. Adhithya	21UST115	III BSc. Statistics	R. Adhithya.
9.	P Pravin Kanna	21UST150	III. B.Sc. Statistics	P. Pravin
10.	A. Mohamed sohail	21UST151	3rd. B.Sc. Statistics	A. Sohail.
11.	S. Aaron Rex	21UST163	3rd BSc. STAT	S. Aaron.
12.	C. Sathish	21UST136	III. Bsc statistics	C. Sathish
13.	W. Tony Amaladas	23UST134	I st BSc. Statistics	W. Tony
14.	A. Partha Sarathi	23UST151	I st BSC statistics	A Partha
15.	N. Sathya Prakash	23UST118	I st B.Sc. Statistics	N. Sathya Prakash
16.	K. K. Mano Ranjan.	23UST164	I st Bsc. Statistics	Mano Ranjan
17.	S. Frankvin	23UST133	I st B.Sc. statistics	S. Frankvin
18.	S. Selva	23UST119	I st B.Sc Statistics	S. Selva
19.	P. Logeshwaran	23UST126	I st B.Sc. Statistics	P. Logeshwaran
20.	Mohamed Yasar Arafath. A	23UST135	I st B.Sc statistics	Yasar. A
21.	Alagesh. V	23UST167	I Bsc statistics	V Alagesh
22.	Tharunkumar M	23UST108	I st Bsc. Statistics	M. Tharunkumar
23.	Srinivasan. S	23UST122	I st B.Sc Statistics	S. Srinivasan
24.	M. Rishek wallace	23UST149	I st Bsc. Statistics	M. Rishek
25.	Rohith fernandas. P	23UST125	I st B.Sc Statistics	P. Rohith

DEPARTMENT: Statistics

DATE: 01.09.2023 TIME: 9.30 AM TOPIC: Managing Negative Emotions

S.NO	NAME	D.NO	CLASS	SIGN
1.	Vinay G	22UST105	II Bsc statistics	
2.	Serena.G	22UST104	II Bsc statistics	
3.	A. Anjela Reni	22 UST117	II Bsc Statistics	
4.	L. POOVIZHA	22UST112	II Bsc Statistics	
5.	Ashly Thangadurai	22UST100	II Bsc. statistics	
6.	M. Keerthana.	22UST163	II BSC. statistics	
7.	P. Swetha	21UST103	III B Sc statistics	
8.	KINGSLIN J	21UST108	III B Sc, Statistics	
9.	CHANTHIA DEVI. M	21UST122	III B Sc, STATISTICS	
10.	V. Japhin	22UST103	II BSC Statistics	
11.	A. Flores Risha	22UST107	II Bsc. Statistics	
12.	V. Jerline.	23UST121	I BSc statistics	
13.	A. Sindhini	23UST117	I Bsc. Statistics	
14.	P. Renuka	23UST111	I BSC. statistics	
15.	R. Suwarinee	22UST152	II B.Sc Statistics	
16.	M. Dharani	22UST139	II B.Sc Statistics	
17.	S. Rishapthiha	22UST124	II Bsc Statistics	
18.	A. MOURISH PREEZY	21UST117	III Bsc statistics	
19.	S. VANITHA LAKSHMI	21UST146	III B Sc STATISTICS	
20.	V. JERNIAH	21UST145	III BSc STATISTICS	
21.	P.V. Nisha	22UST122	II BSC Statistics	
22.	J. Joicy	22UST127	II BSc. Statistics	
23.	B.T. Dhana.	22UST136	II Bsc Statistics	
24.	J. Abinaya	22UST110	II Bsc Statistics	
25.	S. SWETHA	21UST149	III Bsc Statistics	

NAME	D.NO	CLASS	SIGN
APERNA.V	21UST159	III B.Sc STATISTICS	V.Aperna
CAROLENA RUTH.S	21UST106	III B.Sc STATISTICS	S.Carolena Ruth
VINNARASI P	21UST120	III B.Sc STATISTICS	P.Vinn
MALAVIKA.P	21UST124	III B.Sc STATISTICS	P.Malavika
LEKA SUBANU.S	21UST154	III BSc STATISTICS	S.Leka
Anska Roselin	22UST101	II B.Sc Statistics	A.Ros
V.Prathiba	22UST154	II B.Sc. Statistics	~~V.Pra~~
Sakthi Keerthana.G	22UST131	II nd B.Sc Statistics	Sakthikeerthana
Dhanusree.R	22UST132	II nd B.Sc statistics	R.Dhanus.
A.Joice Hettilda	22UST129	II nd BSc.Statistics.	A.Joi

ST. JOSEPH'S COLLEGE, TRICHY

PG DEPARTMENT OF COUNSELLING PSYCHOLOGY & COUNSELLING CENTRE

SEMINAR SERIES - ATTENDANCE LIST

DEPARTMENT: Statistics

DATE: 01.09.2023 TIME: 9.30AM TOPIC: Managing Negative Emotions

S.NO	NAME	D.NO	CLASS	SIGN
1.	A J Jefrina	21UST101	III - Bsc. Statistics	
2.	KAAVEYA BAARATHI M	21UST153	III BSc, Statistics	
3.	Madhumitha .K	21UST155	III Bsc. STATISTICS	K.
4.	HARSHINI B	21UST110	III B.Sc STATISTICS	
5.	Ramya Mary A	21UST104	III BSc statistics	
6.	Neha Linsy J	21UST113	III BSc Statistics	Neha
7.	Catherine Divina A	21UST169	III. B Sc Statistics	
8.	E. Arthi	21UST157	III BSc statistics	E.
9.	J. Sheela Mary	21UST107	III BSc. Statistics	
10.	A. Nancy	21UST143	III. B.Sc. statistics	
11.	D. Harini	21UST164	III - BSc Statistics	D. Harini
12.				
13.				
14.				
15.				

DEPARTMENT: Statistics

DATE: 01.09.2023 TIME: 9.30 AM TOPIC: Managing Negation Emotions

S.NO	NAME	D.NO	CLASS	SIGN
1.	S. Kalpana	23UST162	1st B.Sc Statistics	Kalpana
2.	K. Charumathi	23UST165	1st B.Sc statistics	
3.	P. Nilashini	23UST103	I B.Sc statistics	
4.	k. Yogeshwari	23UST144	I B.Sc. Stat	k. Yogi
5.	S. Infant Reci	23UST116	IB.Sc.Stat	S.
6.	A. Monalisha.	23UST137	I. B. Sc statistics	A. Mon
7.	X. Aashmi	23UST152	I. B.Sc statistics	Ashmi X
8.	S. Shaheena Jose	23UST143	I st Bsc Stat	Shaheena
9.	Radha. V	23UST168	I st Bsc (Statistics)	
10.	R. Arthi	23UST145	I st BSc (statistics)	
11.	M. Sowbakiya	23UST141	I st BSC (Stat)	M. Sowbakiya
12.	A. Remila Jasmine	23UST129	I BSc statistics	Jasmine
13.	S. Stacy Deshasha.	23UST153	I BSC Statistics	Deshasha
14.	M. Arul Jemisha.	23UST128	I. BSC. Statistics	
15.	R. Janani	23UST101	I. B.SC. Statistics	R. Jan
16.	K. Abirami	23UST130	I B.SC. Statistics	K. Abi
17.	Karthi. S	23UST157	I st BSc STATISTICS	
18.	Mystica Rose. D	23UST156	I st Bsc. Statistics	Mystica Rose
19.	Nabisha	23UST155	I BSc Statistics	Nabi
20.	Praveena. R	23UST169	I BSc. Statistics	
21.	Ashvitha. R	23UST158	I BSc. Statistics	
22.	R. Thangamani	23UST140	I st BSc Statistics	Thangamani
23.	R. Sindhuja	23UST120	I st BSc statistics	R Sindhuja
24.				

DEPARTMENT: Statistics

DATE: 01.09.2023 TIME: 9.30 AM TOPIC: Managing Negative Emotions

S.NO	NAME	D.NO	CLASS	SIGN
1.	B. Kevin Das	21UST108	III BSc Stat	B.K
2.	M. Dhineshmoran	21UST170	III. BSc Stat	M.D
3.	S. Prasanna	21UST105	III B.Sc, Stat	S
4.	M. SHITHANDI	21UST142	III B.Sc., STAT	
5.	ROSARIO JEROME SUSAN J	21UST123	III BSc, Stat	
6.	GIRIDHARAN.S	21UST102	III B.SC, STAT	S.
7.				
8.				
9.				
10.				

DEPARTMENT: Statistics

DATE: 01.09.2023 TIME: 9.30 AM TOPIC: Managing Negative Emotions

S.NO	NAME	D.NO	CLASS	SIGN
1.	B Braxton Oreno Anand	23UST105	I B.SC. statistics	B. Braxton Oreno Anand
2.	Jason Samuvel - L	23UST161	I BSc statistics	
3.				
4.				
5.				
6.				
7.				
8.				
9.				
10.				

PG Dept. of Counselling Psychology & Counselling Centre

St. Joseph's College (Autonomous), Trichy - 02

A seminar on

Managing Negative Emotions

for the Department of

Tamil

Resource Person

Rev. Dr. Emmanuel Arockiam, SJ

Head, Dept. of Counselling Psychology

DATE: 11.09.2023 - 09.30 A.M.

VENUE: SAIL HALL

Organizing committee

Ms. Shylin

Ms. Christeela

PG DEPARTMENT OF COUNSELLING PSYCHOLOGY &

COUNSELLING CENTER

ST. JOSEPH'S COLLEGE (Autonomous)

Tiruchirappalli-620 002

Report on 'Managing negative Emotions" – Seminar

Date: 11 September 2023

Audience: Students of Tamil Department

Introduction

A seminar series on topics like "Rising above Addiction," "Maintaining Healthy Relationships," and "Managing negative Emotions" is being organized by the PG Department of Counselling Psychology and the Counselling Centre. Members of the organizing committee were Ms. Christeela and Ms. Shylin. 95 students from Shift I of the Department of Statistics attended the seminar.

About the theme

Negative emotions can come from a triggering event, such as an overwhelming workload. Your thoughts surrounding an event also play a role. The way that you interpret what happened can alter how you experience the event and whether or not it causes stress.

Research has shown that tactics like suppressing your emotions are ineffective and can even be harmful. So instead of trying to ignore your feelings, finding ways to understand, accept, and reframe your emotions is often more helpful.

Making changes in our life can cut down on negative emotions, but it won't eliminate our stress triggers. As we make changes in our life to bring about less

frustration, we will also need to find healthful outlets for dealing with these emotions.

Negative emotions are normal and even expected. The goal isn't to repress these feelings but to find healthier ways of regulating them. Building these coping skills can lead to greater emotional resilience and well-being.

At 9.30 am, the session began with a hymn of prayer at SAIL HALL. The seminar's master of ceremonies was **Ms. Christeela**. **Rev. Dr. Emmanuel Arockiam, SJ**, the resource person, was introduced by Ms. Christeela to lead the session. Fr. Emmanuel discussed the value of having wholesome connections.

This seminar covered a wide range of topics, such as:

- Types of emotions
- Ruminating on emotions
- Poor coping skills
- Regions of brain
- Physiological reactions in the body
- Differences between feelings and emotions
- Healthy ways to handle negative emotions
- Components of Emotional Intelligence

Conclusion

At 11.00 AM, the session came to a close. The attendees in this seminar on "Managing negative Emotions" learned how to spot relationship toxicity and how to treat others with respect and compassion.

Dr. EMMANUEL AROCKIAM, S.J., Ph.D.
DIRECTOR - DEPT OF COUNSELLING PSYCHOLOGY
ST. JOSEPH'S COLLEGE (AUTONOMOUS)
TRICHY-620 002


GPS MAP CAMERA
Dept. of Counselling Psychology &
Counselling Centre, St. Joseph's
Latitude: 10.8284625
Longitude: 78.6904613
Date: 11 Sep 2023
Time: 9:43 AM
Google


GPS MAP CAMERA
Dept. of Counselling Psychology &
Counselling Centre, St. Joseph's
Latitude: 10.8284625
Longitude: 78.6904613
Date: 11 Sep 2023
Time: 9:43 AM
Google


GPS MAP CAMERA
Dept. of Counselling Psychology &
Counselling Centre, St. Joseph's
Latitude: 10.8284625
Longitude: 78.6904613
Date: 11 Sep 2023
Time: 9:43 AM
Google


GPS MAP CAMERA
Dept. of Counselling Psychology &
Counselling Centre, St. Joseph's
Latitude: 10.8284625
Longitude: 78.6904613
Date: 11 Sep 2023
Time: 9:42 AM
Google


GPS MAP CAMERA
Dept. of Counselling Psychology &
Counselling Centre, St. Joseph's
Latitude: 10.8284625
Longitude: 78.6904613
Date: 11 Sep 2023
Time: 9:45 AM
Google


GPS MAP CAMERA
Dept. of Counselling Psychology &
Counselling Centre, St. Joseph's
Latitude: 10.8284625
Longitude: 78.6904613
Date: 11 Sep 2023
Time: 9:43 AM
Google


GPS MAP CAMERA
Dept. of Counselling Psychology &
Counselling Centre, St. Joseph's
Latitude: 10.8284625
Longitude: 78.6904613
Date: 11 Sep 2023
Time: 9:43 AM
Google


GPS MAP CAMERA
Dept. of Counselling Psychology &
Counselling Centre, St. Joseph's
Latitude: 10.8284625
Longitude: 78.6904613
Date: 11 Sep 2023
Time: 9:44 AM
Google

ST. JOSEPH'S COLLEGE, TRICHY

PG DEPARTMENT OF COUNSELLING PSYCHOLOGY & COUNSELLING CENTRE

SEMINAR SERIES – ATTENDANCE LIST

DEPARTMENT: Tamil

DATE: 11.09.2023 TIME: 9.30 A.M. VENUE: SAIL HALL

S.NO	NAME	D.NO	CLASS	SIGN
1.	C. Shanmugapriyan	22UTA132	II - B A TAMIL	C. Shanmugapriyan
2.	A. Allwin Amalraj	22UTA110	II B. A Tamil	A. A
3.	J. Allwin Joe	22UTA134	II B. A. Tamil	[illegible]
4.	S. HEMSURYA	22UTA118	II B.A Tamil	[illegible]
5.	J. PRIJITH.	22UTA126	II BA. Tamil.	[illegible]
6.	A. Stephen Fleming	22UTA102	II B.A Tamil	A. Stephen Fleming
7.	A. Marshal	22UTA143	II B.A. Tamil	A. Marshal
8.	V. Srinivas	22UTA128	II B. A. Tamil	V. Srinivas
9.	P. Dinesh	22UTA130	II B A Tamil	Dinesh
10.	A. Rahul Joseph	22UTA115	II BA Tamil	[illegible]
11.	கா. செல்வக்குமார்	22 UTA 117	II BA Tamil	K. Sk
12.	ச. சேகராஜ்	22UTA111	II. B.A. Tamil	[illegible]
13.	ஜெ. ஜெய் அரவிந்த்	22UTA109	II BA. Tamil	J. [illegible]
14.	ஜெ. பெல்வார்மன்ஆன்டோ	22UTA103	II B.A Tamil	[illegible]
15.	பா. [illegible]	22UTA158	II BA Tamil	[illegible]
16.	ஜெ. பிரதாப்	22UTA140	II BA. Tamil	[illegible]
17.	ச. பிரபாகரன்	22UTA125	II. BA. Tamil	[illegible]
18.	G. Abishek dhoni	22UTA112	II BA Tamil	[illegible]
19.	M. SUDHARSAN	22UTA155	II BA Tamil	M. Sudharsan
20.	R. Raguram	22UTA138	II BA Tamil	R. Ragu[illegible]
21.	[illegible]	22UTA156	II BA Tamil	[illegible]
22.	M. [illegible]	22UTA105	II BA Tamil	[illegible]
23.	ஆ. அருண் சிங்	22UTA141	II BA Tamil	A. G. [illegible]
24.	கு. மகாலிஷ்வா	22UTA145	II BA Tamil	K. Maha[illegible]
25.	து. சுஜித்	22UTA122	II BA. Tamil	D. Sujith
26.	அ. வெங்கடேஷ்	22UTA139	II B.A. Tamil	A. Venkat
27.	ர. ராகுல் ரவி	23UTA169	I B.A TAMIL	[illegible]

ST. JOSEPH'S COLLEGE, TRICHY

PG DEPARTMENT OF COUNSELLING PSYCHOLOGY & COUNSELLING CENTRE

SEMINAR SERIES – ATTENDANCE LIST

DEPARTMENT: TAMIL

DATE: 11.09.23 TIME: 9.30 A.M. VENUE: SAIL HALL

S.NO	NAME	D.NO	CLASS	SIGN
1.	B. Kavin	23UTA131	B.A Tamil I	B. Kavin
2.	V. Jeeckonson	23UTA170	BA Tamil I	V. Jeeckonson
3.	A Manojkumar	23UTA119	B.A Tamil	Manojkumar
4.	M. Ajith kumar	23UTA167	BA Tamil	Ajithkumar
5.	A. Santhosh	23UTA109	B.A. Tamil	A. santhosh
6.	K. Dhanush	23UTA157	B.A Tamil	K. Dhanush
7.	S. MADHAN	23UTA151	B. A. Tamil	S. madhan
8.	V. Balaji	23UTA105	B.A Tamil	V. Balaji
9.	R. Muralitharan.	23UTA152	B.A. Tamil	R. Muralitharan
10.	J. Janakkannan	23UTA158	B.A Tamil	J. Janak
11.	S. Vijay Kayan	23 UTA 107	B.A. Tamil	S. Vijay Kayan
12.	N. Elamaran	23UTA163	B.A Tamil	N. Elamaran
13.	K. Marali	23UTA160	B.A. tamil	M. Marali
14.	S. ASHIK TONY	23UTA129	B.A. tamil	S. Ashik Tony
15.	P. Prabel	23UTA150	BA. Tamil	P. Prabel
16.	B. Ditharson KUMAR	23UTA123	B.A Tamil	B. Ditharson Kumar
17.	G. Gunalan,	23UTA155	B.A. Tamil	G. Gunalan
18.	M. Nagamuthu	23UTA113	B.A. Tamil	M. Nagamuthu
19.	C Karthi	23UTA172	B.A Tamil	Karthi
20.	A. Rajadurai	23 UTA 134	B.A Tamil	A. Rajadurai
21.	S. KUDIyarasu	23UTA180	B.A Tamil	S. Kudiyarasu
22.	J. Ebin Raj.	23UTA117	B.A. Tamil	J. Ebin Raj
23.				
24.				
25.				

ST. JOSEPH'S COLLEGE, TRICHY

PG DEPARTMENT OF COUNSELLING PSYCHOLOGY & COUNSELLING CENTRE

SEMINAR SERIES – ATTENDANCE LIST

DEPARTMENT: TAMIL

DATE: 11.09.23 TIME: 9.30 A.M. VENUE: SAIL HALL

S.NO	NAME	D.NO	CLASS	SIGN
1.	B. Annie Rexitta	23UTA106	I B.A. Tamil	B. Annie Rexitta
2.	Deepa. N	23UTA165	B.A. Tamil I	Deepa. N
3.	G. Tamil Selvi	23UTA162	B.A. Tamil I	G. Tamil Selvi
4.	V. Kopika	23UTA122	B.A Tamil	V. Kopika
5.	J. Mary Valentina	23UTA116	I B.A Tamil	J. Mary Valentina
6.	P. Kalai Selvi	23UTA110	B.A TAMIL	P. Kalai Selvi
7.	J. ASWINI	23UTA165	B.A Tamil	J. ASWINI
8.	M. Aresha Sithika	23UTA143	B.A Tamil	M. Aresha
9.	S. Harini	23UTA118	B.A Tamil	S. Harini
10.	S. Rithika	23UTA112	B.A TAMIL	S. Rithika
11.	G. Sahana	23UTA101	B.A. Tamil I	G. Sahana
12.	S.V. Monisha Rethina Gnaneswari	23UTA115	B.A Tamil-I	S.V. Monisha
13.	R. Varthini	23UTA126	B.A Tamil-I	R. Varthini
14.	S. Mahidhashini	23UTA125	B.A Tamil-I	S. Mahidhashini
15.	E. Anisha Cyril	23UTA132	B.A Tamil-I	E. Anisha Cyril
16.	D. Varsha.	23UTA121	B.A. Tamil	D. Varsha
17.	X. Vimalie	22UTA105	B.A Tamil	X. Vimalie
18.	A. Vithika	22UTA123	BA Tamil	A. Vithika
19.	Ammu Agustin	22UTA153	B.A Tamil	Ammu Agustin
20.	Haily. J	22UTA108	B.A Tamil	Haily. J
21.	Arasi Marlin. S. J.	22UTA104	B.A. Tamil-II	Arasi Marlin. S. J.
22.	A. Santhiya mary	22UTA113	II BA Tamil	A. Santhiya mary
23.	K. Arthi	22UTA136	II BA Tamil	K. Arthi
24.				
25.				

ST. JOSEPH'S COLLEGE, TRICHY

PG DEPARTMENT OF COUNSELLING PSYCHOLOGY & COUNSELLING CENTRE

SEMINAR SERIES – ATTENDANCE LIST

DEPARTMENT: TAMIL

DATE: 11.09.23 TIME: 9.30 A.M. VENUE: SAIL HALL

S.NO	NAME	D.NO	CLASS	SIGN
1.	E. Sureka	21UTA104	III - BA Tamil	E. Sureka
2.	S. Loga Soundharya	21UTA139	III - BA Tamil	S. Loga
3.	Chitrika. S.B	21UTA116	III - BA Tamil	S. B
4.	Madhumith. S	21UTA107	III BA TAMIL	S. Madhumith
5.	Sathya priya. P.	21UTA123	III BA TAMIL	P. Sathya priya
6.	D Staphina Nuresh	21UTA182	III BA TAMIL	D. Staphina.
7.	G. Kalpana chawla	21UTA108	III BA Tamil	G. Kalpana chawla.
8.	P. Subrithra.	21UTA121	III. B.A. Tamil	P. Subrithra
9.	M. Leo priney	21UTA110	III. B.A. Tamil	M. Leo priney
10.	M. Vishalini	21UTA112	III - BA TAMIL	M. Vishalini
11.	A. தமிழ்ச் செல்வி	21UTA106	III - BA தமிழ்	A. தமிழ்ச் செல்வி
12.	S. ஹரிபிரசன்னா வெங்கடேசன்	21UTA167	III - B.A. Tamil	S. Hariprasanna
13.	R. மோகன் ராஜ்	21UTA162	III - B.A. Tamil	R. Mohan
14.	ஏ. மோகன் ராஜ்	21UTA133	III B.A தமிழ்	A. Mohan
15.	J. Daniel	21UTA103	III. BA. தமிழ்	J. Daniel
16.	[redacted]	21UTA105	III B.A. தமிழ்	[redacted]
17.	[redacted]	21UTA129	III. B.A. [redacted]	[redacted]
18.	[redacted]	21UTA117	III - BA Tamil	P. [redacted]
19.	S. Siva Sankaran	21UTA140	III BA. Tamil	S. Siva Sankaran
20.	K Logeshwaran	21UTA145	III B.A. Tamil	K Logeshwaran
21.	S. Mohamed Ali.	21UTA143	III B.A Tamil	S. Mohamed Ali.
22.	A. Roshan	21UTA152	III B.A. [redacted]	A. Roshan
23.	H. Vishanth	21UTA172	III B.A Tamil	H. Vishanth
24.				
25.				

ST. JOSEPH'S COLLEGE (AUTONOMOUS), TRICHY - 620 002

943 responses

Publish analytics

COUNSELLING PSYCHOLOGY - STUDENT SURVEY

PG DEPT. OF COUNSELLING PSYCHOLOGY & COUNSELLING CENTRE

PG Dept. of Counselling Psychology

ST. JOSEPH'S COLLEGE (AUTONOMOUS)

Accredited at A++ Grade (4th Cycle) by NAAC

Special Heritage Status awarded by UGC

TIRUCHIRAPPALLI - 620 002, S. INDIA

www.sjctni.edu **Dept.: counpsychsjc@gmail.com**

+91 94449 03613 **emma.aro@gmail.com**

Dr. Emmanuel Arockiam, S.J., Ph.D.

Director

Respected HoDs/Co-ordinators,

Greetings from the Counselling Centre & the PG Dept. of Counselling Psychology!

We, the Counselling Centre & the PG Dept. of Counselling Psychology, have prepared a student survey questionnaire to get information about them and help them.

The Objectives are:

- To understand students' psychological strengths and weaknesses
- To understand their family background
- To understand their psychological and emotional needs and problems
- To help them if necessary

With the approval of Rev. Dr. Arockiasamy Xavier, S.J., the Principal, we have made the necessary arrangements for the students to take this survey in our college computer labs. We request you to co-operate with us for completing this survey.

Our department will reach you out with the date, time and venue. Kindly send your students when the computer labs are free.

Rev. Dr. Emmanuel Arockiam, SJ
Head, Dept. of Counselling Psychology

For details contact:
Ms. Christeela, Counsellor (Ph- 8637663936)
Ms. Shylin, Counsellor (Ph- 8344665537)

PG Dept. of Counselling Psychology

ST. JOSEPH'S COLLEGE (AUTONOMOUS)

Accredited at A++ Grade (4th Cycle) by NAAC

Special Heritage Status awarded by UGC

TIRUCHIRAPPALLI - 620 002, S. INDIA

www.sjctni.edu Dept.: counpsychsjc@gmail.com

+91 94449 03613 emma.aro@gmail.com

Dr. Emmanuel Arockiam, S.J., Ph.D.

Director

7th August 2023

To Rev. Dr. Arockiasamy Xavier, S.J.
Principal
St. Joseph's College (Autonomous)
Trichy – 620 002

(Sub.: Requesting permission to use the Computer Centres)

Dear Rev. Fr. Principal,

We, the Dept. of Counselling Psychology and the Counselling Centre, are planning to collect data from PG students of our college through a Students Survey Questionnaire. Therefore, could you kindly permit us to use the computer centres? With your permission, we could contact the person-in-charge of the Computer centres.

Thanking you,

Sincerely,

Emmanuel Arockiam, S.J.


GPS MAP CAMERA
Dept. of Maths, St. Joseph's College,
Latitude10.8295817 Longitude78.6926476
Date: 20 Jan 2024 Time: 02:36 PM


GPS MAP CAMERA
Dept. of Maths, St. Joseph's College,
Latitude10.8285817 Longitude78.6926476
Date: 20 Jan 2024 Time: 02:36 PM


GPS MAP CAMERA
Dept. of Maths, St. Joseph's College,
Latitude10.8293817 Longitude78.6926476
Date: 20 Jan 2024 Time: 02:36 PM


GPS MAP CAMERA
Dept. of Maths, St. Joseph's College,
Latitude10.8283817 Longitude78.6920479
Date: 20 Jan 2024 Time: 02:36 PM

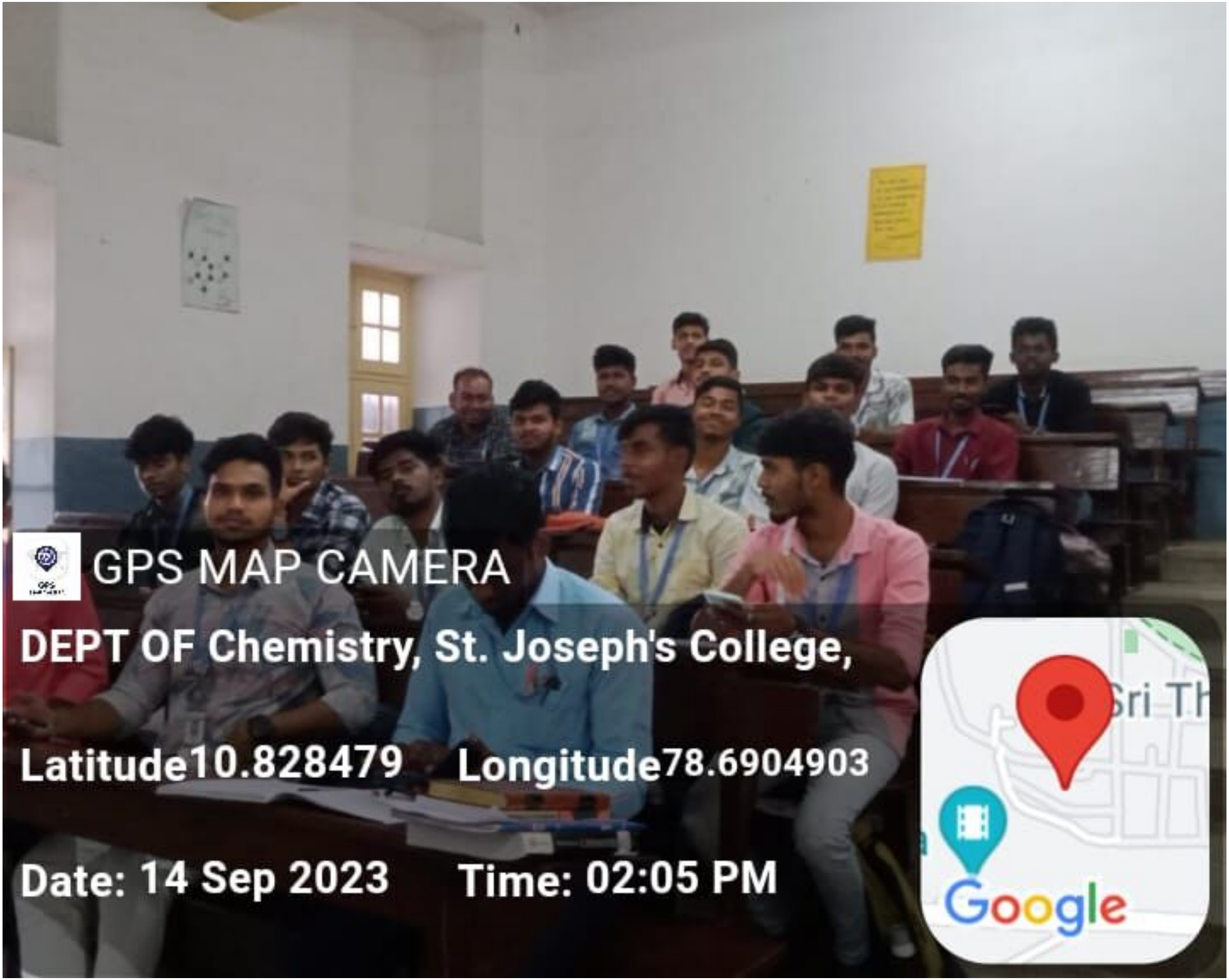
GPS MAP CAMERA
DEPT OF Chemistry, St. Joseph's College,
Latitude10.828479 Longitude78.6904903
Date: 14 Sep 2023 Time: 02:05 PM
Google


GPS MAP CAMERA
DEPT OF Chemistry, St. Joseph's College,
Latitude10.828479 Longitude78.6904903
Date: 14 Sep 2023 Time: 02:05 PM
Google


GPS MAP CAMERA
ECC, St. Joseph's College RMHR+PJX
Latitude10.8293685 Longitude78.6915680
Date: 19 Sep 2023 Time: 02:36 PM
Google


GPS MAP CAMERA
ECC, St. Joseph's College RMHR+PJX
Latitude10.8293685 Longitude78.6915680
Date: 19 Sep 2023 Time: 02:36 PM
Google

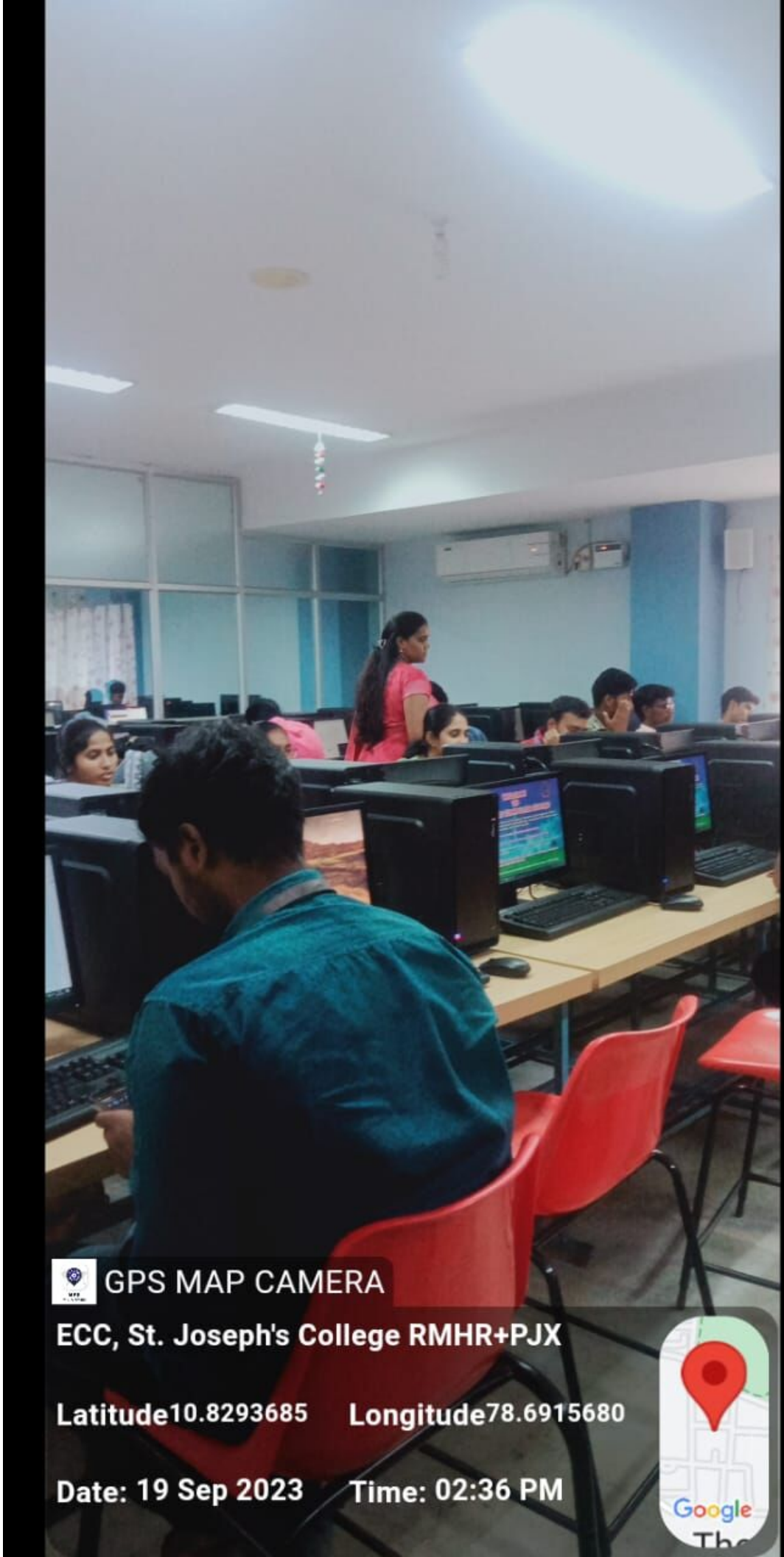
GPS MAP CAMERA
ECC, St. Joseph's College RMHR+PJX
Latitude10.8293685 Longitude78.6915680
Date: 19 Sep 2023 Time: 02:36 PM
Google


GPS MAP CAMERA
ECC, St. Joseph's College RMHR+PJX
Latitude 10.8293685 Longitude 78.6915680
Date: 19 Sep 2023 Time: 12:45 PM
Google


GPS MAP CAMERA
ECC, St. Joseph's College RMHR+PJX
Latitude10.8293685 Longitude78.6915680
Date: 19 Sep 2023 Time: 12:45 PM
Google

PG Dept. of Counselling Psychology

St. JOSEPH'S COLLEGE (Autonomous)

Accredited at A++ Grade (4th Cycle) by NAAC

Special Heritage Status awarded by UGC

TIRUCHIRAPPALLI - 620 002, S. INDIA

www.sjctni.edu Dept.: counpsychsjc@gmail.com

+91 94449 03613

05 October 2023

To

Rev. Dr. Arockiasamy Xavier, S.J.
The Principal
St. Joseph's College (Autonomous)
Trichy – 02

(Subject: Permission to conduct Awareness Activities on Mental Health Day on October 10th)

Respected Fr. Principal,

We, the Dept. of Counselling Psychology and the Counselling Center, request you to kindly permit us to conduct a few simple activities to create Mental Health awareness among students. These activities will not disturb any class. We plan to keep some Affirmation Booths in a number of places with white Flexes on which students and teachers can put up post-it notes, as well as write anonymously something related to mental wellbeing and put the papers in a bottle kept in various places. We will also put up three posters (flexes) connected with mental health awareness. Could you kindly allow us to do these activities on October 10th, the World Mental Health Day?

Thanking you,

Sincerely,

Emmanuel Arockiam, S.J., Ph.D


PG Dept. of Counselling Psychology &
Counselling Centre
St. Joseph's College (Autonomous), Trichy - 02
The Importance of
Mental Health
AWARENESS
It is vital for emotional, psychological and social well-being, and necessary for a healthy and satisfying life.
TAKE CARE OF YOUR MENTAL HEALTH
Your mental health is our priority
WE ARE HERE TO
HELP
The theme for World Mental Health Day 2023 is
'Mental health is a universal human right'.
CONTACT US
9444903613
GPS MAP CAMERA
Dept. of Counselling Psychology & Counselling Centre, St. Joseph's
Latitude: 10.8284625
Longitude: 78.6904613
Date: 12 Oct 2023
Time: 11:37 AM
Google


PG Department of Counselling Psychology & Counselling Centre
St. Joseph's College (Autonomous), Tiruchirappalli - 02
October
Mental Health Awareness Month
Mental health
St. Joseph's College (Autonomous)
Trichy - 620002
PG Department of Counselling Psychology
celebrates
"World Mental Health Day" - 10th Oct 2023.
GPS Map Camera
Tiruchirappalli,TN,India
Uraiyoor, Tiruchirappalli, 620002, TN, India
Lat 10.828602, Long 78.690701
10/10/2023 11:11 AM GMT+05:30
Note : Captured by GPS Map Camera
Maps

PG Dept. of Counselling Psychology & Counselling Centre

St. Joseph's College (Autonomous), Trichy - 02

The Importance of

Mental Health AWARENESS

It is vital for emotional, psychological and social well-being, and necessary for a healthy and satisfying life.

TAKE CARE OF YOUR MENTAL HEALTH

The theme for World Mental Health Day 2023 is

'Mental health is a universal human right'.

Your mental health is our priority

WE ARE HERE TO

HELP

CONTACT US

9444903613

PG Dept. of Counselling Psychology & Counselling Centre

St. Joseph's College (Autonomous), Trichy - 02

Common types of Mental Illness

01. **Anxiety disorders**
include panic disorder, social anxiety disorder, specific phobias.

02. **Mood disorders**
include depression, bipolar disorder, dysthymia, cyclothymic disorder.

03. **Eating disorders**
include anorexia nervosa, bulimia nervosa, binge eating disorder.

04. **Personality disorders (PD)**
include Antisocial PD, Boderline PD, Histrionic PD, Paranoid PD, Narcissistic PD, Avoidant PD, Dependent PD, Obsessive-Compulsive PD.

05. **Psychotic disorders**
including schizophrenia

06 **Post-traumatic stress disorder**

St. Joseph's College (Autonomous)
Tiruchirappalli - 02

PG Department of Counselling Psychology & Counselling Center

Feel better, be better

- Celebrate the counseling profession!
- Mental health is precious.
- Counsellors & psychologists are there to help you.

Counsellor: 9444903613

LEADERS' CHOICE ART WELLNESS TRAINING

13, Arun nagar, Pratiyur post, Trichy -Tamil Nadu- India- 620009.

Contact No: +91 98424 93882 | Email: leaderschoiceartgallery@gmail.com

From
Prof. Hermon Carduz
Director, Leaders' Choice
13, Arun Nagar, Near Dheeran Nagar
Trichy – 620009.

To
Rev. Fr. Emmanuel Arockiam, S.J.,
Head of the Department of Counselling Psychology,
St. Joseph's College
Trichy – 620002.

Reverend Father

Sub: Proposal for the Art Wellness Training workshop – Reg.,

As we discussed on 06 November 2023 regarding the Art and Leadership Training Workshop for the Students Council Members, Class Representatives and the Department of Counselling Psychology. I am writing this training workshop proposal to greatly benefit the students and the college.

Workshop Details:

1. Title : Art Wellness and Leadership Training
2. Dates : 22,23,24 and 27 November 2023
3. Duration : 10:00 AM to 4:30 PM
4. Venue : AV Hall
5. Target Audience : Students Council Members
   Class Representatives
   Department of Counselling Psychology
6. Topics Covered : Neurographic art healing of the Mind
   Teamwork through Painting
   Presentation of Leadership strategies through art
   Power of visualization of goals
   Left/Right Brain Integration
   Reduction of stress and anger
   Enjoyment of colour
   Leadership Art Journaling
   Vision Building through Art

7. Facilitators : Prof. Hermon Carduz
Mr. E. Joseph Antony
Dr. M. Gabriel
Er. Artist. Arun

Engagement Fee:

The estimated cost of this Workshop for **Four Days** is **42,000/-** (Forty Two Thousand Rupees Only). The engagement fee covers the facilitator's fee and transportation charges.

The Leaders' Choice Art Wellness Training programme is the result of 10 years of extensive research with inspirational art and health. It is a non-medical intervention for people in stressful situations, either at work or home, that heals the soul while giving participants a new perspective on life. It is quite different from psycho-metric testing, that creates stereotypes and pigeonholes people to conformist ideology.

Our programme divided into three phases:

Eagle One is designed with Neuro-aesthetics, Neuro-graphic Art and Art therapy activities which help you to realise yourself and to integrate the right/left brain and body.
Eagle Two invokes inspirational leadership strategies through art and team building activities.
Eagle Three is an hour-long meditation on Energy Paintings of India in which the power of visualizing your dreams enhances its realisation.

Just as you don't need to be a musician to enjoy music, you don't need to be an artist to enjoy this workshop.

Thank you for considering our proposal. We look forward to discussing this opportunity with you in more detail. For further details, contact us.

Sincerely,

Prof. Hermon Carduz

PG DEPARTMENT OF COUNSELLING PSYCHOLOGY & WELLBEING
ASSOCIATION OF COUNSELLING PSYCHOLOGY

ST. JOSEPH'S COLLEGE (AUTONOMOUS)

Tiruchirappalli – 620 002

Report on Art Wellness Training Program – One - day Workshop

Place: II M.Sc. Counselling Psychology classroom, St. Joseph's College

Audience: PG students of Counselling Psychology

Date: 27/11/2023

Introduction: PG Department of Counselling Psychology & Counselling Centre collaboratively conducted a one-day workshop on Art Wellness Program.

About the theme: To give an overview of vision building through art and the power of visualization of art in relation to healing of the mind.

Conducted by **REV. Dr. EMMANUEL AROCKIAM SJ,** Asst. Prof, HoD, Counselling Psychology & Library Director, St. Joseph's College (Autonomous), Trichy.

Report:

The session held on November 27, 2023, at St. Joseph's College in the department of counselling psychology was conducted to encourage students in enriching themselves with sufficient knowledge regarding Art Wellness Training Program. There were 38 students participated. The resource person, Prof. Hermon Carduz was warmly welcomed by the efficient professors of Counselling Psychology and was requested to address the students of the first and second -year postgraduate programme on the topic of how art can heal and helps in the reduction of stress and anger. Prof. Hermon Carduz, such an inspiring person, seized the minds of the students with his overwhelming talk about the significance of art and the power of visualization. He spoke about the leadership strategies through art and how neurography art served as a healing to man distressed minds. A brief explanation on Masaru Emoto experiment on frozen water samples to see if any water crystals would be visible and the power of words that have destruction or formation regarding the negative or positive connotation attached to the word. This created awareness on how one's emotions and words affect their mood and life

conditions. The integration of left and right brain featured the need to activate the brain function through brainstorming activities, exercises and practice of reward system that function as a strong indication to the brain to work towards success. The mindfulness practice and focusing the breath by illustrating its rhythm on a paper helped to obtain a sense of calmness in mind. Involving students in art coloring provided stress-free and gain a balance in emotion.

Conclusion:

The students are well-resourced to thrive with the knowledge and experiences shared by Prof. Hermon Carduz. The overall session imbibed a keen understanding of the art and the importance of mindfulness in everyday life. It is very evident that the art has a significant effort in treating the distressed mind and generate positive attitude.

Dr. EMMANUEL AROCKIAM, S.J., Ph.D.
DIRECTOR - DEPT OF COUNSELLING PSYCHOLOGY
ST. JOSEPH'S COLLEGE (AUTONOMOUS)
TRICHY-620 002

PG Dept. of Counselling Psychology
ST. JOSEPH'S COLLEGE (AUTONOMOUS)
Accredited at A++ Grade (4th Cycle) by NAAC
Special Heritage Status awarded by UGC
TIRUCHIRAPPALLI - 620 002, S. INDIA
www.sjctni.edu Dept.: counpsychsjc@gmail.com
+91 94449 03613 emma.aro@gmail.com

Dr. Emmanuel Arockiam, S.J., Ph.D.
Director

Art Wellness & Leadership Training

II M.Sc. Counselling Psychology

22PCP801	Rojimol
22PCP802	Bhuvaneswari
22PCP803	Macrina
22PCP804	Annie Celes
22PCP805	Christy
22PCP806	Ancy
22PCP807	Sarabeshwaraa
22PCP809	Ramya
22PCP810	Laly Chrower
22PCP812	Nandhana
22PCP813	Darwin
22PCP814	Sajeetha
22PCP815	Buvitha
22PCP816	Sathya
22PCP818	Marjiya
22PCP819	Sindhuja
22PCP820	Shobiha
22PCP823	Nirmala · B
22PCP824	Romimol
22PCP826	Shajitha Banu
22PCP828	Nirmala · M
22PCP829	Sasikala
22PCP830	Neha
22PCP837	Raslin
22PCP841	Felishia Ruth

I M.Sc. Counselling Psychology

23PCP801	Manikandan
23PCP802	Kia Graja Priya
23PCP805	Kezia Jakulin
23PCP806	Shama Pearlin
23PCP807	Jeffrin Seba
23PCP808	Nasreen Banu
23PCP809	Shamili
23PCP810	Deborah
23PCP811	Amala Anton
23PCP812	Praveen
23PCP813	Deepika
23PCP814	Varshini
23PCP815	Shanice .

Rev. Dr. Emmanuel Arockiam SJ, Ph.D
Director
Department of Counselling Psychology
St. Joseph's College, Tiruchirappalli-2.


LEADERS' CHOICE
Speaking heart with the art
Art exhibition on colours of life to rejuvenate residents
GPS MAP CAMERA
DEPT OF Counselling Psychology, St. Joseph's College, Tamil Nadu India
Latitude: 10.828479
Longitude: 78.6904903
Date: 27 Nov 2023
Time: 10:48 AM
Google


GPS MAP CAMERA
DEPT OF Counselling Psychology, St. Joseph's College, Tamil Nadu India
Latitude: 10.828479
Longitude: 78.6904903
Date: 27 Nov 2023
Time: 10:46 AM
Google


LEADERS' CHOICE
GPS MAP CAMERA
DEPT OF Counselling Psychology, St. Joseph's College, Tamil Nadu India
Latitude: 10.828479
Longitude: 78.6904903
Date: 27 Nov 2023
Time: 10:51 AM


Speaking heart with the art
GPS MAP CAMERA
DEPT OF Counselling Psychology, St. Joseph's College, Tamil Nadu India
Latitude: 10.828479
Longitude: 78.6904903
Date: 27 Nov 2023
Time: 10:46 AM
Google


GPS MAP CAMERA
DEPT OF Counselling Psychology, St. Joseph's College, Tamil Nadu India
Latitude: 10.828479
Longitude: 78.6904903
Date: 27 Nov 2023
Time: 03:51 PM


Freeze
GPS MAP CAMERA
DEPT OF Counselling Psychology, St. Joseph's College, Tamil Nadu India
Latitude: 10.828479
Longitude: 78.6904903
Date: 27 Nov 2023
Time: 03:51 PM
Google


Freeze
GPS MAP CAMERA
DEPT OF Counselling Psychology, St. Joseph's College, Tamil Nadu India
Latitude: 10.828479
Longitude: 78.6904903
Date: 27 Nov 2023
Time: 04:51 PM
Google


GPS MAP CAMERA
DEPT OF Counselling Psychology, St. Joseph's College, Tamil Nadu India
Latitude: 10.828479
Longitude: 78.6904903
Date: 27 Nov 2023
Time: 03:51 PM
Google

Gmail **Ravindran D <ravindran.da@gmail.com>**

ISCA collaboration for ICIDT-January, 2024

3 messages

Ravindran D <ravindran.da@gmail.com> Fri, Dec 22, 2023 at 2:56 PM
To: Kasmir Raja <svkr157@gmail.com>

Dear Sir,

Wishes from Ravindran.

I am forwarding the letter of request for financial assistance from ISCA for the conduct of the International Conference ICIDT - 2024 at St Joseph's College, Tiruchirappalli

We will meet in Chennai on the evening of 29th Dec 2023, during our visit regarding D S Ravi's 60th-year function. (to be held on 30th)

Thanking you,

with regards,

D Ravindran
Associate Professor in Computer Science,
St Joseph's College,
Tiruchirappalli

Sponsorship Request Letter to ISCA.docx
21K

Kasmir Raja <svkr157@gmail.com> Sat, Dec 23, 2023 at 12:48 PM
To: Ravindran D <ravindran.da@gmail.com>

Dear Dr.Ravindran,
Thank you for your mail.
Hope that the arrangements for the International Conference are going on in full swing.
I will transfer the money on Tuesday or Wednesday next week.
Kindly send the final brochure of the conference to me and also to Dr.Albert, HoD, MCA, SRM.
I wish you all the very best for the success of the conference.
With kind regards
Dr.S.V.Kasmir Raja
[Quoted text hidden]

Ravindran D <ravindran.da@gmail.com> Mon, Feb 12, 2024 at 2:47 PM
To: maheswaran k <mahes161@gmail.com>

[Quoted text hidden]

Sponsorship Request Letter to ISCA.docx
21K

IECD : An institution with HAT-TRICK World Records

0431 - 2332638
2331636
info@iecd.in
www.iecd.in

Prof. E. Ramganesh
M.Sc., PGDCA., Ph.D (CSC).,
M.A. (Psy), M.A. (Phil), M.Ed., M.Phil.,Ph.D (Edn.)
Senior Professor
Dean, Faculty of Arts
Director

IECD
INSTITUTE FOR ENTREPRENEURSHIP AND CAREER DEVELOPMENT
BHARATHIDASAN UNIVERSITY
(Re-Accredited by NAAC with 'A+' Grade in the Third Cycle)
Khajamalai Campus,Tiruchirappalli - 620 023, Tamil Nadu, India

Ref: 2024/051/23.02.2024

To
Rev. Fr. Principal
St. Joseph's College (Autonomous),
Tiruchirappalli - 620 002.

Rev. Father,

Greetings! Let me once again thank you profusely to have helped us in permitting your M.C.A students to serve as Examiner for practical exams of SUITS programme-2023 last year. May I request you to kindly permit 26 of your students of MCA programme to serve as examiner for SUITS programme-2024 from 26.02.2024 to 29.02.2024.

I thank you for your co-operation.

23/2/24

Prof. E. Ramganesh,
Director, IECD

SACRED HEART COLLEGE (AUTONOMOUS)

Accredited by NAAC(4th cycle) with CGPA of 3.31/4 at 'A+ 'Grade
Ranked as 42 college among the colleges of india in NIRF 2023
TIRUPATTUR-635601,TIRUPATTUR DISTRICT,TAMIL NADU,INDIA

PG Department of Computer Science

GitHub

Workshop on

Version Control System Git and GitHub

Resource Person

Prasanth Rao
Python Developer
Cogno AI | Exotel
Bangalore

Date: 07/09/2023
Time: 9.30am to 3.30pm

Venue:Loius Mathias Hall
(John Med Block)

COLLABORATION WITH

Xavier Board of Higher Education in India

ST.JOSEPH'S COLLEGE (Autonomous) Tiruchirappalli,India
Since 1844

AUXILIUM COLLEGE (Autonomous) - NAAC A+ CGPA - 3.55
VELLORE - INDIA

GONZAGA COLLEGE OF ARTS AND SCIENCE FOR WOMEN
Affiliated to Periyar University, Salem
Accredited by NAAC with 'B' Grade

SACRED HEART COLLEGE
(AUTONOMOUS)

Accredited By NAAC (4th Cycle - under RAF) with CGPA of 3.31/4 at 'A+' Grade
42nd Ranked College in India - NIRF 2023

DEPARTMENT OF COMPUTER SCIENCE (SHIFT-II)

ORGANIZES

NATIONAL WORKSHOP ON

MACHINE LEARNING

FOR

DATA SCIENCE

Resource Person

DR.SIVA KUMAR N

M.TECH,PH.D

PROFESSOR IN CSE,
PUDUCHERRY TECHNOLOGICAL UNIVERSITY

FOUNDER&DIRECTOR
TECHMYTHS SOLUTION PVT.LTD

27 NOV 2023 | **9.30 AM** | **KAMARAJAR ARANGAM**

Convener
Mrs.C.Dharma Devi (HOD)

Co-Convener
Mrs.A.Logeshwari

Organizing Secretory
Dr.P.Selva Perumal

Organizing Team
Mr.D.Vigneshwaran
Mrs.R.Ramya

COLLABORATION WITH

GONZAGA COLLEGE OF ARTS AND SCIENCE FOR WOMEN

AUXILIUM COLLEGE (Autonomous) - NAAC 'A' CGPA - 3.55 VELLORE - INDIA

Xavier Board of Higher Education in India

WEBMAIL

Ms. Mary Magdalene. A <marymagdalene_cr2@mail.sjctni.edu>

Request for 4 - Day Placement Training Programme

Alexander Pravindurai <pravindurai@gmail.com> Tue, Aug 1, 2023 at 8:38 PM
To: Aravind ISDC <aravind.cr@isdcglobal.org.uk>, "Mr. J.Camilton" <camilton_co2@mail.sjctni.edu>, "Ms. Mary Magdalene. A" <marymagdalene_cr2@mail.sjctni.edu>, prabakaran_cr2@mail.sjctni.edu, BCom Honours <b.comhonours@mail.sjctni.edu>

Dear Mr. Aravind

Greetings!

The Honours department is planning to organise a 4-Day Placement Training Programme for the final Year students of B.Com Honours similar to the one which was organised by ISDC last year. We would like to have this placement training programme in the last week of August (Starting From 28th August 2023). Please check on this request and let us know about Mr. Hadrine's availability ASAP so that we can make the necessary arrangements. Prof. Camilton will connect with Mr. Hadrine for this programme. You ensure everything goes well from your end.
thank you
Regards

Dr. F. R. Alexander Pravin Durai
Associate Professor and Head
PG and Research Department of Commerce and Honours ACCA
St. Joseph's College (Autonomous)
Special Heritage status College with NAAC A++
Tiruchirappalli - 620 002

WEBMAIL

Ms. Mary Magdalene. A <marymagdalene_cr2@mail.sjctni.edu>

Re: Requesting for Arrangements to be done for Placement Training from 28-Aug-2023 till 31-Aug-2023

Mr. J.Camilton <camilton_co2@mail.sjctni.edu> Wed, Aug 16, 2023 at 12:17 PM
To: Syed Ismail <syed.ismail@isdcglobal.org>
Cc: Aravind ISDC <aravind.cr@isdcglobal.org.uk>, Hadrine H Pereira <hadrine.pereira@isdcglobal.org>, Rajesh Reddy Joseph <rajeshreddy.joseph@isdcglobal.org>, Shone Babu <shone.babu@isdcglobal.org>, Alexander Pravindurai <pravindurai@gmail.com>, BCom Honours <b.comhonours@mail.sjctni.edu>, "Mr. G.PRABAKARAN" <prabakaran_cr2@mail.sjctni.edu>, "Ms. Mary Magdalene. A" <marymagdalene_cr2@mail.sjctni.edu>

Dear Mr.Syed,

Noted. Thanks for your email. Please find attached the Student details of 2021 Batch III B.Com Honours students.

Please feel free to contact me for any further information.

Regards,
Mr.Camilton J,
Assistant Professor & Coordinator,
Department of Commerce Honours,
St.Joseph's College(Autonomous),Tiruchirappalli,Tamil Nadu.
Mob: 9942462632

On Wed, Aug 16, 2023 at 9:41 AM Syed Ismail <syed.ismail@isdcglobal.org> wrote:

> Dear Prof.Camilton Sir,
>
> Greetings from ISDC Global.
>
> Hope you are doing well and safe,It was pleasure talking to you as discussed please find below arrangements required for placement training from 28-Aug-2023 till 31-Aug-2023.
>
> 1. Students List (Required in Advance)
> 2. 3 Cordless Mic
> 3. Projector with Speakers
> 4. 2/3 conference room
> 5. 2-3 Markers
> 6. Good and Stable Internet Connections.
> 7. 3 room for Mock Interviews on 31-Aug-2023.
>
> Appreciate if you could kindly assist us in this regard.
>
> Thanks & Regards
> **Syed Ismail Zabiulla**
> **Assistant Manager-Corporate Relations & Placements**
>
> ISDC International Skill Development Corporation
> Skills for Tomorrow
> www.isdcglobal.org
>
> Global Head Quarters
> The Old Court House
> Hughenden Road
> Buckinghamshire, HP13 5DT
> United Kingdom, Tel : +44 20 376 33333
>
> Regional Office: India
> 10/1, 4th Floor, Lakshmi Narayan Complex
> Palace Road, Vasanth Nagar
> Bengaluru - 560052, Karnataka
> India, Tel : +91 80 4645 8899
>
> Official Education Partner
> 21ST WORLD CONGRESS OF ACCOUNTANTS 2022 18-21 NOVEMBER MUMBAI INDIA
> BUILDING TRUST ENABLING SUSTAINABILITY
>
> Mobile no.+91-8073469616
> linkedin.com/in/ismailzabi007

St.Joseph's College (Trichy) - 2021 Batch Students Data.xlsx
17K

தமிழாய்வுத்துறை

தூய வளனார் கல்லூரி (தன்னாட்சி)

திருச்சிராப்பள்ளி- 02

ஆசா அறக்கட்டளை
சிறப்புச் சொற்பொழிவு & பரிசளிப்பு விழா

26.02.2024, திங்கட்கிழமை, காலை 10.30 மணி

நிகழிடம் : நூலக அரங்கம் (SAIL AUDITORIUM)

வரவேற்புரை : முனைவர் ரெ. நல்லமுத்து
உதவிப்பேராசிரியர்

தலைமை : அருள்முனைவர் ம.ஆரோக்கியசாமி சேவியர் சே.ச.
கல்லூரி முதல்வர்

முன்னிலை : ஆ.கேத்ரின் ஆரோக்கியசாமி
எழுத்தாளர், திருச்சி எழுத்தாளர் சங்கம்.

முனைவர் ஞா.பெஸ்கி
துறைத்தலைவர்

வாழ்த்துரை : அருள்முனைவர் கு. அமல் சே.ச.
கல்லூரிச் செயலர்

சிறப்புரை : பாவலர் அறிவுமதி

பொருண்மை : தமிழும் வீரமாமுனிவரும்

நன்றியுரை : திருமிகு இ.யோகராஜ்
உதவிப்பேராசிரியர்

நிகழ்ச்சி நெறியாளுகை : முனைவர் இரா. முரளி கிருட்டினன்
உதவிப்பேராசிரியர்

அழைப்பின் மகிழ்வில்
முதல்வர் மற்றும் தமிழாய்வுத்துறையினர்

Dr. G. BESCHI
Associate Professor & Head
Department of Tamil
St. Joseph's College (Autonomous)
Tiruchirappalli-620 002.

தமிழாய்வுத்துறை

தூய வளனார் கல்லூரி (தன்னாட்சி)

A++தரத்தகுதியும்செயல்திறன்ஆற்றல்வளத்தனித்தகுதியும்
சிறப்புத்தொன்மைத்தகுதியும்பெற்றது)

திருச்சிராப்பள்ளி – 620 002

அறிக்கை

ஆசா அறக்கட்டளை - சிறப்புச் சொற்பொழிவு *(26.02.2024)*

2024 பிப்ரவரி *09* அன்று தமிழாய்வுத்துறையில் ஆசா அறக்கட்டளை சிறப்புச் சொற்பொழிவு மற்றும் பரிசளிப்பு விழா நடைபெற்றது. அறக்கட்டளை பொறுப்பாளரும் தமிழாய்வுத்துறை உதவிப்பேராசிரியருமான முனைவர் ரெ.நல்லமுத்து வரவேற்புரையாற்றினார். கல்லூரி முதல்வர் அருள்முனைவர் ம. ஆரோக்கியசாமி சேவியர் சே.ச. தலைமை தாங்கி உரையாற்றினார். தமிழாய்வுத்துறைத் தலைவர் முனைவர் ஞா. பெஸ்கி முன்னிலை வகித்தார். கல்லூரிச் செயலர் அருள்முனைவர் கு.அமல், சே..ச. அவர்கள் வாழ்த்துரையாற்றினார். தமிழாய்வுத்துறைத் தலைவர் முனைவர் ஞா. பெஸ்கி திருச்சி எழுத்தாளரும், அறக்கட்டளை நிறுவுநருமான திருமதி கேத்தரீன் ஆரோக்கியசாமி ஆகிய இருவரும் முன்னிலை வகித்தனர். தமிழும் வீரமாமுனிவரும் என்கிற பொருண்மையில் திரைப்பட பாடலாசிரியர் பாவலர் அறிவுமதி சொற்பொழிவாற்றினார். திரைப்பட இயக்குநர் பிருந்தாசாரதி வாழ்த்துரை வழங்கினார். தமிழாய்வுத்துறை உதவிப்பேராசிரியர் இ.யோகராஜ் நன்றியுரையாற்றினார். நிகழ்ச்சிகளை முனைவர் பட்ட ஆய்வாளர் கி.ஜோஸ் ஆல்வின் தொகுத்து வழங்கினார் . பிப்ரவரி *06* ஆம் நடைபெற்ற கட்டுரை, கவிதை, வினாடி வினா மற்றும் பேச்சுப் போட்டிகளில் போட்டிகளில் *18* கல்லுரிகளிலிருந்து மாணவர்கள் பங்கேற்றிருந்தனர். போட்டிகளில் வென்ற மாணவர்களுக்கு பரிசுகள் வழங்கப்பட்டன. இவ்விழாவில் தமிழ் ஆர்வலர்கள், பேராசிரியர்கள், முனைவர் பட்ட ஆய்வாளர்கள், இளநிலை வகுப்புகள் மாணவர்கள் பங்கேற்று சிறப்பித்தனர்.

Dr. G. BESCHI
Associate Professor & Head
Department of Tamil
St. Joseph's College (Autonomous)
Tiruchirappalli-620 002.

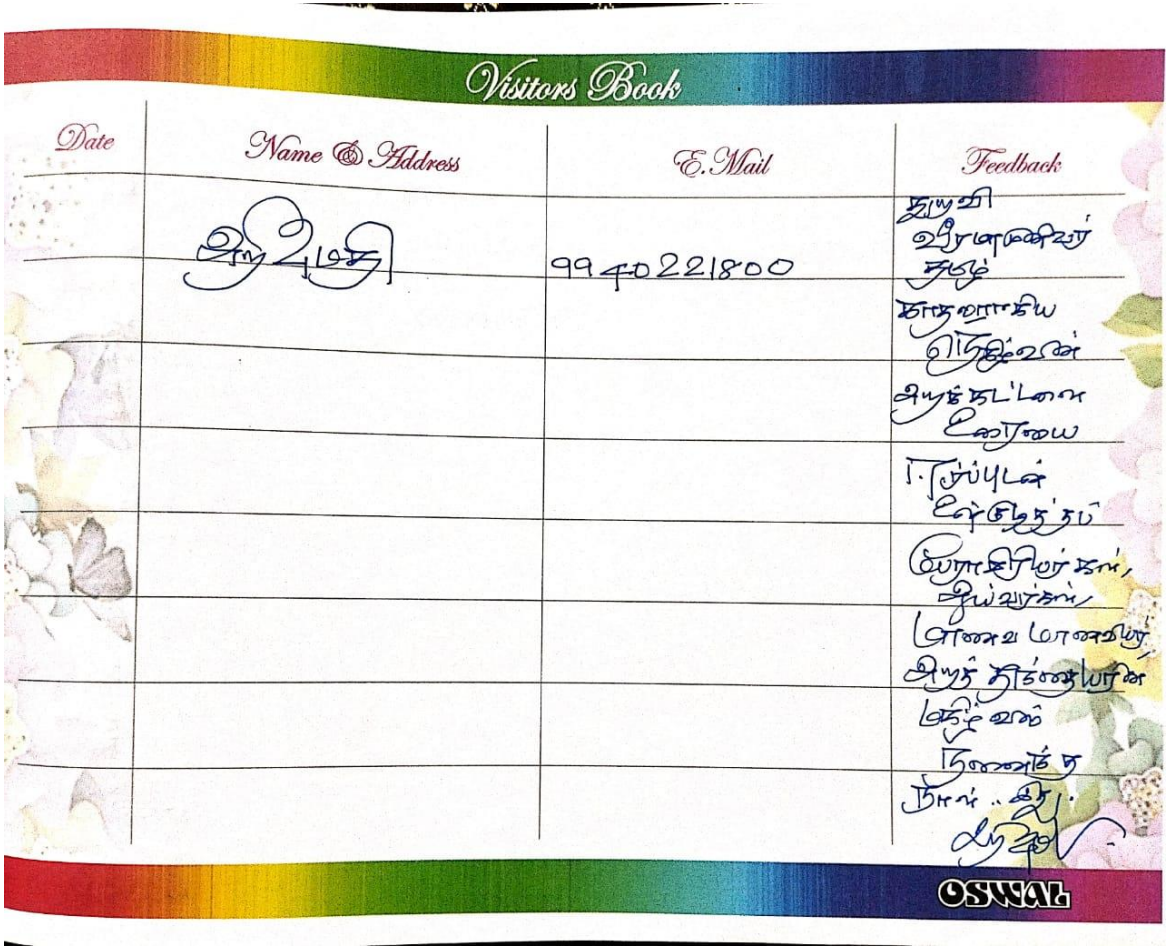

Dr. G. BESCHI
Associate Professor & Head
Department of Tamil
St. Joseph's College (Autonomous)
Tiruchirappalli-620 002.

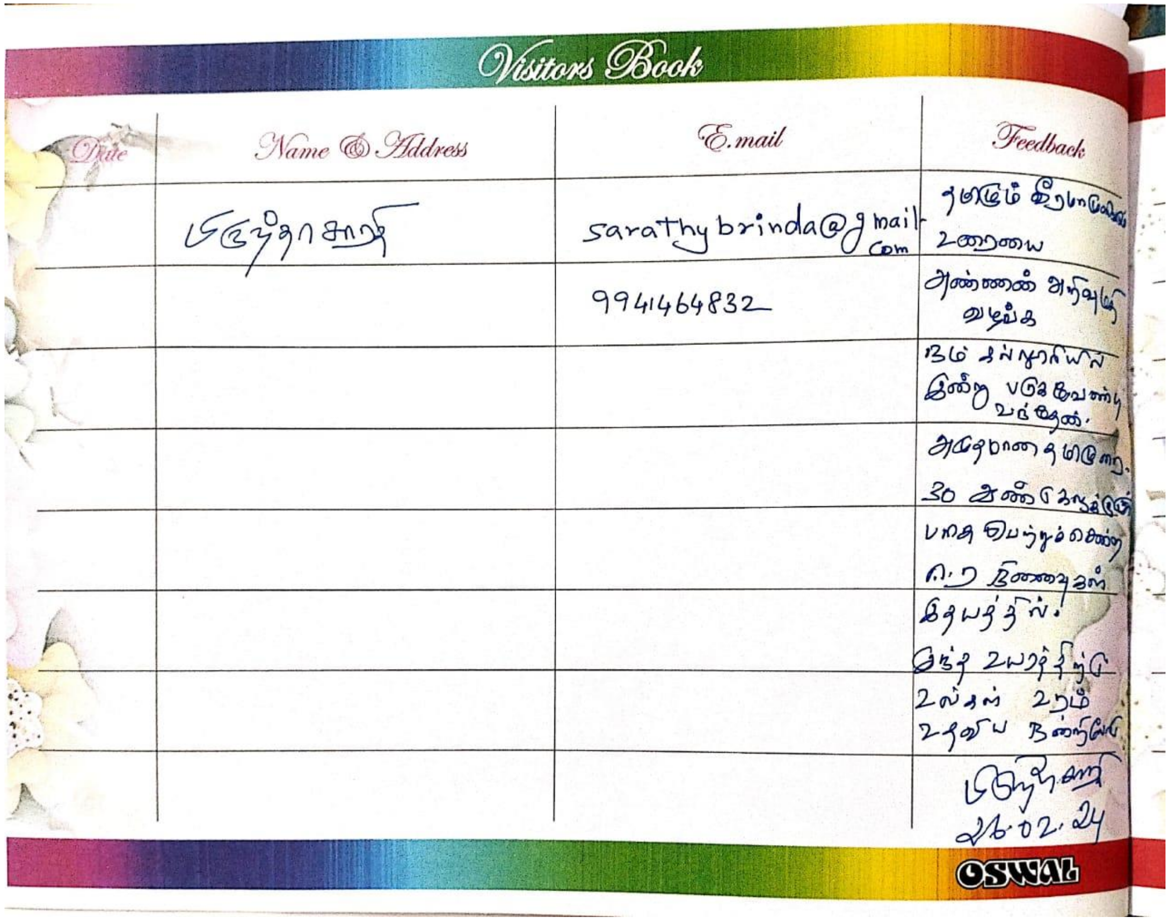

Visitors Book

Date	Name & Address	E.mail	Feedback
	பிருந்தா சாரதி	sarathybrinda@gmail.com	[illegible]
		9941464832	[illegible]
			[illegible]
			[illegible]
			[illegible]
			[illegible]
			[illegible]
			பிருந்தா சாரதி 26.02.24

OSWAL

Dr. G. BESCHI
Associate Professor & Head
Department of Tamil
St. Joseph's College (Autonomous)
Tiruchirappalli-620 002.

Dr. G. BESCHI
Associate Professor & Head
Department of Tamil
St. Joseph's College (Autonomous)
Tiruchirappalli-620 002.

Dr. G. BESCHI
Associate Professor & Head
Department of Tamil
St. Joseph's College (Autonomous)
Tiruchirappalli-620 002.

ஊடகப் பதிவு

திருச்சி செயின்ட் ஜோசப் கல்லூரியில் ஆசா அறக்கட்டளை சிறப்புச் சொற்பொழிவு

திருச்சி, மார்ச் 6-

திருச்சி செயின்ட் ஜோசப் கல்லூரித் தமிழாய்வுத்துறையில் ஆசா அறக்கட்டளை சிறப்புச் சொற்பொழிவு மற்றும் பரிசளிப்பு விழா நிகழ்ச்சி நடைபெற்றது.

அறக்கட்டளை பொறுப்பாளரும், தமிழாய்வுத்துறை உதவிப்பேராசிரியருமான முனைவர் ரெ.நல்லமுத்து வரவேற்புரையாற்றினார். கல்லூரி முதல்வர் அருள்முனைவர் ம.ஆரோக்கியசாமி சேவியர் சே.ச. தலைமை தாங்கி உரையாற்றினார். தமிழாய்வுத்துறைத் தலைவர் முனைவர் ஞா. பெஸ்கி முன்னிலை வகித்தார். கல்லூரிச் செயலர் அருள்முனைவர் கு.அமல், சே..ச. வாழ்த்துரையாற்றினார்.

தமிழாய்வுத்துறைத் தலைவர் முனைவர் ஞா. பெஸ்கி திருச்சி எழுத்தாளரும், அறக்கட்டளையின் நிறுவனருமான கேத்தரீன் ஆரோக்கியசாமி ஆகிய இருவரும் முன்னிலை வகித்தனர். தமிழும் வீரமாமுனிவரும் என்கிற பொருண்மையில் திரைப்பட பாடலாசிரியர் பாவலர் அறிவுமதி சொற்பொழிவாற்றினார். திரைப்பட இயக்குநர் பிருந்தாசாரதி வாழ்த்துரை வழங்கினார். நிகழ்ச்சிகளை முனைவர் பட்ட ஆய்வாளர் கி.ஜோஸ் ஆல்வின் தொகுத்து வழங்கினார். பிப்ரவரி 06 ஆம் நடைபெற்ற கட்டுரை, கவிதை, வினாடி – வினா மற்றும் பேச்சுப் போட்டிகளில் போட்டிகளில் 18 கல்லூரிகளிலிருந்து மாணவர்கள் பங்கேற்றிருந்தனர். போட்டிகளில் வென்ற மாணவர்களுக்கு பரிசுகள் வழங்கப்பட்டன.

இவ்விழாவில் தமிழ் ஆர்வலர்கள், பேராசிரியர்கள், முனைவர் பட்ட ஆய்வாளர்கள், இளநிலை வகுப்புகள் மாணவர்கள் பங்கேற்று சிறப்பித்தனர். தமிழாய்வுத்துறை உதவிப்பேராசிரியர் இ.யோகராஜ் நன்றியுரையாற்றினார்.

தினதொடர், சென்னை 06.03.2024

Dr. G. BESCHI
Associate Professor & Head
Department of Tamil
St. Joseph's College (Autonomous)
Tiruchirappalli-620 002.

தமிழாய்வுத்துறை

தூய வளனார் தன்னாட்சிக் கல்லூரி

(A++ தரத்தகுதியும் செயல்திறன் ஆற்றல் வளத் தனித்தகுதியும்
சிறப்புத் தொன்மைத் தகுதியும் பெற்றது)

திருச்சிராப்பள்ளி - 620 002

தேசியக் கருத்தரங்கம்

தமிழ் இலக்கியத்தில் மேலாண்மை

(Managerial Skills in Tamil literature)

நாள் : 21-02-2024

~~முனைவர்~~ / திருமிகு. தா. மேரிமார்டீனா அவர்கள்

21-02-2024 அன்று திருச்சிராப்பள்ளி தூய வளனார் கல்லூரி தமிழாய்வுத்துறையில் நடைபெற்ற தேசியக் கருத்தரங்கில் பங்கேற்று திருமந்திரத்தில் உடல், உளமேலாண்மை என்னும் தலைப்பில் கட்டுரை வழங்கியதைப் பாராட்டி இச்சான்றிதழ் வழங்கப்படுகின்றது.

This is to Certify that Dr./ Mr./ Ms. .....has participated in the National Seminar on "Managerial Skills in Tamil literature" Organized by the Department of Tamil, St. Joseph's College, Tiruchirappalli on 21st February 2024 and presented a Research paper on .....

முனைவர் கு. அந்தோணி ராஜா
கருத்தரங்கச் செயலர்

முனைவர் ஞா. பெஸ்கி
தமிழாய்வுத்துறைத் தலைவர்

அருள்முனைவர் ம.ஆரோக்கியசாமி சேவியர் சே.ச.
முதல்வர், தூய வளனார் கல்லூரி

Dr. G. BESCHI
Associate Professor & Head
Department of Tamil
St. Joseph's College (Autonomous)
Tiruchirappalli-620 002.

தமிழாய்வுத்துறை

தூய வளனார் கல்லூரி (தன்னாட்சி)
திருச்சிராப்பள்ளி – 620 002

ஆசா அறக்கட்டளை சிறப்புச் சொற்பொழிவு & பரிசளிப்பு விழா

நாள்: 26.02.2024 இடம்: நூலக அரங்கம் (SAIL HALL)

எண்	பெயர்	முகவரி	கையொப்பம்
1.	முனைவர், அ. மரிய தனபால்	உதவிப் பேராசிரியர் தமிழாய்வுத்துறை தூய வளனார் கல்லூரி, திருச்சி – 02.	
2	திரு வ.ம. தனலெட்சுமி	உதவிப் பேராசிரியர், தமிழாய்வுத்துறை, தூய வளனார் கல்லூரி,	
3	ஆ. ஜெயக்கொடிராஜ்	உதவிப் பேராசிரியர், தமிழாய்வுத்துறை, தூய வளனார் கல்லூரி, திருச்சி-02,	

தமிழாய்வுத்துறை

தூய வளனார் கல்லூரி (தன்னாட்சி)
திருச்சிராப்பள்ளி – 620 002

ஆசா அறக்கட்டளை சிறப்புச் சொற்பொழிவு & பரிசளிப்பு விழா

நாள்: 26.02.2024 இடம்: நூலக அரங்கம் (SAIL HALL)

எண்	பெயர்	முகவரி	கையொப்பம்
4	எஸ். ஜெசிலி முனைவர்பட்டஆய்வாளர்	52/2, காந்தி அருகே ஸ்ரீரங்கம் திருச்சி-1	
5	ஆ. இராஜராஜன்	உதவிப் பேராசிரியர் தமிழாய்வுத்துறை தூய வளனார் கல்லூரி திருச்சி	
6	சு. ஜெகிலா பானு	உதவிப் பேராசிரியர் தமிழாய்வுத்துறை	

Dr. G. BESCHI
Associate Professor & Head
Department of Tamil
St. Joseph's College (Autonomous)
Tiruchirappalli-620 002.

தமிழாய்வுத்துறை

தூய வளனார் கல்லூரி (தன்னாட்சி)
திருச்சிராப்பள்ளி – 620 002

ஆசா அறக்கட்டளை சிறப்புச் சொற்பொழிவு & பரிசளிப்பு விழா

நாள்: 26.02.2024 இடம்: நூலக அரங்கம் (SAIL HALL)

எண்	பெயர்	முகவரி	கையொப்பம்
7	முனைவர் கா. [illegible]	உதவிப் பேராசிரியர் தமிழாய்வுத் துறை தூய வளனார் கல்லூரி திருச்சி-2	[illegible]
8	முனைவர் ப. சசிரேகா	உதவிப்பேராசிரியர் தமிழாய்வுத்துறை ~~தூய~~ ~~வ~~ காவேரி மகளிர் கல்லூரி(த) திருச்சி – 620 018	[illegible]
9	கவிஞர். சுமித்ரா தேவி[illegible]	திருச்சி.	M. Smitha

தமிழாய்வுத்துறை

தூய வளனார் கல்லூரி (தன்னாட்சி)
திருச்சிராப்பள்ளி – 620 002

ஆசா அறக்கட்டளை சிறப்புச் சொற்பொழிவு & பரிசளிப்பு விழா

நாள்: 26.02.2024 இடம்: நூலக அரங்கம் (SAIL HALL)

எண்	பெயர்	முகவரி	கையொப்பம்
10	இ. அன்னமேரி ([illegible])	8/27 A மெயின்ரோடு [illegible]. [illegible], அரியலூர் 621722. 9443106828	[illegible]
11	ஜ. யோசுராஜ்	உதவிப்பேராசிரியர் தமிழாய்வுத்துறை தூய வளனார் கல்லூரி திருச்சிராப்பள்ளி -02	[illegible]
12	முனைவர். அ. ஜெய[illegible]	இணைப் பேராசிரியர் தமிழாய்வுத்துறை தூய வளனார் கல்லூரி திருச்சிராப்பள்ளி -02	[illegible]

Dr. G. BESCHI
Associate Professor & Head
Department of Tamil
St. Joseph's College (Autonomous)
Tiruchirappalli-620 002.

ஆசா அறக்கட்டளைச் சிறப்பு சொற்பொழிவு & பரிசளிப்பு விழா - 26.02.2024

எண்	பெயர்	வகுப்பு	துறை எண்	கையொப்பம்
13	ஜா. மேரி வலாண்டினா	இளங்கலை தமிழ் மூன்றாம் ஆண்டு	23UTA116	J. Mary Valantina
14	ப. அனி ரெக்ஸிலட்டா	இளங்கலை தமிழ் மூன்றாம் ஆண்டு	23UTA106	B. Anie Rexilta
15	அ. சங்கவி	இளங்கலை தமிழ் மூன்றாம் ஆண்டு	23UTA138	A. Sangavi
16	ஜா. அஸ்வினி	இளங்கலை தமிழ் மூன்றாம் ஆண்டு	23UTA165	J. Aswini
17	ரெ. வர்ஷினி	இளங்கலை தமிழ் மூன்றாம் ஆண்டு	23UTA126	R. varthini
18	ரா. ஜெயந்தன்	இளங்கலை தமிழ் மூன்றாம் ஆண்டு	23UMA104	R. Jay
19	ஆ. மலைவன் பிரிட்டோ	இளங்கலை கணிதம் மூன்றாம் ஆண்டு	23UMA121	A. Malaivan Britto
20	ச. ரூபன்	இளங்கலை கணிதம் மூன்றாம் ஆண்டு	23UMA107	S. Ruban

ஆசா அறக்கட்டளைச் சிறப்பு சொற்பொழிவு & பரிசளிப்பு விழா - 26.02.2024

எண்	பெயர்	வகுப்பு	துறை எண்	கையொப்பம்
21	B. Robin Niranjan	I. BA. History	23UHS134 History	B Robin
22	K Thanu	I. BA. History	23UHS142	K
23	F. Vincent Raj	I. BA, History	23UHS112	F. Vincent Raj
24	C. Sarma andrews	I. BA. history	23UHS113	C. Sarma Andrews
25	J. Kevin Joseph Raj	I. BA. History	23UHS104	J. Kevin
26	R. Bharathi	I. BA. history	23 UHS 125	R. Bharathi
27	S. Arul vishva	I BA history	23UHS102	S. Arul
28	James Baku. K.	I BA. History	23UHS103	James Baku. K.

Dr. G. BESCHI
Associate Professor & Head
Department of Tamil
St. Joseph's College (Autonomous)
Tiruchirappalli-620 002.

தமிழாய்வுத்துறை

தூய வளனார் கல்லூரி (தன்னாட்சி)
திருச்சிராப்பள்ளி – 620 002

ஆசா அறக்கட்டளை சிறப்புச் சொற்பொழிவு & பரிசளிப்பு விழா

நாள்: 26.02.2024 இடம்: நூலக அரங்கம் (SAIL HALL)

எண்	பெயர்	வகுப்பு	துறை எண்	கையொப்பம்
29	சு. வர்ஷா	B.A. தமிழ் முதலாமாண்டு	23UTA121	DED.
30	வெ. கோமிகா	B.A தமிழ் இளங்கலை முதலாம் ஆண்டு	23UTA122	V. [signature]
31	பெ. கலைச்செல்வி	இளங்கலைத் தமிழ் முதலாம் ஆண்டு	23UTA110	[signature]
32	பெ. சந்தியா	இளங்கலைத் தமிழ் முதலாம் ஆண்டு	23UTA139	P. Santhiya
33	ரா. அகல்யா	இளங்கலைத் தமிழ் முதலாம் ஆண்டு	23UTA137	R. Agalya

ஆசா அறக்கட்டளைச் சிறப்பு சொற்பொழிவு & பரிசளிப்பு விழா - 26.02.2024

எண்	பெயர்	வகுப்பு	துறை எண்	கையொப்பம்
34	ம. சுதர்சன்	II. BA Tamil	22UTA155	M. Sudharsan
35	சு. பாலமுருகன்	II. B.A. Tamil	22UTA151	Balamurugan.
36	பா. பிரவீன்குமார்	II BA Tamil	22UTA158	[signature]
37	ஜே. நிஷாந்த்	III. BA. Tamil	21UTA172	[signature]
38	செ. மணிராஜ்	III. B.A. Tamil	21UTA149	[signature]
39	சி. இளங்கீர்த்தி	III B.A. Tamil	21UTA135	S. [signature]
40	அ. ஹரிசுப்பிரமணி	III BA. Tamil	21UTA147	A. Hari [signature]
41	சு. ஹைபிக்சா யா	II BA. Tamil	22UTA178	S. [signature]

[signature]

Dr. G. BESCHI
Associate Professor & Head
Department of Tamil
St. Joseph's College (Autonomous)
Tiruchirappalli-620 002.

ஆசா அறக்கட்டளைச் சிறப்பு சொற்பொழிவு & பரிசளிப்பு விழா - 26.02.2024

எண்	பெயர்	வகுப்பு	துறை எண்	கையொப்பம்
42	மா.திருஷ்ணா காந்த்	அறிவியல்துறை I-BSC Physics	23UPH112	
43	[illegible]	I st Bsc Physics	23UPH126	
44	ச.சஞ்சய் ஹரிஸ்	I st Bsc physics	23UPH127	S.Sanjay Harish
45	ஆ.திரய ஜோயல்	இயற்பியல் முதல் வருடம்	23UPH128	
46	ச.ஜீஸஸ் ராஜா	I st BSC physics	23UPH145	S.Jesus Raja
47	ந.மோனிஷ் குமார்	I st B.Sc Mathematics	23UMA237	
48	ர.பிரகாஷ்	I st B.Sc Mathematics	23UMA222	R. Prakash
49	ச.வெங்கடேஷ்	I st B.Sc Mathematics	23UMA230	S.Venkatesh

ஆசா அறக்கட்டளைச் சிறப்பு சொற்பொழிவு & பரிசளிப்பு விழா - 26.02.2024

எண்	பெயர்	வகுப்பு	துறை எண்	கையொப்பம்
50	செ.மகிதாஷினி	I-BA Tamil	23UTA125	S. Mahidhashini
51	சு.வ.மோனிஷா தெய்வின கிரிஸ்டி	I-BA Tamil	23UTA115	S.V. Monisha
52	க.துர்க நந்தினி	இளங்கலைத் தமிழ் இரண்டாம் ஆண்டு	21UTA111	G. Durga Nandhini
53	னே.தமிழ்செல்வி	இளங்கலைத் தமிழ் முதலாம் ஆண்டு	23 UTA162	G. Tamil Selvi
54	ந.தீபா.	இளங்கலைத் தமிழ் முதலாம் ஆண்டு	23UTA145	Deepa. N
55	சு.ஹரிணி	இளங்கலைத் தமிழ் முதலாம் ஆண்டு	23UTA118	S. Harini
56	சி.ரித்திகா	இளங்கலை தமிழ் முதலாம் ஆண்டு	23UTA112	S. Rithika
57	மு.அபிஷா ரித்திகா	இளங்கலைத் தமிழ் முதலாம் ஆண்டு	23UTA143	M Abisha

Dr. G. BESCHI
Associate Professor & Head
Department of Tamil
St. Joseph's College (Autonomous)
Tiruchirappalli-620 002.

ஆசா அறக்கட்டளைச் சிறப்பு சொற்பொழிவு & பரிசளிப்பு விழா - 26.02.2024

எண்	பெயர்	வகுப்பு	துறை எண்	கையொப்பம்
58	B. Udhaya prakash	I^st B.Sc Physics 'B'	23UPH242	B. Udhaya prakash
59	G. Raja	I^st Bsc physics 'B'	23UPH248	G. Raja
60	Ezhilnilavan K.S.	I^st BSc physics 'B'	23UPH249	Ezhil.
61	Radha Krishnan. K	I^st BSc physics 'B'	23UPH205	K. Radha
62	RUBAN. V	I^st - B.Sc - physics - B'	23UPH244	V. Ruban
63	S. Sterlin Arco	I^st - B.Sc. Physics - 'B'	23UPH227	S. Sterlin Arco
64	F. Prem deerius	I^st BSc physics 'A'	23UPH102	Prem.
65	J. JOEL NELSON	I^st BSc Physics 'B'	23UPH207	J.

ஆசா அறக்கட்டளைச் சிறப்பு சொற்பொழிவு & பரிசளிப்பு விழா - 26.02.2024

எண்	பெயர்	வகுப்பு	துறை எண்	கையொப்பம்
66	J. Cyriaj	B.Sc. Physics 'A'	23UPH119	Cyriaj
67	J. Richard	I - BSc physics - 'A'	23UPH101	J. Richard
68	Dhana Sekaran. M	B.Sc physics - I'B'	23UPH204	Dhana Sekaran
69	SANJAY. V	I - B.SC Physics 'B'	23UPH224	V. Sanjay
70	I. Jones Anto	I - B.Sc. Physics 'A'	23UPH150	I. Jones Anto
71	S. Dinesh Kumar	I B.Sc. Physics 'A'	23UPH142	S. Dinesh Kumar
72	J. Logeshwaran	I - B.Sc. Physics - 'A'	23UPH147	J.
73	A. Hemildan Dheena	I - B.Sc. Physics - 'A'	23UPH144	Hemildan Dheena

Dr. G. BESCHI
Associate Professor & Head
Department of Tamil
St. Joseph's College (Autonomous)
Tiruchirappalli-620 002.

ஆசா அறக்கட்டளைச் சிறப்பு சொற்பொழிவு & பரிசளிப்பு விழா - 26.02.2024

எண்	பெயர்	வகுப்பு	துறை எண்	கையொப்பம்
74	சு.ஹரிபிரசன்ன வைகுண்டேசன்	இளங்கலைத் தமிழ் மூன்றாம் ஆண்டு	21UTA167	S. Hariprasanna Vaikundesan
75	ஆ.ஜஸ்வின் இருதயராஜ்	இளங்கலைத் தமிழ் மூன்றாம் ஆண்டு	21UTA102	A. Jas Iruthayaraj
76	ர.ர. ஆனந்த்	இளங்கலைத் தமிழ் மூன்றாமாண்டு	21UTA129	26/2/24
77	செ.வினோத் குமார்	இளங்கலைத் தமிழ் மூன்றாம் ஆண்டு	21UTA161	26/2/24
78	அ.ஆல்வின் அல்ரான்	இளங்கலைத் தமிழ் இரண்டாம் ஆண்டு	22UTA110	A. Alwin Alran
79	ஜா: ஆல்வின் ரோஜா	இளங்கலைத் தமிழ் இரண்டாம் ஆண்டு	22UTA134	J. Alwin Roja
80	மு.ஸ்ரீ அகமது	இளங்கலைத் தமிழ் இரண்டாமாண்டு	22UTA114	M. Sri Ahamed
81	ம. பரிதிமாறன்	முதலாம் ஆண்டு இளங்கலை தமிழியல்	23UPH120	M Parithimaran

ஆசா அறக்கட்டளைச் சிறப்பு சொற்பொழிவு & பரிசளிப்பு விழா - 26.02.2024

எண்	பெயர்	வகுப்பு	துறை எண்	கையொப்பம்
82	V Kishore Kumar	B.A TAMIL	23UTA114	V. Kishore Kumar
83	A. Mangj kumar	B.A Tamil	23UTA119	A. Mangj kumar
84	A. Santhosh	I. B.A. Tamil	23UTA109	A. Santhosh
85	P. Thillainathan	I B.A Tamil	23UTA130	P. Thillainathan
86	J. Janarthanan	I B.A Tamil	23UTA158	J. Janarthanan
87	J. Anbu Raj.	I. BA Tamil.	23UTA117	J. Anbu Raj.
88	வ. பாலாஜி	I. BA. Tamil.	23UTA105	V. Balaji
89	S. சூரியா	I BA. Tamil	23UTA140	S. Surya
90.	H. மதுமிதா	III BA TAMIL	21UTA107	H. Madhumitha

Dr. G. BESCHI
Associate Professor & Head
Department of Tamil
St. Joseph's College (Autonomous)
Tiruchirappalli-620 002.

ஆசா அறக்கட்டளைச் சிறப்பு சொற்பொழிவு & பரிசளிப்பு விழா - 26.02.2024

எண்	பெயர்	வகுப்பு	துறை எண்	கையொப்பம்
91	K. ஜெனிபர்	I B.A HISTORY	23UHS170	ஜெனிபர் .k
92	M. kalaiselvi	I BA History	23UHS146	M.[illegible]
93	RENI. V	I. BA History	23UHS105	Reni V
94	ஜெ. ரஷ்மி	I. B.A. History	23UHS 136	[illegible]
95	P. Sugeeswari	I. B.A. History	23UHS107	P. Suji
96	S. Suji	I. B.A. History	23UHS145	S. Suji
97	S. Rexli Dona	I. BA. History	23UHS160	[illegible]
98	Melinda	I. BA. History	23UHS 116	Melinda V

ஆசா அறக்கட்டளைச் சிறப்பு சொற்பொழிவு & பரிசளிப்பு விழா - 26.02.2024

எண்	பெயர்	வகுப்பு	துறை எண்	கையொப்பம்
99	பொ. மாதவன்	I B.A. TAMil	23UTA168	P maathavan
100	நா திலீப்	I st B.A. Tamil	23UTA128	N Dilip
101	சு. திவாகரன்	I st B.A. Tamil	23UTA144	S.D
102	ஆ. மரிய ஜெய்சன்	III B.A. TAMIL	21 UTA 126	A
103	பு. நவீன்	III B.A TAMIL	21UTA150	P Nav
104	மு. நாகமுத்து	காலை நேர தமிழ் முதலாம் ஆண்டு	23UTA113	M. Nagamuthu
105	ரா. ரெங்கராஜன்	I BA. Tamil	23UTA124	R. [illegible]
106	வி. ஜார்ஜ்கென்ஸன்	I BA. Tamil	23UTA170	V. Jarkenson

Dr. G. BESCHI
Associate Professor & Head
Department of Tamil
St. Joseph's College (Autonomous)
Tiruchirappalli-620 002.

ஆசா அறக்கட்டளைச் சிறப்பு சொற்பொழிவு & பரிசளிப்பு விழா - 26.02.2024

எண்	பெயர்	வகுப்பு	துறை எண்	கையொப்பம்
107	மு.ராசித் அகமத	இளங்கலை வரலாறு	23UHS154	
108	க.சந்தோஷ்குமார்	இளங்கலை வரலாறு	23UHS149	
109	ர.கோபிநாத்	இளங்கலை வரலாறு	23UHS171	
110	கி.விக்னேஷ்	இளங்கலை வரலாறு	23UHS152	
111	ஜோ.தாமஸ் அல்வா எழில்ன்	இளங்கலை வரலாறு	23UHS108	
112	அ.ஸ்டீபன் பிரைஸ்லி	இளங்கலைத் தமிழ் இரண்டாமாண்டு தமிழ்	22UTA102	
113	ஜா.பிரிஜித்.	இளங்கலைத் தமிழ் இரண்டாம் ஆண்டு	22UTA126	
114	அசேக் முகம்மது அலி	இளங்கலை வரலாறு	23UHS153	

ஆசா அறக்கட்டளைச் சிறப்பு சொற்பொழிவு & பரிசளிப்பு விழா - 26.02.2024

எண்	பெயர்	வகுப்பு	துறை எண்	கையொப்பம்
115	அ. சகுமார் ஜோன்	I BA History	23UHS114	
116	Sam Samuel Ekka	I BA History	23UHS115	
117	ஜேசுதன் தேவியேர் ராஜ்	I BA History	23UHS111	
118	மா.ஜனகேஸ்வரன்	II BA. Tamil	22UTA105	
119	ரெ.ரகுராம்	II B.A Tamil	22UTA138	
120	அ.சகாயஜெரோம்	I B.A History	23UHS126	
121	இ.தீபக்	I BA. History	23UHS127	
122	சி.அருணாச்சலம்	I BA. History	23UHS173	

Dr. G. BESCHI
Associate Professor & Head
Department of Tamil
St. Joseph's College (Autonomous)
Tiruchirappalli-620 002.

ஆசா அறக்கட்டளைச் சிறப்பு சொற்பொழிவு & பரிசளிப்பு விழா - 26.02.2024

எண்	பெயர்	வகுப்பு	துறை எண்	கையொப்பம்
193	C. தண்முகபிரியன்	இளங்கலைத் தமிழ் இரண்டாம் ஆண்டு	22UTA132	C.Shanmugapriyan
194	ப. ரிஜைத்	இளங்கலைத்தமிழ் இரண்டாம் ஆண்டு	22UTA130	
195	கு. திருக்குமரன்	இளங்கலை தமிழ் இரண்டாம் ஆண்டு	22UTA163	G. Thirukumaran
196	ஆ. மார்ஷல்	இளங்கலை தமிழ் இரண்டாம் ஆண்டு	22UTA143	A. Marshal
197	க. சிவா	இளங்கலை தமிழ் இரண்டாம் ஆண்டு	22UTA127	K. Siva
198	ம. மகாலிங்கா	இளங்கலை தமிழ் இரண்டாம் ஆண்டு	22UTA145	M. Mahalinga
199	ச. மோகன்	இளங்கலை தமிழ் இரண்டாம் ஆண்டு	22UTA125	S. Mohan
130	ஜெ. பரதராஜ்	இளங்கலைத் தமிழ் இரண்டாம் ஆண்டு	22UTA140	J. Bharathraj
வி. ஸ்ரீநிவாஸ்.		இளங்கலைத் தமிழ் இரண்டாம் ஆண்டு	22 UTA 128	V. Srinivas

ஆசா அறக்கட்டளைச் சிறப்பு சொற்பொழிவு & பரிசளிப்பு விழா - 26.02.2024

எண்	பெயர்	வகுப்பு	துறை எண்	கையொப்பம்
131	G- Suriya kumar	I. B.Sc physics 'A'	23UPH104	G. Suriya kumar
132	B. Dayanithi	I. B.Sc physics 'A'	23UPH113	B. Dayanithi
133	P. Chandru Raj	I B.Sc Physics 'A'	23UPH105	P. Chandru Raj
134.	M. Saran	I BSC mathematics	23UMA207	M. Saran
135.	S. Bhuvaneshwaran	I BSC Mathematics	23UMA201	
136.	S. Arun Kumar	I. B.SC MATHEMATICS	23UMA202	
137	S. Varun	I- BSC MATHEMATICS	23UMA213	
138	R. subramaniyan	I- B.sc maths	23UMA222	R. subramaniyan

Dr. G. BESCHI
Associate Professor & Head
Department of Tamil
St. Joseph's College (Autonomous)
Tiruchirappalli-620 002.

ஆசா அறக்கட்டளைச் சிறப்பு சொற்பொழிவு & பரிசளிப்பு விழா - 26.02.2024

எண்	பெயர்	வகுப்பு	துறை எண்	கையொப்பம்
139	மோகனப்பிரியன்.இ	I[st] Bsc Maths	23UMA114	
140	சுனைசேகர்.சு	I[st] BSc. Maths.	23UMA108	26/02/24
141	நசீன் கோர்.ச	I[st] BSc -maths	23UMA115	
142	மேனி ஜான்.ரா	I[st] Bsc Maths	23UMA116	
143	ராகவன்.அ	I[st] Bsc maths	23UMA110	
144	ர.ஜீவன்	I[st] BSC., MATHS	23UMA118	26/Feb/24
145	செ.விஜால்	I BSC. Maths	23UMA129	
146	ஸ்.ஜோஷ்வா சிஜோர்	I B.Sc Maths	23UMA132	

ஆசா அறக்கட்டளைச் சிறப்பு சொற்பொழிவு & பரிசளிப்பு விழா - 26.02.2024

எண்	பெயர்	வகுப்பு	துறை எண்	கையொப்பம்
147	சு.நவீன்	B.Sc physics 'A'	23UPH118	S.Naveen
148	சு.சிவசங்கர்	B.Sc PHYSICS "A"	23UPH140	
149	ர.ரஞ்சித்	B.Sc physics 'A'	23UPH109	
150	வி.மணிசங்கர்	Bsc.Physics 'A'	23UPH115	
151	ச.சஞ்சய்	BSc.Maths 'B'	23UMA211	S.Sanjay
152	ர.ஹரிஹரன்	B.Sc Maths "B"	23UMA231	R.Hariharan
153	செ.அஜாஸ்	B.Sc maths 'B'	23UMA224	
154	ஆ.சேதிய அபிஷேகம்	B.Sc., Maths 'B'	23UMA226	A

Dr. G. BESCHI
Associate Professor & Head
Department of Tamil
St. Joseph's College (Autonomous)
Tiruchirappalli-620 002.

ஆசா அறக்கட்டளைச் சிறப்பு சொற்பொழிவு & பரிசளிப்பு விழா - 26.02.2024

எண்	பெயர்	வகுப்பு	துறை எண்	கையொப்பம்
155	ஹை.செபஸ்டின்	I-B.Sc Physics -'A'	23UPH218	ஹை.செபஸ்டின்
156	சா.பரணிதரன்	I - B.Sc PHYSICS -'B'	23UPH222	சா.பரணிதரன்
157	M. RAKESH	I - B.Sc. Physics -'B'	23UPH223	M. Rakesh
158	ஜீ.சங்கம் குமார்	I-B.sc physics 'B"	23UPH235	ஜீ.சங்கம் குமார்
159	B. MUTHUKUMARAN	I-B.Sc Physics -"B"	23UPH201	B. Muthu
160	கோ.சிசிதேவ்	I.B.Sc. Physics -'B'	23UPH217	கோசிதேவ்
161	பெ.அஜய் ராஜா	I.B.Sc Physics -"A"	23UPH133	பெ.அஜய்ராஜா
162	அல்வின்.ரா	I-BSc Physics -'A'	23UPH147	R. Alwin

ஆசா அறக்கட்டளைச் சிறப்பு சொற்பொழிவு & பரிசளிப்பு விழா - 26.02.2024

எண்	பெயர்	வகுப்பு	துறை எண்	கையொப்பம்
163	ஜா.இளவரசன்	I-B.A.Tamil	23UTA163	ஜா.இளவரசன்
164	Akshitajaiy	I BA Tamil	23UTA129	Akshita
165	I P. தியாகராஜன்	I B.A Tamil	23 UTA 156	P Thyagarajan
166	S. மதன்	I BA Tamil	23UTA151	S. Madhan
167	I.பவுல் பிரசன்னா	I B.A.TAMIL	23UTA108	
168	S.தினகரன்	I.B.A.Tamil	23UTA120	S. Dinakaran
169	DHANABALAN	I BA TAMIL	23UTA146	Dhana
170	S. Vijayabagavathi	I. BA. Tamil	23UTA107	S Vijayabagavathi

Dr. G. BESCHI
Associate Professor & Head
Department of Tamil
St. Joseph's College (Autonomous)
Tiruchirappalli-620 002.

ஆசா அறக்கட்டளைச் சிறப்பு சொற்பொழிவு & பரிசளிப்பு விழா - 26.02.2024

எண்	பெயர்	வகுப்பு	துறை எண்	கையொப்பம்
171	சி. சிவசங்கரன்	இளங்கலைத் தமிழ் மூன்றாம் ஆண்டு	21UTA140	
172	ஆ. சுமீசன் டேனியல்.	இளந்தளைத் தமிழ் மூன்றாம் ஆண்டு.	21UTA106.	
173	இ. கார்யா	"	21UTA173	
174	கு. லோகேஸ்வரன்	"	21UTA145	
175	ம. வைஷாலினி	இளங்கலைத் தமிழ் மூன்றாம் ஆண்டு	21UTA112	
176	ம. லியோதிரின்ஸி	இளங்கலைத் தமிழ் மூன்றாம் ஆண்டு	21UTA110	M. Leoshiny.
177	சி. பு. சித்ரிகா	இளங்கலைத் தமிழ் மூன்றாம் ஆண்டு	21UTA116	
178	பொ. சத்தியபிரியா	இளங்கலைத் தமிழ் மூன்றாம் ஆண்டு.	21UTA123	P. Sathya priya
179	த. சுபிதர்.	இளங்கலைத் தமிழ் மூன்றாம் ஆண்டு.	21UTA121	T. Subitha.

ஆசா அறக்கட்டளைச் சிறப்பு சொற்பொழிவு & பரிசளிப்பு விழா - 26.02.2024

எண்	பெயர்	வகுப்பு	துறை எண்	கையொப்பம்
180	அமிழ் அகஸ்டின்	இளங்கலை தமிழ் இரண்டாம் ஆண்டு	22UTA153	
181	ஹெய்லி. ஜோ	இளங்கலை தமிழ் இரண்டாம் ஆண்டு	22UTA108	
182	கீர்த்தனா. ச	இளங்கலைத் தமிழ் இரண்டாம் ஆண்டு	22UTA107	
183	ஆர்த்தி - கி	இளங்கலைத் தமிழ் இரண்டாம் ஆண்டு	22UTA136	
184	விமலி. ஜ	இளங்கலைத் தமிழ் இரண்டாம் ஆண்டு	22UTA105	Vimala
185	விந்திகா. அ.	இளங்கலைத் தமிழ் இரண்டாம் ஆண்டு	22UTA123	vinthika
186	சுந்தியா மேரி. அ	இளங்கலைத் தமிழ் இரண்டாம் ஆண்டு	22UTA113	Santhiya mary.
187.	ஜெ. ஜா. அரசி மார்லின்	இளங்கலைத் தமிழ் இரண்டாம் ஆண்டு	22UTA104	Arasi marlina

Dr. G. BESCHI
Associate Professor & Head
Department of Tamil
St. Joseph's College (Autonomous)
Tiruchirappalli-620 002.

நிறைவு விழா

09.01.2024 செவ்வாய்க்கிழமை

மதியம் 03.00 மணி

பயிற்சியாளர்கள்

ஓவியக்கவிஞர் **அமுதபாரதி**

கவிஞர் **பாட்டாளி** / கவிஞர் நந்தவனம் **சந்திரசேகரன்**

கவிஞர் **திருவைக்குமரன்** / திண்டுக்கல் **தமிழ்ப்பித்தன்**

திருமிகு **ஜெடிஆர்** / திருமிகு **தினகரன்**

திருமிகு **இரா.தமிழ்தாசன்** / முனைவர் **ஜா.சலேத்**

வரவேற்புரை

முனைவர் **சு.சீனிவாசன்**

ஒருங்கிணைப்பாளர்

தமிழ்த்துறை (பணிமுறை II)

முன்னிலை

திருமிகு **சி. பாக்கிய செல்வரதி**

துணை முதல்வர் பணிமுறை II

பயிற்சி அனுபவப் பகிர்வு பங்கேற்பாளர்கள்

பங்கேற்பாளர்களுக்குப் பாராட்டுச் சான்றிதழ் வழங்கி நிறைவுரை

அருள்முனைவர்

ம.ஆரோக்கியசாமி சேவியர், சே.ச.

முதல்வர், தூய வளனார் கல்லூரி.

நன்றியுரை

முனைவர் **ஜா.சலேத்**

பயிற்சி ஒருங்கிணைப்பாளர்

நிகழ்ச்சித் தொகுப்பு

செல்வி **செ.ஜா. அருசி மார்லின்**

இளங்கலைத் தமிழ் இரண்டாம் ஆண்டு

அழைப்பின் மகிழ்வில்

முதல்வர் & தமிழாய்வுத்துறையினர்

தூய வளனார் கல்லூரி

திருச்சிராப்பள்ளி -2

தமிழாய்வுத்துறை

தூய வளனார் கல்லூரி,

திருச்சிராப்பள்ளி – 2

வேர்கள்

அறக்கட்டளை

வெற்றிமொழி

அங்குசம்

திருச்சிராப்பள்ளி

ராயல் லயன்ஸ் சங்கம்

324 I சங்க எண் : 155083

இணைந்து நடத்தும்

படைப்பிலக்கியப் பயிலரங்கம்

(Workshop on Creative Writing)

08 & 09

ஜனவரி 2024

திங்கள் & செவ்வாய்

நூலக அரங்கம்

(SAIL HALL)

தூய வளனார் கல்லூரி

Dr. G. BESCHI
Associate Professor & Head
Department of Tamil
St. Joseph's College (Autonomous)
Tiruchirappalli-620 002.

படைப்பாற்றல் பயிலரங்கம் 2024

தொடக்க விழா

08.01.2024 திங்கள் கிழமை,
காலை 10.30 மணி

தலைமை

அருள்முனைவர் **பவுல்ராஜ் மைக்கேல்** சே.ச.
அதிபர் தூய வளனார் கல்லூரி நிறுவனங்கள்

எழுத்தாளர்களைச் சிறப்பித்துப் பாராட்டுரை

அருள்முனைவர் **கு.அமல்** சே.ச.
செயலர், தூய வளனார் கல்லூரி

விதைநெல் 2023
இதழை வெளியிட்டுப் பாராட்டுரை

அருள்முனைவர்
ம.ஆரோக்கியசாமி சேவியர், சே.ச.
முதல்வர், தூய வளனார் கல்லூரி.

வரவேற்புரை

முனைவர் **ஆ.ஜோசப் சகாயராஜ்**
ஒருங்கிணைப்பாளர், படைப்பிலக்கிய மன்றம்

அறிமுகவுரை

முனைவர் **ஞா.பெஸ்கி**
தமிழாய்வுத்துறைத் தலைவர்

முன்னிலை

MJF Lion. S. **அடைக்கல ராஜா**
நிறுவுநர், வேர்கள் அறக்கட்டளை

Lion. B. **முகமது ஷபி**
சாசனத்தலைவர்,
திருச்சிராப்பள்ளி ராயல் லயன்ஸ் சங்கம்

சிறப்பிக்கப்படும் எழுத்தாளர்கள்
ஓவியக்கவிஞர் **அமுதபாரதி**
கவிஞர் **பாட்டாளி**
கவிஞர் **திருவைக்குமரன்**

பயிலரங்கைத் தொடங்கி வைத்து
விழாப் பேருரை
''இலக்கும் இலக்கியமும்''
கவிஞர் **ஜெயபாஸ்கரன்**
ஊடகவியலாளர் - எழுத்தாளர்

நன்றியுரை

முனைவர் **ஆ.இராஜாத்தி**
உதவிப்பேராசிரியர், தமிழாய்வுத்துறை

நிகழ்ச்சித் தொகுப்பு

செல்வி **ச.மதுமிதா.**
செல்வி. **ப.ஆனி ரெக்ஸிட்டா**
இளங்கலைத் தமிழ் மாணவர்கள்

Dr. G. BESCHI
Associate Professor & Head
Department of Tamil
St. Joseph's College (Autonomous)
Tiruchirappalli-620 002.

படைப்பிலக்கியப் பயிலரங்கம் (08, 09.01.2024) அறிக்கை

தமிழாய்வுத்துறை, திருச்சிராப்பள்ளி ராயல் லயன்ஸ் சங்கம், திண்டுக்கல் வெற்றிமொழி வெளியீட்டகம், அங்குசம் அறக்கட்டளை மற்றும் அங்குசம் அறக்கட்டளை ஆகிய அமைப்புகளுடன் இணைந்து, கல்லூரி மாணவர்களுக்கானப் படைப்பிலக்கியப் பயிலரங்கை 2024 ஜனவரி 08 மற்றும் 09 ஆகிய தேதிகளில் நடத்தியது.

கல்லூரி அதிபர் **அருள்முனைவர் பவுல்ராஜ் மைக்கேல்** அவர்களின் தலைமையில் நடைபெற்ற இப்பயிலரங்கின் தொடக்கவிழாவில் தமிழகத்தின் மூத்த கவிஞர்களுள் ஒருவரும், தமிழின் முதல் ஹைக்கூ நூலாசிரியர் **ஓவியக்கவிஞர் அமுதபாரதி** அவர்களுக்கு 50 ஆயிரம் பொற்கிழி வழங்கப்பட்டது. பல ஆண்டுகளாக இதழியல் துறையில் சிறப்பாகப் பணியாற்றி வரும் திருச்சிராப்பள்ளி எழுத்தாளர்கள் **கவிஞர் பாட்டாளி** மற்றும் **கவிஞர் திருவைக்குமரன்** ஆகியோரை கல்லூரி முதல்வர் **அருள்முனைவர் ம.ஆரோக்கியசாமி சேவியர்** விருது வழங்கிப் பாராட்டினார்

கல்லூரிச் செயலர் படைப்பிலக்கியப் பயிலரங்கில் ஓலைப்பாயால் அமைக்கப்பட்ட பதாகையை வெகுவாகப் பாராட்டினார். படைப்பிலக்கிய மன்ற ஒருங்கிணைப்பாளர் **முனைவர் ஆ.ஜோசப் சகாயராஜ்** வரவேற்புரையாற்றினார். தமிழாய்வுத்துறைத் தலைவர் **முனைவர் ஞா.பெஸ்கி** அறிமுகவுரையாற்றினார். வேர்கள் அறக்கட்டளை நிறுவுநர் **எம்ஜேஎஃப் லயன் அடைக்கலராஜா,** திருச்சிராப்பள்ளி ராயல் லயன்ஸ் சங்க சாசனத்தலைவர் **லயன் முகமது ஷபி** ஆகியோர் முன்னிலை வகித்தனர்.

Dr. G. BESCHI
Associate Professor & Head
Department of Tamil
St. Joseph's College (Autonomous)
Tiruchirappalli-620 002.

மக்கள் கவிஞர் ஜெயபாஸ்கரன் *கடந்த ஆண்டுப் பயிலரங்கில் மாணவர்கள் எழுதிய படைப்புகள் அடங்கிய விதைநெல் 2023 என்னும் இதழை வெளியிட்டு இலக்கும் இலக்கியமும் என்னும் பொருண்மையில் விழாப்பேருரையாற்றிப் பயிலரங்கைத் தொடங்கி வைத்து* ***ஓவியக்கவிஞர் அமுதபாரதி, கவிஞர் பாட்டாளி, கவிஞர் நந்தவனம் சந்திரசேகரன், கவிஞர் திருவைக்குமரன், கவிஞர் திண்டுக்கல் தமிழ்ப்பித்தன், தினகரன்*** *உட்பட்ட எழுத்தாளர்கள் மற்றும் பத்திரிகையாளர்கள் இந்தப் பயிலரங்கில் பங்கேற்று மாணவர்களுக்குப் பயிற்சியை வழங்கினர்.*

நிறைவில் இப்பயிலரங்கின் ஒருங்கிணைப்பாளர் தூய வளனார் கல்லூரி தமிழாய்வுத்துறை உதவிப் பேராசிரியர் ***முனைவர் ஜா.சலேத்*** *நன்றியுரையாற்றினார். திருச்சிராப்பள்ளியைச் சார்ந்த 34 கல்லூரி மாணவர்கள் இப்பயிலரங்கில் பங்கேற்க ஏற்பாடு செய்யப்பட்டுள்ளது.*

Dr. G. BESCHI
Associate Professor & Head
Department of Tamil
St. Joseph's College (Autonomous)
Tiruchirappalli-620 002.

ஒளிப்படங்கள்

Dr. G. BESCHI
Associate Professor & Head
Department of Tamil
St. Joseph's College (Autonomous)
Tiruchirappalli-620 002.

ஒளிப்படங்கள்

Dr. G. BESCHI
Associate Professor & Head
Department of Tamil
St. Joseph's College (Autonomous)
Tiruchirappalli-620 002.

விதைநெல் - 2023

மாணவர் படைப்புகள்

தமிழாய்வுத்துறை
தூய வளனார் கல்லூரி (தன்னாட்சி)
திருச்சிராப்பள்ளி - 620 002

Dr. G. BESCHI
Associate Professor & Head
Department of Tamil
St. Joseph's College (Autonomous)
Tiruchirappalli-620 002.

ஊடகப் பதிவுகள்

படைப்பிலக்கியப் பயிலரங்கமும்
புல்லாங்குழல்களான மூங்கில்களும்!

திருச்சி தூயவளனார் கல்லூரியின் தமிழாய்வுத்துறை ஏற்பாட்டில், "படைப்பிலக்கியப் பயிலரங்கு" ஜனவரி08,09 ஆகிய இருநாட்கள் நிகழ்வாக கல்லூரி வளாகத்தில் நடைபெற்றது. கல்லூரி வளாகத்தில் .:பிளக்ஸ் பேனர் பயன்படுத்தக்கூடாது என கண்டிப்புடன் கல்லூரி நிர்வாகம் விதித்த தடையைத் தொடர்ந்து கோரைப்பாயில் வரையப்பட்டிருந்த அறிவுப்பு பதாகை அனைவரின் கவனத்தையும் பெற்றது. அங்குசம் இதழ், வேர்கள் அறக்கட்டளை, வெற்றிமொழி வெளியீட்டகம், திருச்சிராப்பள்ளி ராயல் லயன்ஸ் சங்கம் ஆகியவை இணைந்து இப்படைப்பிலக்கியப் பயிலரங்கை நடத்தின.

தூயவளனார் கல்லூரி அதிபர் பவுல்ராஜ் மைக்கேல் தலைமையில் நடைபெற்றநிகழ்வில்,இப்பயிலரங்கை தொடங்கிவைத்துபேருரையாற்றினார், எழுத்தாளரும், கவிஞருமான ஜெய பாஸ்கரன். "வாசிப்பதும், எழுதுவதும் இளைஞர்களின் வழக்கமாக வேண்டும். இலக்கியம் கூறும் அறம் வழி வாழும் படைப்பாளர்களாக மாணவர்கள் உருவாக வேண்டும். கல்வி வழி மனிதம் வளர்க்கும் தூய வளனார் கல்லூரியின் பணி போற்றுதலுக்குரியது." என்றார் அவர்.

> "பாடப் புத்தகங்களின் வழியே, பிழைப்புக்கான கல்வித் தகுதியை வழங்கும் 'தொழிற்சாலை'யாய் அல்லாமல், "அறிவை விரிவு செய், அகண்டமாக்கு" என்ற பாவேந்தனின் வரிகளுக்கேற்ப..."

கடந்த ஆண்டு பயிலரங்கில் பங்கேற்ற மாணவர் கள் படைத்த, "விதை நெல்" என்கிற மாணவர் இதழை வெளியிட்டு கல்லூரி முதல்வர் ஆரோக்கியசாமி சேவியர் உரையாற்றினார்.ஹைக்கூ கவிஞரும் மூத்த ஓவியக்கவிஞருமான அமுதபாரதி அவர்களுக்கு தூயவளனார் கல்லூரி நிர்வாகத்தின் சார்பில் 50,000 பொற்கிழி வழங்கி சிறப்பு செய்தனர்.

இதனைத் தொடர்ந்து, கவிஞர் பாட்டாளி, கவிஞர் திருவைக்குமரன் ஆகியோர் கேடயம் வழங்கி கௌரவிக்கப்பட்டார்கள்.

இவ்விழாவில், திருச்சி ராயல் அரிமா சங்கத்தின் சாசனத் தலைவர் முகமது ஷபி; தூயவளனார் கல்லூரி சார்பில் தமிழ்த்துறைத் தலைவர் முனைவர் பெஸ்கி; பணிமுறை-2இன் துணை முதல்வர் திருமதி சி.பாக்கிய செல்வரதி; படைப்பிலக்கிய மன்ற ஒருங்கிணைப்பாளர் முனைவர் ஆ.ஜோசப்சகாயராஜ்;பேராசிரியர்கள் ஜா.சலேத், ராசாத்தி, சு.சிவிவாசன், கவிஞர் நந்தவனம் சந்திரசேகரன், அங்குசம் இதழின் ஆசிரியர் ஜே.டி.-ஆர். உள்ளிட்டோர் பங்கேற்றனர்.

இதனைத்தொடர்ந்து, கவிஞர் நந்தவனம் சந்திரசேகரன், கவிஞர் பாட்டாளி, கவிஞர் திருவைக் குமரன், கவிஞர் திண்டுக்கல் தமிழ்ப்பித்தன், தமிழ்தாசன், முனைவர் ஜா.சலேத், அங்குசம் இதழின் ஆசிரியர் ஜே.டி.-ஆர்., மற்றும் அங்குசம் இதழின் முதன்மை செய்தியாளர் வே.தினகரன் ஆகியோர் பயிற்சியாளர்களாக பங்கேற்று இருநாள் படைப்பிலக்கியப் பயிலரங்கை நடத்தினர். இருநாள் நிகழ்வையும், தமிழ்த்துறை மாணவர் களான ச.மதுமிதா, ச.ஆஷிக்டோனி மற்றும் செ.ஜா. அரசி மார்வின் ஆகியோர் ஒருங்கிணைத்து வழிநடத்தினர்.

நாளொன்றுக்கு இரண்டு "ஷிப்டுகள்" வீதம் பாடப்புத்தகங்களின் வழியே, பிழைப்புக்கான

அங்குசம் செய்தி ஜனவரி 16 - 31 2024

Dr. G. BESCHI
Associate Professor & Head
Department of Tamil
St. Joseph's College (Autonomous)
Tiruchirappalli-620 002.

கல்வித் தகுதியை வழங்கும் 'தொழிற்சாலை'யாய் அல்லாமல், "அறிவை விரிவு செய், அகண்டமாக்கு" என்ற பாவேந்தரின் வரிகளுக்கேற்ப மாணவர்களை வார்க்க வேண்டுமென்ற நோக்கிலான, தூய வளனார் கல்லூரி நிர்வாகத்தின் முன்னெடுப்பு முன்னுதாரணமானது. திருச்சி, பெரம்பலூர், கரூர் மாவட்டங்களைச் சேர்ந்த பல்வேறு கல்லூரிகளின் சார்பில் பயிலரங்கில் பங்கேற்ற மாணவர்களுள் கணிசமானவர்கள் தமிழ்த்துறை அல்லாத, பிற துறைகளைச் சேர்ந்த மாணவர்கள். அதிலும் சரிபாதிக்கும் மேலானவர்கள் மாணவிகள்.

இசுலாமிய பெண்மணி ஒருவர் எழுதிய முதல் கவிதை; மருத்துவ சிகிச்சையிலிருந்து அப்படியே பயிற்சியில் பங்கேற்ற மாணவி; பகுதிநேர வேலைக்கும் சென்றாக வேண்டும் என்ற நிர்ப்பந்தத்தினூடே பயிற்சியில் பங்கேற்ற மாணவர்; குறிப்பிட்ட அரசியல் பத்திரிக்கை ஒன்றின் பெயரைக் குறிப்பிட்டு, அந்த இதழ் எங்கே கிடைக்கும் என்று விசாரித்த மாணவி ஒருவரது அரசியல் ஆர்வம்; பயிற்சியை முடித்த கூட்டோடு மாணவர் ஒருவர் தனது படைப்புகளை பதிவு செய்வதற்கென்றே பிரத்யேகமாக தொடங்கிய இன்ஸ்டாகிராம் பக்கம் என பயிலரங்கில் பங்கேற்ற மாணவர்களின் படைப்பிலக்கிய ஆர்வம் பிரமிப்பை ஏற்படுத்தின. மிக முக்கியமாக, இவர்களை பின்னிருந்து வழிநடத்தும் பேராசிரியர்களின் பங்களிப்பு குறிப்பிடத்தக்கது. போற்றுதலுக்குரியது!

"இந்தக் காட்டில் எந்த மூங்கில் புல்லாங்குழல்?" என்ற, புகழ்பெற்ற கவிஞர் அமுதபாரதியின் ஹைக்கூ கவிதைக்கு பதிலளிக்கும் விதமாக, "இங்கே வீற்றிருக்கும் மூங்கில்கள் அனைத்துமே நிச்சயம் புல்லாங்குழல்களாக மாறும்" என அனுபவப் பகிர்வில், முத்தாய்ப்பாய் பேசினார் மாணவி ஒருவர். அதனை மெய்ப்பிக்கும் வகையில், நறுக் வார்த்தைகளால் கட்டமைக்கப்பட்ட சமூக அவலங்களை சுட்டும் நேர்த்தியான ஹைக்கூ கவிதைகள்; விமர்சன கண்ணோட்டத்தில் எழுதப் பட்ட அரசியல் கட்டுரைகள்; பெண் வாழ்வியலை மையப்படுத்திய சிறுகதைகள் என ஆகச்சிறந்த படைப்புகளை சமர்ப்பித்து அசத்தினார்கள், பயிற்சியில் பங்கேற்ற மாணவர்கள். தூயவளனார் கல்லூரியின் தமிழ்த்துறைத் தலைவர் முனைவர் பெஸ்கி தலைமையில் நடைபெற்ற நிறைவுவிழாவில், வேர்கள் அறக்கட்டளையின் நிறுவனர் அடைக்கலராஜா அவர்கள், பயிலரங்கில் பங்கேற்ற மாணவர்களுக்கு சான்றிதழ்களையும் அறிவுப் பொக்கிஷங்களான நூல்களையும் வழங்கி பாராட்டினார் ●

◆◆ வே.தினகரன்.

ஃபிளக்ஸ் பேனருக்கு மாற்றாக கோரைப்பாயில் பேனர்!

"ஃப்ளக்ஸ் பேனருக்கு கல்லூரி நிர்வாகம் தடைவித்ததைத் தொடர்ந்து, திண்டுக்கல் ஓவியக்கலைஞர் புஷ்பராஜ் பங்களிப்போடு, இந்த கோரைப்பாய் பதாகையை நிறுவினோம்" என்கிறார், பயிலரங்கின் ஒருங்கிணைப்பாளர் பேராசிரியர் ஜா.சலேத்.

ப்ளக்ஸ் பேனர்களால் சுற்றுச்சூழலுக்கு ஏற்படுத்தும் பாதிப்பு அபாயகரமானது என்பதை சுற்றுச்சூழல் செயற்பாட்டாளர்கள் தொடர்ந்து எச்சரித்து வரும் சூழலில், மிக முக்கியமாக, முந்தைய காலகட்டத்தில் தூரிகை கலைஞர்களாக, சுவரோவியக் கலைஞர்களாக வலம் வந்தவர்களை யெல்லாம், சுண்ணாம்பு அடிக்கும் பெயிண்டர்களாக மாற்றிவிட்ட அவலத்திற்கு மத்தியில், ஃப்ளெக்ஸ் பேனர்களை பயன்படுத்துவதற்கு கல்லூரி நிர்வாகம் விதித்திருக்கும் தடை முக்கியத்துவம் பெறுகிறது.

"ஆஹா! அற்புதம்!" என்ற வகையிலான வார்த்தைகளை உதிர்த்துவிட்டு கடந்து செல்லாமல், அவரவர் தனது வரம்பிற்குட்பட்ட வகையில் ஃப்ளெக்ஸ் பேனர்களின் பயன்பாட்டை தவிர்ப்பதே காலத்தின் தேவை.

அங்குசம் செய்தி ஜனவரி 16 - 31 2024

Dr. G. BESCHI
Associate Professor & Head
Department of Tamil
St. Joseph's College (Autonomous)
Tiruchirappalli-620 002.

படைப்பிலக்கியப் பயிலரங்கம்

8, 9, ஜனவரி 2024

'மக்களை மையப்படுத்திய இலக்கியங்களே வரலாற்றில் வாழும்'

திருச்சி தூய வளனார் கல்லூரியில் தமிழ்த்துறை சார்பில் 2 நாள் படைப்பிலக்கிய பயிலரங்கு நிகழ்ச்சி தொடங்கியது. இந்த பயிலரங்கை தொடங்கி வைத்து எழுத்தாளரும் கவிஞருமான ஜெயபாஸ்கரன் பேசுகையில், இலக்கியங்கள் மனித வாழ்வில் ஒளிரூட்டுவதற்காக உருவாக்கப்பட்டவை. கல்வி வழி மனிதம் வளர்க்கும் தூய வளனார் கல்லூரியின் இந்நிகழ்வு போற்றுதலுக்குரியது. மனிதத்தை உயர்த்தும் பிறக்கும் தமிழ் இலக்கியங்களே வரலாற்றில் இடம் பெறும் தகுதி பெற்றது.

திருச்சி தூய வளனார் கல்லூரியில் தொடங்கிய படைப்பிலக்கிய பயிலரங்கில் கவிஞர் திருவைக்குமாறுக்கு கேடயம் வழங்கி கௌரவித்த (இடமிருந்து) அரிமா சங்கத் தலைவர் முகமது வசிம், கல்லூரி அதிபர் பவுல்ராஜ் ஜைகேல், முதல்வர் ஆரோக்கியசாமி சேவியர், கவிஞர் அமுதபாரதி, கல்லூரிச் செயலர் அமல், கவிஞர் ஜெயபாஸ்கரன்.

வாசிப்பதும் எழுதுவதும் இளைஞர்களின் வழக்கமாக வேண்டும். பாலினச் சமத்துவத்தை பள்ளி பாட்டை சுற்றுச்சூழலைப் போற்றி பாதுகாக்கும் படைப்புகளை உருவாக்கும் படைப்பாளர்களாக மாணவர்கள் உருவாக்க வேண்டும். அறிவியல் படிப்பவர்கள் அந்த தலைமுறையின் சாதனை செய்வர்.

ஆதாம் படிப்பவர்கள் வணிகவியல் குறித்தே சிந்திப்பீர். படைப்பாளர்கள் தான் இலக்கியங்களுக்கு கருவாக அறத்தின் வழிநடை வாழ்க்கையை முன் கொடுப்பர் என்றார் அவர். தொடர்ந்து கல்லூரி அதிபர் பவுல்ராஜ் ஜைகேல் தலைமை வகித்தார். விழாவில் எழுத்தாளர் மாணவர் இதழை வெளியிட்டு கல்லூரி முதல்வர் ஆரோக்கியசாமி சேவியர் உரையாற்றினார். முன்னதாக பெல்சி அரிமுவலாயாற்றினார். தோசியர் ஜா. சவேத் விருதாளர்களை அறிமுகப்படுத்தினார். திருச்சி ராயல் அரிமா சங்கத்தின் சார்பில் தலைவர் முகமது வசிம் முன்னிலை வகித்தார்.

தமிழ்க் கவிதையுலகில் முன்னோடிகளும், வளரக்க கவிதைகள் தரும் வழி தமிழுக்கு அறிமுகப்படுத்தியவருமான ஒவியக்கவிஞர் அமுதபாரதி, கவிஞர் பாட்டாளி, கவிஞர் இருவைக் குமரன் ஆகிய எழுத்தாளர்களுக்கு கேடயம் பரிசுகள் வழங்கி கௌரவிக்கப்பட்டனர். முன்னதாக படைப்பிலக்கிய மன்ற ஒருங்கிணைப்பாளர் முனைவர் ஆ. ஜோசப் சகாயராஜ் வரவேற்று பேசினார்.

நிகழ்ச்சியை, மாணவர்கள் ஆரிக் டோனி, மதுமிதா ஆகியோர் தொகுத்து செய்தனர். தமிழ் ஆர்வலர்கள், எழுத்தாளர்கள், அரிமா சங்க உறுப்பினர்கள், கல்லூரி மாணவர்கள் இப்பயிலரங்கில் பங்கேற்றுப் பயனடைந்தனர். இறுதியாக உதவிப் பேராசிரியர் ஆ. ராஜாத்தி நன்றி கூறினார்.

இந்த பயிலரங்கம், வேர்கள் அறக்கட்டளை, திருச்சி ராயல் அரிமா சங்கம், வெற்றிமொழி வெளியீட்டகம் உள்ளிட்டவை இணைந்து நடத்துவதாக இரண்டாவது நாளாக செவ்வாய்கிழமையும் இந்தப் பயிலரங்கு நடைபெறுகிறது.

தினமணி திருச்சிராப்பள்ளி

09/01/2024

Dr. G. BESCHI
Associate Professor & Head
Department of Tamil
St. Joseph's College (Autonomous)
Tiruchirappalli-620 002.

படைப்பிலக்கிய பயிற்சிப்பட்டறை

— 8, 9 ஜனவரி 2024 —

கல்லூரி மாணவர்களுக்கு நந்தவனம் சந்திரசேகரன் பயிற்சி வழங்கிய போது எடுத்த படம். அருகில் கல்லூரி அதிபர் பவல்ராஜ் மைக்கேல் மற்றும் பலர் உள்ளனர்.

திருச்சி தூய வளனார் கல்லூரியில்

மாணவர்களுக்கு படைப்பிலக்கியப் பயிற்சிப்பட்டறை

நந்தவனம் சந்திரசேகரன் பயிற்சி வழங்கினார்

திருச்சி, ஜன. 9–

திருச்சி தூய வளனார் கல்லூரியில் மாணவர்களுக்கான பயிற்சி வகுப்பு 2 நாட்கள் நடைபெற்றது. இதில் சமகால படைப்புகளின் போக்கு, கதை, கவிதை எழுதுவதற்கான வழிமுறைகள், படைப்பிலக்கியம் நிலம் சமூகத்திற்கு என்ன சொல்லலாம், எழுத்தாளனுக்கு உள்ள கடமைகள்பொறுப்புகள் என்னென்ன என்பது பற்றிய கருத்துக்களை நந்தவனம் சந்திரசேகரன் மாணவர்களுக்கு பயிற்சி அளித்தார்.

கல்லூரி அதிபர் பவல்ராஜ் மைக்கேல் தலைமையில் நடைபெற்ற விழாவில் கவிஞர்கள் அமுதபாரதி, பாட்டாளி, திருவள்ளுவன் ஆகியோருக்கு விருது வழங்கப்பட்டது. கல்லூரியின் செயலர் சு. அமல் பாராட்டுரை வழங்க கல்லூரி முதல்வர் மாணவர்களின் படைப்புகளுடன் வெளியிடப்பட்ட விதைநெல் பத்திரிக்கையை வெளியிட்டார்.

கவிஞர் ஜெயபாஸ்கரன் சிறப்புரையாற்றினார். தமிழ் துறை தலைவர் ஞா. பெஸ்கி வாழ்த்துரை வழங்கினார். ஜா. சலேத் நிகழ்வை ஒருங்கிணைத்தார், முன்னதாக ஆ. ஜோசப் சகாயராஜ் அனைவரையும் வரவேற்றார். முடிவில் அதிராஜ் நன்றி கூறினார்.

இந்த தகவலை ரோட்டரி துணை ஆளுநர் மாவட்டம் 3000த்தின் 2024–25ம் ஆண்டுக்கான மீடியா பப்ளிசிட்டி அதிகார் ரொட்டேரியன் கே. பரினிவாசன் தெரிவித்தார்

மாலைமலர் திருச்சி பதிப்பு

09/01/2024

Dr. G. BESCHI
Associate Professor & Head
Department of Tamil
St. Joseph's College (Autonomous)
Tiruchirappalli-620 002.

தமிழாய்வுத்துறை

தூய வளனார் கல்லூரி, திருச்சிராப்பள்ளி - 2

வேர்கள் அறக்கட்டளை

வெற்றிமொழி

திருச்சிராப்பள்ளி ராயல் லயன்ஸ் சங்கம்
324 F சங்க எண் : 155083

அங்குசம்

இணைந்து நடத்தும்

படைப்பிலக்கியப் பயிலரங்கம்

(Workshop on Creative Writing)

பங்கேற்புச் சான்றிதழ்

2024ஆம் ஆண்டு ஜனவரி 08 மற்றும் 09 ஆகிய நாள்களில் திருச்சிராப்பள்ளி **தூய வளனார் கல்லூரியில்**

நடைபெற்ற **படைப்பிலக்கியப் பயிலரங்கில்** செல்வன் / செல்வி _____

செ. ஜா. அரசி மார்லின் _____ அவர்கள் பங்கேற்றமைக்காகப் பாராட்டி

இச்சான்றிதழ் வழங்கப்படுகிறது.

அருள்முனைவர் **ம.ஆரோக்கியசாமி சேவியர்** M.A.
முதல்வர்

முனைவர் **ஞா.பெஸ்கி**
தமிழாய்வுத்துறைத்தலைவர்

MJF. Lion. S. **அடைக்கலராஜா**
நிறுவனர்,
வேர்கள் அறக்கட்டளை

Lion. B. **முகமது ஷமி**
சாசனத்தலைவர்,
திருச்சிராப்பள்ளி ராயல் லயன்ஸ் சங்கம்

Dr. G. BESCHI
Associate Professor & Head
Department of Tamil
St. Joseph's College (Autonomous)
Tiruchirappalli-620 002.

தமிழாய்வுத்துறை

தூய வளனார் கல்லூரி, திருச்சிராப்பள்ளி - 2

வேர்கள் அறக்கட்டளை | திருச்சிராப்பள்ளி ராயல் லயன்ஸ் சங்கம் | அங்குசம் இணைந்து நடத்தும்

படைப்பிலக்கியப் பயிலரங்கம்

(Workshop on Creative Writing)

08 - 09, ஜனவரி 2024 நூலக அரங்கம், தூய வளனார் கல்லூரி

சிறப்பு அழைப்பாளர்கள்

எண்	பெயர்	முகவரி (அலைபேசி எண்)	கையொப்பம்
1	Fr. K. Amal SJ	செயலர் தூய வளனார் கல்லூரி	
2	அழகுதான்	ஜே-5, பட்டினப் பாக்கம் சென்னை 600028 செல்லை பேசி : 9840 380063	

Dr. G. BESCHI
Associate Professor & Head
Department of Tamil
St. Joseph's College (Autonomous)
Tiruchirappalli-620 002.

தமிழாய்வுத்துறை

தூய வளனார் கல்லூரி, திருச்சிராப்பள்ளி - 2

வேர்கள் அறக்கட்டளை | அங்குசம்

படைப்பிலக்கியப் பயிலரங்கம்

(Workshop on Creative Writing)

08 - 09, ஜனவரி 2024 நூலக அரங்கம், தூய வளனார் கல்லூரி

பயிற்சியாளர்கள்

எண்	பெயர்	முகவரி (அலைபேசி எண்)	கையொப்பம்
3	[illegible]	எண் 17- பாய்க்காரத் தெரு உறையூர், திருச்சி 620003 9443284823	
4	பாமாதேவி	சிந்தனையகம் 9443545262 12, திருவள்ளுவர் தெரு ஆர்.எம்.எஸ் காலனி (அடுக்கு) விடமணைப்பட்டி புதூர் திருச்சி - 620 012	

Dr. G. BESCHI
Associate Professor & Head
Department of Tamil
St. Joseph's College (Autonomous)
Tiruchirappalli-620 002.

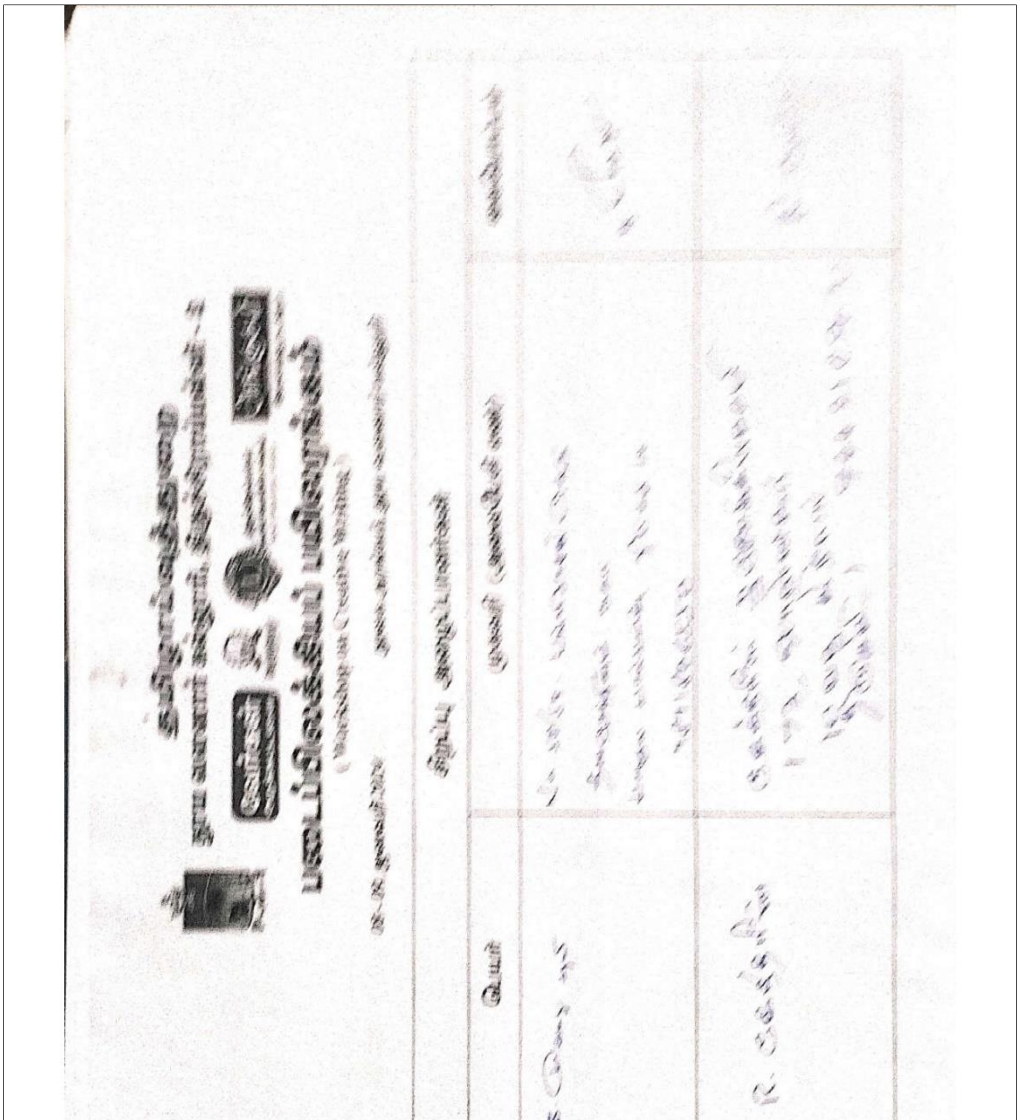

Dr. G. BESCHI
Associate Professor & Head
Department of Tamil
St. Joseph's College (Autonomous)
Tiruchirappalli-620 002.

தமிழாய்வுத்துறை

தூய வளனார் கல்லூரி, திருச்சிராப்பள்ளி - 2.

வேர்கள் அறக்கட்டளை | அங்குசம்

படைப்பிலக்கியப் பயிலரங்கம்

(Workshop on Creative Writing)

08 - 09, ஜனவரி 2024 *நூலக அரங்கம், தூய வளனார் கல்லூரி*

எண்	பெயர், துறை எண்	இல்ல முகவரி (மின் அஞ்சல், அலைபேசி எண்)	கையொப்பம்
1	அ. மாணிக்கம் 23PCC816	341 சுங்கம் தெரியர் தெரு கொங்கை நகர்-630001	அ. மாணிக்கம்
2	சி. டேனியல் 23UEN129	1/75 வடக்கு தெரு பாரதிநகர் திருச்சி-25	சி. டேனியல்
3.	வே. ஜீவசுந்தரி 23PA1456	46/52 பதவி பாண்டியன் தெரு, சரவிராணையபுரம், நாகர்கோவில்-20.	வே. ஜீவசுந்தரி

Dr. G. BESCHI
Associate Professor & Head
Department of Tamil
St. Joseph's College (Autonomous)
Tiruchirappalli-620 002.

தமிழாய்வுத்துறை

தூய வளனார் கல்லூரி, திருச்சிராப்பள்ளி - 2.

வேர்கள் அறக்கட்டளை | திருச்சிராப்பள்ளி ராயல் லயன்ஸ் சங்கம் | அங்குசம் இணைந்து நடத்தும்

படைப்பிலக்கியப் பயிலரங்கம்

(Workshop on Creative Writing)

08 - 09, ஜனவரி 2024 *நூலக அரங்கம், தூய வளனார் கல்லூரி*

எண்	பெயர், துறை எண்	இல்ல முகவரி (மின் அஞ்சல், அலைபேசி எண்)	கையொப்பம்
4.	ஸீ. ஸோனி பீட்ஸா	34/A மேலகிருஸ்ணா புரம், இலாஸ்கிடி, திருச்சி 9361230196 / 8beetsha@gmail.com	
5.	சா. மர்ஜுகா காணம்	81, மேட்டுத் தெரு, உரகனேரி, பாலக்கரை திருச்சி-8. Marjukakanam02@gmail.com 94899 44810	
6.	செ. செல்லமணி தமிழ்த்துறை 23TAM102	78, பாலைக்கரும்பட்டி, மணிலாங்குறிச்சி அஞ்சல், மருங்காபுரி தாலுகா, திருச்சி. 9360555172 / cchellamani708@gmail.com	

Dr. G. BESCHI
Associate Professor & Head
Department of Tamil
St. Joseph's College (Autonomous)
Tiruchirappalli-620 002.

தமிழாய்வுத்துறை

தூய வளனார் கல்லூரி, திருச்சிராப்பள்ளி - 2.

வேர்கள் அங்குசம்

படைப்பிலக்கியப் பயிலரங்கம்

(Workshop on Creative Writing)

08 - 09, ஜனவரி 2024 *நூலக அரங்கம், தூய வளனார் கல்லூரி*

எண்	பெயர், துறை எண்	இல்ல முகவரி (மின் அஞ்சல், அலைபேசி எண்)	கையொப்பம்
7.	ஜே. நெப்சிபா 2K21275 வரலாறு	418 - கோரைப் பாறை மேல்பாதி, புதுக்கோட்டை மாவட்டம். hepsibasv@gmail.com 8778470730	
8.	கு. நாகேஸ்வரி 2K21289 வரலாறு	250, மாரியம்மன் கோயில், பிள்ளையார்பட்டி, திருவெறும்பூர் தாலுகா, புதுக்கோட்டை மாவட்டம் - 622 502 2k21289@hectrichy.ac.in 8012342576	கு. நாகேஸ்வரி
9.	மு. பதீம் மிரியா 2K21291 வரலாறு	17, முத்துக்காடு, திருவெறும்பூர் தாலுகா, புதுக்கோட்டை மாவட்டம் - 622 501 2K21291@hectrichy.ac.in.	மு. பதீம் மிரியா

Dr. G. BESCHI
Associate Professor & Head
Department of Tamil
St. Joseph's College (Autonomous)
Tiruchirappalli-620 002.

தமிழாய்வுத்துறை

தூய வளனார் கல்லூரி, திருச்சிராப்பள்ளி - 2.

வேர்கள் அறக்கட்டளை | அங்குசம் இணைந்து நடத்தும்

படைப்பிலக்கியப் பயிலரங்கம்

(Workshop on Creative Writing)

08 - 09, ஜனவரி 2024 நூலக அரங்கம், தூய வளனார் கல்லூரி

எண்	பெயர், துறை எண்	இல்ல முகவரி (மின் அஞ்சல், அலைபேசி எண்)	கையொப்பம்
10.	ப. சஞ்சீதா 22UMA518	493, தீர்த்தம்பட்டி தெற்குக்காடு, ஆலூர் (Po), பிரான்மலை (TK), புதுக்கோட்டை (DT) - 622515 9025027512 Psanjeetha@gmail.com	P.Sanjeetha
11.	ந. பிரதிபா தேவி 23UMA513	349/277 சுப்பாயிப்பண்ணை, மண்ணச்சநல்லூர் (TK), திருச்சி-621005 pradeepap817@gmail.com 6385755825	N. Pradeepa
12.	கலைவாணி. ப 23UMA504	133/5, தொடர்வண்டி நிலையம் (அருகு), காட்டாங்குளம், தலவாய் (அஞ்சல்), ஆத்தூர் (தாலுகா) அரியலூர் (மாவட்டம்) - 621730 palaniponnu0907@gmail.com 9042862937	kalaivani.P.

Dr. G. BESCHI
Associate Professor & Head
Department of Tamil
St. Joseph's College (Autonomous)
Tiruchirappalli-620 002.

தமிழாய்வுத்துறை

தூய வளனார் கல்லூரி, திருச்சிராப்பள்ளி - 2 .

வேர்கள் அறக்கட்டளை — அங்குசம் இணைந்து நடத்தும்

படைப்பிலக்கியப் பயிலரங்கம்

(Workshop on Creative Writing)

08 - 09, ஜனவரி 2024 — நூலக அரங்கம், தூய வளனார் கல்லூரி

எண்	பெயர், துறை எண்	இல்ல முகவரி (மின் அஞ்சல், அலைபேசி எண்)	கையொப்பம்
13.	பி.கெவின் இன்பியன் பெனடிக் 22UCR536	பிளாட் எண்:6 காந்தி நகர் இரண்டாம் தெரு, கிராப்பட்டி, திருச்சி -620 012 7305734006	
14.	ஜா. முகமது இலியாஸ் 23PA1455	~~காதாடியான் அருகே~~, சிந்தாமணிபட்டி , 7/47 , சிந்தாமணிபட்டி (PO) Karur (DT) , Kadavur (TK) Email : iliyasj2003@gmail.com , 6383481167.	
15	உ. பாபர் முகமது இஸ்மாயில் கான 22PTA002	44, மேட்டு பள்ளி வாசல் வடக்கு தெரு, பழனி (தா) திண்டுக்கல் (மா), தமிழ் நாடு - 624 601. babarmohamed2008@gmail.com 9655783139.	

Dr. G. BESCHI
Associate Professor & Head
Department of Tamil
St. Joseph's College (Autonomous)
Tiruchirappalli-620 002.

தமிழாய்வுத்துறை

தூய வளனார் கல்லூரி, திருச்சிராப்பள்ளி - 2.

படைப்பிலக்கியப் பயிலரங்கம்

(Workshop on Creative Writing)

08 - 09, ஜனவரி 2024 நூலக அரங்கம், தூய வளனார் கல்லூரி

எண்	பெயர், துறை எண்	இல்ல முகவரி (மின் அஞ்சல், அலைபேசி எண்)	கையொப்பம்
16.	[illegible] 22PTA008	5/125, [illegible] — 622107 [illegible]	[illegible]
17.	L. Subhashri [illegible] B.Com	5/173 North Street, [illegible] Srirangam (TK), Trichy [illegible]	[illegible]
18.	[illegible] B.A Tamil	128/1 [illegible] Thirumarudur (TK) Ramanathapuram (Dt) [illegible]	[illegible]

Dr. G. BESCHI
Associate Professor & Head
Department of Tamil
St. Joseph's College (Autonomous)
Tiruchirappalli-620 002.

தமிழாய்வுத்துறை

தூய வளனார் கல்லூரி, திருச்சிராப்பள்ளி - 2.

வேர்கள் அறக்கட்டளை | அங்குசம் இணைந்த நட்பும்

படைப்பிலக்கியப் பயிலரங்கம்

(Workshop on Creative Writing)

08 - 09, ஜனவரி 2024 நூலக அரங்கம், தூய வளனார் கல்லூரி

எண்	பெயர், துறை எண்	இல்ல முகவரி (மின் அஞ்சல், அலைபேசி எண்)	கையொப்பம்
19.	செ.ஜா.அருளி மார்லின் 22UTA104	1/494, சக்தினா நகர், புலாங்குடி காலனி, திருச்சிராப்பள்ளி-620025 Mail: rjaculin@gmail.com Ph no: 9976794546	
80	ப. அன்னி ரெக்ஸிடா 23UTA106	2C, சந்தியாகப்பர் பாலையம், கேம்ஸ்டவுன், திருச்சி - 620 001 Mail: buannie2005@gmail.com ph.no: 9360248618	B. Annie Rexitta
81	தீபா. ந 23UTA145	2/2, அன்னை தெரு, கியமாணிக்கம், திருச்சிராப்பள்ளி - 620025. Mail: nallayandeepa@gmail.com Ph.NO: 7845564768	Deepa.N.

Dr. G. BESCHI
Associate Professor & Head
Department of Tamil
St. Joseph's College (Autonomous)
Tiruchirappalli-620 002.

தமிழாய்வுத்துறை

தூய வளனார் கல்லூரி, திருச்சிராப்பள்ளி - 2.

வேர்கள் அறக்கட்டளை | திருச்சிராப்பள்ளி ராயல் லயன்ஸ் சங்கம் | அங்குசம் இணைந்து நடத்தும்

படைப்பிலக்கியப் பயிலரங்கம்

(Workshop on Creative Writing)

08 - 09, ஜனவரி 2024 — நூலக அரங்கம், தூய வளனார் கல்லூரி

எண்	பெயர், துறை எண்	இல்ல முகவரி (மின் அஞ்சல், அலைபேசி எண்)	கையொப்பம்
௯௨	அ.ச. விக்னேஷ்வர் 23UCH140	64 E/3A கீழ்மாரத்தெரு கல்லுக்குழி, திருச்சி-2 9566367144	Aswignesh
௯௩	செ. அருண் குமார் 23UMA202	2/36, தெற்கு தெரு கரட்டாம்பட்டி 6383711021	S. Arun Kumar..
௯௪	பா. பிரவின்குமார் 22UTA158	92/5 மேலச்செட்டித்தெரு மன்னார்புரம் திருச்சி -2	B. Pravin

Dr. G. BESCHI
Associate Professor & Head
Department of Tamil
St. Joseph's College (Autonomous)
Tiruchirappalli-620 002.

தமிழாய்வுத்துறை
தூய வளனார் கல்லூரி, திருச்சிராப்பள்ளி - 2.

வேர்கள் அறக்கட்டளை | திருச்சிராப்பள்ளி ராயல் லயன்ஸ் சங்கம் | அங்குசம் இணைந்து நடத்தும்

படைப்பிலக்கியப் பயிலரங்கம்
(Workshop on Creative Writing)

08 - 09, ஜனவரி 2024 நூலக அரங்கம், தூய வளனார் கல்லூரி

எண்	பெயர், துறை எண்	இல்ல முகவரி (மின் அஞ்சல், அலைபேசி எண்)	கையொப்பம்
95	மு. மொதுசாமி வரலாற்றுத்துறை 23HI108	5/126, அ. உடையாப்பட்டி மேற்கு, கழுகூர் (Po), திருச்சிறை (Tk), கரூர் (Dt). 639 120. mothusamy201282@gmail.com ph: 7200192506	மு.மொதுசாமி.
96	அ. கிருஷ்ணவேணி தமிழ்த்துறை 23TAM108	மூனையமீபட்டி, கழுகூர் (Po), திருச்சிறை (Tk) கரூர் (Dk) - 639120. Veripriya32H@gmail.com Ph: 6382257910 W.h: 9843382369	A. Krishnaveni
97	வெ. சரண்யா அறிவியல் துறை 23CS122	43, மங்காம்பட்டி, குளித்தலை, கள்ளை (Po) கரூர் (Dk) - 639110 9597970820 , 9944629205	வெ. சரண்யா

Dr. G. BESCHI
Associate Professor & Head
Department of Tamil
St. Joseph's College (Autonomous)
Tiruchirappalli-620 002.

தமிழாய்வுத்துறை

தூய வளனார் கல்லூரி, திருச்சிராப்பள்ளி - 2 .

வேர்கள் அறக்கட்டளை · திருச்சிராப்பள்ளி ராயல் லயன்ஸ் சங்கம் · அங்குசம் இணைந்து நடத்தும்

படைப்பிலக்கியப் பயிலரங்கம்

(Workshop on Creative Writing)

08 - 09, ஜனவரி 2024 நூலக அரங்கம், தூய வளனார் கல்லூரி

எண்	பெயர், துறை எண்	இல்ல முகவரி (மின் அஞ்சல், அலைபேசி எண்)	கையொப்பம்
௨௮	ரே. பிரான்சிஸ் அன்டனி 22UTA101	STT/ சந்தரசன்பட்டி (ஊர், அஞ்சல்) சிவகங்கை - 630555 - 6380883710	
௨௯	மு. வசீர் அகமது 22UTA114	2/6 நீலாவதி நகர் தெரு. கீழக்கரை - 638001	
௩0	ஜா. பெல்லார்மின் அன்டோ 22UTA103	குன்னாங்கரடுத் தோட்டம், கொங்கர்பாளையம், ஈரோடு - 638506	

Dr. G. BESCHI
Associate Professor & Head
Department of Tamil
St. Joseph's College (Autonomous)
Tiruchirappalli-620 002.

தமிழாய்வுத்துறை

தூய வளனார் கல்லூரி, திருச்சிராப்பள்ளி - 2.

வேர்கள் அறக்கட்டளை | திருச்சிராப்பள்ளி மாநகர் லயன்ஸ் சங்கம் | அங்குசம் இணைந்து நடத்தும்

படைப்பிலக்கியப் பயிலரங்கம்

(Workshop on Creative Writing)

08 - 09, ஜனவரி 2024 — *நூலக அரங்கம், தூய வளனார் கல்லூரி*

எண்	பெயர், துறை எண்	இல்ல முகவரி (மின் அஞ்சல், அலைபேசி எண்)	கையொப்பம்
31	வே.தனுஷ்யா,	1/39, கிடிக்கு தெரு, திருவானந்துறை, வேப்பந்தட்டை (TK), பெரம்பலூர் (DT), - 621117 (dhanugopal010@gmail.com 8072034597)	V.Dhanya
32	ப. அபிநயா.	1/19, சிவன் கோவில் தெரு, கல்பாடி, 621 112 பெரம்பலூர் மாவட்டம் - 621 112. (abinayaanbarasee@gmail.com) 8667746387	P.அபிநயா
33	மா. ஷர்மிளா	129/A, எம்.ஜி.ஆர் நகர், அருமடல் (நாமம்), சிறுகுடல் அஞ்சல்துறை, பெரம்பலூர் மாவட்டம் (621 116) Sharmilamanickam8@gmail.com 6374141593	M. Sharmila

Dr. G. BESCHI
Associate Professor & Head
Department of Tamil
St. Joseph's College (Autonomous)
Tiruchirappalli-620 002.

தமிழாய்வுத்துறை

தூய வளனார் கல்லூரி, திருச்சிராப்பள்ளி - 2.

வேர்கள் அறக்கட்டளை | அங்குசம் கைகோர்த்து நடத்தும்

படைப்பிலக்கியப் பயிலரங்கம்

(Workshop on Creative Writing)

08 - 09, ஜனவரி 2024 நூலக அரங்கம், தூய வளனார் கல்லூரி

எண்	பெயர், துறை எண்	இல்ல முகவரி (மின் அஞ்சல், அலைபேசி எண்)	கையொப்பம்
54	ஜா. பேரி வலண்டினா 23UTA116	440, புதுநகர், கதிமாங்கனம், குச்சனூர், புதுக்கோட்டை, 621316 merryvalentina12345@gmail.com 6374449776	J. Mary Valentina
55.	ச. மதுமிதா, 21UTA107	38/50, நெல்லையர் தெரு, முன்னூர், திருச்சிராப்பள்ளி. 620017. madhumithaofficial@gmail.com. 7708399497.	S. Madhumitha

Dr. G. BESCHI
Associate Professor & Head
Department of Tamil
St. Joseph's College (Autonomous)
Tiruchirappalli-620 002.

தமிழாய்வுத்துறை

தூய வளனார் கல்லூரி, திருச்சிராப்பள்ளி - 2

இணைந்து நடத்தும்

படைப்பிலக்கியப் பயிலரங்கம்

(Workshop on Creative Writing)

08 - 09, ஜனவரி 2024 ***நூலக அரங்கம், தூய வளனார் கல்லூரி***

பயிலரங்கத் தொடக்க விழா

08.01.2024, திங்கள் கிழமை முற்பகல் 10.30 மணி

- ***தமிழ்த்தாய் வாழ்த்து***

  தமிழாய்வுத்துறையின் மாணவிகளை அழைக்கிறோம். தமிழ்த்தாய் வாழ்த்திற்கு அனைவரும் எழுந்து நிற்போம்.

- ***வரவேற்புரை***

  வரவேற்புரையாற்ற படைப்பிலக்கிய மன்றத்தின் ஒருங்கிணைப்பாளரும், ஆசிரியர் சங்கத்தின் தலைவரும், தமிழாய்வுத்துறையின் மூத்த பேராசிரியருமான ***முனைவர் ஆ.ஜோசப் சகாயராஜ்*** *அவர்களை அழைக்கிறோம்.*

- ***தலைமையுரை***

  தலைமையுரையாற்ற ***அதிபர் தந்தை*** *அவர்களை உவகையுடன் அழைக்கிறோம்.*

- ***அறிமுகவுரை***

  எண்ணற்ற பணிகளுக்கிடையில் தூய வளனார் கல்லூரி ஏன் படைப்பிலக்கியப் பயிலரங்கை ஆண்டுதோறும் நடத்திட வேண்டும்? தமது துறை மாணவர்களுக்கு மட்டுமின்றி மற்ற துறை மாணவர்களை, மற்ற கல்லூரி மாணவர்களை அழைத்து நடத்த வேண்டும்?... உள்ளிட்ட வினாக்களுக்குத் தம் உரையால் விடையளிக்க வருகிறார் எமது துறைத்தலைவர் அவர்கள். அறிமுகவுரையாற்ற எமது பாசத்துக்குரிய துறைத்தலைவர் ***முனைவர் ஞா.பெஸ்கி ஐயா*** *அவர்களை உவகையுடன் அழைக்கிறோம்.*

- ***விதைநெல் வெளியீடு***

  காகிதத்தை ஆயுதமாகவும் - எழுதுகோலை நெம்புகோலாகவும் ஆக்கும் சீரிய பணியை படைப்பிலக்கியப் பயிலரங்கம் வழியாக நிகழ்த்தும் எமது தமிழாய்வுத்துறை இதற்கு முந்தைய ஆண்டுகளில் பாராட்டுதலுக்குரிய ஒரு பணியை செய்து வருகிறது. அதுவே விதைநெல் வெளியீடு. பயிலரங்கில் மாணவத் தோழர்கள் படைத்த படைப்புகளைத் தொகுத்து விதைநெல் என்னும் பெயரில் அடுத்த பயிலரங்கின் தொடக்க விழாவில் வெளியிடுவதே அந்தப்பணி.

அந்த வரிசையில் விதைநெல் 2001 - விதைநெல் 2002 ஆகிய இதழ்களைத் தொடர்ந்து, கடந்த கல்வியாண்டு நடைபெற்ற படைப்பிலக்கிய பயிலரங்கின் மாணவர்களின் படைப்புகள் அடங்கிய **விதைநெல் 2023** இதழ் அரங்கில் வெளியிடப்படுகிறது. இதழை போற்றுதலுக்குரிய முதல்வர் தந்தை அவர்கள் வெளியிட முதல் பிரதியை தமிழகத்தின் மூத்த கவிஞர் ஐயா அமுதபாரதி அவர்கள் பெற்றுக் கொள்கிறார்கள்.

- **எழுத்தாளர்களை சிறப்பு செய்தல்**

  தமிழ் கூறு நல்லுலகிற்கு தம் எழுத்துக்களால் அரிய பணிகளை முன்னெடுக்கும் முத்தான மூன்று எழுத்தாளர்களை தூய வளனார் கல்லூரித் தமிழாய்வுத்துறை சிறப்பிக்கும் வரலாற்றுத்தருணம் இது. எழுத்தாளர்களை அறிமுகம் செய்து வைக்க தமிழாய்வுத்துறை உதவிப் பேராசிரியர் இப்பயிலரங்கின் ஒருங்கிணைப்பாளர் **முனைவர் ஜா.சலேத்** ஐயா அவர்களை அன்புடன் அடைக்கிறோம்.

- **பாராட்டுரை**
  பாராட்டுரையாற்ற **செயலர் தந்தை** அவர்களை பேரன்புடன் அழைக்கிறோம்.

- **வாழ்த்துரை**
  வாழ்த்துரையாற்ற **முதல்வர் தந்தை** அவர்களை மகிழ்வுடன் அழைக்கிறோம்.

- **சிறப்பு விருந்தினர்களைச் சிறப்பு செய்தல்**

  இது சிறப்பு விருந்தினர்களை சிறப்பு செய்கிற நேரம்.

  1. பயிலரங்கைத் தொடங்கி வைத்து **இலக்கும் இலக்கியமும்** என்கிற பொருண்மையில் விழாப் பேருரையாற்ற வருகை தந்திருக்கும் **கவிஞர் ஜெயபாஸ்கரன்** அவர்களுக்கு நமது போற்றுதலுக்குரிய **அதிபர் தந்தை** அவர்கள் நினைவுப் பரிசு வழங்கி சிறப்பு செய்கிறார்கள்.
  2. ,இப்பயிலரங்க வெற்றிக்குத் தோழமை தந்துள்ள வேர்கள் அறக்கட்டளையின் நிறுவுநர் ***MJF* லயன் அடைக்கலராஜா** அவர்களுக்கு **செயலர் தந்தை** அவர்கள் நினைவுப் பரிசு வழங்கி சிறப்பு செய்கிறார்கள்.
  3. புதிதாக இந்த ஆண்டு பயிலரங்கிற்கு தோழமை அமைப்பாக இணைந்துள்ள திருச்சிராப்பள்ளி ராயல் லயன்ஸ் சங்கத்தின் சாசனத் தலைவர் **லயன் முகமது ஷபி** அவர்களுக்கு **முதல்வர் தந்தை** அவர்கள் நினைவுப் பரிசு வழங்கி சிறப்பு செய்கிறார்கள்.
  4. அங்குசம் செய்தி - பத்திரிகையின் ஆசிரியர் **திரு ஜெ.டிஆர்** அவர்களுக்கு **துறைத்தலைவர்** அவர்கள் நினைவுப் பரிசு வழங்கி சிறப்பு செய்கிறார்கள்.
  5. **அதிபர் தந்தை** அவர்களுக்கு பணிமுறை இரண்டின் துணை முதல்வர் **திருமதி.பாக்கிய செல்வரதி அம்மா** அவர்கள் நினைவுப் பரிசு வழங்கி சிறப்பு செய்கிறார்கள்.
  6. **செயலர் தந்தை** அவர்களுக்கு **பணிமுறை இரண்டின் தமிழ்த்துறை ஒருங்கிணைப்பாளர் முனைவர் சீனிவாசன் ஐயா** அவர்கள் நினைவுப் பரிசு வழங்கி சிறப்பு செய்கிறார்கள்.
  7. **முதல்வர் தந்தை** அவர்களுக்கு தமிழாய்வுத்துறைப் பேராசிரியர் **முனைவர் வில்சன் ஐயா** அவர்கள் நினைவுப் பரிசு வழங்கி சிறப்பு செய்கிறார்கள்.

சிறப்பு செய்தவர்களுக்கும் – சிறப்பினை ஏற்றுக் கொண்டவர்களுக்கும் நன்றி.

- ***விழாப்பேருரை***

  பயிலரங்கைத் தொடங்கி வைத்து ***இலக்கும் இலக்கியமும்*** *என்கிற பொருண்மையில் விழாப் பேருரையாற்ற உலகறிந்த பேச்சாளர்* ***கவிஞர் ஜெயபாஸ்கரன்*** *அவர்களை அன்புடன் அழைக்கிறோம்.*

- ***நன்றியுரை***

  நன்றியுரையாற்ற தமிழாய்வுத்துறைப் மூத்த பேராசிரியர் ***முனைவர் இராஜாத்தி*** *அவர்களை அழைக்கிறோம்.*